

Nanostructure Science and Technology
Series Editor: David J. Lockwood

Ligia Maria Moretto
Kurt Kalcher *Editors*

Environmental Analysis by Electrochemical Sensors and Biosensors

Volume 2: Applications

 Springer

Nanostructure Science and Technology

Series Editor:

David J. Lockwood, FRSC
National Research Council of Canada
Ottawa, Ontario, Canada

More information about this series at <http://www.springer.com/series/6331>

Ligia Maria Moretto • Kurt Kalcher
Editors

Environmental Analysis by Electrochemical Sensors and Biosensors

Applications

Volume 2

 Springer

Editors

Ligia Maria Moretto
Department of Molecular Sciences
and nanosystems
University Ca' Foscari of Venice
Venice, Italy

Kurt Kalcher
Institute of Chemistry
Universität Graz
Graz, Austria

ISSN 1571-5744

ISBN 978-1-4939-1300-8

DOI 10.1007/978-1-4939-1301-5

Springer New York Heidelberg Dordrecht London

ISSN 2197-7976 (electronic)

ISBN 978-1-4939-1301-5 (eBook)

Library of Congress Control Number: 2014949384

© Springer Science+Business Media New York 2015

This work is subject to copyright. All rights are reserved by the Publisher, whether the whole or part of the material is concerned, specifically the rights of translation, reprinting, reuse of illustrations, recitation, broadcasting, reproduction on microfilms or in any other physical way, and transmission or information storage and retrieval, electronic adaptation, computer software, or by similar or dissimilar methodology now known or hereafter developed. Exempted from this legal reservation are brief excerpts in connection with reviews or scholarly analysis or material supplied specifically for the purpose of being entered and executed on a computer system, for exclusive use by the purchaser of the work. Duplication of this publication or parts thereof is permitted only under the provisions of the Copyright Law of the Publisher's location, in its current version, and permission for use must always be obtained from Springer. Permissions for use may be obtained through RightsLink at the Copyright Clearance Center. Violations are liable to prosecution under the respective Copyright Law.

The use of general descriptive names, registered names, trademarks, service marks, etc. in this publication does not imply, even in the absence of a specific statement, that such names are exempt from the relevant protective laws and regulations and therefore free for general use.

While the advice and information in this book are believed to be true and accurate at the date of publication, neither the authors nor the editors nor the publisher can accept any legal responsibility for any errors or omissions that may be made. The publisher makes no warranty, express or implied, with respect to the material contained herein.

Printed on acid-free paper

Springer is part of Springer Science+Business Media (www.springer.com)

Foreword

Electrochemical sensors are transforming our lives. From smoke detectors in our homes and workplaces to handheld self-care glucose meters these devices can offer sensitive, selective, reliable, and often cheap measurements for an ever increasing diversity of sensing requirements. The detection and monitoring of environmental analytes is a particularly important and demanding area in which electrochemical sensors and biosensors find growing deployment and where new sensing opportunities and challenges are constantly emerging.

This manual provides up-to-date and highly authoritative overviews of electrochemical sensors and biosensors as applied to environmental targets. The book surveys the entire field of such sensors and covers not only the principles of their design but their practical implementation and application. Of particular value is the organizational structure. The later chapters cover the full range of environmental analytes ensuring the book will be invaluable to environmental scientists as well as analytical chemists.

I predict the book will have a major impact in the area of environmental analysis by highlighting the strengths of existing sensor technology whilst at the same time stimulating further research.

Oxford University
Oxford, UK

Richard G. Compton

Preface

Dear Reader,

We are pleased that you have decided to use *Environmental Analysis with Electrochemical Sensors and Biosensors* either as a monograph or as a handbook for your scientific work. The manual comprises two volumes and represents an overview of an intersection of two scientific areas of essential importance: environmental chemistry and electrochemical sensing.

Since the invention of the glass electrode in 1906 by Max Cremer, electrochemical sensors represent the oldest type of chemical sensor and are ubiquitously present in all chemical labs, industries, as well as in many fields of our everyday life. The development of electrochemical sensors exploiting new measuring technologies makes them useful for chemical analysis and characterization of analytes in practically all physical phases - gases, liquids and solids - and in different matrices in industrial, food, biomedical, and environmental fields. They have become indispensable tools in analytical chemistry for reliable, precise, and inexpensive determination of many compounds, as single shot, repetitive, continuous, or even permanent analytical devices. Environmental analytical chemistry demands highly sensitive, robust, and reliable sensors, able to give fast responses even for analysis in the field and in real time, a requirement which can be fulfilled in many cases only by electrochemical sensing elements.

The idea for this manual was brought to us by Springer. The intention was to build up an introduction and a concise but exhaustive description of the state of the art in scientific and practical work on environmental analysis, focused on electrochemical sensors.

To manage the enormous extent of the topic, the manual is split into two volumes. The first one, covering the basic concepts and fundamentals of both environmental analysis and electrochemical sensors,

1. gives a short introduction and description of all environments which are subject to monitoring by electrochemical sensors, including extraterrestrial ones, as a particularly interesting and exciting topic;

2. provides essential background information on electroanalytical techniques and fundamental as well as advanced sensor technology;
3. supplies numerous examples of applications along with the concepts and strategies of environmental analysis in all the various spheres of the environment and with the principles and strategies of electrochemical sensor design.

The second volume is more focused on practical applications, mostly complementary to the examples given in volume I, and

1. overviews and critically comments on sensors proposed for the determination of inorganic and organic analytes and pollutants, including emerging contaminants, as well as for the measurement of global parameters of environmental importance;
2. reviews briefly the mathematical background of data evaluation.

We hope that we have succeeded in fulfilling all these objectives by supplying general and specific data as well as thorough background knowledge to make *Environmental Analysis with Electrochemical Sensors and Biosensors* more than a simple handbook but, rather, a desk reference manual.

It is obvious that a compilation of chapters dealing with so many different specialized areas in analytical and environmental chemistry requires the expertise of many scientists. Therefore, in the first place we would like to thank all the contributors to this book for all the time and effort spent in compiling and critically commenting on research, and the data and conclusions derived from it.

Of course, we would like to particularly acknowledge all the people from Springer who have been involved with the process of publication. Our cordial thanks are addressed to Kenneth Howell, who accompanied us during all the primary steps and, later during the process of revision and editing together with Abira Sengupta, was always available and supportive in the most professional and pleasant manner.

Furthermore, we are indebted to a number of our collaborators, colleagues, and friends for kindly providing us literature and ideas, and stimulating us with fruitful discussions. We would also like to thank all the coworkers who did research together with us and under our supervision, as well as all the scientific community working in the field of environmental sensing.

In particular, we would like to express our gratitude to all the persons, especially to our families, who supported us in the period of the preparation of the book.

Last but not least, we will be glad for comments from readers and others interested in this book, since we are aware that some contributions or useful details may have escaped our attention. Such feedback is always welcome and will also be reflected in our future work.

Venice, Italy
Graz, Austria
December 2013

Ligia Maria Moretto
Kurt Kalcher

About the Editors

Ligia Maria Moretto graduated in Chemical Engineering at the Federal University of Rio Grande do Sul, Brazil, and received her Ph.D. in 1994 from the University Ca' Foscari of Venice with a thesis entitled "Ion-exchange voltammetry for the determination of copper and mercury. Application to seawater." Her academic career began at the University of Caxias do Sul, Brazil, and continued at the Research Institute of Nuclear Energy, Sao Paulo, Brazil. In 1996 she completed the habilitation as researcher in analytical chemistry at the University Ca' Foscari of Venice. Working at the Laboratory of Electrochemical Sensors, her research field has been the development of electrochemical sensor and biosensors based on modified electrodes, the study of gold arrays and ensembles of nanoelectrodes, with particular attention to environmental applications. She has published more than 60 papers, several book chapters, and has presented about 90 contributions at international conferences, resulting in more than 1,100 citations. Prof. Moretto collaborates as invited professor and invited researcher with several institutions in Brazil, France, Argentina, Canada, and the USA.

Kurt Kalcher completed his studies at the Karl-Franzens University (KFU) with a dissertation in inorganic chemistry entitled "Contributions to the Chemistry of Cyantrichloride, CINCCl₂"; he also received his Ph.D. in 1980 from the same institution. In 1981 he then did postdoctoral work at the Nuclear Research Center in Jülich (Germany) under the supervision of Prof. Nürnberg and Dr. Valenta, and conducted intensive electroanalytical research while he was there. Prof. Kalcher continued his academic career at KFU with his habilitation on chemically modified carbon paste electrodes in analytical chemistry in 1988. Since then, he has been employed there as an associate professor. His research interests include the development of electrochemical sensors and biosensors for the determination of inorganic and biological analytes on the basis of carbon paste, screen-printed carbon,

and boron-doped diamond electrodes, as well as design, automation, and data handling with small analytical devices using microprocessors. He has published around 200 papers and has presented about 200 contributions at international conferences. These activities have resulted in more than 3,100 citations. Prof. Kalcher has received numerous guest professor position offers in Bosnia-Herzegovina, Poland, Slovenia, and Thailand.

Contents of Volume 1

Part I Environmental Analysis

1 Introduction to Electroanalysis of Environmental Samples	3
Ivan Švancara and Kurt Kalcher	
2 Soil	23
Kenneth A. Sudduth, Hak-Jin Kim, and Peter P. Motavalli	
3 Water	63
Eduardo Pinilla Gil	
4 Atmosphere	93
Andrea Gambaro, Elena Gregoris, and Carlo Barbante	
5 Biosphere	105
Adela Maghear and Robert Săndulescu	
6 Extraterrestrial	131
Kyle M. McElhoney, Glen D. O’Neil, and Samuel P. Kounaves	

Part II Fundamental Concepts of Sensors and Biosensors

7 Electrochemical Sensor and Biosensors	155
Cecilia Cristea, Veronica Hârceagă, and Robert Săndulescu	
8 Electrochemical Sensors in Environmental Analysis	167
Cecilia Cristea, Bogdan Feier, and Robert Sandulescu	
9 Potentiometric Sensors	193
Eric Bakker	
10 Controlled Potential Techniques in Amperometric Sensing	239
Ligia Maria Moretto and Renato Seeber	

11 Biosensors on Enzymes, Tissues, and Cells	283
Xuefei Guo, Julia Kuhlmann, and William R. Heineman	
12 DNA Biosensors	313
Filiz Kuralay and Arzum Erdem	
13 Immunosensors	331
Petr Skládal	
14 Other Types of Sensors: Impedance-Based Sensors, FET Sensors, Acoustic Sensors	351
Christopher Brett	
Part III Sensor Electrodes and Practical Concepts	
15 From Macroelectrodes to Microelectrodes: Theory and Electrode Properties	373
Salvatore Daniele and Carlo Bragato	
16 Electrode Materials (Bulk Materials and Modification)	403
Alain Walcarius, Mathieu Etienne, Grégoire Herzog, Veronika Urbanova, and Neus Vila	
17 Nanosized Materials in Amperometric Sensors	497
Fabio Terzi and Chiara Zanardi	
18 Electrochemical Sensors: Practical Approaches	529
Anchalee Samphao and Kurt Kalcher	
19 Gas Sensors	569
Ulrich Guth, Wilfried Vonau, and Wolfram Oelßner	
Part IV Sensors with Advanced Concepts	
20 Sensor Arrays: Arrays of Micro- and Nanoelectrodes	583
Michael Ongaro and Paolo Ugo	
21 Sensors and Lab-on-a-Chip	615
Alberto Escarpa and Miguel A. López	
22 Electronic Noses	651
Corrado Di Natale	
23 Remote Sensing	667
Tomer Noyhouzer and Daniel Mandler	
Index	691

Contents of Volume 2

Part I Sensors for Measurement of Global Parameters

1 Chemical Oxygen Demand	719
Usman Latif and Franz L. Dickert	
2 Biochemical Oxygen Demand (BOD)	729
Usman Latif and Franz L. Dickert	
3 Dissolved Oxygen	735
Usman Latif and Franz L. Dickert	
4 pH Measurements	751
Usman Latif and Franz L. Dickert	

Part II Sensors and Biosensors for Inorganic Compounds of Environmental Importance

5 Metals	781
Ivan Švancara and Zuzana Navrátilová	
6 Non-metal Inorganic Ions and Molecules	827
Ivan Švancara and Zuzana Navrátilová	
7 Electroanalysis and Chemical Speciation	841
Zuzana Navrátilová and Ivan Švancara	
8 Nanoparticles-Emerging Contaminants	855
Emma J.E. Stuart and Richard G. Compton	

**Part III Sensors and Biosensors for Organic Compounds
of Environmental Importance**

9 Pharmaceuticals and Personal Care Products	881
Lúcio Angnes	
10 Surfactants	905
Elmorsy Khaled and Hassan Y. Aboul-Enein	
11 Determination of Aromatic Hydrocarbons and Their Derivatives	931
K. Peckova-Schwarzova, J. Zima, and J. Barek	
12 Explosives	965
Jiri Barek, Jan Fischer, and Joseph Wang	
13 Pesticides	981
Elmorsy Khaled and Hassan Y. Aboul-Enein	

**Part IV Electrochemical Sensors for Gases of Environmental
Importance**

14 Volatile Organic Compounds	1023
Tapan Sarkar and Ashok Mulchandani	
15 Sulphur Compounds	1047
Tjarda J. Roberts	
16 Nitrogen Compounds: Ammonia, Amines and NO_x	1069
Jonathan P. Metters and Craig E. Banks	
17 Carbon Oxides	1111
Nobuhito Imanaka and Shinji Tamura	

Part V Data Treatment of Electrochemical Sensors and Biosensors

18 Data Treatment of Electrochemical Sensors and Biosensors	1137
Elio Desimoni and Barbara Brunetti	
Index	1153

Part I
Sensors for Measurement of Global
Parameters

Chapter 1

Chemical Oxygen Demand

Usman Latif and Franz L. Dickert

1.1 Introduction

Organic pollution in water can be monitored by measuring an important index called chemical oxygen demand (COD).¹ Different countries such as China and Japan set this parameter as a national standard to investigate the organic pollution in water. The conventional method to measure the COD is the determination of excess oxidizing agent such as dichromate or permanganate left in the sample.² Thus, COD is defined as the number of oxygen equivalents required to oxidize organic materials in water. In the conventional method, a strong oxidant such as dichromate is added to the water sample to digest the organic matter whereas the remaining oxidant is determined titrimetrically by using FeSO_4 as the titrant. However, some drawbacks are associated with this procedure as it requires almost 2–4 h to complete the analysis.^{3,4} Thus, rapid as well as automatic analysis is not possible by using this method. Moreover, skilled workers are required to produce reproducible results. In addition, health issues and safety concerns also arise because of the consumption of expensive (Ag_2SO_4), corrosive (concentrated H_2SO_4), and toxic ($\text{Cr}_2\text{O}_7^{2-}$) chemicals.^{5,6}

The problems associated with the conventional method can be prevented by utilizing electrochemical treatment of wastewater having organic pollutants.^{7,8} The basic principle of this procedure is to electrochemically oxidize organic matter by

U. Latif
Department of Analytical Chemistry, University of Vienna,
Waehringer Strasse 38, 1090 Vienna, Austria

Department of Chemistry, COMSATS Institute of Information Technology,
Tobe Camp, University Road, 22060 Abbottabad, Pakistan

F.L. Dickert (✉)
Department of Analytical Chemistry, University of Vienna,
Waehringer Strasse 38, 1090 Vienna, Austria
e-mail: Franz.dickert@univie.ac.at

applying a high potential. This method will degrade organic pollutants into water and carbon dioxide whereas the amount of charge required for electrochemical oxidation is directly proportional to the value of COD. However, this method is practically impossible by using ordinary electrodes because it requires very high potentials to degrade organic pollutants which results in the oxidation of water. In order to shorten the oxidation time, thin-layer electrochemical cells were also fabricated for complete oxidation of organic pollutants.^{9,10} In these cells a thin layer of the sample (2–100 μm) was allowed to rest on the electrode surface. This thin-layer electrochemical cell realizes time-effective electrolysis of sample layers with a large ratio of electrode area to solution volume. The coulometric analysis of COD via exhaustive oxidation of organic species is still difficult and requires a long time of about 30 min even in the thin-layer electrochemical cell. In order to overcome these problems, a number of electrodes were designed by coating with electrocatalytic materials which lower the oxidation overpotential as well as shorten the reaction time. The determination of COD in water samples is necessary to evaluate its quality because normally in slightly contaminated water the value of COD is 20–25 mg/L of consumed oxygen¹¹ and in extremely contaminated industrial wastewater streams its value may increase to 100,000 mg/L.¹²

1.2 Sensors

1.2.1 *Pt/PbO₂ Ring-Disc Electrode*

The reaction kinetics are very slow when oxidation of the COD pollutants is carried out with oxygen, $\text{K}_2\text{Cr}_2\text{O}_7$, KMnO_4 , and Ce (IV) which leads to an incomplete or even non-occurring oxidation of some organic compounds even when employing a time-consuming refluxing process in the conventional method. Moreover, inorganic compounds such as (Cl^- , Fe^{2+}) may also be oxidized. Thus, the COD values do not actually reflect the actual concentration of organics present in the sample. In order to overcome these problems, there should be such a species as part of a redox system which should oxidize COD pollutants rapidly and selectively. Moreover, this species should have enough lifetime to react with all the organic species present in the sample. The generation of hydroxyl radicals as an unstable intermediate in the oxygen evolution reaction at the electrode is capable to address all the issues concerning COD values.

A rotating ring-disc electrode (RRDE) was utilized for the determination of chemical oxygen demand (COD).³ A PbO_2 layer was deposited on the platinum disc surface of the ring-disc electrode because lead oxide is a promising candidate for the direct oxidation of carbohydrates and amino acids. This device was fabricated in such a way to produce a strong oxidant by in situ formation of an aggressive species which oxidizes the compounds that contribute to COD. The aggressive species which are left behind after oxidizing the compounds react with oxygen

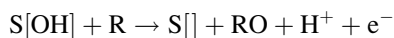
which is monitored at the ring electrode. In such type of COD sensor, a strong oxidant is electrochemically generated at the disc part of the rotating ring-disc electrode. The COD pollutants are exposed to the RRDE, and some of the pollutants will be directly converted to its elementary components (CO_2 and H_2O) at the disc surface while others will be converted indirectly with the generated oxidant at the disc surface. Thus, organic compounds will be degraded via two different paths. Some organic compounds are directly oxidized at a potential where also the oxygen evolution occurs, and then hydroxyl radicals will be produced as an intermediate. These hydroxyl radicals will consume the rest of the organic compounds and excess of hydroxyl will also be oxidized to oxygen. The generation of a strongly oxidizing agent at the electrode surface has the advantage that it would keep the surface clean by avoiding the adsorption of substances.

1.2.2 F-Doped PbO_2 -Modified Electrode

In another approach the electrocatalytic activity of lead oxide was enhanced with fluoride doping. The F-doped lead oxide-modified electrode leads to the fabrication of an electrochemical detection system for flow injection analysis to detect the chemical oxygen demand (COD) in water samples.¹³ The combination of flow injection analysis with electrochemical detection of COD results in the development of a low-cost, rapid, and easily automated detection system with minimum reagent consumption. The basic principle of the F-doped lead oxide electrode is the generation of hydroxyl radicals which are subsequently utilized for the oxidation of COD pollutants in order to determine the COD value. It is a multistep process: at first, hydroxyl radicals will be produced at the surface of the F- PbO_2 electrode by the anodic discharge of water:



These hydroxyl radicals will be adsorbed on the unoccupied surface sites ($\text{S}[\]$) forming $\text{S}[\text{OH}]$ which represents the adsorbed hydroxyl radicals. The electrocatalytic activity of lead oxide is amplified with the doping with F^- because it increases the number of unoccupied surface sites.¹⁴ If the reverse discharging reaction is ignored then the O-transfer step can be represented by the following equation:



The COD pollutants are electrocatalytically oxidized by the surface sites and output current signals are produced which are proportional to the COD value. R represents the organic pollutants which are oxidized to RO by the hydroxyl radical. However, the current efficiency of the O-transfer reaction will be decreased by the

consumption of hydroxyl radicals which results in the evolution of oxygen by the following reaction:



The higher the overpotential of materials for oxygen evolution, the better the reaction compels the physisorbed hydroxyl radicals to oxidize the organics rather than to turn into oxygen.

1.2.3 Rhodium Oxide–Titania Electrode

Dimensionally stable anodes (DSAs) are usually fabricated by depositing metallic oxides on a metal substrate such as titanium. In order to synthesize DSAs, a precursor such as metallic chloride is decomposed in an oven or by electromagnetic induction heating. However, this procedure is very complex and requires a lot of time to complete. These problems can be solved by using the laser as a heat source for developing DSAs via calcination. The designed DSA possesses very unique properties of high corrosion resistance, robustness, and electrocatalytic abilities. The electrocatalytic activity of DSAs is attributed to the formation of hydroxyl radicals at the electrode surface. These physisorbed species, generated by the oxygen evolution reaction, has the ability to oxidize organic pollutants electrochemically. However, a severe side reaction occurs simultaneously which consumes hydroxyl radicals and results in the evolution of oxygen. Thus, this side reaction competes with the oxidative degradation of organic pollutants and lowers the current efficiency. The problem can be solved by using higher overpotential metal oxides for oxygen evolution which preferentially compel hydroxyl radicals to electrocatalytically oxidize organic compounds rather than to release oxygen. A $\text{Rh}_2\text{O}_3/\text{Ti}$ electrode was prepared by laser calcination to develop an amperometric sensor for the determination of COD.¹⁵ Electrocatalytic oxidation of organic compounds could be monitored with this electrode in flow injection analysis. The current responses from the oxidation of the organic contaminants at the electrode surface were proportional to the COD values.

1.2.4 Boron-Doped Diamond Electrode

Boron-doped diamond (BDD) possesses unique properties such as a wide-range working potential, low background current, stable responses, environmental friendliness, and robustness.^{16,17} Thus, boron-doped diamond is an excellent material to design a sensing electrode for electrochemical water treatment.^{18,19} A BDD film can be deposited on a support electrode by microwave plasma chemical vapor deposition.

The BDD electrode was employed as a detecting element for determining COD in combination with flow injection analysis (FIA).²⁰ This continuous flow method led to the development of an online amperometric COD monitoring system which reduced the analysis time significantly. The BDD electrode was deactivated if the applied voltage was very low because of the electropolymerization of some organics such as phenol on the surface of the electrode. This inhibition of electrode could be overcome if a high voltage was applied to hinder the polymerization of organic compounds. The COD values monitored by this rapid online system were closely related to the conventional method. The electrode with BDD acts as a generator for hydroxyl radicals due to its wide electrochemical potential window, and high oxygen evolution potential.²¹ The electrochemical oxidation of organic pollutants in water samples by employing BDD electrode is a direct or a hydroxyl radical-mediated process. However, oxidative degradation of organics is mainly dominated by indirect hydroxyl radicals at high potential. Moreover, the oxidative potential of hydroxyl radicals decreases with an increase in pH. At the same time, the overpotential for oxygen evolution will be lowered when the solution becomes more alkaline which leads to oxygen bubbles at the electrode. The excellent correlation of the BDD-detecting element with the conventional method supports the suitability of the proposed sensor for COD detection.

1.2.5 Nano Copper-Modified Electrode

The electrochemical deposition of Cu nanoparticles on a Cu disc electrode led to the fabrication of a sensor device for chemical oxygen demand (COD).²² The modification of the Cu disc electrode with Cu nanoparticles by using controlled-potential reduction greatly increased the oxidation current signals in comparison to the simple Cu disc electrode. The increase in sensitivity was attributed to the large surface area, and enhanced active sites of nanomaterials in comparison to bulk materials. Thus, nano-Cu exhibited high catalytic activity which resulted in a decrease of the oxidation overpotential and an enhancement of the current signals of the oxidation of organic compounds present in water. In this way, a very sensitive and stable amperometric sensor was developed for the detection of COD.

1.2.6 Activated Glassy Carbon Electrode

A special carbon material called glassy carbon is widely used as electrode material in the field of electrochemistry. The responsive behavior of a glassy carbon electrode (GCE) can be greatly enhanced by means of electrochemical treatment. The GCE can be activated by cyclic sweeps²³ or constant potential oxidation.²⁴ The activation of glassy carbon electrode (GCE) by applying constant potential oxidation tailors its surface morphology, functional groups, and electrochemical activity.

The oxidative activation method introduces thornlike nanostructures as well as hydroxyl groups on the surface of a GCE which will enhance its electrochemical activity.²⁵ This strategy develops a very sensitive, low-cost, and simply fabricated amperometric COD detection system having better practical applicability and accuracy.

1.2.7 Cobalt Oxide-Modified Glassy Carbon Electrode

The modification of a glassy carbon electrode with cobalt oxide led to an excellent sensor for chemical oxygen demand.²⁶ The sensing film of cobalt oxide was prepared on the surface of a glassy carbon electrode via constant potential oxidation. $\text{Co}(\text{NO}_3)_2$ was used as a precursor for the electrochemical deposition of a thin and homogeneous layer. The electrocatalytic ability of the cobalt oxide film was directly related to the potential applied to the electrochemical film deposition. The sensing film which was prepared at an optimized potential (1.3 V vs. SCE) had a high surface roughness, which enhanced its response area and the number of active sites. The high valence cobalt in the sensing film had the capability to catalytically oxidize reduced organic compounds which led to a decrease of the current signal at 0.8 V vs. SCE. The cobalt oxide film was highly useful for COD determinations and the results were reproducible as the response signal decreased sharply after the addition of the wastewater.

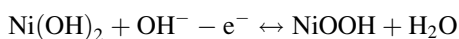
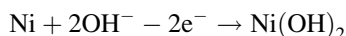
1.2.8 Nickel Nanoparticles

The physical and chemical properties of metal nanoparticles greatly differ from their bulk materials because of their morphology. Nanoparticles show excellent catalytic activity and selectivity towards different analytes if their shape and sizes are properly controlled.²⁷ The convenient and most suitable way for synthesizing metal nanoparticles is electrochemical deposition. Nickel nanoparticles can be deposited on the electrode surface via galvanic or potentiostatic deposition. A process of constant potential reduction was employed for electrochemically depositing nickel nanoparticles on the surface of a glassy carbon electrode by utilizing NiSO_4 as precursor. The sensitive surface fabricated in this way exhibited high electrochemical activity to oxidize reduced organic compounds which resulted in an increase of the oxidation current signals. The catalytic activity of Ni nanoparticles could be enhanced by optimizing the preparation parameters such as reduction potential, deposition time, pH value, and concentration of nickel ions. By optimizing these parameters the shape and sizes of particles were controlled which lead to the fabrication of a sensitive detection tool for the chemical oxygen demand but with poor reproducibility.²⁸

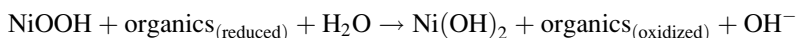
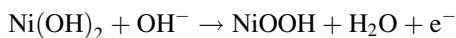
1.2.9 Nickel-Copper Alloy Electrode

An environmentally friendly sensor was developed by fabricating a nickel-copper (NiCu) alloy electrode to determine the chemical oxygen demand.²⁹ The NiCu alloy film was applied to modify the surface of a glassy carbon electrode which led to a very stable detecting element. The surface morphology of NiCu alloy was investigated by atomic force microscopy which confirmed its continuity and uniform thickness over the entire electrode. The chemical composition of the developed NiCu film was evaluated by energy-dispersive X-ray spectrometry which revealed 69 % presence of Ni in the alloy.

Nickel is widely used as an electrode material for electrochemical water treatment as well as in many electrochemical analyses. Moreover, it is an excellent electrocatalyst for oxidizing different organic compounds on the basis of the Ni(OH)₂/NiOOH redox couple. Mixing of Ni with Cu enhances the electrocatalytic activity as well as provides long-term stability to the structure. In addition, a wide range of composition of NiCu alloys is possible because both metals have similar face-centered cubic structure.³⁰ The addition of Cu to the Ni(OH)₂/NiOOH redox couple suppresses the formation of γ -NiOOH and enhances the formation of β -NiOOH which is an excellent electroactive substance. The electrochemical activity of NiCu alloy was evaluated by cyclic voltammetry where the electrochemically relevant reactions were attributed to the Ni(II)/Ni(III) redox couple³¹:



The formation of Ni(OH)₂ at the electrode leaves behind a Cu-enriched surface which can be also oxidized to Cu₂O and finally to Cu(OH)₂. At the end, the surface film will be a mixture of NiOOH and Cu(OH)₂ where the counterions are mobile enough to maintain electroneutrality at the electrode surface during the redox process. When a NiCu alloy-modified electrode comes in contact with organic pollutants present in the sample the Ni(III) species rapidly oxidize them and form Ni(II) species, as follows:



The electrocatalytic activity of the NiCu alloy electrode is higher than of a Ni electrode because the Cu(OH)₂ species enhance the formation of the β -NiOOH phase and suppress the formation of γ -NiOOH. The proposed sensor device based on NiCu alloy is a promising tool for the determination of COD in water quality control and pollution evaluation.

1.3 Total Organic Carbon (TOC)

Total organic carbon is considered as a parameter to assess the organic pollution of a sample.³² In order to measure the TOC in aqueous solutions two digestion procedures³³ are employed such as high-temperature combustion³⁴ and photo-oxidation³⁵ to degrade organics. The basic principle of the abovementioned methods is the complete conversion of organic compounds to carbon dioxide. Then, the evolved carbon dioxide is detected by following traditional analytical techniques such as infrared spectrometry, coulometry, conductivity, flame ionization, or ion chromatography. Both methods demand certain protocols, as oxidation via combustion requires high temperature as well as expensive thermal catalysts. The second method needs UV light of shorter wavelengths in the presence of peroxodisulfate in the sample to completely oxidize organic compounds at moderate temperature. The inexpensive photo-oxidation method has an advantage of measuring lower TOC concentrations in comparison to the combustion method.

References

1. Zhang S, Li L, Zhao H (2009) A portable photoelectrochemical probe for rapid determination of chemical oxygen demand in wastewaters. *Environ Sci Technol* 43(20):7810–7815. doi:[10.1021/es901320a](https://doi.org/10.1021/es901320a)
2. Moore WA, Kroner RC, Ruchhoft CC (1949) Dichromate reflux method for determination of oxygen consumed. *Anal Chem* 21(8):953–957. doi:[10.1021/ac60032a020](https://doi.org/10.1021/ac60032a020)
3. Westbroek P, Temmerman E (2001) In line measurement of chemical oxygen demand by means of multipulse amperometry at a rotating Pt ring—Pt/PbO₂ disc electrode. *Anal Chim Acta* 437(1):95–105. doi:[10.1016/S0003-2670\(01\)00927-8](https://doi.org/10.1016/S0003-2670(01)00927-8)
4. Kim Y-C, Sasaki S, Yano K, Ikebukuro K, Hashimoto K, Karube I (2002) A flow method with photocatalytic oxidation of dissolved organic matter using a solid-phase (TiO₂) reactor followed by amperometric detection of consumed oxygen. *Anal Chem* 74(15):3858–3864. doi:[10.1021/ac015678r](https://doi.org/10.1021/ac015678r)
5. Moore WA, Walker WW (1956) Determination of low chemical oxygen demands of surface waters by dichromate oxidation. *Anal Chem* 28(2):164–167. doi:[10.1021/ac60110a005](https://doi.org/10.1021/ac60110a005)
6. Zhao H, Jiang D, Zhang S, Catterall K, John R (2003) Development of a direct photoelectrochemical method for determination of chemical oxygen demand. *Anal Chem* 76(1):155–160. doi:[10.1021/ac0302298](https://doi.org/10.1021/ac0302298)
7. Sirés I, Oturan N, Oturan MA (2010) Electrochemical degradation of β -blockers. Studies on single and multicomponent synthetic aqueous solutions. *Water Res* 44(10):3109–3120. doi:[10.1016/j.watres.2010.03.005](https://doi.org/10.1016/j.watres.2010.03.005)
8. Y-h C, X-y L, Chen G (2009) Electrochemical degradation of bisphenol A on different anodes. *Water Res* 43(7):1968–1976. doi:[10.1016/j.watres.2009.01.026](https://doi.org/10.1016/j.watres.2009.01.026)
9. Lee K-H, Ishikawa T, McNiven S, Nomura Y, Sasaki S, Arikawa Y, Karube I (1999) Chemical oxygen demand sensor employing a thin layer electrochemical cell. *Anal Chim Acta* 386(3):211–220. doi:[10.1016/S0003-2670\(99\)00041-0](https://doi.org/10.1016/S0003-2670(99)00041-0)
10. Lee K-H, Ishikawa T, Sasaki S, Arikawa Y, Karube I (1999) Chemical oxygen demand (COD) sensor using a stopped-flow thin layer electrochemical cell. *Electroanalysis* 11(16):1172–1179. doi:[10.1002/\(sici\)1521-4109\(199911\)11:16<1172::aid-elan1172>3.0.co;2-j](https://doi.org/10.1002/(sici)1521-4109(199911)11:16<1172::aid-elan1172>3.0.co;2-j)

11. Charef A, Ghauch A, Baussand P, Martin-Bouyer M (2000) Water quality monitoring using a smart sensing system. *Measurement* 28(3):219–224. doi:[10.1016/S0263-2241\(00\)00015-4](https://doi.org/10.1016/S0263-2241(00)00015-4)
12. Puñal A, Lorenzo A, Roca E, Hernández C, Lema JM (1999) Advanced monitoring of an anaerobic pilot plant treating high strength wastewaters. *Water Sci Technol* 40(8):237–244. doi:[10.1016/S0273-1223\(99\)00631-9](https://doi.org/10.1016/S0273-1223(99)00631-9)
13. Li J, Li L, Zheng L, Xian Y, Ai S, Jin L (2005) Amperometric determination of chemical oxygen demand with flow injection analysis using F-PbO₂ modified electrode. *Anal Chim Acta* 548(1–2):199–204. doi:[10.1016/j.aca.2005.05.068](https://doi.org/10.1016/j.aca.2005.05.068)
14. Amadelli R, Armelao L, Velichenko AB, Nikolenko NV, Girenko DV, Kovalyov SV, Danilov FI (1999) Oxygen and ozone evolution at fluoride modified lead dioxide electrodes. *Electrochim Acta* 45(4–5):713–720. doi:[10.1016/S0013-4686\(99\)00250-9](https://doi.org/10.1016/S0013-4686(99)00250-9)
15. Li J, Li L, Zheng L, Xian Y, Jin L (2006) Rh₂O₃/Ti electrode preparation using laser anneal and its application to the determination of chemical oxygen demand. *Meas Sci Technol* 17(7):1995–2000. doi:[10.1088/0957-0233/17/7/044](https://doi.org/10.1088/0957-0233/17/7/044)
16. Wang J, Farrell J (2004) Electrochemical inactivation of triclosan with boron doped diamond film electrodes. *Environ Sci Technol* 38(19):5232–5237. doi:[10.1021/es035277o](https://doi.org/10.1021/es035277o)
17. Jolley S, Koppang M, Jackson T, Swain GM (1997) Flow injection analysis with diamond thin-film detectors. *Anal Chem* 69(20):4099–4107. doi:[10.1021/ac961269x](https://doi.org/10.1021/ac961269x)
18. Cabeza A, Urtiaga AM, Ortiz I (2007) Electrochemical treatment of landfill leachates using a boron-doped diamond anode. *Ind Eng Chem Res* 46(5):1439–1446. doi:[10.1021/ie061373x](https://doi.org/10.1021/ie061373x)
19. Bensalah G, Cañizares P, Sáez C, Lobato J, Rodrigo MA (2005) Electrochemical oxidation of hydroquinone, resorcinol, and catechol on boron-doped diamond anodes. *Environ Sci Technol* 39(18):7234–7239. doi:[10.1021/es050066o](https://doi.org/10.1021/es050066o)
20. Yu H, Ma C, Quan X, Chen S, Zhao H (2009) Flow injection analysis of chemical oxygen demand (cod) by using a boron-doped diamond (BDD) electrode. *Environ Sci Technol* 43(6):1935–1939. doi:[10.1021/es8033878](https://doi.org/10.1021/es8033878)
21. Wang J, Li K, Zhang H, Wang Q, Wang Y, Yang C, Guo Q, Jia J (2012) Condition optimization of amperometric determination of chemical oxygen demand using boron-doped diamond sensor. *Res Chem Intermed* 38(9):2285–2294. doi:[10.1007/s11164-012-0545-6](https://doi.org/10.1007/s11164-012-0545-6)
22. Yang J, Chen J, Zhou Y, Wu K (2011) A nano-copper electrochemical sensor for sensitive detection of chemical oxygen demand. *Sens Actuators B* 153(1):78–82. doi:[10.1016/j.snb.2010.10.015](https://doi.org/10.1016/j.snb.2010.10.015)
23. Du M, Han X, Zhou Z, Wu S (2007) Determination of Sudan I in hot chili powder by using an activated glassy carbon electrode. *Food Chem* 105(2):883–888. doi:[10.1016/j.foodchem.2006.12.039](https://doi.org/10.1016/j.foodchem.2006.12.039)
24. Ahammad AJS, Sarker S, Rahman MA, Lee J-J (2010) Simultaneous determination of hydroquinone and catechol at an activated glassy carbon electrode. *Electroanalysis* 22(6):694–700. doi:[10.1002/elan.200900449](https://doi.org/10.1002/elan.200900449)
25. Wu C, Yu S, Lin B, Cheng Q, Wu K (2012) Sensitive and rapid monitoring of water pollution level based on the signal enhancement of an activated glassy carbon electrode. *Anal Methods* 4(9):2715–2720. doi:[10.1039/c2ay25523e](https://doi.org/10.1039/c2ay25523e)
26. Wang J, Wu C, Wu K, Cheng Q, Zhou Y (2012) Electrochemical sensing chemical oxygen demand based on the catalytic activity of cobalt oxide film. *Anal Chim Acta* 736:55–61. doi:[10.1016/j.aca.2012.05.046](https://doi.org/10.1016/j.aca.2012.05.046)
27. Zhou X, Xu W, Liu G, Panda D, Chen P (2009) Size-dependent catalytic activity and dynamics of gold nanoparticles at the single-molecule level. *J Am Chem Soc* 132(1):138–146. doi:[10.1021/ja904307n](https://doi.org/10.1021/ja904307n)
28. Cheng Q, Wu C, Chen J, Zhou Y, Wu K (2011) Electrochemical tuning the activity of nickel nanoparticle and application in sensitive detection of chemical oxygen demand. *J Phys Chem C* 115(46):22845–22850. doi:[10.1021/jp207442u](https://doi.org/10.1021/jp207442u)
29. Zhou Y, Jing T, Hao Q, Zhou Y, Mei S (2012) A sensitive and environmentally friendly method for determination of chemical oxygen demand using NiCu alloy electrode. *Electrochim Acta* 74:165–170. doi:[10.1016/j.electacta.2012.04.048](https://doi.org/10.1016/j.electacta.2012.04.048)

30. Jafarian M, Forouzandeh F, Danaee I, Gobal F, Mahjani MG (2009) Electrocatalytic oxidation of glucose on Ni and NiCu alloy modified glassy carbon electrode. *J Solid State Electrochem* 13(8):1171–1179. doi:[10.1007/s10008-008-0632-1](https://doi.org/10.1007/s10008-008-0632-1)
31. Jing T, Zhou Y, Hao Q, Zhou Y, Mei S (2012) A nano-nickel electrochemical sensor for sensitive determination of chemical oxygen demand. *Anal Methods* 4(4):1155–1159. doi:[10.1039/c2ay05631c](https://doi.org/10.1039/c2ay05631c)
32. Canals A, del Remedio HM (2002) Ultrasound-assisted method for determination of chemical oxygen demand. *Anal Bioanal Chem* 374(6):1132–1140. doi:[10.1007/s00216-002-1578-2](https://doi.org/10.1007/s00216-002-1578-2)
33. Thomas O, El Khorassani H, Touraud E, Bitar H (1999) TOC versus UV spectrophotometry for wastewater quality monitoring. *Talanta* 50(4):743–749. doi:[10.1016/S0039-9140\(99\)00202-7](https://doi.org/10.1016/S0039-9140(99)00202-7)
34. Jin B, He Y, Shen J, Zhuang Z, Wang X, Lee FSC (2004) Measurement of chemical oxygen demand (COD) in natural water samples by flow injection ozonation chemiluminescence (FI-CL) technique. *J Environ Monit* 6(8):673–678. doi:[10.1039/b404034c](https://doi.org/10.1039/b404034c)
35. Lev O, Tsionsky M, Rabinovich L, Glezer V, Sampath S, Pankratov I, Gun J (1995) Organically modified sol-gel sensors. *Anal Chem* 67(1):22A–30A. doi:[10.1021/ac00097a001](https://doi.org/10.1021/ac00097a001)

Chapter 2

Biochemical Oxygen Demand (BOD)

Usman Latif and Franz L. Dickert

2.1 Introduction

Biochemical oxygen demand (BOD) is a widely used parameter to assess the organic pollution in water systems. This parameter can be detected by the amount of oxygen consumed via microorganisms in aerobic metabolism of organic matter present in the water. The authorized test to analyze biodegradable organic compounds is given by the American Public Health Association Standard Method Committee that is called a 5-day biochemical oxygen demand (BOD₅) test. In this conventional BOD procedure, the analyte is kept in the dark and in properly sealed biological reactors after inoculating with a microbial culture (seed), nutrients, and plenty of oxygen. Afterwards, the amount of oxygen is measured which is consumed by the microorganisms during biological oxidation of organic solutes over a time period of 5 days.¹ Such prolonged analysis makes BOD₅ expensive and requires experienced personnel for reproducible results. This procedure produces good results; however, it cannot be used for rapid analysis such as environmental monitoring and/or process control. The first rapid BOD sensor was proposed by Karube et al. in 1997.² In this approach, microbes were immobilized on a collagen membrane and an oxygen electrode was used as an indicator device. The results were obtained by this method in a short period of time (1 h) and were closely related to BOD estimates (obtained in 5 days).

U. Latif
Department of Analytical Chemistry, University of Vienna,
Währinger Strasse 38, 1090 Vienna, Austria

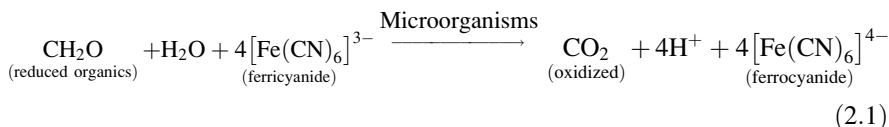
Department of Chemistry, COMSATS Institute of Information Technology,
Tobe Camp, University Road, 22060 Abbottabad, Pakistan

F.L. Dickert (✉)
Department of Analytical Chemistry, University of Vienna,
Währinger Strasse 38, 1090 Vienna, Austria
e-mail: Franz.dickert@univie.ac.at

2.2 Sensors for the Determination of BOD

2.2.1 Ferricyanide-Mediated BOD Sensor

The bacterial catabolism can be monitored with redox mediators. These redox mediators are the species which are able to trap electrons from the redox molecules involved in the electron transport chain.^{3,4} By gaining electrons from the reduced electron transfer chain molecule, the oxidized mediators are reduced. This reduction of mediators is subsequently monitored electrochemically. A biochemical oxygen demand (BOD) sensing method was developed by employing ferricyanide (FC) as a mediator.⁵ This mediator was anchored on an ion-exchangeable polysiloxane. The polysiloxane was synthesized from 3-(aminopropyl) trimethoxysilane by a sol-gel process and ferricyanide was immobilized by ion association and subsequently utilized for electrode modification. Ferricyanide (FC) acts as an efficient mediator for shuttling electrons between the redox centers of reduced bacterial enzymes and the electrode surface.⁶ In the presence of FC as a mediator, electrons derived from the oxidation of organic substrates in aerobic catabolism are transferred to the FC ion which is reduced from ferricyanide to ferrocyanide,⁷ as shown in Eq. (2.1). The reduced form is then re-oxidized to ferricyanide at the working electrode (anode):



FC as a mediator has an advantage over O_2 in designing BOD assays due to its high solubility, linear working range, as well as allowing higher microbial populations. The BOD sensor fabricated by utilizing FC as mediator gives an excellent limit of detection. The results are comparable to the conventional BOD_5 method which proves that the BOD method based on FC is valid for BOD determinations.

2.2.2 Hybrid Material for BOD Sensor

An electrochemical biochemical oxygen demand (BOD) sensor was fabricated by using an organic-inorganic hybrid material.⁸ The hybrid material was synthesized from silica and co-polymerized with poly(vinyl alcohol) and 4-vinylpyridine (PVA-g-P(4-VP)). Afterwards, *Trichosporon cutaneum* strain 2.570 cells were immobilized on the hybrid material. The entrapment of cell strains in extracellular materials provides considerable advantage over free cells such as enhanced metabolic properties and stability. The hybrid materials also protect them from environmental stress and toxicity. The organic-inorganic material provides a biocompatible microenvironment to *T. cutaneum* cells which ensures the long-term viability of

cells proven by confocal laser scanning microscopy (CLSM). The viability of the cells is due to arthroconidia (the state of *Trichosporon cutaneum* when stored) which is produced in the extracellular material.⁹ The arthroconidia state has the ability to resist against environmental stress and toxicity. The proposed sensor by utilizing biocompatible hybrid material could be applied for BOD determinations after activating the arthroconidia in appropriate conditions.

2.2.3 Mediated BOD Sensor

A flow injection biochemical oxygen demand (BOD) analysis system was developed by utilizing a microbial approach.¹⁰ The flow injection technique has advantage over batch analysis due to the ease of rapid and repetitive measurements. A yeast strain was isolated from an activated sludge and was utilized as biological recognition element. This strain was anchored on the substrate made of silica gel particles and packed into a fixed bed reactor. A redox mediator was employed for transporting the electrons from the microbes to the electrode surface. The redox mediators act as electron acceptors from microbes instead of oxygen when organic substrates are decomposed by microbes. Then, these mediators transport the electrons to the electrode surface such as hexacyanoferrate.⁵ The mediators are reduced after accepting the electrons and later are re-oxidized at the electrode surface. The current produced via re-oxidation of the reduced mediator can be related with the concentration of organic contents. Potassium hexacyanoferrate(III) was employed as a mediator. Thus, the mediated BOD sensor device in flow injection mode was fabricated by immobilizing microbes in a reactor which was further coupled to an electrochemical flow cell. The designed detection tool was employed to monitor BOD of *shochu* distillery wastewater (SDW).

2.2.4 Multi-Species-Based BOD Sensor

A BOD detection system containing single-strain microbes shows good stability as well as long lifetime. The single-strain sensors have disadvantages regarding accuracy due to their limited detection capacity for a wide spectrum of substrates. BOD sensors based on multi-species microbes, however, show high detection capacity for a wide spectrum of substrates; but their stability is compromised due to the interference among immobilized multi-species. In the multi-species assay microbial cells are immobilized on a polymer or hydrogel for BOD monitoring systems. If the microbes are immobilized by physical adsorption only, then the activation of the biofilm is very easy but with the disadvantage of limited stability and reproducibility because microorganisms may leak. Proper immobilization of microbes prevents the microorganisms from leaking which provides long-term stability; however, the cross-linked matrix of the hydrogel which entraps the

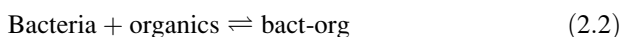
microbes acts as a barrier for the transfer of substrate and oxygen to microbes. Thus, these surfaces required a long activation process.¹¹ The biofilms prepared for the BOD system must be activated¹² before use and this process takes from hours to several days, which is limiting its applicability.

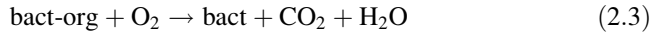
A stable BOD sensor was designed by immobilizing a multi-species BOD seed for wastewater monitoring in a flow system.¹³ The biofilm was synthesized with the BOD seed in an organic–inorganic hybrid material by which the activation time is greatly reduced. The hybrid material was based on a silica sol and co-polymerization was carried out with poly(vinyl alcohol) and 4-vinylpyridine. This organic–inorganic hybrid eliminated problems like cracking and swelling and provided a stable biofilm after immobilizing microbes. The multi-species seed was a commercially available microbial community which was entrapped in the hybrid matrix. The species comprised seven kinds of microbes which were isolated from activated sludge. Thus, immobilizing such multi-species on a hybrid matrix led to a reproducible, long-term stable BOD sensor.

2.2.5 Miniaturized Electrochemical Respirometer

The miniaturization of electrochemical systems is very promising in detecting the analyte of interest. A miniaturized electrochemical respirometer was designed to analyze the organic contents in water samples.¹⁴ This miniaturized device has the ability to monitor the analyte semicontinuously in comparison to other BOD sensors. Thus, the developed sensing tool is based on the concept of a microfluidic respirometer, a microbial fuel cell in an amperometric mode.¹⁵ Thus, it is called a bioreactor—not strictly a biosensor. The BOD detection device contains two twin electrochemical oxygen sensors located in parallel chambers. The protection of electrodes is done by coating with a silicone membrane, and one of them is subsequently modified by an agarose layer containing *Trichosporon cutaneum*, a yeast. The whole system is fabricated by standard microfabrication techniques while the electrochemical oxygen sensors are used to monitor the BOD. The microsystem geometry as well as the coating membranes are optimized to maximize the system output.

The microorganisms consume oxygen in an aerobic process while metabolizing the organic matter present in the sample. In order to understand the function of the miniaturized device, we may assume that the medium is homogeneous. The process can be explained in two steps: At first, bacteria reach an uptake equilibrium with organic matter present in the sample (Eq. 2.2). Then, in a second step they will consume oxygen to metabolize that matter into CO₂ and water (Eq. 2.3):





In the abovementioned equations, bact represents microbial cells without reduced organic matter in their cytosol. The amount of organic matter is represented by organics which will be degraded by microbes by utilizing oxygen. Thus, the amount of oxygen consumed is directly related to the organic contents present in the sample. The term bact-org represents the microbes having reduced organic matter in their cytosol. The respiration of microbial cells is explained by the second equation in which bacteria consume organic matter by utilizing oxygen and produce CO_2 and H_2O . The last part of this miniaturized BOD detection tool is monitoring the amount of oxygen at an electrode expressed in simplified form by Eq. (2.4):



The above mechanism of oxygen detection is rather complex^{16,17} and involves two separate two-electron steps in order to detect the oxygen content by the electrochemical sensor.

2.3 Related Sensors: Bioactivity

Bioactivity sensors (BAS) are related to sensors for the estimation of the BOD, but they are more general in their working concept.^{18–20} They rely on the detection of electroactive metabolites from cultivated biologically active organisms (rather than oxygen in the case of BOD) and may be, therefore, employed under aerobic as well as anaerobic conditions. Bioactivity sensors are useful in quality assessments of wastewaters and may detect the activity of aerobic auto- and heterotrophic biomass, anoxic denitrificants, and anaerobic microorganisms. The working principle is based on a biofuel cell where the electron transfer from the biological component to the anode is the analytically exploitable parameter.

Another assay of bioactivity sensors exploits microorganisms immobilized on electrode surfaces and monitors their activity in dependence on the surrounding conditions.²¹

References

1. Liu J, Mattiasson B (2002) Microbial BOD sensors for wastewater analysis. *Water Res* 36 (15):3786–3802. doi:[10.1016/S0043-1354\(02\)00101-X](https://doi.org/10.1016/S0043-1354(02)00101-X)
2. Karube I, Matsunaga T, Mitsuda S, Suzuki S, Ib TM (2009) Microbial electrode BOD Sensors. *Biotechnol Bioeng* 102(3):659–672. doi:[10.1002/bit.22232](https://doi.org/10.1002/bit.22232)
3. Ertl P, Unterladstaetter B, Bayer K, Mikkelsen SR (2000) Ferricyanide reduction by *escherichia coli*: kinetics, mechanism, and application to the optimization of recombinant fermentations. *Anal Chem* 72(20):4949–4956. doi:[10.1021/ac000358d](https://doi.org/10.1021/ac000358d)

4. Ertl P, Mikkelsen SR (2001) Electrochemical biosensor array for the identification of microorganisms based on lectin–lipopolysaccharide recognition. *Anal Chem* 73(17):4241–4248. doi:[10.1021/ac010324i](https://doi.org/10.1021/ac010324i)
5. Chen H, Ye T, Qiu B, Chen G, Chen X (2008) A novel approach based on ferricyanide-mediator immobilized in an ion-exchangeable biosensing film for the determination of biochemical oxygen demand. *Anal Chim Acta* 612(1):75–82. doi:[10.1016/j.aca.2008.02.006](https://doi.org/10.1016/j.aca.2008.02.006)
6. Morris K, Zhao H, John R (2005) Ferricyanide-mediated microbial reactions for environmental monitoring. *Aust J Chem* 58(4):237–245. doi:[10.1071/CH05038](https://doi.org/10.1071/CH05038)
7. Catterall K, Zhao H, Pasco N, John R (2003) Development of a rapid ferricyanide-mediated assay for biochemical oxygen demand using a mixed microbial consortium. *Anal Chem* 75(11):2584–2590. doi:[10.1021/ac0206420](https://doi.org/10.1021/ac0206420)
8. Liu L, Shang L, Guo S, Li D, Liu C, Qi L, Dong S (2009) Organic–inorganic hybrid material for the cells immobilization: long-term viability mechanism and application in BOD sensors. *Biosens Bioelectron* 25(2):523–526. doi:[10.1016/j.bios.2009.08.004](https://doi.org/10.1016/j.bios.2009.08.004)
9. Li H-M, Du H-T, Liu W, Wan Z, Li R-Y (2005) Microbiological characteristics of medically important *Trichosporon* species. *Mycopathologia* 160(3):217–225. doi:[10.1007/s11046-005-0112-4](https://doi.org/10.1007/s11046-005-0112-4)
10. Oota S, Hatae Y, Amada K, Koya H, Kawakami M (2010) Development of mediated BOD biosensor system of flow injection mode for shochu distillery wastewater. *Biosens Bioelectron* 26(1):262–266. doi:[10.1016/j.bios.2010.06.040](https://doi.org/10.1016/j.bios.2010.06.040)
11. Chan C, Lehmann M, Chan K, Chan P, Chan C, Gruendig B, Kunze G, Renneberg R (2000) Designing an amperometric thick-film microbial BOD sensor. *Biosens Bioelectron* 15(7–8):343–353. doi:[10.1016/S0956-5663\(00\)00090-7](https://doi.org/10.1016/S0956-5663(00)00090-7)
12. Tan TC, Lim EWC (2005) Thermally killed cells of complex microbial culture for biosensor measurement of BOD of wastewater. *Sensors Actuators B Chem* 107(2):546–551. doi:[10.1016/j.snb.2004.11.013](https://doi.org/10.1016/j.snb.2004.11.013)
13. Liu C, Ma C, Yu D, Jia J, Liu L, Zhang B, Dong S (2011) Immobilized multi-species based biosensor for rapid biochemical oxygen demand measurement. *Biosens Bioelectron* 26(5):2074–2079. doi:[10.1016/j.bios.2010.09.004](https://doi.org/10.1016/j.bios.2010.09.004)
14. Torrents A, Mas J, Muñoz FX, del Campo FJ (2012) Design of a microfluidic respirometer for semi-continuous amperometric short time biochemical oxygen demand (BOD_{st}) analysis. *Biochem Eng J* 66:27–37. doi:[10.1016/j.bej.2012.04.014](https://doi.org/10.1016/j.bej.2012.04.014)
15. Chang IS, Jang JK, Gil GC, Kim M, Kim HJ, Cho BW, Byung BH (2004) Continuous determination of biochemical oxygen demand using microbial fuel cell type biosensor. *Biosens Bioelectron* 19(6):607–613. doi:[10.1016/S0956-5663\(03\)00272-0](https://doi.org/10.1016/S0956-5663(03)00272-0)
16. Godino N, Dávila D, Vigués N, Ordeig O, del Campo FJ, Mas J, Muñoz FX (2008) Measuring acute toxicity using a solid-state microrespirometer: Part II. A theoretical framework for the elucidation of metabolic parameters. *Sensors Actuators B: Chem* 135(1):13–20. doi:[10.1016/j.snb.2008.06.056](https://doi.org/10.1016/j.snb.2008.06.056)
17. Lavacchi A, Bardi U, Borri C, Caporali S, Fossati A, Perissi I (2009) Cyclic voltammetry simulation at microelectrode arrays with COMSOL Multiphysics®. *J Appl Electrochem* 39(11):2159–2163. doi:[10.1007/s10800-009-9797-2](https://doi.org/10.1007/s10800-009-9797-2)
18. Holtmann D, Schrader J, Sell D (2006) Quantitative Comparison of the Signals of an Electrochemical Bioactivity Sensor During the Cultivation of Different Microorganisms. *Biotechnol Lett* 28:889–896
19. Holtmann D, Sell D (2002) Detection of the microbial activity of aerobic heterotrophic, anoxic heterotrophic and aerobic autotrophic activated sludge organisms with an electrochemical sensor. *Biotechnol Lett* 24:1313–1318
20. Holtmann D (2005) Elektrochemisches Monitoring biologischer Aktivität. Doctoral thesis, University Magdeburg (Germany) 229
21. Leifheit M, Mohr KH (1997) PTS-Manuskript (PTS-MS 66, PTS-Analytik-Tage: Aktuelle Analyseverfahren) 4/1–4/9

Chapter 3

Dissolved Oxygen

Usman Latif and Franz L. Dickert

3.1 Introduction

Dissolved oxygen (DO) plays a vital role in many industrial^{1,2}, physiological,^{3,4} and environmental processes. The electrochemistry is greatly influenced by the amount of dissolved oxygen because of the reduction of molecular oxygen. Monitoring the percentage of oxygen in cell cultures allows us to screen drugs, cell growth, as well as toxicity analysis. Measurement of dissolved oxygen in the blood reflects the hemoglobin-binding sites occupied by oxygen. If the level of oxygen saturation is low which is called hypoxemia this medical condition is an indication of carbon monoxide poisoning or chronic obstructive pulmonary disease (COPD).⁵

A number of chemical and biological reactions in water also depend on the amount of dissolved oxygen. Monitoring the oxygen in ground or wastewater is an important test in water quality and waste treatment.^{6,7} The quality of water can easily be assessed by the concentration of dissolved oxygen since the metabolic activity and growth rate of microorganisms and aerobic cells depend on their oxygen consumption.⁸

The oxygen present in water systems is due to atmospheric aeration and photosynthetic activity. These common sources maintain an adequate level of oxygen in the aqueous environment which is necessary for the existence and growth of all

U. Latif
Department of Analytical Chemistry, University of Vienna,
Währinger Strasse 38, 1090 Vienna, Austria

Department of Chemistry, COMSATS Institute of Information Technology,
Tobe Camp, University Road, 22060 Abbottabad, Pakistan

F.L. Dickert (✉)
Department of Analytical Chemistry, University of Vienna,
Währinger Strasse 38, 1090 Vienna, Austria
e-mail: Franz.dickert@univie.ac.at

forms of life in water. If the concentration of oxygen in aquatic systems falls below 2 mg/L for some time then it can cause the dying of large fish.⁹ Thus, the amount of dissolved oxygen is a vital parameter to assess water quality.

The DO level should be kept high in order to maintain freshwater streams for swimming or fishing. If the oxygen level drops too low then fish will suffocate and the aqueous environment will be quite favorable for harmful bacteria. There should also be an optimum level of dissolved oxygen in the wastewater treatment process control because the solids in wastewater are allowed to settle and bacteria are added to decompose this solid. If the concentration of oxygen is quite higher than the optimum level more energy is required for aeration and processes will become expensive. If the dissolved oxygen level is low the aerobic bacteria will die and decomposition ceases.

3.2 Membrane-Covered Electrodes

Selectivity can be introduced to an electrode by covering it with a membrane. This membrane helps the specific analyte in reaching the electrode surface and leaves other substances behind. In addition, these membranes also eliminate the problem of electrode poisoning. The best known example is the Clark electrode which is covered with a polytetrafluoroethylene (PTFE) membrane. This porous membrane assists the diffusion of oxygen only. A platinum or gold electrode is first covered with a thin layer of electrolyte. Then, a PTFE porous membrane is placed over it which hinders other species except oxygen to permeate to the electrode, thus avoiding its poisoning. A potential is applied to the working electrode to reduce oxygen. A silver disc serves as a reference electrode.

3.2.1 Clark's Electrode

Leland C. Clark developed this well-known oxygen sensor in 1956 which is widely used for physiological, industrial, and environmental analysis. It is an amperometric sensor which consists of a working electrode, a reference electrode, and the electrolyte as shown in Fig. 3.1.

The working electrode (cathode) is made of noble metals such as platinum or gold, so the cathode material does not take part in the chemical reaction, whereas the anode is Ag in KCl. A negative potential is applied to cathode relative to the anode (reference electrode) in order to reduce the dissolved oxygen present in the solution by the following reaction:

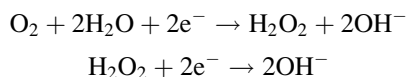
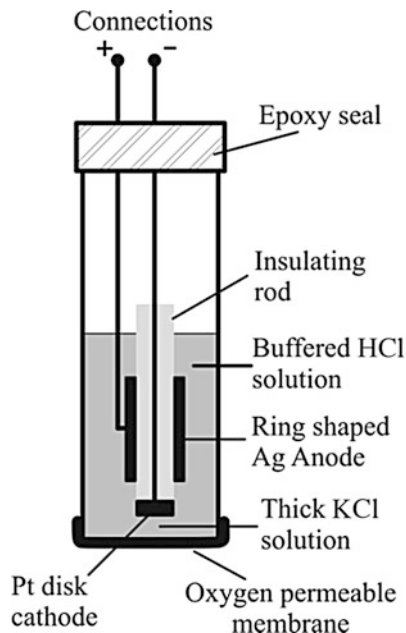


Fig. 3.1 Clark oxygen sensor



The electrode surface is isolated by the oxygen-permeable polymeric membrane in order to avoid the interference of any electroactive species present in the solution along with DO. As a result, only dissolved oxygen present in the sample will diffuse through the membrane and be reduced at the cathode surface due to a negative external potential which will produce an electric current. At a specific value of polarization potential which depends on the cathode material the current is linearly proportional to the oxygen concentration.

3.2.2 *Pt-LaF₃-Sensing Membrane*

Xingbo and co-workers designed a device to determine the DO content¹⁰ with a sensor based on metal insulator semiconductor field effect (MISFET) structure. A LaF₃ crystal exhibits extraordinary sensing capability towards oxygen which makes it an attractive material for researchers.¹¹ In order to fabricate the device, carbon paste with a Pt-LaF₃ mixture film was used as a sensing membrane. The sensor was assessed with different oxygen concentrations (5–12 ppm) and output voltage signals were obtained at different temperatures and different biases. The device with Pt-LaF₃ sensor film exhibited excellent sensitivity towards DO concentrations. The sensor responded to a change in oxygen concentration producing a

gate voltage shift of the MISFET which was used to measure DO concentrations. The gate of the sensor device was developed by following N-type metal oxide semiconductor (NMOS) technology. Then, the sensing film of Pt-LaF₃ was prepared by a carbon paste film. Paraffin wax was used as an adhesive and by melting it at 60 °C it was spread equally on the surface of the gate which helped in preparing the film with the sensing mixture after drying.

The device was operated at a constant drain-source current and voltage. The measurement was carried out with a feedback loop by regulating the reference voltage.¹² The sensor output signals in terms of gate voltage shift were measured as a function of the DO concentration by a digital voltmeter.

LaF₃ was also employed as solid electrolyte while using Pt as a sensing electrode to develop a potentiometric oxygen sensor.¹³

3.2.3 PIDS or TiO₂ Membrane-Coated Sensor

A potentiometric sensor was developed by Martinez-Manez and co-workers in thick film technology.¹⁴ RuO₂ was used as sensitive material whereas this active electrode surface was covered with a semipermeable polymeric (polyisophthalamide diphenylsulfone, PIDS) or ceramic-based (TiO₂) membrane. The measurement of DO could only be carried out effectively if other redox processes were excluded except the desired reaction which was produced by oxygen.¹⁵ This was achieved by covering the active electrode with a semipermeable polymeric or ceramic membrane which allowed to pass DO and excluded any other redox-active species present in solution. A schematic view of the DO potentiometric sensor is displayed in Fig. 3.2.

This DO electrode consisted of (1) a substrate made of isolating material, (2) a layer of conductive material with (2a) as the terminal side of this material, (3) a layer of sensitive material (RuO₂), (4) a layer of a polymer or ceramic as oxygen-permeable membrane, and (5) an isolating layer exposing the active and terminal sides and covering the rest. The response of the TiO₂-coated RuO₂ electrode was monitored in the presence of oxygen in an aqueous environment. Variations in the

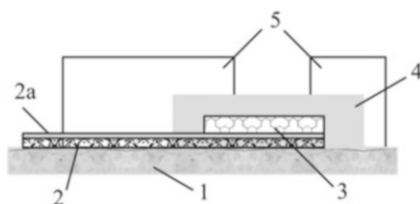


Fig. 3.2 Schematic representation of MISFET for dissolved oxygen electrode: (1) substrate, (2) layer of conductive material, (2a) terminal area, (3) layer of material sensible to oxygen, (4) layer consisting of a membrane ideally permeable to oxygen and non-permeable to ions, and (5) isolating layer, adapted from reference [14]

emf of the active electrode versus an Ag/AgCl reference electrode as a function of DO concentrations in water were obtained. A linear response with a Nernstian slope of 59.4 mV per decade was observed in 0.5–8 ppm DO concentration range. This reaction involved only one electron per oxygen molecule in the reduction process indicating that superoxide (O_2^-) was produced by the reaction $\text{O}_2 + 1e^- = \text{O}_2^-$.

Excellent emf variations were observed if the active electrode was covered with an oxygen-permeable membrane because the typical interfering species was the proton. Non-coated active electrodes gave a linear response against proton concentrations in comparison to the oxygen-permeable membrane-coated electrode which showed a much lower variation of the potential against pH. The PIDS-coated RuO_2 also exhibited a linear response as a function of DO concentrations in the range from 0.8 to 8 ppm and showed negligible influence from pH, but the only drawback was the inferior adherence of the PIDS membrane in comparison to the titania membrane.

3.3 Modified Electrodes

Aside from covering their surface with a membrane, electrodes can be modified with an electroactive species. These modifiers act as mediators which help with the electron transfer between the analyte and the electrode. Moreover, this modification also helps in lowering the potential needed to reduce oxygen at the electrode surface. The modified electrodes can be prepared by direct adsorption of electroactive species or by physically covering the electrode surface. In some cases, linkers are also employed in order to immobilize the mediators to the electrode surface. Chapter 16.2 of the volume 1 is dedicated to the many different aspects of modified electrodes.

3.3.1 *Poly(Nile Blue)-Modified Electrode*

Electrodes modified with electroactive polymers exhibit considerable sensitivity and may lower the reduction potential for the detection of oxygen.¹⁶ Actually, the direct reduction of oxygen at solid electrodes requires a highly negative potential. Electroactive metal complexes such as metal-porphyrins or metal-free organic compounds can act as electron transfer mediators and are suitable for electrode modification to determine oxygen.¹⁷ Nile blue is a well-known electroactive mediator for electron transfer. Poly(nile blue) film can easily be immobilized on a glassy carbon electrode by electropolymerization. The resulting layer is very stable which is attributed to the presence of conjugated aromatic rings in the dye. The poly(nile blue) layer possesses significant affinity for dissolved oxygen. By the electrocatalytic activity of this compound oxygen is reduced in a two-electron-two-proton process at a lower potential as shown in Fig. 3.3.¹⁸

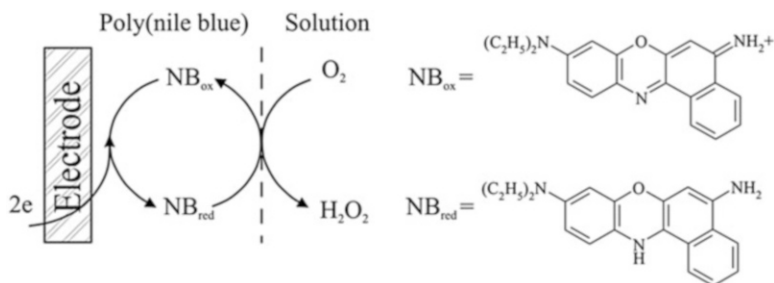


Fig. 3.3 Electrocatalytic action of poly(nile blue) for the reduction of oxygen, adapted from reference [18]

3.3.2 Metalloporphyrin-Modified Electrode

Porphyrins and metalloporphyrins possess distinct properties which make them attractive as a class of material suitable for modifying electrodes.¹⁹ These properties include electrocatalytic activity, or photoreactivity. Hydrolysis and subsequent condensation of silanes with metalloporphyrins create a silica matrix in which metalloporphyrins are covalently bound. The iron(III)-tetra-*o*-ureaphenylporphyrino silica matrix ((*o*)-FeTUPPS) is an excellent mediator for electron transfer; it is obtained by anchoring iron porphyrin tetraurea to a silica matrix²⁰; the resulting layer is highly stable due to the covalent attachment of the porphyrin to the silica backbone.²¹

Modification of the electrode surface with (*o*)-FeTUPPS leads to the formation of active sites available for the reduction of oxygen which occurs at a less negative potential in comparison to the unmodified graphite electrode. If metalloporphyrins are used for electrode modification, then the reduction of dissolved oxygen can occur via two mechanisms: reduction of oxygen to hydrogen peroxide by a transfer of two electrons, or direct reduction to water when four electrons take part in the process. (*o*)-FeTUPPS as a modifier catalyzes the two-electron process which leads to the formation of H_2O_2 which is determined by a rotating disk electrode.

3.3.3 Cobalt Tetrasulfonate Phthalocyanine (CoTSPc)-Modified Electrode

In another approach, a DO sensor was proposed by modifying a glassy carbon (GC) electrode with cobalt tetrasulfonate phthalocyanine (CoTSPc).²² The direct reduction of oxygen at a solid electrode is a slow process and also requires a high negative potential which can be lowered by electron transfer mediators that can shuttle the electrons between oxygen and electrode. Among these mediators, phthalocyanines acquired a lot of attention because of their catalytic ability and

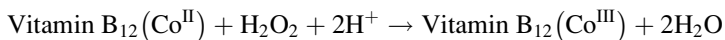
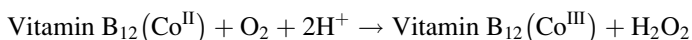
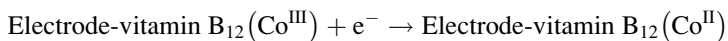
stability.^{23,24} CoTSPc was immobilized by using a poly-L-lysine (PLL) film which acted as an excellent stabilizer for CoTSPc modifier.²⁵ This polyelectrolyte avoids leaching of the electrocatalyst due to ion-pair attraction between the amino group of PLL and the sulfonic acid group of CoTSPc. The PLL film alone does not create any effect in reducing dissolved oxygen; the catalytic effect is solely attributed to [Co(II)TSPc]⁴⁻ as the active site present in the PLL film.

The influence of CoTSPc and PLL amount in the sensor response was analyzed and best results were obtained when using 0.8 mmol L⁻¹ of CoTSPc and 0.12 mmol L⁻¹ of PLL. The measurements were carried out by differential pulse voltammetry (DPV) and chronoamperometry. With the latter technique a linear response was observed for 0.2–8 mg L⁻¹ DO in solution.

In the DPV measurements, the peak current increased with scan rates from 0.005 to 0.02 V s⁻¹ but accompanied by a broadening of peaks. Best sensitivity was achieved with a pulse amplitude of 0.075 V and a scan rate of 0.02 V s⁻¹. The DPV measurements showed a linear response at optimized conditions for concentrations from 0.2 to 8 mg L⁻¹ oxygen in solution. The device with modified GC exhibited excellent catalytic activity and shifted the reduction potential of DO by 200 mV towards less negative value.

3.3.4 Vitamin B₁₂-Modified Electrode

Cobalt-based macrocyclic complexes are some of the catalysts that exhibit significant catalytic activity against DO.²⁶ Vitamin B₁₂ is a cobalt-based complex and inherits excellent electrocatalytic properties.²⁷ It can be easily screen printed to modify the electrode providing DO sensors better than the Clark-type electrode. The latter should be covered with a permeable membrane and must be properly maintained. Modifying the electrode with vitamin B₁₂ creates a membrane-free DO sensor. Tedious maintenance is not required with this kind of sensor. Moreover, poisoning of the membrane is not an issue anymore. The electrochemical behavior of the vitamin B₁₂-modified electrode involved in the reduction of oxygen can be explained by the following equations²⁸:

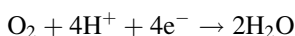
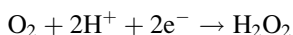


These equations clearly show the electrocatalytic properties of vitamin B₁₂. The electrocatalytic reduction of oxygen leads to the formation of hydrogen peroxide by the electrode; H₂O₂ is then further reduced to water molecules by vitamin B₁₂.

3.3.5 *Manganese Phthalocyanine-Modified Electrode*

A mixed oxide matrix comprises a porous framework which makes it a perfect substrate for the immobilization of electroactive species.²⁹ The surface of the mixed oxide network is covered with hydroxyl (-OH) groups which allow functionalization with electroactive species. The electrochemical properties, electrical conductivity, as well as stability of transition metal complexes make them a promising candidate for designing an electrochemical sensor for dissolved oxygen.³⁰ These properties are associated with the electrons of conjugated bonds and on the central metal atom as well. The manganese phthalocyanine (MnPc) complex can be immobilized on a porous network of a mixed oxide matrix consisting of SiO₂/SnO₂³¹ to which the mechanical stability of the film is attributed. Chemical stability results from the strong confinement of electroactive species in the pores of the oxide framework which prevents its leaching over a long time when being in contact with the solution. Moreover, the confinement of metal complexes in the pores ensures a homogeneous layer of electroactive species over the whole-electrode surface.

The reduction of oxygen can occur in two different ways, either involving two electrons yielding H₂O₂ or through reduction to water with four electrons:



The estimation of the number of electrons involved in oxygen reduction and the product obtained can be assessed by rotating ring-disk electrode experiments. This technique proved the involvement of four electrons when MnPc complex was used for the modification of electrodes.

3.3.6 *Poly(Methylene Blue)-Modified Electrode*

Some organic dyes show high electroactivity which makes them useful electron mediators.³² The electrochemical activity of dyes, such as methylene blue, methylene green, neutral red, and pyronin B, is attributed to their conjugated ring structure.³³ Modification of electrodes with these electroactive compounds (e.g., methylene blue) for the detection of dissolved oxygen yields excellent results. However, problems are associated with their anchoring on the electrode surface because they will leach if they are not properly attached. Many organic dyes can be immobilized on the electrode surface by carbon nanotubes, zeolite, Nafion, silane, or electropolymerization.

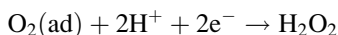
Electrodes which are modified with a dye-polymer exhibit usually good stability, conductivity, and enhanced electrochemical sensing behavior. Among a lot of other significant properties silica nanoparticles possess a large surface area and open space for the immobilization of organic dyes without affecting their inherent

properties. These nanostructures incorporate dye molecules inside their matrix avoiding their leaching. The dye molecules trapped in silica nanoparticles are able to form a polymer which will form a nanocomposite called polymer(dye)-doped silica nanoparticles. The nanocomposite is electrocatalytically active and exhibits conductive properties as well. The reduction of oxygen in such a nanostructured environment involves three steps³⁴:

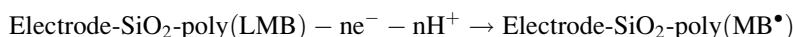
1. Diffusion of oxygen molecules into the polymeric structure
2. Adsorption of oxygen molecules at the active sites
3. Reduction of oxygen with the aid of the electrocatalyst

Hence, the mechanism of oxygen reduction on polymethylene blue-doped silica nanoparticles (PMB@SiO₂) is described by the following reaction sequence³⁵:

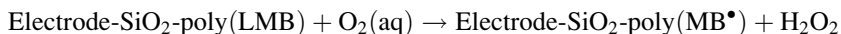
Oxygen diffuses into the polymeric structure and subsequently adsorbs at the active sites. Afterwards, it is reduced via electron transfer by the following equation:



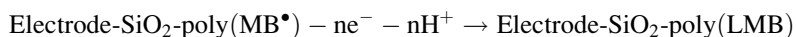
where the reduced leuco form of methylene blue (LMB) acts as the catalyst:



The overall reaction can be summarized as



Leucomethylene blue is regenerated again from the deprotonated form of methylene blue (MB[•]) by electrochemical reduction:



3.3.7 Nickel-Salen-Modified Electrode

Electrocatalysts which assist multi-electron transfers are of great interest for the reduction of oxygen because this process involves multiple electron transfer steps.³⁶ These electrocatalysts facilitate crossing over the activation energy barriers involved in this process.

Transition metal complexes with Schiff bases as ligands attracted a great interest in this respect. These metal complexes can easily be immobilized on electrode surfaces via electropolymerization³⁷ generating an electrically conductive polymeric film.³⁸ The reactivity of metal complexes depends on the nature of the metal as well as on the ligand attached.

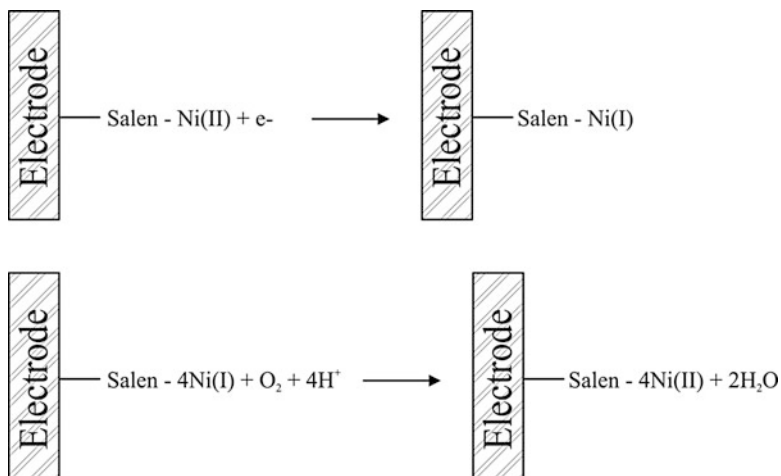


Fig. 3.4 The reduction mechanism of oxygen at Ni-salen-modified platinum electrode, adapted from reference (41)

A thin film of Ni-salen (salen = *N, N'*-ethylenebis(salicylideneiminato)) polymer on a platinum electrode exhibits a high rate of electron transfer and can be the platform for a highly sensitive system for the determination of oxygen.³⁹

The Ni-salen polymer promotes the reduction of oxygen via the Ni(II)/Ni(I) redox couple. Oxygen is reduced directly to water involving four electrons at a significantly decreased potential.⁴⁰ The reduction proceeds in two steps as shown in Fig. 3.4⁴¹:

1. Ni(II) is reduced to Ni(I).
2. Ni(I) reduces oxygen and is oxidized to Ni(II).

The output of the sensor will be in the form of current which is controlled by oxygen diffusion.

3.3.8 Anthraquinone-Modified Electrode

The high overpotential of the oxygen reduction can be significantly lowered with electrocatalysts which also improve the speed of electron transfer.⁴² p-Quinones are recognized as such type of compounds which can transfer electrons in biological systems. Thus, among others, anthraquinones attract considerable interest in this respect because of their p-quinoid substructure which can be easily reduced. In addition, anthraquinones are also conductive and can be shaped into monolayers. Thus, anthraquinones can be used for the modification of electrodes for the reversible electron transfer which is attributed to the p-quinones group.⁴³ However, these

electrocatalysts require to be attached covalently; otherwise these they cannot be used for long-term operation.

The anthraquinone moieties on the surface of electrode show excellent electrocatalytic ability towards oxygen. The reaction involves the reduction of anthraquinone to dihydranthraquinone via two electrons and two protons.⁴⁴ Afterwards, dihydranthraquinone reacts with oxygen and converts it to hydrogen peroxide while anthraquinone is regenerated.

3.4 Miniaturized Dissolved Oxygen Sensors

3.4.1 Solid-State Oxygen Sensor

McLaughlin and co-workers designed a microfabricated solid-state oxygen sensor.⁴⁵ The device consisted of microfabricated electrodes overlaid by a solid-state proton conductive matrix. It was further encapsulated in a bio-inert polytetrafluoroethylene (PTFE) film. The sensor characteristics exhibited a linear response to oxygen over a concentration range from 0 to 601 μM . It was a Clark-type oxygen sensor matrix consisting of a matrix working electrodes with diameters of 10, 20, 40, and 80 μm ; each element of the matrix consisted of a working, reference, and counter electrode having a surface area ratio of 1:5:25 in order to gain higher current density at the working electrode (Fig. 3.5). Afterwards, a proton conductive matrix (PCM) was deposited on the electrode matrix which was a Nafion-perfluorinated ion-exchange resin. The hydrophobic structure of the PCM was permeable to oxygen whereas its hydrophilic region acted as proton transport site. The device was finally encapsulated with a bio-inert PTFE film which was oxygen permeable.

The fabricated sensor device reduced dissolved oxygen electrochemically and monitored the resulting current. This sensor could also be used to measure the oxygen concentration in blood because the electrodes were encapsulated in a bio-inert oxygen-permeable PTFE membrane. The electrochemical reduction of

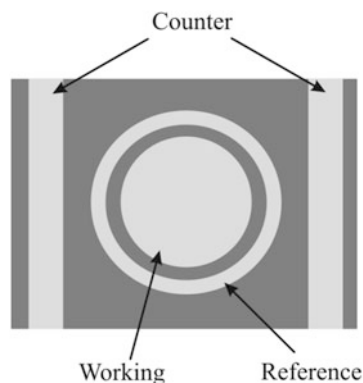
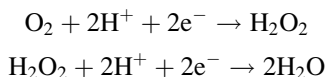


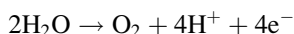
Fig. 3.5 Illustration of an element of the matrix of electrodes, adapted from reference [45]

oxygen is a two-step process which occurs at the working electrode whereas the counter electrode converts it back into reactants.⁴⁶

The mechanism of the oxygen reduction at the working electrode (cathode) is described in the following two equations:



The products formed at working electrode are converted back into reactants at the counter electrode (anode) by the following process:



This sensor is better than a conventional Clark's device because there is no net consumption of any electrode. Both cyclic voltammetric and chronoamperometric measurements were carried out to analyze the performance of the microfabricated DO sensor. Good linearity was observed when using 80 μm diameter electrode sets.

3.4.2 *Microelectrodes*

Microelectrodes are among the most advanced, reliable, and excellent sensing systems.⁴⁷ A needle-type microelectrode array (MEA) was also designed for measuring the concentration of dissolved oxygen in solution.⁴⁸ The MEA was fabricated by following microelectromechanical system (MEMS) technologies. The needle-type nature of the DO sensor allowed the device to penetrate into the environmental sample. The microelectrodes were made of gold due to its potential use in measuring DO⁴⁹ as well as a large number of other analytes.⁵⁰ The DO-MEA consisted of four 1 cm long electrically isolated microelectrodes. The DO microelectrodes were characterized by using a calibration cell with a commercial Ag/AgCl reference electrode.

The microelectrode array was polarized before calibration with a negative voltage to reduce the amount of oxygen to zero on the cathode of the microelectrode surface which eliminated any disturbances caused by any residual oxygen. Different salinities of water samples produced different sensitivities of the microelectrode array.

The developed dissolved oxygen sensor was capable to operate in multi-species aerobic films.⁵¹ The horizontal and vertical movement of the microelectrodes was controlled by a micromanipulator. Thus, the MEA could measure microprofiles of dissolved oxygen in biofilms. The results depicted that the DO concentration was high at an interface of air-saline solution due to oxygen diffusion. The DO concentration decreased within the saline-biofilm.

References

1. Zhang H-T, Zhan X-B, Zheng Z-Y, Wu J-R, English N, Yu X-B, Lin C-C (2012) Improved curdlan fermentation process based on optimization of dissolved oxygen combined with pH control and metabolic characterization of *Agrobacterium* sp. ATCC 31749. *Appl Microbiol Biotechnol* 93(1):367–379. doi:[10.1007/s00253-011-3448-3](https://doi.org/10.1007/s00253-011-3448-3)
2. El-Sedawy HF, Hussein MMM, Essam T, El-Tayeb OM, Mohammad FHA Scaling up for the industrial production of rifamycin B.; optimization of the process conditions in bench-scale fermentor. *Bulletin of Faculty of Pharmacy, Cairo University* (0). doi:[10.1016/j.bfopcu.2013.02.002](https://doi.org/10.1016/j.bfopcu.2013.02.002)
3. Bowyer JN, Booth MA, Qin JG, D'Antignana T, Thomson MJS, Stone DAJ (2013) Temperature and dissolved oxygen influence growth and digestive enzyme activities of yellowtail kingfish *Seriola lalandi* (Valenciennes, 1833). *Aquacul Res* 1–11. doi:[10.1111/are.12146](https://doi.org/10.1111/are.12146)
4. Evans SM, Koch CJ (2003) Prognostic significance of tumor oxygenation in humans. *Cancer Lett* 195(1):1–16. doi:[10.1016/S0304-3835\(03\)00012-0](https://doi.org/10.1016/S0304-3835(03)00012-0)
5. Pison CM, Wolf JE, Levy PA, Dubois F, Brambilla CG, Paramelle B (1991) Effects of captopril combined with oxygen therapy at rest and on exercise in patients with chronic bronchitis and pulmonary hypertension. *Respiration* 58(1):9–14
6. Rai R, Upadhyay A, Ojha CS, Singh V (2012) Water pollution. In: *The Yamuna River Basin*, vol 66. Water science and technology library. Springer Netherlands, pp 245–275. doi:[10.1007/978-94-007-2001-5_9](https://doi.org/10.1007/978-94-007-2001-5_9)
7. Chen Y-P, Liu S-Y, Yu H-Q (2007) A simple and rapid method for measuring dissolved oxygen in waters with gold microelectrode. *Anal Chim Acta* 598(2):249–253. doi:[10.1016/j.aca.2007.07.045](https://doi.org/10.1016/j.aca.2007.07.045)
8. Ansa-Asare OD, Marr IL, Cresser MS (2000) Evaluation of modelled and measured patterns of dissolved oxygen in a freshwater lake as an indicator of the presence of biodegradable organic pollution. *Water Res* 34(4):1079–1088. doi:[10.1016/S0043-1354\(99\)00239-0](https://doi.org/10.1016/S0043-1354(99)00239-0)
9. Zhao L, Li D, Ma D, Ding Q (2010) An portable intelligent measurement instrument for dissolved oxygen in aquaculture. *Sens Lett* 8(1):102–108
10. Na X, Niu W, Li H, Xie J (2002) A novel dissolved oxygen sensor based on MISFET structure with Pt–LaF₃ mixture film. *Sensors Actuators B Chem* 87(2):222–225. doi:[10.1016/S0925-4005\(02\)00238-1](https://doi.org/10.1016/S0925-4005(02)00238-1)
11. Miura N, Hisamoto J, Yamazoe N, Kuwata S, Salardenne J (1989) Solid-state oxygen sensor using sputtered LaF₃ film. *Sensors Actuators* 16(4):301–310. doi:[10.1016/0250-6874\(89\)85001-2](https://doi.org/10.1016/0250-6874(89)85001-2)
12. Hendrikse J, Olthuis W, Bergveld P (1999) The EMOSFET as an oxygen sensor: constant current potentiometry. *Sensors Actuators B Chem* 59(1):35–41. doi:[10.1016/S0925-4005\(99\)00195-1](https://doi.org/10.1016/S0925-4005(99)00195-1)
13. Sun G, Wang H, Zhuangde J, Junqiang R (2011) A potentiometric oxygen sensor based on LaF₃ using Pt micro grid as the sensing electrode. In: *Nano/Micro Engineered and Molecular Systems (NEMS), 2011 I.E. International Conference on*, 20–23 Feb. 2011 pp 53–56. doi:[10.1109/nems.2011.6017293](https://doi.org/10.1109/nems.2011.6017293)
14. Martínez-Máñez R, Soto J, Lizondo-Sabater J, García-Breijo E, Gil L, Ibáñez J, Alcaina I, Alvarez S (2004) New potentiometric dissolved oxygen sensors in thick film technology. *Sensors Actuators B Chem* 101(3):295–301. doi:[10.1016/j.snb.2004.03.008](https://doi.org/10.1016/j.snb.2004.03.008)
15. Kohler H, Göpel W (1991) Mixed valent tungsten oxides: new electrode materials for the potentiometric detection of dissolved oxygen at temperatures below 35 °C. *Sensors Actuators B Chem* 4(3–4):345–354. doi:[10.1016/0925-4005\(91\)80134-6](https://doi.org/10.1016/0925-4005(91)80134-6)
16. Mao L, Jin J, L-n S, Yamamoto K, Jin L (1999) Electrochemical Microsensor for In vivo measurements of oxygen based on nafion and methylviologen modified carbon fiber microelectrode. *Electroanalysis* 11(7):499–504. doi:[10.1002/\(sici\)1521-4109\(199906\)11:7<499::aid-elan499>3.0.co;2-8](https://doi.org/10.1002/(sici)1521-4109(199906)11:7<499::aid-elan499>3.0.co;2-8)

17. Collman JP, Denisevich P, Konai Y, Marrocco M, Koval C, Anson FC (1980) Electrode catalysis of the four-electron reduction of oxygen to water by dicobalt face-to-face porphyrins. *J Am Chem Soc* 102(19):6027–6036. doi:[10.1021/ja00539a009](https://doi.org/10.1021/ja00539a009)
18. Ju H, Shen C (2001) Electrocatalytic reduction and determination of dissolved oxygen at a poly(nile blue) modified electrode. *Electroanalysis* 13(8–9):789–793. doi:[10.1002/1521-4109\(200105\)13:8/9<789::aid-elan789>3.0.co;2-g](https://doi.org/10.1002/1521-4109(200105)13:8/9<789::aid-elan789>3.0.co;2-g)
19. Trévin S, Bedioui F, Devynck J (1996) New electropolymerized nickel porphyrin films. Application to the detection of nitric oxide in aqueous solution. *J Elec Chem* 408(1–2):261–265. doi:[10.1016/0022-0728\(96\)04540-8](https://doi.org/10.1016/0022-0728(96)04540-8)
20. Ribeiro ES, Gushikem Y, Biazzotto JC, Serra OA (2002) Electrochemical properties and dissolved oxygen reduction study on an iron(III)-tetra(o-ureaphenyl)porphyrinosilica matrix surface. *J Porphyrins Phthalocyanines* 06(08):527–532. doi:[10.1142/S1088424602000658](https://doi.org/10.1142/S1088424602000658)
21. Ciuffi KJ, Sacco HC, Biazzotto JC, Vidoto EA, Nascimento OR, Leite CAP, Serra OA, Iamamoto Y (2000) Synthesis of fluorinated metalloporphyrinosilica imprinted with templates through sol–gel process. *J Non-Cryst Solids* 273(1–3):100–108. doi:[10.1016/S0022-3093\(00\)00149-6](https://doi.org/10.1016/S0022-3093(00)00149-6)
22. Luz RCS, Damos FS, Tanaka AA, Kubota LT (2006) Dissolved oxygen sensor based on cobalt tetrasulphonated phthalocyanine immobilized in poly-L-lysine film onto glassy carbon electrode. *Sensors Actuators B Chem* 114(2):1019–1027. doi:[10.1016/j.snb.2005.07.063](https://doi.org/10.1016/j.snb.2005.07.063)
23. Phougat N, Vasudevan P (1997) Electrocatalytic activity of some metal phthalocyanine compounds for oxygen reduction in phosphoric acid. *J Power Sources* 69(1–2):161–163. doi:[10.1016/S0378-7753\(97\)02567-6](https://doi.org/10.1016/S0378-7753(97)02567-6)
24. Baranton S, Coutanceau C, Roux C, Hahn F, Léger JM (2005) Oxygen reduction reaction in acid medium at iron phthalocyanine dispersed on high surface area carbon substrate: tolerance to methanol, stability and kinetics. *J Electroanal Chem* 577(2):223–234. doi:[10.1016/j.jelechem.2004.11.034](https://doi.org/10.1016/j.jelechem.2004.11.034)
25. Oyama N, Anson FC (1980) Catalysis of electrode processes by multiply-charged metal complexes electrostatically bound to polyelectrolyte coatings on graphite electrodes, and the use of polymer-coated rotating disk electrodes in diagnosing kinetic and conduction mechanisms. *Anal Chem* 52(8):1192–1198. doi:[10.1021/ac50058a009](https://doi.org/10.1021/ac50058a009)
26. Ng BW, Lenigk R, Wong YL, Wu X, Teng Yu N, Renneberg R (2000) Poisoning Influence of Cyanide on the Catalytic Oxygen Reduction by Cobalt(III) Tetra(3-methoxy-4-hydroxyphenyl) Porphyrin Modified Electrode. *J Electrochem Soc* 147(6):2350–2354. doi:[10.1149/1.1393535](https://doi.org/10.1149/1.1393535)
27. Njue CK, Nuthakki B, Vaze A, Bobbitt JM, Rusling JF (2001) Vitamin B12-mediated electrochemical cyclopropanation of styrene. *Electrochem Commun* 3(12):733–736. doi:[10.1016/S1388-2481\(01\)00255-7](https://doi.org/10.1016/S1388-2481(01)00255-7)
28. Lin MS, Leu HJ, Lai CH (2006) Development of Vitamin B12 based disposable sensor for dissolved oxygen. *Anal Chim Acta* 561(1–2):164–170. doi:[10.1016/j.aca.2005.12.048](https://doi.org/10.1016/j.aca.2005.12.048)
29. Canevari TC, Arguello J, Francisco MSP, Gushikem Y (2007) Cobalt phthalocyanine prepared in situ on a sol–gel derived SiO₂/SnO₂ mixed oxide: Application in electrocatalytic oxidation of oxalic acid. *J Electroanal Chem* 609(2):61–67. doi:[10.1016/j.jelechem.2007.06.006](https://doi.org/10.1016/j.jelechem.2007.06.006)
30. Santos LSS, Landers R, Gushikem Y (2011) Application of manganese (II) phthalocyanine synthesized in situ in the SiO₂/SnO₂ mixed oxide matrix for determination of dissolved oxygen by electrochemical techniques. *Talanta* 85(2):1213–1216. doi:[10.1016/j.talanta.2011.06.003](https://doi.org/10.1016/j.talanta.2011.06.003)
31. Canevari TC, Luz RCS, Gushikem Y (2008) Electrocatalytic determination of nitrite on a rigid disk electrode having cobalt phthalocyanine prepared in situ. *Electroanalysis* 20(7):765–770. doi:[10.1002/elan.200704082](https://doi.org/10.1002/elan.200704082)
32. Arvand M, Sohrabnezhad S, Mousavi MF, Shamsipur M, Zanjanchi MA (2003) Electrochemical study of methylene blue incorporated into mordenite type zeolite and its application for amperometric determination of ascorbic acid in real samples. *Anal Chim Acta* 491(2):193–201. doi:[10.1016/S0003-2670\(03\)00790-6](https://doi.org/10.1016/S0003-2670(03)00790-6)
33. Khoo SB, Chen F (2002) Studies of sol – gel ceramic film incorporating methylene blue on glassy carbon: an electrocatalytic system for the simultaneous determination of ascorbic and uric acids. *Anal Chem* 74(22):5734–5741. doi:[10.1021/ac0255882](https://doi.org/10.1021/ac0255882)

34. Khomenko V, Frackowiak E, Béguin F (2005) Determination of the specific capacitance of conducting polymer/nanotubes composite electrodes using different cell configurations. *Electrochim Acta* 50(12):2499–2506. doi:[10.1016/j.electacta.2004.10.078](https://doi.org/10.1016/j.electacta.2004.10.078)
35. Xiao X, Zhou B, Tan L, Tang H, Zhang Y, Xie Q, Yao S (2011) Poly(methylene blue) doped silica nanocomposites with crosslinked cage structure: Electropolymerization, characterization and catalytic activity for reduction of dissolved oxygen. *Electrochim Acta* 56 (27):10055–10063. doi:[10.1016/j.electacta.2011.08.095](https://doi.org/10.1016/j.electacta.2011.08.095)
36. Zuo G, Yuan H, Yang J, Zuo R, Lu X (2007) Study of orientation mode of cobalt-porphyrin on the surface of gold electrode by electrocatalytic dioxygen reduction. *J Mol Catal A Chem* 269 (1–2):46–52. doi:[10.1016/j.molcata.2006.11.041](https://doi.org/10.1016/j.molcata.2006.11.041)
37. Demetgül C, Deletoğlu D, Karaca F, Yalçinkaya S, Timur M, Serin S (2010) Synthesis and characterization of a Schiff base derived from 2-aminobenzylamine and its Cu(II) complex: electropolymerization of the complex on a platinum electrode. *J Coord Chem* 63 (12):2181–2191. doi:[10.1080/00958972.2010.496852](https://doi.org/10.1080/00958972.2010.496852)
38. Dadamos TRL, Teixeira MFS (2009) Electrochemical sensor for sulfite determination based on a nanostructured copper-salen film modified electrode. *Electrochim Acta* 54 (19):4552–4558. doi:[10.1016/j.electacta.2009.03.045](https://doi.org/10.1016/j.electacta.2009.03.045)
39. Martin CS, Dadamos TRL, Teixeira MFS (2012) Development of an electrochemical sensor for determination of dissolved oxygen by nickel–salen polymeric film modified electrode. *Sensors Actuators B Chem* 175:111–117. doi:[10.1016/j.snb.2011.12.098](https://doi.org/10.1016/j.snb.2011.12.098)
40. Šljukić B, Banks CE, Compton RG (2005) An overview of the electrochemical reduction of oxygen at carbon-based modified electrodes. *JICS* 2(1):1–25. doi:[10.1007/bf03245775](https://doi.org/10.1007/bf03245775)
41. Dadamos TR, Martin CS, Teixeira MFS (2011) Development of nanostructured electrochemical sensor based on polymer film nickel–salen for determination of dissolved oxygen. *Procedia Eng* 25:1057–1060. doi:[10.1016/j.proeng.2011.12.260](https://doi.org/10.1016/j.proeng.2011.12.260)
42. Zon A, Palys M, Stojek Z, Sulowska H, Ossowski T (2003) Supramolecular derivatives of 9,10-anthraquinone. *Electrochemistry at regular- and low ionic strength and complexing properties*. *Electroanalysis* 15(5–6):579–585. doi:[10.1002/elan.200390072](https://doi.org/10.1002/elan.200390072)
43. Manisankar P, Gomathi A (2005) Electrocatalytic reduction of dioxygen at the surface of carbon paste electrodes modified with 9,10-anthraquinone derivatives and dyes. *Electroanalysis* 17(12):1051–1057. doi:[10.1002/elan.200403213](https://doi.org/10.1002/elan.200403213)
44. Tiwari I, Singh M, Gupta M, Aggarwal SK (2012) Electroanalytical properties and application of anthraquinone derivative-functionalized multiwalled carbon nanotubes nanowires modified glassy carbon electrode in the determination of dissolved oxygen. *Mater Res Bull* 47 (7):1697–1703. doi:[10.1016/j.materresbull.2012.03.031](https://doi.org/10.1016/j.materresbull.2012.03.031)
45. McLaughlin GW, Braden K, Franc B, Kovacs GTA (2002) Microfabricated solid-state dissolved oxygen sensor. *Sensors Actuators B Chem* 83(1–3):138–148. doi:[10.1016/S0925-4005\(02\)00021-7](https://doi.org/10.1016/S0925-4005(02)00021-7)
46. Maruyama J, Inaba M, Ogumi Z (1998) Rotating ring-disk electrode study on the cathodic oxygen reduction at Nafion(R)-coated gold electrodes. *J Electroanal Chem* 458(1):175–182
47. Wightman RM (2006) Probing cellular chemistry in biological systems with microelectrodes. *Science* 311(5767):1570–1574. doi:[10.1126/science.1120027](https://doi.org/10.1126/science.1120027)
48. Lee J-H, Seo Y, Lim T-S, Bishop PL, Papautsky I (2007) MEMS needle-type sensor array for in situ measurements of dissolved oxygen and redox potential. *Environ Sci Technol* 41 (22):7857–7863. doi:[10.1021/es070969o](https://doi.org/10.1021/es070969o)
49. Linsenmeier RA, Yancey CM (1987) Improved fabrication of double-barreled recessed cathode O₂ microelectrodes. *J Appl Physiol* 63(6):2554–2557
50. McRipley MA, Linsenmeier RA (1996) Fabrication of a mediated glucose oxidase recessed microelectrode for the amperometric determination of glucose. *J Electroanal Chem* 414 (2):235–246. doi:[10.1016/0022-0728\(96\)04692-X](https://doi.org/10.1016/0022-0728(96)04692-X)
51. Lee J-H, Lim T-S, Seo Y, Bishop PL, Papautsky I (2007) Needle-type dissolved oxygen microelectrode array sensors for in situ measurements. *Sensors Actuators B Chem* 128 (1):179–185. doi:[10.1016/j.snb.2007.06.008](https://doi.org/10.1016/j.snb.2007.06.008)

Chapter 4

pH Measurements

Usman Latif and Franz L. Dickert

4.1 Introduction

pH represents the hydrogen-ion activity of a solution by which we can evaluate the chemical properties of the solution. This concept was introduced by the Danish biochemist S.P.L. Sorensen in 1909, director of the Chemical Department of the Carlsberg laboratories.¹ The term pH expresses the solution pressure of hydrogen ions in aqueous solution called as pondus Hydrogenii or potentia Hydrogenii and represented as $P_{\text{H}} = -\log(c_{\text{H}}/\text{mol dm}^{-3})$. According to IUPAC, the activity of hydrogen ions in solution or pH can be defined in terms of molality:

$$\text{pH} = -\log a_{\text{H}} = -\log \frac{m_{\text{H}}\gamma_{\text{H}}}{m_0}$$

where

m_{H} = molality of hydrogen ion H^+

γ_{H} = molal activity coefficient of hydrogen ion H^+

$m_0 = 1 \text{ mol kg}^{-1}$

The pH is an important parameter when we deal with environmental pollution, analyzing the quality of water, and even in clinical diagnosis.^{2,3} This vital parameter

U. Latif

Department of Analytical Chemistry, University of Vienna,
Waehring Strasse 38, 1090 Vienna, Austria

Department of Chemistry, COMSATS Institute of Information Technology,
Tobe Camp, University Road, 22060 Abbottabad, Pakistan

F.L. Dickert (✉)

Department of Analytical Chemistry, University of Vienna,
Waehring Strasse 38, 1090 Vienna, Austria
e-mail: Franz.dickert@univie.ac.at

contributed a lot and still is contributing in advancing different fields such as pharmacy, chemistry, biology, medicine, industry, agriculture, biochemistry, and environment.

4.2 Glass Electrode

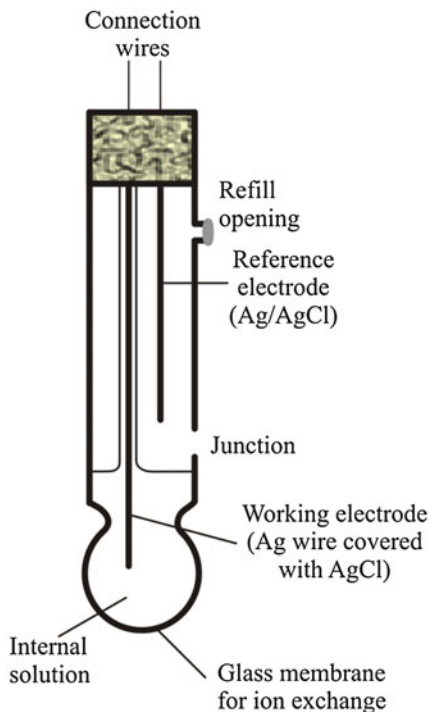
The glass electrode is a most successful electrochemical sensor which is used to determine the activity of hydrogen ions H^+ in solution. In 1906, Cremer⁴ discovered that an electrical potential will be generated by using a thin glass membrane between two aqueous solutions. This was the basic concept by which a pH meter was developed by F. Haber and Z. Klemensiewicz in 1909.⁵ The basic principle of a potentiometric setup consists of an electrolytic cell, which contains two electrodes dipped into a test solution. The classical method to measure the pH value is based on the glass electrode. This is a convenient and widely used method to measure the hydrogen ion activity, its effective concentration, of a solution. The glass electrode is made up of a silver/silver chloride electrode which is prepared by coating an Ag wire with AgCl. The electrode is dipped in a solution of 0.1 M HCl having a fixed pH to complete the electrical circuit. The Ag/AgCl electrode is confined in a thin glass membrane whose advantage is that its permeability is to hydrogen ions only. The concentration of the internal HCl is kept constant which will maintain the potential of the Ag/AgCl electrode at a constant value. The potential will only vary between the outer surface of the glass bulb and the test solution which is governed by the hydrogen ion activity of test solution. The glass membrane with the internal Ag/AgCl electrode in 0.1 M HCl (working electrode) is a half cell which is combined with a reference half cell. The Ag/AgCl is mostly used as a reference half cell usually immersed in a saturated solution of potassium chloride.

The potential of the glass electrode is directly related to the hydrogen ion activity of the test solution. A voltmeter between the two half cells gives a direct reading of pH of the solution in which it is placed. As the output is a voltage, the voltmeter is calibrated for pH reading by using one or more solutions of known pH. The commercial pH electrodes which are commonly available on the market are structured in a single handling unit, initially suggested by W. Ingold in 1952, by combining the glass electrode and the reference half cell in a single casing as shown in Fig. 4.1.

The overall electromotive force (e.m.f.) is determined by:

- The electrode potential (E_1) of the internal Ag/AgCl electrode exposed to a solution of fixed pH.
- The potential (E_2) setup across ion-selective glass membrane due to the two solutions having different hydrogen ion concentrations.
- The electrode potential (E_3) of the reference electrode.

Fig. 4.1 Combination glass electrode, adapted from reference [8]

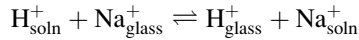


The electrode potentials E_1 and E_3 remain constant. Thus, the e.m.f. of the glass electrode is totally attributable to the hydrogen ion activity of the solution being analyzed. However, many problems are associated with this glass electrode such as large size, shape, cost, and fragility. These factors limit its applications to specific environments.⁶

For proper functioning of the glass electrode, the most important part is the glass membrane. At first, glass was composed of SiO_2 , Na_2O , and CaO to manufacture the glass electrode. It gives satisfactory results over the pH range 1–9 but produces an error in solutions of high alkalinity. This was called an “alkaline error,” at which the glass electrode gives too low values for the pH. The value for error varies with the alkali-metal ions in solution. Its value is greater when sodium ions are present and becomes smaller in solutions containing lithium, potassium, barium, or calcium ions. Thus, glasses with different composition were tested which should be free from alkaline errors, and better results were found if most of the sodium content was replaced by lithium.

The response mechanism as well as the basis of alkaline error can be understood from the following discussion. The inner side of a glass bulb contains a fixed concentration of HCl which leads to a constant potential of Ag/AgCl immersed in it. Thus, it is the outer side of glass bulb which governs the potential depending on the hydrogen ion concentration in the test solution. When the glass electrode is soaked in water it will form a hydrated layer on the outer surface of glass.

This hydrated layer facilitates the ion exchange process. When it is brought in contact with a solution of definite pH, then the exchange processes of ions commence. The sodium ions present in glass exchange with the hydrogen ions present in the solution by the following equilibrium:



Thus, due to the ion exchange process the conductivity of the silicate lattice changes which is related to the pH of the test solution. According to the abovementioned equilibrium, also the alkaline error can be understood. If a high concentration of sodium ions is present in the test solution then the ions will pass into the hydrated layer and provoke a lower pH indicated for the test solution.

In 1930, McInnes worked on the improvement of pH selectivity of the glass membrane, and now the presently used pH-selective glasses contain 63 % SiO₂, 28 % LiO₂, 5 % BaO, and 2 % La₂O₃. Other metal oxides are also used in order to improve the performance of the glass membrane in alkaline solutions. Another improvement of the pH meter was induced by replacing the liquid electrolyte by a gel electrolyte. This replacement was tossed by Ingold in 1986 which inhibits a loss of electrolyte into the external solution and improves the lifetime of the pH meter.

A conventional pH electrode contains a pH-sensitive glass membrane. Thus, a number of efforts were put forward in order to replace the glass membrane with other pH-sensitive materials such as metal oxides, polymers, and carbon nanotubes.

The first dielectric material that was used on open gates of field effect transistors (ion-sensitive field effect transistor, ISFET) was silicon dioxide by Bergveld⁷ in 1970. The problem in the ISFET structure is the poor insulation between the device and the solutions. The ISFET structure was improved by using ion-sensitive electrodes (ISE). With field effect transistors the gate area can be extended by using a conductive wire covered with the sensitive membrane. This new approach helps in enhancing the stability, sensitivity, and flexibility in shaping i.e., miniaturization of pH-sensitive devices.

4.3 Solid-State pH Sensors

The development of a solid-state glass electrode for the determination of pH of analyte is complicated. A number of ion-selective field effect transistors have been designed since 1970 initiated by Bergveld. The signal output of these ISFET pH sensors is still not so precise as that of glass electrodes but a number of problems have been overcome by them such as size, cost, and robustness. The principle by which the ISFET detects changes in pH is that the gate is covered with an ion-sensitive layer. As the gate is between the drain and the source of the FET, it controls the flow of the source-drain current. When this solid-state pH electrode (ISFET) is exposed to either acidic or basic solution, the ion-sensitive layer coated

on the gate will be protonated or deprotonated. Due to the interaction with the surrounding solution an electrostatic field is generated (altering the gate voltage) which controls the flow of current between drain and source and gives a current output which is interpreted as pH of the test solution. A number of materials are used to cover the gate of the FET as ion-sensitive films, such as (1) metallic layers (e.g., Pt), (2) ceramic layers (e.g., alumina, zirconia, silicon nitride, gallium nitride), (3) polymer materials (e.g., polypyrrole, polyethylene, polytetrafluoroethylene), and (4) non-polymeric organic films such as valinomycin.

4.4 Metallic Electrodes

Some metals are also sensitive to H^+ ion concentrations. Insoluble hydroxides are formed when these metals come in contact with aqueous solutions. These hydroxide-covered metallic surfaces can be used to analyze the change in pH values. The redox potential of these electrodes directly relates to the proton concentration in solution. Table 4.1 summarizes different metallic electrodes along with their redox potentials which are pH dependent.⁸

Table 4.1 pH dependent potentials of metal-metal oxide electrodes

Group	Material	Redox equilibrium $Ox + ze^- \rightleftharpoons Red$	E^0/V (pH 0)	E^0/V (pH 14)
IVa	Tin	$SnO_2 + 4H^+ + 4e^- \rightleftharpoons Sn + 2H_2O$	-0.117	-0.945
	Lead	$HPbO_2^- + H_2O + 2e^- \rightleftharpoons Pb + 3OH^-$	(-0.36)	-0.537
Va	Arsenic	$As_2O_3 + 6H^+ + 6e^- \rightleftharpoons 2As + 3H_2O$	+0.234	-0.68
	Antimony	$Sb_2O_3 + 6H^+ + 6e^- \rightleftharpoons 2Sb + 3H_2O$	+0.152	-0.639
	Bismuth	$Bi_2O_3 + 3H_2O + 6e^- \rightleftharpoons 2Bi + 6OH^-$	+0.317	-0.46*
Ib	Copper	$Cu_2O + H_2O + 2e^- \rightleftharpoons 2Cu + 2OH^-$	(+0.34)	-0.36*
	Silver	$Ag_2O + H_2O + 2e^- \rightleftharpoons 2Ag + 2OH^-$	(+0.80)	+0.342
	Gold	$H_2AuO_3^- + H_2O + 3e^- \rightleftharpoons Au + 4OH^-$	+1.50	+0.70
IIb	Zinc	$ZnO + H_2O + 2e^- \rightleftharpoons Zn + 2OH^-$	(-0.497)	(-1.260)*
	Mercury	$HgO + H_2O + 2e^- \rightleftharpoons Hg + 2OH^-$	+0.860	+0.098
Vb	Tantalum	$Ta_2O_3 + 10H^+ + 10e^- \rightleftharpoons 2Ta + 5H_2O$	-0.750	-1.578
VIb	Tungsten	$WO_2 + 4H^+ + 4e^- \rightleftharpoons W + 2H_2O$	-0.119	(-0.946)
VIIb	Rhenium	$Re_2O_3 + 6H^+ + 6e^- \rightleftharpoons 2Re + 3H_2O$	+0.227	-0.600
VIIIb	Iron	$Fe_3O_4 + 8H^+ + 8e^- \rightleftharpoons 3Fe + 4H_2O$	(-0.085)	-0.912*
	Nickel	$NiO + 2H^+ + 2e^- \rightleftharpoons Ni + H_2O$	(+0.110)	-0.717*
	Osmium	$OsO_4 + 8H^+ + 8e^- \rightleftharpoons Os + 4H_2O$	+0.838	(\approx 0.00)
	Rhodium	$RhOH^{2+} + H^+ + 3e^- \rightleftharpoons Rh + H_2O$	+0.83	\approx 0.00
	Iridium	$Ir_2O_3 + 3H_2O + 6e^- \rightleftharpoons 2Ir + 6OH^-$	+0.923	+0.098
	Platinum	$PtO_2 + 4H^+ + 4e^- \rightleftharpoons Pt + 2H_2O$	+1.0	+0.14

Metals with $E^0 < 0$ V dissolve in aqueous solution. The values which are presented in parentheses represent unstable oxides at these conditions.

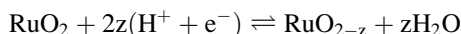
*represents those metals whose hydroxides exist in alkaline solutions

4.5 Metal Oxide Probes

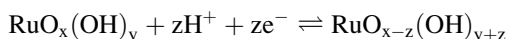
Metal oxides are also promising materials to design pH-sensitive chemical sensors. In these devices an electric charge is set up at the electrode-electrolyte interface. The change in electric charge at their interfaces is used to detect the pH of the solution. Different hydrogen-sensitive metal oxides are in use, such as cobalt oxide, zinc oxide, tin oxide, molybdenum oxide, tungsten oxide, manganese oxide, ruthenium oxide, and iridium oxide. The pH response of these metal oxides originates from their oxygen defect stoichiometry which makes them both electronic and ionic conducting materials. The mechanism of the pH sensitivity in these materials does not involve redox transitions but ion exchanges at the surface sites.

4.5.1 Ruthenium Oxide

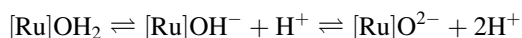
Metal oxides are promising candidate in designing pH-sensitive devices as explained by Fog and Buck.⁹ The ruthenium oxide thin film is very sensitive to hydrogen ions and can be used as a sensitive surface in H⁺-ion-selective electrodes (ISE). The film of ruthenium oxide can be deposited by different methods such as sputtering,¹⁰ pulsed-laser deposition,¹¹ sol-gel route,¹² and chemical vapor deposition.¹³ The general sensing mechanism of ruthenium oxide is reported by McMurray by considering “oxygen intercalation” which can be expressed as follows¹⁴:



Apart from the intercalation, the responsive nature of ruthenium oxide is due to ion exchange in a surface layer containing OH groups. This proton exchange mechanism was explained by Trasatti¹⁵ as follows:



The responsive behavior of ruthenium oxide is analogous to that of platinum oxides explained schematically in Fig. 4.2:



Water molecules will be adsorbed on metal oxide surfaces to compensate the oxygen defects in the lattice. Afterwards, water molecules will dissociate and the surface of ruthenium oxide is covered with hydroxide groups. When this layer is exposed to an electrolyte a Helmholtz double layer is formed at the electrode-electrolyte interface which is responsible for the electrochemical potential of the electrode attributed to the pH of the solution.

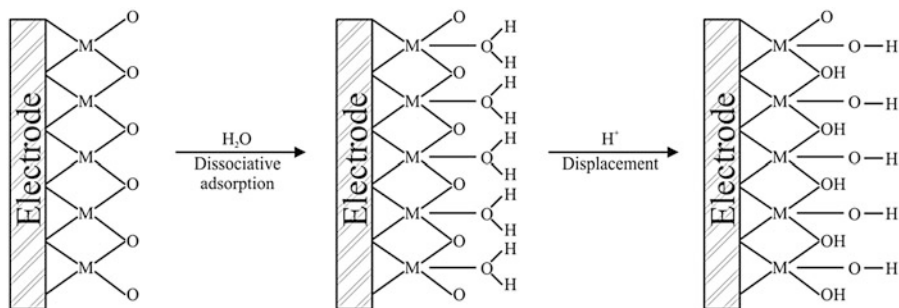


Fig. 4.2 Dissociative adsorption of water at platinum metal oxides and proton conductivity, adapted from reference [8]

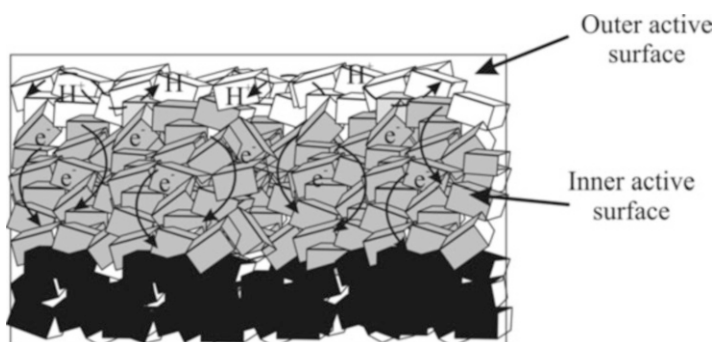


Fig. 4.3 Cu_2O -doped RuO_2 -SE showing paths of charge carriers to the Pt support (*black*), adapted from reference [16]

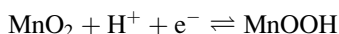
4.5.2 Cu_2O -Doped RuO_2

In order to design a pH-sensing electrode (SE) of ruthenium oxide it can be doped with other metal oxides such as copper oxide.¹⁶ Suitable doping as well as optimizing the microstructures and thickness will generate a highly sensitive electrode surface of high surface-to-volume ratio with required morphology and porosity.¹⁷ The sensing mechanism of this type of electrode is depicted in Fig. 4.3. It can be seen that the SE contains a complex of metal oxides where the surface of the electrode is separated by highly defective regions. The doping of ruthenium oxide will generate paths to transfer the charge carriers. The picture clearly shows three sections of SE electrode. The first two interfaces are greatly concerned with the performance of electrode. The outer surface is mainly in contact with the solution and interacts with the protons. The liquid also penetrates into the pores and interacts with the inner active surface which is responsible for the electronic charge transport. The third interface is the support of the oxide layer.

4.5.3 *MnO₂*

MnO₂ is a nonstoichiometric compound and exists in different crystal forms. The better electrochemical behavior and low cost make MnO₂ a promising candidate to be used in dry and alkaline batteries.¹⁸ The redox properties of MnO₂ are attributed to its crystal structure which facilitates the diffusion of hydrogen ions and electrons into its lattice.¹⁹ Moreover, the surface of manganese oxide exhibits ion-exchange characteristics when hydroxidized.²⁰ These properties make MnO₂ an interesting candidate as a pH-sensitive electrode material.

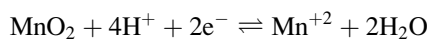
The potentiometric sensor for measuring pH was fabricated by using manganese dioxide as sensitive layer.²¹ The MnO₂/MnOOH redox system is pH dependent. When it is exposed to either acidic or basic solutions, MnO₂/MnOOH redox equilibrium is established. The sensing mechanism of sensitive surface is given by



In alkaline medium, manganese oxyhydroxide is a stable species and the abovementioned sensing mechanism holds. However, in acidic medium MnOOH is not stable and a disproportionation reaction occurs where Mn⁺² ions are formed:



Thus, in acidic medium, a MnO₂/Mn⁺² redox equilibrium is established which is represented by the following equation:



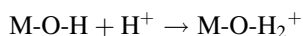
The two electrochemical systems are established by similar metal oxide-sensitive layer. One operates in basic medium and the other in acidic medium.

Such a behavior of MnO₂ is not very suitable for measuring the pH because a good Nernst response cannot be achieved. In order to solve this problem the sensitive surface of the metal oxide is covered with a Nafion membrane which protects the surface from complex matrices. In the presence of Nafion, a perfect MnO₂/Mn²⁺ redox system is present because Nafion is a superacid (from which Nafion membrane is synthesized). In basic media, only the MnO₂/MnOOH redox couple will exist but in the presence of Nafion (superacid-acidic media) Mn²⁺ ions will be produced due to disproportionation of MnOOH which leads to the formation of the MnO₂/Mn²⁺ redox couple for pH sensing.

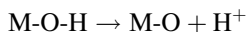
4.5.4 *Titanates*

Lithium lanthanum titanates, also called LLTO, are sensitive to pH of the aqueous solutions.²² These perovskite ceramics show pH-sensitive properties if sintered at optimum temperature.²³ The pH sensitivity of these ceramics (LLTO) depends on

their surface properties.²⁴ The pH-sensitive surfaces show a number of hydrophilic characteristics which are attributed to the presence of hydroxyl (OH) groups on the perovskite ceramic surfaces. The LLTO behave as ionic conductive ceramics and represent a promising sensitive element in potentiometric devices.²⁵ These ceramic conductors allow the exchange of ions between analyte solution and ceramic oxide. The sensitive behavior of these ceramics originates by enhancing their acido-basic surface characters by heat treatment. The ceramic surfaces contain basic hydroxyl (OH) groups which can be converted to active hydroxyl groups by proper heat treatment.²⁶ These active hydroxyl groups show higher electronegativity than non-active hydroxyl groups and become sensitive to protons present in aqueous solution. The higher hydrophilic properties of ceramic surfaces are attributed to these active hydroxyl groups. An array of hydroxyl groups is developed on oxide ceramics by immersing them in aqueous solution. These hydroxyl groups are attached to cations which show an amphoteric character to which the pH sensitivity of these ceramics is attributed. The sensitive behavior of the surfaces can be explained by the following mechanism as the hydroxyl groups interact with protons while exposed to acidic solutions:



and in alkaline medium they behave as follows:



The hydrophilic character of the LLTO surface is dependent on the presence of hydroxyl groups. These hydroxyl groups on the surface are formed by the adsorption or dissociation of water molecules on the LLTO ceramics.²⁷ The oxide ceramic is able to adsorb water molecules while at high temperature a defective surface is formed which helps in dissociation of water molecules. When LLTO oxide ceramics are exposed to an aqueous solution they first adsorb water molecules. Afterwards, at high temperature, water is decomposed on the surface. The hydroxyl groups which come from water decomposition will attach to the metal cations present on the surface. The remaining H groups from decomposed water will link to oxygen atoms, adjacent to the metal cations of the surface. The electronegativity and basic character of hydroxyl groups are attributed to the covalency of the (O-H) group. It also depends on the oxygen coordination.²⁸ In LLTO ceramic structures, an O atom present in the bulk of the material is more coordinated to the metal cations in comparison to an O atom present on the material surface. Thus surface oxygen atoms have a basic character.

Figure 4.4 explains the formation of different hydroxyl groups with different basic character depending on the O coordination. The hydroxyl group whose oxygen is attached to one metal cation and is di-coordinated exhibits a more basic character, whereas the O atom of a hydroxyl group which belongs to the LLTO lattice and is multi-coordinated is less basic than the former one. Due to different surrounding environments, five different -OH groups are present on the surface of ceramics as shown in Fig. 4.5.²⁹

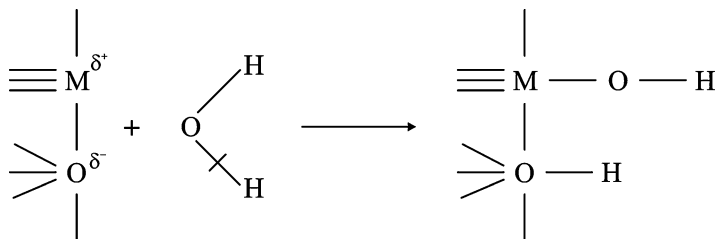


Fig. 4.4 The presence of different hydroxyl groups on metal oxide surfaces, adapted from reference [22]

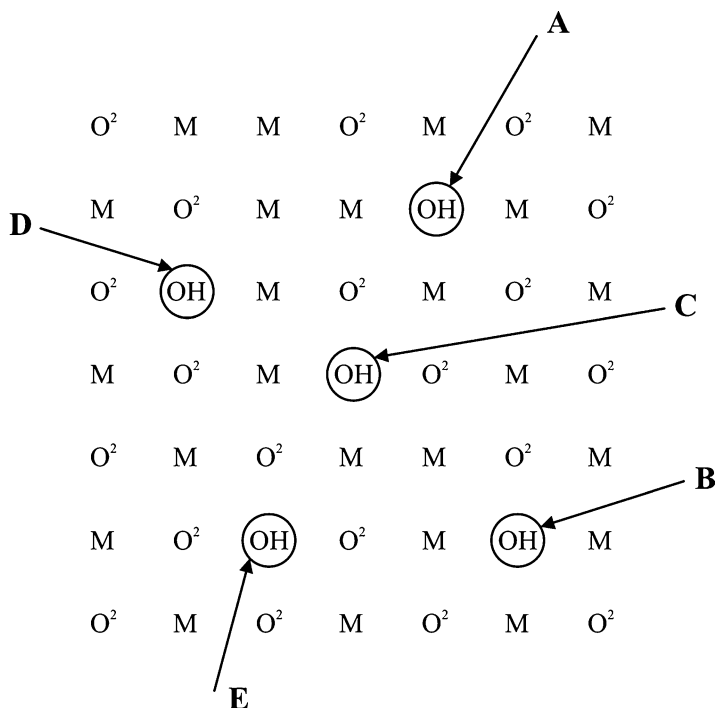


Fig. 4.5 The hydroxyl groups on an oxide surface exhibit different acido-basic character depending on surrounding ions. From A to E, the sites become more basic and less acidic. “M” denotes metal ions on the layer below the surface, adapted from reference [22]

Ti was also used as a dopant in different materials such as Gd_2O_3 (as Gd_2TiO_5) in order to develop a pH-sensing membrane for ISFETs.³⁰ This doping improves the crystalline structure of materials which results in fabricating a highly sensitive, selective, and a low drift pH-sensing system.

4.5.5 *Titania Nanotubes*

The surface morphology, crystal structure, and hydrophilicity of titania nanotubes make them a promising candidate to design a pH-sensitive device.³¹ Moreover, amorphous titania nanotubes show better pH response in comparison to anatase titania nanotubes. Nanotubes have larger surface areas than thin films. The electrode covered with titania nanotubes shows greater roughness and comes up with enhanced interaction sites. This phenomenon explains the profound sensitivity of an amorphous titania nanotube-modified electrode. The hydrophilic properties of titania are induced by UV illumination. UV light will create a large concentration of Ti^{+3} or oxygen vacancies on the rough surfaces of titanium.³² These modifications will make titania favorable to adsorb hydroxyls from water or air. In this way the titania-sensitive surface will be more susceptible to diffusion of H^+ ions into its lattice which explains its response mechanism. Thus, the sensitivity and reversibility of titania nanotubes are greatly enhanced by UV illumination which introduces surface hydroxyl groups and increases its hydrophilic behavior. The hydrophilic character of the surface will change to hydrophobic by interacting with oxygen; this will change the oxidation character from +3 to +4.³³

4.5.6 *Zinc Oxide*

ZnO was also employed to develop a pH sensor by structuring it in the form of nanorods and nanotubes.³⁴ These materials are very sensitive to the pH of the solution with good reproducibility and stability.³⁵ Nanotubes exhibit higher sensitivity in comparison to nanorods. The higher response of nanotube towards pH of electrolyte solution is attributed to the increased effective surface area whereas the surface-to-volume ratio of nanorods is a bit less than of nanotubes. The electrochemical potential of a pH sensor depends on the number of active sites which will generate the pH-dependent signal. The ZnO nanotubes take lead on nanorods because of the high density of oxygen vacancies as active sites due to a greater surface area. The response mechanism of ZnO as ion-sensitive material is explained that the active sites interact with H^+ ions present in an electrolyte solution to generate a surface potential which corresponds to the pH of the desired electrolyte. Actually a Helmholtz layer is formed when the ZnO material is brought in contact with an electrolyte solution. The interaction between electrolyte-nanotubes or electrolyte-nanorods leads to the establishment of the Helmholtz layer. This interaction originates from the adsorption of electrolyte ions or dipoles on the metal oxide surface. Moreover, ZnO is an amphoteric oxide due to which it shows both acidic and basic properties and can interact with either of them. To create a pH response, the Zn atoms in the amphoteric oxide must be electropositive to induce enough negative charge on oxygen to strip H^+ ions from H_3O^+ . However, when the

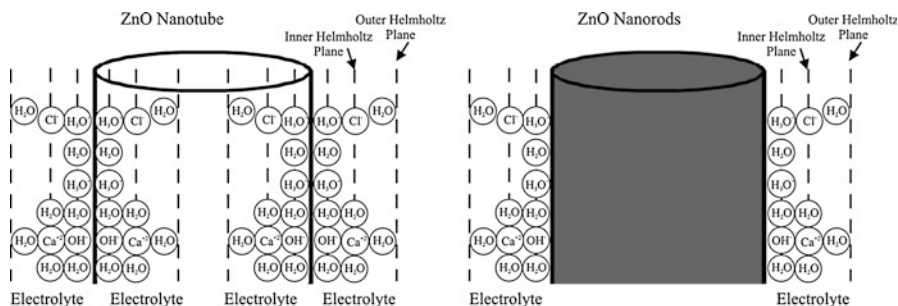
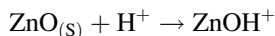


Fig. 4.6 Comparison of the response mechanism of ZnO nanorods and nanotubes, adapted from reference [34]

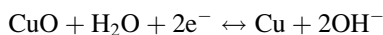
amphoteric oxide comes in contact with hydroxyl ions (OH^-) then metal atoms must be sufficiently electronegative to accept an electron from OH^- ions present in solution, i.e.,



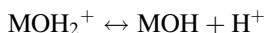
The ZnO nanotubes are more responsive as pH-sensitive materials in comparison to ZnO nanorods. The enhanced sensitivity of nanotubes is explained by its higher surface-to-volume ratio due to its hollow structure.³⁶ Thus, in nanotubes a large effective surface area is exposed to interact with the ions of analyte solution. Figure 4.6 shows the responsive nature of both structures of ZnO while immersed in a CaCl_2 electrolyte. This picture shows the charge distribution at ZnO nanotubes and nanorods.

4.5.7 CuO

CuO materials exhibit pH-sensitive sites which generate an electrochemical response when exposed to the analyte solution. This metal oxide may be structured as nano-flower shape which enhances its sensitivity and reproducibility, and shortens the response time.³⁷ The response mechanism of CuO can be described by the following reaction:



The sensing mechanism of metal oxides is dependent on their surface chemistries. These surface morphologies control the potential of the sensing electrode. The active sites originate from the protonation-deprotonation of water molecules attached to the metal (M) ions:

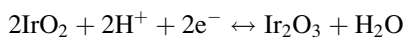
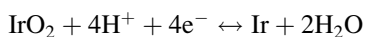
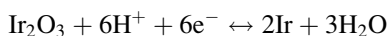


The MOH species which is present on the surface of the metal oxide is amphoteric in nature and has a tendency to attract both acidic and basic species. These active groups interact with either OH^- or H^+ groups of the analyte solution. These surface interactions lead to a protonation or deprotonation of the MOH groups and develop a surface charge which is equal to the pH of the analyte solution. The ion-sensitive CuO film thus contains surface sites which can specifically interact with H^+ ions (hydrogenate) after interaction with an electrolyte solution. The CuO surface charge and surface potential depend on the protonation or deprotonation of these sites which is equal to the pH of electrolyte solution.

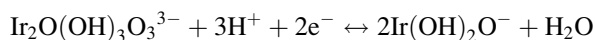
Copper oxide (CuO) nanowires also form a pH-sensitive material.³⁸ The sensitivity of this metal oxide nanowires is ascribed to their enhanced surface-to-volume ratio.

4.5.8 Iridium Oxide

Iridium oxide thin films coated on the working electrode serve as pH-sensitive material.³⁹ Iridium is covered with adsorbed oxygen atoms. This oxide is prepared by either anodic oxidation or heating the metal in an oxygen atmosphere. The developed metal oxide exhibits improved redox properties involving hydrogen ions. The pH response of the iridium oxide electrode is attributed to Ir(IV)/Ir(III) redox transitions due to the release or uptake of protons. This metal oxide-coated electrode in combination with a reference electrode will provide an electrochemical signal which is related to the pH of the solution. The possible mechanisms by which iridium oxide generates an electric potential when it comes in contact with a solution of definite pH are expressed by the following equations:



These redox reactions exhibit the two oxidation states of iridium oxide by which it is able to create an electrochemical potential as a pH sensor being similar to the conventional glass electrode. If there is any variation in the stoichiometry of the metal oxide then its pH response behavior will also be changed. If the metal oxide contains hydroxyl (OH^-) groups at its surface the pH response will also be generated due to ion exchange:



Iridium oxide films (IROF) were also fabricated on silicon-based thin-film platinum microelectrodes. These electrodes can also measure the pH of the test solution with high sensitivity by intercalating the protons into their structure.⁴⁰

4.6 Nano-Structured Material-Based pH Sensors

4.6.1 Silicon Nanowires

Silicon nanowires (SiNW) are also promising candidates in order to fabricate a pH sensor with good stability, and sensitivity. The device was developed on the principle of a field effect transistor (FET).⁴¹ Si is doped with boron to make it a p-type material. The SiNW were further covered with a silicon nitride passivation layer to insulate the nanowires. This insulating layer also behaves as ion blocker. The detection principle is sketched in Fig. 4.7. The charge carriers in the SiNW are holes, and a sufficient number of holes is present if the pH of the solution is neutral. If the SiNW is exposed to acidic solutions the Fermi level difference between the holes or mobile carriers and outer charges induces a downward bending of the flatband energy.⁴² Thus, depletion of mobile carriers is produced near the surface. This happens due to the protonation of the outer surface of SiNW because the concentration of H^+ ions is very high at lower pH, whereas a higher pH causes the deprotonation of the SiNW surface which provokes the accumulation of mobile charge carriers due to the upward bending of energy bands.

In the pH-sensitive device, the introduction of a SiN insulating layer on the nanowires decreases the diffusion of H^+ ions from the fluid to the sensitive wires. The insulation of the sensitive surface is carried out to increase the stability and repeatability of the pH sensor. The passivation layer not only separates the surface charge from mobile charge carriers of the p-type SiNW but also is responsive to the solution pH to induce a depletion or accumulation of mobile charge carriers.

4.6.2 Silica Nanoparticles

Silica nanoparticles enhance the electrochemical sensitivity as well as linearize the pH behavior of semiconducting nanomaterial thin-film devices.⁴³ These devices may be either a resistor or ion-sensitive field-effect transistor (ISFET).

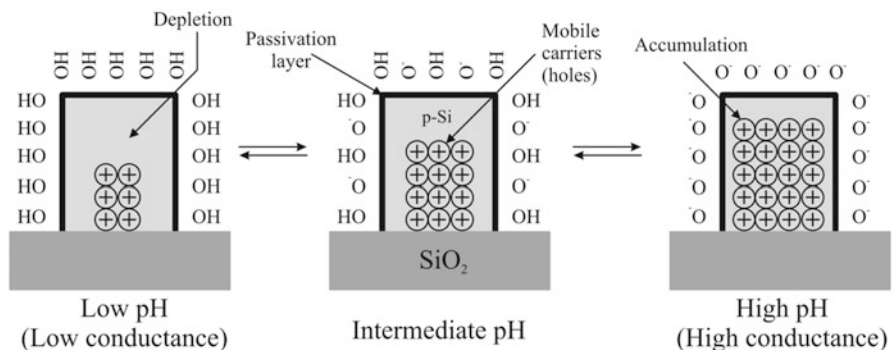
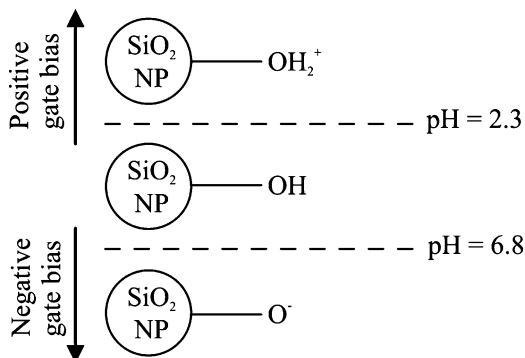


Fig. 4.7 Principle of pH detection with SiNW, adapted from reference [41]

Fig. 4.8 Scheme of pH-responsive surface functional groups in SiO_2 NPs, adopted from reference [43]



Silica nanoparticles contain surface hydroxyl groups which can be protonated or deprotonated corresponding to the pH of the solution. Thus, silica nanoparticles act as a charge collector as shown in Fig. 4.8. At low pH the charge will shift towards positive due to protonation and vice versa at high pH. In acidic medium, the OH or O^- species are protonated whereas a basic environment causes the deprotonation of OH_2^+ or OH groups. Thus, the protonation of OH or O^- species induces a positive shift in the pH gating voltage which leads to a decrease in conductance of the underlying semiconductor material (SWCNTs). However, deprotonation causes a negative shift and thereby increases the conductance. At low pH, the doping of holes in the semiconductor material results in an increase of the conductance but the conductance decreases due to positive biasing induced by the silica nanoparticles. In this way, the surface layer of silica nanoparticles on top of functional nanomaterials linearizes the signal output as well as modulates the sensitivity which increases at low pH. In SWCNT resistors, the surface-coated silica nanoparticles increase the resistance by adsorption and thus linearize the pH sensitivity due to a positive shift in the gating voltage of the p-type semiconductor.

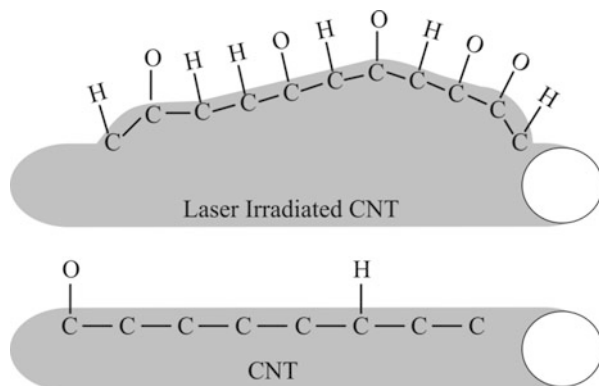
4.6.3 SnO_2 Nanorods

SnO_2 is also utilized as a sensitive surface to fabricate a pH sensor device by using extended-gate field-effect transistors (EGFET).⁴⁴ SnO_2 is employed in the form of nanorods which show better sensitivity attributed to a high surface-to-volume ratio. These nanorods have a high effective sensing area meaning a high number of interaction sites for the ions present in solution.

4.6.4 Carbon Nanotubes as Sensitive Coatings

Carbon nanotubes (CNTs) are very sensitive to different analytes which makes them a very promising candidate in fabricating a pH-sensitive device. The electrical

Fig. 4.9 CNT network sensing mechanism: non-irradiated CNT network (*below*) and laser-irradiated CNT network (*above*), adapted from reference [46]



properties of CNTs attached to sensitive electrodes depend on the pH of the analyte solution.⁴⁵ When the OH groups come in contact with CNTs the energy gap is greatly reduced which in turn enhances the conductivity of CNTs. The concentration of OH groups can be calculated from the pH value of the solution. Thus, an increase or decrease in conductivity of CNTs is dependent on the OH concentration and in this way the pH value of a solution can be determined.

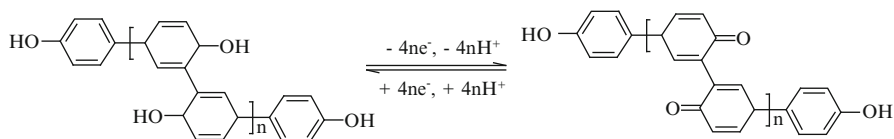
The sensitivity of carbon nanotubes (CNTs) was further enhanced by irradiating them with a laser.⁴⁶ The laser energy improves the electrical and sensing properties of carbon tubes by modifying their walls into a number of graphite layers.

The irradiation of MWCNT with laser results in expanding the CNT layer as well as broadening the conducting pathways as shown in Fig. 4.9. Thus, the overall electrical behavior and the surface area of CNTs are greatly enhanced. The energy of laser irradiation would convert the CNT network into a number of graphite layers and dangling bonds at the edges of these graphite layers are converted to carbonyl functional groups and C–H bonds. These are the sensing sites by which the modified CNTs interact with hydronium or hydroxyl ions in solution. The C–O bond will adsorb H^+ ions (acidic solution) whereas, in an alkaline environment, C–H bonds will interact with OH^- groups and will change the sensing surface potential. Thus, the laser-irradiated CNTs show profound sensing properties which are attributed to increases in conductance as well as uniform interaction sites for ion bonding.

4.7 Polymer-Based pH Sensors

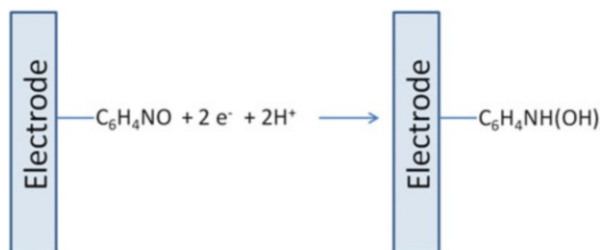
Some polymer materials which exhibit reversible redox activities respond to the pH of the test solution. Bisphenol-A polymer containing benzoquinonyl and hydroquinonyl groups not only shows electrochemical activities but also demonstrates a change in its conductance when changing the pH of the surrounding media. The conductance of polybisphenol-A (PBPA) is attributed to both ionic and

electronic behavior of the polymer.⁴⁷ When comparing a commercial glass electrode with a PBPA electrode, both show a wide response range but the PBPA-based electrodes are very easy to produce, cheaper, and much more stable and selective. The mechanism of the redox reaction of PBPA films is explained by the following equation. The redox reaction reveals the involvement of H^+ ions in order to produce an output signal which corresponds to the pH of the solution.⁴⁸



The PBPA electrodes possess an H^+ ion-sensitive surface, and the conductivity of the film depends on the degree of protonation or deprotonation as a function of pH.⁴⁹ This electrochemical mechanism of PBPA films when interacting with protons of the solution is analogous to the quinone/hydroquinone redox system.⁵⁰

The pH-dependent redox potential of surface-bound nitrosophenyl groups was exploited to construct a pH electrode. A screen-printed electrode was modified with nitrosophenyl groups which lead to a highly sensitive pH sensor for a wide range of pH values. The mechanism of nitrosophenyl reduction can be explained by the following reaction, which is responsible for the sensitivity to the pH of the test solution⁵¹:

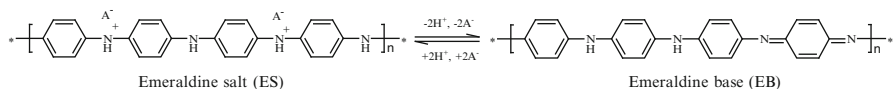


The surface-bound nitrosophenyl group is reversibly reduced to the hydroxylaminephenyl group involving two electrons and two protons. A redox system of nitrosophenyl/hydroxylaminephenyl couples will be established which is very sensitive to pH.

Polyaniline (PANI) was also utilized to develop a conductometric pH sensor.⁵² The response mechanism of the polymer film originates from the deprotonation of the polymer backbone nitrogen atoms when exposed to aqueous environments. In acidic solution, emeraldine polyaniline exists in the form of a salt (ES), and in alkaline solution it is converted to the base form (EB). The function of the sensor depends on the change in different forms of polyaniline which arises due to the deprotonation of nitrogen atoms.⁵³ Thus, the conductivity of the sensitive layer is changed when PANI interacts with the hydronium or hydroxyl ions present in the solution. PANI is an amorphous film, and the electrolyte penetrates into the film and interacts with individual particles of the polymer. The charge carriers can pass

easily through the salt form of PANI because particles are in close contact with each other. In alkaline solution, the base form of PANI becomes insulating which reduces the conduction path. Thus, the sensitivity of the polyaniline polymer is greatly reduced when it changes its form from salt to base.⁵⁴

Polyaniline is also employed to develop an electrochemical measuring system to analyze the pH of a solution amperometrically. The measurement principle of the sensor is again dependent on the transition of PANI from ES-EB as explained by the following equation and corresponding potential variations are recorded.



Poly(propylene imine) dendrimer (PPID) multilayered with nickel tetrasulfonated phthalocyanine (NiTsPc) was also employed as sensitive membranes in extended-gate field-effect transistor pH sensors.⁵⁵ These porous membranes were fabricated on different substrates such as quartz, glass, indium tin oxide (ITO), or gold-covered glass. The nanostructured membranes on ITO showed better sensitivity in comparison to other substrates.

4.8 Graphene-Based pH Sensor

The unique quantum properties of graphene⁵⁶ and the two-dimensional character of the carbon-based platform make it a valuable candidate to design ultrafast electronics.⁵⁷ Moreover, simple fabrication of graphene as well as its miniaturized size lead to design sensor devices for micro/nano applications. Graphene shows ambipolar characteristics and is very sensitive to both hydroxyl (OH^-) and hydronium ions (H_3O^+).⁵⁸ These properties of graphene make it possible to modulate the channel conductance of a field-effect transistor (FET) by doping “holes” or “electrons” when in contact with acidic or basic solutions. When graphene is exposed to an electrolyte solution then an electrochemical double layer is established at the graphene/electrolyte interface as shown in Fig. 4.10. The electrochemical double layer is formed at the graphene/solution interface which is attributed to its ambipolar character by which graphene attracts charged species, e.g., hydronium or hydroxyl ions. The formation of the Helmholtz layer involves capacitive charging of the sensitive surface when in contact with H_3O^+ or OH^- because graphene is ambipolar and contains both “holes” and “electrons.” When the graphene layer is exposed to an acid, the adsorbed ions are primarily hydronium ions (H_3O^+) whereas in alkaline medium, hydroxyl ions (OH^-) are adsorbed on the graphene surface. The adsorption of ions is purely capacitive which means that the positive or negative charges do not permeate across the graphene/electrolyte interface. An electrochemical double layer is formed at the graphene/solution interface because the graphene film behaves as n-doped material when in contact with hydronium ions and as p-doped while exposed to hydroxyl ions.⁵⁹

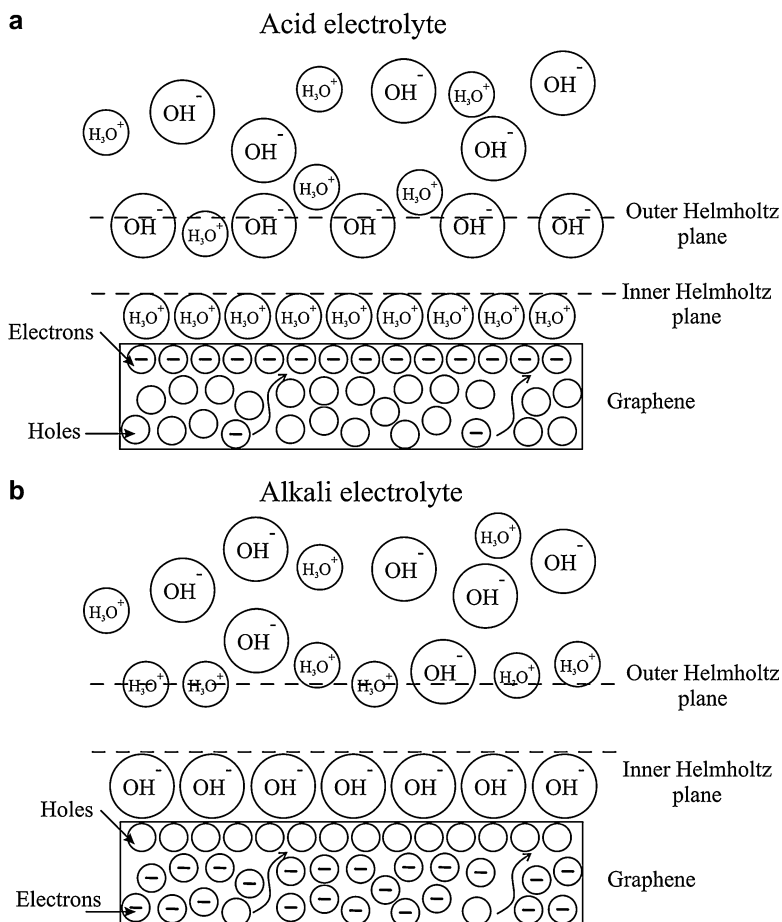


Fig. 4.10 (a) H_3O^+ from an acidic electrolyte attached to the inner Helmholtz plane, which attracts graphene “electrons”; (b) OH^- from an alkaline electrolyte attached to the inner Helmholtz plane, which attracts graphene “holes” as countercharges, adapted from reference [59]

4.9 Miniaturized pH Sensors

4.9.1 Antimony Nanowires for pH Sensors

The precise and accurate pH value detection is of great interest in a large number of fields such as biological research, clinical diagnostics, electrochemistry, and industry. To measure the pH, a number of devices or methods are available which are bulky in nature like glass bulb electrodes or field-effect transistors. The large size of these pH-measuring devices makes them unsuitable in invasive diagnostics and intervention in medicine, e.g., analyzing the pH of blood, wound, and gastric

fluids. Thus miniaturized pH sensors are the only devices which are appropriate for these kinds of tasks.

One approach that was used to miniaturize pH devices was focused on metallic pH-sensitive electrodes. Antimony was considered as an electrode material for pH measurement because of its high sensitivity, robustness, and, most importantly, its biocompatibility.^{60,61} In some respect, the use of Sb as electrode material is of great advantage in comparison to glass under certain circumstances, such as measuring the proton concentration of HF-containing solutions. A Sb metallic electrode can withstand an HF environment where the glass electrode cannot be employed. Sb was used in the form of nanostructures in order to increase its sensitive nature towards proton determination. Antimony was shaped in the form of nanowires (NW) to form a microscale pH electrode.

Sb can be shaped into NW by a number of approaches, e.g., pulsed electrodeposition,⁶² patterning of nanoparticles,⁶³ microwave-induced formation,⁶⁴ and by using focused ion beams (FIB).⁶⁵ For developing nanowires of Sb for pH measurements, the FIB technology was used. The material was exposed to a Ga^+ ion beam under high vacuum at room temperature. This procedure led to the formation of tangled Sb rods which formed a porous network of NW.

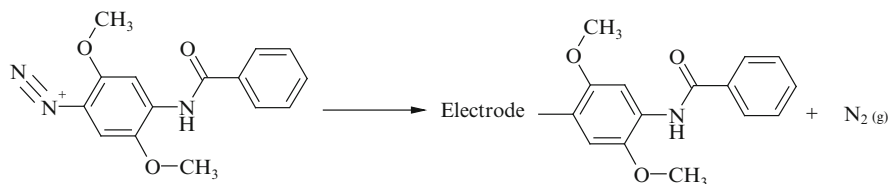
For the construction of the miniaturized pH device, the complementary metal oxide semiconductor (CMOS) approach was utilized. The Si substrate (p-doped) with a CMOS material was covered with a Sb film.⁶⁶ This layer was converted to NW by exposing it to the ion beam. An Ag pad atop of the oxide was also deposited which was afterwards converted to a Ag/AgCl reference electrode by applying a ferric chloride solution. Thus, the final microscale pH sensor contained Sb-NWs as the working electrode and Ag/AgCl as the reference electrode. These electrodes were separated by a SiO_2 insulation layer and could measure the electromotive force developed between these two electrodes while exposing them to an analyte solution.

4.9.2 Carbon Fiber Microelectrode

Another miniaturized pH-measuring device was manufactured by modifying a carbon-fiber electrode to develop a reagentless sensor system to measure *in vivo* pH values. Carbon-based electrodes are ideal candidates to fabricate such devices due to their biocompatibility. In addition, carbon-fiber electrodes are conductive and their surface can easily be modified as desired, in this case by ion-selective materials. A number of methods are available for tethering the ion-selective molecules such as acidic oxidation in combination with plasma treatment,⁶⁷ physical adsorption,⁶⁸ and covalent bonding of amines via oxidation⁶⁹ or bonding of diazonium groups via reduction.⁷⁰

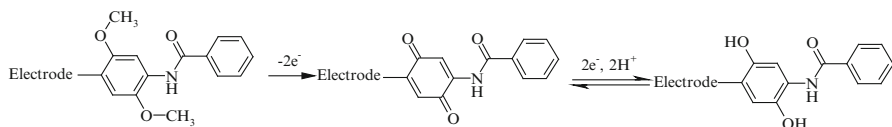
A microelectrode was designed to measure the real-time pH changes in physiological environments, even small pH changes in the central nervous system (CNS) of a micro-analytical model organism, *Drosophila melanogaster*.⁷¹

The miniaturized pH-sensing device was manufactured by modification of the carbon microfiber surface with a diazonium salt of Fast Blue RR (FBRR) via electrochemical cycling. The mechanism by which the diazonium salt was attached to the carbon surface is given by following scheme. Radicals of the diazonium salt are formed electrochemically by reduction and afterwards, they are covalently attached to the carbon-fiber electrode by evolution of nitrogen.



Catecholamines and indolamines are present in the central nervous system and different physiological and behavioral functions of the brain are based on these chemical messengers. These species are actively involved in the neurotransmission processes of the CNS. Neurosecretion is associated with the metabolic activities which occur in the brain. These metabolic processes stimulate pH fluctuations in the CNS. Thus, secretion of neurotransmitters is accompanied with endogenous species such as protons or ascorbate ions which alter the behavior of redox-active chemical messengers, e.g., catecholamines and indolamines.⁷²

The recognition sites of the modified carbon microelectrode were used to detect these electrochemically active compounds which are associated with pH fluctuations. Fast Blue RR (FBRR) contains a hydroquinoid structure. The fabricated probe was able to measure the redox activity of p-quinone to detect the real-time pH values in biological microenvironments associated with the physiological changes.⁷³ A number of other quinone-based compounds are available which can respond to pH fluctuations but all these compounds are not biocompatible and efficient to detect pH changes in biological environments.



Thus, the diazonium salt of FBRR is an attractive quinone-based material which possesses all the characteristics which make it fit for the design of a miniaturized pH device for the detection of small pH changes that occur in a fly brain. The proposed mechanism of quinone-based pH-sensitive compounds is given in the scheme above. This process exhibits that this compound is oxidized to a p-quinone analogue from the p-methoxy compound which involves two electrons. This quinone then converts to the hydroxy derivative of the molecule by chemical reduction involving a two-electron/two-proton system. This scheme indicates the involvement of outer-sphere electron transfer of FBRR by which in vivo dynamic pH

fluctuations of nerve tissue can be monitored. The real-time measurements were conducted by inserting the carbon-fiber-modified microelectrode into the brain of an adult fly by microsurgery. The flies are sensitive to blue light which stimulates the dopamine neurosecretion accompanied with pH fluctuations in the CNS due to the release of neurotransmitters. The modified carbon surface with FBRR material yielded a very efficient measuring device for the real-time detection of pH fluctuations in a physiological environment.

4.10 Tattoo-Based Ion-Selective Electrode

An innovation in miniaturized pH-measuring systems is the fabrication of ion-selective electrodes on tattoo paper.⁷⁴ A tattoo paper can easily be applied on the skin to direct epidermal pH monitoring and the textile geometry of the designed sensor makes it capable to withstand against repeated mechanical stress. The sensor should bear this stress and produce good results according to the wearer's routine. Carbon fibers were embedded in the tattoo structure to achieve robustness of the tattoo-based sensor by which it could withstand against mechanical stress while working as a potentiometric sensor. These fibers induced the elasticity in the structure as well as increased the tensile strength. The tattoo-based potentiometric pH sensor was developed by combining a polymer-based ion-selective electrode with commercially available tattoo paper.⁷⁵ The tattoo was shaped in the form of "smiley face" consisting of one eye as pH-sensitive polyaniline electrode whereas the second eye served as reference electrode. Polyaniline (PANi) was used as a pH-sensitive polymer based on its emeraldine salt (ES)/emeraldine base (EB) electrochemical active system.⁷⁶ The redox system switches between these forms while being exposed to acidic or basic environments. Apart from its pH sensitivity, PANi was selected on the basis of its other characteristics such as its biocompatibility, minimal cytotoxicity, and easily synthesizable thin films. These characteristics were key features in developing a pH-sensitive device for measuring epidermal pH. Moreover, the insertion of carbon fibers made this device to perform efficiently under practical scenarios. The pH values of human perspiration alter under different respiration conditions. Thus, ion-selective polyaniline-based electrodes which were combined with tattoo paper were capable to detect the pH fluctuations in human perspiration during complex body motions such as fitness and athletic routines.

4.11 Textile-Based pH Sensor

The recovery process of a wound is an important issue in point-of-care treatment. The proper healing of wounds depends on its assessment. The pH of a wound is one of the various physiological parameters to assess the healing process of wounds.⁷⁷

An inflammation can alter wound exudate properties and also change the pH along with other physiological parameters. There is a direct relationship between wound pH and its healing process. If the wound is not properly treated then complications may arise such as infections of the wound which can cause the pathogens to penetrate into the body and even into the bloodstream. In order to avoid these complications, a miniaturized sensor device is needed to monitor the healing process continuously. Along with other properties the miniaturized pH sensor should be biocompatible. Thus, a textile-based pH-measuring device was fabricated which showed high integration, flexibility, and stability, and had a simple readout system.⁷⁸ These features were embedded in the device by shaping the electrodes in the form of a thread. The electrodes were adjusted in such a way that lateral movement was ceased which made it a highly stable sensor setup. This device was used to measure the impedance between the electrodes. The electrodes were insulated by a hydrogel which also acted as a pH-sensitive layer. The hydrogel was synthesized by poly(vinyl alcohol)/poly(acrylic acid) (PVA/PAA) which exhibited very sensitive pH-dependent swelling behavior.

The pH of the wound was determined by measuring the impedance of the sensor. This impedance was directly related to the distance between electrodes which depended on the swelling behavior of the hydrogel. The latter was directly related to the pH of the test solution which in turn changed the impedance of the sensor. The biggest advantage of this pH-sensitive fiber was its integratability into wound dressings by applying a simple textile procedure.⁷⁹ These features make this sensor a perfect candidate which meets all the requirements for monitoring wound pH in real time.

References

1. Nørby JG (2000) The origin and the meaning of the little p in pH. *Trends Biochem Sci* 25(1):36–37, [http://dx.doi.org/10.1016/S0968-0004\(99\)01517-0](http://dx.doi.org/10.1016/S0968-0004(99)01517-0)
2. Shao Q, R-h Q, M-w S, Zhou Q, Ma DDD, Lee S-T (2011) Shape controlled flower-like silicon oxide nanowires and their pH response. *Appl Surf Sci* 257(13):5559–5562, <http://dx.doi.org/10.1016/j.apsusc.2011.01.038>
3. Fang X, Zhai T, Gautam UK, Li L, Wu L, Bando Y, Golberg D (2011) ZnS nanostructures: from synthesis to applications. *Prog Mater Sci* 56(2):175–287, <http://dx.doi.org/10.1016/j.pmatsci.2010.10.001>
4. Cremer M (1906) Über die Ursache der elektromotorischen Eigenschaften der Gewebe, zugleich ein Beitrag zur Lehre von den polyphasischen Elektrolytketten. *Z Biol* 47:562–608
5. Haber F, Klemensiewicz Z (1909) Ueber elektrische Phasengrenzkraft. *Z Phys Chem* 67:385–431
6. Eftekhari A (2003) pH sensor based on deposited film of lead oxide on aluminum substrate electrode. *Sensors Actuators B Chem* 88(3):234–238, [http://dx.doi.org/10.1016/S0925-4005\(02\)00321-0](http://dx.doi.org/10.1016/S0925-4005(02)00321-0)
7. Bergveld P (1970) Development of an Ion-sensitive solid-state device for neurophysiological measurements. *IEEE Trans Biomed Eng BME-17*(1):70–71. doi:10.1109/tbme.1970.4502688
8. Kurzweil P (2009) Metal oxides and Ion-exchanging surfaces as pH sensors in liquids: state-of-the-art and outlook. *Sensors* 9(6):4955–4985

9. Fog A, Buck RP (1984) Electronic semiconducting oxide as pH sensors. *Sensors Actuators* 5(2):137–146
10. Jevtić MM, Jelenković EV, Tong KY, Pang GKH (2006) Noise and structural properties of reactively sputtered RuO₂ thin films. *Thin Solid Films* 496(2):214–220, <http://dx.doi.org/10.1016/j.tsf.2005.08.265>
11. Hiratani M, Matsui Y, Imagawa K, Kimura S (2000) Growth of RuO₂ thin films by pulsed-laser deposition. *Thin Solid Films* 366(1–2):102–106, [http://dx.doi.org/10.1016/S0040-6090\(99\)01111-6](http://dx.doi.org/10.1016/S0040-6090(99)01111-6)
12. Armelao L, Barreca D, Moraru B (2003) A molecular approach to RuO₂-based thin films: sol-gel synthesis and characterisation. *J Non-Cryst Solids* 316(2–3):364–371, [http://dx.doi.org/10.1016/S0022-3093\(02\)01636-8](http://dx.doi.org/10.1016/S0022-3093(02)01636-8)
13. Lee D-J, Kang S-W, Rhee S-W (2002) Chemical vapor deposition of ruthenium oxide thin films from Ru(tmhd)₃ using direct liquid injection. *Thin Solid Films* 413(1–2):237–242, [http://dx.doi.org/10.1016/S0040-6090\(02\)00439-X](http://dx.doi.org/10.1016/S0040-6090(02)00439-X)
14. McMurray HN, Douglas P, Abbot D (1995) Novel thick-film pH sensors based on ruthenium dioxide-glass composites. *Sensors Actuators B Chem* 28(1):9–15, [http://dx.doi.org/10.1016/0925-4005\(94\)01536-Q](http://dx.doi.org/10.1016/0925-4005(94)01536-Q)
15. Trasatti S (1991) Physical electrochemistry of ceramic oxides. *Electrochim Acta* 36(2):225–241
16. Zhuykov S, Kats E, Kalantar-zadeh K, Breedon M, Miura N (2012) Influence of thickness of sub-micron Cu₂O-doped RuO₂ electrode on sensing performance of planar electrochemical pH sensors. *Mater Lett* 75:165–168, <http://dx.doi.org/10.1016/j.matlet.2012.01.107>
17. Zhuykov S, Kats E, Marney D, Kalantar-Zadeh K (2011) Improved antifouling resistance of electrochemical water quality sensors based on Cu₂O-doped RuO₂ sensing electrode. *Progress Organic Coatings* 70(1):67–73, <http://dx.doi.org/10.1016/j.porgcoat.2010.10.003>
18. Desai BD, Fernandes JB, Dalal VNK (1985) Manganese dioxide—a review of a battery chemical Part II. Solid state and electrochemical properties of manganese dioxides. *J Power Sources* 16(1):1–43, [http://dx.doi.org/10.1016/0378-7753\(85\)80001-X](http://dx.doi.org/10.1016/0378-7753(85)80001-X)
19. Kozawa A, Yeager JF (1965) The cathodic reduction mechanism of electrolytic manganese dioxide in alkaline electrolyte. *J Electrochem Soc* 112(10):959–963. doi:[10.1149/1.2423350](https://doi.org/10.1149/1.2423350)
20. Johnson RS, Vosburgh WC (1952) The reproducibility of the manganese dioxide electrode and the change of electrode potential with p H. *J Electrochem Soc* 99(8):317–322. doi:[10.1149/1.2779743](https://doi.org/10.1149/1.2779743)
21. Cachet-Vivier C, Tribollet B, Vivier V (2010) Cavity microelectrode for studying manganese dioxide powder as pH sensor. *Talanta* 82(2):555–559, <http://dx.doi.org/10.1016/j.talanta.2010.05.006>
22. Roffat M, Noël O, Soppera O, Bohnke O (2009) Investigation of the perovskite ceramic Li_{0.30}La_{0.56}TiO₃ by Pulsed Force Mode AFM for pH sensor application. *Sensors Actuators B Chem* 138(1):193–200, <http://dx.doi.org/10.1016/j.snb.2008.12.031>
23. Pham QN, Bohnke O, Bohnke C (2006) Potentiometric measurements and impedance characteristics of Li_{0.30}La_{0.57}TiO₃ membrane in lithium anhydrous solutions. *Electrochim Acta* 51(27):6186–6193, <http://dx.doi.org/10.1016/j.electacta.2005.12.050>
24. Catti M, Sommariva M, Ibberson RM (2007) Tetragonal superstructure and thermal history of Li_{0.3}La_{0.567}TiO₃ (LLTO) solid electrolyte by neutron diffraction. *J Mater Chem* 17(13):1300–1307
25. Bohnke O, Bohnke C, Fourquet JL (1996) Mechanism of ionic conduction and electrochemical intercalation of lithium into the perovskite lanthanum lithium titanate. *Solid State Ionics* 91(1–2):21–31, [http://dx.doi.org/10.1016/S0167-2738\(96\)00434-1](http://dx.doi.org/10.1016/S0167-2738(96)00434-1)
26. Stramare S, Thangadurai V, Weppner W (2003) Lithium lanthanum titanates: a review. *Chem Mater* 15(21):3974–3990. doi:[10.1021/cm0300516](https://doi.org/10.1021/cm0300516)
27. Henderson MA (2002) The interaction of water with solid surfaces: fundamental aspects revisited. *Surf Sci Rep* 46(1–8):1–308, [http://dx.doi.org/10.1016/S0167-5729\(01\)00020-6](http://dx.doi.org/10.1016/S0167-5729(01)00020-6)

28. Boehm HP (1971) Acidic and basic properties of hydroxylated metal oxide surfaces. *Discuss Faraday Soc* 52:264–275
29. Boehm H-P (1978) *The Chemical Physics of Surfaces*. Von S. R. Morrison. Plenum Press, New York—London 1977. XVII, 415 S., div. Abb. und Tab., geb. \$ 47.40. *Angew Chem* 90 (6):500–501. doi:10.1002/ange.19780900640
30. Kao CH, Wang JC, Lai CS, Huang CY, Ou JC, Wang HY (2012) Ti-doped Gd₂O₃ sensing membrane for electrolyte–insulator–semiconductor pH sensor. *Thin Solid Films* 520 (10):3760–3763, <http://dx.doi.org/10.1016/j.tsf.2011.11.063>
31. Zhao R, Xu M, Wang J, Chen G (2010) A pH sensor based on the TiO₂ nanotube array modified Ti electrode. *Electrochim Acta* 55(20):5647–5651, <http://dx.doi.org/10.1016/j.electacta.2010.04.102>
32. Wang R, Hashimoto K, Fujishima A, Chikuni M, Kojima E, Kitamura A, Shimohigoshi M, Watanabe T (1997) Light-induced amphiphilic surfaces. *Nature* 388(6641):431–432
33. Sakai N, Wang R, Fujishima A, Watanabe T, Hashimoto K (1998) Effect of ultrasonic treatment on highly hydrophilic TiO₂ surfaces. *Langmuir* 14(20):5918–5920. doi:10.1021/la980623e
34. Fulati A, Usman Ali S, Riaz M, Amin G, Nur O, Willander M (2009) Miniaturized pH sensors based on zinc oxide nanotubes/nanorods. *Sensors* 9(11):8911–8923
35. Batista PD, Mulato M (2005) ZnO extended-gate field-effect transistors as pH sensors. *Appl Phys Lett* 87(14):143508–143503
36. Qiu Y, Yang S (2008) Kirkendall approach to the fabrication of ultra-thin ZnO nanotubes with high resistive sensitivity to humidity. *Nanotechnology* 19(26):265606. doi:10.1088/0957-4484/19/26/265606
37. Zaman S, Asif MH, Zainelabdin A, Amin G, Nur O, Willander M (2011) CuO nanoflowers as an electrochemical pH sensor and the effect of pH on the growth. *J Electroanal Chem* 662 (2):421–425, <http://dx.doi.org/10.1016/j.jelechem.2011.09.015>
38. Chang S-P, Yang T-H (2012) Sensing performance of EGFET pH sensors with CuO nanowires fabricated glass substrate. *Int J Electrochem Sci* 7(6):5020–5027
39. Huang W-D, Cao H, Deb S, Chiao M, Chiao JC (2011) A flexible pH sensor based on the iridium oxide sensing film. *Sensors Actuators A Phys* 169(1):1–11, <http://dx.doi.org/10.1016/j.sna.2011.05.016>
40. Prats-Alfonso E, Abad L, Casañ-Pastor N, Gonzalo-Ruiz J, Baldrich E (2013) Iridium oxide pH sensor for biomedical applications. Case urea–urease in real urine samples. *Biosens Bioelectron* 39(1):163–169, <http://dx.doi.org/10.1016/j.bios.2012.07.022>
41. Choi S, Park I, Hao Z, Holman H-Y, Pisano A (2012) Quantitative studies of long-term stable, top-down fabricated silicon nanowire pH sensors. *Appl Phys A* 107(2):421–428. doi:10.1007/s00339-011-6754-9
42. Colinge J-P, Lee C-W, Afzaljan A, Akhavan ND, Yan R, Ferain I, Razavi P, O'Neill B, Blake A, White M, Kelleher A-M, McCarthy B, Murphy R (2010) Nanowire transistors without junctions. *Nat Nano* 5(3):225–229, http://www.nature.com/nnano/journal/v5/n3/supinfo/nnano.2010.15_S1.html
43. Lee D, Cui T (2012) A role of silica nanoparticles in layer-by-layer self-assembled carbon nanotube and In₂O₃ nanoparticle thin-film pH sensors: Tunable sensitivity and linearity. *Sensors Actuators A Phys* 188:203–211, <http://dx.doi.org/10.1016/j.sna.2012.01.004>
44. Hung-Hsien L, Wei-Syuan D, Jung-Chuan C, Huang-Chung C (2012) An extended-gate field-effect transistor with Low-temperature hydrothermally synthesized SnO_2 nanorods as pH sensor. *Electron Device Lett IEEE* 33(10):1495–1497. doi:10.1109/led.2012.2210274
45. Lei KF, Lee K-F, Yang S-I (2012) Fabrication of carbon nanotube-based pH sensor for paper-based microfluidics. *Microelectron Eng* 100:1–5, <http://dx.doi.org/10.1016/j.mee.2012.07.113>
46. Yun-Shan C, Wan-Lin T, Lee IC, Jung-Chuan C, Huang-Chung C (2012) A novel pH sensor of extended-gate field-effect transistors with laser-irradiated carbon-nanotube network. *Electron Device Lett IEEE* 33(11):1622–1624. doi:10.1109/led.2012.2213794

47. Bobacka J (1999) Potential stability of All-solid-state Ion-selective electrodes using conducting polymers as Ion-to-electron transducers. *Anal Chem* 71(21):4932–4937. doi:[10.1021/ac990497z](https://doi.org/10.1021/ac990497z)
48. Li Q, Li H, Zhang J, Xu Z (2011) A novel pH potentiometric sensor based on electrochemically synthesized polybisphenol A films at an ITO electrode. *Sensors Actuators B Chem* 155(2):730–736, <http://dx.doi.org/10.1016/j.snb.2011.01.038>
49. Aquino-Binag CN, Kumar N, Lamb RN, Pigram PJ (1996) Fabrication and characterization of a hydroquinone-functionalized polypyrrole thin-film pH sensor. *Chem Mater* 8(11):2579–2585. doi:[10.1021/cm9506114](https://doi.org/10.1021/cm9506114)
50. Scholz F, Steinhardt T, Kahlert H, Pörksen JR, Behnert J (2005) Teaching pH measurements with a student-assembled combination quinhydrone electrode. *J Chem Educ* 82(5):782. doi:[10.1021/ed082p782](https://doi.org/10.1021/ed082p782)
51. Xiong L, Batchelor-McAuley C, Compton RG (2011) Calibrationless pH sensors based on nitrosophenyl and ferrocenyl co-modified screen printed electrodes. *Sensors Actuators B Chem* 159(1):251–255, <http://dx.doi.org/10.1016/j.snb.2011.06.082>
52. Gill E, Arshak A, Arshak K, Korostynska O (2010) Response mechanism of novel polyaniline composite conductimetric pH sensors and the effects of polymer binder, surfactant and film thickness on sensor sensitivity. *Eur Polym J* 46(10):2042–2050, <http://dx.doi.org/10.1016/j.eurpolymj.2010.07.012>
53. Gill E, Arshak K, Arshak A, Korostynska O (2008) Mixed metal oxide films as pH sensing materials. *Microsyst Technol* 14(4–5):499–507. doi:[10.1007/s00542-007-0435-9](https://doi.org/10.1007/s00542-007-0435-9)
54. Gill EI, Arshak A, Arshak K, Korostynska O (2009) Investigation of thick-film polyaniline-based conductimetric pH sensors for medical applications. *Sensors J IEEE* 9(5):555–562. doi:[10.1109/jsen.2009.2016608](https://doi.org/10.1109/jsen.2009.2016608)
55. Fernandes EGR, Vieira NCS, de Queiroz AAA, Guimarães FEG, Zucolotto V (2010) Immobilization of poly(propylene imine) dendrimer/nickel Phthalocyanine as nanostructured multilayer films to be used as gate membranes for SEG-FET pH sensors. *J Phys Chem C* 114(14):6478–6483. doi:[10.1021/jp9106052](https://doi.org/10.1021/jp9106052)
56. Novoselov KS, Geim AK, Morozov SV, Jiang D, Katsnelson MI, Grigorieva IV, Dubonos SV, Firsov AA (2005) Two-dimensional gas of massless Dirac fermions in graphene. *Nature* 438(7065):197–200
57. Gu G, Nie S, Feenstra RM, Devaty RP, Choyke WJ, Chan WK, Kane MG (2007) Field effect in epitaxial graphene on a silicon carbide substrate. *Appl Phys Lett* 90(25):253507–253503
58. Ang PK, Chen W, Wee ATS, Loh KP (2008) Solution-gated epitaxial graphene as pH sensor. *J Am Chem Soc* 130(44):14392–14393. doi:[10.1021/ja805090z](https://doi.org/10.1021/ja805090z)
59. Lei N, Li P, Xue W, Xu J (2011) Simple graphene chemiresistors as pH sensors: fabrication and characterization. *Meas Sci Technol* 22(10):1–6. doi:[10.1088/0957-0233/22/10/107002](https://doi.org/10.1088/0957-0233/22/10/107002)
60. Stock JT, Purdy WC, Garcia LM (1958) The antimony-antimony oxide electrode. *Chem Rev* 58(4):611–626. doi:[10.1021/cr50022a001](https://doi.org/10.1021/cr50022a001)
61. Cafilisch CR, Pucacco LR, Carter NW (1978) Manufacture and utilization of antimony pH electrodes. *Kidney Int* 14(2):126–141
62. Zhang Y, Li G, Wu Y, Zhang B, Song W, Zhang L (2002) Antimony nanowire arrays fabricated by pulsed electrodeposition in anodic alumina membranes. *Adv Mater* 14(17):1227–1230. doi:[10.1002/1521-4095\(20020903\)14:17<1227::aid-adma1227>3.0.co;2-2](https://doi.org/10.1002/1521-4095(20020903)14:17<1227::aid-adma1227>3.0.co;2-2)
63. Wang YW, Hong BH, Lee JY, Kim J-S, Kim GH, Kim KS (2004) Antimony nanowires self-assembled from Sb nanoparticles. *J Phys Chem B* 108(43):16723–16726. doi:[10.1021/jp047375h](https://doi.org/10.1021/jp047375h)
64. Zhou B, Hong J-M, Zhu J-J (2005) Microwave-assisted rapid synthesis of antimony dendrites. *Mater Lett* 59(24–25):3081–3084, <http://dx.doi.org/10.1016/j.matlet.2005.05.026>
65. Schoendorfer C, Lugstein A, Hyun Y-J, Bertagnolli E, Bischoff L, Nellen PM, Callegari V, Pongratz P (2007) Focused ion beam induced synthesis of a porous antimony nanowire network. *J Appl Phys* 102(4):044308–044305
66. Avdic A, Lugstein A, Schondorfer C, Bertagnolli E (2009) Focused ion beam generated antimony nanowires for microscale pH sensors. *Appl Phys Lett* 95(22):223106–223103

67. Li X, Horita K (2000) Electrochemical characterization of carbon black subjected to RF oxygen plasma. *Carbon* 38(1):133–138, [http://dx.doi.org/10.1016/S0008-6223\(99\)00108-6](http://dx.doi.org/10.1016/S0008-6223(99)00108-6)
68. Runnels PL, Joseph JD, Logman MJ, Wightman RM (1999) Effect of pH and surface functionalities on the cyclic voltammetric responses of carbon-fiber microelectrodes. *Anal Chem* 71(14):2782–2789. doi:[10.1021/ac981279t](https://doi.org/10.1021/ac981279t)
69. Adenier A, Chehimi MM, Gallardo I, Pinson J, Vilà N (2004) Electrochemical oxidation of aliphatic amines and their attachment to carbon and metal surfaces. *Langmuir* 20(19):8243–8253. doi:[10.1021/la049194c](https://doi.org/10.1021/la049194c)
70. Pinson J, Podvorica F (2005) Attachment of organic layers to conductive or semiconductive surfaces by reduction of diazonium salts. *Chem Soc Rev* 34(5):429–439
71. Piyanekarage SC, Augustin H, Grosjean Y, Featherstone DE, Shippy SA (2008) Hemolymph amino acid analysis of individual drosophila larvae. *Anal Chem* 80(4):1201–1207. doi:[10.1021/ac701785z](https://doi.org/10.1021/ac701785z)
72. Adams RN (1990) In vivo electrochemical measurements in the CNS. *Prog Neurobiol* 35(4):297–311, [http://dx.doi.org/10.1016/0301-0082\(90\)90014-8](http://dx.doi.org/10.1016/0301-0082(90)90014-8)
73. Makos MA, Omiatek DM, Ewing AG, Heien ML (2010) Development and characterization of a voltammetric carbon-fiber microelectrode pH sensor. *Langmuir* 26(12):10386–10391. doi:[10.1021/la100134r](https://doi.org/10.1021/la100134r)
74. Durst RA (2012) Ion-selective electrodes—the early years. *Electroanalysis* 24(1):15–22. doi:[10.1002/elan.201100429](https://doi.org/10.1002/elan.201100429)
75. Bandodkar AJ, Hung VWS, Jia W, Valdes-Ramirez G, Windmiller JR, Martinez AG, Ramirez J, Chan G, Kerman K, Wang J (2013) Tattoo-based potentiometric ion-selective sensors for epidermal pH monitoring. *Analyst* 138(1):123–128
76. Zhang X, Ogorevc B, Wang J (2002) Solid-state pH nanoelectrode based on polyaniline thin film electrodeposited onto ion-beam etched carbon fiber. *Anal Chim Acta* 452(1):1–10, [http://dx.doi.org/10.1016/S0003-2670\(01\)01435-0](http://dx.doi.org/10.1016/S0003-2670(01)01435-0)
77. Schneider L, Korber A, Grabbe S, Dissemond J (2007) Influence of pH on wound-healing: a new perspective for wound-therapy? *Arch Dermatol Res* 298(9):413–420. doi:[10.1007/s00403-006-0713-x](https://doi.org/10.1007/s00403-006-0713-x)
78. Nocke A, Schroter A, Cherif C, Gerlach G (2012) Miniaturized textile-based multi-layer ph-sensor for wound monitoring applications. *Autex Res J* 12(1):20–22. doi:[10.2478/v10304-012-0004-x](https://doi.org/10.2478/v10304-012-0004-x)
79. McColl D, Cartlidge B, Connolly P (2007) Real-time monitoring of moisture levels in wound dressings in vitro: an experimental study. *Int J Surg* 5(5):316–322, <http://dx.doi.org/10.1016/j.ijssu.2007.02.008>

Part II
Sensors and Biosensors for Inorganic
Compounds of Environmental Importance

Chapter 5

Metals

Ivan Švancara and Zuzana Navrátilová

5.1 Frequently Determined Heavy Metals and Metalloids

When reviewing the literature on electrochemical environmental analysis of inorganic ionic species, six of most common heavy metals, namely zinc, cadmium, lead, copper, mercury and thallium, have attracted the greatest attention, together with another two metalloids, i.e. arsenic and selenium (see, e.g., references (1–3)). The environmental importance and toxicological profile of all these species are, in fact, very similar in character, when considering their ultimate impact on the living organisms^{4,5} with severe or even fatal consequences. Perhaps, except zinc and copper whose harmfulness is somewhat lower, all the above-listed elements are highly toxic at trace concentration level, most of them being able of effective bioaccumulation^{6–10} in plant and animal tissues. Moreover, the corresponding ionic and complex species are involved in the environmental, geochemical, and biochemical cycles, “ensuring” their transport and distribution in the lithosphere and hydrosphere with an intensity that reflects the extent of pollution of a region or a locality.

I. Švancara (✉)

Department of Analytical Chemistry, Faculty of Chemical Technology,
University of Pardubice, 532 10 Pardubice, Czech Republic
e-mail: Ivan.Svancara@upce.cz

Z. Navrátilová

Department of Chemistry, Faculty of Science, University of Ostrava,
30. dubna 22, 701 03 Ostrava, Czech Republic
e-mail: Zuzana.Navratilova@osu.cz

5.1.1 Choice of the Individual Methods and Procedures

In Table 5.1 a representative collection of electroanalytical methods for the determination of metals is given, gathering typical classical approaches, as well as some other highly effective or otherwise interesting procedures. The individual entries are characterised by means of basic facts and experimental data from the respective original literature—see references (11–32).

5.1.2 Basic Principles and Mechanisms

Concerning heavy metal ions, Table 5.1 intentionally surveys several types and variants of methods that can be classified as typical and, in most cases, thoroughly proven in electroanalytical practice (see, e.g., references (30–35) and references therein). Moreover, the principles of many methods are often very similar, allowing one to sketch general schemes like those given below.

1. Electrolytical Deposition with Subsequent Electrochemical Detection

The principal basis is a two-step faradic (redox) transformation at the electrode surface by means of potentiostatic electrolysis (Eq. 5.1a) with reduction of metal ion to the elemental state and its subsequent re-oxidation (Eq. 5.1b),



while the electrochemical detection can be accomplished either by voltammetric scanning (preferably with the DPV and SWV ramp within an anodic stripping protocol^{33,36}) or in the form of dt/dE-vs.-E curves recorded in the stripping (chrono)potentiometric mode after chemical oxidation with a suitable reagent (in PSA³⁷) or by imposing a positive constant current (in constant current stripping analysis, CCSA³⁸); the individual alternatives having their pros and cons.

The effectiveness of electrolytic accumulation depends substantially upon the choice of the working electrode. Normally, the surface of bare solid electrodes is not optimal due to a poorer adherence of most of the heavy metal deposits. Of course, exceptions can be found represented by some materials with particular surface conditions, which is the case of boron-doped diamond (see, e.g., references (14, 39))

In electroanalysis, electrolytic deposition/accumulation has been predominantly performed at mercury-based electrodes—here, of course, as reduction only—i.e. with the dropping mercury electrode (DME^{40,41}), the hanging mercury drop electrode (HMDE^{41,42}), mercury film (plated) electrodes (MFES^{43,44}) and eventually chemically modified electrodes (CMEs) containing a Hg^{II} compound immobilised on the electrode surface⁴⁵ or dispersed as a solid in the electrode bulk.⁴⁶

Table 5.1 Determination of toxic heavy metals and metalloids in environmental samples. Selected methods and their specification

Ions/species	Working el. (modifier)	Reference el.; auxiliary el.	Technique (mode)	Measuring principles (method sequences)	Experimental conditions: (selection)	Analytical characteristics (with "c" given in mol·l ⁻¹)	Sample(s)	Ref (s)
Cd ²⁺ , Cu ²⁺ , Pb ²⁺ , Zn ²⁺ , Bi ³⁺	MF-GCE (as RDE)	SCE	ASV	<ul style="list-style-type: none"> - Electrolytic preconcentration: Meⁿ⁺ + ne⁻ + xHg → Me(Hg)_x - Subsequent anodic stripping: Me(Hg)_x → Meⁿ⁺ + ne⁻ + xHg 	SS: for Cd, Pb, Cu, and Bi: acidified sea water (10 M HCl), E _{dep} -0.9 V, t _{dep} 30 min SE: for Zn: 1 M HCl + 2 M sodium acetate, E _{dep} -1.3 V, t _{dep} 30 min SE: acidified water sample + 2-4 mg l ⁻¹ Hg ²⁺	(LR: model calibrations at concentration levels required for reliable detection of all metal elements of interest)	Seawater	11
Cd ²⁺ , Cu ²⁺ , Pb ²⁺ , Zn ²⁺	TMF (GC-support)	SCE; Pt foil	S(C)P (PSA)	<ul style="list-style-type: none"> - Electrolytic preconcentration: Meⁿ⁺ + ne⁻ + xHg → Me(Hg)_x - Subsequent anodic stripping: Me(Hg)_x → Meⁿ⁺ + ne⁻ + xHg 		LOD: 4.6 × 10 ⁻¹⁰ M (for Zn), 2.7 × 10 ⁻¹⁰ M (Cd), 4.8 × 10 ⁻¹¹ M (Pb), 3.1 × 10 ⁻¹⁰ M (Cu); all for t _{acc} 75 min	Seawater	12
Cd ²⁺ , Cu ²⁺ , Pb ²⁺	HMDE	Ag/AgCl	DPCSV	<ul style="list-style-type: none"> - Adsorptive collection of Cd^{II}, Cu^{II}, Pb^{II}-complexes with 8-hydroxyquinoline - Subsequent cathodic stripping (with reduction of Me^N → Me⁰) 	SE: 0.01 M buffer HEPES (pH 7.5-8) + 8 × 10 ⁻⁶ M 8-hydroxyquinoline, E _{ads} -1.1 V, t _{ads} 1-12 min; E _{in} -0.3 V	LR: 0.2-25 nM (Cd), 3-90 nM (Cu), 0.3-60 nM (Pb) LOD (3σ, t _{ads} 1 min): 0.12 nM (Cd), 0.24 nM (Cu), 0.45 nM (Pb) InR: Triton (0.5 mg l ⁻¹); Sb, V, U (100:1)	Seawater	13
Cu ²⁺ , Pb ²⁺	BDDF (G-substrate)	SCE	ASV	<ul style="list-style-type: none"> - Nucleation deposition of the corresponding metal - Subsequent anodic stripping 	SE: 0.1 M HNO ₃	LR: 2.5 × 10 ⁻⁶ to 10 ⁻⁴ M (for both Cu + Pb)	Model solutions	14

(continued)

Table 5.1 (continued)

Ions/ species	Working el. (modifier)	Reference e.l.; auxiliary e.l.	Technique (mode)	Measuring principles (method sequences)	Experimental conditions: (selection)	Analytical characteristics (with "c" given in mol·l ⁻¹)	Sample(s)	Ref (s)
Cu ²⁺ , Pb ²⁺	MFuE (C-substrate)	Ag/AgCl/ sat.	ASV	- Electrolytic preconcentration: Me ⁿ⁺ + ne ⁻ + xHg → Me(Hg) _x - Subsequent anodic stripping: Me(Hg) _x → Me ⁿ⁺ + ne ⁻ + xHg	SS: real waters pH < 6 or acidified to pH 1 (HNO ₃) Presence of Cl ⁻ < 1 mM	LR: calibrationless (the content calculated from equations: (0.48–4.8) × 10 ⁻⁷ M (Pb), (0.47– 4.7) × 10 ⁻⁷ M (Cu)) RR: ±5 %	Well water, rain (water)	15
Cd ²⁺ , Pb ²⁺	BIFE (SP-substrate)	Ag/AgCl (screen printed)	S(CP) CCSA	- Electrolytic preconcentration: Me ⁿ⁺ + ne ⁻ + xBi → Me(Bi) _x - Subsequent chemical strip- ping: Me(Bi) _x → Me ⁿ⁺ + ne ⁻ + xBi	SE: 0.1 M HCl + ammonium acetate (pH 4.6), E _{dep} -1.0 V, t _{dep} 120 s, I _{CCSA} : 1 μA	LR: (0.18–2.7) × 10 ⁻⁶ M (Cd), 9.7 × 10 ⁻⁸ – 1.4 × 10 ⁻⁶ M (Pb); LOD (3σ): 7.1 × 10 ⁻⁸ M (Cd) and 4.8 × 10 ⁻⁸ M (Pb) InR: Cu (1:4) RR: ±5.1 % (Cd), ±4.5 % (Pb)	Wastewaters, soil extracts	16
Cd ²⁺ , Pb ²⁺	MWCNTs-Na ₂ Bi (composite film- modified GCE)	Ag/AgCl/ 3 M NaCl; Pt wire	DPASV	- Electrolytic preconcentration: Me ⁿ⁺ + ne ⁻ + xBi → Me(Bi) _x - Subsequent anodic stripping: Me(Bi) _x → Me ⁿ⁺ + ne ⁻ + xBi	SE: 0.1 M acetate buffer pH 4.5, E _{dep} -1.2 V	LR: 1.3 × 10 ⁻⁹ to 1.6 × 10 ⁻⁶ M (Cu), 2.4 × 10 ⁻¹⁰ to 4.8 × 10 ⁻⁷ M (Pb) LOD (3σ, t _{dep} 2 min): 3.6 × 10 ⁻¹⁰ M (for Cd), 1.2 × 10 ⁻¹⁰ M (Pb) RR: ±1.7 % (Cd), ±1.8 % (Pb) InR: SCN ⁻ , Cl ⁻ , F ⁻ , SO ₄ ²⁻ , NO ₃ ⁻ (500:1), Hg ₂ ²⁺ (5:1), surfactants (slightly)	Tap water	17

Pb ²⁺	(M)CPE (modifier: resin QuadraPure™, TU)	Ag/AgCl/ 3 M KCl; Pt plate	SWASV	<ul style="list-style-type: none"> - Pb²⁺ + R-NH-C(-NH₂)=S → PbS + 2e⁻ (chelating) - Reduction of Pb^{II} → Pb⁰ - Subsequent anodic stripping: Pb⁰ → Pb²⁺ + 2e⁻ 	SE: 0.1 M acetate buffer pH 4.5 open-circuit accumulation, t _{dep} 15 min E _{dep} -1.0 V (reduction step)	LR: 2.4 × 10 ⁻⁸ to 2.4 × 10 ⁻⁵ M (1.2 × 10 ⁻⁴ M) InR: Bi ³⁺ (1:1, 10:1)	Water samples Sewage sludge	18
Cd ²⁺ , Cu ²⁺ , Pb ²⁺ , Tl ⁺	MFE BiFE	Ag/AgCl/ 3 M KCl; GC tip	ASV (SWV ramp)	<ul style="list-style-type: none"> - Me⁰ deposition onto mercury or bismuth films - Subsequent anodic stripping - Me⁰ → Meⁿ⁺ + ne⁻ 	SS: highly saline samples (ca 0.4 M NaCl) acidified with conc. HCl, E _{dep} -0.9 V, t _{dep} 60 s	MFE: LR: (0-3.6) × 10 ⁻⁶ M (Cd) ^{ab} , (0-1.9) × 10 ⁻⁶ M (Pb) ^{ab} , (0-6.3) × 10 ⁻⁶ M (Cu) ^{ab} , (0-2.4) × 10 ⁻⁶ M (Tl) ^{ab} , (0-2.6) × 10 ⁻⁶ M (Cd) ^c , (0-1.4) × 10 ⁻⁶ M (Pb) ^c , (0-4.7) × 10 ⁻⁶ M (Cu) ^c , (0-2) × 10 ⁻⁶ M (Tl) ^c LODs (3σ, t _{dep} 60 s): 4.4 × 10 ⁻¹⁰ M (Cd) ^{ab} , 6.2 × 10 ⁻¹⁰ M (Cd) ^c , 4.8 × 10 ⁻¹⁰ M (Pb) ^{ab,c} , 2.4 × 10 ⁻⁹ M (Cu) ^{ab} , 7.9 × 10 ⁻⁹ M (Cu) ^c , 3.4 × 10 ⁻⁹ M (Tl) ^{ab} , 4.4 × 10 ⁻⁹ M (Tl) ^c	Seawater ^a Hydrothermal fluids ^b Dialysis concentrates ^c	19

(continued)

Table 5.1 (continued)

Ions/species	Working el. (modifier)	Reference el.; auxiliary el.	Technique (mode)	Measuring principles (method sequences)	Experimental conditions: (selection)	Analytical characteristics (with "c" given in mol·l ⁻¹)	Sample(s)	Ref (s)
Tl ⁺	MFE (GC substrate)	SCE	S(CP (PSA)	<ul style="list-style-type: none"> Electrolytic preconcentration: Tl⁺ + e⁻ + xHg → Tl(Hg)_x Subsequent reoxidation: Tl(Hg)_x → Tl⁺ + e⁻ + xHg 	SE: 0.02–0.07 M HNO ₃ + 0.02 M CH ₃ COONa + 0.001 M EDTA + 6 × 10 ⁻⁵ M HgCl ₂ , E _{dep} -0.9, t _{dep} 5–30 min	LR: 2.5 × 10 ⁻⁹ to 2.5 × 10 ⁻⁸ M, t _{dep} 3 min, 2.5 × 10 ⁻¹⁰ to 2.5 × 10 ⁻⁹ M, t _{dep} 15 min, 2.5 × 10 ⁻¹¹ to 2.5 × 10 ⁻¹⁰ M, t _{dep} 30 min LOD (3σ, t _{dep} 30 min): 5 × 10 ⁻¹¹ M	CRMs: tap and rain water, river sediment, sewage sludge	20
Tl ^{III}	(M)CPE (modifier: anion exchanger Amberlite LA-2)	SCE; Pt wire	DPASV	<ul style="list-style-type: none"> Open-circuit preconcentration: Tl^{III} as [TlCl₄]⁻ Intermediate reduction: [TlCl₄]⁻ + 3e⁻ → Tl⁰ + 4Cl⁻ Subsequent reoxidation Tl⁰ → Tl^I 	SE: MEX, (1) deposition: 0.1 M HCl, (2) DPV: 0.001 M HCl + 0.047 M KCl	LR: (0–4.9) × 10 ⁻⁴ M (t _{prec} 15 s), (0–4.9) × 10 ⁻⁵ M (t _{prec} 60 s), (0–4.9) × 10 ⁻⁶ M (t _{prec} 300 s) LOD: 9.8 × 10 ⁻⁸ M RR: ±0.7%	(Coal) fly ash	21
Hg ^{II}	Au twin disc (as RDE)	SCE; Pt coil	DPASV (with subtraction)	<ul style="list-style-type: none"> Electrolytic preconcentration: Hg²⁺ + 2e⁻ → Hg⁰ Subsequent anodic stripping: Hg⁰ → Hg²⁺ + 2e⁻ (after MEX, with elimination of undesired background) 	SE: MEX, (a) deposition: in sample solution, (b) ASV: 0.1 M HClO ₄ + 2–3 M NaCl, t _{prec} (up to) 15 min	LR: 2 × 10 ⁻¹⁰ to 2 × 10 ⁻⁸ M (10 min)	Seawater, inland water	22

Hg^{II}	Au disc (as RDE)	Ag/AgCl; Pt-wire	DPASV	– Electrolytic preconcentration: $\text{Hg}^{2+} + 2e^- \rightarrow \text{Hg}^0$ – Subsequent anodic stripping: $\text{Hg}^0 \rightarrow \text{Hg}^{2+} + 2e^-$	SE: MEX, (a) deposition: in sample solution, (b) DPV: 0.1 M HClO_4 + 2.5 HCl $E_{\text{acc}} -0.2 \text{ V}$, $t_{\text{prec}} 40-60 \text{ min}$, $v_{\text{RDE}} = 1,500 \text{ rpm}$ SS: sample + 2–2.5 ml of SE containing 2.5 M NaCl; 0.25 M sodium acetate + 0.25 M acetic acid + 0.001 M KMnO_4 + Cu^{2+} (2 mg l^{-1}); $E_{\text{acc}} -0.7 \text{ V}$, $t_{\text{prec}} 8 \text{ min}$	LR: 5×10^{-11} to $2 \times 10^{-10} \text{ M}$ LOD: 10^{-11} M	Seawater	23
	GCE (bare)	SCE; Pt foil	S(C)/P (PSA)	– Electrolytic preconcentration: $\text{Hg}^{2+} + 2e^- \rightarrow \text{Hg}^0$ (presence of Cu) + subsequent oxidation by KMnO_4 : $\text{Hg}^0 \rightarrow \text{Hg}^{2+} + 2e^-$		LR 5×10^{-9} to 10^{-3} M (1–60 min) LOD: $5 \times 10^{-9} \text{ M}$ (64 min); RR: $\pm 6.5 \%$ In: Ag, oxidizable species	Seawater	24
Hg^{II}	(M)GCE, (<i>Kryptofix-222</i>)	SCE	SWASV	– Complexation with modifier – Intermediate reduction of the complex (with $\text{Hg}^{\text{II}} \rightarrow \text{Hg}^0$) – Subsequent reoxidation to Hg^{II}	SE: sample buffered with acetate	LR: 2×10^{-12} to $2 \times 10^{-10} \text{ M}$ LOD: $< 1 \times 10^{-12} \text{ M}$ (10 min)	Sea water, waste water	25
As^{III} , As^{V}	Au (as RDE)	NCE; Pt wire	DPASV	– Electrolytic deposition/stripping: $\text{As}^{3+} + 3e^- \rightarrow \text{As}^0 \rightarrow \text{As}^{3+} + 3e^-$ – As^{V} determined after reduction to As^{III} with SO_2 (g)	SS: sample + 20 mg ascorbic acid + 1 ml 96 % H_2SO_4 + 0.1 ml 30 % HCl, $E_{\text{dep}} -0.3 \text{ V}$, $t_{\text{dep}} 2 \text{ min}$	LR: 2.7×10^{-9} to $1.3 \times 10^{-7} \text{ M}$ LOD (4 min): $2.7 \times 10^{-9} \text{ M}$ RR: 6 % ($2.7 \times 10^{-8} \text{ M}$)	Seawater	26
	Au film (Pt fibre as support)	Ag/AgCl	PSA (FIA)	– Electrolytic deposition: $\text{As}^{\text{V}} + 5e^- \rightarrow \text{As}^0$ – Subsequent oxidative stripping: $\text{As}^0 \rightarrow \text{As}^{3+} + 3e^-$	SE: 4 M HCl + 2.5 M CaCl_2 , $E_{\text{dep}} -1.6 \text{ V}$, $t_{\text{dep}} 60 \text{ s}$	LOD (3σ): $1.3 \times 10^{-9} \text{ M}$ (for 60 s)	Seawater Urine	27

(continued)

Table 5.1 (continued)

Ions/species	Working el. (modifier)	Reference el.; auxiliary el.	Technique (mode)	Measuring principles (method sequences)	Experimental conditions: (selection)	Analytical characteristics (with "c" given in mol·l ⁻¹)	Sample(s)	Ref (s)
As ^{III}	Au film (CP support)	SCE; Pt wire	CCSA	– Electrolytic deposition/stripping: As ³⁺ + 3e ⁻ → As ⁰ /→ As ³⁺ + 3e ⁻ – As ^V determined after reduction to As ^{III} with α-cysteine	SE: 10 M HClO ₄ + 2 M HCl, E _{dep} -0.4 V, t _{dep} 15 s (Note: Solutions stabilised by addition of N ₂ H ₅ ⁺ ions)	LR: 6.7 × 10 ⁻⁸ to 1.3.7 × 10 ⁻⁶ M LOD (3σ, 15 s): 2.7 × 10 ⁻⁸ M As ³⁺ , 6.7 × 10 ⁻⁹ M As ^V , red RR: 6 %	River water	28
Se ^{IV}	HMDE		DPCSV	– Electrolytic reductive deposition of Cu(I) ₂ Se complex – Subsequent cathodic stripping (with detection of Cu ^{II} → Cu ⁰)	SS: sample acidified to pH 1.6 + 40 μM Cu	InR: Hg, Ag, Se (10:1), Cu (5:1) LR: 0–200 nM LOD (15 min): 0.01 nM	Seawater	29

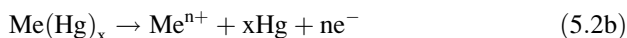
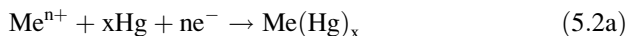
Abbreviations:

Symbols and general abbrevs.: *c* concentration/content; *E_{acc}* accumulation/deposition potential; *el.* electrode; *EP* peak potential; (*g*) gas, gaseous; *ICCSA* constant current (in CCSA mode); *In(R)* interference (ratio); *LOD* limit of detection; *LR* linear range; *M* molar concentration (mol per litre); *mini* minute(s); *RR* reproducibility/repeatability; *sat.* saturated; *SE* supporting electrolyte; *SS* sample solution; *t_{acc}* accumulation/deposition/pre-concentration time; *v* velocity
Electrodes: *BDDF* boron-doped diamond film, *BiFE* bismuth film electrode, *C* carbon, *GC(E)* glassy carbon substrate (electrode), *HMDE* hanging mercury drop electrode, (*M/CPE*) (modified) carbon paste electrode, *MFE* mercury film electrode, *MWCNTs-Na/Bi* multiwall carbon nanotubes dispersed in Nafion used in combination with Bi, *SCE* saturated calomel electrode, *RDE* rotated/rotating disc electrode, *SMDE* static mercury drop electrode, *SP-BiFE* screen-printed bismuth film electrode, *WE* working electrode

Techniques: *ASV* anodic stripping voltammetry, *AdCSV* adsorptive cathodic stripping voltammetry, *SWASV* square-wave anodic stripping voltammetry, *CCSA* constant current stripping analysis, *DCASV* direct current ASV, *DPASV* differential pulse anodic stripping voltammetry, *DPCSV* differential pulse cathodic stripping voltammetry, *DPV* differential pulse voltammetry, *PSA* potentiometric stripping analysis (with chemical oxidation), *S(C)/P* stripping (chrono)potentiometry, *SWASV* square-wave anodic stripping voltammetry
Chemicals and reagents: *HEPES* *N*-2-hydroxy-ethylpiperazine-*N'*-2-ethane sulphonic acid, *Tropolone* 2-hydroxy-cyclo-hepta-2,4,6-trienone, *Kryptofix-222* 4.7.13,16,21,24-hexaoxa-1,10-diazabicyclo[8.8.8] hexacosane

Other abbrevs.: *CRM(s)* certified reference material(s), *ME_x* medium exchange, *TMF* thin mercury film

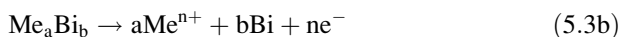
All these types of mercury electrodes enable a particularly effective pre-concentration, when the driving force is further enhanced by amalgamation—dissolution of the reduced metal in liquid mercury (Eq. 5.2a) and its anodic reoxidation (Eq. 5.2b):



The amalgam-forming processes may substantially enhance the sensitivity and selectivity of an ASV or a PSA measurement because there is quite different willingness of metallic elements to form an alloy with mercury.⁴⁷ Heavy metals, in general, belong to those whose affinity towards liquid mercury is quite high⁴⁴; nevertheless, there are also some nuances. For instance, the mutual affinity of Hg to Zn, Cd or Tl is well developed, but much less pronounced than that between Hg and Pb. As a consequence, extraordinarily efficient pre-concentration of Pb^{2+} ions at mercury electrodes in combination with the proper electrochemical detection results in achieving extremely low concentrations (down to the pM range), positioning the corresponding methods to the front of the most sensitive measurements ever proposed and employed in instrumental analysis of water samples for the determination of lead.⁴⁸

Recently, a similar mechanism was utilised in electroanalysis with bismuth-based electrodes (BiEs^{49,50}) that have already become successful competitors, as well as real alternatives, of electrodes from liquid mercury (HMDE and DME) or from highly toxic Hg(II) precursors needed to prepare MFEs. (By the way, thanks to the environmentally friendlier character of bismuth, bismuth film electrodes, BiFEs, and related configurations are now aspiring after the role of the first true “green electrodes”.⁵¹)

The proper mechanism of comparably effective pre-concentration onto Bi(F)Es is based on spontaneous formation of (low melting) bismuth alloys⁵² (Eq. (5.3a)), their deposition as specific crystalline layers,⁵³ followed by disintegration during the re-oxidation step (Eq. 5.3b):



2. Non-electrolytic Pre-concentrations^{54–64}

In principle, such accumulations are not necessarily associated with electron transfer and current flow and can, therefore, be performed under open-circuit conditions, with the working electrode optionally disconnected from the cell and electric circuit.⁵⁵

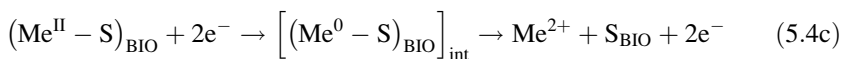
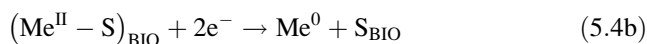
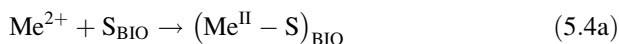
Concerning the particular mechanisms in the individual procedures of electrochemical stripping analysis (ESA), one can utilise the following processes: adsorption,⁵⁴ extraction,^{55,56} ion-pairing or ion-exchange^{55,57–60} and bioaccumulation.^{61,62} To complete the list of applicable physicochemical

phenomena, the electrocatalysis-assisted detection^{63,64} can also be quoted, although it normally accompanies the stripping step regardless of which type of pre-concentration is used.

In the case of heavy metals, non-electrolytic accumulation is not widely used. Perhaps, adsorptive pre-concentration is more frequent for the determination of copper (see references (55, 57–60) plus references therein), whereas the other heavy metals and both metalloids are preferably determined by ESA with electrolytic deposition (see Table 5.1) and the choice of other methodologies is rather a research topic than practical routine.

Except the bioaccumulation of heavy metals that is quite efficient for these toxic elements, further discussion on non-electrolytic pre-concentrations is given below in association with other metals, for which such principles are typical in methods employed in practical analyses.

Bioaccumulative behaviour of most of the heavy metal is mainly important from a toxicological point of view^{4–10}; nevertheless, it has been the subject of interest in some special studies with invertebrate and plant tissues, dried and grinded to a fine mass and applied as a bulk modifier. This was the case of various algae (see reference (61) and references therein) or mosses and lichens.⁶² In a scheme, the process of bioaccumulation onto a bio-substrate, “S_{BIO}”, can be sketched as follows (Eq. 5.4a):



where the reduction either is the measurement reaction (Eq. 5.4b) or provides an intermediate INT during the accumulation which is oxidized during the voltammetric scan (Eq. 5.4c). With regard to the electroanalytical characterisation, bioaccumulation of heavy metals can be rather selective, but not very sensitive to be applicable to environmental samples in a wider extent.

The use of bio-organic material for accumulation is rather rare, whereas various tissues of mushrooms, fruits or vegetables are frequently employed as natural sources of enzymes in the configurations of biosensors.⁵⁵

3. Zero-Current Measurements for the Determination of Heavy Metals

In this category, direct potentiometry with ion-selective electrodes (ISEs) has to be mentioned. Unfortunately, traditional ISEs can be operated at the trace concentration level only scarcely⁶⁵ and, therefore, their employment for real samples containing heavy metals is limited.

Outside the commercial market for ISEs, some research activities have shown that equilibrium potentiometry can be employed also in environmental monitoring of heavy metals. More specifically, there are the so-called non-Nernstian ISEs⁶⁶ which, reportedly, may offer outstanding analytical performance being

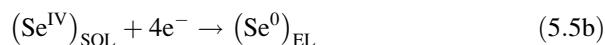
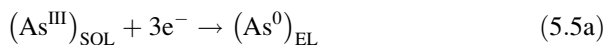
able to indicate equilibrium potential changes for concentrations at trace or even ultratrace level (e.g., down to 1×10^{-12} M for Pb^{2+} ; reference (67)).

4. Other Possibilities

Finally, among occasionally chosen approaches in analysis of samples with heavy metal ions, one can quote, for example, simultaneous determination with metalloid(s),⁶⁸ detection in flowing streams (FIA and HPLC; see references (69–71) and references therein), use of hydrodynamic mode with rotated disc electrodes (RDEs) for improvement of accumulation (see references (11, 22, 23) in Table 5.1), array of microelectrodes¹⁵ and some indirect methods like an orientation assay for natural waters heavily polluted with mercury, when the measurement relies upon the decrease of the signal of a special marker—here, the $[\text{B}(\text{C}_5\text{H}_6)_4]^-$ anion—whose quite sensitive oxidation is suppressed by concurrent reaction with Hg^{II} .⁷²

Concerning the principles of the determination of the two metalloids, arsenic and selenium, a concise summarisation of the individual methods is rather difficult; nevertheless, some principal aspects and associations can be outlined, whereas the corresponding mechanisms, method sequences and schemes are given in Table 5.1.

Both As and Se as elements show practically no affinity to mercury and, also, their deposition onto solid compact surfaces is problematic and usually poorly reproducible. An exception is gold and hence, gold-based electrode configurations are the primary choice for the proper determination of both semimetals.^{26–29,68} In these cases, the deposition of both (Eqs. 5.5a and 5.5b) requires the particular valence of the corresponding species:



where the subscripts “SOL” and “EL” mean “solution” and “electrode”, respectively.

This has to be considered in the case of samples containing these two metalloids in species with maximal valence, i.e. as arsenate, $\text{HAs}^{\text{V}}\text{O}_4^{2-}$, and selenate, SeO_4^{2-} . Both anions are extraordinarily stable and, normally, cannot be reduced at the electrode,²⁷ requiring chemical reduction by SO_2 (g) or cysteine for $\text{As}^{\text{V}} \rightarrow \text{As}^{\text{III}}$ (see also Table 5.1) and $\text{Na}_2\text{S}_2\text{O}_4$ or $\text{Na}_2\text{H}_2\text{PO}_2$ for $\text{Se}^{\text{VI}} \rightarrow \text{Se}^{\text{IV}}$ to obtain electrochemically active species prior to electroanalytical measurements.^{28,29} It is advisable to stabilise such chemically pre-reduced arsenic by adding a mild reductant (e.g. N_2H_5^+ or NH_3OH^+) to the sample as also mentioned in the table.

Finally, some methods are also based on the selective formation of binary adducts, Mt_AMe_B (where “Mt” means metalloid and “Me” metal, usually, copper), whose electrode transformations are correlated with the quantity of the respective metalloid.²⁹

5.1.3 *Electroanalysis of Heavy Metals and Environmental Samples*

Zinc, cadmium and lead can be determined simultaneously as shown in many methods of ESA (see, e.g., Table 5.1,^{11–13,19}). This is possible due to their close physicochemical properties and, of course, satisfactorily resolved peak potentials, E_p . Certain problems can be encountered when differentiating between Cd and Pb, whose E_p values at some electrodes may be very similar, whereas that for zinc is almost always separated due to the more negative re-oxidation of Zn compared to both Cd and Pb. If such difficulties occur, there are several possible ways of how to influence the actual resolution of Cd and Pb peaks. Probably the most frequent is the choice of the supporting electrolyte and the selection of a slightly different accumulation potential for each element. A potentially viable route is also masking of one of the two ions prior to deposition, but this is not very common due to the quite limited number of reagents whose Cd^{II} and Pb^{II} complexes would have sufficiently different stability.⁷³ There are also some procedures capable of separating the Cd and Pb peaks via post-experimental treatment of stripping curves by mathematical processing of the overlapped signals.^{74,75} Finally, there is also the option to exchange the supporting electrolyte, to change the working electrode or to significantly alter its deposition/stripping performance, e.g. by rearranging the plating regime for ex situ-generated metallic films.⁵³

Regarding the sensitivity of commonly used electrodes and sensors towards the individual metals, it depends, of course, upon the electrode used. Nonetheless, a majority of them respond in the order “Pb → Cd → Zn”, when the difference between the first and last one can be substantial with respect to their determination in trace analysis. These three metals can be also simultaneously determined together with copper, where care has to be taken not to have too high concentration of zinc and copper because of formation of their intermetallics (see below).

The electrochemistry of thallium is rather specific given by the fact that this element exists in two forms, the monovalent Tl^+ ion²⁰ and as trivalent thallate.²¹ A well-known tendency of Tl^+ not to form complexes⁷³ is exploited for a selective determination of this highly toxic element, when the metal ions with similar stripping characteristics (Cd^{2+} , Pb^{2+} and In^{3+}) can be effectively masked by EDTA in an acetate buffer at pH ~ 4.³⁵ (Less well known is a finding that such a masking can be performed also in acidic solutions of the wet-digested samples, containing ca. 0.05 M HNO_3 as the residual concentration after mineralisation and diluting, but still enabling to form Cd^{II} and Pb^{II} chelates with EDTA despite already weakened complexing properties of its protonated molecules.²⁰) Furthermore, worth of mentioning is the behaviour of Tl^{I} at some metallic film electrodes in basic media of ammonia buffer,⁷⁶ giving rise to a pair of stripping peaks, each of them being proportional to concentration and, in certain extent, available for calibration. When thallium in the sample is converted into its trivalent form and a suitable anion of the $[\text{Tl}^{\text{III}}\text{X}_4]^-$ type, the pre-concentration at the electrode takes place via ion pairing, followed by immediate reduction to Tl^0 and subsequent anodic stripping (see Table 5.1 and reference (21)).

Within common heavy metals, certain specificity can be attributed to copper and mercury, due to their nobler character and somewhat different behaviour compared to the previous metals. Namely, Cu^{2+} ions (or Cu^{II} species, respectively) can be reduced to the metal in one-electron steps in alkaline media, $\text{Cu}^{2+} + \text{e}^- \rightarrow \text{Cu}^+ + \text{e}^- \rightarrow \text{Cu}^0$,^{30,31} and, in the same way, re-oxidised. Some of the metals may form intermetallic adducts that may seriously interfere in many determinations using ESA, especially, at metallic film electrodes.^{44,52}

With regard to mercury, one should not forget about the instability of very diluted solutions, in which originally present Hg^{2+} can be reduced by impurities to Hg_2^{2+} dismutating to $\text{Hg}^{2+} + \text{Hg}^0$, thus allowing the elemental form to evaporate away. This loss must be prevented by stabilisation with MnO_4^- or $\text{Cr}_2\text{O}_7^{2-}$, whenever the sample for trace analysis is to be stored for longer time.²² Yet another peculiarity is that Hg^{2+} ions are hard to release from naturally occurring complexes, requiring a very thorough decomposition of the samples,⁷⁷ in some cases rather with high-pressure ashing (HPA) than by using common and often routinely applied microwave-assisted (wet) digestion.

HMDE vs. MFE

For long time, the hanging mercury drop and the mercury film electrode, HMDE and MFE, respectively, have represented by far the most frequent electrodes in environmental analysis of heavy metals.^{34,35} Although both configurations are from the same electrode material, they may differ considerably in the overall performance. Firstly, there is a completely different size of Hg droplets. MFEs, and especially those operated in situ,⁴³ are functioning via a very thin film of Hg droplets (with diameter of 10–100 nm^{53,78}) which is readily saturated with intermetallic adducts, interfering during experiments. Compared to this, the HMDE is less vulnerable and usually does not need special treatments like a MFE,⁴⁴ when determinations of Zn, Cd and Pb in the presence of higher contents of Cu^{II} require addition of Ga^{III} (see Fig. 5.1 and reference (79)) or masking of Cu^{2+} in a specific complex or a precipitate (e.g. with SCN^- ⁷³).

Then, there are notable differences in the reproducibility of measurements. At the HMDE, this parameter commonly is below 1 % rel., whereas similar experiments with a MFE vary in an interval of 3–5 % rel.^{44,80} Of course, in this case, such values are still excellent if one considers typical levels of precision for measurements in trace analysis (normally, with recovery rates within 90–110 % as stated in numerous scientific papers).

A further issue is the mechanical stability of both HMDE and MFE, which is in favour of the latter and, for instance, for hydrodynamic measurements with the rotating disc electrode (RDE, see Table 5.1 and reference (11)) or that in improvised shipboard laboratories,⁸¹ the reliable use of an HMDE with its dropping mechanism is hardly imaginable, perhaps, except for some special and purposely constructed automated analysers.⁸²

Finally, the use of liquid mercury is contradictory to green analytical chemistry.⁵¹ If some predictions come true and this trend will pursue some administrative acts of this sort, the only choice will be the MFE being prepared from mercury

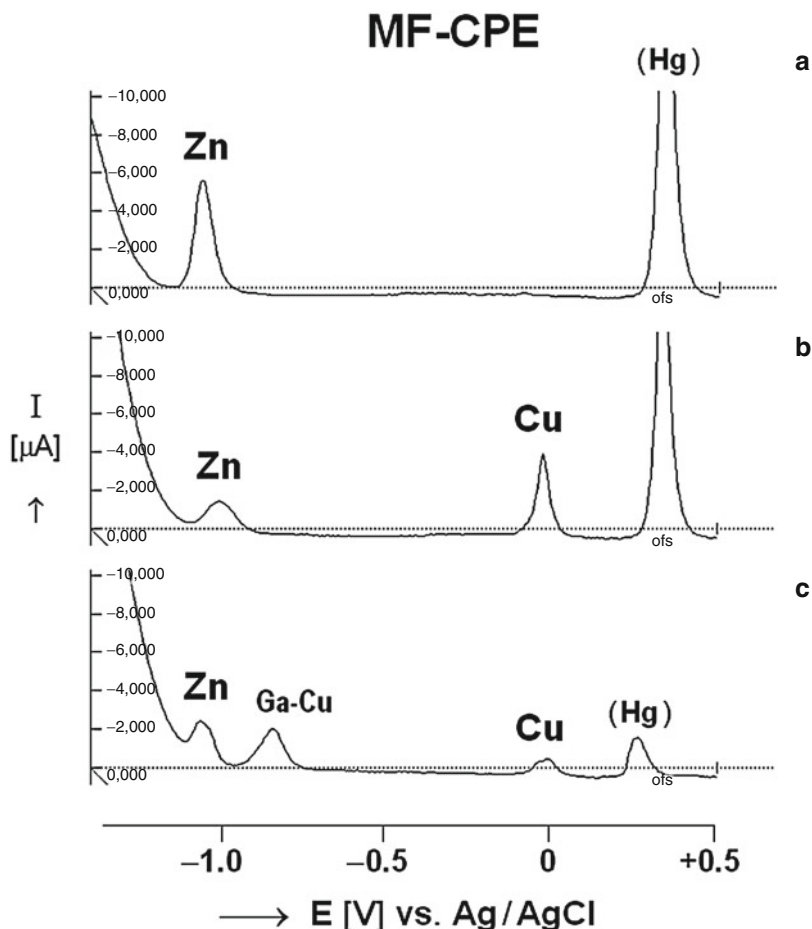


Fig. 5.1 Anodic stripping voltammetry of Zn^{2+} and Cu^{2+} (model mixture) at mercury film-plated carbon paste electrode (MF-CPE) in the presence of Ga^{3+} ions. An initial study. Legend: (a) Zn (II) [$E_p(\text{Zn}) = -1.14$ V, $I_p(\text{Zn}) = 5.7$ μA]; (b) Zn(II) + Cu(II) [$E_p(\text{Zn}) = -1.11$ V, $I_p(\text{Zn}) = 1.3$ μA ; $E_p(\text{Cu}) = -0.06$ V, $I_p(\text{Cu}) = 4.2$ μA]; (c) Zn(II) + Cu(II) + Ga(III) [$E_p(\text{Zn}) = -1.14$ V, $I_p(\text{Zn}) = 1.5$ μA ; $E_p(\text{Ga-Cu}) = -0.91$ V, $I_p(\text{Ga-Cu}) = 2.1$ μA ; $E_p(\text{Cu}) = -0.03$ V, $I_p(\text{Cu}) = 0.8$ μA]. Experimental conditions: differential pulse anodic stripping voltammetry (DPASV); supporting electrolyte, acetate buffer (0.2 M CH_3COOH + 0.2 M CH_3COONa , pH 4.2); $c(\text{Hg}) = 5 \times 10^{-5}$ mol l^{-1} , $c(\text{Zn}, \text{Cu}) = 1 \times 10^{-6}$ mol l^{-1} ; $c(\text{Ga}) = 1 \times 10^{-5}$ mol l^{-1} ; accumulation time, $t_{\text{ACC}} = 30$ s; equilibration time, $t_{\text{EQ}} = 10$ s; initial potential, $E_{\text{INT}} = -1.5$ V ve. ref.; final potential, $E_{\text{FIN}} = +0.5$ V; scan rate, $\nu = 20$ mV s^{-1} ; pulse height, $\Delta E = -50$ mV (taken, adapted and rearranged from reference (79))

(II) salts that, in paradox, have not been included in the already existing official bans.⁸³

MFES vs. Bi(F)Es

Similar to the previous paragraph, it is also possible to compare these two related designs. Apart from the already emphasised ecological associations^{51,83} and some

obvious physicochemical characteristics, there are some notable nuances in the electrochemical behaviour of both MFEs and BiFEs (see references (44, 50–52) and references therein).

With respect to the determination of heavy metals, the use of a BiFE offers a somewhat better resolution of the stripping peaks of Cd and Pb, together with markedly higher sensitivity to cadmium. Both phenomena are explained by different affinities of Cd and Pb to Bi in the corresponding alloy(s) compared to similar interaction during amalgamation at the MFE. Further, in the square-wave anodic stripping voltammetric (SWASV) mode, BiFEs can be operated in non-deoxygenated solutions, which is another distinct advantage compared to mercury analogues. Furthermore, BiFEs can be prepared in situ and operated in highly alkaline media, where—in contrast to precipitation of $\text{HgO}\cdot x\text{H}_2\text{O}$ hindering the formation of a mercury film—the Bi^{III} species are kept soluble as $[\text{Bi}(\text{OH})_4]^-$ complex that can be reduced during the deposition step and thus employed, for example, for selective resolution of the Tl^+ signal from the responses of $\text{Cd}^{2+} + \text{Pb}^{2+}$.

Last but not least, it should also be mentioned that the fundamental configuration of bismuth film electrodes, BiFEs, has a number of derived varieties and modifications (see references (50–52) and references therein), as well as some related counterparts.^{84,85} Concerning the former, there are the bismuth bulk electrode (BiBE), heterogeneous carbon-based electrodes modified with bismuth powder, bismuth nanoparticles, bismuth alloys or various bismuth(III) compounds, such as Bi_2O_3 , BiOCl , $(\text{BiO})_2\text{CO}_3$, specially encapsulated $\text{Bi}(\text{NO}_3)_3$, BiF_3 and NH_4BiF_4 .

The electrodes related to BiFEs or BiEs, respectively, are mainly lead film-plated electrodes (PbFEs^{84}) and antimony film electrodes (SbFEs^{85}) plus their possible variants. Especially the arrangement of SbFEs may offer surprisingly good performance in the determination of Cd and Pb in water samples requiring acidification to pH 2, which is not very suitable for BiFEs responding optimally in acetate-buffered solutions.⁵²

Nafion[®]-Coated MFEs and BiEEs

Generally higher vulnerability of both MFEs and BiFEs towards the interferences from foreign species can be effectively suppressed by coating their surface with Nafion[®].^{86–88} This perfluorinated polymer (commonly supplied in alcoholic solutions) is carefully applied onto the surface of the ex situ-plated film electrode yet prior to measurement(s). The resultant protective layer or membrane has been shown to be fairly effective against otherwise disastrous effects of industrial surfactants and other macromolecular substances. Moreover, according to reference (88) the presence of Nafion may also enhance the resultant sensitivity of BiFEs towards Zn, Cd and Pb, reflected in markedly improved signal-to-noise characteristics.

Analysis of Environmental Samples

Due to the great diversity of environmental samples, the matrix, its actual composition and its effect upon the determination of heavy metals have to be considered individually, from case to case.

Natural sweet waters, as samples with apparently the simplest matrix, can be analysed directly by stripping potentiometry, where solely appropriate buffering is needed (see references (37, 38, 48) and references therein). Compared to this, voltammetry usually requires mild digestion, such as UV irradiation²⁸; however, this operation is not even needed if highly selective pre-concentrations are available (e.g. those utilising non-electrolytic principles, open circuit and/or medium exchange; see Table 5.1 and reference (21)).

Sea and brackish waters, containing generally higher concentrations of salts (about 3 % NaCl), may represent a challenge; nevertheless, thanks to the already existing systematic investigations of some specialised teams,^{34,89,90} there is a vast archive of practically proven procedures utilising the principles of electrochemical stripping analysis and maintained for all the specificities of saline waters when applicable to each heavy metal (Table 5.1), including their mutual combinations and occurrence in various complex species.

Heavily polluted, industrial and waste waters usually undergo a thorough decomposition by modern wet-digestion methods, UV irradiation in the presence of oxidants or some special operations, such as extraction or column separation, enabling to isolate either too resistant matrix constituent(s) or the analyte itself. In electroanalytical determinations of heavy metals, all these approaches have already been successfully applied (see, e.g., references (30–33) and (16, 25) in Table 5.1).

Soil (aqueous) extracts represent another group of potentially interesting samples, providing important information about the geochemical cycles of heavy metals in the environment.^{1,6,7} The corresponding solutions contain higher concentrations of mineral acids (HNO₃, HCl and occasionally also HF, H₂SO₄ and H₃PO₄), which either have to be buffered or the target ions are isolated by extraction. Of similar nature can also be air samples or the samples of gases as such, obtained by using special sorption units and giving rise to sample solutions where the gas of interest is entrapped via a suitable reagent or in a medium with appropriately adjusted pH.

Solid specimens represented by a wide spectrum of materials, such as river/lake sediments, sewage sludge, fly ashes or various biological tissues (dried or pre-decomposed and stored in a fridge, freezer or liquid nitrogen^{20, 35}), require standard mineralisation by means of wet or dry digestion. For electroanalytical determinations, the resultant digest solutions are treated in the same way like aqueous samples.

5.2 Iron Metals and Metals from Group III–VII of the Periodical System of the Elements

Another environmentally important group of elements includes the iron metals, i.e. iron, cobalt and nickel, and some more commonly occurring metals from group III to VII from the PSE (see, e.g., references (1–3)), namely manganese, chromium,

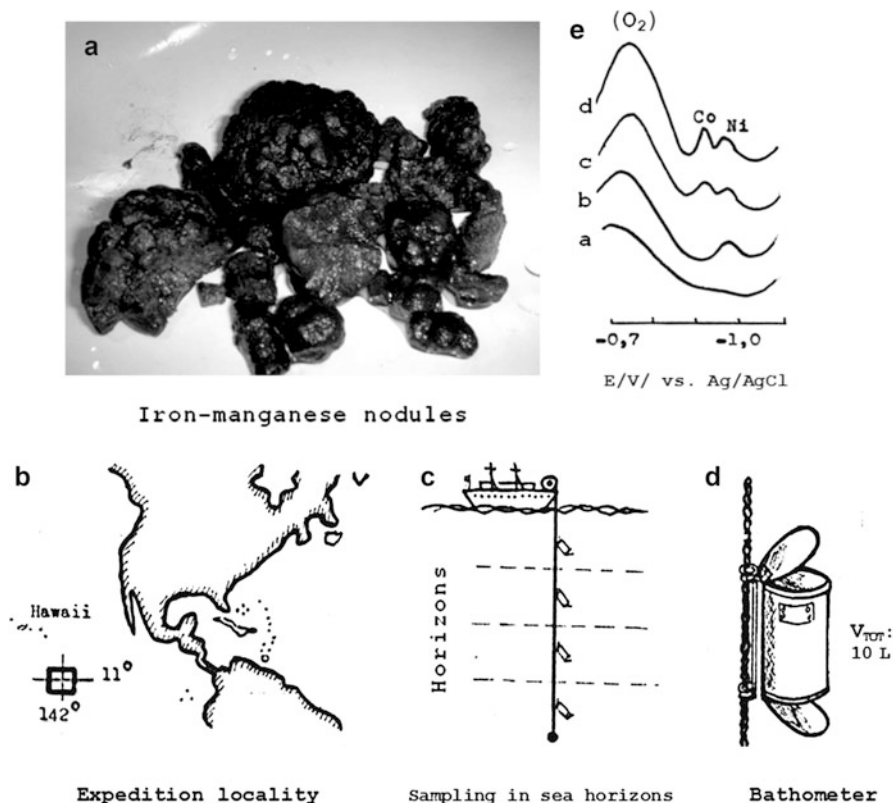


Fig. 5.2 Determination of Ni(II) and Co(II) in seawater under expeditional conditions. Legend: (a) Real appearance of the iron-manganese nodules after being explored from sea bottom; (b) main operational region of the expedition ship; (c) way of collecting samples using a series of bathometers hung upon a steel line and positioned in the different sea horizons; (d) construction of the bathometer (sampling vessel) with automated closing option, a sketch; (e) typical DPASV curves for the determination of Ni^{II}+Co^{II} at a mercury-film-plated carbon paste electrode (MF-CPE), study on the peak resolution, (a) blank, (b) model sample of synthetic seawater (buffered, containing addition of dimethylglyoxime, and spiked with Ni^{II}, (c)+(d) two additions of Co^{II} standard (taken and rearranged from references (81, 91–93); photo “a” reproduced with permission,⁹¹ images “b, d, e”,⁸¹ and scheme “c” from 93 or authors’ archives)

molybdenum, vanadium, titanium and aluminum, as well as cerium and scandium like the most abundant elements among rare earths.

A majority of metallic elements listed above belong to the so-called metals of strategic importance and their impact on the environment and human health is of continuing interest.^{4,5} Whereas, surface mining and industrial use of these metals are widely known, there are also special occurrences, such as (iron-)manganese nodules^{91,92} (see also Fig. 5.2, image “a”) —rock concretions on the sea bottom being of volcanic origin and containing, besides the two main constituents, notably high contents of Co, Ni and Cu. A potential exploitation of this raw material in

some demarcated localities is a great challenge for lengthy decades, initiating also some special expedition projects where environmental monitoring has played one of the key roles.⁹³

5.2.1 Choice of Methods and Their Basic Principles

In Table 5.2, a selected overview of typical electroanalytical methods for the determination of the above-stated elements is given.^{94–110}

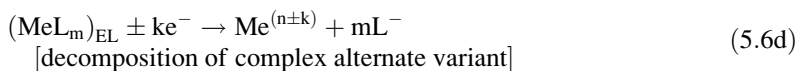
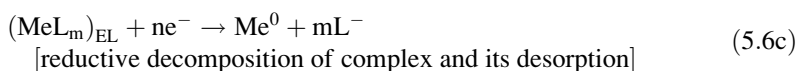
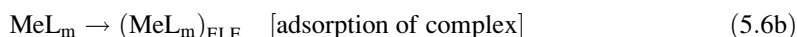
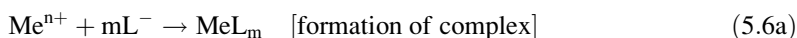
1. Electrolytic Depositions

In contrast to heavy metals mentioned before, there is apparently no practically applicable procedure that employed the accumulation of elemental Fe, Co, Ni, Mn, Cr, etc. at mercury, gold, platinum or (bare) carbon-based electrodes. The reason is poor or even impossible deposition of these metals at the electrode in ASV or PSA (see, e.g., the discussion in reference (111)). Thus, successful determination has to be accomplished via non-electrolytic accumulation with the exception of manganese which can be accumulated fairly well as MnO₂ at positive potentials.

2. Non-electrolytic Pre-concentrations with Subsequent Reductive or Oxidative Detection

Adsorptive Pre-concentration

A model procedure involving adsorption of a metallic ion can be formulated in three consecutive steps (Eqs. 5.6a–5.6d)^{54,55}:



where the index “_{EL}” means the electrode surface, “m” a stoichiometric coefficient and “Me^(n±k)” is the reduced or oxidised form of the metal (e.g. Fe^{III} → Fe²⁺ in reference (94) or Ce^{IV} → Ce³⁺ in reference (108); in both cases the resultant ions are released into the solution).

This direct adsorption of the target substance (often performed in situ, after precipitation with a reagent added to the sample) can be controlled via some experimental factors, such as actual surface conditions or homogeneity of the electrode.⁵⁴ As pointed out by numerous authors, mercury drops available with a HMDE or the array of tiny droplets of MFES are the materials of choice offering nearly an ideal surface by liquid mercury. Both configurations have been many

Table 5.2 Determination of metals of the iron and III.–VII. group of the periodical system: Selected methods and their specification

Ions/ species	Working el. (modifier)	Reference el.; auxiliary el.	Technique (mode)	Measuring principles (method sequences)	Experimental conditions: (selection)	Analytical characteristics (with $^{+}c^*$ given in mol·l ⁻¹)	Sample(s)	Ref (s)
Fe ³⁺	HMDE	Ag/AgCl	AdSV	– Adsorptive preconcentration of Fe ^{III} -catechol complexes – Subsequent cathodic stripping	SE: SS (adjusted at pH 6.9) + (PIPES buffer) + 0.1 M catechol E _{acc} –0.1 V, t _{acc} 1–5 min	LR: 6×10^{-10} to 5×10^{-8} M (3 min) LOD (t _{acc} = 3 min): 6×10^{-10} M InR.: Pb (>10 ⁻⁷ M)	Seawater	94
Fe ²⁺	MF-CFIE (in FIA cell)	SCE	S(C)P (CCSA)	– Adsorptive preconcentration of Fe ^{II/III} -SVRS complexes – Subsequent stripping by CC	SE: SS (adjusted at pH 4.5) + 1 M sodium acetate) + 0.001 M SVRS E _{acc} –0.42 V, t _{acc} 8 s	LR: 0.72×10^{-7} M LOD: 1.8×10^{-9} M In: Sn, Fe ²⁺ , Ti, Zr	Tap water	95
Ni ²⁺ , Co ²⁺	Wall-jet GCE with TMF	Ag/AgCl/ 3 M KCl; Pt tube	AdCISV (SWV, FIA)	– Electrolytic preconcentration: Me ⁿ⁺ + ne ⁻ + xHg → Me(Hg) _x – Subsequent anodic stripping: Me(Hg) _x → Me ⁿ⁺ + ne ⁻ + xHg (likely catalysed by ClO ₄ ⁻)	SE: 30 mM HEPES + 0.1 M NaClO ₄ + 10 ⁻⁴ M Hg ²⁺ E _{ads} –0.7 V, t _{acc} 60 s	LR: – LOD: 1 nM	Model solutions	96
Ni ²⁺ , Co ²⁺	Hg(Ag)FE	Ag/AgCl/ 3MKCl; Pt wire	AdSV	– Adsorptive preconcentration of Me ^{II} -ioxime complexes – Subsequent cathodic stripping reduction (of complexes)	SE: 0.1 M ammonia buffer+ 50 μM cyclohexanedione dioxime E _{ads} –0.7 V, t _{acc} 30 s	LR: 1.7×10^{-10} to 1.2×10^{-7} M (Co) (30 s), 1.7×10^{-9} to 1.7×10^{-7} M (Ni) (30 s) LOD (3σ, t _{acc} 60 s): 5.8×10^{-11} M (Co), 2.2×10^{-10} M (Ni) RR: ±5.8 % (Co), ±5.6 % (Ni) InR.: surf. (0.5 mg l ⁻¹)	CRM: rain water	97
Co ²⁺	SMDE	Ag/AgCl/ 3MKCl; Pt wire	AdCISV	– Adsorptive preconcentration of Co ^{II} -DMG complex – Subsequent detection of Co ^{II} reduction assisted by catalysis with NO ₂ ⁻	SE: 0.1 M ammonia buffer + 1×10^{-4} M DMG + 0.5 M NaNO ₂ E _{acc} –0.7 V, t _{acc} 30 s	LR: 1×10^{-10} to 8×10^{-9} M (30 s) LOD (3σ, t _{acc} 30 s): 4×10^{-11} M InR.: Zn (10 ⁴ :1), Ni (20:1)	Model solutions	98

(continued)

Table 5.2 (continued)

Ions/ species	Working el. (modifier)	Reference el.; auxiliary el.	Technique (mode)	Measuring principles (method sequences)	Experimental conditions: (selection)	Analytical characteristics (with ^{65}Zn given in $\text{mol}\cdot\text{L}^{-1}$)	Sample(s)	Ref (s)
Mn^{2+}	BIDDE	SCE; Pt wire	CSV	<ul style="list-style-type: none"> Electrolytic deposition Subsequent cathodic stripping 	<p>SE: 0.5 M NH_4NO_3 (pH 7) + 8-hydroxy-quinoline (<i>Oxzin</i>) E_{acc} +0.85 V, t_{acc} 60 s</p>	<p>LR: 1.25–25 μM LOD (3σ, t_{dep} 60 s) : 7.4×10^{-7} M</p>	Marine sediments	99
Cr^{VI}	(M)CPE (in situ modifiers: <i>Septonex</i> [®] , CTAB, CPyB)	Ag/AgCl/3MKCl; Pt plate	DPCSV	<ul style="list-style-type: none"> Ion-pairing/extractive pre-concentration of chromate ion associate(s) Subsequent cathodic stripping 	<p>SE: 0.1–0.3 M HCl + 0.1 M NaCl + 2.5–25 μM modifier E_{acc} +0.7 V, t_{acc} 300 s</p>	<p>LR: 0.5–50 μM (300 s) LOD (3σ, t_{acc} 300 s): 8×10^{-8} M (Septonex), 4×10^{-8} M (CTAB), 1×10^{-8} M (CPB) RR: 8–14 %</p>	CRMs: tea, bush, leaves, clover	100
Cr^{3+}	BIF-GCE	Ag/AgCl; Pt	AdSV (SWV)	<ul style="list-style-type: none"> Non-electrolytic accumulation of Cr^{III}-<i>Cupferron</i> complex Subsequent cathodic stripping 	<p>SE: 0.2 M PIPES buffer + 1 M KCl + 0.01 M <i>Cupferron</i> E_{acc} -0.7 V, t_{acc} 60–150 s</p>	<p>InR: Γ, Au, Ti (2:1) LR: 9.6×10^{-9} to 6.7×10^{-8} M (150 s), 3.8×10^{-8} to 2.7×10^{-7} M (60 s) LOD (3σ, t_{acc} 120 s): 1.9×10^{-9} M RR: ± 3.6 % InR: surf.(1,000:1), Zn(50:1) Ti (2:1)</p>	Tap water, tobacco, soil	101
Mo^{VI}	HMDE	Ag/AgCl/sat. KCl	AdSV (DPV)	<ul style="list-style-type: none"> Non-electrolytic accumulation of Mo^{VI}-8-hydroxy-quinoline Subsequent cathodic stripping 	<p>SE: 0.45 M HCl + 0.2 M 8-hydroxyquinoline (<i>Oxzin</i>) E_{acc} -0.2 V, t_{acc} 1–2 min</p>	<p>4×10^{-9} $\text{M}\cdot\text{L}^{-1}$ to 3×10^{-7} $\text{M}\cdot\text{L}^{-1}$ LOD (t_{acc} 10 min): 10^{-10} $\text{M}\cdot\text{L}^{-1}$</p>	Seawater	102
Mo^{VI}	BIFE (GC substrate)	Ag/AgCl; Pt wire	AdSV (SWV)	<ul style="list-style-type: none"> Synergistic pre-concentration of Mo^{VI}-chloranilate complex by electrolysis and chemisorption Subsequent cathodic stripping 	<p>SE: 0.05 M acetate buffer + 50 μM chloranilate acid + 8-hydroxyquinoline E_{acc} -0.55 V, t_{acc} 1–10 min</p>	<p>LR: 5.2×10^{-8} to 5.2×10^{-7} M (1 min) LOD (t_{acc} 10 min): 2×10^{-9} M (10 min) RR: ± 2.6 % V (20:1)</p>	Seawater	103

Mo ^{VI} , V ^V , Ti ^{IV}	(M)CPE (in situ modifier CTAB)	SCE; Pt wire	AdSV (DPV)	<ul style="list-style-type: none"> - Ion-pairs based accumulation of Me⁸⁺ as anionic oxalate in ion-associates with CTAB - Subsequent anodic stripping (with oxidation of C₂O₄²⁻) 	<p>SE for Ti: 0.05 M acetate buffer + 0.01 M oxalic acid + 10⁻⁴ M CTAB, E_{acc} = -1.2 V, for V: 0.01 M oxalic acid + 2.5 × 10⁻⁴ M CTAB, E_{acc} = -0.9 V; for Mo: 0.01 M oxalic acid + 7.5 × 10⁻⁵ M CTAB; E_{acc} = -1.2 V, t_{acc} (for all) 2–10 min</p>	<p>LR: Ti: 1 × 10⁻⁷ to 3.3 × 10⁻⁶ M (2 min)</p> <p>LOD (3σ, t_{acc} 10 min): 2 × 10⁻⁹ M</p> <p>RR: ±4 %; Me-oxalates (50:1)</p> <p>V: 4.8 × 10⁻⁸ to 2 × 10⁻⁶ M (2 min)</p> <p>LOD (3σ, t_{acc} 10 min): 1.4 × 10⁻⁹ M</p> <p>RR: ±3.5 %</p> <p>InR: Br⁻ (500:1), Me-oxalates (50:1), Zn-oxalate (500:1) Mo: 2.6 × 10⁻⁸ to 2.1 × 10⁻⁶ M (2 min)</p> <p>RR: ±3.9 %</p> <p>LOD (3σ, t_{acc} 10 min): 4.2 × 10⁻¹⁰ M</p> <p>InR: anions slightly (500:1), Ga, TI (50:1)</p>	Stone wool, fuel oil, steel	104,105
								V ^V
Al ³⁺	HMDE		AdSV (DPV)	<ul style="list-style-type: none"> - Adsorption of the Al^{III}-DASA chelate - Subsequent cathodic stripping and reduction of the ligand(s) 		<p>LR: –</p> <p>LOD: 1 nM (tads 45 s)</p>	Seawater, fresh water	107
Ce ³⁺	(M)CPE (modi- fier NHMF)	Ag/AgCl/ sat. KCl; Pt wire	AdSV	<ul style="list-style-type: none"> - Accumulation of Ce^{III}-NHMF complex - Subsequent anodic stripping (with oxidation Ce^{III} → Ce^{IV}) 	<p>SE: 0.05 M phosphate buffer (pH 7)</p> <p>E_{acc} = -0.2 V, t_{acc} 350 s</p>	<p>LR: 0.5 × 10⁻⁹ to 90 × 10⁻⁹ M</p> <p>LOD (3σ, t_{acc} = 350 s): 0.8 × 10⁻⁹ M</p> <p>RR: ±5.6 %</p> <p>In: La, Sm (50 × 10⁻⁹ M)</p>	Phosphate rock, wastewater	108

(continued)

Table 5.2 (continued)

Ions/species	Working el. (modifier)	Reference el.; auxiliary el.	Technique (mode)	Measuring principles (method sequences)	Experimental conditions: (selection)	Analytical characteristics (with "c" given in mol.l ⁻¹)	Sample(s)	Ref (s)
Sc ³⁺	CPE	SCE	AdSV	- Adsorption of Sc ^{III} -Alizarin Complexan chelate - Subsequent reduction of ligand (s) in the complex	SE: buffer pH 5.4-0.04 M acetate +0.016 M bipthalate	LR: 1×10^{-9} to 6×10^{-7} M LOD: 6×10^{-10} M RR: ± 4.34 %	Mineral samples	109
Rare earths ^a (Me _{re-L} , Me _{re-H})	CPE	SCE	AdSV (LSV)	- Adsorptive accumulation of Me _{re} -Alizarin Complexan chelates - Subsequent oxidation of the complexes	SE: 0.12 M HAAC + NaAc + 0.3 M bipthalate (pH 5) E _{acc} -0.2 V; t _{acc} up to 120 s	LR: 5×10^{-10} to 2×10^{-7} M (Ho) LOD (3 σ , t _{acc} 120 s): 6×10^{-10} M (Ho) RR: ± 3.8 %	Nodular cast iron	110

Abbreviations:

Symbols and general abbrevs.: c concentration/content, *Eacc*(*ads*/*dep* accumulation/adsorption/deposition/potential, *el.* electrode, *In*(*R*) interference (ratio), *LOD* limit of detection, *LR* linear range, *M* molar concentration (mol per litre), *min* minute(s), *RR* reproducibility/repeatability, *sat.* saturated, *SE* supporting electrolyte, *SS* sample solution, *tacc*/*dep* accumulation/deposition time

Electrodes: *BDDE* boron-doped diamond electrode, *BiFE* bismuth film electrode, *BiFE* carbon fibre electrode, *CPE* carbon paste electrode, *GCE* glassy carbon electrode, *HMDE* hanging mercury drop electrode, *Hg(Ag)/FE* silver-amalgam film electrode, *(M)CPE* (modified) carbon paste electrode, *MFE* mercury film electrode, *MWCNTs-Na/Bi* multiwall carbon nanotubes dispersed in Nafion used in combination with Bi, *SCE* saturated calomel electrode, *SMDE* static mercury drop electrode, *SP-BiFE* screen-printed bismuth film electrode

Techniques: *ASV* anodic stripping voltammetry, *Ad(C)SV* adsorptive (cathodic) stripping voltammetry, *AdCtSV* adsorptive catalytic stripping voltammetry, *CSV* cathodic stripping voltammetry, *CCSA* constant current stripping analysis, *DCASV* direct current anodic stripping analysis, *DPASV* differential pulse anodic stripping voltammetry, *DPCSV* differential pulse cathodic stripping voltammetry, *DPV* differential pulse voltammetry, *FIA* flow injection analysis, *PSA* potentiometric stripping analysis (with chemical oxidation), *S(C)P* stripping (chrono)potentiometry, *SWASV* square-wave anodic stripping voltammetry, *SWV* square-wave voltammetry
Chemicals and reagents: *CPyB* cetylpyridinium bromide, *CTAB* cetyltrimethylammonium bromide, *DASA* 1,2-dihydroxyanthraquinone-3-sulphonic acid, *NHMF* *N*-(2-hydroxy-phenyl)methylidene]-2-fluorohydrazone, *DMG* dimethylglyoxime, *HEPES* *N*-2-hydroxyethylpiperazine-*N*'-2-ethanesulphonic acid, *PIPES* piperazine-*N*, *N*'-bis-2-ethanesulphonic acid, *SVRS Solochrome violet RS*

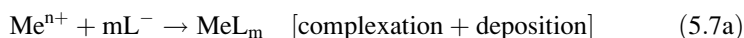
Miscellaneous: *CRM*(s) certified reference material(s), *NaAc* + *HAAC* acetate buffer, *TMF* thin mercury film

^aLight rare earths (Me_{re-L}) Y, Sc, Sm, Eu, Gd and Tb, heavy rare earths (Me_{re-H}): Dy, Ho, Er, Tm, Yb and Lu

times proven to be the most convenient substrates for adsorption/desorption processes.^{43,44,54,112}

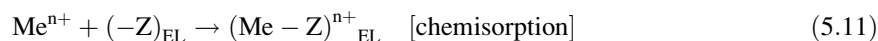
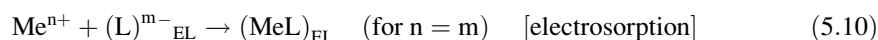
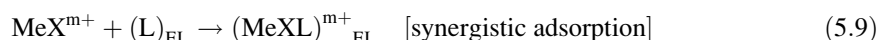
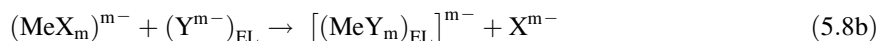
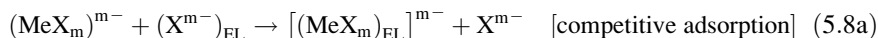
Thus, classical electrochemical stripping analysis (ESA) had spawned an offspring—adsorptive stripping voltammetry (AdSV) that became soon one of the most frequent techniques in electrochemical trace determination of metals (see, e.g., reference (113) and references therein). The determinations by AdSV and the related potentiometric method, constant current (adsorptive) stripping analysis, CCSA, are characterised by high selectivity which can be yet improved in the open-circuit arrangement and/or medium exchange.^{54,55} AdSV also offers remarkable detection capabilities down to the nanomolar level (see Table 5.2 and references (94, 97, 108, 110)).

Sometimes, adsorptive accumulation is accompanied by electrolytic pre-reduction to the elemental state (Eqs. 5.7a and 5.7b) prior to the electrochemical detection (Eq. 5.7c), e.g.



In the model equation sequence, stoichiometric coefficients are equal, $n = m$, whereas “CC” means the positive constant current of the μA intensity. This mechanism is quite typical for heavy metals due to their deposition affinity; see Table 5.1.^{18,21,25}

According to the previous classifications,^{54,55,57,114} also other adsorption processes can be distinguished—mainly for chemically modified electrodes, CMEs—depending on the accumulation principles, electrode surface conditions and actual chemical equilibria (always, in close relation with solubility products, pK_s , or conditional stability constants⁷³). Together with the already introduced schemes (Eqs. 5.6a–5.6c), there are the following possible sorption mechanisms (Eqs. 5.8a–5.11):



where the subscript “EL” means the electrode surface, and “-Z” a functional group, other abbreviations and symbols being obvious or already explained.

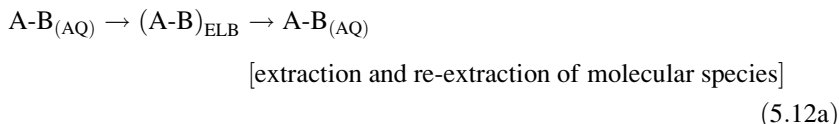
The individual mechanisms are essential for many popular methods, including the pre-concentration of Ni^{II} - and/or Co^{II} -dimethylglyoximates,^{81,93,98,115–118} Ni^{II} - and Co^{II} -nioximates,⁹⁷ $\text{Co}^{\text{II/III}}$ -1-nitroso-2-naphthol,⁸¹ Me^{N} -alizarin

complexans,^{109,110} Fe^{III}-catecholate⁹⁴ and Cr^{III}-cupferron.¹⁰¹ Regarding synergistic processes (Eqs. 5.8a, 5.8b, and 5.9), they can be represented by adsorption/extraction accumulation (e.g. reference (100)), whereas electrosorption (Eq. 5.10)—i.e. entrapment of electrically charged species via van der Waals forces—may accompany ion pairing.^{104,105} Otherwise, one can speak about synergistic adsorption when an uncharged complex of the MeX type is formed in the solution and, in parallel, interacting with another ligand (“L”) being then firmly adsorbed onto the electrode surface and rearranged into a MeXL adduct anchored by adsorption as well.⁵⁵ Finally, chemisorption (Eq. 5.11) can be utilised after immobilisation of an analyte during redox reactions¹⁰³ or, eventually, at some CMEs employing the function of inorganic/organic hybrids with reactive functional groups (“-Z”) that are able of effectively complex-binding the respective ion, Meⁿ⁺ (for typical examples, see references (55, 58–60) and references therein).

Apart from diverse mechanisms of adsorptive pre-concentrations, there is yet another valuable aspect of this process—its applicability to indirect methods, in which hardly reducible or even totally irreducible metal ions can be determined via redox transformations of ligand(s) in complexes with such metals. Typical examples are Al³⁺ (reference (119)); on HMDE, however, determinable also via direct reduction¹⁰⁷, Sc³⁺ (reference (109)) Be²⁺ (reference (120)) or ions of alkaline metals (e.g. Li⁺, Na⁺, K⁺ and Cs⁺ in reference (121)).

Extractive Accumulation

This applies to another possible way of non-electrolytic accumulation, based on spontaneous transfer and distribution of a species between two liquid phases, typically from an aqueous solution into a non-polar medium, when the role of exchanged species can be attributed to neutral molecules or ion associates with compensated charge. This is accomplished with the liquid binder in carbon paste mixtures^{55,56,122} or by liquid membranes coating the tips of potentiometric or amperometric sensors.^{123–125} In both cases, extraction (Eq. 5.12a) and the reverse process, re-extraction, take place in the electrode bulk (“ELB”) before the release from the interior to the aqueous phase (“AQ”) and the final disintegration during detection (Eq. 5.12b):



which gives rise to characteristically broad voltammetric signals or long-time responding potentiometric cells.^{122,123} Instructive information can be found in the literature.^{55,56,122}

Ion Pairing and Ion Exchange

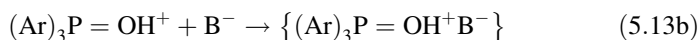
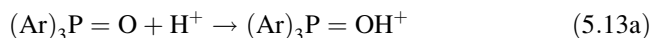
Both processes are based on electrostatic interactions between the charged analyte and a correspondingly charged reagent, either dissolved in solution or embedded in the electrode material as a bulk modifier.⁵⁵ Frequently, ion exchange and ion pairing act together or even mean the same process, which is also evident from various mechanisms reported in the literature (see reference (55) and references therein).

Compared to adsorption and extraction, the resultant effectiveness of the ion-pairing process primarily depends upon the reagent involved, whereas the “quality” of the electrode (substrate) is of lesser importance.^{55,56} A straightforward approach of ion exchange accumulation is *in situ* modification employing an ion exchanger not sooner than during the measurement, which can be advantageous if one does not want to prepare specially modified electrodes *extra* but uses a common bare sensor.

Secondly, ionic analytes of opposite charge can be immobilized and pre-concentrated by ion pairing with highly lipophilic and voluminous moieties, such as anion-attracting tetraalkyl ammonium salts (e.g. CTAB, see Table 5.2 and references (100, 104, 105)) or the long-chain alkyl-sulphonic acids for coupling with cations. Also this type of pre-concentration can be accomplished *in situ* and due to this, it can be classified as a particular case of the previous one.

Other strategies already require the preparation of CMEs containing the respective ion-pairing agent. As surveyed recently,⁵⁵ this can be achieved by two fundamental ways: (1) the direct incorporation of a solid ion exchanger into the electrode bulk, or (2) the use of liquid ion exchangers in the carbon paste configuration, where such a substance acts in a dual role—it replaces the pasting liquid/binder while being also as an ion-pairing agent.¹²⁶ Regarding both approaches, the latter is apparently more convenient because it ensures a better homogeneity of the modified electrode materials, which applies not only to CPEs, but also to the carbon inks used in manufacturing of screen-printed electrodes and sensors.^{80,127–129}

A model pathway of ion-pairing mechanisms can be shown on the above-mentioned, dually acting carbon paste binder tricresyl phosphate (TCP) as an example. This mixture of isomers is commercially available and, in electroanalysis with CPEs, an already well-established pasting liquid.¹³⁰ Abbreviating the *o,m,p*-dimethylbenzene groups by “Ar”, the process can be described by Eqs. (5.13a) and (5.13b):



where “B[−]” is the anion of interest and the structure in brackets the ion associate formed. The scheme indicates that the TCP molecule has to be protonated prior to ion pairing.¹²⁶

Finally, it should be emphasised again that the ion-pairing process is often spontaneously accompanied by extraction because all the ion pairs and ion associates bear compensated charges and—as each neutral species—naturally tend to be extracted.^{55,56,122} Similarly, a combination of ion pairing with adsorption is feasible in situations when a compact (and not penetrable) electrode substrate is being employed.

Intercalation Inside a Crystalline Structure

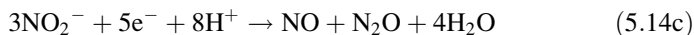
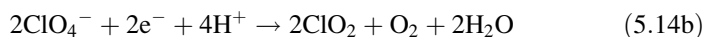
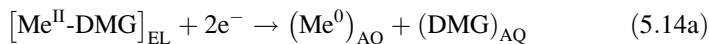
Such an insertion of a suitable substrate/modifier belongs to indeed rare non-electrochemical processes and there are only a few examples of such methods used in practical electroanalysis. Their attractiveness can be seen in its capability to determine some almost inert metal ions, such as Li^+ .¹³¹

Electrocatalytically Assisted Detections

In contrast to the previous phenomena, catalytic processes represent a relatively frequent principal approach on how to significantly enhance the resultant sensitivity of voltammetric detections.^{63,64} Actually, it had also given rise to a special technique known under the abbreviation AdCtSV, i.e. “adsorptive catalytic stripping voltammetry”.⁶⁴ In such measurements, a catalyst (or a mediator in biological reactions¹²⁵) generally accelerates and amplifies the electrode redox transformation of an analyte and the transfer of electrons, acting as a special marker (analogically to classic H_2 waves in polarography¹³²). In some processes, the resultant responses exhibit extraordinary intensities, explaining why electrocatalysis-assisted detections can be remarkably sensitive.^{63,64,98}

Evidently, (electro)catalytic measurements are the domain of CMEs,⁵⁵ when the catalyst of choice can be applied as a solid incorporated in the electrode bulk, adsorbed onto the surface, or even immobilized chemically.

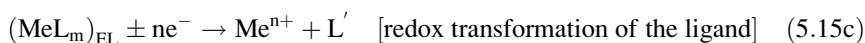
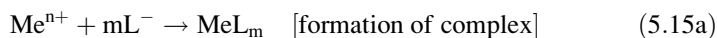
In Table 5.2, electrocatalytically assisted methods are illustrated by two characteristic examples,^{96,98} when the detection is based on the reduction of Ni^{II} - and/or Co^{II} -dimethylglyoximate (“DMG”; Eq. 5.14a) catalysed by parallel reduction of perchlorate (reference (96) Eq. 5.14b) or nitrite (reference (98) and Eq. 5.14c):



when, in both cases, the sensitivity is enhanced more than one order. According to more detailed investigations also the ligand is electrochemically converted and contributes to the current flow. As seen in the table, catalysing chemicals can be present in the solution, which is advantageous with respect to possible selection of their optimal concentration compared to a control via the content in the electrode bulk. Nevertheless, it should be mentioned that the term “catalytic”, though accepted in the literature, is somehow doubtful because the “catalyst” is consumed in the reaction. In the literature this expression is also used for mediators (modifiers at the electrode surface) whose action is mainly to decrease overpotentials.

3. Other Possibilities

In environmental electroanalysis, some less frequent approaches are potentiometric determinations with ISEs, for instance, Al^{3+} in water samples¹³³; Ca^{2+} , Mg^{2+} and K^{+} in soil extracts^{134,135}; or—with some promise—also Rb^{+} and Cs^{+} .^{136,137} Furthermore, there are setups in flowing streams^{96,116} or relatively abundant indirect methods in the AdSV mode^{104,105,107,109,110} which complete the previously introduced concepts (Eqs. 5.6a–5.11) with the following schemes (Eqs. 5.15a–5.15c):



where “L'” is the ligand after reduction (e.g. references (107, 109)) or in an oxidised form^{104,105,110} and “ Me^{n+} ” denotes the ionic form of the metal (either the original one or after release from the complex and having unchanged valence).

5.2.2 Electrochemical Methods for Environmental Analysis

Iron, cobalt and nickel belong to the most common metal elements on earth, occurring in ores and minerals, in natural waters as well as in industrial products, and their chemistry is known in detail. For these three metals, typical and widely used electroanalytical methods combine traditional principles with modern instrumentation and latest advances.

Exemplary cases are the use of classical reagents like polyhydroxy-benzenes or Solochrome violet for Fe (see Table 5.2 and references (94, 95)), 1-nitroso-2-naphthol (also known as “N-N” or “Iliinskii’s reagent”¹³⁸) for Co and mainly dimethylglyoxime (DMG or “Tschugaeff’s reagent”¹³⁹) for Ni, designed for HMDE (e.g. references (98, 115)), MFE,^{93,96,117} Ag-amalgam,⁹⁷ BiFE,¹¹⁸ CPE modified with DMG¹¹⁷ or GCE⁹⁶ in AdSV^{93,115,117} or CCSA,^{116,118} as batch measurement^{93,115–118} or FIA arrangement,⁹⁶ occasionally with some special in-field and expedition adaptations,⁸¹ the latter being documented on a collage in Fig. 5.2 (from references (81, 91–93)).

Manganese, chromium, molybdenum, vanadium, titanium, aluminium and some rare earths represent, in fact, metals of rather wavering interest, nevertheless still belonging to a portfolio of permanently monitored pollutants.

Their corresponding electroanalytical methods cannot be easily schematized; nevertheless, many of them utilise again various classical reagents like cupferron (see Table 5.2 and reference (101)), oxin¹⁰² or alizarine^{109,110} and the already discussed adsorption/desorption stripping models. In these cases, the individual determinations may be complicated by mutual interferences and therefore, a very careful optimisation of experimental conditions is almost

mandatory, especially, with respect to the supporting electrolyte composition, pH and the parameters of the potential ramp. If this is taken into account, then it is possible to elaborate and carry out numerous simultaneous determinations; see Table 5.2 and references (93, 97, 98, 104, 105, 110).

Alkaline earths (mainly Be, Mg, Ca) and alkaline metals (Li, Na, K) seem to be of somewhat marginal topic with respect to their environmental monitoring and compared to, for example, clinical and pharmaceutical analysis.^{65,140} Electrochemistry of these otherwise abundant elements is scanty and framed by a few potentially applicable ISEs^{65,133–135} or, occasionally, by some indirect methods with amperometric detection and based on the ion-exchange/exclusion principle.¹²¹ However, as shown recently, more effective use of stripping voltammetry can also be the case, namely for the determination of lithium in natural waters by DPASV.¹³¹ The sophisticated procedure utilises the reduction $\text{Mn}^{\text{IV}} \rightarrow \text{Mn}^{\text{III}}$ in manganese dioxide used as a bulk modifier of carbon paste (ca. 25 % m/m) and the consequent intercalation/insertion of Li^+ ions into the spinel structure of $\gamma\text{-MnO}_2$.

5.3 Precious Metals and Some Other Heavy-Metal Elements

The third group of chemical elements reviewed in this chapter comprises two precious metals, silver and gold, plus the sextet of Pt metals: ruthenium, rhodium, palladium, osmium, iridium and platinum. Considered will be also some less frequent heavy metals, i.e. antimony, bismuth, indium, tin (by some authors referred to as “stannum”) and uranium.

The selected elements represent the remaining environmentally important metals and, at the same, they also possess some related physicochemical and electrochemical properties. They may be related also with some associations and consequences of principal importance.¹⁴¹ Starting with silver, its environmental impact is connected now with massively popularised nanoforms of silver,¹⁴² in which the long-time known disinfectant properties of the Ag^+ species are apparently undergoing a new renaissance. In this context, the already reported hypotheses should be remembered that some toxic effects of nanosilver are due to a combination of specific properties of Ag nanoparticles with their capability to release Ag^+ ions.¹⁴²

Concerning gold, there are mainly the aspects of its surface or undersurface mining¹⁴³ apart from the fact that the respective processes are the classic procedures with its extraction by means of cyanide or elemental mercury or some more modern and environmentally friendlier ways.

Platinum metals are eventually coming into the focus with the continuing progress of their use in automobile catalysts with potential tendencies for environmental and biological accumulation.^{144,145} This concerns predominantly Pt, Pd and Rh, whereas the remaining elements are used in much minor extent. Available

evidence from analysed tissues from sediment-dwelling invertebrates and some fish exposed to polluted water with contact to road dust indicates clearly that Pt metals, especially Pd, are readily transported to biological materials and are accumulated, for example, in the human body in liver and kidneys.¹⁴⁴ A considerable danger associated with Pt metals can be attributed to their distinct catalytic properties that may initiate some mutagenic processes, including cancer. Also disposals and excretions of pharmaceuticals containing platinum, such as the chemotherapeutic agent “*cis*-platinum”, should be considered. As already quoted, the analytics of Pt metals are becoming a challenge and one of the anticipated problems in the future.

Other heavy metals including uranium also have unquestionable environmental significance, on one side bismuth as a representative of “green elements”,^{50–52} and on the other, indium and uranium as toxic elements whose more abundant occurrence in the environment is generally undesirable and, locally or even regionally, still more intensively monitored (see, e.g., references (3–5)).

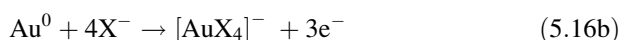
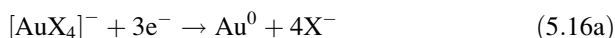
5.3.1 Choice of the Methods and Their Basic Principles

Table 5.3 summarises key facts and data from selected methods^{146–160} for the determination of the Pt metals, as well as for the other metal elements mentioned above.

1. Electrolytic Depositions

According to some authors^{55,161,162} both silver(I) and gold(III) are the best accumulation-able species among all the metals at bare carbonaceous materials like glassy carbon, pyrolytic graphite or even carbon paste. This is explained mainly by very favourable deposition/dissolution potentials positioned within the range of easily accessible positive potentials (ca. +0.1 to +0.7 V vs. Ag/AgCl), where such carbon-based electrodes offer, in general, superb signal-to-noise characteristics.¹⁶¹

Thus, many electroanalytical methods designed for electrochemical stripping have employed this type of pre-concentration (Table 5.3 and references (146, 147, 149)). Whereas the reaction pathway of Ag⁺ single ions is analogous to that shown in Eqs. (5.1a) and (5.1b) (for heavy metals), the deposition and stripping of gold are sketched in Eqs. (5.16a) and (5.16b), because trivalent gold exists mainly as an anion (tetrahalaurate):



An interesting method for the determination of silver utilizes potentiostatic deposition combined with pre-activation of the working electrode and exploiting the assistance of ion pairing which results in detection capabilities at the ubiquitous level of silver (Fig. 5.3 and reference (146)).

Table 5.3 Determination of precious metals, Pt metals and some other heavy metal elements: Selected methods and their specification

Ions/ species	Working el. (modifier)	Reference el.; auxiliary el.	Technique (mode)	Measuring principles (method sequences)	Experimental conditions: (selection)	Analytical characteristics ("c" given in mol.l ⁻¹)	Sample(s)	Ref (s)
Ag ⁺	(M)CPE (active binder: tricresyl phosphate)	SCE; Pt wire	DPASV	– Electrolytic preconcentration: $\text{Ag}^+ + \text{e}^- \rightarrow \text{Ag}^0_{\text{surf}}$ – Subsequent anodic stripping (after MEX): $\text{Ag}^0_{\text{surf}} \rightarrow \text{Ag}^+_{\text{sol}} + \text{e}^-$	SE: 0.02 M ace- tate buffer + 8.3×10^{-5} M sodium heptylsulfonate + 0.003 M EDTA $E_{\text{acc}} - 0.2$ V, t_{acc} 30 s–120 min	LR: 6.7×10^{-13} to 1.4×10^{-7} M (after cathodic activation of CPE, with t_{acc} 30 s– 120 min) LOD (15 min): 2.5×10^{-12} M InR: Bi, Cu, hg, Pt, Ir (100:1), Au(10:1)	Tap/drink- ing water	146
Ag ⁺	MF-CFIE	(–)	S(C)P (CCSA, FIA)	– Electrolytic preconcentration: $\text{Ag}^+ + \text{e}^- \rightarrow \text{Ag}^0$ – Subsequent stripping: $\text{Ag}^0 \rightarrow \text{Ag}^+ + \text{e}^-$	SE: acetonitrile + 0.2 M HClO ₄ 8.3×10^{-5} M sodium heptylsulfonate	LR: down to 5×10^{-9} M LOD(3σ): 2.2×10^{-9} M (30 min)	Model solutions	147
Ag ⁺	ISE with solid membrane (Ag ⁺ - ionofor "TBCx")	Ag/AgCl (with salt bridge)	POT (as FIA)	– Chemical equilibrium: $(\text{Ag}^+)_{\text{AQ}} + \text{Na}^+ \text{-resin} \rightarrow$ $(\text{Na}^+)_{\text{AQ}} + \text{Ag}^+ \text{-resin}$ – Potentiometric indication	SE: 1×10^{-5} M LiNO ₃ Rgn: 1×10^{-4} M AgNO ₃ (24 h)	LOD: 1×10^{-5} M (Ag ⁺) RR: ±8 % InS: nearly none form Li ⁺ , Na ⁺ , K ⁺	Model solutions	148
Au ^{III}	MF-CFIE (or Pt FIE)	SMDE	S(C)P (CCSA, FIA)	– Electrolytic preconcentration: $\text{Au}^{\text{III}} + 3\text{e}^- + \text{xHg} \rightarrow \text{Au}$ (Hg) _x – Subsequent anodic strip- ping: Au $(\text{Hg})_{\text{x}} \rightarrow \text{Au}^{\text{III}} + 3\text{e}^- + \text{xHg}$	SE: 2 M HCl + 1– 5 mg l ⁻¹ Hg ²⁺ , Cu ²⁺ $E_{\text{acc}} - 0.6$ V	LR: – LOD(3σ, 15 min): 5×10^{-9} M	Model solutions	149

Au ^{III}	CPE (with TCP, active binder)	Ag/AgCl/ Pt plate	DP(C)SV	<ul style="list-style-type: none"> - Ion-pairing of AuCl₄⁻ with protonated TCP (in SE) + - Extraction into the CP-bulk - Cathodic (reductive) stripping 	SE: 1 M HCl + 0.1 M EDTA (in open circuit) Rgn: mechanical	LR: 1×10^{-7} to 1×10^{-5} M LOD: 8×10^{-8} (10 min)	Industrial products (Au-plated components)	150
Au ^{III}	(M)CPE (montmorillonite)	Ag/AgCl/ 3 M KCl; Pt wire	DPASV	<ul style="list-style-type: none"> - Open-circuit preconcentration: $Au^{III}_{sol} \rightarrow Au^{III}_{surf}$ - Reduction: $Au^{III}_{surf} \rightarrow Au^0_{surf}$ - Subsequent anodic stripping: $Au^0_{surf} \rightarrow Au^{III}_{sol} + 3e^-$ 	SE: (a) 0.001 M HCl, MEx (b) 0.1 M KCl (pH 4.7) t_{prec} 5–10 min	LR: 8.12×10^{-7} to 6.1×10^{-6} M LOD(10 min): 8.12×10^{-7} M InR: SCN ⁻ (1:10 ⁻³), Al, Fe (1:10), Hg (1:100)	Tap and table water (model samples)	151
Pt ^{IV} , Rh ^{III}	HMDE	Ag/AgCl/ 3 M KCl; GCE	AdCtSV	<ul style="list-style-type: none"> - Adsorption of Pt^{IV}- and Rh^{III}-complexes - Subsequent cathodic stripping of Me^N-complexes 	SE: 0.2 M HCl + 0.6 M H ₂ SO ₄ + 1.2 mM N ₂ H ₅ ⁺ + 0.6 mM HCHO Pt: E _{ads} ¹ 0 V, t _{ads} ¹ 90 s Rh: E _{ads} ² -0.8 V, t _{ads} ² 120 s	LR: 0 to 3×10^{-11} M (Pt) LR: 0 to 4.9×10^{-12} M (Rh) LOD(3σ, 90 s): 1×10^{-13} M (Pt) LOD(3σ, 120 s): 5.4×10^{-14} M (Rh)	Spruce shoots	152
Pt ^{IV} , Ir ^{III} , Os ^{IV}	(M)CPE (in situ modifiers: Septonex, CTAB, CPyB)	Ag/AgCl/ 3 M KCl; GCE	DP(C)SV	<ul style="list-style-type: none"> - Accumulation of PtCl₄²⁻, IrCl₆³⁻, OsCl₆³⁻ via their ion-pairs with modifier - Subsequent cathodic stripping 	SE: 0.1 M acetate buffer + 0.15 M KCl E _{acc} +0.8 V, t _{acc} 30 s	LR: 1×10^{-6} to 10×10^{-6} M (Pt, Ir) LR: 0.1×10^{-7} to 6×10^{-7} M (Os) RR: ± 8–15 % (Pt, Ir), ± 5 % (Os) LOD(3σ): 7×10^{-7} M (Pt), 9×10^{-7} M (Ir), 5×10^{-9} M (Os)	Waste water	153

(continued)

Table 5.3 (continued)

Ions/ species	Working el. (modifier)	Reference el.; auxiliary el.	Technique (mode)	Measuring principles (method sequences)	Experimental conditions: (selection)	Analytical characteristics ("c", given in mol.l ⁻¹)	Sample(s)	Ref (s)
Pd ²⁺	Hg(Ag)FE	Ag/AgCl/ 3 M KCl; Pt wire	SWAdSV	– Accumulation of Pd ^{II} -DMG complex with modifier – Subsequent cathodic stripping	SE: 0.1 M acetate buffer (pH 4.4) + 2 × 10 ⁻⁴ DMG E _{acc} -0.45 V, t _{acc} 60 s	LR: 9 × 10 ⁻⁹ to 4.7 × 10 ⁻⁷ M RR: ±3 % LOD(3σ, 60 s): 1.4 × 10 ⁻⁹ M In: surf. 0.5 mg l ⁻¹	Tap water (spiked)	154
Sb ^{III} , Sb ^V	AuF-AuFiE	Ag/AgCl	S(C)P (CCSA, FIA)	– Electrolytic deposition: Sb ³⁺ + 3e ⁻ → Sb ⁰ – Subsequent oxidative strip- ping (with positive constant current)	SE: deposition: redox buffer with 0.01 M Fe ²⁺ in 0.1 M HCl E _{dep} -0.4 V, t _{dep} 0.5–10 min SE: stripping: 2 M HCl or 4 M HCl/4 M CaCl ₂	LR: down to 1 × 10 ⁻⁸ M RR: ±6.5 % for 5.2 × 10 ⁻⁹ M	CRMs: river water, seawater	155
Bi ³⁺	MF-GCE (as RDE)	SCE	S(C)P (PSA)	– Electrolytic deposition after acidification (by 0.1 M HCl) or oco-precipitation with Mg(OH) ₂ – Subsequent chemical stripping	SS: acidified— 0.1 M HCl E _{dep} -0.9 V, t _{dep} 8 min	LR: — LOD (2σ): 0.6 nM (0.003 nM)	Seawater	156
In ³⁺	(a) HMDE (b) MFE (GC-support)	SCE	(a) DPASV (b) DPASV	– Electrolytic preconcentration: In ³⁺ + 3e ⁻ + xHg → In(Hg) _x – Subsequent anodic strip- ping: In(Hg) _x → In ³⁺ + 3e ⁻ + xHg	SE: (a) 1 M HCl, t _{dep} 5 min SE: (b) acetate - bromide (pH 4.7) t _{dep} 5 min	LOD (3σ, t _{dep} 60 s): 4.4 × 10 ⁻⁸ M InR: Mo, Pt, PO ₄ ³⁻ (5:1), Cu (50:1)	River water	157

Sn^{2+}	SMDE	Ag/AgCl/ 3 M KCl	Ad(C)SV	– Adsorptive collection of $\text{Sn}^{\text{II/IV}}$ complexes with <i>Tropolone</i> – Subsequent cathodic stripping	SE: pH 2.1 (HCl 1:1) + 40 μM <i>Tropolone</i> E_{ads} –0.8 V, t_{ads} 5–10 min RR: $\pm 1\%$ (for 1 nM, $\pm 3\%$ (30 pM)	LR: 0–60 nM (t_{ads} 1 min) LOD (t_{ads} 10 min): 5 pM RR: $\pm 1\%$ (for 1 nM, $\pm 3\%$ (30 pM)	Estuarine water	158
U^{VI}	(M)CPE (modifier: propyl gallate	Ag/AgCl; Pt wire	DPCSV	– Accumulation of U^{VI} -propyl gallate complex – Subsequent cathodic stripping	SE: 0.002 M acetate buffer (pH 4.5) E_{acc} +0.2 V, t_{acc} 5–20 s	LR: 8.4×10^{-7} to 6.7×10^{-6} M LOD(3 σ , 60 s): 4.2×10^{-7} M In: Fe, Cr, Ti 1 mg l $^{-1}$	Ground water	159
U^{VI}	BIF-CFIE	Ag/AgCl; Pt wire	SW(C)SV	– Accumulation of U^{VI} - <i>Cupferron</i> complex – Subsequent cathodic stripping	SE: 0.1 M acetate buffer pH 4.6 + 75 μM <i>Cupferron</i> E_{acc} –0.3 V, t_{acc} 2 min	LR: 4.2×10^{-8} to 2.1×10^{-7} M RR: $\pm 3.8\%$ LOD(3 σ , 10 min): 1.3×10^{-9} M InR: Cu, Ti (2:1), phosphate (0.001 M)	Seawater	160

Abbreviations:

Symbols and general abbrevs.: *c* concentration/content, *Eacc/ads/depl* accumulation/adsorption/deposition potential, *el* electrode, *I_h(R)* interference (ratio), *h* hour(s), *LOD* limit of detection, *LR* linear range, *M* molar concentration (mol per litre), *min* minute(s), *R_{gn}* regeneration, *RR* reproducibility/repeatability, *sat.* saturated, *SE* supporting electrolyte, *SS* sample solution, *tacc/ads/depl/prec* accumulation/adsorption/deposition/pre-concentration time
Electrodes: *AuF* gold film, *AuF/IE* gold fibre electrode, *CFIE* carbon fibre electrode, *CPE* carbon paste electrode, *BiF* bismuth film, *GCE* glassy carbon electrode, *HMD* hanging mercury drop electrode, *Hg(Ag)FE* silver-amalgam film electrode, *(M)CPE* (modified) carbon paste electrode, *MF(E)* mercury film (electrode), *Pt-FIE* Platinum fibre electrode, *RDE* rotating/rotated disc electrode, *SCE* saturated calomel electrode, *SMDE* static mercury drop electrode
Techniques: *ASV* anodic stripping voltammetry, *Ad(C)SV* adsorptive (cathodic) stripping voltammetry, *AdCSV* adsorptive catalytic stripping voltammetry, *AdSV* adsorptive stripping voltammetry, *CCSA* constant current stripping analysis, *DPA* differential pulse anodic stripping voltammetry, *DPCSV* differential pulse cathodic stripping voltammetry, *DPV* differential pulse voltammetry, *FIA* flow injection analysis, *PSA* potentiometric stripping analysis (with chemical oxidation), *S(C)/P* stripping(chrono)potentiometry, *SW/ASV* square-wave anodic stripping voltammetry, *SW/AdSV* square-wave adsorptive stripping voltammetry, *SW(C)SV* square-wave (cathodic) stripping analysis
Chemicals and reagents: *CPyB* cetylpyridinium bromide, *CTAB* cetyltrimethylammonium bromide, *DMG* dimethylglyoxime, *TCP* tricresyl phosphate, *TBCxO*, *O'*-bis[2-(methylthio)ethyl]-*tert*-butylcalix[4]arene
Miscellaneous: *CRMs* certified reference materials, *MEx* medium exchange, “–” not specified

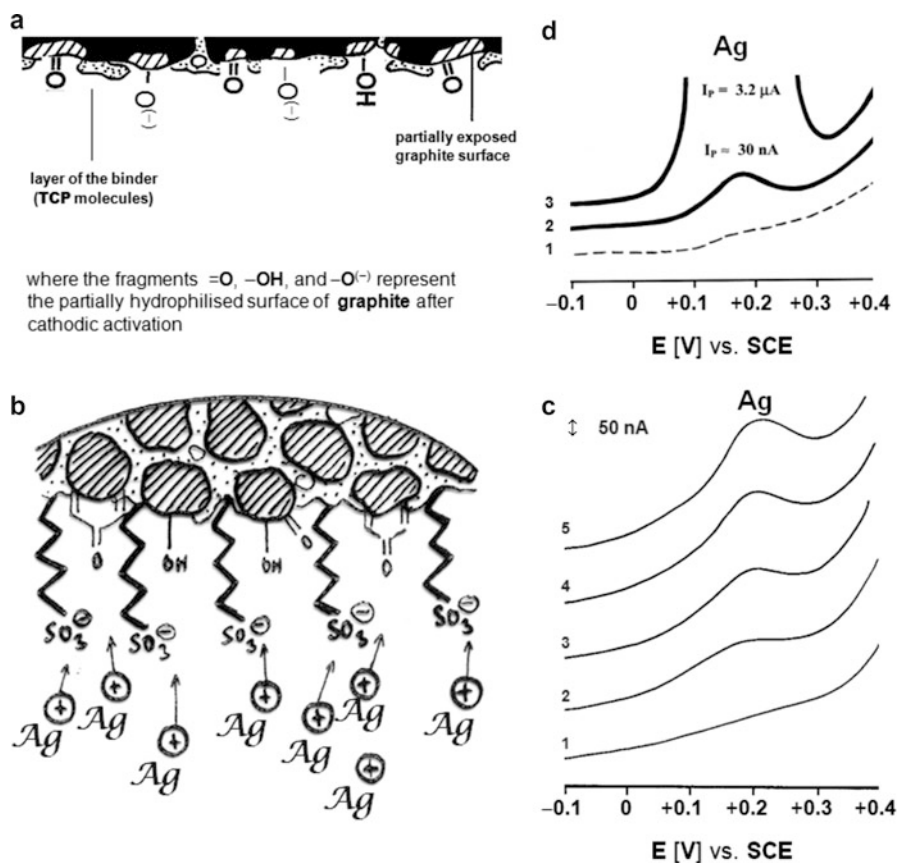


Fig. 5.3 Determination of Ag^+ ions at the ultratrace level at the activated carbon paste electrode containing tricresyl phosphate as a binder and additionally modified in situ with alkyl-sulphonate. Legend: (a) The surface states at the pre-cathodised electrode, a scheme; (b) synergistic accumulation of $\text{Ag}^{(+)}$ ions via electrolytic reduction of the single ions with $\text{Ag}^{(+)}\text{-R-SO}_3^{(-)}$ ion pairs pre-concentrated in parallel; (c) model calibration of Ag^+ ions in the DPASV regime, with pre-concentration time for 120 min, (1) baseline/blank, (2–5) $c(\text{Ag}^+)$ from 7×10^{-13} to $3 \times 10^{-12} \text{ mol L}^{-1}$; (d) special test on detection capabilities of the method, (1) blank, (2) ca. $1 \times 10^{-12} \text{ mol L}^{-1}$, (3) $1 \times 10^{-9} \text{ mol L}^{-1}$ (images “a, b, d” compiled and rearranged from the authors’ archives; “c” reproduced with permission,¹⁴⁶ for other details on experimental conditions and instrumental parameters, see the same source)

2. Non-electrolytic Pre-concentrations

In the case of Ag, Au, Pt metals and the remaining title metals, various suitably chosen non-faradaic processes and mechanisms may provide a very powerful methodical basis applicable also in environmental analysis.

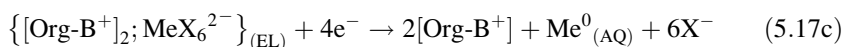
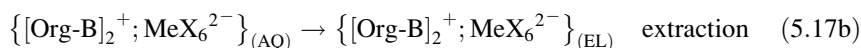
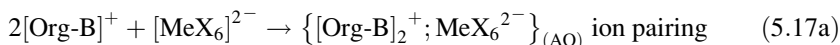
Adsorptive pre-concentration

In Table 5.3, adsorption is the main accumulation principle in several procedures, such as determination of Pd^{II} via its DMG-chelate¹⁵⁴ exploiting its formation and stability at acidic pH different to Ni^{II} or Co^{II} ¹¹⁷ pre-concentration of tin by means of

purpurocatechol (or tropolone, see reference (158)) and determination of U^{VI} via the uranyl ion, UO_2^{2+} (reference (159, 160)) whose affinity towards some classic reagents is comparable to that of other metals discussed in Sects. 5.1 and 5.2.

Extractive and ion-pairing accumulation

In many methods both mechanisms act simultaneously or one after the other.^{55,145} In any case, an anionic species, e.g. $[Me^{IV}X_6]^{2-}$, is involved and the corresponding ESA mechanism which can be formulated in the following way:



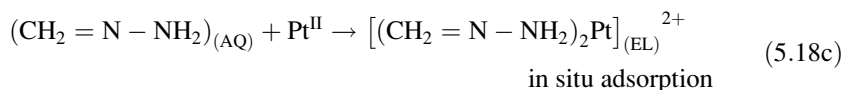
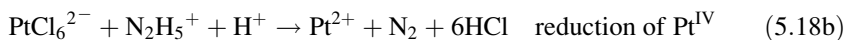
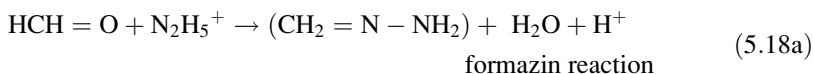
where “Org-B” represents a large cation with lipophilic organic skeleton. The same reaction pathway (Eqs. 5.17a and 5.17b) accompanied by the reductive stripping (Eq. 5.17c) was presented in reference (153).

The mechanism enabled to determine simultaneously Os, Ir and Pt, where the ion-pairing reagent was found especially efficient for Os, resulting in a LOD below the nanomolar level.¹⁶³

Electrocatalysis / Catalysis-Assisted Detection

This is a very typical feature of Pt metals, is involved in a palette of methods, which is the case of the determination of platinum via the Pt^{II} -formazon complex or similar adducts,¹⁵² representing the most frequently chosen approach to determine platinum (e.g. reference (145) and citations herein).

The original variant of the method¹⁶⁴ is based on a mutual reaction between formaldehyde and hydrazinium ions in acidic media directly in the sample solution yielding an unstable intermediate, formazin (Eq. 5.18a), that instantaneously reacts with Pt^{II} (formed meanwhile from Pt^{IV} by reduction with one of the reagent Eq. (5.18b), giving rise to the resultant complex (Eq. 5.18c):



where the subscripts “AQ” and “EL” have the same meaning like before. The complex adsorbs strongly onto the electrode surface, causing large catalytic hydrogen waves as the resultant signals to be recorded. Among the Pt metals, the whole procedure is almost specific and achieves remarkable detection limits

(far below the nM level), which has inspired some authors for elaborating further modifications and adaptations,¹⁴⁵ including those with the formation of Pt^{II}-thiosemicarbazone,¹⁶⁵ Pt^{II}-formaloxime¹⁶⁶ or Pt^{II}- and Rh^{III}-HCH=O adducts^{167,168}; all of them being capable of generating respective H₂ waves, the latter reaction is fairly applicable to detect simultaneously rhodium and platinum. Similar (electro)catalytic procedures can also be applied to determine osmium in the sample solution containing dispersed OsO₄ and BrO₃⁻ ions¹⁶⁹ or iridium via the Ir^{IV}-malachite-green complex in the presence of IO₄⁻.¹⁷⁰

Bioaccumulation of gold(III) should not be omitted at the end of this brief survey of non-electrochemical preconcentration schemes. More specifically, a green alga (*Chlorella pyrenoidosa* sp.,¹⁷¹) or thoroughly pre-dried antheral cells from *Datura innoxia* (a plant species known also as “moonflower”,¹⁷²) were shown to be the modifiers of choice for fairly selective determinations via purely bioaccumulative principles.

3. Other Possibilities

In Table 5.3 one example is included presenting the results of a study with a “non-Nernstian” ion-selective electrode¹⁴⁸; otherwise, the methods based on principles differing from those commented in points (1) and (2) are scarce (e.g. references (30–33, 55, 145)).

5.3.2 Other Electroanalytical Methods and Simultaneous Determinations

Concerning silver and gold, despite the existence of numerous sophisticated methods for their voltammetric determination (see, e.g., references (146, 150, 151)), both precious metals can be determined simply but still simultaneously using the already mentioned direct deposition at (bare) carbonaceous electrodes. The resolution of the corresponding stripping peaks is sufficient, with E_p(Ag) ca. +0.2 V vs. SCE and E_p(Au) +0.7 V, for their detection down to the nM level in LSV mode.¹⁶² Quite atypical employment of an HPLC-EC system for the determination of Ag⁺ was described recently¹⁷³ in an environmental study on the role of Ag⁺ ions in growth of some underwater plants via their reaction with –SH groups. Such thiolic compounds are also the reagents of choice in various methods with adsorptive accumulation of Ag (see, e.g., reference (174)), whereas ion pairing can be accomplished with quaternized polyvinylpyridine with immobilised [Fe(CN)₆]⁴⁻, [Mo(CN)₈]⁴⁻ and [Ir(Cl)₆]³⁻ anionic species.¹⁷⁵ In contrast to this, electrocatalytic procedures for determinations of Ag^I and Au^{III} are very rare (e.g. reference (176)).

For platinum metals, most typical approaches have already been summarized; a bio-assay can be mentioned still for the determination of platinum with a DNA-modified biosensor¹⁷⁷ operated in amperometric mode and potentially applicable to environmental samples of biological origin.

Some other and alternate methods are available also for the remaining heavy metals. For instance, in stripping voltammetry, antimony and bismuth exhibit close stripping characteristics and their dissolution signals may overlap.³⁰ To avoid this, both metals are accumulated as ion associates via the respective iodo-complexes, SbI_4^- and BiI_4^- ,¹²⁶ of which the latter is more stable,⁷³ thus permitting selective accumulation of Bi^{III} and its subsequent cathodic stripping (with reduction to Bi^0) in the presence of a tenfold concentration excess of Sb^{III} species. It has already been shown that a bismuth-film electrode, BiFE, can substitute the mercury counterparts for the determination of indium (see Table 5.3). Electrolytic deposition at BiFEs is also feasible for the determination of tin if one ensures highly acidic and/or highly saline media (e.g. 2 M HCl¹⁷⁸ or 2.5 M NaBr¹⁷⁹) that stabilise Sn^{2+} ions against hydrolysis, enhance the selectivity against potentially interfering Pb^{2+} , Cd^{2+} and Tl^+ species, as well as prevent possible oxidation of Sn^{II} to $\text{Sn}^{\text{IV}}\text{O}^{2+}$. Finally, for uranium, the use of AdSV is almost obligatory as confirmed in a recent report on its determination with the lead-film electrode, PbFE,¹⁸⁰ successfully verified on a certified reference material of natural water.

References

1. Manahan SE (2001–2012) Fundamentals of environmental chemistry, 1st–3rd edn. CRC Press, Boca Raton, FL
2. Patnaik P (1997) Handbook of environmental analysis: chemical pollutants in air, water, soil, and solid wastes. CRC Press, Boca Raton, FL
3. Reimann C, De Caritat P (1998) Chemical elements in the environment: factsheets for the geochemists and environmental scientists. Springer, Berlin
4. Manahan SE (2002) Toxicological chemistry and biochemistry, 3rd edn. Taylor & Francis, Boca Raton, FL
5. Fraga CG (2005) Relevance, essentiality and toxicity of trace elements in human health. *Mol Asp Med* 26:235–244
6. Paquin PR (ed) (2003) Metals in aquatic systems: a review of exposure, bioaccumulation, and toxicity models, Metals and the environmental series. Society of Environmental Toxicology and Chemistry (SETAC) Press, Pensacola, FL
7. Bryan GW, Langston WJ (1992) Bioavailability, accumulation and effects of heavy metals in sediments with special reference to United Kingdom estuaries: A review. *Environ Pollut* 76:89–131
8. Gadd GM (1993) Interaction of fungi with toxic metals. *New Phytol* 124:25–60
9. Goodyear KL, McNeill S (1999) Bioaccumulation of heavy metals by aquatic macro-invertebrates of different feeding guilds: a review. *Sci Total Environ* 229:1–19
10. Vinodhini R, Narayanan M (2008) Bioaccumulation of heavy metals in organs of fresh water fish *Cyprinus carpio* (common carp). *Int J Environ Sci Technol* 5:179–182
11. Florence TM (1972) Determination of trace metals in marine samples by anodic stripping voltammetry. *J Electroanal Chem* 35:237–245
12. Jagner D, Aren K (1979) Potentiometric stripping analysis for zinc, cadmium, lead and copper in sea water. *Anal Chim Acta* 107:29–35
13. Van den Berg CMG (1986) Determination of copper, cadmium and lead in seawater by cathodic stripping voltammetry of complexes with 8-hydroxyquinoline. *J Electroanal Chem* 215:111–121

14. Prado C, Wilkins SJ, Marken F, Compton RG (2002) Simultaneous electrochemical detection and determination of lead and copper at boron-doped diamond film electrodes. *Electroanalysis* 14:262–272
15. Daniele S, Bragato C, Baldo AM (1997) An approach to the calibrationless determination of copper and lead by anodic stripping voltammetry at thin mercury film microelectrodes. Application to well water and rain. *Anal Chim Acta* 346:145–156
16. Kadara RO, Tothill IE (2004) Stripping chronopotentiometric measurements of lead(II) and cadmium(II) in soils extracts and waste waters using a bismuth film screen-printed electrode assembly. *Anal Bioanal Chem* 378:770–775
17. Xu H, Zeng L-P, Xing S-J, Xian Y-Z, Shi G-Y, Jin L-T (2008) Ultrasensitive voltammetric detection of trace lead(II) and cadmium(II) using MWCNTs-Nafion/bismuth composite electrodes. *Electroanalysis* 20:2655–2662
18. Mikysek T, Švancara I, Vytřas K, Banica FG (2008) Functionalised resin-modified carbon paste sensor for the voltammetric determination of Pb(II) within a wide concentration range. *Electrochem Commun* 10:242–245
19. De Carvalho LM, do Nascimento PC, Koschinsky A, Bau M, Stefanello RF, Spengler C, Bohrer D, Jost C (2007) Simultaneous determination of Cd, Pb, Cu, and Tl in highly saline samples by anodic stripping voltammetry using mercury-film and bismuth film electrodes. *Electroanalysis* 19:1719–1726
20. Švancara I, Ostapczuk P, Arunachalam J, Emons H, Vytřas K (1997) Determination of thallium in environmental samples using potentiometric stripping analysis. Method development. *Electroanalysis* 9:26–31
21. Diewald W, Kalcher K, Neuhold C, Cai X-H, Magee RJ (1993) Voltammetric behavior of thallium(III) on carbon paste electrodes chemically modified with an anion exchanger. *Anal Chim Acta* 273:237–244
22. Sipos L, Valenta P, Nurnberg HW, Branica M (1977) Applications of polarography and voltammetry to marine and aquatic chemistry. A new voltammetric method for study of mercury traces in sea and inland waters. *J Electroanal Chem* 77:263–266
23. Gustavsson I (1986) Determination of mercury in sea water by stripping voltammetry. *J Electroanal Chem* 214:31–36
24. Jagner D (1979) Potentiometric stripping analysis for mercury. *Anal Chim Acta* 105:33–41
25. Turyan I, Mandler D (1994) Electrochemical determination of ultralow levels (below 10–12 M) of mercury by anodic stripping voltammetry using a chemically modified electrode. *Electroanalysis* 6:838–843
26. Bodewig FG, Valenta P, Nurnberg HW (1982) Trace determination of As(III) and As(V) in natural waters by differential pulse anodic stripping voltammetry. *Fresenius' Z Anal Chem* 311:187–191
27. Huang H-L, Jagner D, Renman L (1988) Flow potentiometric and constant current stripping analysis for arsenic(V) without prior chemical reduction to arsenic(III): application to the determination of total arsenic in seawater and urine. *Anal Chim Acta* 207:37–46
28. Švancara I, Vytřas K, Bobrowski A, Kalcher K (2002) Determination of arsenic at a gold-plated carbon paste electrode using constant current stripping analysis. *Talanta* 58:45–55
29. Van den Berg CMG, Khan S-H (1990) Determination of selenium in seawater by adsorptive cathodic stripping voltammetry. *Anal Chim Acta* 231:221–229
30. Vydra F, Štulík K, Juláková E (1976) *Electrochemical stripping analysis*. Ellis Horwood, Chichester
31. Brainina Kh, Neiman E (1993) *Electroanalytical stripping methods*. Wiley, New York
32. Wang J (1982) Anodic stripping voltammetry as an analytical tool. *Environ Sci Technol* 16:104A–109A
33. Wang J (1985) *Stripping analysis: principles, instrumentation, and application*. VCH Publishers, Deerfield Beach, FL

34. Florence TM (1989) Electrochemical techniques for trace element speciation in waters. In: Batley GE (ed) Trace element speciation: analytical methods and problems. CRC Press, Boca Raton, FL, pp 77–116
35. Ostapczuk P, Froning M (1992) Advanced electrochemical techniques for the determination of heavy metals in specimen bank materials. In: Rossbach M, Schlodot JD, Ostapczuk P (eds) Specimen banking—environmental monitoring and modern analytical approaches. Springer, Berlin, pp 153–165
36. Compton RG, Banks CE (2011) Understanding voltammetry, 2nd edn. Imperial College Press, London
37. Jagner D (1982) Potentiometric stripping analysis: a review. *Analyst (UK)* 107:593–599
38. Graabæk AM, Jeberg B (1992) Trace element analysis by computerized stripping potentiometry. *Intern Labor* 22:33–38
39. Compton RG, Foord JS, Marken F (2003) Electroanalysis at diamond-like and doped-diamond electrodes. *Electroanalysis* 15:349–363
40. Heyrovský J (1922) Electrolysis with a mercury drop cathode (in Czech). *Chem Listy XVI*:258–264
41. Nurnberg HW (1977) Potentialities and applications of advanced polarographic and voltammetric methods in environmental research and surveillance of toxic metals. *Electrochim Acta* 22:935–949
42. Kemula W, Kublik Z (1958) The hanging mercury drop electrode. *Anal Chim Acta* 18:104–108
43. Florence TM (1970) Anodic stripping voltammetry with a glassy carbon electrode mercury-plated in situ. *J Electroanal Chem* 27:273–278
44. Economou A, Fielden PR (2003) Mercury film electrodes: developments, trends and potentialities for electroanalysis. *Analyst (UK)* 128:205–212
45. Prabakar SJ, Sakthivel C, Narayanan SS (2011) Hg(II) immobilized MWCNT graphite electrode for the anodic stripping voltammetric determination of lead and cadmium. *Talanta* 85:290–297
46. Metelka R, Vytřas K, Bobrowski A (2000) Effect of the modification of mercuric oxide on the properties of mercury films at HgO-modified carbon paste electrodes. *J Solid State Electrochem* 4:348–352
47. Gumiński C (1989) Selected properties of simple amalgams. A review. *J Mater Sci* 24:2661–2676
48. Ostapczuk P (1993) Present potentials and limitations in the determination of trace elements by potentiometric stripping analysis. *Anal Chim Acta* 273:35–40
49. Wang J, Lu J-M, Hočevár SB, Farias PAM, Ogorevc B (2000) Bismuth-coated carbon electrodes for anodic stripping voltammetry. *Anal Chem* 72:3218–3222
50. Švancara I, Prior C, Hočevár SB, Wang J (2010) A decade of bismuth-modified electrodes in electroanalysis. *Electroanalysis* 22:1405–1420
51. Yáñez-Sedeño P, Pingarrón JM, Hernández L (2012) Bismuth electrodes. In: De la Guardia M, Garrigues S (eds) Handbook of green analytical chemistry. Wiley, New York, p 262–268 and 282–284
52. Economou A (2005) Bismuth-film electrodes: recent developments and potentialities for electroanalysis. *Trends Anal Chem* 24:334–340
53. Švancara I, Baldrianová L, Tesařová E, Vlček M, Vytřas K, Sotiropoulos S (2007) Microscopic studies with bismuth-modified carbon pastes: morphological changes of bismuth microstructures and related observations. In: Vytřas K, Kalcher K (eds) Sensing in electroanalysis, vol 2. University of Pardubice, Czech Rep, pp 35–58
54. Paneli MG, Voulgaropoulos A (1993) Applications of adsorptive stripping voltammetry in the determination of trace and ultratrace metals. *Electroanalysis* 5:355–373
55. Švancara I, Kalcher K, Walcarius A, Vytřas K (2012) Electroanalysis with carbon paste electrodes. CRC Press, Boca Raton, FL

56. Zima J, Švancara I, Pecková K, Barek J (2009) Carbon paste electrodes for the determination of detrimental substances in drinking water. In: Lefèbvre MH, Roux MM (eds) *Progress on drinking water research*. Nova, Hauppauge, NY, pp 1–54
57. Kalcher K (1990) Chemically modified carbon paste electrodes in voltammetric analysis. *Electroanalysis* 2:419–433
58. Walcarius A (1999) Zeolite-modified electrodes in electroanalytical chemistry. *Anal Chim Acta* 384:1–16
59. Walcarius A (2001) Electroanalysis with pure, chemically modified, and sol-gel-derived silica-based materials (an overview). *Electroanalysis* 13:701–718
60. Walcarius A (2008) Electroanalytical applications of microporous zeolites and mesoporous (organo)silicas: recent trends. *Electroanalysis* 20:711–738
61. Torresday JG, Darnall D, Wang J (1988) Bioaccumulation and measurement of copper at an alga-modified carbon paste electrode. *Anal Chem* 60:72–76
62. Dempsey E, Smyth MR, Richardson DHS (1992) Application of lichen-modified carbon paste electrodes to the voltammetric determination of metal ions in multi-element and speciation studies. *Analyst (UK)* 117:1467–1470
63. Bobrowski A, Zarebski J (2000) Catalytic systems in adsorptive stripping voltammetry: a review. *Electroanalysis* 12:1177–1186
64. Bobrowski A, Zarebski J (2008) Catalytic adsorptive stripping voltammetry at film electrodes. *Curr Anal Chem* 4:191–201
65. Veselý J, Weis D, Štulík K (1978) *Analysis with ion-selective electrodes*. E. Horwood, Chichester
66. Bakker E, Pretsch E (2005) Potentiometric sensors for trace level analysis. *Trends Anal Chem* 24:199–207
67. Sokalski T, Ceresa A, Zwickl T, Pretsch E (1997) Large improvement of the lower detection limit of ion-selective polymer membrane electrodes. *J Am Chem Soc* 119:11347–11348
68. Gil EP, Ostapczuk P (1994) Potentiometric stripping determination of mercury(II), selenium (IV) copper(II) and lead(II) at a gold film electrode in water samples. *Anal Chim Acta* 293:55–65
69. Štulík K, Pacáková V (1987) *Electroanalytical measurements in flowing liquids*. Ellis Horwood, Chichester
70. Wang J (1990) Modified electrodes for electrochemical detection in flowing streams. *Anal Chim Acta* 234:41–48
71. Luque de Castro MD, Izquierdo A (1991) Flow-injection stripping analysis. A review. *Electroanalysis* 3:457–467
72. Švancara I, Vytřas K, Hua C, Smyth MR (1992) Voltammetric determination of mercury (II) at a carbon paste electrode in aqueous solutions containing tetra-phenylborate ion. *Talanta* 39:391–396
73. Kotrlý S, Šůcha L (1985) *Handbook of chemical equilibria in analytical chemistry: tables and diagrams*. Ellis Horwood, Chichester
74. Trnková L (2005) Identification of current nature by elimination voltammetry with linear scan. *J Electroanal Chem* 582:258–266
75. Mocák J, Janiga I, Rievaj M, Bustin D (2007) The use of fractional differentiation or integration for signal improvement. *Meas Sci Rev* 7(1):39–42
76. Švancara I, Baldrianova L, Tesarova E, Mikysek T, Vytřas K (2007) Anodic stripping voltammetry at bismuth-modified electrodes in ammonia-buffered media. *Sci Pap Univ Pardubice A* 12:5–19
77. Ostapczuk P (1994/1995) Personal communication
78. Zakharchuk NF, Brainina KZ (1998) The surface morphology of mercury plated glassy carbon electrodes and stripping voltammetry of heavy metals. *Electroanalysis* 10:379–386
79. Švancara I, Fairouz M, Ismail K, Metelka R, Vytřas K (2003) A contribution to the characterisation of mercury- and bismuth film carbon paste electrodes in stripping voltammetry. *Sci Pap Univ Pardubice A* 9:31–48

80. Švancara I, Metelka R, Tesařová E (2006) Stripping voltammetry at mercury film plated carbon paste- and screen-printed electrodes. Ten years of advanced laboratory practice for students at the University of Pardubice. *Sci Pap Univ Pardubice A* 11:343–361
81. Renger F, Švancara I, Šuška M (1992) Voltammetric determination of nickel(II) and cobalt (II) at a carbon paste electrode and its application under expedition conditions. *Sb Ved Pr, Vys Sk Chemickotechnol, Pardubice* 56:5–19
82. Achterberg EP, van den Berg CMG (1994) Automated voltammetric system for shipboard determination of metal speciation in sea water. *Anal Chim Acta* 284:463–471
83. Navrátil T, Švancara I, Mrázová K, Nováková K, Šestáková I, Heyrovský M, Pelclová D (2011) Mercury and mercury electrodes: the ultimate battle for the naked existence (a consideration). In: Kalcher K, Metelka R, Švancara I, Vytřas K (eds) *Sensing in electroanalysis*, vol VI. University Press Centre, Pardubice, Czech Rep, pp 23–53
84. Korolczuk M, Tyszczyk K, Grabarczyk M (2005) Adsorptive stripping voltammetry of Ni and Co at in-situ plated lead film electrode. *Electrochem Commun* 7:1185–1189
85. Hočevar SB, Švancara I, Ogorevc B, Vytřas K (2007) Antimony film electrode for electrochemical stripping analysis. *Anal Chem* 79:8639–8643
86. Economou A, Fielden PR (1993) Adsorptive stripping voltammetry on mercury film electrodes in the presence of surfactants. *Analyst (UK)* 118:1399–1403
87. Wang J, Deo RP, Thongngamdee S, Ogorevc B (2001) Effect of surface-active compounds on the stripping voltammetric response of bismuth film electrodes. *Electroanalysis* 13:1153–1156
88. Kefala G, Economou A, Voulgaropoulos A (2004) A study of nafion-coated bismuth-film electrodes for the determination of trace metals by anodic stripping voltammetry. *Analyst (UK)* 129:1082–1090
89. Van den Berg CMG (1983) Trace metal speciation in seawater (a review). *Anal Proc* 20:458–460
90. Bond AM, Heritage ID, Thormann W (1986) Strategy for trace metal determination in seawater by anodic stripping voltammetry using a computerized multitime-domain measurement method. *Anal Chem* 58:1063–1066
91. (Anonymous) (2013) Wikipedia: Manganese nodule. http://en.wikipedia.org/wiki/Manganese_nodule. Downloaded 5 July 2013
92. (Anonymous) (2013) CENSIN resources: The future of iron-manganese nodules. <http://www.censin.com/manganese-nodules-mines/>. Downloaded 5 July 2013
93. Švancara I (1988) Application of carbon paste electrodes in voltammetric determination of low concentrations of nickel(II) and cobalt(II) ions. MSc dissertation (in Czech), University of Chemical Technology, Pardubice, Czech Rep.
94. Van den Berg CMG, Huang ZQ (1984) Determination of iron in seawater using cathodic stripping voltammetry preceded by adsorptive collection with the hanging mercury drop electrode. *J Electroanal Chem* 177:269–280
95. Hua C, Jagner D, Renman L (1988) Constant-current stripping analysis for iron(III) by adsorptive accumulation of its solochrome violet RS complex on a carbon-fiber electrode. *Talanta* 35:597–600
96. Brett CMA, Garcia MBQ, Lima JLFC (1996) Square-wave adsorptive stripping voltammetry of nickel and cobalt at wall-jet electrodes in continuous flow. *Electroanalysis* 8:1169–1173
97. Kapturski P, Bobrowski A (2008) The silver amalgam film electrode in catalytic adsorptive stripping voltammetric determination of cobalt and nickel. *J Electroanal Chem* 617:1–6
98. Bobrowski A, Bond AM (1992) Exploitation of the nitrite catalytic effect to enhance the sensitivity and selectivity of the adsorptive stripping voltammetric method for the determination of cobalt with dimethylglyoxime. *Electroanalysis* 4:975–979
99. Banks CE, Kruusma J, Moore RR, Tomčík P, Peters J, Davis J, Komorosky-Lovrić Š, Compton RG (2005) Manganese detection in marine sediments: anodic vs. cathodic stripping voltammetry. *Talanta* 65:423–429

100. Švancara I, Foret P, Vytrás K (2004) A study on the determination of chromium as chromate at a carbon paste electrode modified with surfactants. *Talanta* 64:844–852
101. Chatzitheodorou E, Economou A, Voulgaropoulos A (2004) Trace determination of chromium by square-wave adsorptive stripping voltammetry on bismuth film electrodes. *Electroanalysis* 16:1745–1754
102. Van den Berg CMG (1985) Direct determination of molybdenum in seawater by adsorption voltammetry. *Anal Chem* 57:1532–1536
103. Wang J, Thongngamdee S, Lu D-L (2006) Adsorptive stripping voltammetric measurements of trace molybdenum at Bi-film electrode. *Electroanalysis* 18:59–63
104. Stadlober M, Kalcher K, Raber G (1998) Voltammetric determination of titanium, vanadium, and molybdenum using a carbon paste electrode modified with cetyltrimethylammonium bromide. *Sci Pap Univ Pardubice A* 3:103–137
105. Stadlober M, Kalcher K, Raber G, Neuhold C (1996) Anodic stripping voltammetric determination of titanium(IV) using a carbon paste electrode modified with cetyltrimethylammonium bromide. *Talanta* 43:1915–1924
106. Van den Berg CMG, Zi QH (1984) Direct electrochemical determination of dissolved vanadium in seawater by cathodic stripping voltammetry with the hanging mercury drop electrode. *Anal Chem* 56:2383–2386
107. Van den Berg CMG, Murphy K, Riley JP (1986) The determination of aluminum in seawater and fresh-water by cathodic stripping voltammetry. *Anal Chim Acta* 188:177–185
108. Javanbakht M, Khoshafar H, Ganjali MR, Norouzi P, Adib M (2009) Adsorptive stripping voltammetric determination of nanomolar concentration of cerium(III) at a carbon paste electrode modified by N' -[(2-hydroxyphenyl) methylidene]-2-furo-hydrazide. *Electroanalysis* 21:1605–1610
109. Li J, Yi F, Shen D, Fei J (2002) Adsorptive stripping voltammetric study of scandium-alizarin complexan complex at a carbon paste electrode. *Anal Lett* 35:1361–1372
110. Li J, Liu S, Mao X, Gao P, Yan Z (2004) Trace determination of rare earths by adsorption voltammetry at a carbon paste electrode. *J Electroanal Chem* 561:137–142
111. Olson C, Adams RN (1963) Carbon paste electrodes: application to cathodic reductions and anodic stripping voltammetry. *Anal Chim Acta* 29:358–363
112. Van den Berg CMG (1989) Adsorptive cathodic stripping voltammetry of trace elements in sea water. *Analyst (UK)* 114:1527–1530
113. Kalvoda R (1994) Review of adsorptive stripping voltammetry—assessment and prospects. *Fresenius J Anal Chem* 349:565–570
114. Lovrić M (2002) Stripping voltammetry. In: Scholz F (ed) *Electroanalytical methods: guide to experiments and applications*. Springer, Berlin, pp 200–203
115. Pihlar B, Valenta P, Nurnberg HW (1981) New high-performance analytical procedure for the voltammetric determination of nickel in routine analysis of waters, biological materials and food. *Fresenius' Z Anal Chem* 307:337–346
116. Baldwin RP, Christensen JK, Kryger L (1986) Voltammetric determination of traces of nickel (II) at a chemically modified electrode based on dimethylglyoxime-containing carbon paste. *Anal Chem* 58:1790–1798
117. Gil EP, Ostapczuk P (1993) Nickel and cobalt determination by constant current stripping potentiometry: 1. Method development & 2. Modifications and check of the method. *Fresenius J Anal Chem* 346:952–956, 957–960
118. Hutton EA, Hočevár SB, Ogorevc B, Smyth MR (2003) Bismuth film electrode for simultaneous adsorptive stripping analysis of trace cobalt and nickel using constant current chronopotentiometric and voltammetric protocol. *Electrochem Commun* 5:765–769
119. Cai QT, Khoo SB (1993) Differential pulse voltammetric determination of aluminum at a 8-hydroxyquinoline modified carbon paste electrode. *Bull Singapore Natl Inst Chem* 21:157–170

120. Sun CL, Wang JY, Hun W, Xie TA (1992) Adsorption voltammetry of beryllium in the presence of 4-[(4-diethylamino-2-hydroxyphenyl)azo]-5-hydroxy-naphthalene-2,7-disulphonic acid (Beryllon III). *Anal Chim Acta* 259:319–323
121. Walcarius A, Mariaulle P, Louis C, Lamberts L (1999) Amperometric detection of nonelectroactive cations in electrolyte-free flow systems at zeolite modified electrodes. *Electroanalysis* 11:393–400
122. Švancara I, Schachl K (1999) Testing of unmodified carbon paste electrodes. *Chem List* 93:490–499
123. Vytřas K, Švancara I (2007) Carbon paste-based ion-selective electrodes. In: Vytřas K, Kalcher K (eds) *Sensing in electroanalysis*, vol 2. Univ. Pardubice Press Centre, Pardubice, Czech Rep, pp 7–22
124. De Marco R, Clarke G, Pejcic B (2007) Ion-selective electrode potentiometry in environmental analysis. *Electroanalysis* 19:1987–2001
125. Badihi Mossberg M, Buchner V, Rishpon J (2007) Electrochemical biosensors for pollutants in the environment. *Electroanalysis* 19:2015–2028
126. Švancara I, Vytřas K (1993) Voltammetry with carbon paste electrodes containing membrane plasticizers used for PVC-based ion-selective electrodes. *Anal Chim Acta* 273:195–204
127. Kalcher K, Schachl K, Švancara I, Vytras K, Alemu H (1997) Recent progress in the development of electrochemical carbon paste sensors. *Sci Pap Univ Pardubice A* 3:57–85
128. Hart JP, Wring SA (1997) Recent developments in the design and application of screen-printed electrochemical sensors for biomedical, environmental and industrial analyses. *Trends Anal Chem* 16:89–103
129. Hart JP, Crew A, Crouch E, Honeychurch KC, Pemberton RM (2004) Some recent designs and developments of screen-printed carbon electrochemical sensors/bio-sensors for biomedical, environmental, and industrial analyses. A review. *Anal Lett* 37:789–830
130. Guzvány V, Papp ZS, Švancara I, Vytřas K (2012) Electroanalysis of insecticides at carbon paste electrodes with particular emphasis on neonicotinoid derivatives. In: Perveen F (ed) *Insecticides: advances in integrated pest management*. INTECH/Open Access Publisher, Rijeka, Croatia, pp 541–578
131. Teixeira MFS, Bergamini MF, Bocchi N (2004) Lithium ions determination by selective pre-concentration and differential pulse anodic stripping voltammetry using a carbon paste electrode with a spinel-type manganese oxide. *Talanta* 62:603–609
132. Heyrovský J, Kůta F (1966) *Principles of polarography*. Academic, New York
133. Arvand M, Asadollah Zadeh SA (2008) Ion-selective electrode for the aluminum determination in pharmaceutical substances, tea leaves, and water samples. *Talanta* 75:1046–1054
134. Cheng K-L, Hung J-C, Prager DH (1973) Determination of exchangeable calcium and magnesium in soil by ion-selective electrode method. *Microchem J* 18:256–261
135. Cieřla J, Ryzak M, Bieganowski A, Tkaczyk P, Walczak RT (2007) Use of ion selective electrodes for determination of content of potassium in Egner-Rhiem soil extracts. *Res Agric Eng* 53:29–33
136. Hyun M-H, Piao M-H, Cho Y-J, Shim Y-B (2004) Ionophores in rubidium ion-selective membrane electrodes. *Electroanalysis* 16:1785–1790
137. Cadogan A, Diamond D, Smyth MR, Svehla G, McKervey MA, Seward EM, Harris SJ (1990) Caesium-selective poly(vinyl chloride) membrane electrodes based on calix[6]arene esters. *Analyst* 115:1207–1210
138. Iliinskii M (1884) *Ber.** 17:2581–2593. *) “Chemische Berichte”
139. Tschugaeff L (1905) About a new sensitive reagent for nickel (in German). *Berichte Deutsch Chem Gesellschaft* 38:2520–2522
140. Ozkan SA (2012) *Electrochemical methods in pharmaceutical analysis and their validation*. HNB Publishing, New York
141. Adren AW, Bober TW (eds) (2002) *Silver in the environment: transport, fate, and effects*. SETAC Press, Pensacola, FL

142. Wijnhoven SWP, Peijnenburg WJGM, Herberts CA, Hagens WI, Oomen AG, Heugens EHW, Roszek B, Bisschops J, Gosens I, van de Meent D, Dekkers S, deJong WH, van Zijverden M, Sips AJAM, Geertsma RE (2009) Nano-silver: a review of available data and knowledge gaps in human and environmental risk assessment. *J Nanotoxicol* 3:109–138
143. (Anonymous) (2013) EU-Commission: The environmental impact of gold production. <http://ec.europa.eu/environment/integration/research/newsalert/pdf/302na5.pdf>. Downloaded 10 July 2013
144. Ek KH, Morrison GM, Rauch S (2004) Environmental routes for platinum group elements to biological materials: a review. *Sci Total Environ* 334–335:21–38
145. Locatelli C (2007) Voltammetric analysis of trace levels of platinum group metals: principles and applications (a review). *Electroanalysis* 19:2167–2175
146. Švancara I, Kalcher K, Diewald W, Vytřas K (1996) Voltammetric determination of silver at ultratrace levels using a carbon paste electrode with improved surface characteristics. *Electroanalysis* 8:336–342
147. Huang HL, Jagner D, Renman L (1988) Flow potentiometric and constant-current stripping analysis for silver(I) with carbon-fiber and platinum-fiber electrodes. *Anal Chim Acta* 207:27–35
148. Ceresa A, Radu A, Peper S, Bakker E, Pretsch E (2002) Rational design of potentiometric trace level ion sensors: a Ag(+)-selective electrode with a 100 ppt detection limit. *Anal Chem* 74:4027–4036
149. Huang HL, Jagner D, Renman L (1988) Computerized flow constant-current stripping analysis for gold(III) with carbon or platinum fiber electrodes. *Anal Chim Acta* 208:301–306
150. Vytřas K, Švancara I, Renger F, Srey M, Vaňková R, Hvizdalová M (1993) Voltammetric and potentiometric determination of gold in gold-plated electrotechnical components. *Collect Czechoslov Chem Commun* 58:2039–2046
151. Navrátilová Z, Kula P (2000) Determination of gold using clay modified carbon paste electrode. *Fresenius J Anal Chem* 367:369–372
152. Leon C, Emons H, Ostapczuk P, Hoppstock K (1997) Simultaneous ultratrace determination of platinum and rhodium by cathodic stripping voltammetry. *Anal Chim Acta* 356:99–104
153. Švancara I, Galík M, Vytřas K (2007) Stripping voltammetric determination of platinum metals at a carbon paste electrode modified with cationic surfactants. *Talanta* 72:512–518
154. Bobrowski A, Gawlicki M, Kapturski P, Mirceski V, Spasovski F, Zarebski J (2009) The silver amalgam film electrode in adsorptive stripping voltammetric determination of palladium(II) as its dimethyldioxime complex. *Electroanalysis* 21:36–40
155. Huang HL, Jagner D, Renman L (1987) Flow constant-current stripping analysis for antimony(III) and antimony(V) with gold fiber working electrodes. Application to natural waters. *Anal Chim Acta* 202:123–129
156. Eskilsson H, Jagner D (1982) Potentiometric stripping analysis for bismuth in sea water. *Anal Chim Acta* 138:27–33
157. Florence TM, Batley GE, Farrar YJ (1974) Determination of indium by anodic stripping voltammetry. Application to natural waters. *J Electroanal Chem* 56:301–309
158. Van den Berg CMG, Khan SH, Riley JP (1989) Determination of tin in sea-water by adsorptive cathodic stripping voltammetry. *Anal Chim Acta* 222:43–54
159. Wang J, Lu J, Larson DD, Olsen K (1995) Voltammetric sensor for uranium based on the propyl gallate-modified carbon paste electrode. *Electroanalysis* 7:247–250
160. Lin L, Thongngamdee S, Wang J, Lin H-Y, Sadik OA, Ly S-Y (2005) Adsorptive stripping voltammetric measurements of trace uranium at the bismuth film electrode. *Anal Chim Acta* 535:9–13
161. Adams RN (1969) *Electrochemistry at solid electrodes*. Marcel Dekker, New York
162. Jacobs ES (1963) Anodic stripping voltammetry of gold and silver with carbon paste electrodes. *Anal Chem* 25:2112–2115
163. Galík M, Cholota M, Švancara I, Bobrowski A, Vytřas K (2006) A study on stripping voltammetric determination of osmium(IV) at a carbon paste electrode modified in situ with cationic surfactants. *Electroanalysis* 18:2218–2224

164. Zhao Z-F, Freiser H (1986) Differential pulse polarographic determination of trace levels of platinum. *Anal Chem* 58:1498–1501
165. Huszal S, Kowalska J, Krzeminska M, Golimowski J (2005) Determination of platinum with thiosemicarbazide by catalytic adsorptive stripping voltammetry. *Electroanalysis* 17:299–304
166. Huszal S, Kowalska J, Sadowska M, Golimowski J (2005) Simultaneous determination of platinum and rhodium with hydroxylamine and acetone oxime by catalytic adsorptive stripping voltammetry. *Electroanalysis* 17:1841–1846
167. Locatelli C, Melucci D, Torsi G (2005) Determination of platinum-group metals and lead in vegetable environmental bio-monitors by voltammetric and spectroscopic techniques: critical comparison. *Anal Bioanal Chem* 382:1567–1573
168. Locatelli C (2006) Simultaneous square wave stripping voltammetric determination of platinum group metals (PGMs) and lead at trace and ultratrace concentration level: application to surface water. *Anal Chim Acta* 557:70–77
169. Ensafi AA, Zarei K (1999) Determination of ultratrace amounts of osmium using catalytic wave of OsO_4 -bromate system by voltammetric method. *Anal Sci (Japan)* 15:851–855
170. Zhi-Liang J (1992) A novel and highly sensitive catalytic method with oscillopolarographic detection for the determination of ultratrace amounts of iridium. *Talanta* 39:1317–1321
171. Gardea Torresdey J, Darnall D, Wang J (1988) Bioaccumulation and voltammetric behavior of gold at alga-containing carbon paste electrodes. *J Electroanal Chem* 252:197–208
172. Wang J, Tian B-M, Rayson GD (1992) Bioaccumulation and voltammetry of gold at flower-biomass modified electrodes. *Talanta* 39:1637–1642
173. Mikelová R, Baloun J, Petřlová J, Adam V, Havel L, Petřek J, Horna A, Kizek R (2007) Electrochemical determination of Ag-ions in environment waters and their action on plant embryos. *Bioelectrochemistry* 70:508–518
174. Sugawara K, Tanaka S, Taga M (1991) Voltammetry of silver(I) using a carbon-paste electrode modified by 2,2'-dithiodipyridine. *J Electroanal Chem* 304:249–255
175. Lorenzo E, Abruña HD (1992) Determination of silver with polymer-modified electrodes. *J Electroanal Chem* 328:111–125
176. Ha K-S, Kim J-H, Ha Y-S, Lee S-S, Seo M-L (2001) Anodic stripping voltammetric determination of silver(I) at a carbon paste electrode modified with S_2O_2 -donor podand. *Anal Lett* 34:675–686
177. Babkina SS, Ulakhovich NA, Zyavkina YI (2000) Determination of platinum in pharmaceuticals and biological objects using an amperometric biosensor based on deoxyribonucleic acid. *Ind Labor (Russia)* 66:779–781
178. Švancara I, Baldrianová L, Tesařová E, Mikysek T, Vytřas K (2005) Determination of tin (II) at bismuth-modified carbon paste electrodes. Initial study (in Czech). In: Vytřas K, Kellner J, Fischer J (eds) *Monitoring of environmental pollutants*, vol VII. Univ. Pardubice Press Centre, Pardubice, Czech Rep, pp 139–148
179. Prior C, Walker GS (2006) Use of the bismuth film electrode for anodic stripping voltammetric determination of tin. *Electroanalysis* 18:823–829
180. Korolczuk M, Tyszczyk K, Grabarczyk M (2007) Determination of uranium by adsorptive stripping voltammetry at a lead film electrode. *Talanta* 72:957–961

Chapter 6

Non-metal Inorganic Ions and Molecules

Ivan Švancara and Zuzana Navrátilová

In this chapter, inorganic non-metallic analytes are overviewed, comprising selected inorganic anions (namely NO_3^- , NO_2^- , N_3^- , HPO_4^{2-} , SO_4^{2-} , CN^- , F^- , I^- plus IO_3^- , ClO_4^- , and OH^-), cations (H^+ , NH_4^+ , N_2H_5^+), and inorganic molecules (O_2 , H_2O_2 , and common toxic gases like H_2S , SO_2 , NO_x , and Cl_2) (Table 6.1, data from references 1–20). Additionally, some other species from the individual categories will be shortly presented throughout the text in an effort to cover briefly most analytes which deserve some attention with respect to their environmental occurrence and possible impact on the biosphere. Gaseous sulphur and nitrogen compounds will be considered in separate chapters; therefore their summary here will be only short and complementary.

A straightforward classification of non-metallic inorganic pollutants with respect to their role in the environment would be rather fragmented, but there is one connecting point; it is the fact that the great majority of such substances are of anthropogenic origin, coming from industrial plants, agriculture, food production, as the flue gases from power plants, from public and/or household heating systems, automobile exhausts, etc.^{21–25}

I. Švancara (✉)

Faculty of Chemical Technology, Department of Analytical Chemistry,
University of Pardubice, 532 10, Pardubice, Czech Republic
e-mail: Ivan.Svancara@upce.cz

Z. Navrátilová

Faculty of Science, Department of Chemistry, University of Ostrava,
30. dubna 22, 701 03, Ostrava, Czech Republic
e-mail: Zuzana.Navratilova@osu.cz

Table 6.1 Determination of (non-metal) inorganic ions and molecules: Selected methods and their specification

Ions/species	Working el. (modifier)	Reference el.; auxiliary el.	Technique (mode)	Measuring principles (method sequences)	Experimental conditions: (selection)	Analytical characteristics ("c" given in mol·l ⁻¹ , for gases ppb, ppm)	Sample(s)	References
NO ₃ ⁻	Cu plated BDD (microelectrode array)	SCE; Pt-wire	LSWV	Electrocatalytic effect of Cu ^{II} on the reduction of NO ₃ ⁻	SE: 0.1 M Na ₂ SO ₄ + 0.002 M CuSO ₄	LR: 1.2–124 μM, LOD: 0.76 μM	Drinking water, river water	1
	(M)CPE (modifier: Amberlite LA2)	SCE; -	DPV	Preconcentration NO ₃ ⁻ via TiCl ₄ ⁻ + Ti ^{III} → Ti ⁰ Reoxidation Ti ⁰ → Ti ⁺ by nitrate (equivalent to NO ₃ ⁻)	Open-circuit arrangement (with MEX)	LR: 8.1 × 10 ⁻⁷ to 9.7 × 10 ⁻⁴ M, LOD: -	Drinking water	2
NO ₂ ⁻	(M)CPE (modifier: Aliquat 336)	SCE; Pt-wire	DPASV	Open-circuit accumulation via ion-pairing process: NO ₂ ⁻ (sol) → NO ₂ ⁻ (surf)	Open-circuit arrangement (with MEX)	LR: 0–2.2 × 10 ⁻⁷ M (I _{prec} 3 min)	Water (model solutions)	3
						LR: 0–2.2 × 10 ⁻⁶ M (I _{prec} 2 min)		
						LR: 0–2.2 × 10 ⁻⁵ M (I _{prec} 30 s)		
						LR: 0–2.2 × 10 ⁻⁴ M (I _{prec} 5 s)		
						RR: ±7 % (1.1 × 10 ⁻⁶), LOD: 6.5 × 10 ⁻⁹		
N ₃ ⁻ (together with Pb ²⁺)	DMTE (t _{Hg} 3–5 s)	Hg/ Hg ₂ SO ₄ / 1 M H ₂ SO ₄	POL (LSP)	Subsequent oxidation	(a) SS: sample	LR: 0.2–1.2 meq·L ⁻¹ , LOD: - where "meq": molecular weight equivalent stability of st. solutions: up to 30 days	Pb(N ₃) ₂ (s) (solubilised and stabilised)	4
					(b) SE: 20 ml water + 0.04 ml KCl (sat. soln.)			
					SE: 0.1 M KNO ₃ + 0.002 % Triton X-100			
					E _p (N ₃): +0.27 V vs ref. (E _p (Pb): -0.38 V)			

NH ₄ ⁺	HIMDE	Ag/AgCl/ 3MKCl; Pt-wire	ADSV (DPV)	Adsorption of the intermediate CH ₂ = NH, formed by reaction of NH ₄ ⁺ with HCHO) Subsequent (stripping) reduction of methylenimine	SE: pH 3.8 + 13 % (w/v) HCHO E _{anod} -0.85 V, t _{anod} 60 s	LR: 10–3,000 nM, LOD: 4 nM	Lake water, seawater	5
	(M)GCE (modifier: DBH)	Ag/AgCl;	CHA (WE used as remote sensor)	Electrocatalytic effect of DBH on oxidation of -NH-NH ₂	SE: 0.05 M phosphate buffer (pH 7.4)	LR: 5–40 μM RR: ±3.7 % LOD (3σ): 5 × 10 ⁻⁷ M	River water, lake water, groundwater	6
HPO ₄ ²⁻	ISE-CPE (modifier: HDTMA-modified zeolite particles)	Ag/AgCl/ sat;	POT (direct)	Open-circuit accumulation of HPO ₄ ²⁻ by ion exchange with HDTMA Measurement of equilibrium potential	SE: pH 4–12 (adjusted by HCl and NaOH)	LR: 1.58 × 10 ⁻⁵ to 1 × 10 ⁻² M RR: ±3.7 % LOD: 1.58 × 10 ⁻⁵ M; In: AsO ₄ ³⁻	Industrial fertiliser	7
	(M)CPE (Cr ^{III} -SBC)	SCE (with sat. KCl)	POT (direct, titration)	Chemical equilibria at the liquid membrane saturated with modif.: SO ₄ ²⁻ ↔ [Cr-SB-SO ₄] adduct	SS: Buffered to pH 4–9 (SBC ... Schiff base: N,N'-ethylene-bis(5-hydroxy-salicylidene-iminate); titrant: 0.01 M Ba ²⁺)	LR: 2 × 10 ⁻⁶ to 0.05 M LOD(t _{pot} = 10 s): 1 × 10 ⁻⁶ M	Mineral water, natural water	8
CN ⁻	(M)μE (enzyme: HRP)	–	CND (direct)	Indication of titration end-point Competitive inhibition of bio-reaction releasing H ₂ O ₂ (and catalysed by HRP) Indirect conductivity sensing	SS: Buffered to pH 4–5 (HRP ... horseradish peroxidase)	LR: 4 × 10 ⁻⁶ to 0.1 M LOD(t _{res} 3 min) 0.1 μM	Water, air (model samples)	9

(continued)

Table 6.1 (continued)

Ions/species	Working el. (modifier)	Reference el.; auxiliary el.	Technique (mode)	Measuring principles (method sequences)	Experimental conditions: (selection)	Analytical characteristics ("c" given in mol·l ⁻¹ , for gases ppb, ppm)	Sample(s)	References
F ⁻	F ⁻ -ISE (commercial type)	SCE	POT (direct, STM)	Effect of the lattice defect in La(Eu)F ₃ crystal in the solid membrane of F/ISE Chemical equilibria indication (interaction with single F ⁻ ions)	SS: No treatment (without buffering) STM: Standard addition method	LR: 1 × 10 ⁻⁶ to 0.1 M LOD: – InR: No effect from Al ^{III} and Fe ^{III}	Seawater (synthetic and natural samples)	10
I ⁻ (IO ₃ ⁻)	(M)CPE (active binder: TCP)	Ag/AgCl/ 0.1 M KCl; Pt plate	DP(C)SV S(C)P (CCSA)	Potentiostatic accumulation via ion pairing with TCP Immense oxidation: 2I ⁻ - 2e ⁻ → I ₂	SE: 0.5 M NaCl + 0.1 M HCl E _{acc} +0.7 (or +0.8 V), t _{acc} 60 s to 5 min (IO ₃ ⁻ reduced chem.: with N ₂ H ₅ ⁺)	Water samples: LR: 5 × 10 ⁻⁶ to 1 × 10 ⁻⁷ M LOD(3σ _{1,acc} 5 min): 7.5 × 10 ⁻⁸ M; Salt samples: LR: 4 × 10 ⁻⁷ to 2 × 10 ⁻⁵ M LOD(3σ _{1,acc} 5 min): 1.5 × 10 ⁻⁷ M; InR: Br ⁻ , SCN ⁻ (100:1), Cl ⁻ (1:10 ⁶)	Mineral water, seawater (model SS) commercial table salts (with iodide or iodate)	11–13
ClO ₄ ⁻	(M)CPE (modifier: anion exchanger)	Ag/AgCl	Catalytic voltammetry	Subsequent cathodic stripping Catalytic effect based on reoxidation of Ti ^{IV} (generated by presence of ClO ₄ ⁻)	SE: Diluted HCl + TiCl ₄ ⁻	LR: – LOD(3σ _{1,acc} 12 min):: 25 × 10 ⁻⁴ M	Drinking water (spiked)	14
H ⁺ (pH-sensing)	BPPG modified with Mts*		CV, SWV	Voltammetric response of immobilised material (resulting from carbon powder modified with Mts ^a)	SS: Media of various pH	LR: pH 1–12 LOD: –	Model solutions	15
OH ⁻	Au microdisk Au RDE	SCE	LSV	Oxidation of OH ⁻ (to H ₂ O ₂ and H ₂ O)	SE: 0.1 M Na ₂ SO ₄	LR: 0.05–10 mM (AuRDE) LOD: 0.05 mM	Model solutions	16

H ₂ O ₂	(M)CPE (modifier: MnO ₂ -film)	FIA amperometry	Oxidation of H ₂ O ₂ (mediated by MnO ₂)	SE: ammonia/aq. solutions	LR: 1.5×10^{-4} to 1.3×10^{-2} M LOD(3 σ): 1.4×10^{-4} M	Rain water	17
O ₂ (dissolved)	GrPE	Ag-wire	Reduction of dissolved oxygen (to H ₂ O ₂ and H ₂ O)	SE: 0.01 M KCl	LR: 1.6×10^{-5} to 6.3×10^{-4} M LOD: –	Tap water, natural water	18
SO ₂ (g)	CPE	Ag/AgCl	Reduction of Fe ³⁺ in complex with phen Detection at E _{CONST}	SE: Fe ^{III} -phen complex	LR: 0.3–14 ppm (v/v) RR: ± 3 %	Air samples	19
NO ₂ , SO ₂ , H ₂ S, Cl ₂ (g)	(M)CPE (modifier: TP-phen)	AD (FIA)	Electrocatalytic effect (enhancing the original current detection)	SS: Gases absorbed in buffered media	LR: 1 ppb to 1 ppm (v/v) LOD: –	Air samples	20

Abbreviations:

Symbols and general abbreviations: *aq.* aqueous, *c* concentration/content, *chem.* chemically, *Eacc/ads* accumulation/adsorption/potential, *el.* electrode, *(g)* gas, gaseous, *LOD* limit of detection, *LR* linear range, *M* molar concentration (mol-per-litre), *min* minute(s), *ppb* parts per billion, *ppm* parts per million, *RR* reproducibility/repeatability, *sat.* saturated, *SE* supporting electrolyte, *soln.* solution, *SS* sample solution, *t_{acc/ads/prec}* accumulation/adsorption/precipitation time, *v/v* volume/volume

Electrodes: *BDD(E)* boron-doped diamond (electrode), *BPPG* basal plane pyrolytic graphite, *BiFE* bismuth film electrode, *CPE* carbon paste electrode, *DME* (Heyrovský) dropping mercury electrode, *GrPE* graphite paste electrode, *HMDE* hanging mercury drop electrode, *ISE* ion-selective electrode, *(M)CPE* (modified) carbon paste electrode, *MFE* mercury film electrode, *(M)GCE* modified glassy carbon electrode, *(M)SPE* (modified) screen-printed electrode, *RDE* rotated/rotating disc electrode, *SCE* saturated calomel electrode, *WE* 1x(55)working electrode, μ E microelectrode

Techniques: *AD* amperometric detection, *Ad(C)SV* adsorptive (cathodic) stripping voltammetry, *ASV* anodic stripping voltammetry, *DPV* differential pulse voltammetry, *CCSA* constant current stripping analysis, *CV* cyclic voltammetry, *CHA* chronoamperometry, *CND* conductometry, *DCSV* differential pulse cathodic stripping voltammetry, *DPSV* differential pulse anodic stripping voltammetry, *DPAV* differential pulse anodic voltammetry, *DPCSV* differential pulse cathodic stripping voltammetry, *SWV* square-wave voltammetry

Chemicals and reagents: *CoPc* cobalt phthalocyanine, *DBH* 3,4-dihydroxybenzaldehyde, *HDTMA* hexadecyltrimethyl ammonium bromide, *phen* 1,10-phenanthroline, *TCP* tricresyl phosphate, *TP-phen* tris[4,7-diphenyl-1,10-phenanthroline]Fe(II) perchlorate, *Triton X-100*[®] commercial non-ionic surfactant

Miscellaneous: *Ar* aromatic, *aryl* MEx medium exchange

^{*} *Mts* materials prepared by derivatisation of carbon powder with the individual substances being as follows: anthracene, azobenzene, diphenylamine, 9,10-diphenylanthracene, 1,3-diphenyl quinidine, fluorescein, methylene blue, 3-nitrofluoroanthene, 6-nitrochrysene, 9-nitroanthracene, 9,10-phenanthraquinone, thionin, triphenylamine, and 2,5-dimethoxy-4-[(4-nitrophenyl)azo]-benzenediazonium chloride

Regarding nitrates and phosphates or sulphates, their main users are agriculture (mainly as fertilisers) and water-treatment stations. Sulphite is of interest mainly in food analysis. Nitrite, iodide, and fluoride are also more typical for the food and pharmaceutical industry but, in some extent, they are monitored in the environment (e.g. nitrite is used in syntheses of explosives, together with nitrates, azides, and perchlorates). A severe industrial pollutant is undoubtedly cyanide, mainly for its extreme toxicity and well-known ability to participate in numerous complex-forming reactions. Hydroxide is needed in many industrial processes as being involved in various pH-dependent reactions, unless of quoting that pH measurement itself—i.e., the determination of H^+ ions—represents a routine laboratory operation needed almost anywhere.

Ammonium comes into environment via fertilisers, but it is also the key indicator of biological decay in natural waters. Highly toxic hydrazinium and hydroxylammonium ions are normally found in localities with special productions, where their monitoring seems to be of constant interest. The list of inorganic molecules continues with gaseous pollutants, NO_x , SO_2 , H_2S , and Cl_2 , whose list can further be extended with other globally occurring common gases, such as CO , CO_2 , and ozone, O_3 , whose environmental monitoring is not so frequent.

Hydrogen peroxide, H_2O_2 , together with organic peroxides, is involved in a number of biological pathways, where this molecule is frequently monitored, but also plays an important role in many industrial processes. Last but not least, the environmental importance of (di)oxygen, O_2 , is obvious and does not need any special comment, perhaps, a remark that, in environmental determinations by electrochemical methods, the respective procedures are predominantly dealing with its determination in water samples.

6.1 Choice of the Methods and Their Basic Principles

6.1.1 Redox (Faradaic) Transformations

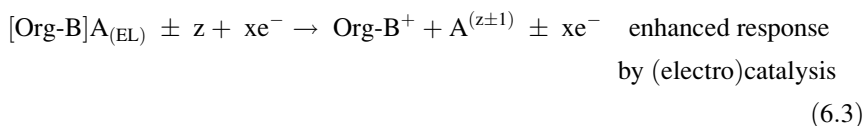
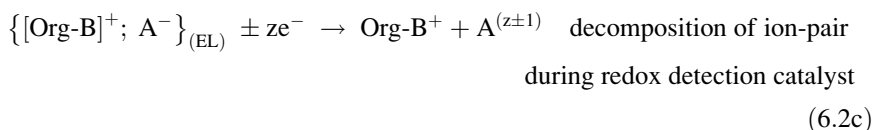
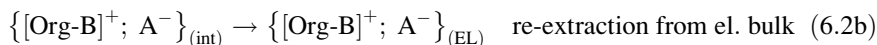
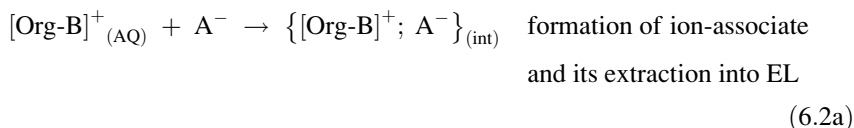
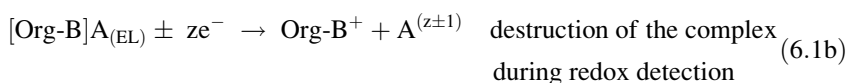
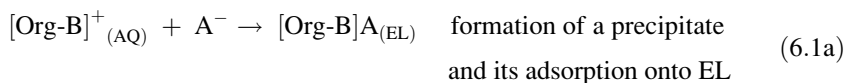
A majority of non-metallic species of environmental significance is electrochemically active and the respective cations, anions, or molecules involved in the electrode processes are connected with the electron transfer.^{26–30} Thus, in this category, the current measurement-based techniques dominate apart from the fact if a single redox or a synergistic process is to be measured.

Normally, when using stripping techniques for non-metallic species, there is *no deposition* comparable to the amalgamation at mercury electrodes or alloying for bismuth alternatives; nevertheless, a possible accumulation step cannot be simplified to a pure oxidation and/or reduction. As documented in the table, such a case is only seldom (e.g. in references 16,18), whereas the prevailing accumulations utilise

parallel non-faradic processes, facilitating or even enabling inevitable adherence of an analyte onto the electrode surface. Due to this, typical examples of such combined processes are given next.

6.1.2 (Accompanying) Non-electrolytic Processes

When considering the relevant data in Table 6.1, three most typical variants of the combined mechanisms can be sketched as follows:



where the respective stoichiometric coefficients are, for simplicity, assumed to be “ $m = n - 1$ ”; other abbreviations and symbols have the same meaning as in Chap. 5. In the table, schemes by Eqs. (6.1a, 6.1b) correspond roughly to the mechanism reported in references 4,5. Eqs. (6.2a–6.2c) then describe the pathway in references,^{3,7,11–13} whereas the (electro)catalytic detection, indicated by Eq. (6.3), can be attributed to references 6,14,17.

6.1.3 Other Possibilities

Table 6.1 includes also methods or their sequences that cannot be classified according to the schemes presented above. There are two examples on zero-current measurements by (equilibrium) potentiometry: the use of classic F^- -ISE, when the

special adaptation of standard addition procedure had allowed the authors to analyse seawater without buffering¹⁰ and the determination of redox indifferent sulphate by means of membrane ion-exchange with a Me-Org-SO₄ adduct.⁸

Furthermore, in the table, one can also find direct reduction (without accumulation) of an anion initiated by a catalyst,¹ intermediate oxidation of the analyte before its reductive stripping,^{11–13} precipitation and dissolution of the electrode material during oxidative scanning,⁴ or indirect detection of the analyte, causing the inhibition of an enzyme-catalysed biological reaction.⁹

As already mentioned for metal-based ionic species, the intermediate reduction to the elemental state is occasionally made in order to improve the adherence of the deposit to the electrode surface. However, there can also be another reason, which is the case of some methods for the determination of iodide that utilise the reversible process $2\text{I}^- \rightleftharpoons \text{I}_2 + 2\text{e}^-$ and, mainly, the extraction capabilities of molecular iodine involved in this reaction. And if one has at hand an electrode enabling to incorporate the extraction/re-extraction step, e.g. a CPE with liquid binder serving as extraction medium, the overall mechanism obtains the additional benefit of markedly improved selectivity^{11–13} compared to similar approaches based on ion pairing at CMEs with compact electrode substrate which does not permit such extraction pathway. A method utilising the ion pairing of I⁻ anion, its oxidation to I₂ with subsequent extraction/re-extraction in the carbon paste bulk, is sketched in Fig. 6.1, assembled from the authors' presentations and reports.^{11–13,30–32} The figure shows the oxidation of the ion pair formed (a) and its subsequent extractive pathway (b). The method itself has been shown to be extraordinarily selective and, besides its applications quoted in Table 6.1, allows the determination of iodide also in seawater at its typical concentration level (see Fig. 6.1c).

6.2 Electroanalysis of Non-metallic Species and Molecules

6.2.1 *Alternate Approaches to the Determination of the Title Analytes and Some Related Substances*

Among nitrogen-derived compounds hydroxylammonium salts, NH₃OH⁺A⁻ are occasionally used as selective reductants (see, e.g., reference 11) representing also highly toxic species occasionally distributed in the hydrosphere due to their excellent solubility in water.³³ The respective, highly sensitive determination of NH₃OH⁺ can be performed amperometrically with a Pd-powder-modified electrode.³⁴ Another interesting nitrogen-based structure is the azide anion, [N=N=N]⁻, whose environmental significance is associated not only with well-known production of primary explosives, but also with its widespread use in

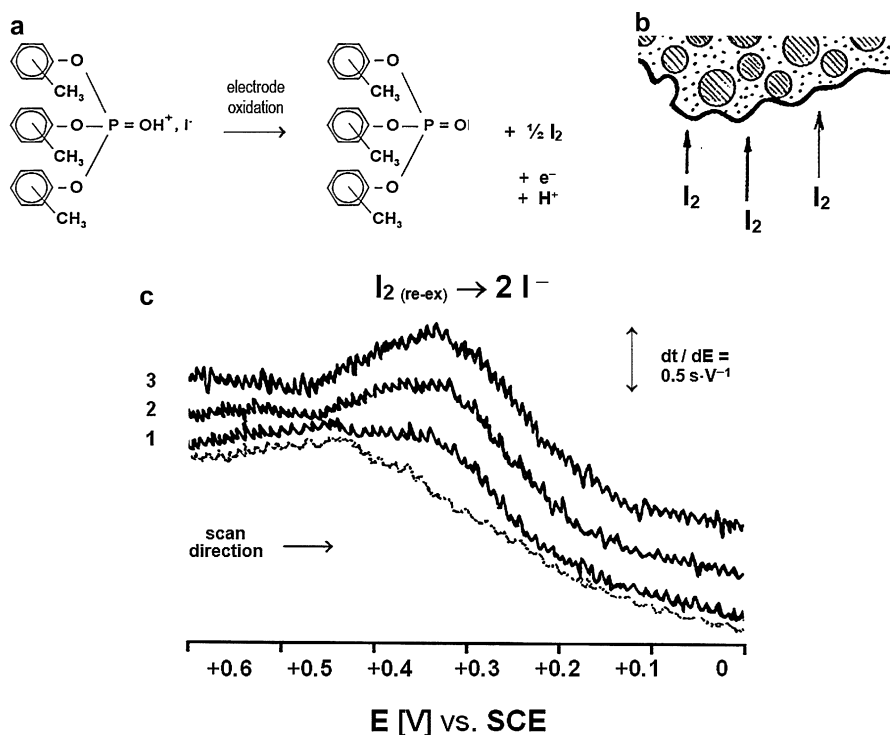


Fig. 6.1 Determination of iodide via its ion pairing and subsequent extraction/re-extraction at the tricresyl-phosphate-based carbon paste electrode (TCP-CPE). (a) Electrode oxidation of the ion pair formed between the protonated TCP and iodide; (b) extraction of the released iodine into the carbon paste bulk, a scheme; (c) determination of iodide in seawater (synthetic and spiked sample) by stripping potentiometry, *dotted line*: baseline (blank), *full lines*: 1) sample + 0.1 M HNO_3 (pH 1); (2, 3) two standard additions as two aliquots, $c(I^-) = 50 \mu g L^{-1}$. Mode: constant current stripping analysis with TCP-CPE; $E_{DEP} = +0.8$ V vs. ref. for 10 min; the stripping limits: $+0.6 \rightarrow -0.2$ V vs. ref., constant current, $I = -1 \mu A$; $I_2(re-ex)$ —iodine released by re-extraction from CPE (adapted and rearranged from references 11–13,30–32)

automobile airbag propellants.³⁵ Despite kinetically driven reaction, azide is readily oxidisable and thus, it can be determined at various electrodes, including those made of carbon paste³⁶ or boron-doped diamond.³⁷

In environmental analysis of the recent period, there is increasing attention paid to phosphates that exist, according to actual pH, as $H_2PO_4^-$ and HPO_4^{2-} species, whereas the PO_4^{3-} ion exists only in highly alkaline media^{23,24,38}, or also in the form of the poly-*meta*-phosphates, $(PO_3)_n^-$, used in washing powder formulations. Steadily growing interest in phosphates is undoubtedly associated with their role in providing favorable conditions for the expansion of toxic green algae in sweet-water systems in the due of global warming and climate changes.³⁹ Since phosphate is typically an electrochemically inactive ion,^{26–29} the effective electroanalytical

methods are based on chemical equilibrium processes at ISEs,^{40,41} or, newly, upon mediated or inhibited bioreactions (see, e.g., 42) plus some special principles like electrochemiluminescence detection.⁴³

Sulphate, SO_4^{2-} , appears in the environment partially from natural sources (via leaching of sulphate ores and minerals), and partially due to the activities by human population (residua from fertilisers or as acid rains).⁴⁴ Similarly to phosphate also the electrochemistry of the SO_4^{2-} ion does not participate in any redox reactions and its detection has to be carried out alternately, mainly, via indications of its involvement in chemical equilibria.⁴⁵ Sulphite, SO_3^{2-} , holds a prominent position mainly in food analysis; nevertheless, a few methods for its monitoring in environmental samples have also been proposed.⁴⁶

Of continuing interest is monitoring of fluoride, F^- , equally in seawater and sweet water,⁴⁷ where, despite the principal progress of modern instrumental analysis, still the most popular methods for its determination are based on the classical F^- -ISE, applicable not only to reliable quantification (see Table 6.1, reference 10), but also for speciation of some fluoride complexes (of the $\text{Me}^{\text{II}}\text{F}^+$ type, where “Me” is Mg, Ca, Sr, Ba), detectable at the decimolar level.⁴⁸ As certain rarity, an amperometric biosensor for F^- can also be mentioned,⁴⁹ being modified with a flower tissue and having utilised the above-mentioned bio-inhibition mechanism.

Environmental associations of cyanide, CN^- , are summarised in an excellent review in this topic⁵⁰ and, besides reference 9 (see Table 6.1), yet another method presented as an example of an approach employing indeed unusual modifier–liquid crystals.⁵¹

Finally, some electrochemical methods for the determination of carbon monoxide, CO ,⁵² carbon dioxide, CO_2 ,⁵³ and ozone, O_3 ,⁵⁴ can also be mentioned.

References

1. Ward-Jones S, Banks CE, Simm AO, Li J, Compton RG (2005) An in-situ copper plated boron-doped diamond microelectrode array for the sensitive electrochemical detection of nitrate. *Electroanalysis* 17:1806–1815
2. Neuhold C, Kalcher K, Diewald W, Cai X-H, Raber G (1994) Voltammetric determination of nitrate with a modified carbon paste electrode. *Electroanalysis* 6:227–236
3. Kalcher K (1986) A new method for the voltammetric determination of nitrite. *Talanta* 33:489–494
4. Bryant JI, Kemp MD (1960) Simultaneous polarographic determination of lead and azide ions of lead azides in aqueous media. *Anal Chem* 32:758–760
5. Harbin AM, van den Berg CMG (1993) Determination of ammonia in seawater using catalytic cathodic stripping voltammetry. *Anal Chem* 65:3411–3416
6. Wang J, Chen Q, Cepria G (1996) Electrocatalytic modified electrode for remote monitoring of hydrazines. *Talanta* 43:1387–1391
7. Ejhieh AN, Masoudipour N (2010) Application of a new potentiometric method for determination of phosphate based on a surfactant-modified zeolite carbon-paste electrode (SMZ-CPE). *Anal Chim Acta* 658:68–74

8. Soleymanpour A, Asl EH, Nasser MA (2006) Chemically modified carbon paste electrode for determination of sulfate ion, SO_4^{2-} , by potentiometric method. *Electroanalysis* 18:1598–1604
9. Bouyahia N, Hnaïen M, Hamlaoui ML, Kherrat R, Lagarde F, Jaffrezic-Renault N (2009) A novel conductometric biosensor based on horseradish peroxidase for cyanide detection. *Sensors Lett* 7:739–744
10. Rix CJ, Bond AM, Smith JD (1976) Direct determination of fluoride in sea water with a fluoride ion-selective electrode by a method of standard additions. *Anal Chem* 48:1236–1239
11. Konvalina J, Švancara I, Vytřas K, Kalcher K (1997) Study of conditions for voltammetric determinations of iodine at carbon paste electrodes. *Sci Pap Univ Pardubice Ser A* 3:153–162
12. Švancara I, Konvalina J, Schachl K, Kalcher K, Vytřas K (1998) Stripping voltammetric determination of iodide with synergistic accumulation at a carbon paste electrode. *Electroanalysis* 10:435–441
13. Švancara I, Ogorevc B, Novič M, Vytřas K (2002) Simple and rapid determination of iodide in table salts by stripping potentiometry with a carbon paste electrode. *Anal Bioanal Chem* 372:795–800
14. Neuhold CG, Kalcher K, Cai X-H, Raber G (1996) Catalytic determination of perchlorate using a modified carbon paste electrode. *Anal Lett* 29:1685–1704
15. Leventis HC, Streeter I, Wildgoose GG, Lawrence NS, Li J, Jones TGJ, Compton RG (2004) Derivatized carbon powder electrodes: reagentless pH sensors. *Talanta* 63:1039–1051
16. Abdelsalam ME, Denuault G, Baldo MA, Bragato C, Daniele S (2001) Detection of hydroxide ions in aqueous solutions by steady-state voltammetry. *Electroanalysis* 13:289–294
17. Schachl K, Alemu H, Kalcher K, Ježková J, Švancara I, Vytřas K (1997) Flow injection determination of hydrogen peroxide using a carbon paste electrode modified with a manganese dioxide film. *Anal Lett* 30:2655–2673
18. Guzman SQ, Baudino OM, Cortinez VA (1987) Design and evaluation of an electrochemical sensor for determination of dissolved oxygen in water. *Talanta* 34:551–554
19. Rios A, Luque de Castro MD, Valcarcel M, Mottola HA (1987) Electrochemical determination of sulphur dioxide in air samples in closed-loop flow injection system. *Anal Chem* 59:666–670
20. Bonakdar M, Mottola HA (1989) Electrocatalysis at chemically modified electrodes. Detection/determination of redox gaseous species in continuous-flow systems. *Anal Chim Acta* 224:305–313
21. Manahan SE (2001–2012) *Fundamentals of environmental chemistry*, 1st–3rd edn. CRC, Boca Raton, FL
22. Patnaik P (1997) *Handbook of environmental analysis: chemical pollutants in air, water, soil, and solid wastes*. CRC, Boca Raton, FL
23. Reimann C, De Caritat P (1998) *Chemical elements in the environment: Factsheets for the geochemists and environmental scientists*. Springer, Berlin
24. Manahan SE (2002) *Toxicological chemistry and biochemistry*, 3rd edn. Taylor & Francis, Boca Raton, FL
25. Fraga CG (2005) Relevance, essentiality and toxicity of trace elements in human health. *Mol Aspects Med* 26:235–244
26. Vydra F, Štulík K, Juláková E (1976) *Electrochemical stripping analysis*. Ellis Horwood, Chichester, UK
27. Brainina K, Neiman E (1993) *Electroanalytical stripping methods*. Wiley, New York
28. Wang J (1982) Anodic stripping voltammetry as an analytical tool. *Environ Sci Technol* 16:104A–109A
29. Wang J (1985) *Stripping analysis: principles, instrumentation, and application*. VCH Publishers, Deerfield Beach, FL
30. Švancara I, Kalcher K, Walcarius A, Vytřas K (2012) *Electroanalysis with carbon paste electrodes*. CRC, Boca Raton, FL

31. Zima J, Švancara I, Pecková K, Barek J (2009) Carbon paste electrodes for the determination of detrimental substances in drinking water. In: Lefèbvre MH, Roux MM (eds) *Progress on drinking water research*. Nova Science Publishers, Hauppauge, NY, pp 1–54
32. Švancara I, Vytřas K (2001) Determination of iodide in potassium iodide-dosage tablets using cathodic stripping voltammetry with a carbon paste electrode. *Sci Pap Univ Pardubice Ser A* 7:5–15
33. Gross P, Smith RP (1985) Biologic activity of hydroxylamine: a review. *Crit Rev Toxicol* 14:87–99
34. Cai X-H, Kalcher K, Lintschinger J, Neuhold CG, Tykarski J, Ogorevc B (1995) Electrocatalytic amperometric detection of hydroxylamine with a palladium-modified carbon paste electrode. *Electroanalysis* 7:556–559
35. Betterton EA (2003) Environmental fate of sodium azide derived from automobile airbags. *Crit Rev Environ Sci Technol* 33:423–458
36. Samo AR, Khahawer MY, Arbani SA, Qureshi GA (1993) Quantitation of azide and lead in lead azide by voltammetric method. *J Chem Soc Pak* 15:187–190
37. Xu JS, Swain GM (1998) Oxidation of azide anion at boron-doped diamond thin-film electrodes. *Anal Chem* 70:1502–1510
38. Kotrlý S, Šúcha L (1985) *Handbook of chemical equilibria in analytical chemistry: tables and diagrams*. Ellis Horwood, Chichester, UK
39. Warwick C, Guerreiro A, Soares A (2013) Sensing and analysis of soluble phosphates in environmental samples: a review. *Biosens Bioelectron* 41:1–11. doi:10.1016/j.bios.2012.07.012
40. Veselý J, Weis D, Štulík K (1978) *Analysis with ion-selective electrodes*. E. Horwood, Chichester, UK
41. Bakker E, Pretsch E (2005) Potentiometric sensors for trace level analysis. *Trends Anal Chem* 24:199–207
42. Quintana JC, Idrissi L, Palleschi G, Albertano P, Amine A, El Rhazi M, Moscone D (2004) Investigation of amperometric detection of phosphate: application in seawater and cyanobacterial biofilm samples. *Talanta* 63:567–574
43. Xue Y, Zheng XW, Li GX (2007) Determination of phosphate in water by means of a new electrochemiluminescence technique based on the combination of liquid–liquid extraction with benzene-modified carbon paste electrode. *Talanta* 72:450–456
44. Chou I-M, Seal-II RR, Wang A (2013) The stability of sulfate and hydrated sulfate minerals near ambient conditions and their significance in environmental and planetary sciences. *J Asian Earth Sci* 62:734–758
45. Lee YK, Kim CK, Park JT, Kim KS, Whang KJ (1985) Potentiometry with carbon paste-based ion-selective electrode for the determination of sulphate. *J Korean Air Pollut Res Assoc* 1:99–103
46. De Castro MDL, Fernández Romero JM (1995) Development of an optical flow-through biosensor for the determination of sulphite in environmental samples. *Anal Chim Acta* 311:281–287
47. Ozsvath DL (2009) Fluoride and environmental health: a review. *Rev Environ Sci Bio-Technol* 8:59–79
48. Bond AM, Hefter G (1971) Use of the fluoride ion-selective electrode for the detection of weak fluoride complexes. *J Inorg Nuclear Chem* 33:429–434
49. Liawruangrath S, Oungpipat W, Watanesk S, Liawruangrath B, Dongduen C, Purachat P (2001) *Asparagus*-based amperometric sensor for fluoride determination. *Anal Chim Acta* 448:37–46
50. Barnes DE, Wright PJ, Graham SM, Jones-Watson EA (2000) Techniques for the determination of cyanide in a process environment: a review. *Geostandards Newsl* 24:183–195
51. Ulakhovich NA, Zakieva DZ, Galyametdinov YG, Budnikov GK (1993) Voltammetric determination of cyanide by use of preconcentration at a carbon-paste electrode modified with liquid crystals. *J Anal Chem (Moscow)* 48:1048–1052

52. Zaromb S, Stetter JR, O'Gorman D (1983) Determination of carbon monoxide in air by dynamic coulometry. *J Electroanal Chem* 148:279–287
53. Roberts JL Jr, Sawyer DT (1959) Voltammetric determination of carbon dioxide using dimethylsulfoxide as a solvent. *J Electroanal Chem* 9:1–7
54. Knake R, Hauser PC (2002) Sensitive electrochemical detection of ozone. *Anal Chim Acta* 459:199–207

Chapter 7

Electroanalysis and Chemical Speciation

Zuzana Navrátilová and Ivan Švancara

7.1 Basic Definitions and Terms

The greatest concern for speciation of the elements relates to their impact on biological systems depending on their physical and chemical form,^{1,2} occurrence, behaviour, and actual circulation in the environment (see scheme in Fig. 7.1; and reference (3)), toxicological profile,⁴⁻⁷ and bioactivity and bioavailability.⁵⁻⁷

In terms of the official terminology and IUPAC recommendation,⁸ speciation analysis can be defined as a tool to find and identify the individual forms for a given element and to determine their concentration level in the sample, both with a goal to define the actual distribution of the respective species.

For instance, in the case of metal ions, speciation analysis classifies *three basic forms*:

1. Single/free ions of various valence, e.g. Me^{n+} and $\text{Me}^{(n+1)}$
2. Hydrated/labile forms $[\text{Me}^{\text{N}}(\text{H}_2\text{O})_m]^{n+}$, $[\text{Me}^{\text{N}}(\text{OH})_2(\text{H}_2\text{O})_{m-2}]^{n+}$
3. Complex stable structures of either inorganic or organic origin, such as the anionic species $[\text{Me}^{\text{N}}\text{L}_m]^{(m-n)-}$

The total content of the metal to be analysed is then given as a sum of the concentrations of all its forms found out in the sample.

Z. Navrátilová (✉)

Faculty of Science, Department of Chemistry, University of Ostrava, 30.
dubna 22, 701 03 Ostrava, Czech Republic
e-mail: Zuzana.Navratilova@osu.cz

I. Švancara (✉)

Faculty of Chemical Technology, Department of Analytical Chemistry
University of Pardubice, 532 10 Pardubice, Czech Republic
e-mail: Ivan.Svancara@upce.cz

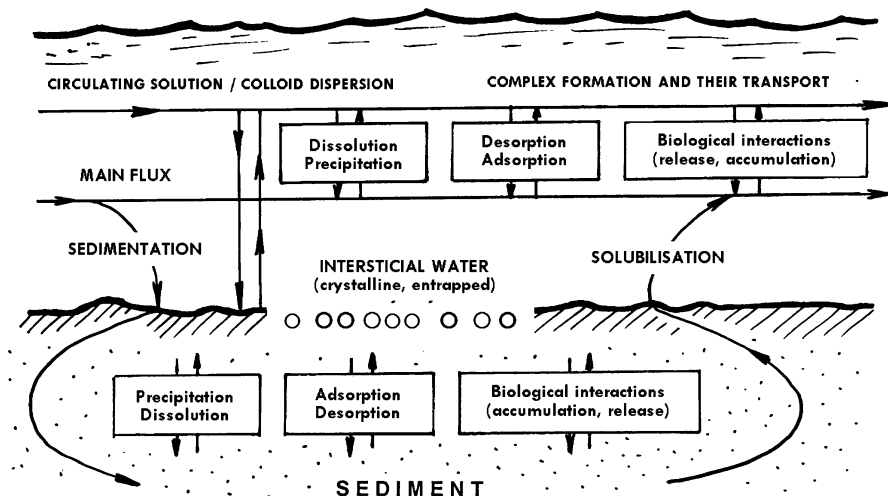


Fig. 7.1 Physicochemical processes of inorganic species in the environmental cycle of life. A scheme (adapted and rearranged from reference (3))

7.2 Electrochemical Measurements

In combination with electrochemical principles, speciation has a long tradition and at least since the last third of the twentieth century^{9–15} this special area skilfully utilises the ability of electroanalysis to indicate the changes in chemical equilibrium and redox state of various substances, which allows—together with determinations of their total content—the identification and quantification of the individual forms and their actual distribution—a problematic deal for many other instrumental techniques. In this respect, specialised teams have elaborated to a remarkable extent mainly the electrochemistry of natural aquatic systems, covering for two decades the dominant part of chemical speciation in environmental electroanalysis (see, e.g., references (15, 16)).

Concerning the most convenient electrochemical techniques for speciation analysis, there is (equilibrium) potentiometry and, mainly, stripping techniques with the effective pre-concentration step for accumulating many species at a high concentration level.

7.2.1 Potentiometry with Ion-Selective Electrodes (ISEs)¹⁷

This is the traditional technique for indication of the changes in chemical equilibrium and requires zero-current conditions. This may be advantageous with respect to the high selectivity achieved; however, common potentiometric measurements are not sufficiently sensitive to be used for monitoring at the trace concentration

level typical for environmental samples, except for special types of ISEs with non-Nernstian responses, reportedly able of operating even at the nanomolar level or even below (see, e.g., reference (18) and references therein).

7.2.2 *Anodic and Cathodic Stripping Voltammetry (ASV and CSV^{19, 20})*

This technique coupled with differential-pulse or square-wave potential ramp (DPASV and SWASV) is able to detect extremely low concentration levels (down to 1×10^{-11} mol/L⁻¹), when still distinguishing the labile and non-labile fractions of the corresponding metal(s). Electrochemical deposition within the stripping procedure enables to accumulate onto the electrode the labile forms of metal(s) under controlled—usually, constant—potential, when the effectiveness of such depositions is strongly dependent upon the type of electrode and the composition of supporting/background electrolytes (type of major components, pH, ionic strength, the presence of complex-forming anions or other ligands).

7.2.3 *Stripping (Chrono)potentiometry*

Stripping (chrono)potentiometry in its two common variants, potentiometric stripping analysis (with chemical oxidation, PSA^{21,23}) and constant current stripping analysis (CCSA^{21,22}) closely related to both ASV and CSV, is also convenient for studying metal complexation because it offers comparable sensitivity to stripping voltammetry; moreover, it is less vulnerable to the undesirable phenomena as adsorption of metal species or insufficient availability of a ligand during the measurement.^{24,25} Furthermore, PSA has been shown to be a useful tool for studying the stability and kinetics of metal ions bound by heterogeneous ligands (e.g. fulvic acid), especially thanks to the operability at a wide range of the ligand-to-metal ratio.²⁴ Yet another advantage of (chrono)potentiometry is its capability to eliminate the induced adsorption of metal ions and to minimise a ligand concentration excess.²⁵

7.2.4 *Working Electrodes for Electroanalytical Speciation*

Similarly like in other areas of applied electrochemistry, the leading scientists and teams^{9,10,12–15} were usually preferring the reliable constructions of commercially available mercury-drop-based electrodes, i.e. Kemula's HMDE and occasionally also Heyrovský's DME (see Chap. 1), or their mercury-film alternative, MFE.^{21,23}

In a lesser scope, the applicability of some carbonaceous and metallic materials as the electrodes of choice was also reported; for instance, the bare glassy carbon²⁶ or easily renewable (unmodified) carbon pastes.^{27,28} For special determinations, (solid) gold-disc,²⁹ gold-film,²⁷ screen-printed gold,³⁰ or lithographically sputtered bismuth³¹ electrodes were successfully used, too.

The second large group of frequently used working electrodes is represented by chemically modified electrodes (CMEs) expanding substantially the possibilities in chemical speciation thanks to selectively acting modifiers entrapped at the electrode surface or in the electrode bulk as a suitable ligand,³² ion exchanger,³³ or even enzyme.³⁴

Ligands immobilized in these ways form complexes with metals in solution; the electrochemical response of a given metal can then be directly related to the stability constant of a given complex. Such modified electrodes have been applied to investigate the complex-forming properties of humic substances,^{33,35,36} for example, by using them in solid form for direct modification of a CPE and, in this way, proving the formation of Cu^{II} complex structures with solid humic acids/salts.³⁶ In this study, Cu^{II}-humate complexes exhibited labile or slow dissociation character in dependence of pH. Similarly, a formation of Cu^{II} complexes with humic acid and humates at the surface layer of CPE(s) containing these substances also in the bulk could be used to quantify the respective metal ions.³⁷ These complexes were proved by IR spectra indicating the existence of COOH groups. Finally, the heterogeneous stability constant of the Cu^{II}-humic acid complex could also be determined with the aid of such modified CPE.³⁸

7.3 Basic Strategies in Electroanalytical Speciation

In environmental analysis, representing the prevailing but not exclusive applications, several fundamental approaches can be noticed as documented in the following sections.

7.3.1 *Speciation of Metal Forms and Their Overall Distribution in Aquatic Systems*^{9-16,39-41}

In brief, there are four fundamental forms of metal species: (1) free metal ions, (2) hydrated metal ions, (3) metal complexes with inorganic and/or organic ligands, and finally (4) metal species adsorbed/entrapped onto solids or colloidal particles.

The early methods for assessment of such metal fractions had employed mainly voltammetric techniques,^{9,10,12-15,39} later supplemented or also altered by stripping (chrono)potentiometry.^{24,25,42} The corresponding procedures were designed as more or less uniform schemes combining the identification and determination of

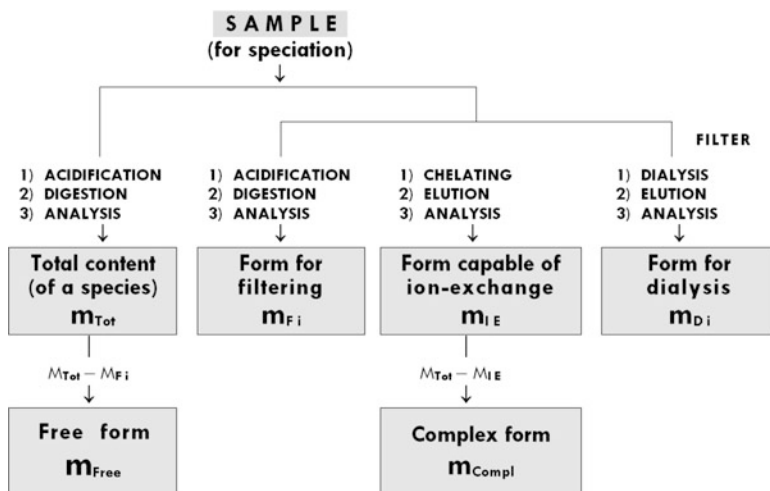


Fig. 7.2 Algorithm for chemical speciation of water samples in electroanalysis (drawn and rearranged from reference (44))

the individual metal species in untreated natural water, in acidified sample, and after the UV irradiation of the sample. In detail, a typical speciation procedure for the metal classification in natural waters was proposed by Nürnberg,¹⁴ one of the true legends of environmental analysis and co-founder of the “Environmental Specimen Banking” programme (see Chap. 1). During such speciation, the natural water is being subjected to the following steps and operations:

- Filtration to remove and analyse solid matter (with filter porosity: $0.45 \mu\text{m}$) → filtrate is subjected to analyses described in the subsequent steps (b), (c), and (d).
- Voltammetric determination of heavy metals in filtrate at natural pH → information on the dissolved metal species (free ions, hydrated cations, labile complexes with inorganic ligands).
- Voltammetric determination of heavy metals in filtrate after acidifying to pH 2 → amount of heavy metals related to their complexes (with dissolved organic matter or metals in colloids).
- Voltammetric determination of heavy metals after UV irradiation of the acidified filtrate → amount of heavy metals relating to their stable and non-labile complexes with organic ligands.

Eventually, the above-described procedure was further adapted for the use of chelating resins,⁴¹ or amended with the use of (transfer) stripping voltammetry with medium exchange,⁴³ when one might, e.g., suppress the undesirable interferences from some matrix constituents. Subsequently, as depicted by the scheme in Fig. 7.2 (sketched after Hart et al.; see reference (44)), the procedures had become yet more sophisticated after incorporation of additional separations in an ion-exchange column or by membrane dialysis, nevertheless, having still pursued the basic idea

of separation and differentiation of two ultimate forms with free and complexed/bound species.

In aquatic systems chemical equilibrium processes and their qualitative and quantitative characterisation by means of dissociation constants (pK_A), stability and conditional stability constants (K_{ML} and K'_{ML} , respectively), solubility products (pK_S), distribution pH diagrams, or reaction rate data have been studied into detail and well defined (see, e.g., reference (45)), which had inspired some scientists to combine these databases with modern computation modelling and chemometric methods.

One of the results of such efforts is shown in Tables 7.1 and 7.2, presenting a model composition of natural river water (Table 7.1) and of seawater (Table 7.2) with respect to all the chemical species that could be identified and determined by suitable instrumental techniques. In contrast to the original way of presentation,⁴⁶ the values listed in both parts have been rearranged in a reader-friendly form illustrating explicitly the abundance of the individual ions and complexes together with their corresponding contents in relation to the distribution for each chemical element and, at the same, with respect to the grand total of all the species in the water model given.

All the methods and procedures dealing with the metal speciation and distribution were mostly used for speciation of Cu, Cd, Pb, and Zn in natural waters—in these cases, predominantly with mercury electrodes (see, e.g., references (9–15) and references therein)—and speciation of Hg and As at gold electrodes,^{27,47,48} as well as various types of CMEs^{32,35,36,41} and biosensors.³⁴

Concerning the former group of heavy metals, it is worth of to mention, e.g., a systematic study on the complexing capacity of Cu(II), Cd(II), and Pb(II) towards various complexing agents (fulvic acid, alginic acid, tannic acid, surfactant Triton X[®]) while incorporating the double-acidification procedure of polluted natural waters and synthetic wastes.¹⁶ Also, electroanalytical speciations focused on organometallic and organosemimetallic species are always attractive, especially those like $(CH_3)_2Hg$ and $CH_3Hg^{+34,49}$; $(CH_3)_4Pb$, $(CH_3)_3Pb^+$, $(CH_3)_2Pb^{2+}$, $(C_2H_5)_4Pb$, etc.⁵⁰; nearly twenty organostannic compounds, including $(C_6H_5)_4Sn$, $(C_6H_5)_3Sn^+$, and $(C_4H_9)_4Sn^{51}$; and some organoarsenic derivatives.⁵²

7.3.2 Differentiation of the Valence/Oxidation State

Certain elements and their single ions or complex forms are of interest with respect to this specific feature,¹ potentially playing a principal role in the final toxicity and bioactivity^{4–7} with the subsequent impact on environmental and biological systems.

In electroanalysis, differentiation between two or even more oxidation states has been in focus mainly in the case of (1) arsenic (As^{III} and As^V ,⁴⁸ occasionally also As^{-III} (53)), (2) chromium (Cr^{III} and Cr^{VI} in chromates),⁵⁴ and in lesser extend also (3) mercury (Hg_2^{2+} and Hg^{II} (55)) and some other metallic elements like

Table 7.1 Chemical species in river water and their overall distribution^{a-c}

Major constituents				Minor/trace constituents			
Element	Form (species)	Content		Element	Form (species)	Content	
		(mg kg ⁻¹)	%			(µg kg ⁻¹)	%
<i>Metals</i>				<i>Metals</i>			
Na	Na ⁺	12,065	99.6	Fe	Fe ²⁺	8,880	88.3
	NaHCO ₃ ⁰	0.025	0.2		FeOH ⁺	1,165	11.6
	NaSO ₄ ⁻	0.025	0.2		Fe(OH) ₄ ⁻	0.006	0.1
Ca	Ca ²⁺	11,825	92.1		Fe ³⁺	5 × 10 ⁻¹²	–
	CaHCO ₃ ⁺	0.505	4.0	Mn	Mn ²⁺	3,460	96.5
	CaSO ₄ ⁰	0.385	3.0		MnSO ₄ ⁰	0.090	2.5
	CaCO ₃ ⁰	0.125	0.9		MnOH ⁺	0.035	1.0
Mg	Mg ²⁺	7,340	91.2	Ni	Ni ²⁺	1,175	38.2
	MgSO ₄ ⁰	0.425	5.3		NiCO ₃ ⁰	1,900	61.8
	MgHCO ₃ ⁺	0.270	3.4	Zn	Zn ²⁺	0.410	44.8
	MgCO ₃ ⁰	0.010	0.1		ZnCO ₃ ⁰	0.375	41.0
K	K ⁺	1,450	99.8		Zn(HS) ₂ ⁰	0.130	14.2
	KSO ₄ ⁻	0.003	0.2	Al	Al(OH) ₄ ⁻	0.380	100
Bi	BiO ⁺	0.015	–		Al ³⁺	3 × 10 ⁻⁷	–
	<i>Non-metals</i>				Cu	Cu ²⁺	0.060
C	HCO ₃ ⁻	72,135	99.6	Cd		Cd ²⁺	0.055
	CO ₃ ²⁻	0.300	0.4	Pb	CdOH ⁺	0.001	1.8
Si	H ₄ SiO ₄ ⁰	28,360	–		PbCO ₃ ⁰	0.035	93.8
Cl	Cl ⁻	10,005	–		PbOH ⁺	0.002	5.4
	S	SO ₄ ²⁻	7,115	–	Pb ²⁺	0.001	0.8
B	H ₃ BO ₃ ⁰	0.270	91.5	Ag	AgHS ⁰	0.055	100
	B(OH) ₄ ⁻	0.025	8.5		Ag ⁺	2 × 10 ⁻⁸	–
F	F ⁻	0.095	–	Cr	Cr ³⁺	5 × 10 ⁻¹¹	–
O	OH ⁻	0.005	–	Hg	Hg ²⁺	2 × 10 ⁻¹²	–
H	H ⁺	1 × 10 ⁻⁵	–	<i>Non-metals and semimetals</i>			
				N	NO ₃ ⁻	895	86.9
					NH ₄ ⁺	135	13.1
				P	HPO ₄ ²⁻	150	85.7
					H ₂ PO ₄ ⁻	25	14.3
				As	HAsO ₄ ²⁻	3.5	–
				I	I ⁻	2.0	–
					S	HS ⁻	1.5
				H ₂ S ⁰		0.2	11.8
				Se ^d	HSeO ₄ ⁻	1 × 10 ⁻¹⁰	–

^aPrepared from the results published in Batley GE (ed) (1989) *Trace Element Speciation*, CRC Press. For full citation, see the reference list and item⁴⁶

^bAll data given for t = 25 °C. Further, the individual values are recalculated to the content in mg L⁻¹ or µg L⁻¹, resp., when considering the density of seawater of ρ_w = 1.0 kg L⁻¹

^cPercentage, when all the species listed give the grand total of 100 %

^dData from another source (see reference (3))

Table 7.2 Chemical species in seawater and their overall distribution^{a-c}

Major constituents				Minor/trace constituents			
Element	Form (species)	Content		Element	Form (species)	Content	
		(mg kg ⁻¹)	%			(μg kg ⁻¹)	%
<i>Metals</i>				<i>Metals</i>			
Na	Na ⁺	10,900	93.5	Li	Li ⁺	170	–
	NaSO ₄ ⁻	750	6.4	Rb	Rb ⁺	120	–
	NaHCO ₃ ⁰	15	0.1	Ba	Ba ²⁺	20	–
Mg	Mg ²⁺	1,090	61.3	Al	Al(OH) ₄ ⁻	3.90	74.3
	MgSO ₄ ⁺	660	37.5		Al(OH) ₃ ⁰	1.35	25.7
	MgHCO ₃ ⁺	15	0.9		Al ³⁺	3 × 10 ⁻⁹	–
	MgCO ₃ ⁰	5	0.2	Zn	Zn ²⁺	2.05	56.2
	MgF ⁺	3	0.1		ZnCO ₃ ⁰	1.60	43.8
K	K ⁺	410	95.3	Ni	NiCl ₂ ⁰	1.05	38.2
	KSO ₄ ⁻	20	4.7		NiCO ₃ ⁰	0.95	34.6
Ca	Ca ²⁺	380	48.0		Ni ²⁺	0.75	27.2
	CaCl ⁺	270	34.1	Mn	MnCl ⁺	0.15	71.4
	CaSO ₄ ⁰	135	17.1		Mn ²⁺	0.06	28.6
	CaHCO ₃ ⁺	4	0.5	Cd	CdHS ⁺	0.115	45.5
	CaCO ₃ ⁰	2	0.3		CdCl ₂ ⁰	0.075	29.6
Sr	Sr ²⁺	7	–		CdCl ⁺	0.060	23.7
					Cd ²⁺	0.003	1.2
<i>Non-metals</i>				Pb	PbCO ₃ ⁰	0.045	67.2
Cl	Cl ⁻	19,900	–		PbI ₂ ⁰	0.015	22.4
S	SO ₄ ²⁻	1,350	–		Pb ²⁺	0.007	10.4
				Hg	HgCl ₃ ⁻	0.040	100
C	HCO ₃ ⁻	75	97.4		Hg ²⁺	2 × 10 ⁻¹⁵	–
	CO ₃ ²⁻	2	2.6	Cu	Cu(OH) ₂ ⁰	0.031	96.9
Br	Br ⁻	70	–		Cu ²⁺	0.001	3.1
B	H ₃ BO ₃ ⁰	20	80.0	Ag	AgCl ₄ ³⁻	0.003	100
	B(OH) ₄ ⁻	5	20.0		Ag ⁺	1 × 10 ⁻⁷	–
Si	H ₄ SiO ₄ ⁰	7	–	Cr	Cr ³⁺	5 × 10 ⁻¹⁸	–
F	F ⁻	0.80	–		<i>Non-metals and semimetals</i>		
O	OH ⁻	0.04	–	N	NO ₃ ⁻	297	99.7
H	H ⁺	8 × 10 ⁻⁶	–		NH ₄ ^{+e}	3.0	0.3
					NO ₂ ^{-e}	1 × 10 ⁻⁵	–
				I	I ⁻	65	–
					P	HPO ₄ ²⁻	10
				H ₂ PO ₄ ⁻		0.40	3.9
				PO ₄ ³⁻		0.01	0.1
				As	HAsO ₄ ²⁻	2.05	–

^{a-c}See footnote in Table 7.1, except for the seawater density, which is ρ = 1.3 kg L⁻¹

(4) antimony (Sb^{III} and Sb^{V} ⁽⁵⁶⁾), (5) iron (Fe^{II} and Fe^{III} , ⁽⁵⁷⁾ or (6) vanadium (V^{III} , V^{IV} , and V^{V} ⁽⁵⁸⁾).

After basic studies on the speciation of arsenic by polarography with the DME (see, e.g., references (52, 59)), recent methods are based on more efficient electrochemical stripping analysis with gold electrodes, ^{42,48} either in the disc configuration ²⁹ or as the gold-film-plated carbon electrode support. ²⁷ However, differentiation between As^{III} and As^{V} in freshwater can also be performed on the HMDE ⁶⁰ in combination with CSV via varying the supporting electrolyte composition and using mannitol (polyalcohol) as the activator for the electroreduction of $\text{As}^{\text{V}} \rightarrow \text{As}^{\text{III}}$ with the consecutive determination of the latter after medium exchange.

Similarly, an electrolyte with varied pH enabled to determine first As^{III} (with an LOD of 0.2 nM, pH 8) and afterwards the total content of arsenic, i.e. $\text{As}^{\text{III}} + \text{As}^{\text{V}}$ (LOD: 0.3 nM, pH 1), both when employing ASV and a gold microwire electrode. ⁶¹ An analogous approach to determine total arsenic as As^{III} after chemical reduction of As^{V} (in this case, using α -cysteine) and, in the second step, As^{III} alone utilised the above-mentioned AuF-CPE in combination with CCSA. ²⁷ The respective method was particular in a simple regeneration of the gold electrode used, as well as by finding that the CCSA signals for As^{III} differed notably in shape and overall appearance from those obtained for chemically pre-reduced As^{V} , apparently caused by the effect of residual reductant.

Finally, again by employing CCSA, one can determine pentavalent arsenic directly ⁶² by imposition of extremely negative deposition potential (close to -2 V vs. SCE) where the otherwise almost impossible electrode reduction of $\text{As}^{\text{V}} \rightarrow \text{As}^0$ is initiated, assisted, and propelled—in the right sense of this word—by the hydrogen bubbles formed during the pre-concentration process.

Concerning the speciation of chromium, one can choose from two fundamental approaches: (1) definition of the actual valence/redox state with the aid of direct electrochemical measurement of one of the two oxidation states (either Cr^{VI} in chromates ⁵⁴ or $\text{Cr}^{\text{III}}/\text{Cr}^{3+}$ ⁽⁶³⁾) with previous pre-concentration of the respective form and (2) redox-state specification by separation (via ion exchange, chromatography, or micro-extraction), enabling the selective isolation of one particular chromium species and the subsequent (unspecific) electrochemical determination. ⁶⁴ From the individual methods, one can quote catalytically assisted adsorptive stripping voltammetric determination combined with tangential flow filtration ⁶⁵ enabling the speciation of Cr^{III} and Cr^{VI} as well as the partitioning of chromium ions between the dissolved and colloidal forms in river water. Two other examples manifest the portability of electrochemical instrumentation for the field monitoring enabling the analysis immediately after sampling, minimising possible contamination during transport and storage of the samples. Such remote and fully automated electrochemical analysers were described in the reports of van-den-Berg's ⁶⁶ and "Joe" Wang's ⁶⁷ teams. The former had been employed at a shipboard laboratory, where the vertical depth profile was analysed with respect to the content of Cr^{III} , Cr^{VI} , and total Cr in a locality in the Mediterranean Sea.

Last but not least, speciation of mercury represents a global and, for lengthy decades, challenging problem of environmental analysis. Particular interest attracts methylmercury species, CH_3Hg^+ , representing the ultimate product in metabolism of marine fauna^{4,6} and also the main reason for a mass poisoning in Japan in the mid-1950s (the so-called Minamata disease⁶⁸ having left almost 2,500 victims). As already mentioned, the typical mercury species are Hg^{2+} , Hg^{II} (i.e. non-dissociated HgCl_2 and related HgCl_3^-) and CH_3Hg^+ .^{6,34,47,49,55} Further details on inorganic, organic, and organometallic forms of mercury are beyond the scope of this text, but some examples on the determination of Hg were quoted in the previous chapter (see Tables 6.3 and 7.1, and references (69–71)).

In many cases, speciation of mercury is made with CMEs, e.g. those based on modification with silicates that, in general, exhibit strong adsorption capacity towards inorganic forms of mercury—namely HgCl_3^- , HgCl_4^{2-} , and $\text{Hg}(\text{OH})_3^-$ —often occurring in aquatic systems.⁷² Similarly, clay-modified CPEs could be also used to study the cationic forms of Cu^{II} (Cu^{2+} , CuAc^+) and the anionic forms of Hg^{II} (HgAc_4^{2-} , HgCl_4^{2-} , HgCl_3^-) and Au^{III} (AuCl_4^-), where “Ac” means acetate.⁷³

7.3.3 Chemical Speciation with the Aid of the DGT

This special approach concerns a relatively new method for metal speciation in the presence of natural organic ligands and is named *diffusive gradients in thin films (DGT)*.^{74–76} Largely based on the transport of substances through a gel, the individual forms of metals and their complexes are distributed via their sizes on the gels with specific porosity, when inorganic species can pass through whereas larger complexes with organic ligands cannot. After such elimination, an ASV method or a similar procedure is then applied to determine the corresponding metal forms. Here, it can be quoted yet that although the DGT method is being co-named “in situ” because of a direct speciation of metals in natural waters, the real outdoor operation is sampling only, while the proper electrochemical analysis usually takes place in laboratories.

7.4 Concluding Remarks

As can be seen in a collection of reviews published since the beginning of the new millennium,^{77–82} speciation analysis by means of electrochemical measurements is now a firmly established area of special environmental analysis capable of pursuing the newest trends and absorbing almost all progressive achievements.

At present, many methods for electroanalytical speciation involve miniaturised and portable instrumentation,^{77,81} electrodes and sensors made by modern printing and sputtering technologies^{77,81} in configurations with various nanoparticles,⁸¹ or

utilising in more extent environmentally friendly materials⁷⁹ when satisfactory ecological profile can be attributed to the respective procedures themselves.^{78,80}

Thus, it can be concluded that electrochemical measurements employing various types of traditional as well as new electrodes are fully compatible with the latest trends and may compete with highly sophisticated instrumental techniques like ET-AAS, CV-AAS, ICP-MS, CE, or HPLC-NAA. This statement applies pretty well to chemical speciation, where electrochemical principles belong for lengthy decades among the most flexible and powerful tool in inorganic environmental analysis.

References

1. Reimann C, De Caritat P (1998) Chemical elements in the environment: factsheets for the geochemists and environmental scientists. Springer, Berlin
2. Siegel FR (2002) Environmental geochemistry of potentially toxic metals. Springer, Berlin
3. Helán V (ed) (1999) Inorganic environmental analysis: a book of proceedings (in Czech). Ing. Václav Helán, Český Těšín, Czech Rep, p 145
4. Manahan SE (2002) Toxicological chemistry and biochemistry, 3rd edn. Taylor & Francis, Boca Raton, FL
5. Fraga CG (2005) Relevance, essentiality and toxicity of trace elements in human health. *Mol Aspects Med* 26:235–244
6. Wood JM, Fanchiang YT, Ridley WP (1978) The biochemistry of toxic elements. *Q Rev Biophys* 11:467–479
7. Chowdhury B (1987) Biological and health implications of toxic heavy metal and essential trace element interactions. *Prog Food Nutr Sci* 11:55–113
8. Templeton DM, Arise F, Cornelis R, Danielsson LG, Muntau H, van Leeuwen HP, Lobynski R (2000) Guidelines for terms related to chemical speciation and fractionation of elements. Definitions, structural aspects, and methodological approaches. *Pure Appl Chem* 72:1453–1470
9. Van den Berg CMG (1983) Trace metal speciation in seawater (a review). *Anal Proc* 20:458–460
10. Bond AM, Heritage ID, Thormann W (1986) Strategy for trace metal determination in seawater by anodic stripping voltammetry using a computerized multitime-domain measurement method. *Anal Chem* 58:1063–1066
11. Batley GE, Florence TM (1976) Novel scheme for classification of heavy metal species in natural waters. *Anal Lett* 9:379–388
12. Florence TM, Batley GE (1980) Chemical speciation in natural waters (a review). *Crit Rev Anal Chem* 9:219–296
13. Hart BT (1981) Trace metal complexing capacity of natural waters: a review. *Environ Technol Lett* 2:95–110
14. Nurnberg HW (1983) Investigations on heavy metal speciation in natural waters by voltammetric procedures. *Fresenius Z Anal Chem* 316:557–565
15. Van den Berg CMG (1991) The reality of speciation measurements in natural waters. *Anal Proc* 28:58–59
16. Florence TM (1992) Trace element speciation by anodic stripping voltammetry. *Analyst* 117:551–553
17. Veselý J, Weis D, Štulík K (1978) Analysis with ion-selective electrodes. E. Horwood, Chichester, UK

18. Bakker E, Pretsch E (2005) Potentiometric sensors for trace level analysis. *Trends Anal Chem* 24:199–207
19. Wang J (1985) *Stripping analysis: principles, instrumentation, and application*. VCH Publishers, Deerfield Beach, FL
20. Mirčeski V, Komorsky-Lovrić Š, Lovrić M (2007) *Square-wave voltammetry*. Springer, Berlin
21. Ostapczuk P (1993) Present potentials and limitations in the determination of trace elements by potentiometric stripping analysis. *Anal Chim Acta* 273:35–40
22. Estela JM, Tomás C, Cladera A, Cerdà V (1995) Potentiometric stripping analysis: a review. *Crit Rev Anal Chem* 25:91–141
23. Jagner D (1982) Potentiometric stripping analysis: a review. *Analyst (UK)* 107:593–599
24. Town RM (1998) Chronopotentiometric stripping analysis as a probe for copper(II) and lead (II) complexation by fulvic acid: limitations and potentialities. *Anal Chim Acta* 363:31–43
25. Van Leeuwen HP, Town RM (2003) Electrochemical metal speciation analysis of chemically heterogeneous samples: the outstanding features of stripping chrono-potentiometry at scanned deposition potential. *Environ Sci Technol* 37:3945–3952
26. Lowe TA, Hedberg J, Lundin M, Wold S, Wallinder IO (2013) Chemical speciation measurements of silver ions in alkaline carbonate electrolytes using differential pulse stripping voltammetry on glassy carbon compared with ion-selective electrode measurements. *Int J Electrochem Sci* 8:3851–3865
27. Švancara I, Vyřas K, Bobrowski A, Kalcher K (2002) Determination of arsenic at a gold-plated carbon paste electrode using constant current stripping analysis. *Talanta* 58:45–55
28. Liu A, Wong J-L (2000) Chemical speciation of nickel in fly ash by phase separation and carbon paste electrode voltammetry. *J Hazard Mater* 74:25–35
29. Bodewig FG, Valenta P, Nurnberg HW (1982) Trace determination of As(III) and As(V) in natural waters by differential pulse anodic stripping voltammetry. *Fresenius Z Anal Chem* 311:187–191
30. Rueda Holgado F, Bernalte E, Palomo Marín MR, Calvo Blázquez L, Cereceda Balic F, Pinilla Gil E (2012) Miniaturized voltammetric stripping on screen-printed gold electrodes for field determination of copper in atmospheric deposition. *Talanta* 101:435–439
31. Kokkinos C, Economou A, Raptis I, Efstathiou CE, Speliotis T (2007) Novel disposable bismuth-sputtered electrodes for the determination of trace metals by stripping voltammetry. *Electrochem Commun* 9:2795–2800
32. Cha SK, Abruna HD (1990) Determination of copper at electrodes modified with ligands of varying coordination strength: a preamble to speciation studies. *Anal Chem* 62:274–278
33. Labuda J, Korgová H, Vaníčková M (1995) Theory and application of chemically modified carbon paste electrode to copper speciation determination. *Anal Chim Acta* 305:42–48
34. Amine A, Cremisini C, Palleschi G (1995) Determination of mercury(II), methyl-mercury and ethylmercury in the ng/ml range with an electrochemical enzyme glucose probe. *Microchim Acta* 121:183–190
35. Labuda J, Bučková M, Halamová L (1997) Sensor-analyte interaction kinetics as a metal speciation criterion. *Electroanalysis* 9:1129–1131
36. Navrátilová Z, Kula P (1993) Modified carbon paste electrodes for the study of metal-humic substances complexation. *Anal Chim Acta* 273:305–311
37. Lopez da Silva WT, Thobie-Gautier C, Rezende MOO, El Murr N (2002) Electrochemical behavior of Cu(II) on carbon paste electrode modified by humic acid, cyclic voltammetry study. *Electroanalysis* 14:71–77
38. Wang C, Zhu B, Li H (1999) Theoretical analysis and determination of the heterogeneous stability constant of copper(II)-humic acids complex at chemically modified carbon paste electrode. *Electroanalysis* 11:183–187
39. Florence TM (1989) Electrochemical techniques for trace element speciation in waters. In: Batley GE (ed) *Trace element speciation: analytical methods and problems*. CRC, Boca Raton, FL, pp 77–116

40. Tercier M-L, Buffle J (1993) In-situ voltammetric measurements in natural waters: future prospects and challenges. *Electroanalysis* 5:187–200
41. Bott AW (1995) Voltammetric determination of trace concentrations of metals in the environment. *Curr Sep* 14:24–30
42. Muñoz E, Palmero S (2005) Analysis and speciation of arsenic by stripping potentiometry: a review. *Talanta* 65:613–620
43. Florence TM, Mann KJ (1987) Anodic stripping voltammetry with medium exchange in trace element speciation. *Anal Chim Acta* 200:305–312
44. Ran Y, Fu J-M, Sheng G-Y, Beckett R, Hart BT (2000) Fractionation and composition of colloidal and suspended particulate materials in rivers. *Chemosphere* 41:33–43
45. Stumm W, Morgan JJ (1996) *Aquatic chemistry: chemical equilibria and rates in natural waters*, 3rd edn. Wiley-Interscience, Weinheim
46. Waite TD (1989) Mathematical modeling of trace element speciation. In: Batley GE (ed) *Trace element speciation: analytical methods and problems*. CRC, Boca Raton, FL, pp 117–140
47. Colilla M, Mendiola MA, Procopio JR, Sevilla MT (2005) Application of a carbon paste electrode modified with a Schiff base ligand to mercury speciation in water. *Electroanalysis* 17:933–940
48. Hung D-Q, Nekrassova O, Compton RG (2004) Analytical methods for inorganic arsenic in water: a review. *Talanta* 64:269–277
49. Ribeiro F, Neto MM, Rocha MM, Fonseca IT (2006) Voltammetric studies on the electrochemical determination of methylmercury in chloride medium at carbon micro-electrodes. *Anal Chim Acta* 579:227–234
50. Colombini MP, Fuoco R, Papoff P (1984) Electrochemical speciation and determination of organometallic species in natural waters. *Sci Total Environment* 37:61–70
51. Markušová K, Kladeková D, Žežula I (1980) Electrochemical behaviour of organotin compounds. *Chem Zvesti/Chem Papers (Slovakia)* 34:726–739
52. Watson A, Svehla Gy (1975) Polarographic studies on some organic compounds of arsenic. Part I: arsonic acids and Part II: phenyl arsenoxide analyst 100. pp. 489–502 and 573–583
53. Greschonig H (1997) Electrochemical behaviour and electroanalytical methods for the determination of arsenic compounds. *Sci Pap Univ Pardubice Ser A* 3:293–305
54. Švancara I, Foret P, Vytřas K (2004) A study on the determination of chromium as chromate at a carbon paste electrode modified with surfactants. *Talanta* 64:844–852
55. Agraz R, Sevilla MT, Hernández L (1995) Voltammetric quantification and speciation of mercury compounds. *J Electroanal Chem* 390:47–57
56. Huang HL, Jagner D, Renman L (1987) Flow constant-current stripping analysis for antimony (III) and antimony(V) with gold fiber working electrodes. Application to natural waters. *Anal Chim Acta* 202:123–129
57. Lu M, Rees NV, Kabakaev AS, Compton RG (2012) Determination of iron: electro-chemical methods. *Electroanalysis* 24:1693–1702
58. Grigoreva MF, Ivanko MG (1997) Simultaneous determination of vanadium(III, IV, V) in chloride melts. *Vestn S Peterb Univ Ser 4 (Ukraine)* 1:98–102
59. Arnold JP, Johnson RM (1969) Polarography of arsenic. *Talanta* 16:1191–1207
60. Henze G, Wagner W, Sander S (1997) Speciation of arsenic(V) and arsenic(III) by cathodic stripping voltammetry in fresh water samples. *Fresenius J Anal Chem* 358:741–744
61. Salaun P, Planer-Friedrich B, van den Berg CMG (2007) Inorganic arsenic speciation in water and seawater by anodic stripping voltammetry with a gold microelectrode. *Anal Chim Acta* 585:312–322
62. Huang H-L, Jagner D, Renman L (1988) Flow potentiometric and constant current stripping analysis for arsenic(V) without prior chemical reduction to arsenic(III): application to the determination of total arsenic in seawater and urine. *Anal Chim Acta* 207:37–46
63. Chatzitheodorou E, Economou A, Voulgaropoulos A (2004) Trace determination of chromium by square-wave adsorptive stripping voltammetry on bismuth film electrodes. *Electroanalysis* 16:1745–1754

64. Harzdorf AC (1987) Analytical chemistry of chromium species in the environment and interpretation of results. *Int J Environ Anal Chem* 29:249–261
65. Bobrowski A, Bas B, Dominik J, Niewiara E, Szalinska E, Vignati D, Zarebski J (2004) Chromium speciation study in polluted waters using catalytic adsorptive stripping voltammetry and tangential flow filtration. *Talanta* 63:1003–1012
66. Achterberg EP, van den Berg CMG (1994) Automated voltammetric system for shipboard determination of metal speciation in sea water. *Anal Chim Acta* 284:463–471
67. Wang J, Chen Q, Cepria G (1996) Electrocatalytic modified electrode for remote monitoring of hydrazines. *Talanta* 43:1387–1391
68. Anonymous (2013) Minamata disease. http://en.wikipedia.org/wiki/Minamata_disease. Accessed on 30 May 2013
69. Sipos L, Valenta P, Nurnberg HW, Branica M (1977) Applications of polarography and voltammetry to marine and aquatic chemistry. A new voltammetric method for study of mercury traces in sea and inland waters. *J Electroanal Chem* 77:263–266
70. Gustavsson I (1986) Determination of mercury in sea water by stripping voltammetry. *J Electroanal Chem* 214:31–36
71. Jagner D (1979) Potentiometric stripping analysis for mercury. *Anal Chim Acta* 105:33–41
72. Walcarius A, Etienne M, Delacote C (2004) Uptake of inorganic Hg(II) by organically modified silicates: influence of pH and chloride concentration on binding pathways and electrochemical monitoring of the process. *Anal Chim Acta* 508:87–98
73. Navrátilová Z, Kula P (2000) Cation and anion exchange on clay modified electrodes. *J Solid State Electrochem* 4:342–347
74. Zhang H, Davison W (2000) Direct in situ measurements of labile inorganic and organically bound metal species in synthetic solutions and natural waters using diffusive gradients in thin films. *Anal Chem* 72:4447–4457
75. Zhang H (2004) In-situ speciation of Ni and Zn in freshwaters: comparison between DGT measurements and speciation models. *Environ Sci Technol* 38:1421–1427
76. Sébastien M, Odzak N, Behra R, Sigg L (2004) Speciation of copper and zinc in natural freshwater: comparison of voltammetric measurements, diffusive gradients in thin films (DGT) and chemical equilibrium models. *Anal Chim Acta* 510:91–100
77. Taillefert M, Luther GV III, Nuzzio DB (2000) The application of electrochemical tools for in-situ measurements in aquatic systems. *Electroanalysis* 12:401–412
78. Emons H (2002) Artefacts and facts about metal(loid)s and their species from analytical procedures in environmental biomonitoring. *Trends Anal Chem* 21:401–411
79. Wang J (2002) Real-time electrochemical monitoring: toward green analytical chemistry. *Acc Chem Res* 35:811–816
80. Reeder RJ, Schoonen MAA, Lanzirotti A (2006) Metal speciation and its role in bioaccessibility and bioavailability. *Rev Miner Geochem* 64:59–113
81. Miró M, Hansen EH (2012) Recent advances and future prospects of mesofluidic lab-on-a-valve platforms in analytical sciences. A review. *Anal Chim Acta* 750:3–15
82. Li C-M, Hu W-H (2013) Electroanalysis in micro- and nano-scales. *J Electroanal Chem* 688:20–31

Chapter 8

Nanoparticles-Emerging Contaminants

Emma J.E. Stuart and Richard G. Compton

8.1 Introduction: Nanoparticles in the Environment and the Need for Monitoring

A nanoparticle is widely considered to be a particle with at least one dimension that is less than 100 nm as reflected in the IUPAC definition¹ that a nanoparticle is a “microscopic” particle, often restricted to the so-called nanosized particles. The definition partially overlaps that of colloids which are dispersions in a fluid medium of particles between 1 nm and 1 μm in size. More usefully the term “nanoparticle” often implies a particle of sufficiently small size in contrast to bulk media of the same chemical composition such that one or more of its properties—optical, electronic, mechanical, . . .—is size dependent.

Environmental nanoparticles primarily originate from natural sources or from human manufacturing activities. The former includes particles from forest fires or volcanic emissions and some of those made of humic materials as well as biological particles such as bacteria and viruses. The incidence of manufactured nanoparticles reflects the huge growth in the nanotechnology industries in recent years with continued expansion expected such that the US National Science Foundation predicts a global \$1 trillion market with two million workers in the nanotechnology area by 2015² with broad and diverse applications in materials science, medicine, energy, communication and the environment.³ Nanomaterials feature in consumer products such as electronic components, cosmetics, cigarette filters, antimicrobial and stain-resistant fabrics,³ more specifically as batteries, skin-care products, paints, wound dressings, food additives, toothpastes, etc.⁴ Indeed no less than ca. 15 % of all global consumer products are estimated to be “nano-enabled”.⁵ Nanoparticles have also been employed in environmental remediation to improve

E.J.E. Stuart • R.G. Compton (✉)

Department of Chemistry, Oxford University, Oxford, United Kingdom

e-mail: emma.stuart@hertford.ox.ac.uk; richard.compton@chem.ox.ac.uk

the quality of air, water and soils. The US Environmental Protection Agency (EPA) allocated \$1 billion for environmental remediation in 2009.^{3,6} As an illustration magnetic iron oxides have been used to remove arsenic from drinking water. The ions adsorb on the nanoparticle surface and then a magnetic field is used to separate the complex from the water.⁷ Gold nanoparticles supported on alumina have been used to remove inorganic mercury from drinking water⁸ whilst iron nanoparticles have been used to remove metals such as Cr(VI), U(IV and VI) and Co(II).^{9–11} The latter have also been used to degrade organic pollutants as have TiO₂ nanoparticles.²

“Incidental nanoparticles” are produced as a side product of anthropogenic processes such as in automobile exhausts. One interesting but unexpected source of incidental nanoparticles relates to the discovery¹² that silver and copper metallic nanoparticles are formed spontaneously on the surface of manmade objects (made of Ag and Cu) that humans have long been in contact with and that macroscale objects represent a potential source of nanoparticles in the environment.

The most important environmental nanoparticles are carbon nanotubes (CNTs), fullerenes (such as C₆₀), nanowires, TiO₂, ZnO, CeO₂, SiO₂ (silica), iron oxides, alumina, hydroxyapatite and metallic nanoparticles such as Fe, Ag and Au.⁴ World production of TiO₂ is estimated to be in excess of 40,000 tons per annum with most of the material being nano-sized.¹³

Because of their size nanoparticles can display significantly changed behaviour in comparison with the corresponding macroscopic materials. Most notably the reduced size leads to high surface area-to-volume ratios, high absolute surface areas and changed electronic properties arising from quantum effects leading to changed chemical and physical properties such as³ aggregation, electrical conductivity, heat conduction, catalytic activity, surface chemistry, mechanical strength and solubility.

An implication of the changed reactivity between the macro- and nanoscale is that the documentation and understanding of the effects of nanoparticles on human health as well as on plants and other animals are at a relatively immature stage. There is evidence that nanoparticles are usually more toxic than larger particles of the same material.^{14,15} Origins of some nanotoxicity have been suggested to lie in the ability of for example Fe nanoparticles to generate radical species, coupling into the chemistry of reactive oxygen species and the generation of oxidative stress or removal of antioxidants.¹⁶ In other cases the changed physical and chemical properties from the macroscale can make materials behave quite differently from the bulk analogs. In some cases positive effects, for example the beneficial role of CNTs on mustard plant growth, have been documented.¹⁷

Given the absolute and increasing scale of production of nanomaterials allied to their uncertain effects on human health it is important that the presence of nanoparticles in the environment can be measured and monitored along with their chemical identification and concentration. The quantification of environmental nanoparticles represents a significant analytical challenge.¹³ In the next section (8.2), we very briefly outline existing non-electrochemical methods before considering in detail electrochemical alternatives in Sect. 8.3.

8.2 Non-electrochemical Approaches to the Quantification of Environmental Nanoparticles and Their Limitations

The application of existing analytical methodology to the quantification of environmental nanoparticles has been summarised in an excellent review by Howard¹³ who identifies the importance of techniques as follows: analyte enrichment (centrifugation, density gradient centrifugation, split-flow thin-cell fractionation); particle visualisation (scanning electron microscopy (SEM), transmission electron (TEM) and helium ion microscopy, atomic force microscopy); particle sizing in nanoparticle suspensions (disc centrifugation, nanoparticle tracking analysis, dynamic light scattering (DLS), UV-visible and fluorescence) and separation methods (flow cytometry, disc centrifuge, field-flow fractionation, hydrodynamic chromatography, size-exclusion chromatography, electrophoresis).

In comparison with the above, electrochemical methods are relatively under-explored but offer scope for chemical identification, low cost and ease of portability.

8.3 Electrochemical Approaches to the Quantification of Nanoparticles

8.3.1 Stripping Voltammetry of Nanoparticles

The simplest approach to the electrochemical (voltammetric) analysis of nanoparticles is to first separate and isolate the nanoparticles from the sample of interest and then immobilise them on a suitable substrate electrode and conduct stripping voltammetric analysis. This approach can be illustrated by the elegant work of Giovanni and Pumera¹⁸ on molybdenum metallic nanoparticle detection using cyclic and differential pulse voltammetry. They formed Mo nanoparticle-modified glassy carbon electrodes by depositing a small amount of colloidal suspension on the surface of a glassy carbon electrode and then letting the solvent (dimethylformamide) evaporate to dryness. Voltammograms were then recorded in phosphate buffer of neutral pH and these are shown in Fig. 8.1. Clearly defined oxidation features are discernible, fingerprinting the nanoparticles as Mo. A similar approach has been applied by the same group to Ni¹⁹ and Ag²⁰ nanoparticles. Such analyses promise application in bioassays with the possibility that different nanoparticles can be used to label (tag) different species. For example CdS nanoparticles can be directly detected electrochemically in much the same way as Mo²¹ and have been used to label DNA.²²

In the case of Au nanoparticles a more indirect approach was taken.²³ First the Au nanoparticles were physically adsorbed on the surface of a glassy carbon electrode at open circuit. Subsequently electrochemical oxidation of the colloidal Au nanoparticles to AuCl_4^- in 0.1 M aqueous HCl was carried out. Immediately

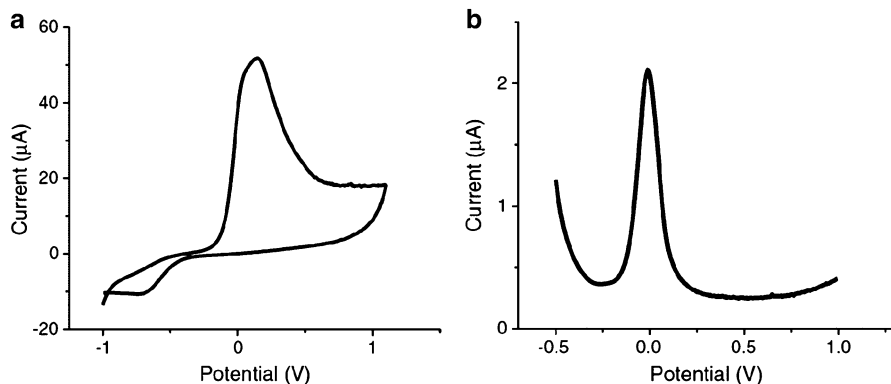
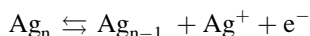


Fig. 8.1 (a) Cyclic voltammogram for a glassy carbon electrode modified with 0.25 μg of molybdenum nanoparticles recorded in 50 mM phosphate buffer (pH 7.4) at a scan rate of 100 mV s^{-1} . (b) Differential pulse voltammetric response for the oxidation of 0.1 μg of molybdenum nanoparticles in 50 mM phosphate buffer (pH 7.4). Reprinted from reference (18) with permission from Elsevier

following this step the AuCl_4^- formed was detected and quantified via differential pulse voltammetry.

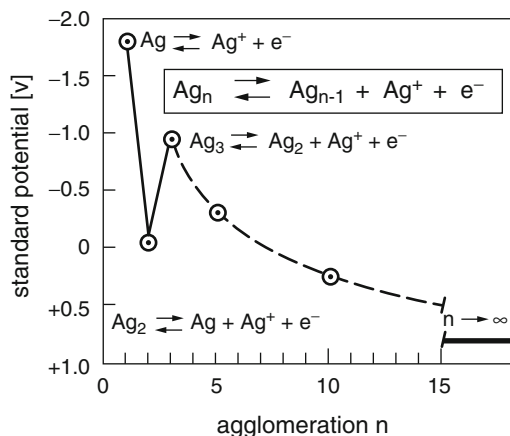
There are several reports that the electrochemical oxidation of nanoparticles can be size dependent with both Ag^{20,24} and Pt nanoparticles studied.²⁵ Ivanova and Zamborini immobilised different sized citrate-capped Ag nanoparticles ranging in size from 8 to 50 nm onto an amine-functionalised indium tin oxide (ITO)-coated glass electrode via electrostatic attachment to the protonated amine group. The largest diameter particles studied showed an oxidation potential in 0.1 M aqueous sulphuric acid ca. 100 mV more positive than that of the smallest nanoparticles studied.

The size dependency of the electrochemical oxidation of metal nanoparticles can be partially understood in the light of several different considerations.^{24–30} First, data deriving from work on small silver clusters, Ag_n , formed in aqueous solution via pulse radiolysis coupled with other information such as mass spectroscopic equilibrium data and Gibbs energies of sublimation of silver has led to the estimation of the standard electrode potential of the redox couple



For large values of n the potential approaches that expected for the Ag/Ag^+ redox couple (+0.799 V). However at small values of n there is a strong size dependence²⁷ with a value of -1.8 V calculated for the special case of a single atom of silver ($n = 1$).^{26–28} In between these limits the electrode potential varies as shown in Fig. 8.2 with a strong oscillation in the $n = 1\text{--}3$ range—the silver atom being strongly electron donating whereas the dimer ($n = 2$) is being almost “noble”²⁷ (-0.1 V) with the trimer again having a very negative value. The ease of oxidation of Ag_n as n increases is evident in Fig. 8.2.

Fig. 8.2 Variation of the standard electrode potential for the Ag/Ag⁺ redox couple with agglomeration of silver atoms. Reprinted with permission from reference (27). Copyright 1993 American Chemical Society

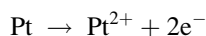


For larger clusters approaching nanoparticle dimensions Plith²⁶ considered surface Gibbs energies reflecting the fact that metal atoms in the surface of a small particle are in less energetically favourable positions compared to those in bulk material. He obtained the following equation for the difference in electrode potential between the dispersed (colloidal) metal as compared with the bulk material:

$$\Delta E \propto -\frac{\gamma}{r}$$

where the particles were considered to be spheres of radius r , γ is the surface energy (J m^{-2}) and the analysis was considered to apply to particles of ca 0.7 nm or larger in radius (corresponding to 100 atoms or so). Application of the theory required knowledge of surface energy values and this limited the application of the theory in real systems. Figure 8.3 however shows the results of some model calculations²⁶ and that significant shifts of redox potential can be seen for particles as large as 10 nm.

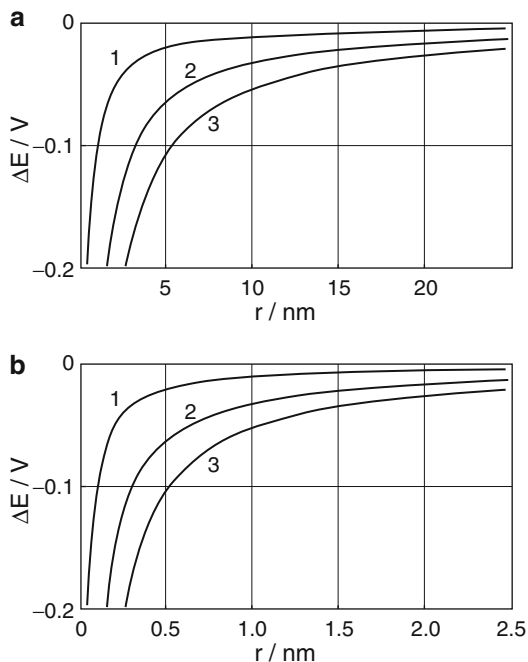
Developing from this type of approach Tang and colleagues²⁵ used first principle electronic structure calculations of the surface energy of Pt nanoparticles to develop size-dependent potential pH diagrams and to show, supported by experimental electrochemical scanning tunnelling microscopy, that Pt nanoparticles of diameter less than ~4 nm dissolve oxidatively via the direct electrochemical dissolution:



whereas larger nanoparticles form oxide layers.

A further consideration pertaining to size-dependent electrochemical oxidation of metal nanoparticles supported on a conductive electrode surface relates to the size-dependent concentration profiles of the metal ions produced during oxidation as they diffuse away from the electrode surface.²⁹⁻³¹ In order to identify the effects

Fig. 8.3 Cathodic shift in redox potential for a metal electrode as a function of particle size (a) particle radius $r < 25$ nm, (b) particle radius $r < 2.5$ nm for surface energy values of 0.5 J m^{-2} (curve 1), 1.5 J m^{-2} (curve 2) and 2.5 J m^{-2} (curve 3). Adapted with permission from reference (26). Copyright 1982 American Chemical Society



of diffusion on the voltammetric stripping signal from an electrode partially covered with the nanoparticles (of a uniform size) being stripped, the formal potential for the oxidation was assumed constant in simulations made to isolate the effects of diffusion.^{29–31} Under these conditions theory predicts that for electrochemically irreversible kinetics (slow electron transfer requiring an overpotential) the peak potential will be independent of the metal coverage but will shift to more negative potentials as the nanoparticle radius shrinks in size. If a range of nanoparticle sizes is present then this is reflected by the broadening of the stripping peak as observed experimentally for Bi nanoparticles being stripped from the surface of a boron-doped diamond electrode.³¹

In contrast for an electrochemically reversible stripping process it is predicted, again assuming no influence of particle size on the standard electrode potential of the stripping process, that assuming the diffusion layers surrounding each nanoparticle overlap so as to produce overall planar diffusion of the stripped ions away from the electrode, the peak potential will depend on the total metal coverage but not the nanoparticle size. In the opposite limit, where the diffusion layers do not overlap particle size effects are predicted. Experiments reported³⁰ for the electrochemically reversible stripping of silver nanoparticles supported on a basal plane pyrolytic graphite electrode showed the expected dependence on the metal loading but not the particle size.

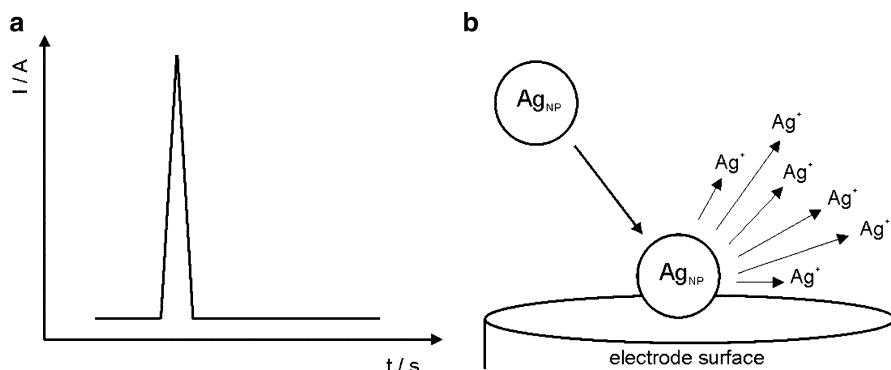


Fig. 8.4 Schematic diagram of (a) the spike observed in the current-time transient when a silver nanoparticle collides with a potentiostated electrode and is oxidatively destroyed (b)

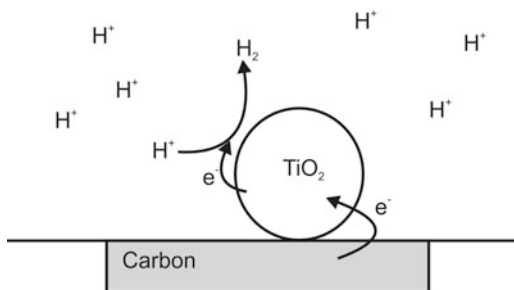
In summary, stripping voltammetry can be used to identify the presence of oxidisable nanoparticles, thus allowing fingerprinting and, with suitable calibration, their quantification although care is required in the interpretation of the peak potential with sensitivity to particle size and possible loadings.

8.3.2 Nanoparticle: Electrode Impacts

An alternative and at least in principle much simpler and easier electrochemical approach to that of the previous section, in which nanoparticles are sequentially isolated, immobilised on an electrode and then analysed via stripping voltammetry, is the direct study of the nanoparticles suspended in a solution phase into which an electrode under potentiostatic control is introduced. The movement of the nanoparticles in the solution is expected to approximate to Brownian which from time to time will bring the nanoparticles close to or in physical contact with the electrode to which they can either stick or rebound, unless the electrode is held at a potential corresponding to the oxidation or reduction of the nanoparticles or at least the surface of the nanoparticles. In the latter case, the nanoparticle impacts on the electrode are revealed by a pulse of current, as shown schematically in Fig. 8.4. These spikes can be used to identify (“fingerprint”) the nanoparticles (by virtue of their “onset potentials”), measure their concentrations and to size them as discussed in more detail below. This type of measurement is currently subject to significant levels of interest (see reference (32) for an early review).

The original work in the area was carried out by Heyrovský and colleagues^{33–36} using mercury electrodes to electro-*reduce* particles of metal oxides. They examined the voltammetry of polydisperse “colloidal” solutions of the oxides SnO₂, TiO₂ and Fe₂O₃ in aqueous solution. The voltammograms measured reflected the summation of the contribution of groups of particles of different sizes and they were able³⁶ to

Fig. 8.5 The indirect nanoimpact process studied by Heyrovský et al. in reference (35) where protons are reduced on the surface of impacting TiO_2 particles.⁽³²⁾ Adapted by permission of The Royal Society of Chemistry



voltammetrically determine the approximate composition of Fe(III)-doped TiO_2 colloids. The work was subsequently extended, again exclusively with mercury electrodes, to the reduction of oxide layers on the surfaces of “metal powders” (Cu, Fe, Ni, Mo, W),³⁷ on copper/copper oxide “ultrafine powders”³⁸ and finally on aluminium “nanoparticles”.³⁹ In 35 the authors report the reduction of protons in acid solutions occurring on the surface of TiO_2 particles for the duration of their impacts with the electrode surface. This experiment is the forerunner of the “indirect processes” now studied more widely (see below and Fig. 8.5).

Innovative experiments were carried out by Scholz⁴⁰ in which the range of impact experiments were usefully extended to study the collisions of liposomes with a mercury electrode in aqueous solution at pH 7. Sharp current transients, of ca. 1–20 ms duration, were seen as the liposomes contacted, broke up and then spread over the electrode surface. However, unlike the experiments of Heyrovský, the current spikes were deduced to be non-faradaic in character with capacitive origins: the frequency of the transient signals was found to be a minimum at the potential of zero charge, pzc, and to increase with potentials negative or positive of the pzc. In subsequent work the kinetics of liposome adhesion were explored and also the impact of montmorillonite clay particles on a mercury electrode was studied.^{41,42}

Related experiments were carried out by present authors’ group using suspensions of oil droplets and solid particles in aqueous solutions induced into motion by power ultrasound and allowed to impact solid electrodes (Au, Pt).^{43–46} Current transients of microsecond duration were seen corresponding to the much faster speed of the impacting particles as compared to those in the Scholz experiments, leading to a greatly reduced contact time between particle and electrode. The amount of charge passed in the impact transients scaled with the size and conductivity of the impacting particle and the sign of the current transient inverted at the pzc of the substrate electrode as shown in Fig. 8.6. Charge transfer between the particle and the electrode and/or the deformed double layer and the electrode was inferred but at the microsecond timescales resulting from insonation it was concluded that faradaic charge transfer was not operative and experiments using large insonated metal particles confirmed no such activity.

A significant advance was made in which similar experiments were performed using silver nanoparticles, Ag_n , but without insonation, rather using natural Brownian

Fig. 8.6 Current spikes observed for graphite powder (diameter 2–20 μm) impacting a gold microdisc electrode under sonication in 0.1 M perchloric acid. Reprinted with permission from reference (45). Copyright 2004 American Chemical Society

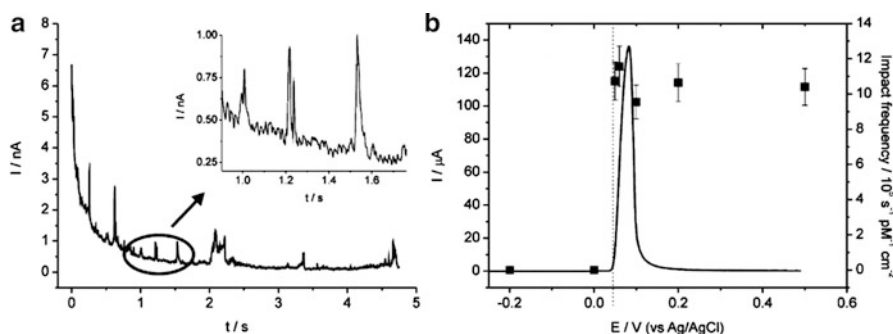
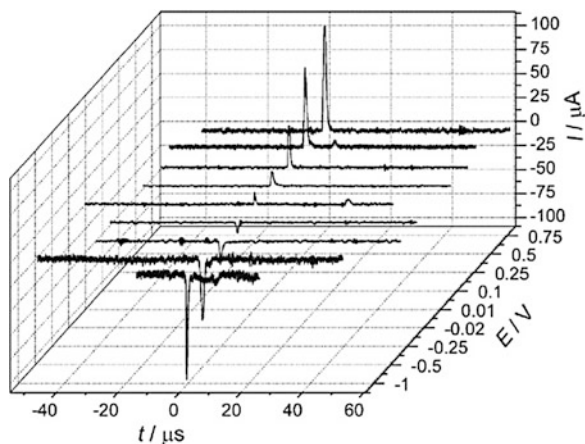
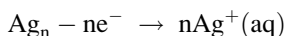


Fig. 8.7 (a) Impact spikes observed when silver nanoparticles are directly oxidised upon collision with a potentiostated carbon microelectrode surface in 10 mM citrate/90 mM KCl. (b) Stripping voltammogram for a silver nanoparticle-modified glassy carbon electrode in 10 mM citrate/90 mM KCl (*left axis*) overlaid with the observed frequency of nano-impacts (*right axis*) at a carbon microelectrode in the same solution at varying potentials. Reproduced from reference (47). Copyright © 2013 WILEY-VCH Verlag GmbH & Co. KGaA, Weinheim

motion to give rise to the impact with an electrode surface.^{47,48} Using a carbon electrode it was found that sharp current spikes of ca. 1–10 ms durations were seen (Fig. 8.7) when the electrode was potentiostatted at a value more positive than that required for the process in which the nanoparticles were oxidised to aqueous silver cations:



The onset potential for the observation of the spikes corresponded closely to the peak potential recorded if the same Ag nanoparticles were immobilised on a glassy carbon electrode (as in Sect. 8.3.1 above) and subjected to anodic stripping analysis (Fig. 8.7b). Furthermore, in the former experiments the frequency of the measured

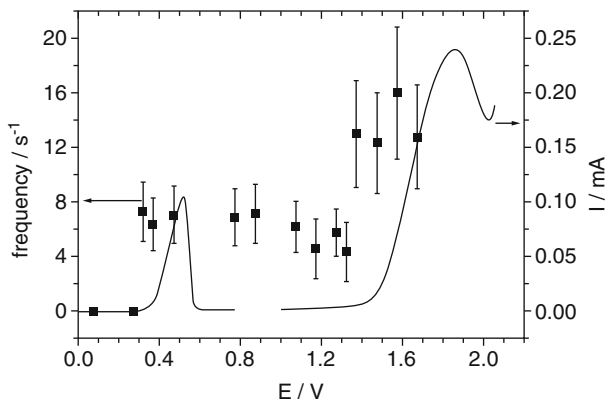


Fig. 8.8 Overlay plot of stripping voltammetry for a glassy carbon electrode modified with silver (peak potential = +0.5 V) and nickel nanoparticles (peak potential = +1.8 V) with impact frequency of the nanoparticle mixture at a carbon microelectrode in 10 mM HClO_4 /100 mM NaClO_4 . The onset potential of spikes at 0.3 V corresponds to the direct oxidation of silver nanoparticles whilst the later switch on potential (+1.4 V) is caused by the mixed nanoparticles.⁵³ Reproduced by permission of The Royal Society of Chemistry

impacts scaled with the nanoparticle concentration in solution. Analogous experiments were conducted for the electro-oxidation of diverse other metal nanoparticles: gold,⁴⁹ copper⁵⁰ and nickel.^{51,52} The different onset potential for the appearance of the oxidative spikes allowed mixtures of nanoparticles to be analysed, for example, mixtures of silver and nickel nanoparticles⁵³ as shown in Fig. 8.8.

It is evident that such experiments can provide information about the chemical identity of the impacting nanoparticles by virtue of the onset potential for the appearance of oxidative spikes. However it was additionally discovered that the oxidation of the nanoparticles is quantitative, so that all of the atoms in a particle become oxidised on impact even for a large nanoparticle of 100 nm in diameter.^{47,48} This was understood in terms of a model⁵⁴ explicitly invoking Brownian motion interpreting the observed millisecond timescale current “spikes” as each resulting from a cluster of very rapidly consecutive encounters of the nanoparticle with the electrode, in each of which partial oxidation of the nanoparticle takes place, but such as to bring about the overall complete oxidation of the nanoparticle. Calculations suggested that it was unlikely that partially oxidised nanoparticles would survive on the observed millisecond timescale. It follows that the charge passed during the current spikes was directly and quantitatively linked with the number of atoms in the nanoparticles (Faraday’s first law of electrolysis!) and hence with the nanoparticle size. Figure 8.9 shows the size distribution for nickel nanoparticles determined via oxidative electrode impacts (“anodic particle coulometry”, APC) and that measured from SEM⁵³ where the nanoparticle radius has been inferred from the charge passed under the spikes on the assumption that the particle is spherical. Excellent and quantitative agreement is apparent.

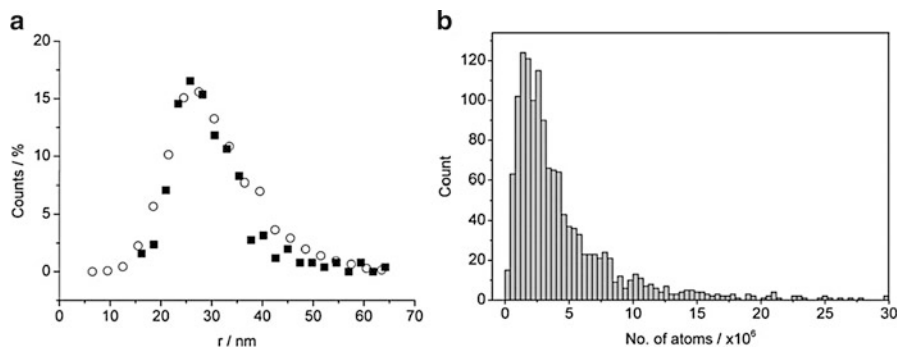


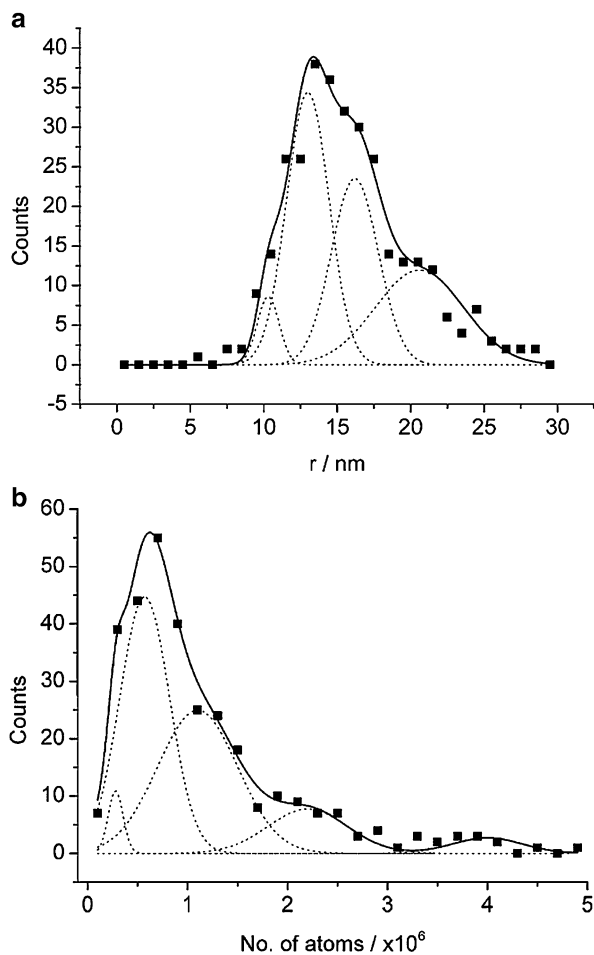
Fig. 8.9 (a) Size distribution for nickel nanoparticles determined via anodic particle coulometry (*open circle*) overlaid with a distribution for the same nanoparticles determined using SEM (*filled square*). A radius (r) of approximately 26 nm is inferred. (b) Size distribution for nickel nanoparticles in terms of the number of atoms making up each nanoparticle colliding with the electrode surface.⁵³ Reproduced by permission of The Royal Society of Chemistry

The nickel nanoparticles used in the experiments⁵³ to generate Fig. 8.9 did not undergo any significant aggregation on the timescale of the voltammetric measurements. This is in contrast to silver and gold nanoparticles where it was found that the electrochemical measurements revealed the presence of aggregation in solution.^{48,49} Figure 8.10 shows the atom counting and sizing for gold nanoparticles measured in 0.1 M aqueous HCl solution. The nanoparticles were sized as 20 nm in diameter via SEM; the electrochemistry shows the presence of some single nanoparticles (radius 10.5 ± 0.5 nm) as well as clusters of two or more nanoparticles,⁴⁹ thus revealing the occurrence of aggregation of the nanoparticles in aqueous solution. Similar observations were made for silver nanoparticles.⁴⁸ Thus APC allows not only particle sizing (number of atoms, radius of the nanoparticle if assumed spherical) but also, in principle, the extent and rate of nanoparticle aggregation in real time.

A detailed study was performed to investigate the capabilities of APC for nanoparticle agglomeration studies.⁵⁵ Agglomeration of silver nanoparticles in a citrate/potassium chloride solution was monitored by sizing the nanoparticles, in terms of the number of atoms contained in each silver nanoparticle, using APC. The analysis performed on the APC data took into consideration the link between the underlying normal distribution of a silver nanoparticle monomer and its agglomerates, ensuring that no physical meaning was lost during data fitting. In addition, nanoparticle tracking analysis (NTA), a commercially available nanoparticle-sizing device, was used to provide a critical comparison of the nanoparticle sizing results gained via APC.

As shown in Fig. 8.11, an excellent agreement was achieved between the two sizing techniques; moreover the electrochemical sizing technique was found to present a number of advantages over NTA, which can suffer from drawbacks commonly associated with optical sizing techniques such as the inability to measure the agglomeration state of non-spherical nanoparticles without performing a

Fig. 8.10 Size distribution for APC measurements of gold nanoparticles expressed as (a) radius (r) and (b) the number of atoms in an impacting nanoparticle.⁴⁹ Reproduced by permission of The Royal Society of Chemistry



correction as well as having limited application to nanoparticles contained in non-transparent solutions. A further study performed by our group found that it is possible to successfully achieve a slower rate of silver nanoparticle agglomeration/aggregation for a range of different sized particles when a high concentration of trisodium citrate is selected as the electrolyte thanks to its nanoparticle-stabilising properties.⁵⁶

With the APC method having been shown to be effective for the detection and sizing of a variety of metal nanoparticles, an obvious progression of this work and the earlier work performed by Heyrovský^{33–36} was to test the application of cathodic particle coulometry (CPC) for the detection of metal oxides. Fe₃O₄ nanoparticles were detected and sized using CPC with SEM employed to confirm the accuracy of this electrochemical sizing method.⁵⁷ Furthermore, it was discovered that using both CPC and APC in conjunction with one another (Fig. 8.12)

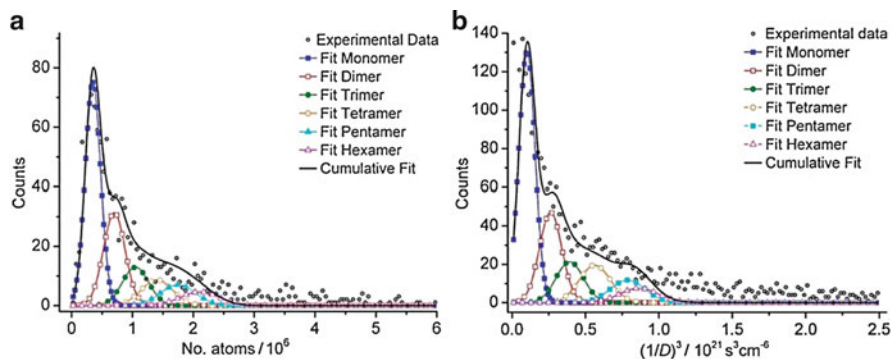


Fig. 8.11 Distribution of silver nanoparticle size in 10 mM citrate/90 mM KCl detected by (a) APC and (b) NTA. The individual Gaussian distributions for nanoparticle monomers (*filled square*), dimers (*open square*), trimers (*filled circle*), tetramers (*open circle*), pentamers (*filled triangle*) and hexamers (*open triangle*) are overlaid to achieve the overall data fit (*continuous line*). Reproduced from reference (55). Copyright © 2013. The Authors. ChemistryOpen published by WILEY-VCH Verlag GmbH & Co. KGaA, Weinheim. This is an open-access article under the terms of the Creative Commons Attribution Non-Commercial License, which permits use, distribution and reproduction in any medium, provided the original work is properly cited and is not used for commercial purposes

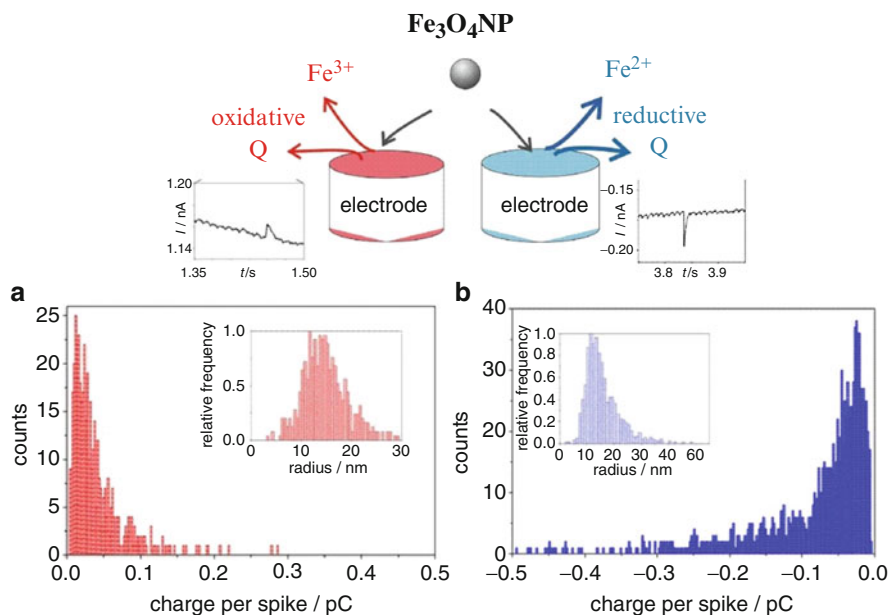


Fig. 8.12 Schematic for the two electrochemical routes used to size Fe_3O_4 nanoparticles and the resulting charge and size (*inset*) distributions gained from (a) APC experiments and (b) CPC experiments. Reproduced from reference (57). Copyright © 2013 Tsinghua University Press and Springer-Verlag Berlin Heidelberg

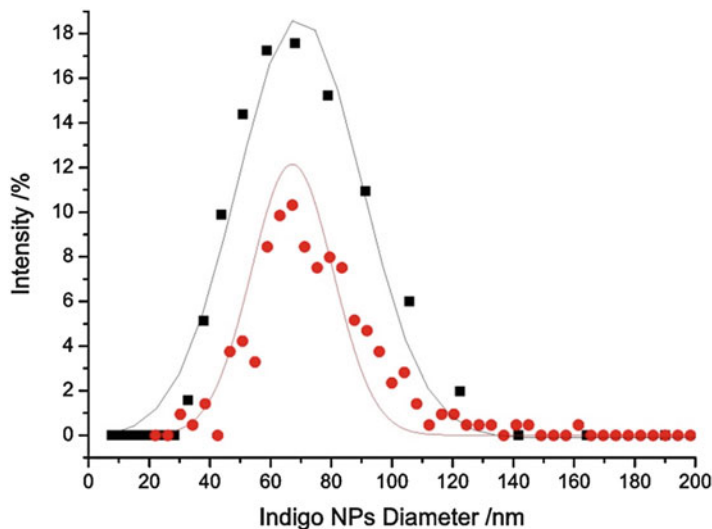


Fig. 8.13 Overlaid distributions for indigo nanoparticle sizing measured via CPC (*filled circle*) and DLS (*filled square*). Reproduced from reference (58). Copyright © 2013 WILEY-VCH Verlag GmbH & Co. KGaA, Weinheim

provides a suitably accurate and thorough nanoparticle characterisation method, rendering the use of optical techniques for verification of these electrochemical sizing methods redundant.

One type of nanoparticles that are particularly difficult to size using currently available techniques is organic nanoparticles. Experiments were conducted to investigate the suitability of CPC as an alternative to existing techniques (e.g. SEM, TEM, DLS, ultracentrifugation) used for organic nanoparticle sizing, with indigo nanoparticles used as a model system.⁵⁸ Figure 8.13 shows the size distribution gained for the electro-reduction of indigo nanoparticles via CPC in comparison with the size analysis of the same batch of nanoparticles determined using DLS. It can be seen that the resulting size distributions from both techniques are in excellent agreement, with a mean diameter of the indigo nanoparticles investigated being 68 nm.

The viability of the impact approach has been demonstrated in authentic seawater media. Figure 8.14a shows oxidative current-time transients of citrate-capped silver nanoparticles (13 ± 2 nm in radius) dispersed in seawater measured at a carbon microelectrode of radius ca. $6 \mu\text{m}$ ⁵⁹ whilst Fig. 8.14b shows the size distribution of the nanoparticles in terms of the number of atoms making up each nanoparticle inferred from the charge passed during transients such as those in Fig. 8.14a. From the independently measured average nanoparticle size of 13 nm radius it can be estimated that a single silver nanoparticle of this size contains ca. 5.4×10^5 atoms. It is evident from Fig. 8.14 that the nanoparticles must be extensively aggregated in the seawater (on the timescale studied which was ca. 40 min from the addition of the nanoparticles); deconvolution of the distribution

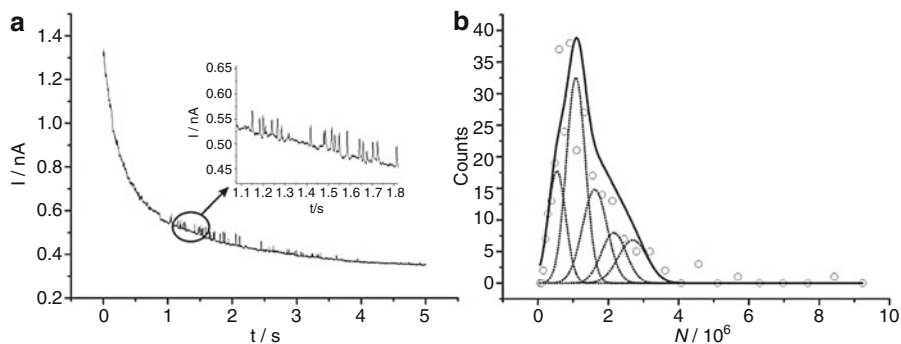


Fig. 8.14 (a) Oxidative impact spikes for silver nanoparticles in authentic seawater media. (b) Size distribution for silver nanoparticles in seawater obtained via APC expressed as the number of atoms (N) per impacting nanoparticle and deconvoluted to reveal contributions from aggregates.⁵⁹ Reproduced (a) and adapted (b) by permission of The Royal Society of Chemistry

in Fig. 8.14b suggested significant contributions from not only single nanoparticles but also aggregates of 2, 3, 4 and 5 nanoparticles corresponding to 1.08×10^6 , 1.62×10^6 , 2.16×10^6 and 2.70×10^6 atoms, respectively.

The types of nanoparticles used for APC/CPC experiments have either been synthesised in-house (Ag, Au) or purchased directly from chemical companies (Cu, Fe_3O_4). With the number of nanoparticle-based products available to purchase on the market increasing, it is typically the nanoparticles contained in these products that are leaching into the environment and posing a risk to the ecosystem. Therefore, it is these nanoparticles in consumer goods for which the need for effective detection and characterisation techniques suitable for use in the field is great. As a result, one such product, a colloidal silver disinfectant spray, was selected to determine if the nanoparticles contained within it could be studied using APC.⁶⁰ It was found that APC was effective at successfully detecting and sizing the silver nanoparticles contained in the disinfectant spray in both a standard electrolyte solution ($\text{radius}_{\text{NP}} = 11 \text{ nm}$) and seawater ($\text{radius}_{\text{NP}} = 10.3 \text{ nm}$). Figure 8.15 shows the size distributions achieved via APC and NTA methods and the excellent agreement between the two for both solutions in which the nanoparticles were dispersed.

In addition to particle identification and sizing, the impact method can also be used to measure the concentration of nanoparticles in solution. This is best done by measuring oxidative impacts at a micro-disc electrode, typically made of carbon. The current (I)-time transient at such an electrode following the application of a potential sufficient to oxidise species under diffusion control in an n -electron process is

$$I = 4nFCDr_e f(\tau)$$

where F is the Faraday constant, C is the bulk concentration of the electroactive species, D is the diffusion coefficient of the latter and $f(\tau)$ is a dimensionless time.

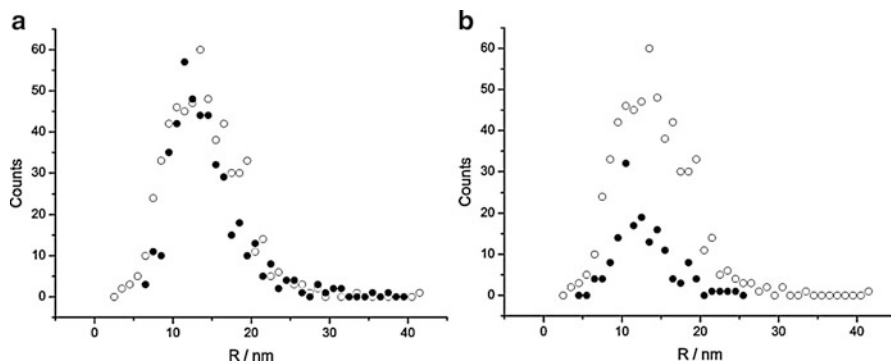


Fig. 8.15 Size distributions for the radius (R) of silver nanoparticles contained in a commercially available disinfectant cleaning spray determined via NTA (*open circle*) and APC (*filled circle*) in (a) 0.1 M NaClO_4 and (b) authentic seawater media. Reproduced from reference (60)

The latter is defined by $\tau = 4Dt/r_e^2$ where r_e is the microdisc radius and t is time. This expression is very well established for molecular species where the form of $f(\tau)$ has been given by Shoup and Szabo⁶¹ where at short times the flux to the electrode surface is linear and a Cottrellian transient behaviour is seen where $I \propto Cr_e^2(D/t)^{1/2}$ whilst for longer times, where convergent diffusion is established, $f \rightarrow 1$ so that $I \propto Cr_e D$. The implication of the differing dependences on D in the limiting forms is that if measurements are made to span the timescales of both linear and convergent diffusion then fitting of the transient allows the separate determination of the terms (nC) and D . In the molecular context, it follows that if one of n or C is known then both the unknown parameter (n or C) and D can be found via the measurement of a potential step chronoamperometric transient. The power of this approach is well documented allowing, in effect, coulometry (the measurement of n) on the voltammetric timescale without the need for exhaustive electrolysis as pertains at macro-sized electrodes.⁶²

In the context of nano-impact data such as that in Fig. 8.7a it is best expressed as a plot of the cumulative number of impacts as a function of time. This can then be compared with an integrated form of the Shoup-Szabo expression.⁵³ Fitting the latter to the former so as to determine C , the unknown concentration of nanoparticles, requires a knowledge of r_e (which can be found by independent electrochemical calibration) and D , the nanoparticle diffusion coefficient. Given the large size of the nanoparticles the latter can be reliably calculated from the Stokes-Einstein equation

$$D = \frac{k_B T}{6\pi\eta r_{np}}$$

where r_{np} is the radius of the nanoparticle, k_B is the Boltzmann constant and η is the solvent viscosity. Note that this approach is inappropriate for molecules because they are too small to reliably use the Stokes-Einstein equation. In the case of nanoparticles, r_{np} can be reliably determined from the APC experiment as noted above.

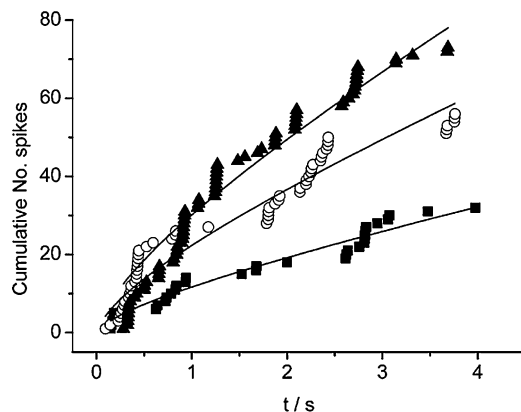


Fig. 8.16 Fitting the accumulative number of spikes as a function of time with an integrated form of the Shoup-Szabo expression for a nanoimpact experiment using varying concentrations of nickel nanoparticles, (*filled square*) 28 pM, (*open circle*) 54 pM and (*filled triangle*) 77 pM, in 10 mM HClO_4 and 100 mM NaClO_4 .⁵³ Reproduced by permission of The Royal Society of Chemistry

Figure 8.16 shows data for the cumulative number of impacts versus time obtained for three different samples of Ni nanoparticles of known concentrations— 28 ± 4 , 54 ± 8 and 77 ± 11 pM. The theoretical lines shown in the figure arise from the best fit of the integrated form of the Shoup and Szabo flux equation with the nanoparticle diffusion coefficient estimated by the Stokes-Einstein equation using the APC-determined value of r_{np} . The best fit concentration values were 30, 60 and 80 pM in excellent agreement with the known values, thus validating the use of nano-impacts as a means of measuring nanoparticle concentrations. The method was extended to systems in which aggregation was present.⁵³

The above suggests the following general strategy for both sizing and measuring the unknown concentration of nanoparticles in a single experiment. First current-time transients are recorded—such as those in Fig. 8.7a—and the data analysed first to give the average charge per “spike”. The latter can, in the absence of aggregation, then be converted into a nanoparticle radius assuming that the nanoparticles are approximately spherical. With a knowledge of r_{np} , an estimate of the nanoparticle diffusion coefficient can be made from the Stokes-Einstein equation. The original data can then be converted into a plot of the cumulative number of impacts as a function of time and fitted using the integrated Shoup-Szabo equation and the estimated diffusion coefficient to give the sought unknown concentration. By way of caveat, it might be noted that this approach is approximate in the sense that it assumes that the nanoparticle diffusion coefficient is equivalent to that in the bulk solution at all points adjacent to the electrode. In practice, nanoparticles suffer “hindered diffusion” near solid surfaces,^{63,64} with the local diffusion coefficient reduced below its bulk value; however this has been shown to have a relatively negligible effect on the analysis suggested.⁶⁵

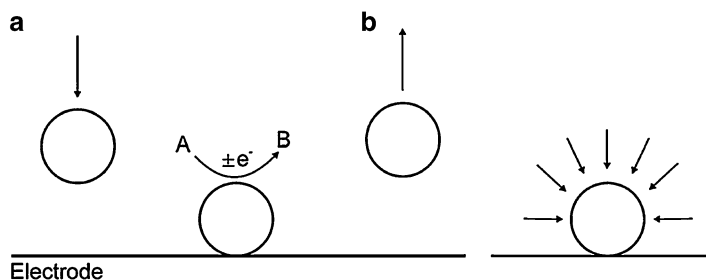


Fig. 8.17 (a) Schematic of an indirect process involving a redox reaction occurring on the surface of the nanoparticle when it is in contact with the electrode. (b) Upon impact convergent diffusion to the nanoparticle occurs almost instantaneously meaning a steady-state current is established for the electrocatalytic reaction occurring on the nanoparticle surface. Reprinted from reference (68) with permission from Elsevier

The above impact experiments involve the exhaustive electro-oxidation of metal nanoparticles. An alternative non-destructive method for nanoparticle identification and sizing has been proposed^{66,67} in which the surface of metal nanoparticles such as silver or gold is “tagged” by the adsorptive attachment of redox active molecules onto the surfaces of the nanoparticles. The tagged nanoparticles are allowed to impact an electrode surface just as in APC except that now the electrode potential is held at a value such as to reduce or oxidise the tag. Typical tags might contain nitrophenyl⁶⁶ or ferrocenyl groups which, respectively, undergo reduction or oxidation in aqueous media. Thiol groups can be used to anchor the tags on silver or gold nanoparticle surfaces. In the case where a full monolayer of tag covers the nanoparticle surfaces then the average charge passed under the “spikes” measured in an impact experiment provides information about the average surface area of the nanoparticles and hence, under the assumption that the particles are spherical, an indication of the nanoparticle size (radius). Radii inferred via this approach were in excellent agreement with those obtained for the same nanoparticles using APC.⁶⁷

In the nano-impact experiments discussed to date the electron transfer to or from the nanoparticles is a direct transfer. It is worth noting that, building on Heyrovský's³⁵ observations of proton reduction on the surface of TiO₂ nanoparticles impacting mercury electrodes, considerable progress has been made on the study of “indirect” electron transfers. Figure 8.17 schematically shows the concept underlying this experiment. As before Brownian motion of nanoparticles brings them into contact with an electrode under potentiostatic control. Whilst a nanoparticle is in contact, usually for a period of 1–10 ms, it adopts the potential of the electrode so that if redox active molecules are present in solution they can undergo electrolysis on the surface of the nanoparticle. If the nanoparticle-electrode combination is carefully selected then at some potential values electrolysis can be exclusively confined to the nanoparticles. For the case of silver nanoparticles suspended in aqueous acid solution impacting a carbon electrode,⁶⁸ the reduction of protons on the impacting silver nanoparticles can be seen as current “spikes” at potentials less cathodic than needed for their reduction on the underlying carbon electrode.

The analysis of the potential dependence of the current spikes allows for the deduction of electron transfer kinetics of redox couples at single nanoparticles via appropriate modelling^{51,68,69} treating the impacted nanoparticle as a sphere on a flat surface, and recognising that the time needed to set up steady-state electrolysis at the nanoparticle surface is tiny compared to the duration of the impacts so that the nanoparticle-confined electrolysis can be accurately treated as being at steady state. It should however be recognised that some nanoparticles can “stick” to the electrode surface which thus gradually changes its chemical (and electrochemical nature) over the course of time; values for the sticking probabilities have been measured.^{70,71} Other chemical examples of these indirect processes are given by Bard in a review of his group’s work in the area.⁷² In the case of electrochemically irreversible processes the potentials needed to see the process taking place on the nanoparticles can be shifted to significantly higher potentials than required on macro-electrodes made of the corresponding material because of the much enhanced diffusional mass transport at the nanoscale, leading to a greater overpotential for the redox reaction of interest.⁶⁸

Similar considerations, most notably treating the transport to an impacted sphere as being at steady state, also allow the modelling of the APC type of impact experiment where the nanoparticle is exhaustively oxidised and in particular the prediction of the onset potential for the appearance of current “spikes”. Different behaviour is predicted for fast or slow (electrochemically reversible or irreversible) charge transfer kinetics.^{50,52} Copper⁵⁰ and nickel⁵² nanoparticles showed slow electron transfer kinetics whereas silver nanoparticles showed reversible kinetics.⁵² The latter observation explains the fact that the onset potential for the appearance of oxidation “spikes” for the silver nanoparticles approximately matches the peak potential in the stripping voltammetry when the same particles are immobilised on an electrode.

8.3.3 Nanoparticle Detection at “Sticky” Surfaces

For the application of the nanoparticle-electrode impact methods described in Sect. 8.3.2 to environmental monitoring one major drawback is that the environmental samples to be tested would have to be isolated and transported to a laboratory before the nanoparticles within the selected sample can be detected via APC/CPC. Here, the user would run the risk of the nanoparticles within the sample changing (e.g. aggregating) before analysis can be performed. Therefore, an in situ nanoparticle detection method is desirable for this type of field work. One such method is to immobilise nanoparticles in solution on an electrode surface under open-circuit conditions before oxidatively stripping off the nanoparticles using anodic stripping voltammetry to reveal the amount of nanoparticles that have adhered to the surface and therefore providing information on the concentration of nanoparticles in solution.⁷³ Again, the potential of the stripping peak can be used to identify the type of nanoparticles present.

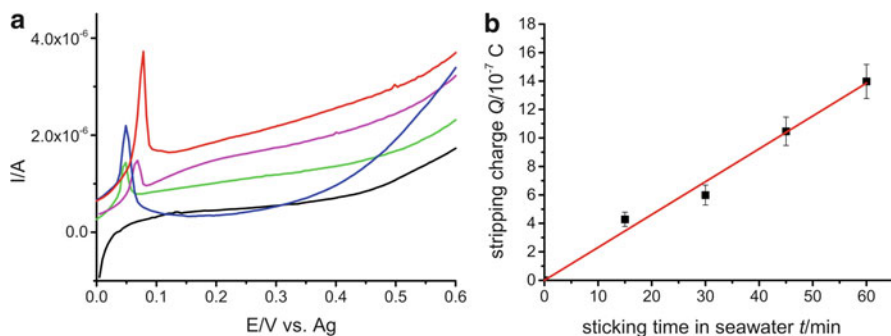


Fig. 8.18 (a) Anodic stripping voltammograms for the oxidation of silver nanoparticles contained in a commercially available colloidal silver spray cleaning product that had become adhered to a screen-printed carbon electrode in authentic seawater media after 0 min (black line), 15 min (green line), 30 min (pink line), 45 min (blue line) and 60 min (red line). (b) A plot of the stripping charge for the silver nanoparticle stripping peaks vs. time. Reproduced from reference (74)

It is possible to increase the adhesion extent and rate of nanoparticle adsorption on the electrode surface by modifying the surface so that it becomes “sticky”. The electrochemical modification of a glassy carbon electrode surface with cysteine was found to increase the ability of silver nanoparticles in 0.1 M NaClO₄ to stick onto the surface of the electrode, with larger stripping peaks observed at much shorter times in comparison to sticking experiments at an unmodified substrate.⁷³ Figure 8.18 shows how the same cysteine “sticky” electrodes were found to be suitable for the detection of silver nanoparticles contained in a commercially available colloidal silver disinfectant spray using disposable carbon electrodes immersed in authentic seawater media.⁷⁴

8.4 Outlook

The study of nanoparticles is in its infancy and that is especially the case for the electrochemistry of these environmentally important species, where measurements can be expected to reveal important information about the redox behaviour of nanoparticles as well as provide analytical methods for their characterisation. That said, to date, voltammetric methods have been developed for the identification of nanoparticles as well as offering the possibility for sizing them, monitoring their aggregation in real time and measuring their concentrations. Already electrochemical methods are providing significant insights into the behaviour of naturally occurring environmental nanoparticles^{75–79} and an explosion of growth in this area and related areas is to be expected in the near future.

References

1. Duffus JH, Nordberg M, Templeton DM (2007) Glossary of terms used in toxicology, 2nd ed. *Pure Appl Chem* 79:1153–1344
2. Sanchez A, Recillas S, Font X, Casals E, Gonzalez E, Puentes V (2011) Ecotoxicity of, and remediation with, engineered inorganic nanoparticles in the environment. *Trends Anal Chem* 30:507–516
3. Chen Z, Yadghar AM, Zhao L, Mi Z (2011) A review of environmental effects and management of nanomaterials. *Toxicol Environ Chem* 93:1227–1250
4. Zanker H, Schierz A (2012) Engineered nanoparticles and their identification among natural nanoparticles. *Annu Rev Anal Chem* 5:107–132
5. Kumar P, Kumar A, Lead JR (2012) Nanoparticles in the Indian environment: known, unknowns and awareness. *Environ Sci Technol* 46:7071–7072
6. Karn B, Kuiken T, Otto M (2009) Nanotechnology and in situ remediation: a review of the benefits and potentials risks. *Environ Health Perspect* 117:1823–1831
7. Yavuz CT, Mayo JT, Yu WW, Prakash A, Falkner JC, Yean S, Cong L, Shipley HJ, Kan A, Tomson M, Natelson D, Colvin VL (2006) Low-field magnetic separation of monodisperse Fe₃O₄ nanocrystals. *Science* 314:964–969
8. Lisha KP, Pradeep T (2009) Towards a practical solution for removing inorganic mercury from drinking water using gold nanoparticles. *Gold Bull* 42:144–149
9. Dickinson M, Scott TB (2010) The application of zero-valent iron nanoparticles for the remediation of a uranium-contaminated waste effluent. *J Hazard Mater* 178:171–178
10. Xu YH, Zhao DY (2007) Reductive immobilization of chromate in water and soil using stabilized iron nanoparticles. *Water Res* 41:2101–2110
11. Üzüüm Ç, Shahwan T, Eroğlu AE, Lieberwirth I, Scott TB, Hallam KR (2008) Application of zero-valent iron nanoparticles for the removal of aqueous Co²⁺ ions under various experimental conditions. *Chem Eng J* 144:213–218
12. Glover RD, Miller JM, Hutchison JE (2011) Generation of metal nanoparticles from silver and copper objects: nanoparticle dynamics on surfaces and potential sources of nanoparticles in the environment. *ACS Nano* 5:8950–8957
13. Howard AG (2010) On the challenge of quantifying man-made nanoparticles in the aquatic environment. *J Environ Monit* 12:135–142
14. Donaldson K, Stone V, Tran CL, Kreyling W, Borm PJ (2004) Nanotoxicology. *Occup Environ Med* 61:727–728
15. Moos PJ, Chung D, Woessner M, Honegger M, Cutler NS, Veranth JM (2010) ZnO particulate matter requires cell contact for toxicity in human colon cancer cells. *Chem Res Toxicol* 23:733–739
16. Burello E, Worth AP (2010) A theoretical framework for predicting the oxidative stress potential of oxide nanoparticles. *Nanotoxicology* 5:228–235
17. Mondal M, Basu R, Das S, Nandy P (2011) Beneficial role of carbon nanotubes on mustard plant growth: an agricultural prospect. *J Nanoparticle Res* 13:4519–4528
18. Giovanni M, Pumera M (2011) Molybdenum metallic nanoparticle detection via differential pulse voltammetry. *Electrochem Commun* 13:203–204
19. Giovanni M, Ambrosi A, Pumera M (2012) The inherent electrochemistry of nickel/nickel-oxide nanoparticles. *Chem Asian J* 7:702–706
20. Giovanni M, Pumera M (2012) Size dependant electrochemical behaviour of silver nanoparticles with sizes of 10, 20, 40, 80 and 107 nm. *Electroanalysis* 24:615–617
21. Merkoçi A, Marcolino LH, Marin S, Fatibello-Filho O, Alegret S (2007) Detection of cadmium sulphide nanoparticles by using screen-printed electrodes and a handheld device. *Nanotechnology* 18:035502
22. Marin S, Merkoçi A (2009) Direct electrochemical stripping detection of cystic-fibrosis-related DNA linked through cadmium sulfide quantum dots. *Nanotechnology* 20:055101

23. Pumera M, Aldavert M, Mills C, Merkoçi A, Alegret S (2005) Direct voltammetric determination of gold nanoparticles using graphite-epoxy composite electrode. *Electrochim Acta* 50:3702–3707
24. Ivanova OS, Zamborini FP (2010) Size-dependent electrochemical oxidation of silver nanoparticles. *J Am Chem Soc* 132:70–72
25. Tang L, Li X, Cammarata RC, Friesen C, Sieradzki K (2010) Electrochemical stability of elemental metal nanoparticles. *J Am Chem Soc* 132:11722–11726
26. Plieth W (1982) Electrochemical properties of small clusters of metal atoms and their role in surface enhanced raman scattering. *J Phys Chem* 86:3166–3170
27. Henglein A (1993) Physicochemical properties of small metal particles in solution: “micro-electrode” reactions, chemisorption, composite metal particles, and the atom-to-metal transition. *J Phys Chem* 97:5457–5471
28. Henglein A (1977) The reactivity of silver atoms in aqueous solutions (a γ -radiolysis study). *Ber Bunsenges Phys Chem* 81:556–561
29. Ward Jones SE, Chevallier FG, Paddon CA, Compton RG (2007) General theory of cathodic and anodic stripping voltammetry at solid electrodes: mathematical modelling and numerical simulations. *Anal Chem* 79:4110–4119
30. Ward Jones SE, Campbell FW, Baron R, Xiao L, Compton RG (2008) Particle size and surface coverage effects in the stripping voltammetry of silver nanoparticles: theory and experiment. *J Phys Chem C* 112:17820–17827
31. Ward Jones SE, Toghiani KE, Zheng SH, Morin S, Compton RG (2009) The stripping voltammetry of hemispherical deposits under electrochemically irreversible conditions: a comparison of the stripping voltammetry of bismuth on boron-doped diamond and Au(III) electrodes. *J Phys Chem C* 113:2846–2854
32. Rees NV, Zhou Y-G, Compton RG (2012) Making contact: charge transfer during particle-electrode collision. *RSC Adv* 2:379–384
33. Heyrovský M, Jirkovský J (1995) Polarography and voltammetry of ultrasmall colloids: introduction to a new field. *Langmuir* 11:4288–4292
34. Heyrovský M, Jirkovský J, Müller BR (1995) Polarography and voltammetry of aqueous colloidal SnO₂ solutions. *Langmuir* 11:4293–4299
35. Heyrovský M, Jirkovský J, Štruplová-Bartáčková M (1995) Polarography and voltammetry of aqueous colloidal TiO₂ solutions. *Langmuir* 11:4300–4308
36. Heyrovský M, Jirkovský J, Štruplová-Bartáčková M (1995) Polarography and voltammetry of mixed titanium(IV) oxide/iron(III) oxide colloids. *Langmuir* 11:4309–4312
37. Korshunov AV, Heyrovský M (2006) Voltammetry of metallic powder suspensions on mercury electrodes. *Electroanalysis* 18:423–426
38. Korshunov A, Heyrovský M (2009) Electrochemical behaviour of copper metal core/oxide shell ultra-fine particles on mercury electrodes in aqueous dispersions. *J Electroanal Chem* 629:23–29
39. Korshunov A, Heyrovský M (2010) Voltammetry of aluminium nanoparticles in aqueous media with hanging mercury drop electrode. *Electroanalysis* 22:1989–1993
40. Hellberg D, Scholz F, Schauer F, Weitschies W (2002) Bursting and spreading of liposomes on the surface of a static mercury drop electrode. *Electrochem Commun* 4:305–309
41. Scholz F, Hellberg D, Harnisch F, Hummel A, Hasse U (2004) Detection of the adhesion events of dispersed single montmorillonite particles at a static mercury drop electrode. *Electrochem Commun* 6:929
42. Hellberg D, Scholz F, Schubert F, Lovrić M, Omanović D, Hernández VA, Thede R (2005) Kinetics of liposome adhesion on a mercury electrode. *J Phys Chem B* 109:14715–14726
43. Banks CE, Rees NV, Compton RG (2002) Sono-electrochemistry in acoustically emulsified media. *J Electroanal Chem* 535:41–47
44. Banks CE, Rees NV, Compton RG (2002) Sono-electrochemistry understood via nanosecond voltammetry: sono-emulsions and the measurement of the potential of zero charge of a solid electrode. *J Phys Chem B* 106:5810–5813

45. Rees NV, Banks CE, Compton RG (2004) Ultrafast chronoamperometry of acoustically agitated solid particulate suspensions: nonFaradaic and Faradaic processes at a polycrystalline gold electrode. *J Phys Chem B* 108:18391–18394
46. Clegg AD, Rees NV, Banks CE, Compton RG (2006) Ultrafast chronoamperometry of single impact events in acoustically agitated solid particulate suspensions. *ChemPhysChem* 7:807–811
47. Zhou Y-G, Rees NV, Compton RG (2011) The electrochemical detection and characterization of silver nanoparticle in aqueous solutions. *Angew Chem Int Ed* 50:4219–4221
48. Rees NV, Zhou Y-G, Compton RG (2011) The aggregation of silver nanoparticles in aqueous solution investigated via anodic particle coulometry. *ChemPhysChem* 12:1645–1647
49. Zhou Y-G, Rees NV, Pillay J, Tshikhudo R, Vilakazi S, Compton RG (2012) Gold nanoparticles show electroactivity: counting and sorting nanoparticles upon impact with electrodes. *Chem Commun* 48:224–226
50. Haddou B, Rees NV, Compton RG (2012) Nanoparticle-electrode impacts: the oxidation of copper nanoparticles has slow kinetics. *Phys Chem Chem Phys* 14:13612–13617
51. Zhou Y-G, Rees NV, Compton RG (2013) Electrochemistry of nickel nanoparticles is controlled by surface oxide layers. *Phys Chem Chem Phys* 15:761–763
52. Zhou Y-G, Haddou B, Rees NV, Compton RG (2012) The charge transfer kinetics of the oxidation of silver and nickel nanoparticles via particle-electrode impact electrochemistry. *Phys Chem Chem Phys* 14:14354–14357
53. Stuart EJE, Zhou Y-G, Rees NV, Compton RG (2012) Determining unknown concentrations of nanoparticles: the particle-impact electrochemistry of nickel and silver. *RSC Adv* 2:6879–6884
54. Dickinson EJE, Rees NV, Compton RG (2012) Nanoparticle-electrode collision studies: brownian motion and the timescale of nanoparticle oxidation. *Chem Phys Lett* 528:44–48
55. Ellison J, Tschulik K, Stuart EJE, Jurkschat K, Omanović D, Uhlemann M, Crossley A, Compton RG (2013) Get more out of your data: a new approach to agglomeration and aggregation studies using nanoparticle impact experiments. *ChemistryOpen* 2:69–75
56. Lees JC, Ellison J, Batchelor-McAuley C, Tschulik K, Damm C, Omanović D, Compton RG (2013) Nanoparticle impacts show high-ionic-strength citrate avoids aggregation of silver nanoparticles. *ChemPhysChem* 14:3895–3897
57. Tschulik K, Haddou B, Omanović D, Rees NV, Compton RG (2013) Coulometric sizing of nanoparticles: cathodic and anodic impact experiments open two independent routes to electrochemical sizing of Fe₃O₄ nanoparticles. *NanoResearch* 6:836–841
58. Cheng W, Zhou X-F, Compton RG (2013) Electrochemical sizing of organic nanoparticles. *Angew Chem Int Ed* 52:12980–12982
59. Stuart EJE, Rees NV, Cullen JT, Compton RG (2013) Direct electrochemical detection and sizing of silver nanoparticles in seawater media. *Nanoscale* 5:174–177
60. Stuart EJE, Tschulik K, Omanović D, Cullen JT, Jurkschat K, Crossley A, Compton RG (2013) Electrochemical detection of commercial silver nanoparticles: identification, sizing and detection in environmental media. *Nanotechnology* 24:444002
61. Shoup D, Szabo A (1982) Chronoamperometric currents at finite disk electrode. *J Electroanal Chem* 140:237–245
62. Paddon CA, Bhatti FL, Donohoe TJ, Compton RG (2006) Cryo-electrochemistry in tetrahydrofuran: the electrochemical reduction of a phenyl thioether: [(3-{{trans-4-(Methoxymethoxy)cyclohexyl}oxy}propyl)thio]benzene. *J Electroanal Chem* 589:187–194
63. Brenner H (1961) The slow motion of a sphere through a viscous fluid towards a plane surface. *Chem Eng Sci* 16:242–251
64. Bevan MA, Prieve DC (2000) Hindered diffusion of colloidal particles very near to a wall: revisited. *J Chem Phys* 113:1228–1236
65. Barnes EO, Compton RG (2013) The rate of adsorption of nanoparticles on microelectrode surfaces. *J Electroanal Chem* 693:73–78

66. Zhou Y-G, Rees NV, Compton RG (2012) The electrochemical detection of tagged nanoparticles via particle-electrode collisions: nanoelectroanalysis beyond immobilisation. *Chem Commun* 48:2510–2512
67. Rees NV, Zhou Y-G, Compton RG (2012) The non-destructive sizing of nanoparticles via particle-electrode collision: tag-redox coulometry (TRC). *Chem Phys Lett* 525:69–71
68. Kahk JM, Rees NV, Pillay J, Tschikhudo R, Vilakazi S, Compton RG (2012) Electron transfer kinetics at single nanoparticles. *Nano Today* 7:174–179
69. Ward KR, Lawrence NS, Hartshorne RS, Compton RG (2012) Modelling the steady state voltammetry of a single spherical nanoparticle on a surface. *J Electroanal Chem* 683:37–42
70. Zhou Y-G, Rees NV, Compton RG (2011) Electrode-nanoparticle collisions: the measurement of the sticking coefficient of silver nanoparticles on a glassy carbon electrode. *Chem Phys Lett* 514:291–293
71. Zhou Y-G, Stuart EJE, Pillay J, Vilakazi S, Tshikhudo R, Rees NV, Compton RG (2012) Electrode-nanoparticle collisions: the measurement of the sticking coefficients of gold and nickel nanoparticles from aqueous solution onto a carbon electrode. *Chem Phys Lett* 551:68–71
72. Bard AJ, Zhou H, Kwon SJ (2010) Electrochemistry of single nanoparticles via electrocatalytic amplification. *Israel J Chem* 50:267–276
73. Tschulik K, Palgrave R, Batchelor-McAuley C, Compton RG (2013) ‘Sticky electrodes’ for the detection of silver nanoparticles. *Nanotechnology* 24:295502
74. Cheng W, Stuart EJE, Tschulik K, Compton RG (2013) A disposable sticky electrode for the detection of commercial silver nanoparticles in seawater. *Nanotechnology* 24:505501
75. Bura-Nakić E, Krznarić D, Helz GR, Ciglencečki I (2012) Characterization of iron sulfide species in model solutions by cyclic voltammetry. Revisiting an old problem. *Electroanalysis* 23:1376–1382
76. Bura-Nakić E, Viollier E, Jézéquel D, Thiam A, Ciglencečki I (2009) Reduced sulfur and iron species in anoxic water column of meromictic crater Lake Pavin (Massif Central, France). *Chem Geol* 266:311–317
77. Helz GR, Ciglencečki I, Krznarić D, Bura-Nakić E (2011) Voltammetry of sulphide nanoparticles and the FeS(aq) problem. *Aquat Redox Chem* 1071:265–282
78. Krznarić D, Helz GR, Bura-Nakić E, Jurašin D (2008) Accumulation mechanism for metal chalcogenide nanoparticles at Hg⁰ electrodes; Cu sulfide example. *Anal Chem* 80:742–749
79. Bura-Nakić E, Krznarić D, Jurašin D, Helz GR, Ciglencečki I (2007) Voltammetric characterization of metal sulfide particles and nanoparticles in model solutions and natural waters. *Anal Chim Acta* 594:44–51

Part III
Sensors and Biosensors for Organic
Compounds of Environmental Importance

Chapter 9

Pharmaceuticals and Personal Care Products

Lúcio Angnes

9.1 Introduction

9.1.1 A Brief Chronology

When the industrial revolution started, there was a consensus that rivers, lakes, and mainly the oceans were able to absorb and transform entirely the pollution produced by the humans. In the next century, particularly after the Second World War, an impressive “turnover” in the human population-growing factor was observed. The main reasons for this huge expansion of the population were the exponential production of foods, which passed from manual to mechanized process and the development of important drugs, in special the antibiotics, penicillin being the most representative example. The mechanization in the agriculture reduced significantly the needs of labor force in the cultivated lands, oppositely to the requests of the modern industry. This reality brings about a strong emigration of peoples from the field to the cities. Besides a rapid and non-organized growing of the population, the modern industrial processes pass to demand quantities of water never before utilized and consequently leave behind ever-growing amounts of wastewater.

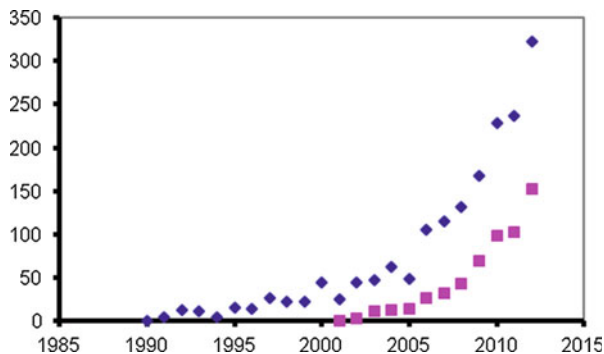
Until the middle of the twentieth century, there was no conscience about the potential problems related to any inorganic or organic compound wasted in soil, rivers, lakes, and oceans or even in the atmosphere. Probably the Minamata disaster was the starting point of concern about the effects of pollution. In the following years, the conscience of the Americans was waked up for DDT problems. In sequence, peoples realized that the capacity of our rivers, lakes, oceans, soil, and atmosphere to accept all kinds of pollutants is finite and started to look with more care for all aspects involving our environment.

L. Angnes (✉)

Instituto de Química, University of São Paulo, São Paulo, SP, Brazil

e-mail: luangnes@iq.usp.br

Fig. 9.1 Number of research publications per year using “emerging contaminants” with (■) and without quotation marks (◆) using the Web of Science database



In the following years, with the evolution of the analytical instrumentation, the limits of detection were lowered tremendously and in consequence the number of compounds monitored in water grew remarkably. Many “new” compounds are now referred as “emerging compounds”; once among these new analytes, pharmaceutical and products of personal care started to be monitored in waters with increasing frequency in the last years.

A search in the Web of Sciences presents some interesting aspect. Using the words emerging contaminants, a total of 1,836 papers were found (May 30, 2013), this designation being utilized for the first time in 1990. Between this year and the end of 2012, there are 1,712 papers. Making the same search putting “emerging contaminants” between quotation marks, a total of 564 papers were found till the end of 2012, being the first from 2001. Figure 9.1 depicts both series of data and demonstrates the exponential growing of research on the topic in question.

9.1.2 What Are and Why Study Emerging Compounds?

There is not a clear definition but, in principle, almost all the species synthesized for applications in the modern life can be classified as emerging compounds. All these compounds represent a potential risk for the environment, especially considering its extraordinary diversity. Nowadays, about three million synthetic compounds are known and this number is still growing at an accelerated rate and about 100,000 of these compounds are produced regularly for the most diverse applications, equivalent to 200 million tons per year. From this impressive amount, 20–30 % are estimated that attain the aquatic environment and we know almost nothing about the effects of these compounds individually or in association with other compounds on the environment. There are aspects as embryonary defects, DNA damage, cancer, or even fish sex exchange attributed to different emerging compounds. We need to understand exactly the sources of these compounds, their reactivity, distribution, lifetime, secondary products, and even environmental problems unrevealed until now, involving, short-, medium-, or long-term processes.

9.1.3 *Scope of This Chapter*

Emerging contaminants is a theme extremely ample and in this chapter we are restricted to pharmaceuticals and personal care products in water. Even restricting to these two issues, the subject of this chapter remains complex and difficult to cover in details. In this sense, this chapter is limited to discuss the development of voltammetric methods focused in the quantification of pharmaceuticals and personal care products.

9.2 Overview

Pharmaceuticals and personal care products are used for many centuries but their monitoring and the evaluation of their effects on the environment and on humans is still a relatively new subject. Until the starting of the 1990s, the main attention was focused on the heavy metals and the persistent organic pollutants. In the industrialized countries, this problem decreased significantly due to the strong control of the pollution sources. At this time, many scientists realized that there are a myriad of man-made chemicals, utilized in the industry, agriculture, and also pharmaceuticals and personal care products that are still unregulated and potentially can produce adverse effects on the environment and on the humans.

Only in the pharmaceutical area, there are more than 3,000 pharmaceutically active compounds (analgesics, anti-inflammatory drugs, antibiotics and antihistamines, β -blockers, lipid regulators, contraceptives, antidiabetics, antipsychotics, estrogens, antidepressants, anticonvulsants, antiepileptics, stimulants, impotence drugs, etc.) that are used in human medicine. The main part of these pharmaceuticals is excreted in urine and feces and attains the aquatic environment water via wastewater and the effects of all these products alone or in combination are still not well known. In association with the pharmaceuticals, personal care products are normally studied and the acronym PPCP was coined and adopted by many authors.¹

Books,^{1,2} reports,³⁻⁵ and reviews⁶⁻¹¹ dealing with different aspects of emerging contaminants discuss their potential sources, the complexity of their removal, and the importance of significantly increasing research efforts related to these issues. The majority of the researchers that are working in this area utilize pre-concentration processes associated with separation techniques, such as solid-phase extraction-liquid chromatography-electrospray-tandem mass spectrometry (SPE-LC-ESI-MS/MS),¹² ultraperformance liquid chromatography-mass spectrometry (UPLC-MS/MS),¹³ liquid chromatography coupled to fluorescence detection¹⁴ or combining gas chromatography/mass spectrometry (GC/MS), and liquid chromatography/quadrupole time-of-flight mass spectrometry (LC-QTOF-MS)¹⁵ among other alternatives. Even so, some authors demonstrate that mass

spectroscopy needs also many improvements, once the databases and libraries presently available have mostly been developed for the metabolomic field.¹⁶

Even taking into account that the techniques mentioned above produce very reliable data, Greenwood and col.¹⁷ detach that the infrequent spot (bottle) sampling is unlikely to fulfill the developing needs. Representative sampling is a key requisite to generate precise information about water quality and the authors detach that a range of alternative tools are emerging and even considering the fact that these ones do not have the same low level of uncertainty, they can provide more representative data, often at lower cost. The electroanalytical technique is one of the most promising possibilities, until now not adequately explored.

9.3 Voltammetric Analysis

Electroanalytical techniques are well established and their applications are rapidly growing, spreading to the most different fields, among them the pharmaceutical area. The extraordinary advances obtained with the modern instruments and techniques turned electroanalysis more sensitive, rapid, and also more selective to solve many analytical problems. For the quantification of pharmaceutical and personal care products (PPCP), the literature presents many research articles describing the use of different voltammetric techniques, mainly focusing the quantification of products in their unprocessed form or in the final commercial form, or quantifying pharmaceuticals and/or their metabolites in human body fluids, but until now there are only few studies focusing on the analysis of these compounds in surface water, groundwater, wastewater, or drinking water. Many of these studies present very good sensitivity and have potential to be employed in the analysis of these compounds in aqueous matrix. In the following sections we discuss the (relatively small number of) studies involving the determination of PPCP in water, as also selected examples, demonstrating the applicability of the electroanalytical techniques for the analysis for this purpose.

In the literature, a series of good reviews about the use of electroanalytical methods for determination of pharmaceuticals,¹⁸ the utilization of chemical-modified electrodes,¹⁹ or even focusing on the utilization of voltammetric techniques in association with flow injection analysis²⁰ demonstrate the great potentialities of the use of electroanalysis for quantification of low levels of pharmaceutical compounds. In the following sections, these aspects are addressed and selected examples are presented. A classification based on the electrode materials was chosen for giving the lecturer an outlook of the developments in the area.

9.3.1 Mercury Electrodes

Mercury electrodes were determinant for the development in the early days of electroanalytical techniques. Starting by polarography developed by Heyrovsky in 1922, mercury electrodes were fundamental for the development of many electroanalytical methods. The elevated purity attainable for metallic mercury, the excellent overpotential for hydrogen reduction, and the fact that the electrode is renewable turn this electrode very attractive for the analysis of pharmaceutical compounds. The first paper was published in 1948.²¹ In the following years the number of articles that appeared was relatively small, but with the evolution of the instrumentation and especially with the advent of the hanging mercury drop electrode (HMDE), the applications utilizing mercury electrodes associated to adsorptive processes spread out and the number of studies grew significantly.

Adsorptive processes on mercury electrodes are very favorable techniques for the quantification of low concentrations of a series of organics, among them pharmaceutical compounds. The perfectly smooth surface of mercury associated with the very reproducible electrode area turns HMDE the electrode of choice for adsorptive processes, with the peculiar advantage of be completely renewable just by the opening (and closing) of the mercury flow.

Using HMDE, the analysis of triamcinolone acetonide (TAA) was performed by square-wave voltammetry (SWV) and a detection limit of $3.0 \times 10^{-10} \text{ mol L}^{-1}$ was attained.²² The method was successfully applied for the analysis of TAA in tablets and in serum, without pretreatment of the samples. The quantification of haloperidol was performed under controlled adsorptive accumulation onto HMDE and was applied in low concentrations of the bulk form to pharmaceutical formulations and human fluids. A limit of quantification (LOQ) of $3.83 \times 10^{-10} \text{ mol L}^{-1}$ was calculated by the authors.²³ In another study of the same research group, ethinylestradiol was investigated and a detection limit of $5.9 \times 10^{-10} \text{ mol L}^{-1}$ was reported.²⁴ The analysis of cefoperazone in pharmaceutical formulations and in human plasma was carried by pre-concentration followed by SWV onto an HMDE, attaining a detection limit of $4.5 \times 10^{-10} \text{ mol L}^{-1}$.²⁵ The analysis of the antifungal antibiotic griseofulvin, used for treatment of pathogenic mycotic diseases, was performed by adsorptive stripping analysis using HMDE and a limit of quantification of $5.8 \times 10^{-10} \text{ mol L}^{-1}$ was reported.²⁶ In another study, the same author developed methodology for gatifloxacin analysis, attaining detection limits of 1.5×10^{-9} and $2.2 \times 10^{-9} \text{ mol L}^{-1}$ in the bulk form and in human serum, respectively.²⁷ The analysis of tobramycin, a broad-spectrum antibiotic against Gram-positive bacteria, was performed utilizing linear sweep voltammetry and a limit of quantification of $3.44 \times 10^{-9} \text{ mol L}^{-1}$ was attained.²⁸ In a study focused on the quality control of tinidazole, a drug utilized for treatment of trichomonas infection, methodology for quantification of this drug was developed and applied for tablets and also in biological fluids and the detection limit attained was $4.5 \times 10^{-10} \text{ mol L}^{-1}$. In this study, it was observed that the addition of CTAB increases significantly the voltammetric signal of tinidazole.²⁹ The association of

ASV and square-wave voltammetry for the analysis of rosiglitazone was explored in human urine and plasma samples. The detection limit attained for this drug was $3.2 \times 10^{-11} \text{ mol L}^{-1}$ using only 120 s of pre-concentration.³⁰ Our search indicates that presently there are studies on HMDE for the quantification of insecticides and metals in wastewater, groundwater, superficial water, and drinking water, but any study involving real samples.

9.3.2 Other Metallic Electrodes

The use of other metals for electroanalytical purposes is nowadays very frequent and still growing. All solid electrodes, compared to mercury electrodes, present some disadvantages such as difficulty to control the reproducibility and the renovation of its surface can be a challenge. Conversely, mercury can be used only in a limited anodic potential region, and this hampers the oxidation of many organic molecules. Many solid electrodes can be utilized in this region and this is an aspect that can be explored with these electrodes. The use of metals as electrodes for the quantification of pharmaceutical compounds was considerably explored in the last years and their use is still growing. Among the noble metals (normally considered inert) platinum and gold are more widely used, followed by palladium. Applications involving copper, lead, silver, and ruthenium are also reported in the literature.

Gold electrodes were utilized for the quantification of tetracycline, chlorotetracycline, and oxytetracycline using a screen-printed electrode (SPE) in a flow cell. The limit of detection for the three cyclones was $9.6 \times 10^{-7} \text{ mol L}^{-1}$, $5.8 \times 10^{-7} \text{ mol L}^{-1}$, and $3.5 \times 10^{-7} \text{ mol L}^{-1}$, quantified in pharmaceutical products and foods.³¹ Gold electrodes can also be easily modified with self-assembled monolayers (SAMs) and in some occasions the structure formed on the surface of the electrode can favor the electrochemical process. The quantification of vitamin B-12 was done on a gold electrode modified by a monolayer of mercaptoacetic acid and the limit of quantification attained in this case was $1.0 \times 10^{-9} \text{ mol L}^{-1}$.³² The quantification of the antidepressant trazodone was done using a static and a rotating platinum disk electrode and the detection limits attained were $2.5 \times 10^{-6} \text{ mol L}^{-1}$ for the static electrode and $1.72 \times 10^{-6} \text{ mol L}^{-1}$ for the rotating electrode.³³ The deposition of platinum over gold electrodes and its association with flow injection analysis (FIA) allow to perform 90-analysis per hour and detection limit of $7.8 \times 10^{-7} \text{ mol L}^{-1}$.³⁴

Palladium was electrodeposited on gold electrodes constructed from recordable CDs and was utilized for dipyrone quantification under flow injection analysis. The limit of detection attained was $1 \times 10^{-7} \text{ mol L}^{-1}$, the volume utilized in the FIA was only 100 μL , and the time required for each analysis was 40 s.³⁵ Arrays of microelectrodes modified by electrodeposition of palladium, platinum, and a mixture of platinum + palladium were utilized for the quantification of the components of a mixture containing ascorbic acid, dopamine, epinephrine, and dipyrone.³⁶ Lead

films plated on glassy carbon or gold electrodes point to a promising way to determine low levels of pharmaceutical products. Very low detection levels for the quantification of testosterone, trimethoprim, sildenafil citrate, folic acid, rutin, glipizide, and rifampicine, situated between 2×10^{-8} and 9×10^{-11} mol L⁻¹ were reported in different studies carried out by the same research group.³⁷

The formation of Cu(III) on the surface of the electrode in alkaline medium was explored to catalyze the oxidation of acetyl salicylic acid. The quantification of this compound in pharmaceutical formulations was done using amperometric measurements in association with batch injection analysis (BIA). A detection limit of 4.8×10^{-7} mol L⁻¹ and a frequency of 60-determination per hour were reported.³⁸ There is a series of studies where silver is involved in the quantification of pharmaceutical products, mainly as nanoparticle or in the form an insoluble compound, sometimes amalgamated. One interesting study involving solid silver electrodes describes the determination of trihalomethanes (THMs) in waters and utilizes a very clever process. On the silver electrode maintained as cathode, the THM is electrolyzed to release the halide (chloride or bromide). In a second step, the previously freed halide ions are collected on the second silver electrode, and anodically polarized, forming the corresponding silver halide film, which adheres to this electrode surface. In sequence, the collected film is reduced using differential pulse voltammetry (DPV). The detection limit reported was 12 nmol L⁻¹ for bromoform and 50 nM L⁻¹ for chloroform.³⁹ Thioridazine was quantified utilizing cyclic voltammetric measurements with ruthenium, platinum, and glassy carbon electrodes. The best results were obtained with ruthenium and the linear region was situated in the concentration range of 5×10^{-5} and 1×10^{-3} mol L⁻¹.⁴⁰

Bismuth film electrode (BiFE) was developed to replace mercury film electrodes. More recently, BiFEs were also utilized for the quantification of vitamin B-12 in pharmaceutical products, with a detection limit of 3.3×10^{-8} mol L⁻¹ after a pre-concentration of only 30 s.⁴¹ Sildenafil citrate was quantified on BiFE films prepared ex situ using a glassy carbon electrode as substrate. A limit of detection of 1.8×10^{-8} mol L⁻¹ was attained with 120 s of deposition.⁴²

9.3.3 Carbon Electrodes

9.3.3.1 Conventional Carbon Electrodes

Carbon electrodes usually present good conductivity, broad potential windows, and low background current. Its wider potential window compared with the other classes of electrodes confers them an ample set of applications in electroanalysis. The origin and the treatment of its surface can be determinant of electron transfer reactivity, so as the predominance of edge plane toward basal plane in this surface will determine faster electron transfer kinetics. A variety of treatments to improve the electrode performance and to obtain reproducible surfaces have been proposed, but there is not a “definitive prescription.”

Glassy carbon electrodes (GCE) are the most used electrodes for many applications, including PPCP analysis, due to their properties such as excellent electrical conductivity and mechanical stability, wide potential range, impermeability to gases, chemical inertness (even to concentrated acids), and reproducible performance.⁴³ There are many studies where GCE was employed for quantification of very low concentration of pharmaceuticals and representative examples are the following: For the quantification of tegaserod, this compound was adsorbed on the glassy carbon electrode at open circuit, at pH 9.0. After this step, the medium is exchanged and the DPV is processed. A detection limit of 3.0×10^{-10} mol L⁻¹ was obtained under 3-min pre-concentration.⁴⁴ The association of amperometry and BIA for isoniazid quantification leads to a very sensitive response, with a detection limit calculated as 4×10^{-9} mol L⁻¹ and an unusual linear region of response situated from 5×10^{-8} to 1.0×10^{-3} mol L⁻¹.⁴⁵ Adsorptive accumulation was explored for the direct quantification of levofloxacin in human urine, which was only diluted (1,000 times) before the measurements in acetate buffer (pH 5.0). A detection limit of 5×10^{-9} mol L⁻¹ was obtained utilizing 5 min of pre-concentration at +0.4 V.⁴⁶ Trimetazidine was quantified in tablet dosage form and in urine. Both samples were diluted in buffer solution and the analyte was pre-concentrated on the electrode for 300 s, at open circuit, under vigorous stirring. In sequence, the solution was replaced for another, with the same buffer and the square-wave voltammogram was recorded. A detection limit of 2×10^{-8} mol L⁻¹ was attained.⁴⁷ The antihypertensive and antianginal agent amlodipine besylate in pharmaceutical, urine, and serum was quantified exploring cyclic and square-wave voltammetry. The best pH encountered was 11.0, the ideal pre-concentration potential was determined as 0.0 V, and the deposition time established as ideal was 180 s. Under these conditions a detection limit of 1.4×10^{-8} mol L⁻¹ was reached.⁴⁸ The quantification of amisulpride was optimized for quantification in dosage forms, serum, urine, and gastric juice by oxidation using DPV and SWV. The response obtained at pH 7.0 was the most favorable and the detection limits attained were 2.2×10^{-8} mol L⁻¹ using DPV and 3.6×10^{-8} mol L⁻¹ when SWV was the technique utilized.⁴⁹ The same authors' research group also developed studies involving vardenafil present in dosage forms and in serum. The detection limits determined in electrolyte solutions were calculated as 2.27×10^{-8} mol L⁻¹ using DPV and 6.56×10^{-8} mol L⁻¹ using SWV. In the presence of serum the detection limits achieved were evaluated as 2.53×10^{-8} mol L⁻¹ using DPV and 2.69×10^{-8} mol L⁻¹.⁵⁰ The analysis of levodopa and carbidopa in mixtures was developed, based on the reductive peak of first and the oxidative peak of the second when in mixture. In this study, the analysis of levodopa was not affected by the presence of carbidopa, whereas for the quantification of this last, it was necessary to utilize a nafion, turning the surface selective to carbidopa. The detection limit obtained for levodopa was 4.2×10^{-8} mol L⁻¹ and for carbidopa (using the nafion film) was 3.8×10^{-7} mol L⁻¹.⁵¹

Pyrolytic graphite electrodes have also been utilized for quantification of very low levels of pharmaceutical compounds. The quantification of acetyl salicylic acid and caffeine was done employing an edge plane pyrolytic graphite electrode.

Detection limits for acetyl salicylic acid were 1×10^{-8} mol L⁻¹ and for caffeine 8×10^{-9} mol L⁻¹.⁵² A comparative study involving pyrolytic graphite with different surfaces (basal \times edge planes) was carried out for hydrocortisone. The edge plane electrode showed a better performance, with greater sensitivity, and for hydrocortisone the detection limit attained was 8.8×10^{-8} mol L⁻¹. The same electrode was utilized to quantify hydrocortisone in blood plasma and any interference was observed.⁵³ Diclofenac was studied by SWV using edge plane pyrolytic graphite. A detection limit of 6×10^{-9} mol L⁻¹ was evaluated for this analyte.⁵⁴ The surface of pyrolytic graphite favors the adsorption of many different catalytic species on its surface and the majority of the recent papers involve the utilization of some modifiers on its surface.

Screen printing electrodes (SPE) are gaining preference for many applications, in special for screening procedures outside of a conventional laboratory. The construction of SPE makes use of thick-film technology and it is a very convenient form of mass production of disposable electrochemical sensors (units with individual electrodes or more commonly comprised by an arrangement with the three electrodes). These electrodes are constructed by deposition of conductive carbon inks on the surface of an inert substrate (PVC and ceramic materials are preferred). To obtain reproducible units, the film dimensions should be identical. Advantages such as the very low cost of these electrodes, the possibility of printing a large number of units (with the same ink to obtain similar electrodes or with different inks producing differentiated units), and the possibility of mix modifier to tailor the characteristics of the electrode are attractive aspects of this kind of electrodes.

Applications of SPE have been growing in the last years and in some cases the quantification attained is 10^{-8} mol L⁻¹. The quantification of sildenafil was performed by SWV at pH 4.5, the detection limit was calculated as 5.5×10^{-8} mol L⁻¹ and the method was successfully applied to pharmaceuticals and to spiked urine samples.⁵⁵ The direct oxidation of methionine was achieved on SPE in a multivitamin complex, without noticeable interferences, and the detection limit calculated was 9.5×10^{-6} mol L⁻¹.⁵⁶ The quantification of the anticancer drug flutamide was performed by DPV on bare SPE and a detection limit of 8×10^{-7} mol L⁻¹ was reported.⁵⁷ The association of amperometry and FIA was explored for the rapid quantification of procaine in pharmaceutical formulations using SPE. A frequency of 36 analysis was attained and the limit of detection was calculated as 6.0×10^{-6} mol L⁻¹.⁵⁸

9.3.3.2 Carbon Paste Electrodes

Carbon paste electrodes (CPE) were introduced by Adams in 1958⁵⁹ and along the years the applications of this kind of electrodes have grown tremendously. Initially it was prepared by the mixture of mineral oil and graphite powder but with time the group of heterogeneous electrodes grew tremendously. The main reasons for this fantastic expansion are the simplicity of preparation of carbon pastes, the facility to renew the electrode surface, the versatility for the introduction of new constituents

in the paste, and the very low costs of basic materials (mineral oil and carbon powder) to prepare CPE. Studies involving unmodified paste electrodes are nowadays not so common, and the reasons are easy to understand, once researchers have access to a several modifiers that can improve CPE signal. An excellent revision focused on the electroanalysis of organic compounds at CPE⁶⁰ covered the years 2004–2008. In this period, 80 % of the papers reported modified CPEs. Even unmodified electrodes can lead to very good results, as can be seen in the following examples: For the analysis of melatonin, the adsorption of this compound was explored in association with alternating current voltammetry and a detection limit of 9×10^{-11} mol L⁻¹ was attained.⁶¹ For the quantification of the diuretic drug indapamide CPEs were explored using different techniques. Exploring the adsorption of the compound on the electrode and DPV, a detection limit of 5×10^{-9} mol L⁻¹ was reported.⁶² For the determination of physcion the adsorptive process on the CPE was also explored, but during the potential scan the reduced product was immediately oxidized by the dissolved oxygen and consequently was available for a new reduction. This enhanced significantly the sensitivity of the method and a detection limit of 8×10^{-11} mol L⁻¹ was obtained.⁶³

Besides the classical CPE, there are almost infinite possibilities related to modifications of the paste, as also related to the “inert” mineral oil. Recent papers describe the utilization of modified electrodes with porphyrins, able to detect 1.6×10^{-13} mol L⁻¹ dopamine in pharmaceuticals⁶⁴ or even 1.1×10^{-14} mol L⁻¹ for ascorbic acid in beverages and pharmaceutical samples.⁶⁵

9.3.3.3 Boron-Doped Diamond Electrodes

Synthetic diamonds are basically produced by chemical vapor deposition (CVD) or by the high-pressure/high-temperature (HPHT) processes and date from 1952 and 1955, respectively. In the 1980s, researchers developed the process to implant ions on these diamonds, turning the films much more conductive. In 1992 the first paper presenting the polycrystalline boron-doped diamond (BDD) electrodes was published⁶⁶ and in the following years the applications of these electrodes grew exponentially, and many of the applications were devoted to pharmaceutical quantification. The preference for this kind of electrodes is attributed to many properties such as the following: low and reproducible background current, almost unaffected by adsorptive processes, elevated electrochemical stability in both alkaline and acidic medium, and owns one of the widest usable potential windows. These properties are induced by morphologic factors, crystallographic orientation, and presence of impurities (non-diamond sp² carbon), which turns these electrodes significantly different from the other conventional carbon-based electrodes discussed before.

The utilization of BDD for analysis of nitrofurantoin was performed with electrodes recovered with different amounts of boron and a detection limit of 8.15×10^{-9} mol L⁻¹ of the studied compound was related.⁶⁷ Naproxen was oxidized on BDD in nonaqueous medium and this electrochemical process was

explored for the accurate quantification of this compound in pharmaceutical formulations. DPV was the most favorable technique, allowing the quantification of low concentrations of naproxen. The detection limit was calculated as $3 \times 10^{-8} \text{ mol L}^{-1}$.⁶⁸ Tetracycline and its derivatives were quantified in drug formulation using GC, as-deposited BDD, and anodized BDD associated with FIA + amperometry. The anodized BDD leads to the best signals and to the lowest detection limit, calculated as $1 \times 10^{-8} \text{ mol L}^{-1}$ of tetracycline.⁶⁹

Another important field of application for BDDs is in the electrolytic degradation processes, where the wider potential window provided by these electrodes is fundamental for an efficient process. There are more than 200 studies dealing with BDD and electrolysis, 13 of them focusing on the decomposition of pharmaceuticals, all of them published after 2001. For application in large scale (as in a wastewater treatment) there are still challenges such as the construction of large electrodes and the design of cells of high performance.

9.3.3.4 Fullerenes, Graphenes, and Nanotubes

Fullerenes, graphenes, and nanotubes are new forms of carbon that present many interesting properties and have emerged as the most investigated nanostructure materials of the last years. Fullerenes emerged in the end of the 1980s and started to be produced commercially in 1991. The existence of nanotubes was mentioned in the 1950s, but only in 1991 this material was separated from the soot of arc discharge and in sequence was obtained using a CVD process. The existence of graphene was also previewed before middle of the last century, but only in 2004 its production was started.

A myriad of sensors utilizing these carbon forms were intensely developed in these relatively short period and due to their special structural features and unique electronic properties, upstanding results were attained for many applications. Glassy carbon electrodes modified with fullerene-C-60 were utilized for methylprednisolone quantification in pharmaceuticals and human biological fluids. The presence of C-60 produced a marked enhancement of the DPV signal in comparison with the bare electrode. The detection limit was estimated as $5.6 \times 10^{-9} \text{ mol L}^{-1}$.⁷⁰ Enhanced electrochemical response for carbamazepine was achieved with a GCE modified with a nanostructured film of C-60. Utilizing DPV, the limit of detection obtained was $1.62 \times 10^{-8} \text{ mol L}^{-1}$ and the method was satisfactorily applied to pharmaceutical formulations, spiked human serum, and urine samples.⁷¹ The electrochemical response to acyclovir was also improved when a glassy carbon electrode was modified with fullerene-C-60. Under optimized conditions, a detection limit of $1.48 \times 10^{-8} \text{ mol L}^{-1}$ of this antiviral drug was attained.⁷²

Carbon nanotube electrodes (single- and multi-wall) present characteristics that make them very attractive for many voltammetric applications. Their utilization for quantification of pharmaceutical compounds is significant, and advantages such as high sensitivity and stability, good repeatability, lower oxidation potential, and absence of fouling effect are reported. Electrodes modified with nanotubes can lead

to very sensitive responses, such as the ones obtained for the quantification of trifluoperazine using a GCE modified with multi-walled carbon nanotubes. According to the authors,⁷³ an adsorptive process was explored for enhancement of the signal and after the optimization of the process, a detection limit of 7.49×10^{-10} mol L⁻¹ was attained. The quantification of the antiviral drug vanganciclovir was performed using a multi-walled carbon nanotube-modified GCE. Adsorptive accumulation process enhanced significantly the signal obtained and a detection limit of 1.52×10^{-9} mol L⁻¹ was attained for this compound.⁷⁴ Triamcinolone, a doping agent prohibited for athletes, was quantified using an edge plane pyrolytic graphite electrode modified with single-wall carbon nanotubes and using the same pyrolytic graphite electrode modified with fullerene-C-60. The authors concluded that electrode modified with the nanotubes was more sensitive than the one modified with fullerenes. A detection limit of 8.9×10^{-10} mol L⁻¹ was attained when the single-walled carbon nanotube-modified electrode was utilized.⁷⁵ Analysis of pharmaceuticals and real urine samples was performed, with good agreement with chromatographic analysis.

Graphene presents a freestanding 2D structure with one-atom thickness and rapidly is becoming one of the hottest topics in the field of material science, physics, chemistry, and nanotechnology since it was first isolated in 2004. Applications of graphene to tailor sensors of differentiated performance are growing rapidly and will be a hot topic in the following years, as will be illustrated. For the quantification of paracetamol, a GCE was recovered with graphene that produced an intense decrease in the oxidation potential of this analyte and an excellent electrocatalysis for the determination of this pharmaceutical compound. A detection limit of 3.2×10^{-8} mol L⁻¹ was calculated for this compound.⁷⁶ Lower detection limits were obtained utilizing composites containing graphene. For the quantification of rutin, a composite based on cyclodextrin/reduced graphene/naion leads to detection limits of 2×10^{-9} mol L⁻¹ of rutin.⁷⁷ A composite containing gold nanoparticles/L-cysteine/graphene/naion deposited on GCE was utilized for the quantification of theophylline. Responses in a wide linear range (4×10^{-9} to 6×10^{-5} mol L⁻¹) were recorded and the detection limit for this electrode was calculated as 4×10^{-10} mol L⁻¹ of theophylline.⁷⁸ For the quantification of quercetin, a composite of p-aminothiophenol-functionalized graphene oxide/gold nanoparticles produced amazing sensitivity. For this compound, a detection limit of 3×10^{-13} mol L⁻¹ was obtained using SWV.⁷⁹

A comparison between the development of sensors based on these new forms of graphite shows that nanotubes are at this moment the most utilized material and this probably can be attributed to the facility of acquisition and utilization of this material. Graphene, even being the “youngest” of these materials, in few years surpassed the fullerenes use as sensing material, probably due to the fact that this last requires chemical modification before its utilization.

9.3.3.5 Other Electrodes

Besides the solid metallic electrodes, the utilization of metal films, nanoparticles, and insoluble compounds immobilized on the solid electrodes is a field with plenty of opportunities and there are many aspects to be explored. Noble metals are able to catalyze many electrochemical reactions. Mercury and gold are the most favorable surfaces to explore adsorptive pre-concentration,^{80,81} which allow detection in the 10^{-12} mol L⁻¹ region. Mercury is still among the best sensors and in the starting of the last century, polarography was responsible for the popularity of electroanalytical techniques. Unfortunately many countries are considering the possibility of discontinuing the use of mercury electrodes. Alternative ways are the utilization of mercury films or mercury amalgams. The use of mercury film on carbon fiber microelectrodes was explored for the quantification of folic acid and mitoxantrone, obtaining detection limits of 9×10^{-10} and 5×10^{-10} mol L⁻¹, respectively.⁸² Silver amalgam was utilized for the quantification of folic acid and the detection limit calculated was 5×10^{-10} mol L⁻¹.⁸³

Low detection limits were also attained using gold electrodes modified by thio-compounds. A study involving simultaneous self-assembled films containing corrole-SH and other thiol derivatives generated a very sensitive sensor for dopamine, free from interferences of species commonly present in blood. A detection limit of 5.3×10^{-12} mol L⁻¹ was obtained for a direct determination of dopamine in human plasma 80 times diluted.⁸⁴ The grafting of molecular imprinting polymers (MIPs) was executed via photopolymerization of acrylamide and trimethylolpropane trimethacrylate on a gold electrode surface. A sensor with wide concentration working region (10^{-9} to 10^{-3} mol L⁻¹) was obtained and its detection limit was calculated as 1×10^{-10} mol L⁻¹.⁸⁵

The use of carbon paste electrodes (CPE) for the quantification of trace amounts of pharmaceuticals has been also explored due to the versatility of this electrode, an attractive aspect many times considered by the researchers. The intense adsorption of vardenafil on CPE was explored for its quantification in commercial formulations and in human serum with high sensitivity, attaining a detection limit of 3×10^{-10} mol L⁻¹.⁸⁶ CPE modified with dysprosium hydroxide nanowires⁸⁷ or lanthanum hydroxide nanowires^{88,89} also presented sensitivities in the 10^{-10} mol L⁻¹ region. CPE modified with carbon nanotubes and DNA was explored for the quantification of DL-alpha-tocopherol. A detection limit of 1.3×10^{-10} mol L⁻¹ was attained in this study.⁹⁰ The utilization of clay in the CPE produced an effective improvement in the quantification of nifedipine (LOD: 3.9×10^{-10} mol L⁻¹) and nimodipine (LOD: 4.8×10^{-10} mol L⁻¹).⁹¹ Octyl-bonded silica (C-8) was introduced in a CPE to enhance the quantification of doxazosin (LOD: 7.4×10^{-10} mol L⁻¹).⁹² The use of 1,2-dibromocyclohexane as the paste binder created an ingenious way to obtain a self-catalytic carbon paste electrode for the detection of vitamin B-12. A detection limit of 8.5×10^{-10} mol L⁻¹ was attained⁹³ for this vitamin.

There are many other studies that can be found in the literature, but the aim of this chapter is to give to the readers an overlook concerning to what was developed until now and about the potential represented by the electroanalytical techniques for the continuous monitoring of emerging pollutants in water and wastewater. Unfortunately, the number of applications to real samples is still very reduced (as will be seen in the next section) but a significant increase in these applications can be expected in the future.

9.4 Voltammetric Determination of PPCP

The number of papers dedicated to the electrochemical quantification of the constituents of commercial products is remarkably significant in comparison with the ones dealing with their determination in natural waters and wastewater. This huge difference is motivated by many factors, among them: The need of analytical control of these components is essential for the quality of the products manufactured; procedures for the analysis of these products were established for relatively long time in their matrixes, but still to be established in wastewater; the conscience about emerging contaminants is relatively new and the direct analysis of these compounds in wastewater can be more complex than in pharmaceutical products. An evaluation on the papers dedicated to analysis of PPCP in water indicates some preference for sensors containing the new forms of graphite (nanotubes, graphenes, and fullerenes—particularly considering their relatively short life).

Multiwalled carbon nanotubes (MWCNT) deposited on GC were explored for the quantification of carbamazepine in wastewater and in pharmaceuticals.⁹⁴ The results compared well with the ones obtained by chromatography and the detection limit attained using linear sweep voltammetry was 4×10^{-8} mol L⁻¹ for carbamazepine. GC covered with MWCNT was utilized for quantification of the dihydroxybenzene isomers (hydroquinone, catechol, and resorcinol) in artificial wastewater.⁹⁵ The electrocatalytic proprieties afforded by the MWCNT produce an intense anticipation of the oxidation peaks, so as a good separation between them, allowing the direct quantification of the three compounds. In another study, composites containing epoxy and MWCNT and epoxy + MWCNT + silver-modified zeolites were utilized for the quantification of ibuprofen by different techniques. The authors verified better responses for the composite containing silver-modified zeolites, reporting a detection limit of 4×10^{-7} mol L⁻¹ ibuprofen.⁹⁶ According to them, this electrode presents potential both for degradation and simultaneously its control. A study comparing the performance of BDD, GC, and MWCNT-epoxy composites for the degradation of ibuprofen demonstrated a superior performance of the composite electrode.⁹⁷ The authors verified an additional enhancement in the performance of this electrode in the presence of chloride ions. In another study, the potential of MWCNT for the removal of natural and synthetic endocrine disrupting estrogens was also evaluated in a kinetic and mechanistic

study.⁹⁸ The authors concluded that nanotubes present good potential for removal of estrogens from aqueous phase at relatively lower concentrations.

Graphene was immobilized on gamma Fe_2O_3 nanoparticles and presented high performance in removal processes of endocrine-disrupting compounds from water.⁹⁹ This strategy minimizes the graphene-graphene interaction, and maintained a very high graphene active area. An additional advantage is the fact that the resulting material favors its magnetic separation after the adsorption of the endocrine disruptors. Graphene was associated to platinum nanoparticles to form a composite on a GC electrode after electropolymerization of mercaptopnicotinic acid in the presence of 17 beta-estradiol. After the removal of the template, the electrode presented good linear response in the range of $4\text{--}60 \times 10^{-9} \text{ mol L}^{-1}$, the limit of detection being calculated as $2 \times 10^{-9} \text{ mol L}^{-1}$. The sensor was applied for 17 beta-estradiol quantification in mackups with good recovery.¹⁰⁰ Recently, the favorable characteristics of graphene were also explored to adsorb pharmaceuticals and personal care products from wastewater and their quantification by gas chromatography-mass spectrometry.¹⁰¹ The limit of quantification calculated for nine different pharmaceutical products was situated between 13 and 115 ng L^{-1} .

Fullerene-C-60 was immobilized on glassy carbon by evaporation of a CH_2Cl_2 solution. The adsorbed fullerene was cycled in 1 M NaOH for its reduction and the electrode was utilized for bisphenol quantification in wastewater.¹⁰² The detection limit was determined as $3.7 \times 10^{-9} \text{ mol L}^{-1}$. The association of fullerenes and MWCNT was explored for the quantification of the endocrine disruptor vinclozolin in wastewater. A glassy carbon electrode was polished and a solution containing both carbon forms (MWCNT:C-60 = 2:1) were cast on the electrode that was dried at air. This electrode was applied for vinclozolin in optimized conditions, attaining a detection limit of $9.1 \times 10^{-8} \text{ mol L}^{-1}$.¹⁰³ This sensor was successfully applied to the detection of vinclozolin in wastewater, obtaining a recovery ranging from 97.6 to 103.6 %.

Glassy carbon electrodes were also utilized for pharmaceutical quantification in wastewater. The redox characteristics of domperidone were critically investigated by DPV and CV. The limit of quantification of this compound was evaluated as $6.1 \times 10^{-7} \text{ mol L}^{-1}$.¹⁰⁴ The procedure proposed shown a good recuperation for the pure form ($98.2 \pm 3.1 \%$) and a very satisfactory value for wastewater ($95.0 \pm 2.9 \%$). The quantification of triclosan on glassy carbon was studied in the presence of sodium dodecyl sulfate, which contributes for the enhancement of the voltammetric signal. The detection limit calculated was $1.73 \times 10^{-8} \text{ mol L}^{-1}$.¹⁰⁵ The procedure was successfully applied to analyze wastewater and personal care product samples.

Screen-printed electrodes were also used for quantification of PPCP in waters, wastewater, and sewage samples. A screen-printed carbon electrode was utilized for quantification of bisphenol A in river water and sewage samples, without pretreatment of the samples.¹⁰⁶ The presence of cetyltrimethylammonium bromide was very favorable, acting as antifouling and preconcentrating agent. A limit of detection of $5.1 \times 10^{-8} \text{ mol L}^{-1}$ was obtained in this study. A screen-printed silver electrode was utilized to quantify the content of aluminum chlorohydrate content in

antiperspirant deodorants. A single drop (50 μL) was sufficient for the analysis.¹⁰⁷ The detection limit was calculated as 3.03 mg L^{-1} .

Mercury electrode was utilized for the quantification of pyriithione in seawater. The cathodic stripping analysis was performed in the presence of Triton X-100, with the aim of separating the desired peak from the signal from the interfering thiol compounds. A detection limit of $1.5 \times 10^{-9} \text{ mol L}^{-1}$ was attained using 60-s pre-concentration.¹⁰⁸

Silver electrodes and its amalgam were also explored for analytical purposes. Trihalomethanes were quantified at submicromolar concentrations in water, using a three-step stripping process. The trihalomethane was reduced on a silver cathode, forming halides, which were captured at a silver halide anode. The insoluble AgX formed was then reduced using differential pulse voltammetry. Using this procedure, bromoform and chloroform can be detected in the 1.2×10^{-8} and $5 \times 10^{-8} \text{ mol L}^{-1}$ in water.³⁹ Silver amalgam was employed for quantification of ketoconazole in pharmaceuticals and in shampoos. The best conditions were determined, a detection limit of $1.2 \times 10^{-7} \text{ mol L}^{-1}$ was calculated, and the method was applied to shampoos and cream samples with good recovery.¹⁰⁹ Composites involving nanoparticles were also explored for the determination of different compounds. Zinc hydroxide nanoparticles were utilized for the quantification of 21 different parabens in aqueous solution. The detection limit was situated in the low micromolar region.¹¹⁰

Biosensors, immunosensors, and aptosensors present elevated selectivity or even specificity for a distinct target. This aspect is an important advantage in very complex matrixes such as wastewater or sewage water. Enzymes can be utilized both for the generation of a detectable species¹¹¹ or to eliminate some target of interest¹¹² in the complex sample. The use of immunosensors can produce very sensitive and selective responses. Recombinant single-chain antibody fragments were utilized for constructing a very sensitive sensor for atrazine, using a screen-printed electrode incorporating a conducting polymer, which enables direct mediatorless reaction.¹¹³ This sensor presented very high sensitivity and its detection limit was $4.6 \times 10^{-10} \text{ mol L}^{-1}$. An aptosensor for tetracycline detection was developed using an ssDNA aptamer that selectively binds to tetracycline as recognition element. To immobilize the ssDNA aptamer, it was biotinylated and bonded to the streptavidin-modified surface of a gold screen-printed electrode.¹¹⁴ The detection limit was calculated as $1 \times 10^{-8} \text{ mol L}^{-1}$.

Microelectrodes (single or arrays) also can be explored for the monitoring of species of interest in natural waters. An array of amalgamated gold microelectrodes was utilized to evaluate biogeochemical response of native sediments following its capping with a clean layer of a "clean" material.¹¹⁵ In this study it was observed that the oxygen penetration into sand capping material extend only a few centimeters, maintaining so the sediment anaerobic. This kind of sensor arrangement is very important for better understanding the biogeochemical processes that affect natural water reservoirs. The possibility of measure *in situ* processes that occur in the seafloor is of great importance for understanding aspects of the sediment biogeochemistry and about the exchanges that occur in the ocean.¹¹⁶ Information about the

flux of metallic and organic compounds can contribute for a better understanding of the multiple processes that occur there. Microelectrodes can be very versatile, favoring even the determination of analytes in very small samples. One interesting example that illustrates this aspect is the study dealing with the effects of the makeup based on lead salts, utilized by ancient Egyptians.¹¹⁷ Measurements made with only few cells demonstrate that the low solubility of the metal was sufficient to activate the specific oxidative stress responses of keratinocytes, producing more nitrogen monoxide and stimulating immunological defenses.

For the future, many progresses can be envisioned. The use of arrays of different electrodes and the treatment of the data so obtained with chemometrics will increase the power of the obtained information. New nanostructured materials will amplify the possibilities for this purpose.

9.5 Final Remarks

Studies focused on emerging contaminants are still in its beginning and constitute a field plenty of challenges to be faced. There are a myriad of aspects to be studied and will require huge efforts to rationalize the multifaceted aspects involving these compounds. Emerging contaminants can be found almost everywhere (air, water, soil, waste, foods, drinks, tissues, plants, milk, etc.) and its real number is unknown (pharmaceuticals, creams, pesticides, hormones, veterinary products, illicit drugs, surfactants, plasticizers, solvents, plastics components, catalyzers, etc.).

Only recently the deleterious effects caused by emerging contaminants started to be considered seriously and it is urgent to take actions to control or at least minimize their effects. The development of strategies to screen continuously these compounds in water is an important task to bring valuable information, which is essential to take decisions. Analytical data will be also fundamental for the optimization of treatment processes, such as the ones which utilize strong oxidants (chlorination, ozonation, H₂O₂), processes which employ electro-oxidation, retention processes based in membranes (reverse osmosis, membranes for nano-filtration), and bioreactors or even active sludge—all can be benefited with precise and continuous monitoring of the income and the outcome of emerging compounds. And the electroanalytical methods can strongly contribute in this direction.

References

1. Barceló D, Petrovic M (eds) (2008) *Emerging contaminants from industrial and municipal waste. Occurrence, analysis and Effects*. Springer, Berlin
2. Bhandari A, Surampalli RY, Adams CD, Champagne P, Ong SK, Tiagi RD, Zhang TC (2009) *Contaminants of emerging environmental concern*. ASCE Publications, American Society of Civil Engineers, Preston, VA, 495 p. http://ascelibrary.org/doi/pdf/10.1061/9780784410141_fm. Accessed 30 Jun 2013

3. Tremblay LA, Stewart M, Peake BM, Gadd JB, Norhcott G (2011) Review of the risks of emerging contaminants and potential impacts to Hawke's Bay—Prepared for Hawke's Bay Regional Council. Cawthron Report No. 1973. 39 p. <http://www.envirolink.govt.nz.pdf>. Accessed 30 Jun 2013
4. Holtz S (2006) There is no "Away". Pharmaceuticals, personal care products and endocrine-disrupting substances: emerging contaminants detected in water—Canadian Institute for Environmental Law and Policy. 82 p. <http://www.cielap.org/pdf/NoAway.pdf>. Accessed 30 Jun 2013
5. Stuart ME, Manamsa K, Talbot JC et al (2011) Emerging contaminants in groundwater. British Geological Survey, Groundwater Science Program—Open Report OR/11/013. 111p. <http://nora.nerc.ac.uk/14557/1/OR11013.pdf>. Accessed 30 Jun 2013
6. Richardson SD, Ternes TA (2001) Water analysis: emerging contaminants and current issues. *Anal Chem* 83:4614–4648
7. Jurado A, Vázquez-Suñé E, Carrera J et al (2012) Emerging organic contaminants in groundwater in Spain: a review of sources, recent occurrence and fate in a European context. *Sci Total Environ* 440:82–94
8. Deblonde T, Cossu-Leguille C, Hartemann P (2011) Emerging pollutants in wastewater: a review of the literature. *Int J Hyg Environ Health* 214:442–448
9. Giger W (2009) Hydrophilic and amphiphilic water pollutants: using advanced analytical methods for classic and emerging contaminants. *Anal Bioanal Chem* 393:37–44
10. Narvaez JF, Jimenez C (2012) Pharmaceutical products in the environment: sources, effects and risks. *Rev Facult Quim Farm* 19:93–108
11. Lopez-Serna R, Jurado A, Vázquez-Suñé E et al (2001) Occurrence of 95 pharmaceuticals and transformation products in urban groundwaters underlying the metropolis of Barcelona, Spain. *Environ Pollut* 174:305–315
12. Bailly E, Levi Y, Karolak S (2013) Calibration and field evaluation of polar organic chemical integrative sampler (POCIS) for monitoring pharmaceuticals in hospital wastewater. *Environ Pollut* 174:100–105
13. Paiga P, Santos LH, Amorim CG et al (2013) Pilot monitoring study of ibuprofen in surface waters of north of Portugal. *Environ Sci Pollut Res* 20:2410–2420
14. Smital T, Terzc S, Loncar J et al (2001) Prioritisation of organic contaminants in a river basin using chemical analyses and bioassays. *Environ Sci Pollut Res* 20:1384–1395
15. Gonzalez-Marino I, Quintana JB, Rodríguez I et al (2012) Screening and selective quantification of illicit drugs in wastewater by mixed-mode solid-phase extraction and quadrupole-time-of-flight liquid chromatography-mass spectrometry. *Anal Chem* 84:1708–1717
16. Zedda M, Zwiener C (2012) Is nontarget screening of emerging contaminants by LC-HRMS successful? A plea for compound libraries and computer tools. *Anal Bioanal Chem* 9:2493–2502
17. Greenwood R, Mills GA, Roig B (2007) Introduction to emerging tools and their use in water monitoring. *Trends Anal Chem* 26:263–267
18. Uslu B, Ozkan SA (2011) Electroanalytical methods for the determination of pharmaceuticals: a review of recent trends and developments. *Anal Lett* 44:2644–2702
19. Radi AE (2010) Recent updates of chemically modified electrodes in pharmaceutical analysis. *Comb Chem High Throughput Screening* 13:728–752
20. Felix FS, Angnes L (2010) Fast and accurate analysis of drugs using amperometry associated with flow injection analysis. *J Pharm Sci* 99:4784–4804
21. Duncan JB, Christian JE (1948) Polarographic determination of folic acid and zinc salts in pharmaceuticals. *J Am Pharm Assoc* 37:507–509
22. Hammam E (2007) Determination of triamcinolone acetonide in pharmaceutical formulation and human serum by adsorptive cathodic stripping voltammetry. *Chem Anal (Warsaw)* 52:43–53
23. El-Desoky HS, Ghoneim MM (2005) Assay of the anti-psychotic drug haloperidol in bulk form, pharmaceutical formulation and biological fluids using square-wave adsorptive stripping voltammetry at a mercury electrode. *J Pharm Biomed Anal* 38:543–550

24. Ghoneim EM, El-Desoky HS, Ghoneim MM (2006) Adsorptive cathodic stripping voltammetric assay of the estrogen drug ethinylestradiol in pharmaceutical formulation and human plasma at a mercury electrode. *J Pharm Biomed Anal* 40:255–261
25. Hammam E, El-Attar MA, Beltagi AM (2006) Voltammetric studies on the antibiotic drug cefoperazone—quantification and pharmacokinetic studies. *J Pharm Biomed Anal* 42:523–527
26. El-Desoky HS (2005) A validated voltammetric procedure for quantification of the antifungal drug griseofulvin in bulk form, tablets, and biological fluids at a mercury electrode. *Anal Lett* 38:1783–1802
27. El-Desoky HS (2009) Stability indicating square-wave stripping voltammetric method for determination of gatifloxacin in pharmaceutical formulation and human blood. *J Braz Chem Soc* 20:1790–1799
28. Sun N, Mo WM, Shen ZL et al (2005) Adsorptive stripping voltammetric technique for the rapid determination of tobramycin on the hanging mercury electrode. *J Pharm Biomed Anal* 38:256–262
29. Jain R, Rather JA (2011) Stripping voltammetry of tinidazole in solubilized system and biological fluids. *Colloids Surf A Physicochem Eng Asp* 378:27–33
30. Al-Ghamdi AF, Hefnawy MM (2012) Electrochemical determination of rosiglitazone by square-wave adsorptive stripping voltammetry method. *Arab J Chem* 5:383–389
31. Masawat P, Slater JM (2007) The determination of tetracycline residues in food using a disposable screen-printed gold electrode (SPGE). *Sens Actuators B Chem* 124:127–132
32. Yang NJ, Wan QJ, Wang XX (2005) Voltammetry of Vitamin B-12 on a thin self-assembled monolayer modified electrode. *Electrochim Acta* 50:2175–2180
33. Dogrukol-Ak D, Zaimouglu V, Tuncel M (1999) Voltammetry of trazodone by platinum electrode and its determination in tablets using DP technique in the rotating conditions. *Eur J Pharm Sci* 7:215–220
34. Munoz RAA, Matos RC, Angnes L (2001) Gold electrodes from compact discs modified with platinum for amperometric determination of ascorbic acid in pharmaceutical formulations. *Talanta* 55:855–860
35. Munoz RAA, Matos RC, Angnes L (2001) Amperometric determination of dipyrone in pharmaceutical formulations with a flow cell containing gold electrodes from recordable compact discs. *J Pharm Sci* 90:1972–1977
36. Matos RC, Angnes L, Araújo MCU et al (2000) Modified microelectrodes and multivariate calibration for flow injection amperometric simultaneous determination of ascorbic acid, dopamine, epinephrine and dipyrone. *Analyst* 125:2011–2015
37. Tyszczyk K, Korolczyk M (2010) Analysis of organic compounds using an in situ plated lead film electrode. *Comb Chem High Throughput Screening* 13:753–757
38. Quintino MDM, Corbo D, Bertotti M et al (2002) Amperometric determination of acetylsalicylic acid in drugs by batch injection analysis at a copper electrode in alkaline solutions. *Talanta* 58:943–950
39. Peverly AA, Peters DG (2012) Electrochemical determination of trihalomethanes in water by means of stripping analysis. *Anal Chem* 84:6110–6115
40. Biryol I, Dermis S (1998) Voltammetric determination of thioridazine hydrochloride. *Turk J Chem* 22:325–333
41. Kreft GL, de Braga OC, Spinelli A (2012) Analytical electrochemistry of vitamin B-12 on a bismuth-film electrode surface. *Electrochim Acta* 83:125–132
42. Sopha H, Hocevar SB, Pihlar B et al (2012) Bismuth film electrode for stripping voltammetric measurement of sildenafil citrate. *Electrochim Acta* 60:274–277
43. Wang J (Ed) (2006) *Electroanalytical chemistry*, 3rd ed., Wiley-VCH Pub., New Jersey
44. Radi A (2004) Preconcentration and differential pulse voltammetry of tegaserod at a glassy carbon electrode. *Anal Lett* 37:1103–1113
45. Quintino MSM, Angnes L (2006) Fast BIA-amperometric determination of isoniazid in tablets. *J Pharm Biomed Anal* 42:400–404

46. Radi A, El-sherif Z (2002) Determination of levofloxacin in human urine by adsorptive square-wave anodic stripping voltammetry on a glassy carbon electrode. *Talanta* 58:319–324
47. Ghoneim MM, Khashaba PY, Beltagi AM (2002) Determination of trimetazidine HCl by adsorptive stripping square-wave voltammetry at a glassy carbon electrode. *J Pharm Biomed Anal* 27:235–241
48. Gazy AAK (2004) Determination of amlodipine besylate by adsorptive square-wave anodic stripping voltammetry on glassy carbon electrode in tablets and biological fluids. *Talanta* 62:575–582
49. Ozkan SA, Uslu B, Senturk Z (2004) Electroanalytical characteristics of amisulpride and voltammetric determination of the drug in pharmaceuticals and biological media. *Electroanalysis* 16:231–237
50. Uslu B, Dogan B, Ozkan SA et al (2005) Electrochemical behavior of vardenafil on glassy carbon electrode: determination in tablets and human serum. *Anal Chim Acta* 552:127–134
51. Quintino MSM, Yamashita M, Angnes L (2006) Voltammetric studies and determination of levodopa and carbidopa in pharmaceutical products. *Electroanalysis* 18:655–661
52. Goyal RN, Bishnoi S, Agrawal B (2011) Electrochemical sensor for the simultaneous determination of caffeine and aspirin in human urine samples. *J Electroanal Chem* 655:97–102
53. Goyal RN, Chatterjee S, Rana ARS (2010) A comparison of edge- and basal-plane pyrolytic graphite electrodes towards the sensitive determination of hydrocortisone. *Talanta* 83:149–155
54. Goyal RN, Chatterjee S, Agrawal B (2010) Electrochemical investigations of diclofenac at edge plane pyrolytic graphite electrode and its determination in human urine. *Sens Actuators B Chem* 145:743–748
55. Farghali RA, Ahmed RA (2012) A novel electrochemical sensor for determination of sildenafil citrate (Viagra) in pure form and in biological and pharmaceutical formulations. *Int J Electrochem Sci* 7:13008–13019
56. Gomez-Mingot M, Iniesta J, Montiel V et al (2011) Direct oxidation of methionine at screen printed graphite macroelectrodes: towards rapid sensing platforms. *Sens Actuators B Chem* 155:831–836
57. Hamman E, El-Desoky HS, El-Beradie KY et al (2004) Three validated stripping voltammetric procedures for determination of the anti-prostate cancer drug flutamide in tablets and human serum at mercury electrode. *Canadian J Chem* 82:1386–1392
58. Bergamini MF, Santos AL, Stradiotto NR et al (2007) Flow injection amperometric determination of procaine in pharmaceutical formulation using a screen-printed carbon electrode. *J Pharm Biomed Anal* 43:315–319
59. Adams RN (1958) Carbon paste electrodes. *Anal Chem* 30:1576
60. Zima J, Svancara I, Barek J et al (2009) Recent advances in electroanalysis of organic compounds at carbon paste electrodes. *Crit Rev Anal Chem* 39(204):227
61. Cortujo-Antuna JL, Martinez-Montequin S, Fernandez-Abedul MT et al (2003) Sensitive adsorptive stripping voltammetric methodologies for the determination of melatonin in biological fluids. *Electroanalysis* 15:773–778
62. Radi A (2001) Stripping voltammetric determination of indapamide in serum at castor oil-based carbon paste electrodes. *J Pharm Biomed Anal* 24:413–419
63. Ding YL, Li J, Fei J (2005) Adsorptive catalytic voltammetry of physcion in the presence of dissolved oxygen at a carbon paste electrode. *Microchim Acta* 150:125–130
64. Balasoju SC, Stefan-van-Staden RI, van Staden JF et al (2010) Carbon and diamond paste microelectrodes based on Mn(III) porphyrins for the determination of dopamine. *Anal Chim Acta* 668:201–207
65. Stefan-van-Staden R-I, Balasoju SC, van Staden JF et al (2012) Microelectrodes based on porphyrins for the determination of ascorbic acid in pharmaceutical samples and beverages. *J Porphyrins Phthalocyanines* 16:809–816
66. Patel K, Hashimoto K, Fujishima A (1992) Application of boron-doped cvd-diamond film to photoelectrode. *Denki Kagaku* 60:659–661

67. de Lima-Neto P, Correia AN, Portela RR et al (2010) Square wave voltammetric determination of nitrofurantoin in pharmaceutical formulations on highly boron-doped diamond electrodes at different boron-doping contents. *Talanta* 80:1730–1736
68. Suryanarayan V, Zhang Y, Yoshihara S et al (2005) Voltammetric assay of naproxen in pharmaceutical formulations using boron-doped diamond electrode. *Electroanalysis* 17:925–932
69. Wangfuengkanagul N, Siangproh W, Chailapakul O (2004) A flow injection method for the analysis of tetracycline antibiotics in pharmaceutical formulations using electrochemical detection at anodized boron-doped diamond thin film electrode. *Talanta* 64:1183–1188
70. Goyal RN, Bachheti N, Tyagi A (2007) Differential pulse voltammetric determination of methylprednisolone in pharmaceuticals and human biological fluids. *Anal Chim Acta* 605:34–40
71. Kalanur SS, Jaldappagari S, Balakrishnan S (2012) Enhanced electrochemical response of carbamazepine at a nano-structured sensing film of fullerene-C-60 and its analytical applications. *Electrochim Acta* 56:5295–5301
72. Shetti NP, Malode SJ, Nandibewoor ST (2012) Electrochemical behavior of an antiviral drug acyclovir at fullerene-C-60-modified glassy carbon electrode. *Bioelectrochemistry* 88:76–83
73. Dogan-Topal B (2013) Electrooxidative behavior and determination of trifluoperazine at multiwalled carbon nanotube-modified glassy carbon electrode. *J Solid State Electrochem* 17:1059–1066
74. Dogan-Topal B, Bozal-Palabiyik B, Uslu B et al (2013) Multi-walled carbon nanotube modified glassy carbon electrode as a voltammetric nanosensor for the sensitive determination of anti-viral drug valganciclovir in pharmaceuticals. *Sens Actuators B Chem* 177:841–847
75. Goyal RN, Gupta VK, Chatterjee S (2009) A sensitive voltammetric sensor for determination of synthetic corticosteroid triamcinolone, abused for doping. *Biosens Bioelectron* 24:3562–3568
76. Kang XH, Wang J, Wu H et al (2010) A graphene-based electrochemical sensor for sensitive detection of paracetamol. *Talanta* 81:754–759
77. Liu KP, Wei JP, Wang CM (2011) Sensitive detection of rutin based on beta-cyclodextrin@chemically reduced graphene/Nafion composite film. *Electrochim Acta* 56:5189–5194
78. Zi LJ, Li JJ, Mao YX et al (2012) High sensitive determination of theophylline based on gold nanoparticles/L-cysteine/Graphene/Nafion modified electrode. *Electrochim Acta* 78:434–439
79. Yola ML, Atar N, Ustundag Z et al (2013) A novel voltammetric sensor based on p-aminothiophenol functionalized graphene oxide/gold nanoparticles for determining quercetin in the presence of ascorbic acid. *J Electroanal Chem* 698:9–16
80. Skrzypek S, Ciesielski W, Sokolowski A et al (2005) Square wave adsorptive stripping voltammetric determination of famotidine in urine. *Talanta* 66:1146–1151
81. Daneshgar P, Norouzi P, Ganjali MR (2009) Rapid determination of bisacodyl in flow injection system combination by a novel sensitive adsorptive square-wave voltammetry. *Sens Actuators B Chem* 136:66–72
82. Delgado JA, Garcia AC, Blanco PT (1993) Adsorptive stripping voltammetry on mercury-coated carbon-fiber ultramicroelectrode. *Anal Chim Acta* 273:101–109
83. Bandzuchova L, Selesovska R, Navratil T et al (2011) Electrochemical behavior of folic acid on mercury meniscus modified silver solid amalgam electrode. *Electrochim Acta* 56:2411–2419
84. Kurzatowska K, Dolusic E, Dehaen W et al (2009) Gold electrode incorporating corrole as an ion-channel mimetic sensor for determination of dopamine. *Anal Chem* 81:7397–7405
85. Wang ZH, Li JS, Liu XL et al (2013) Preparation of an amperometric sensor for norfloxacin based on molecularly imprinted grafting photopolymerization. *Anal Bioanal Chem* 405:2525–2533

86. Ghoneim MM, Hassanein AM, Salahuddin NA et al (2013) Trace determination of vardenafil hydrochloride in commercial formulation and human serum by adsorptive anodic stripping voltammetry at a carbon paste electrode. *J Solid State Electrochem* 17:1891–1902
87. Daneshgar P, Norouzi P, Dousty F et al (2009) Dysprosium hydroxide nanowires modified electrode for determination of rifampicin drug in human urine and capsules by adsorptive square wave voltammetry. *Curr Pharm Anal* 5:246–255
88. Liu L, Song JF, Yu PF et al (2007) Sensing system integrating lanthanum hydroxide nanowires with Copper(II) ion for uracil and its application. *Anal Lett* 40:2562–2573
89. Liu L, Song JF, Yu PF et al (2006) A novel electrochemical sensing system for inosine and its application for inosine determination in pharmaceuticals and human serum. *Electrochem Commun* 8:1521–1526
90. Ly SY (2008) Voltammetric analysis of DL-alpha-tocopherol with a paste electrode. *J Sci Food Agric* 88:1272–1276
91. Reddy TM, Reddy SJ (2004) Differential pulse adsorptive stripping voltammetric determination of nifedipine and nimodipine in pharmaceutical formulations, urine, and serum samples by using a clay-modified carbon-paste electrode. *Anal Lett* 37:2079–2098
92. Arranz A, Moreda JM, Arranz JF (2000) Preconcentration and voltammetric determination of the antihypertensive doxazosin on a C-8 modified carbon paste electrode. *Mikrochim Acta* 134:69–75
93. Tomcik P, Banks CE, Davies TJ et al (2004) A self-catalytic carbon paste electrode for the detection of vitamin B-12. *Anal Chem* 76:161–165
94. Veiga A, Dordio A, Palace Carvalho AJ et al (2010) Ultra-sensitive voltammetric sensor for trace analysis of carbamazepine. *Anal Chim Acta* 2010(674):182–189
95. Ding YP, Liu WL, Wu QS et al (2005) Direct simultaneous determination of dihydroxybenzene isomers at C-nanotube-modified electrodes by derivative voltammetry. *J Electroanal Chem* 575:275–280
96. Motoc S, Remes A, Pop A et al (2013) Electrochemical detection and degradation of ibuprofen from water on multi-walled carbon nanotubes-epoxy composite electrode. *J Environ Sci* 25:838–847
97. Motoc S, Manea F, Pop A (2012) Electrochemical degradation of pharmaceutical effluents on carbon-based electrodes. *Environ Eng Manag J* 11:627–634
98. Kumar AK, Mohan SV (2012) Removal of natural and synthetic endocrine disrupting estrogens by multi-walled carbon nanotubes (MWCNT) as adsorbent: kinetic and mechanistic evaluation. *Sep Purif Technol* 87:22–30
99. Sinha A, Jana NR (2013) Graphene-based composite with gamma-Fe₂O₃ nanoparticle for the high-performance removal of endocrine-disrupting compounds from water. *Chem Asian J* 8:786–791
100. Wen TT, Xue C, Li Y et al (2012) Reduced graphene oxide-platinum nanoparticles composites based imprinting sensor for sensitively electrochemical analysis of 17 beta-estradiol. *J Electroanal Chem* 582:121–127
101. Yu Y, Wu LS (2013) Application of graphene for the analysis of pharmaceuticals and personal care products in wastewater. *Anal Bioanal Chem* 405:4913–4919
102. Rather JA, De Wael K (2013) Fullerene-C-60 sensor for ultra-high sensitive detection of bisphenol-A and its treatment by green technology. *Sens Actuators B Chem* 176:110–117
103. Rather JA, De Wael K (2012) C-60-functionalized MWCNT based sensor for sensitive detection of endocrine disruptor vinclozolin in solubilized system and wastewater. *Sens Actuators Chem B* 171:907–915
104. El Shahawi MS, Bahaffi SO, El-Mogy T (2007) Analysis of domperidone in pharmaceutical formulations and wastewater by differential pulse voltammetry at a glassy-carbon electrode. *Anal Bioanal Chem* 387:719–725
105. Fotouhi L, Shahbaazi HR, Fatehi A et al (2010) Voltammetric determination of triclosan in waste water and personal care products. *Int J Electrochem Sci* 5:1390–1398

106. Brugnera MF, Trindade MAG, Zanoni MVB (2010) Detection of bisphenol on a screen-printed carbon electrode in CTAB miscelar medium. *Anal Lett* 43:2823–2836
107. Zen JM, Yang TH, Kumar AS et al (2009) Detection of aluminum chlorohydrate content in antiperspirant deodorants using screen-printed silver electrodes by one drop analysis. *Electroanalysis* 21:2272–2276
108. Mackie DS, van den Berg CMG, Readman JW (2004) Determination of pyriithione in natural waters by cathodic stripping voltammetry. *Anal Chim Acta* 511:47–53
109. Dantas AND, De Souza D, de Lima JES et al (2010) Voltammetric determination of ketoconazole using a polished silver solid amalgam electrode. *Electrochim Acta* 55:9083–9089
110. Hasanzadeh M, Shadjou N, Saghatforoush L et al (2012) Eletrocatalytic oxidation of selected parabens on zinc hydroxide nanoparticles. *Cat Commun* 19:10–16
111. Campanella L, Roversi R, Sammartino MP et al (1998) Hydrogen peroxide determination in pharmaceutical formulations and cosmetics using a new catalase biosensor. *Pharm Biomed Anal* 18:105–116
112. Matos RC, Pedrotti JJ, Angnes L (2001) Flow-injection system with enzyme reactor for differential amperometric determination of hydrogen peroxide in rainwater. *Anal Chim Acta* 441:73–79
113. Grennan K, Strachan G, Porter AJ et al (2003) Atrazine analysis using an amperometric immunosensor based on single-chain antibody fragments and regeneration-free multi-calibrant measurement. *Anal Chim Acta* 500:287–298
114. Kim YJ, Kim YS, Niazi JH et al (2010) Electrochemical aptasensor for tetracycline detection. *Bioprocess Biosyst Eng* 33:31–37
115. Himmelheber DW, Taillefert M, Pennell DD et al (2008) Spatial and temporal evolution of biogeochemical processes following in situ capping of contaminated sediments. *Environ Sci Technol* 42:4113–4120
116. Viollier E, Rabouille C, Apitz SE et al (2003) Benthic biogeochemistry: state of the art technologies and guidelines for the future of in situ survey. *J Exp Marine Biol Ecol* 285:5–31
117. Tapsoba I, Arbault S, Walter P et al (2010) Finding out Egyptian Gods' secret using analytical chemistry: biomedical properties of Egyptian black makeup revealed by amperometry at single cells. *Anal Chem* 82:457–460

Chapter 10

Surfactants

Elmorsy Khaled and Hassan Y. Aboul-Enein

Surfactants are the active ingredients in personal hygiene products and detergents for industrial and household cleaning. There are four classes (cationic, anionic, amphoteric, and nonionic) based on the ionic charge (if present) of the hydrophilic portion of the surfactant in an aqueous solution. The annual global production of surfactants was 13 million metric tons in 2008, about 70 % represent anionic ones. Surfactants are among the most important components in the group of highly toxic substances that affect environmental conditions in marine ecosystems.

The determination of surfactants in the environment is important not only because they are toxic, but also for their biodegradation metabolites that are more persistent. The routine procedure for surfactants analysis is based on a two-phase titration method. While this method is sensitive, it has many disadvantages such as limitation of application to strongly colored and turbid samples, time-consuming, toxicity of organic chlorinated solvents used, and formation of emulsions during titration which could disturb the visual end-point detection. In view of its disadvantages, other alternative analytical techniques have been developed such as spectrophotometry, thin layer chromatography, and capillary electrophoresis.

However, increasing environmental concerns have fostered the development of automated analytical systems for environmental monitoring with added features for in situ, real time and remote operation. The use of electrochemical sensors as detectors integrated in automated flow systems has proved to achieve simple, robust, and automatic analyzers for environmental monitoring.

E. Khaled (✉)

Microanalysis Laboratory, National Research Centre, Dokki, Giza, 12262 Egypt
e-mail: elmorsykhaled@yahoo.com

H.Y. Aboul-Enein

Pharmaceutical and Medicinal Chemistry Department, National Research Centre,
Dokki, Giza, 12262 Egypt

This chapter presents an overview of electrochemical techniques applied for the determination of surfactants. Special focus will be put on both potentiometric and amperometric sensors and biosensors.

10.1 Introduction

Surfactants form a unique class of organic compounds. A surfactant molecule contains a hydrophilic head group and a hydrophobic chain (or tail). The polar or ionic head group usually interacts strongly with an aqueous environment, in which case it is solvated via dipole–dipole or ion–dipole interactions. Surfactants have a remarkable ability to influence the properties of surfaces and interfaces, and thereby have an impact on industrial processes and products. Applications of surfactants in industry area are quite diverse and have a great practical importance. Surfactants may be used in the production and processing of foods, agrochemicals, pharmaceuticals, personal care and laundry products, petroleum, mineral ores, fuel additives and lubricants, paints, coatings and adhesives, and in photographic films.^{1–6} They can also be found throughout a wide spectrum of biological systems and medical applications, soil remediation techniques, and other environmental, health, and safety applications.⁶

The nature of the polar head group is used to divide surfactants into different categories.⁶ Anionic surfactants are dissociated in water in an amphiphilic anion, and a cation (metal or quaternary ammonium ions). They are the most commonly used surfactants as they account for about 50 % of the world production. Examples for anionic surfactants include alkylbenzene sulfonates (detergents), soaps (fatty acids), lauryl sulfate (foaming agent), di-alkyl sulfosuccinate (wetting agent), lignosulfonates (dispersants), etc. On second position behind anionic surfactants, nonionic surfactants represent about 45 % of the overall industrial production. They do not ionize in aqueous solution, because their hydrophilic group is of a non-dissociable type, such as alcohol, phenol, ether, ester, or amide. A large proportion of these nonionic surfactants are made hydrophilic by the presence of a polyethylene glycol chain, obtained by polycondensation of ethylene oxide. They are called polyethoxylated nonionics. Cationic surfactants dissociate in water into an amphiphilic cation and an anion, most often of the halogen type. A very large proportion of this class corresponds to nitrogen compounds such as fatty amine salts and quaternary ammoniums, with one or several long chain of the alkyl type, often coming from natural fatty acids.

Surfactants are widely used in everyday personal care and household products as well as in a variety of industrial applications. As a result, large amounts of surfactants are commonly discharged in large quantities to sewage treatment plants or directly to the aquatic environment in areas where there is no sewage treatment. The toxicity and persistence of surfactants is now fairly predictable for a variety of environmental situations and several reviews are available.^{7–11} Under aerobic conditions many surfactants are readily biodegraded, while anaerobic

biodegradation generally proceeds more slowly. The toxicity of surfactants naturally depends greatly upon their structure. Increasing the alkyl chain length in the hydrophobic group will generally increase the toxicity, whereas increasing the ethylene oxide (EO) numbers with the same hydrophobic group will generally decrease the toxicity.⁶ Because many surfactants are ubiquitous,¹² the potential toxic effects of these chemicals have attracted much research attention in the past several decades.^{13–15}

10.2 Determination of Surfactants

The widespread importance of surfactants in industrial applications, and scientific interest in their nature and properties have been reflected on a wealth of published literature on surfactant analysis.^{16–31} Probably the most common analytical method for ionic surfactants is Epton's two-phase titration.^{32–34} Here, the surfactant is extracted into an organic hydrophobic solvent (CHCl_3) when a lipophilic ion-pair formed with the titrant. The latter is generally a surfactant of opposite charge. The titration is carried out in the presence of an ionic dye (or a mixture of ionic dyes) which colors the organic layer differently in the presence of an excess of anionic or cationic surfactants. Nonionic surfactants can be titrated after the addition of an activator to form a charged complex.³⁵ Although this procedure was currently used as a standard method; Gerlache et al.³⁰ reported several drawbacks such as formation of an emulsion during titration (risks of errors in visual end-point detection), lack of efficiency for a surfactant having a short carbon chain length, turbidity of the solution when analyzing a complex sample, toxicity of the chlorinated organic solvent (CHCl_3), time-consuming, and difficulty of automation. So it seems necessary to search for alternatives of the aforementioned method in order to increase the laboratory productivity and operator safety and comfort and to reduce drastically the reagents consumption and waste production.

This chapter was intended to provide an overview of different electroanalytical methods for surfactant analysis. Surfactant sensors are usually divided into potentiometric, voltammetric, and amperometric sensors and biosensors. While amperometric sensors and biosensors are very few for the determination of surfactants, potentiometric sensors are the most common due to their simplicity and versatility.

10.2.1 Potentiometric Surfactant Sensors

Potentiometric surfactant sensors are usually used as titration end-point indicator electrodes, although some direct potentiometric surfactant electrodes have also been reported.^{20–23,29–31} All surfactant titrations are based on the so-called antagonistic reaction, where an ionic surfactant reacts with an oppositely charged ion (mainly surfactant, too) forming a water insoluble salt (ion-pair).^{21,29} Before the

equivalent point, the analyte is in excess and, afterwards, the titrant is in excess. The electrode may be sensitive to the analyte or to the titrant. The electroactive material is usually an ion associate A^+B^- in the sensing element in which B^- is an anionic surfactant and A^+ is usually a cationic surfactant.^{21,29} Simply, the ion associate can be prepared by mixing adequate volumes of an aqueous solution containing the anionic surfactant with a solution containing an equimolar amount of the cationic one. The precipitate is filtered, washed thoroughly with distilled water, and dried under vacuum at 25 °C for at least 24 h; afterwards it is ground to a fine powder. Potentiometric sensors are suitable for the determination of ionic (cationic and anionic) as well as nonionic surfactants after activation of the latter with barium chloride.³⁶

Investigations of surfactant-sensitive potentiometric electrodes began in the 1970s.³⁷ Since surfactant ion-selective electrodes have been developed by Gavach and Seta,³⁸ the development of potentiometric surfactant sensors is an area of interest. Several excellent articles^{20,21,29,30,39,40} review the use of different types of electrodes for surfactant analysis. When compared with other analytical methods, ion-selective electrodes (ISEs) are simple, relatively inexpensive, robust, durable, and ideal for their use in field environments. Some other advantages involve that they can be used very rapidly, that they allow continuous monitoring, and that they are not affected by turbidity or color of a sample.

In this part, different potentiometric ion-selective electrodes for the determination of surfactants will be discussed including liquid membrane electrodes, conventional polyvinyl chloride membrane electrodes (PVC), solid contact electrodes, carbon paste electrodes (CPEs), and more recently disposable screen-printed electrodes (SPEs).

10.2.1.1 Liquid Membrane Electrodes

The customary type of a liquid membrane electrode is a design in which the sensitive membrane is composed of a water-immiscible organic solvent containing the ion of interest in the form of ion associate. The membrane is interposed between a standard (internal) and a test (external) ion solution.^{41–43} In early types of liquid membrane electrodes, an organic phase as a membrane is placed between two aqueous phases in bulk or with the support of a thin, porous cellulose sheet, sintered glass, or similar lamellas. Nitrobenzene is the popular membrane solvent; other organic solvents are also applied such as *o*-nitrotoluene, 4-ethylnitrobenzene, 4-nitro-*m*-xylene, and *p*-nitrocoumarin.

Gavach et al.⁴⁴ were probably the first to apply liquid membrane-based ion-selective electrodes (ISEs) for the titration of long chain alkyl methyl ammonium salts with sodium tetraphenyl borate. Birch et al.^{45,46} were also among the first researchers to use liquid ion-exchange electrodes responsive to ionic surfactants in 1972.

A solution of a surfactant ion associate dissolved in a hydrophobic organic solvent (nitroaromatic derivatives) was used as a sensitive liquid membrane

electrode for the determination of surfactants.^{25,26} The inner body of the electrode was filled with a chloride solution of a diluted anionic surfactant and a Ag/AgCl reference electrode was dipped into this internal solution.

Ishibashi et al.⁴⁷ used a Crystal Violet salt in nitrobenzene or 1,2-dichloromethane as the active sensing part for aromatic sulfonates. As reported, the presence of hydrophobic groups in the Crystal Violet molecule limited the dissolution of the sensing solution in aqueous samples.

A comparison of the results obtained with surfactant selective electrodes⁴⁸ and the two-phase titration procedure reveals great accuracy for both techniques. However, the analysis of commercial cosmetic products and washing powders gave better results with the potentiometric titration method.

Sap et al.⁴⁹ used an Fe (II) bis [2,4,6-tri(2-pyridyl)]-1,3,5-triazine complex embedded in the sensor for the determination of dodecyl sulfate (DS). Linear response was in the concentration range between 7×10^{-6} and 1.5×10^{-6} mol L⁻¹. No interference from inorganic ions was noticed while some other organic ions did. The potential jump magnitude increases with the alkyl chain length of the surfactant (formation of a more hydrophobic ion-pair).

A supported liquid and a PVC-based membrane selective for dodecyl sulfate (DS⁻) ion was described by Arvand-Barmchia et al.⁵⁰ The electroactive element was a membrane containing a dissolved ion association complex of DS⁻ with cetylpyridinium (CP⁺) cation dissolved in acetophenone. Nernstian response towards the DS⁻ anion was achieved over the concentration range from 8.3×10^{-3} to 1.0×10^{-6} M at 25 °C. The proposed electrode also showed good selectivity and precision (RSD about 2.0 %), and was usable within the pH range of 4.0–6.8. The liquid membrane electrode could find application in the direct determination of DS by the standard addition method at pH 5.0, and exhibited useful analytical characteristics for the determination of sodium dodecyl sulfate (SDS) in detergents and real samples.

Two major problems encountered with liquid membrane electrodes are the drift of the potentiometric signal with time and a risk of membrane dissolution in the aqueous phase when the concentration of the surfactant approaches the critical micelle concentration (CMC).

10.2.1.2 Conventional Polymeric Membrane ISEs (PVC)

Moody et al.⁵¹ introduced a more convenient approach for liquid membrane electrodes, where the membrane components (electroactive material, supporting polymer and plasticizer) were dissolved in tetrahydrofuran or cyclohexanone at room temperature. The cocktail was poured in a Petri dish, where the slow evaporation of the solvent left a flexible master sheet of 10–100 μm thickness. The membrane was cut with a cork borer and mounted at the end of a plastic tube. The electrode body was filled with a standard internal solution of the target ion and saturated KCl as desired for establishing the potential of the internal reference electrode. Since these membranes contained ~70 % (w/w) plasticizer and because

the plasticized polymer behaved like a viscous liquid, the properties of the electrode were very similar to the original liquid membrane electrode. However, the polymeric matrix could be considered as a microporous net or a close netting, respectively, the vacancies of which were occupied by the plasticizer in which the electroactive material was dissolved.⁴¹ Many polymers were used as a polymeric support such as polyvinyl chloride (PVC), polyurethane, silicone rubber, polystyrene, and polymethyl methacrylate.⁵² PVC was the most commonly used polymer matrix as it gave homogeneous, solid and flexible membranes with electrochemical compatibility with a host of sensor material cocktails based on liquid ion exchanger and their appropriate plasticizing solvent mediators.⁵³ The role of plasticizers in plastic membrane electrode might be considered analogous to that of organic solvent in liquid membrane electrodes, as it would determine the electrode selectivity towards the ion of interest, the slope of the calibration graph, as well as the membrane resistance.

Moody and coworkers^{54,55} and Buschmann and coworkers^{36,39} were leaders in constructing efficient surfactant sensors. ISEs containing PVC membranes with ortho-nitrophenyloctyl ether (*o*-NPOE) as a plasticizer were suitable for the determination of amphoteric (ZS) and cationic (CS) surfactants. At pH < 1.5, the ZS reacts as a CS and can be titrated by a bulky counter ion such as tetraphenylborate.⁵⁶ Complexation of the ethoxylated part of nonionic surfactants with a bivalent cation such as Ba²⁺ allows potentiometric titration with tetraphenyl borate.³⁶ Jones et al.⁵⁴ report a detection limit of 1×10^{-7} mol L⁻¹ for Antarox 880.

A potentiometric flow injection determination method for DS⁻ ion was proposed by utilizing a flow-through type ion-selective electrode detector. The sensing membrane of the electrode was a PVC membrane plasticized with *o*-NPOE without added ion exchanger.⁵⁷ A linear relationship was found between peak height and logarithmic concentration of the DS⁻ ion with a Nernstian slope of 52 mV decade⁻¹ in a concentration range from 1.0×10^{-5} to 1.0×10^{-3} mol L⁻¹; the detection limit was 5×10^{-7} mol L⁻¹ and the relative standard deviation 1.3 %. The method was free from the interference of nonionic surfactants and inorganic electrolytes for the determination of the DS⁻ ion. The same author applied a plasticized PVC membrane electrode sensitive to dodecylbenzene sulfonate (DBS) ion for the determination of anionic polyelectrolytes by potentiometric titration, using a solution of (Cat-floc) as a titrant. A linear relationship between the concentration of anionic polyelectrolytes and the end-point volume of the titrant existed in the concentration range from 2×10^{-5} to 4×10^{-4} mol L⁻¹ for potassium polyvinyl sulfate (PVSK), alginate, and carrageenan.⁵⁸ In a more recent publication, a PVC membrane electrode sensitive to octadecylammonium (stearyltrimethylammonium) ion for the determination of cationic polyelectrolytes or Cat-floc by potentiometric titration was published.⁵¹ A linear relationship between the concentration of cationic polyelectrolyte and the end-point volume of the titrant existed in the concentration range from 2×10^{-5} to 4×10^{-4} mol L⁻¹ for Cat-floc, glycol chitosan, and methylglycol chitosan.

A sensor for anionic surfactants with a membrane consisting of 33 % (m:m) PVC, 66 % dioctylphthalate (DOP) plasticizer, and 1 % tridodecylmethylammonium

chloride (TDMAC) was developed and used for flow injection analysis.⁵⁹ The sensor displayed a working response range from 5×10^{-7} to 5×10^{-3} mol L⁻¹ DBS with a Nernstian slope of 58.5 ± 0.2 mV decade⁻¹, a response time of 30 s and a detection limit of 1.5×10^{-7} mol L⁻¹. The sensor was used to measure anionic surfactants (DBS) in different wastewater samples, commercial detergent products, and for monitoring the rate of surfactant biodegradation in sewage treatment plants. The results obtained agreed fairly well with the data obtained by the standard spectrophotometric method.

Three other kinds of ion-selective polymeric membranes (ISEs) sensitive to cationic surfactants were fabricated and characterized by Campanella et al.⁶⁰ They use benzyltrimethylhexadecylammonium-reineckate, dodecyltrimethylammonium-reineckate, or hexadecyl-pyridinium-phosphotungstate as exchanger. ISEs displayed a linearity range for common cationic surfactants between about 10^{-6} and 10^{-4} mol L⁻¹, satisfactory fast response (60 s) and moderately sub-Nernstian slope values. An electrode based on PVC membrane containing trioctylhydroxybenzene sulfonic acid as an ion exchanger and dibutylphthalate (DBP) as a plasticizer was used for the determination of low concentrations of cationic surfactants in antiseptic formulations, by potentiometric titration with sodium tetraphenyl borate.⁶¹

A cetylpyridinium chloride (CPC)-selective membrane sensor consisting of CPC-ferric thiocyanate ion pairs in a PVC matrix plasticized with DOP was described by Mostafa.⁶² The electrode showed a stable, near-Nernstian response for 10^{-3} to 10^{-6} mol L⁻¹ CPC at 25 °C over the pH range of 1–6 with a slope of 57.5 ± 0.4 mV decade⁻¹. There is negligible interference from many cations, anions, and pharmaceutical excipients; however, cetyltrimethylammonium bromide (CTAB) interfered significantly. The direct determination of CPC in Ezaflour mouthwash gave results that compare favorably with those obtained by the British Pharmacopoeia method.

Badawy et al.⁶³ prepared a cetyltrimethylammonium (CTA) cation sensitive polymeric membrane electrode. The electroactive material was the ion-association complex of the cation (CTA)⁺ with phosphotungstic acid (PTA). The electrode was applied for the determination of CTAB in aqueous solutions by standard additions and by potentiometric titration with PTA. The response was nearly Nernstian between 3.2 and 830 μM and was unaffected by pH changes. Recoveries of CTAB from a disinfectant solution were 102.8 and 97 % by the standard addition and the potentiometric method, respectively. The same group fabricated a PVC membrane electrode selective for the CTA⁺ ion using the CTA-trinitrobenzene sulfonate (TNBS) ion pair as electroactive material. The electrode showed a near-Nernstian response within the CTA⁺ concentration range from 1.08×10^{-6} to 8×10^{-4} M at 25 ± 1 °C, good selectivity and precision (RSD = 1.0 %); it was usable within the pH range 2.5–10.2. The electrode was used for the direct determination of CTAB either by the standard addition method or by potentiometric titration with TNBS at pH 7.⁶⁴ In another publication, the same author⁶⁵ prepared a PVC membrane electrode selective for the cetyltrimethylammonium ion (CDEA). The active element was a plasticized PVC membrane

containing the ion associate complex of CDEA with phosphotungstic acid. Near-Nernstian response within the concentration range of 10^{-6} to 10^{-4} mol L⁻¹ CDEA was achieved.

A polyvinyl chloride (PVC) membrane⁶⁶ electrode based on hexadecylpyridinium-phosphotungstate (HDP-PTA) ion associate was constructed for the determination of HDP ion in some antiseptic and disinfecting preparations by standard addition or potentiometric titration methods. The electrode showed a Nernstian response over the concentration range of 6.3×10^{-6} and 3.1×10^{-3} mol L⁻¹ of HDP at 25 °C over a wide pH range.

Patil et al.⁶⁷ fabricated PVC electrodes sensitive to dodecyltri-methylammonium ions (DTA⁺) and tetradecyltrimethylammonium ions (TTA⁺). The electrode was used for determination of critical micelle concentration of TTAB in water. Moreover the electrode was tested in the presence of nonaqueous polar solvents, i.e., dimethylformamide (DMF) and dimethylsulphoxide (DMSO).

A sensitive potentiometric surfactant sensor was prepared based on the highly lipophilic 1,3-didecyl-2-methyl-imidazolium cation in the form of its tetraphenylborate associate.⁶⁸ The sensor responded fast and showed a Nernstian response for the following surfactants under investigation: CPC, CTAB, and hyamine with slope values of 59.8, 58.6, and 56.8 mV decade⁻¹, respectively. The sensor served as an end-point detector in ion-pair surfactant potentiometric titrations using sodium tetraphenylborate as titrant. Several technical grade cationic surfactants and a few commercial disinfectant products were also titrated, and the results were compared with those obtained from a two-phase standard titration method. The results, compared to those obtained using a commercial surfactant electrode with the standard two-phase titration method, exhibited satisfactory mutual agreement.

A membrane with the hexadecyltrioctadecylammonium-tetraphenylborate (HDTA-TPB) ion pair was used for the preparation of a potentiometric sensor for anionic surfactants, such as DS⁻.⁶⁹ The sensor exhibited a Nernstian response of 58.1 mV decade⁻¹ between 3×10^{-7} and 3×10^{-3} mol L⁻¹. The interfering effect of several inorganic and organic anions, most frequently used in formulated products, was investigated. The homologous series of C7–C12 alkane sulfonates and some commercial detergent products were successfully titrated.

More recently,⁷⁰ a PVC membrane electrode selective to HDTA⁺ and DS⁻ was constructed using modified single-walled carbon nanotubes (SWCNTs). The membrane electrodes exhibited a Nernstian response (59.5 mV/decade) for DS⁻ and a near-Nernstian response (57.2 mV decade⁻¹) for CTAB over a wide concentration range below their critical micelle concentrations (CMC). The electrodes showed a fast response time ($t_{90\%} = 30$ s) and could be used for 3 months without any divergence in potentials. The ion-selective electrode could determine SD⁻ down to concentrations as low as 1.9×10^{-6} mol L⁻¹ and CTA⁺ to 5.2×10^{-6} mol L⁻¹. This method for determining anionic surfactants was found to be quite accurate when compared with classical methods.

An installation for the rapid determination of surfactants in seawater using ion-selective electrodes was developed by Stepanets et al.⁷¹ The installation was tested under on-site conditions on shipboard in the course of integrated marine

studies of environmental conditions in the Baltic Sea. Maximum marine pollution levels were detected in the near-shore zone; this fact can be explained by waste discharges from sites where surfactants are in wide residential and industrial use.

Generally, potentiometric sensors incorporated with ion-pair associates are plagued by limited selectivity and their applications are restricted to more challenging matrices; therefore more selective molecular recognition components are clearly required. Chemically modified electrodes (CMEs) were suggested for improving the electroanalytical performance through application of molecular recognition species selective to the target analyte.^{72,73} Different types of molecular recognition elements have been proposed including crown ethers, calixarenes, cyclodextrins (CDs), or porphyrins.^{74,75} Cyclodextrins are naturally occurring macrocyclic oligosaccharides formed of 1,4-glucosidic bond-linked D(+) glucopyranose oligomers of 6, 7, and 8 glucose units yielding α -, β -, and γ -CDs, respectively. CDs can form inclusion complexes with different types of guest molecules without the formation of chemical bonds or changing their structure, where the binding forces are attributed to a number of weak interactive forces, such as hydrophobic forces, hydrogen bonding, and other factors such as size of the cavity and shape of the guest molecule.⁷⁶

Functionalized, lipophilic α -, β -, and γ -cyclodextrins were synthesized and their suitability as onium ion-selective potentiometric sensors was investigated. The proposed electrodes showed Nernstian responses for acetylcholine chloride, dopamine hydrochloride, and the surfactant myristyltrimethylammonium bromide (MTMAB). In each instance, the electrode response was substantially enhanced and stabilized by the presence of the lipophilic cyclodextrin.⁷⁷

A PVC membrane ion-selective electrode suitable for the potentiometric end-point detection in the titration of cationic surfactants was constructed by Khalil et al.⁷⁸ The active substance of the electrode was the neutral carrier dibenzo-18-crown-6 using diisooctyl phthalate as plasticizer. The electrode had a pH working range from 2.0 to 12.0 with a Nernstian behavior between 6.0×10^{-6} and 1.6×10^{-3} mol L⁻¹ of hyamine 1622. Katsu and Nishimura⁷⁹ evaluated eight dioxadicarboxylic diamides as ionophores in PVC membrane electrodes for the detection of hexylammonium ions. As reported, near-Nernstian response was achieved and the selectivities were much better than those of the dibenzo-18-crown-6-electrode.

A cyclic aza-oxa-cycloalkane, 7,13-bis(*n*-octyl)-1,4,10-trioxa-7,13-diazacyclopentadecane (L1), was characterized and its interaction with anionic surfactants studied.⁸⁰ Different PVC membrane anionic surfactant-selective electrodes were prepared using L1 as ionophore and *o*-NPOE, bis(2-ethylhexyl) sebacate (BEHS) or DBP as plasticizers. The PVC-based membrane electrode containing *o*-NPOE as plasticizer showed a Nernstian response with a slope of 57.7 ± 0.2 mV decade⁻¹ for lauryl sulfate (LS) in a concentration range from 3.3×10^{-6} to 6.7×10^{-3} mol L⁻¹ with a detection limit of 2.2×10^{-6} mol L⁻¹. The fabricated electrode was used for the determination of anionic surfactants in several mixtures, and the results obtained were compared to those found using a commercially available electrode. A similar ligand (7-methyl-7,13-di-octyl-1,4,10-trioxa-13-aza-7-azonia-cyclopentadecane)

was used as ionophore in the development of a LS ion-selective electrodes.⁸¹ The characteristic performances of the sensor were as follows: the potentiometric response was Nernstian with 59.5 mV decade⁻¹ in a range of concentrations from 1.3×10^{-6} to 6.8×10^{-3} mol L⁻¹ with a detection limit of 6.0×10^{-7} mol L⁻¹. Moreover, the cyclam derivative 1,4,8,11-tetra(*n*-octyl)-1,4,8,11-tetraazacyclotetradecane (L) was used as a carrier for the preparation of PVC-based membrane ion-selective electrodes for anionic surfactants in the presence of tetra-*n*-octylammonium bromide (TOAB) as cationic additive.⁸² The electrode composition was as follows: 56 % DBP, 3.4 % ionophore, 3.8 % TOAB, and 36.8 % PVC. This electrode displays a Nernstian slope of 60.0 ± 0.9 mV decade⁻¹ in the concentration range from 2.0×10^{-3} to 7.9×10^{-6} mol L⁻¹ DS⁻ and a poor response to common inorganic cations and anions. The selective sequence found was DS⁻ > ClO₄⁻ > HCO₃⁻ > SCN⁻ > NO₃⁻ \approx CH₃COO⁻ \approx I⁻ > Cl⁻ > Br⁻ > IO₃⁻ \approx NO₂⁻ \approx SO₃²⁻ > HPO₄²⁻ > C₂O₄²⁻ > SO₄²⁻, i.e., basically following the Hoffmeister series except for the hydrophilic anion bicarbonate. The electrode could be used for 144 days without showing significant changes in the value of the slope or the working range. The electrode showed a selective response to DS and a poor response to common inorganic cations and anions.

Although symmetric ISEs have found a wide range of applications,⁵⁴⁻⁸³ they still have certain inherent limitations; they are mechanically complex, and thus difficult to be miniaturized. The internal reference solution increases the system's impedance and the electrode response time, in addition to a shorter lifetime due to leaching of the electroactive material throughout both solutions in contact with the membrane, and finally due to the internal compartment, which cannot withstand high pressure.⁸⁴

10.2.1.3 Solid Contact Electrodes

The increased interest in using ISEs has led to the development of new sensor materials that show high selectivity for a variety of anions and cations and new approaches for electrode construction. Several attempts have been made to eliminate the internal reference electrode resulting in a solid-state sensor design. Examples of these types of sensors include coated wire electrodes, graphite rods, graphite-based electrodes, and ion-selective field-effect transistors (ISFETs).

A new kind of all solid-state sensors was first reported by Cattrall and Freiser in 1971 in which the internal reference element was in direct contact with the sensing membrane and thus contained no aqueous solution. The first group of such simplified sensors was those of the so-called coated wire construction type (CWE). In this approach, a metal wire was dipped with a solution of PVC in THF containing also a suitable electroactive material. During evaporation of the solvent, a PVC film on the metal wire surface was formed.⁸⁵ Although different materials such as platinum, silver or silver chloride, and aluminum could serve as central conductors, the nature of the wire support had no substantial influence on the electrode performance if it did not react with the membrane components.⁸⁶

Cottrell was the first who used a PVC-coated wire electrode for the determination of low concentrations of surfactants.⁸⁷ Extensive articles and excellent overviews on CWEs for the determination of surfactants were published by Vytras's group, who were very active in developing simple coated wire electrodes for cationic and ampholytic surfactants especially during the 1980s.^{21,29,43,88-95}

A method was described for the determination of nonionic surfactants containing poly(oxyethylene) chains with sodium tetraphenylborate, based on the precipitation of ternary compounds in the presence of bivalent metal ions (barium salts). Titrations were monitored potentiometrically with a simple PVC membrane-coated aluminum wire electrode plasticized with 2,4-dinitrophenyloctyl ether.⁹⁴

Cations of the homologous series of *N*-alkyl-*N*-ethylpyrrolidinium salts were determined with a good precision by a titration using sodium tetraphenylborate using a simple CWE.⁹⁵ The magnitude of both, the potential break and sharpness at the inflexion point of the titration curve, was predetermined by the solubility of the corresponding ion-pair in the membrane solvent and was affected by the nature of the membrane plasticizer. The results showed that *o*-NPOE gave the highest ΔE , which might be due to its high polarity. The author reported that the value of the potentiometric titration break depended on the number of carbon atoms in the alkyl chain.

More recently, a new, simple, sensitive, low cost, and rapid potentiometric method for direct determination of ultra-trace amounts of SDS with a new DS^- selective electrode was reported.⁹⁶ The electrode was prepared by electropolymerization of aniline on the surface of a Pt electrode in acidified solutions containing DS^- ions. The sensor showed a Nernstian behavior response of 59.0 ± 2.3 mV decade⁻¹ over a very wide linear range from 1.0×10^{-9} to 3.0×10^{-6} mol L⁻¹. The electrode exhibited high selectivity to DS^- over other ions and could be used for 4 weeks without any major deviations in the pH range of 3.5–9.8. The proposed electrode was applied to the determination of DS^- in mouth washing solution and tap water samples. The potentiometric behavior of coated wire electrodes based on DBS-doped polypyrrole (PPy-DBS) and hyamine as ion exchanger was investigated by Shafiee-Dastjerdi and Alizadeh.⁹⁷ Two types of coated wire electrodes made of PVC-PPy-DBS and PVC-hyamine-DBS, plasticized with *o*-NPOE, showed Nernstian behavior (with respective calibration slopes of about 58 and 60 mV per decade) within a concentration range of 3.0×10^{-6} to 1.1×10^{-3} and 5.0×10^{-6} to 1.3×10^{-3} mol L⁻¹ DBS^- , respectively. The potentiometric response was independent from the pH of the test solution in the range of 3–10. The response time of electrodes was fast (10 s for both types of electrode), and the electrodes could be used for at least 3 months without any significant changes in the potential. DBS^- was determined in some commercial detergents with results in satisfactory agreement with those obtained by a standard method (two-phase titration).

Data for cationic surfactant ions in common cleaners as determined with CWEs were presented by Plesha et al.⁹⁸ Dinonylnaphthalene sulfonic acid, tetraphenylborate, and tetrakis (4-chlorophenyl)borate were examined as ion exchangers, from which dinonylnaphthalene sulfonic acid showed to be the favorable agent. The

ISEs exhibited approximately Nernstian behavior down to the 10^{-6} mol L⁻¹ with lifetimes over 50 days when used continuously, and a shelf life of over 100 days.

Selig was the first who used a spectroscopic graphite rod coated with a solution of PVC and DOP in tetrahydrofuran for the potentiometric titration process.⁹⁹ An interesting membrane was constructed by Dowle and coworkers,^{100,101} where a graphite rod was coated with PVC containing tritolylyl phosphate (TPP) and an appropriate ionophore (tetradecylammonium dodecyl sulfate) which is sensitive to anionic surfactants. The fabricated electrode showed a linear measuring range from 10^{-2} to 10^{-6} mol L⁻¹ SDS with fast response time of 30 s. The sensor operated well in ethanolic solutions (20 % v/v) and could be used under flow conditions such as in HPLC. The disadvantages were a relatively poor lifetime and the need to calibrate the electrode several times per day.

Nineteen quaternary ammonium salts including CTAB and 25 basic dyes were potentiometrically titrated against Orange IV.¹⁰² The indicator electrode was a carbon rod coated with a PVC membrane containing triheptyldodecylammonium iodide (THDAI). The ammonium compounds containing alkyl groups of 14–18 carbon atoms showed well-defined titration curves with sensitivity in the concentration range from 10^{-5} to 10^{-4} mol L⁻¹.

An alternative approach for construction of solid contact electrodes can be also applied by casting the sensitive membrane directly on the surface of a conductor such as silver or a conductive carbon resin. Thus, two surfactant sensors were prepared using hyamine 1622 or tetradodecylammonium (TDA) as cationic and DBS as anionic surfactant.¹⁰³ The sensing materials were incorporated in a PVC matrix containing *o*-NPOE as a solvent mediator and applied on a support of a conductive resin without inner reference solution. The responses of these electrodes to DS and DBS as well as the interferences of several common inorganic anions and anionic surfactants were examined. The membranes showed good performance for use as a general potentiometric sensor responsive to anionic surfactants.

An automated FIA system with a throughput of 85 samples/h for the determination of low concentration levels of anionic surfactants in river water and wastewater was developed by Saad et al.¹⁰⁴ The system used specially constructed tubular flow-through all solid-state ion-selective electrodes as potentiometric sensors and on-line pre-concentration techniques. They showed a general response to anionic surfactants with a lower detection limit of approximately 10^{-5} mol L⁻¹. Potentially interfering substances such as chloride, nitrate, and nonionic surfactants were proved not to interfere. Matesic-Puac et al.¹⁰⁵ prepared an all solid-state surfactant-sensitive electrode based on a teflonized graphite conducting substrate coated with a plasticized PVC membrane containing tetrahexyldecylammonium dodecylsulfate (THDADS) as an anionic surfactant-sensing material. The electrode was used as end-point indicator for potentiometric titrations.

An automated electronic tongue consisting of an array of potentiometric sensors and an artificial neural network (ANN) was developed to resolve mixtures of anionic surfactants. The sensor array was formed by five different flow-through sensors for anionic surfactants, based on polyvinyl chloride membranes having cross-sensitivity features.¹⁰⁶

ISFETs work as varieties of CWEs, incorporating the ion sensing membrane directly on the gate of a FET. The construction is based on the technology to prepare small multisensor systems with multiple gates, for sensing several ions simultaneously, while their small size permits the *in vivo* determination of analytes. An ISFET device selective to anionic detergents, based on a PVC-sebacate membrane, containing benzyldimethylcetylammmonium cholate (BSCAC) as the ion exchanger was characterized and applied for the determination of some anionic surfactants by Campanella et al.¹⁰⁷ The linearity range extended over 3–4 concentration decades depending on the examined surfactant, within the range between about 10^{-6} and 10^{-3} mol L⁻¹ in all cases. The proposed electrode could determine anionic surfactants in standard aqueous solutions and in authentic matrices (lake and sea water). The same author¹⁰⁸ described three new ISFET devices based on polymeric selective membranes sensitive to cationic surfactants. These sensors use a PVC-sebacate matrix incorporating as exchanger benzyldimethylhexadecylammmonium-reineckate (BDHC-RN), dodecyltrimethylammmonium-reineckate (DTA-RN), and hexadecylpyridinium-phosphotungstate (HDP-PT), respectively. A characterization of the ISFETs was performed and the analytical results were compared with those obtained using other sensors such as ISEs equipped with the same exchanger or using a biosensor responsive to cationic and anionic surfactants. Determinations of cationic surfactants in aqueous matrices of environmental interest were carried out using the sensor with the best performance. Furthermore, the critical micellar concentration (CMC) of some cationic surfactants was also evaluated.

Sanchez and coworkers¹⁰⁹ reported a new ISFET sensor for the determination of anionic surfactants by titrations. The developed devices showed a lifetime longer than 4 months, improving the reported values of PVC membrane-ISFETs. Other characteristics were Nernstian slopes from 59 to 62 mV decade⁻¹, with detection limits of about 10^{-6} mol L⁻¹. In a comparative study, there were no significant differences between the results produced with the standard two-phase titration method and the proposed potentiometric titration method. In a following publication, ISFETs based on a photocurable membrane sensitive to anionic surfactants SDBS and DS were reported.¹¹⁰ The determination of the concentrations of the surfactants was performed following a standard addition methodology using ISFETs as sensors without any previous separation stages.

Mainly due to the sacrifice of the internal reference solution, solid contact electrodes exhibit interesting properties: they can be machined in any shape, exhibit faster responses, and facilitate the possibility to be operated in higher pressure environments where symmetric ISEs might be damaged. Drawbacks of the above construction are the poor reproducibility of the electrode potential and a drift that can be related to the asymmetric membrane with no internal reference electrode and filling solution. There is an ill-defined thermodynamic charge transfer at the blocked interface (phase boundary) between the ion sensitive membrane with ionic conductivity and the conducting substrate with electronic conductivity.¹¹² For this reason, CWEs are better applied under hydrodynamic conditions, e.g., in flow injection analysis, where the contact of the sample plug with the electrode surface is brief.

10.2.1.4 Carbon Paste Electrodes (CPEs)

Carbon paste electrodes (CPEs) were firstly reported by Adams in 1958 as a new sensor material to overcome limitations of the dropping mercury electrode (DME) caused by anodic dissolution of Hg at more positive potentials.¹¹² Carbon pastes are usually prepared by mixing of graphite powder and a pasting liquid (binder), using an agate mortar and a pestle. The resulting paste with fine consistency is packed into a piston driven electrode holder offering easy and quick surface regeneration which is the most frequently emphasized advantage of CPEs. In addition, carbon paste has advantages of ease of bulk modification compared with surface modification which is usually more complex and time-consuming.^{42,113–115} The binder, or pasting liquid, behaves similar to the plasticizer of the membrane electrodes. From among the substances currently used, tricresyl phosphate (TCP) was recommended in case of ISE potentiometry.¹¹⁶ Earlier, CPEs were classified as a special type of solid and/or carbon electrodes. From the potentiometric point of view, the electrodes are now classified as ion-selective electrodes with a liquid membrane as the pasting liquid is present as a very thin film surrounding the carbon particles and exhibits usually good extraction ability against ion associates composed of lipophilic species.^{117,118}

Concerning the determination of surfactants, in 1997 Vytras's group demonstrated that carbon paste-based electrodes could also be used as potentiometric sensors to monitor titrations of surfactants.^{117,119} When compared to PVC and CW electrodes, CPEs had the advantages of very low Ohmic resistance, very short response time in addition to the ease of fabrication and regeneration as well as long functional lifetime. Jezkova et al.¹¹⁶ used perchlorate and fluoroborate ion-selective carbon paste electrodes for both direct potentiometric measurements and potentiometric titration of perchlorate or fluoroborate with 0.1 M CPC. The electrodes had a rapid response, low Ohmic resistance, and limits of detections and selectivity similar to the limits of commercial membrane electrodes. A carbon paste electrode incorporated with the ion association of CPC–thallium halo complexes was applied as indicator electrode with the potentiometric titration of surfactants.¹²⁰

10.2.1.5 Screen-Printed Electrodes

While CPEs continued to play a major role in the development of analytical procedures applicable in laboratory or to test new analytical methodologies,^{113–115} their relatively large size diminishes commercialization. Over the past few years, interest has been growing in the application of simple, rapid, inexpensive disposable sensors for clinical, environmental, and industrial analysis. Screen printing seems to be one of the most promising technologies allowing sensors to be produced on a large scale with the advantages of optimized manufacturing repeatability. Mass production at low cost makes them ideal for industrial commercialization with long shelf-life time and applications in the field with portable small

instruments.^{113,121–125} Historically, the first reports on single-use disposable strip electrodes were dealing with amperometric biosensors by Wring and coworkers.¹²⁶

Screen-printed electrodes (SPEs) are devices that are produced by printing different inks on a suitable substrate. Through the application of this technique, it is possible to fabricate a chip containing working, reference, and auxiliary electrode or even multisensory array. Electrode fabrication requires an ink as a precursor, which is typically a mixture containing at least three components¹¹³ (see also Chap. 16 of Volume I):

1. Conductive particles having electroactive sites.
2. A polymer that can bind together these particles.
3. A solvent in which the ink components are dissolved or dispersed.

The mixture is liquid at room temperature, while after printing and curing at suitable temperatures, a solid conductive film with surface electroactive sites is produced. Commercially available inks are already tested and optimized under various conditions.

In a comprehensive study, Khaled et al.¹²⁷ fabricated a simple disposable potentiometric sensor for the determination of surfactants. The proposed disposable sensor, containing both working and reference electrodes, was fabricated by screen printing technology using a homemade printing ink composed of carbon particle and a plasticizer dissolved in a PVC/THF solution. It was expected that, when such sensors were immersed in a stirred aqueous suspension of the ion-pair formed during the potentiometric titration, their organic solvents (plasticizers) became gradually saturated with the ion pair and there was no need for the addition of the electroactive material to the electrode matrix.

Analytical performances of the printed electrodes were compared with those of carbon paste, coated wire, coated graphite, and PVC polymeric membrane electrodes. The printed electrodes showed very short response time reaching 3 s with adequate shelf-life (6 months). The disposable sensor was successfully applied for the potentiometric titration of five different cationic surfactants, namely CPC, hexadecyltrimethylammonium bromide (HDTAB), DTAB, didodecyldimethylammonium bromide (DDMAB), and septonex with NaTPB. Concerning the titration process, the total potential changes and potential jump at the end-point were large (between 528 and 234 mV with potential jump ranging between 2,035 and 650 mV mL⁻¹ titrant) which allowed the determination of 90 µg surfactant. The total potential change decreased proportionally with decreasing hydrophobicity of the molecule yielding the following series: CPC > HDTAB > Septonex > DDMAB > DTAB (Fig. 10.1).

The proposed disposable strips were successfully used for the potentiometric titration of cationic and anionic surfactants, pharmaceutical preparations, detergents, and water samples with sensitivities comparable with the official method; they also have the ability of field measurements using a portable titration system (Fig. 10.2).

Similar sensors were fabricated using screen-printed electrodes for the determination of CPC,¹²⁸ CTAB,¹²⁹ and Septonex¹³⁰ using different thick films modified

Fig. 10.1 Potentiometric titration of different cationic surfactants with 10^{-2} mol L $^{-1}$ NaTPB using SPCPEs as potentiometric sensor. (Reprint with permission from reference (127). Copyright (2008) Elsevier

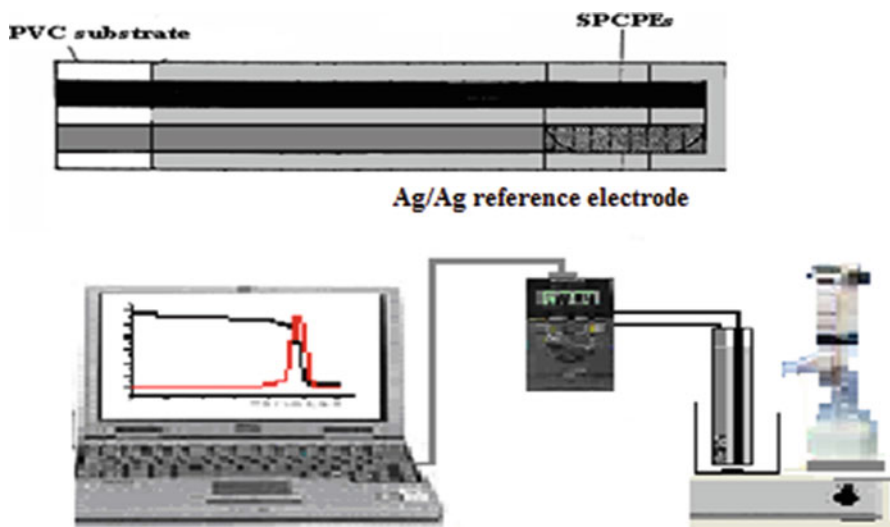
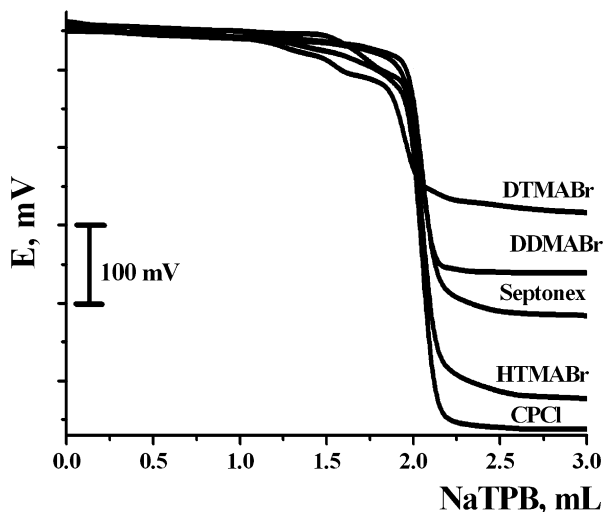


Fig. 10.2 Schematic diagram of a portable system manifold used for the potentiometric titration of surfactants in the field. (Reprint with permission from reference (127). Copyright (2008) Elsevier

by the corresponding ion associates of the surfactant with tetraphenyl borate. The fabricated electrodes showed a stable, near-Nernstian response for 1×10^{-2} to 1×10^{-6} mol L $^{-1}$ CPC at 25 °C over the pH range 2–8 with a slope of 60.66 ± 1.10 mV decade $^{-1}$.

10.2.1.6 Commercial Surfactants Potentiometric Electrodes

In parallel to research considering surfactants sensors, some commercially surfactant selective electrodes have been launched into the market. Orion model 93-42,¹³¹ ASTEC model TSE 01:91,¹³² and Metrohm “High Sense Tenside” are examples with considerable long operational life time^{38,55} and is the most promising specimen on the market.^{39,56} It is stable over a wide pH range and its use permits differentiation between some detergents in mixtures simply by changing the pH of the analyzed sample.

The polyoxyethylene portion of nonionic surfactants forms pseudo-crown compounds in the presence of barium ions which can be titrated with sodium tetraphenylborate using the Orion surfactant electrode as an end-point indicator electrode. An average recovery of 96.4 % can be obtained for the determination of three standard detergents.¹³¹ The described method has been used successfully in the routine determination of nonionic surfactants.

A commercially available fluoroborate ion-selective indicator electrode was used for the potentiometric titration of surfactants and soaps.¹³² The titrants were HDTAC, hexadecylpyridinium chloride (HDPC), and diisobutylphenoxyethoxyethyl-(dimethyl)benzylammonium chloride (DIPEBC).¹³³ Similarly, Benoit et al.¹³⁴ titrated CTAB with sodium tetraphenylborate potentiometrically using a commercial ClO_4^- selective electrode. The method proved to be precise exhibiting a relative standard deviation of 1.1 %.

10.2.2 Voltammetric and Amperometric Sensors

A surfactant is usually not electroactive from voltammetric and amperometric view; therefore, it is necessary to apply an indirect technique using a solution with a certain amount of an electroactive species (a marker) which is oxidized or reduced at the working electrode. The current of the marker decreases in the presence of a surfactant, which inhibits the electronic transfer at the electrode surface, and the concentration of the analyte can be related to the magnitude of the current decrease. For instance, Skoog et al.¹³⁵ studied different surfactants by their influence on the amperometric and cyclic voltammetric responses of hexacyanoferrate. In a flow system, they noted that the presence of nonionic surfactants had an irreversible blocking effect on the electrode response. The suppression effect by a surfactant on the adsorptive voltammetric response of the nickel dimethylglyoxime complex was also reported by Adeloju and Shaw^{136,137} using different types of working electrodes, such as an HMDE, a mercury-film electrode, or a dropping mercury electrode. CPC and CTAB could be determined at ultra-trace levels by indirect stripping voltammetry on a hanging Hg drop electrode. The calibration graphs were linear up to 65, 5, and 0.5–3 mg L^{-1} for CPC, CTAB, and DBS, respectively. The method was applied to the determination of the

aforementioned surfactants in disinfectants, lozenges, and mouth wash. In some cases the sample solution was subjected to cleanup through a chromatographic column before analysis to eliminate matrix interference.

The study of the inhibition of parahydroquinone oxidation at a graphite electrode in the presence of a surfactant (phospholipid) was reported by Schmidt and Emons.¹³⁸ The decrease of the parahydroquinone oxidation peak was related to the surfactant concentration. In a similar approach, using ferrocene in a CPE as a redox tracer, Kim et al.¹³⁹ determined different surfactants via modification of the ferrocene redox behavior. In the presence of DS, the oxidation peak current of ferrocene was enhanced by a factor of 3.5. A limitation of the technique was the analysis time because the electrode-solution contact period was 1 h. Similarly, anionic polyelectrolytes were determined by adsorptive stripping voltammetry (ADSV) at a carbon paste electrode in the presence of 11-ferrocenyltrimethylundecyl ammonium ions.¹⁴⁰ The ion-association complex between an anionic polyelectrolyte and the ferrocenyl cationic surfactant was adsorptively accumulated at the electrode in the absence of an applied potential. The concentration of the anionic surfactant was indirectly evaluated from the oxidation wave of the ferrocenyl cationic surfactant. By means of AdSV, levels of anionic surfactants of 10^{-7} mol L⁻¹ could be measured with good selectivity.

The combination of ion-pair extraction and differential pulse polarography was shown to be a method suitable for the determination of 10^{-7} mol L⁻¹ of organic quaternary ammonium bases using Orange II as an appropriate polarographically active counter ion.¹⁴¹ The proposed method was used for the determination of tetrapentylammonium bromide (TPAB), Septonex, and codeine. An indirect voltammetric method for determination of CPC was proposed by Simunkova via the extraction of the electroactive CP-picrate as a 1:1 ion associate into chloroform. After drying the equivalent amount of picric acid in the extracted ion associate was determined by differential pulse voltammetry (DVP) on a hanging mercury drop electrode.¹⁴² The limit of determination was 0.136 mg L⁻¹ with a relative standard deviation less than 6 %. The CPC content in pastilles of an antiseptic medicament ("Halset") was determined with good accuracy. Moreover, other simple extractive procedures were suggested for the determination of anionic surfactants.^{143,144} The methods involved the formation of an extractable complex between the synthetic surfactant anion and the bis-(ethylenediamine)-diaqua-copper(II) cation. It was extracted into chloroform and then back-extracted into dilute acid. The resulting Cu(II) ions were determined by AAS and ASV with good correlation. A limit of detection of 5.0 µg L⁻¹ anionic surfactant was observed with a linear calibration from 5.0 to 500 µg L⁻¹ in the sample.

In addition, few direct voltammetric procedures were suggested for the quantification of surfactants. Zhao and Zeng¹⁴⁵ noticed that, in presence of L-cysteine, CPC exhibited a sensitive cathodic stripping peak at about ~1.2 V. (vs. SCE). The square root of the peak height was linear to the CPC concentration in the range of 2–50 µM. A flow injection voltammetric method was developed for the determination of surfactants and ethanol.¹⁴⁶ Surfactants in waters and ethanol in alcoholic drinks were determined.

10.2.3 Surfactant Biosensors

During the last decades, many biosensors have been developed for monitoring environmental parameters.^{145–148} With respect to surfactants, several biosensors have been proposed that employ microorganisms, cells, or enzymes. In this way, a bioreactor-type electrochemical sensor for the determination of linear alkylbenzene sulfonates (LASs) was described.¹⁴⁹ The detection principle is based on the fact that, when LASs are biodegraded by certain bacteria, their respiratory activity in solution increases with a concomitant decrease in dissolved oxygen. The latter can be followed by an oxygen electrode positioned on-line in an appropriate flow setup. A linear response up to 6 mg L^{-1} of LAS could be achieved in less than 15 min. Applications to the determination of surfactants in river pollution were suggested.

Bacterial degraders as the base of an amperometric biosensor for the detection of anionic surfactants were investigated by Taranova et al.¹⁵⁰ Several strains belonging to genera *Pseudomonas* and *Achromobacter* were characterized by their ability to degrade anionic surfactants; they were tested as potential bases of microbial biosensors. For each strain the author studied the substrate specificity and stability of the sensor signals. Maximal signals were observed with anionic surfactants. The lower limit of detection for DS used as a model surfactant in the field was $1 \text{ }\mu\text{M}$ for all strains. The microbial biosensor can extend the practical possibilities for rapid evaluation of surfactants in water media.

A *Pseudomonas rathonis* T-based amperometric biosensor was constructed for the detection of anionic surfactants.¹⁵¹ Microorganisms contained the plasmid for the degradation of surfactant. The sensor had high sensitivity to DS (the lower limit of DS detection was within the range from 0.25 to 0.75 mg L^{-1}); the responses to other detergents—volgonat, decylbenzene sulfonate, metaupon, toluene sulfonate, and alkylbenzene sulfonate—were 82, 36, 20, 10, and 10 % of response to SDS, respectively. As reported, the measurement time did not exceed 5 min.

The effect of nonionic surfactants in textile and tannery wastewater on the bacterium *Escherichia coli*, immobilized in an Anopore membrane on the surface of a screen printed carbon electrode, was studied.¹⁵² The amperometric response of the sensor was monitored at +550 mV versus a chloridized silver wire electrode in a vial with the neutralized sample and ferricyanide as a redox mediator. Toxicity was measured by determining the degree of inhibition of the biosensor signal after an exposure of 35 min. The observed toxicity of wastewater samples was attributed to nonionic surfactants.

Some studies have recently indicated that some surfactants may inhibit cholinesterase (ChE) activity in aquatic animals.^{153,154} Indeed, the chemical properties of surfactants can alter enzyme activities by binding or disrupting the enzyme structure.¹⁵⁵ Evtugyn et al.¹⁵⁶ investigated the influence of nonionic surfactants on the response of cholinesterase-based potentiometric biosensors. The effect of surface-active compounds depended on the hydrophilic properties and porosity of the enzyme support material and the inhibition mechanism. In the range of mass per volume (m/V) ratio 0.002–0.3 % the surfactants showed a reversible inhibiting

effect on the biosensor response. At lower concentrations (down to mass per volume ratio 10^{-4}) the surfactants alter the analytical characteristics of reversible and irreversible inhibitor determination.

References

1. (1966–2002) Surfactant science series, vol 1–109. Dekker, New York
2. Wasan DT, Ginn ME, Shah DO (eds) (1988) Surfactants in chemical/process engineering. Dekker, New York
3. Myers D (1988) Surfactant science and technology. VCH, New York
4. Porter MR (1991) Handbook of surfactants. Blackie, Glasgow
5. Karsa DR (ed) (1999) Industrial applications of surfactants IV. Royal Society of Chemistry, Cambridge
6. Schramm LL, Stasiuk EN, Marangoni DG (2003) Surfactants and their applications. *Annu Rep Prog Chem Sect C* 99:3–34
7. Maddin CM (1991) Proceedings of the international conference on health safety and environment. Society of Petroleum Engineers, Richardson, TX, SPE paper 23354
8. Arthur D. Little, Inc (1991) Environmental and human safety of major surfactants. Vol. I. Anionic surfactants. A final report to The Soap and Detergent Assoc. Arthur D. Little, Inc, Cambridge, MA
9. Hutzinger O (ed) (1992) Handbook of environmental chemistry. Springer, Berlin
10. Swisher D (1987) Surfactant biodegradation. Dekker, New York
11. Karsa DR, Porter MR (eds) (1995) Biodegradability of surfactants. Blackie Academic, London
12. Ying GG, Williams B, Kookana R (2002) Environmental fate of alkylphenols and alkylphenol ethoxylates—a review. *Environ Int* 28:215–226
13. Abel PD (1974) Toxicity of synthetic detergents to fish and aquatic invertebrates. *J Fish Biol* 6:279–298
14. Lewis MA (1991) Chronic and sublethal toxicities of surfactants to aquatic animals: a review and risk assessment. *Water Res* 25:101–113
15. Lewis MA, Suprenant D (1983) Comparative acute toxicities of surfactants to aquatic invertebrates. *Ecotoxicol Environ Saf* 7:313–322
16. Rosen MJ, Goldsmith HA (1972) Systematic analysis of surface-active agents. Wiley, New York
17. Cross J (ed) (1977) Anionic surfactants—chemical analysis. Dekker, New York
18. Cross J (ed) (1986) Non-ionic surfactants—chemical analysis. Dekker, New York
19. Porter MR (ed) (1991) Recent developments in the analysis of surfactants. Elsevier, Essex
20. Birch BJ, Cockcroft RN (1981) Analysis of ionic surfactants in the detergent industry using ion-selective electrodes. *Ion Sel Electrode Rev* 4:1–41
21. Vytras K (1985) Potentiometry. In: Encyclopedia of pharmaceutical technology. Swarbic J, Boylan JC. Marcel Dekker (eds), New York 12:347–388
22. Toei K (1987) Ion association reagents. *Anal Sci* 3:479–488
23. Cullum DC, Platt P (1991) Recent developments in the analysis of surfactants, vol 32. Elsevier, New York
24. Aboul-Kassim TA, Simonei BRT (1993) Detergents: a review of the nature, chemistry, and behavior in the aquatic environment. Part I. Chemical composition and analytical techniques. *Crit Rev Environ Sci Technol* 23:325–376
25. Schmitt TM (1994) Analysis of surfactants, 2nd edn. Dekker, New York
26. Cullum DC (ed) (2001) Introduction to surfactant analysis. Blackie, London

27. Schmitt TM (2001) Analysis of surfactants, vol 96, Surfactant science series. Marcel Dekker, New York
28. Hummel DO (2000) Handbook of surfactant analysis: chemical physico-chemical and physical methods. Wiley, New York
29. Vytras K (1991) Coated wire electrodes in the analysis of surfactants of various types: an overview. *Electroanalysis* 3:343–347
30. Gerlache M, Kauffmann JM, Quarin G, Vire JE, Bryant GA, Talbot JM (1996) Electrochemical analysis of surfactants: an overview. *Talanta* 43:507–519
31. Sak-Bosnar M, Grabaric Z, Grabari BS (2004) Surfactant sensors in biotechnology part 1—electrochemical sensors. *Food Technol Biotechnol* 42:197–206
32. Epton SR (1947) A rapid method of analysis for certain surface-active agents. *Nature* 160:795–796
33. Glazer J, Smith TD (1952) Determination of sodium oleate in dilute aqueous solution. *Nature* 169:497–498
34. Greenberg AF, Clesceri LS, Eaton AD (eds) (1992) Standard methods for the examination of water and wastewater, 18th edn. American Public Health Association, Washington, DC, p 5, Section 5540 C
35. De Caro CA (1998) Automated surfactant titration: a review of various techniques. *Riv Ital Sostanze Grasse* LXXV:197–205
36. Buschmann N, Gors U, Schulz R (1993) Comparison of different cationic titrants for the potentiometric determination of anionic surfactants. *Comun Jorn Com Esp Deterg* 24:469–476
37. International Organization for Standardization (1989) Surface active agents, detergents, determination of anionic-active matter by manual or mechanical direct two-phase titration procedure, ISO 2271. International Organization for Standardization, Geneva
38. Gavach C, Seta P (1970) Dosage potentiometrique des ions alkyl-trimethylammonium a longue chaine et tetrabutyl-ammonium. *Anal Chim Acta* 50:407–412
39. Buschmann N, Schultz R (1993) Comparison of different ion-sensitive electrodes for the titrimetric determination of ionic surfactants. *Tenside Surf Det* 30:18–23
40. Buschmann N, Schultz R (1992) Development of an ion-sensitive electrode for the titration of surfactants. *Comun Jorn Com Esp Deterg* 23:323–328
41. Ma TS, Hassan SSM (1982) Organic analysis using ion-selective electrode, vol 1 and 2. Academic, London
42. Wang J (2000) Analytical electrochemistry, 2nd edn. Wiley VCH, New York
43. Vytras K (1995) Potentiometry. In: Swarbic J, Boylan JC (eds) Encyclopedia of pharmaceutical technology. Marcel Dekker, New York, pp 347–388
44. Gavach C, Bertrand C (1971) Electrodes specifiques d'anions a longue chaine hydro-carbonee: Application au dosage potentiométrique de détergents anioniques. *Anal Chim Acta* 55:385–393
45. Birch BJ, Clarke DE (1972) An electrode selective to the dodecyl sulphate anion: comments on the application of direct potentiometry to c.m.c. measurements. *Anal Chim Acta* 61:159–162
46. Birch BJ, Clarke DE, Lee RS, Oakes J (1974) Surfactant-selective electrodes: Part III. Evaluation of a dodecyl sulphate electrode in surfactant solutions containing polymers and a protein. *Anal Chim Acta* 70:417–423
47. Ishibashi N, Kohara H, Horinouchi K (1973) Aromatic sulphonate ion-selective electrode membrane with crystal violet as ion-exchange site. *Talanta* 20:867–874
48. Anghel DF, Popescu G, Niculescu F (1980) Analytical applications of surfactant selective electrodes-I. Cosmetic products. *Tenside Surf Det* 17:171–173
49. Sap P, Anghel DF, Luca C (1983) Electrochemical sensors for anionic surfactants. I. The electrode based on bis[2,4,6-tris(2-pyridyl)-1,3,5-triazine]iron(II) dodecyl sulfate. *Rev Roum Chim* 28:883–890
50. Arvand-Barmchia M, Mousavi ME, Zanjanchi MA, Shamsipur M (2003) A new dodecylsulfate-selective supported liquid membrane electrode based on its *N*-cetylpyridinium ion-pair. *Microchem J* 74:149–156
51. Moody GJ, Oke RP, Thomas JDR (1970) A calcium-sensitive electrode based on a liquid ion exchanger in a poly(vinyl chloride) matrix. *Analyst* 95:910–918

52. Fiedler U, Ruzicka J (1973) Selectrode—the universal ion-selective electrode: Part VII. A valinomycin-based potassium electrode with nonporous polymer membrane and solid-state inner reference system. *Anal Chim Acta* 67:179–193
53. Davies G, Moody GJ, Thomas JDR (1988) Optimization of poly(vinyl chloride) matrix membrane ion-selective electrodes for ammonium ions. *Analyst* 113:497–500
54. Jones DL, Moody GJ, Moody GJ, Birch BJ (1981) Barium-polyethoxylate complexes as potentiometric sensors and their application to the determination of non-ionic surfactants. *Analyst* 106:974–984
55. Alexander PHV, Moody GJ, Thomas JDR (1987) Electrode membrane and solvent extraction parameters relating to the potentiometry of polyalkoxylates. *Analyst* 112:113–120
56. Buschmann N, Schulz R (1992) Determination of cationic and zwitterionic surfactants using ion selective electrodes. *Tenside Surf Det* 29:128–130
57. Masadome T, Imato T, Hachiya H, Asano Y (1998) Flow injection determination of dodecylsulfate-selective plasticized poly (vinyl chloride) membrane electrode detector. *J Flow Injection Anal* 15:242–247
58. Masadome T, Imato T, Asano Y (1999) End point detection of potentiometric titration for anionic polyelectrolytes using an anionic surfactant-selective plasticized poly (vinyl chloride) membrane electrode and anionic surfactant as a marker. *Fres J Anal Chem* 363:241–245
59. Hassan SSM, Badr IHA, Abd-Rabboh HSM (2004) Potentiometric flow injection analysis of anionic surfactants in industrial products and wastes. *Microchim Acta* 144:263–269
60. Campanella L, Aiello L, Colapicchioni C, Tomassetti M (1996) New ion selective polymeric membrane for cationic surfactant analysis. *Analisis* 24:387–391
61. Egorov VV, Repin VA, Kaputskii VA (1996) Determination of cationic surface-active antiseptics by ion-selective electrodes. *J Anal Chem* 51:986–988
62. Mostafa GAE (2001) PVC matrix membrane sensor for potentiometric determination of cetylpyridinium chloride. *Anal Sci* 17:1043–1048
63. Badawy SS, Shoukry AF, Farghaly RA (1989) A cetyltrimethyl-ammonium cation-sensitive polymeric membrane electrode based on the cetyltrimethylammonium-phosphotungstate ion association. *Microchem J* 40:181–186
64. Issa YM, Badawy SS, El-Hawary WF, Ashour MS (1999) Cetyltrimethylammonium-selective PVC electrode based on its trinitrobenzene sulfonate ion-pair. *Electroanalysis* 11:1063–1067
65. Badawy SS, Issa YM, El-Hawary WF, Ashour MS (2001) Cetyltrimethylammonium-selective PVC electrode based on its ion-associate with phosphotungstic acid. *Mikrochim Acta* 136:1–17
66. Shoukry AF, Badawy SS, Farghaly RA (1988) Hexadecyl-pyridinium-phosphotungstate ion association in construction of a hexadecylpyridinium cation selective electrode. *Anal Chem* 60:2399–2402
67. Patil SR, Rokshit AK (2004) Membrane electrode sensitive to a cationic surfactant in aquo-organic media. *Anal Chim Acta* 518:87–91
68. Madunic-Cacic D, Sak-Bosnar M, Galovic O, Sakac N, Matesic-Puac R (2008) Determination of cationic surfactants in pharmaceutical disinfectants using a new sensitive potentiometric sensor. *Talanta* 76:259–264
69. Madunic-Cacic D, Sak-Bosnar M, Matešić-Puac R (2011) A new anionic surfactant-sensitive potentiometric sensor with a highly lipophilic electroactive material. *Int J Electrochem Sci* 6:240–253
70. Najafi M, Maleki L, Rafati AA (2011) Novel surfactant selective electrochemical sensors based on single walled carbon nanotubes. *J Mol Liq* 159:226–229
71. Stepanets OV, Soloveva G, Mikhailova AM, Kulapin AI (2001) Rapid determination of anionic surfactants in seawater under shipboard conditions. *J Anal Chem* 56:290–293
72. Cox JA, Tess ME, Cummings TE (1996) Electroanalytical methods based on modified electrodes: a review of recent advances. *Rev Anal Chem* 15:173–223

73. Zen J, Kumar AS, Tasi D (2003) Recent updates of chemically modified electrodes in analytical chemistry. *Electroanalysis* 15:1073–1086
74. Shahgaldian P, Pieleś U (2006) Cyclodextrin derivatives as chiral supramolecular receptors for enantioselective sensing. *Sensors* 6:593–615
75. Ogoshi T, Harada A (2008) Chemical sensors based on cyclodextrin derivatives. *Sensors* 8:4961–4982
76. Astray G, Gonzalez-Barreiro C, Mejuto JC, Rial-Otero R, Simal-Gandara (2009) A review on the use of cyclodextrins in foods. *Food Hydrocolloids* 23:1631–1640
77. Bates PS, Kataký R, Parker D (1994) Functionalized cyclodextrins as potentiometric sensors for onium ions. *Analyst* 119:181–186
78. Khalil MM, Anghel DF, Luca CC (1986) Poly (vinyl chloride) containing dibenzo-18-crown-6 as an ion-selective membrane for hyamine 1622. *Anal Lett* 19:807–824
79. Katsu TK, Nishimura N (2000) Organic ammonium ion-selective electrodes using acyclic neutral carriers developed for inorganic-selective electrodes. *Anal Sci* 16:523–526
80. Seguí MJ, Lizondo-Sabater J, Martínez-Manez R, Pardo T, Sancenón F, Soto J (2004) Ion-selective electrodes for anionic surfactants using a new aza-oxa-cycloalkane as active ionophore. *Anal Chim Acta* 525:83–90
81. Seguí MJ, Lizondo-Sabater J, Benito A, Martínez-Manez R, Pardo T, Sancenón F, Soto J (2007) A new ion-selective electrode for anionic surfactants. *Talanta* 71:333–338
82. Lizondo-Sabater J, Martínez-Manez R, Sancenón F, Seguí MJ, Soto J (2008) Ion-selective electrodes for anionic surfactants using a cyclam derivative as ionophore. *Talanta* 75:317–325
83. Masadome T, Imato T (2003) Use of marker ion and cationic surfactant plastic membrane electrode for potentiometric titration of cationic polyelectrolyte. *Talanta* 60:663–668
84. Müller B, Hauser PC (1996) Effect of pressure on the potentiometric response of ion-selective electrodes and reference electrodes. *Anal Chim Acta* 320:69–75
85. Cattrall RW, Freiser H (1971) Coated wire ion selective electrodes. *Anal Chem* 43:1905–1906
86. Vytras K, Kalous J, Simickova B, Cerna J, Silena I (1988) Potentiometric titration of palladium (II) halide complex anions based on ion-pair formation. *Anal Chim Acta* 209:357–361
87. Cotrell R (1973) IUPAC, book of papers, international symposium on ion-selective electrodes, Cardiff
88. Vytras K (1977) Titration of organic cations with sodium tetraphenylborate indicated by K^+ ion selective electrode. *Collect Czech Chem C* 42:3168–3174
89. Vytras K, Remeš M, Kubešová-Svobodová H (1981) Coated-wire organic ion-selective electrodes in titrations based on ion-pair formation: determination of arenediazonium salts with sodium tetraphenylborate. *Anal Chim Acta* 124:91–98
90. Vytras K, Djakova M, Mach V (1981) Coated-wire organic ion-selective electrodes in titrations based on ion-pair formation: Part 2. Determination of ionic surfactants. *Anal Chim Acta* 127:165–172
91. Vytras K, Kalous J, Vosmanská M (1985) Ion-selective electrodes in titrations involving azo-coupling reactions: Part 5. Determination of arenediazonium salts of ampholytic character. *Anal Chim Acta* 175:313–317
92. Vytras K (1984) Determination of some pharmaceuticals using simple potentiometric sensors of coated-wire type. *Mikrochim Acta* 3:139–148
93. Vytras K, Kalous J, Symerský J (1985) Determination of some ampholytic and cationic surfactants by potentiometric titrations based on ion-pair formation. *Anal Chim Acta* 177:219–223
94. Vytras K, Dvořáková V, Zeman I (1989) Titrations of non-ionic surfactants with sodium tetraphenylborate using simple potentiometric sensors. *Analyst* 114:1435–1441
95. Vytras K, Tomáš Čapoun T, Haláček E, Souček J, Štajerová B (1990) Potentiometric ion-pair formation titrations of N-alkyl-N-ethylpyrrolidinium cations using plastic membrane electrodes. *Collect Czech Chem C* 55:941–950
96. Mousavi MF, Shamsipur M, Riahi S, Rahmanifar MS (2002) Design of a new dodecylsulfate-selective electrode based on conductive polyaniline. *Anal Sci* 18:137–140

97. Shafiee-Dastjerdi L, Alizadeh N (2004) Coated wire linear alkylbenzenesulfonate sensor based on polypyrrole and improvement of the selectivity behavior. *Anal Chim Acta* 505:195–200
98. Plesha MA, Van Wie BJ, Mullin JM, Kidwell DA (2006) Measuring quaternary ammonium cleaning agents with ion selective electrodes. *Anal Chim Acta* 570:186–194
99. Selig W (1982) A simple sensor for potentiometric titrations. *Anal Lett* 15:309–329
100. Dowle CJ, Cooksey BG, Ottaway JM, Campbell WC (1987) Development of ion-selective electrodes for use in the titration of ionic surfactants in mixed solvent systems. *Analyst* 112:1299–1302
101. Dowle CJ, Cooksey BG, Ottaway JM, Campbell WC (1988) Determination of ionic surfactants by flow injection pseudotitration. *Analyst* 113:117–119
102. Pan J, Cao L, Li B, Fan H (1986) Potentiometric titration curves of the Orange IV-basic dye or quaternary ammonium salt systems. *Yingyong Huaxue* 3:39–43
103. Baro-Roma J, Sanchez J, del Valle M, Alonso J, Bartroli J (1993) Construction and development of ion-selective electrodes responsive to anionic surfactants. *Sens Actuators B Chem* 15:179–183
104. Saad B, Ariffin MM, Saleh MI (1997) Paraquat sensors containing membrane components of high lipophilicities. *Anal Chim Acta* 338:89–96
105. Matesic-Puac R, Sak-Bosnar M, Bilic M, Grabaric S (2005) Potentiometric determination of anionic surfactants using a new ion-pair-based all-solid-state surfactant sensitive electrode. *Sens Actuators B Chem* 106:221–228
106. Ecker C, Calvo D, del Valle M (2008) Potentiometric determination of anionic surfactants using a new ion-pair-based all-solid-state surfactant sensitive electrode. *J Pharm Biomed Anal* 46:213–218
107. Campanella L, Battilotti M, Borraccino A, Colapicchioni C, Tomassetti M, Visco G (1994) A new ISFET device responsive to anionic detergents. *Sens Actuators B Chem* 19:321–328
108. Campanella L, Aiello L, Colapicchioni C, Tomassetti M (1997) Analysis of cationic surfactants in environmental aqueous matrices by new ISFET devices. *Anal Lett* 30:1611–1629
109. Sanchez J, Beltran A, Alonso J, Jimenez C, del Valle M (2000) Development of a new ion-selective field-effect transistor sensor for anionic surfactants: application to potentiometric titrations. *Anal Chim Acta* 382:157–164
110. Sanchez J, del Valle M (2001) Photocurable ISFET for anionic surfactants. Monitoring of photodegradation processes. *Talanta* 54:893–902
111. Fibbioli M, Morf WE, Badertscher M, de Rooij NF, Pretsc E (2000) Potential drifts of solid-contacted ion-selective electrodes due to zero-current ion fluxes through the sensor membrane. *Electroanalysis* 12:1286–1292.
112. Adams RN (1958) Carbon paste electrode. *Anal Chem* 30:1576
113. Kalcher K, Švancara I, Metelka R, Vytras K, Walcarius A (2006) In: Grimes CA, Dickey EC, Pishko MV (eds) *Encyclopedia of sensors*, vol 4. American Scientific Publishers, Stevenson Ranch, pp 283–430. ISBN 1-58883-060-8
114. Svancara I, Vytras K, Kalcher K, Walcarius A, Wang J (2009) Carbon paste electrodes in facts, numbers, and notes: a review on the occasion of the 50-years jubilee of carbon paste in electrochemistry and electroanalysis. *Electroanalysis* 21:7–28
115. Svancara I, Kalcher K, Walcarius A, Vytras K (2012) *Electroanalysis with carbon paste electrodes*. CRC Press, Boca Raton, FL
116. Jezkova J, Musilova J, Vytras K (1997) Potentiometry with perchlorate and fluoroborate ion-selective carbon paste electrodes. *Electroanalysis* 9:1433–1436
117. Vytras K, Kalous J, Jezkova J (1997) Automated potentiometry as an ecologic alternative to two-phase titration of surfactants. *Egypt J Anal Chem* 6:107–128
118. Svancara I, Hvizdolova M, Vytras K, Kalcher K, Novotny R (1996) A microscopic study on carbon paste electrodes. *Electroanalysis* 8:61–65
119. Vytras K, Jezkova J, Dlabka V, Kalous J (1997) Studies on potentiometric titrations using liquid membrane-based electrodes: coated wires vs. carbon paste. *Sci Pap Univ Pardubice Ser A* 3:307–323
120. Vytras K, Khaled E, Jezkova J, Hassan HNA, Barsoum BN (2000) Studies on potentiometric thallium (III)-selective carbon paste electrodes and its possible applications. *Fres J Anal Chem* 367:203–207

121. Hart JP, Wring SA (1997) Recent developments in the design and application of screen-printed electrochemical sensors for biomedical, environmental and industrial analyses. *Trends Anal Chem* 16:89–103
122. Honeychurch KC, Hart JP (2003) Screen-printed electrochemical sensors for monitoring metal pollutants. *Trends Anal Chem* 22:456–469
123. Hart JP, Crew A, Crouch E, Honeychurch KC, Pemberton RM (2004) Some recent designs and developments of screen-printed carbon electrochemical sensors/biosensors for biomedical, environmental and industrial analyses (review). *Anal Lett* 37:789–830
124. Renedo OD, Alonso-Lomillo MA, Martinez MJ (2007) Recent developments in the field of screen-printed electrodes and their related applications. *Talanta* 73:202–219
125. Li M, Li Y, Li D, Long Y (2012) Recent developments and applications of screen-printed electrodes in environmental assays—a review. *Anal Chim Acta* 743:31–44
126. Wring SA, Hart JP, Bracey L, Birch BJ (1990) Development of screen-printed carbon electrodes, chemically modified with cobalt phthalocyanine, for electrochemical sensor applications. *Anal Chim Acta* 231:203–212
127. Khaled E, Mohamed GG, Ali TA (2008) Disposal screen-printed carbon paste electrodes for the potentiometric titration of surfactants. *Sens Actuators B Chem* 135:74–80
128. Mohamed GG, Ali TA, El-Shahat MF, Al-Sabagh AM, Migahed MA, Khaled E (2010) Potentiometric determination of cetylpyridinium chloride using a new type of screen-printed ion selective electrodes. *Anal Chim Acta* 673:79–87
129. Mohamed GG, Ali TA, El-Shahat MF, Al-Sabagh AM, Migahed MA (2010) New screen-printed ion-selective electrodes for potentiometric titration of cetyltrimethylammonium bromide in different civilic media. *Electroanalysis* 22:2587–2599
130. Mohamed GG, El-Shahat MF, Al-Sabagh AM, Migahed MA, Ali TA (2011) Septonex–tetraphenylborate screen-printed ion selective electrode for the potentiometric determination of Septonex in pharmaceutical preparations. *Analyst* 136:1488–1495
131. Selig S (1980) The potentiometric titration of surfactants and soaps using ion-selective electrodes. *Fres J Anal Chem* 300:183–188.
132. Gallegos RD (1993) Titrations of non-ionic surfactants with sodium tetraphenylborate using the Orion surfactant electrode. *Analyst* 118:1137–1141
133. Szczepaniak W (1990) Mercurated polystyrene as a sensor for anionic surfactants in ion-selective polymeric membrane electrodes. *Analyst* 115:1451–1455
134. Benoit E, Leroy P, Nicolas A (1985) Use of an electrode selective for perchlorate ions in the potentiometric analysis of quaternary ammonium by tetraphenylborate ions. *Ann Pharm Fr* 43:177–182
135. Skoog M, Kronkvist K, Johansson G (1992) Blocking of chemically modified graphite electrodes by surfactants. *Anal Chim Acta* 269:59–64
136. Adeloju SB, Shaw SJ (1994) Indirect determination of surfactants by adsorptive voltammetry: Part 1: determination of trace and ultratrace concentrations of sodium dodecylbenzene sulfonate. *Electroanalysis* 6:639–644
137. Adeloju SB, Shaw SJ (1994) Indirect determination of surfactants by adsorptive voltammetry: Part 2: determination of hexadecyltrimethyl ammonium bromide and cetylpyridinium chloride in industrial and consumer products. *Electroanalysis* 6:645–649
138. Schmidt T, Emons H (1994) Tensammetric and indirect amperometric detection of phospholipids. *Electroanalysis* 3:543–551
139. Kim OS, Shiragami S, Kusuda K (1994) Increase of the redox current in cyclic voltammetry of a compound dissolved in Nujol by contacting with a surface active compound in an aqueous solution. *J Electroanal Chem* 367:271–273
140. Toshiaki H, Kenji O (2002) Determination of anionic polyelectrolytes by adsorptive voltammetry using 11-fluorocetyltrimethylundecyl ammonium ion at a carbon past. *Bunseki Kagaku* 51:1171–1174
141. Koula V, Kucova D, Gasparic J (1992) Determination of organic bases by ion-pair extraction polarography using Orange II as counter ion. *Collect Czech Chem C* 57:2272–2278

142. Simunkova-Kulova P, Kotoucek M (2003) Indirect voltammetric determination of cetylpyridinium chloride using ion pair extraction. *Acta Univ Palacki Olomuc* 42:51–60
143. Spencer MJ, Wallace GG, Crisp PT, Lewis TW (1991) Determination of anionic surfactants by bis(ethylenediamine) copper(II) extraction and anodic stripping voltammetry. *Anal Chim Acta* 244:197–200
144. John R, Lord D (1999) Determination of anionic surfactants using atomic absorption spectrometry and anodic stripping voltammetry. *J Chem Edu* 76:1256–1258
145. Zhao FQ, Zeng BZ (2002) Voltammetric determination of cetylpyridinium chloride with a silver electrode. *Anal Lett* 35:1603–1615
146. Sawamoto H, Gamoh K (1991) Determination of the compounds which are neither oxidized or reduced at electrodes by a flow injection voltammetric methods. *Anal Sci* 7:1707–1709
147. Andreescu S, Marty J (2006) Twenty years research in cholinesterase biosensors: from basic research to practical applications. *Biomol Eng* 23:1–15
148. Amine A, Mohammadi H, Bourais I, Palleschi G (2006) Enzyme inhibition-based biosensors for food safety and environmental monitoring. *Biosens Bioelectron* 21:1405–1423
149. Rogers KR (2006) Recent advances in biosensor techniques for environmental monitoring. *Anal Chim Acta* 568:222–231
150. Rodriguez-Mozaz S, de Alda MJL, Marco M, Barceló D (2005) Biosensors for environmental monitoring: a global perspective. *Talanta* 65:291–297
151. Nomura Y, Ikebukuro K, Yokoyama K, Takeuchi T, Arikawa Y, Ohno S, Karube L (1994) A novel microbial sensor for anionic surfactant determination. *Anal Lett* 27:3095–3108
152. Taranova L, Semenchuk I, Manolov T, Iliasov P, Reshetilov A (2002) Bacteria-degraders as the base of an amperometric biosensor for detection of anionic surfactants. *Biosens Bioelectron* 17:635–640
153. Reshetilov AN, Semenchuk IN, Iliasov PV, Taranova LA (1997) The amperometric biosensor for detection of sodium dodecyl sulfate. *Anal Chim Acta* 347:19–26
154. Farre M, Pasini O, Alonso MC, Castillo M, Barcelo D (2001) Toxicity assessment of organic pollution in wastewaters using a bacterial biosensor. *Anal Chim Acta* 426:155–165
155. Guilhermino L, Lacerda MN, Nogueira AJ, Soares AM (2000) In vitro and in vivo inhibition of *Daphnia magna* acetylcholinesterase by surfactant agents: possible implications for contamination biomonitoring. *Sci Total Environ* 247:137–141
156. Garcia LM, Castro B, Ribeiro R, Guilhermino L (2000) Characterization of cholinesterase from guppy (*Poecilia reticulata*) muscle and its in vitro inhibition by environmental contaminants. *Biomarkers* 5:274–284
157. Cserhati T, Forgacs E, Oros G (2002) Biological activity and environmental impact of anionic surfactants. *Environ Int* 28:337–348
158. Evtugyn GA, Budnikov HC, Nikolskaya EB (1996) Influence of surface-active compounds on the response and sensitivity of cholinesterase biosensors for inhibitor determination. *Analyst* 121:1911–1915

Chapter 11

Determination of Aromatic Hydrocarbons and Their Derivatives

K. Peckova-Schwarzova, J. Zima, and J. Barek

Aromatic hydrocarbons and their derivatives are important environmental pollutants. This chapter is devoted to their detection using either boron-doped diamond film electrodes or carbon paste electrodes. Boron-doped diamond is a fascinating new electrode material with extremely broad potential window, low noise, and high resistance to passivation that make it very useful for environmental applications, based both on anodic oxidations and cathodic reductions depending on the functional groups present in target analyte. This is illustrated by numerous examples given in Sect. 11.1. Carbon paste electrodes are well-established sensors in the field of environmental analysis and their capability for detection of organic compounds is well known. In this case, applications based on anodic oxidations prevail because of problems with elimination of signal of oxygen contained in carbon paste. Easy surface renewal, chemical modification, user friendliness, and broad spectrum of described applications make carbon paste electrodes very popular sensors in environmental detection of aromatic hydrocarbons and their derivatives which is documented by Sect. 11.2.

K. Peckova-Schwarzova • J. Zima • J. Barek (✉)
Department of Analytical Chemistry, UNESCO Laboratory of Environmental
Electrochemistry, Faculty of Science, University Research Centre “Supramolecular
Chemistry”, Charles University in Prague, Albertov 6, Prague 2 128 43, Czech Republic
e-mail: barekj096@seznam.cz

11.1 Determination of Aromatic Hydrocarbons and Their Derivatives at Boron-Doped Diamond Thin-Film Electrodes

11.1.1 Preparation, Characterization, and Properties of Boron-Doped Diamond Thin Films

The introduction of boron-doped diamond (BDD) thin films in 1992 by Fujishima¹ started a new era in electrochemical research. Over the past 20 years, it has become apparent that the diamond-based electrodes are in many ways ideal as electrode materials for electrochemistry and four main directions of their use have been established: (1) electrochemical oxidation of environmental pollutants at BDD anodes proposed for their quantitative conversion or destruction in wastewaters, (2) electrochemical disinfection of drinking and bathing water, (3) use of BDD electrodes in electroanalysis as electrochemical sensors employed in voltammetric methods or liquid flow methods (high-performance liquid chromatography (HPLC), flow injection analysis (FIA), capillary electrophoresis (CE)) for detection of organic and inorganic species in environmental, biological, and pharmaceutical matrices), and (4) electrochemical synthesis, in particular in the production of strong oxidizing agents and in electroorganic synthesis.^{2–5} These four application proposals were developed based on advantageous electrochemical, physical, and mechanical properties of BDD thin films, e.g., very low capacitance resulting in low and stable background current, wide potential range in aqueous and nonaqueous media, resistance to fouling resulting in good responsiveness for many redox analytes without pretreatment, corrosion resistance, high thermal conductivity, high hardness, and chemical inertness.^{6–9}

For these purposes, various types of BDD electrodes differing in conductive support and surface termination or its modification are produced. In general, diamond thin films are grown from dilute mixtures of a hydrocarbon gas (e.g., methane) in hydrogen using one of several energy-assisted chemical vapor deposition (CVD) methods, the most popular being hot-filament and microwave plasma-assisted CVD. In these processes, a carbon-containing gas is energetically activated to decompose the molecules into methyl radicals and atomic hydrogen and deposited on a suitable substrate, most frequently conductive silica wafers.

The growth methods mainly differ in the manner in which the gas activation is accomplished. Typical growth conditions are as follows: 0.3–1.0 % CH₄ in H₂, pressures of 10–150 Torr, substrate temperatures of 700–1,000 °C, and microwave powers of 1,000–1,300 W, or filament temperatures up to ~2,800 °C, depending on the methods used. The film grows by nucleation at rates in the 0.1–2 μm h⁻¹ range. For the substrates to be continuously coated with diamond, the nominal film thickness must be ~1 μm. Boron doping is accomplished from the gas phase by mixing boron-containing compounds such as B₂H₆, trimethylborane, or B₂O₃ with the source gases, or from the solid state by gasifying a piece of hexagonal-boron nitride (h-BN). The doping level can be as high as 15,000 ppm of boron in the gas phase, resulting in boron carrier concentration in the final film 1 × 10¹⁸ cm⁻³ to 1 × 10²¹ cm⁻³ or greater resulting in film resistivities <0.1 Ω cm.^{9,10}

The working procedure and conditions during CVD influence fundamentally the quality and properties of BDD thin films: The boron-doping level, structural defects in the diamond film, content of non-diamond (sp^2) impurities, size of diamond crystallites and crystallographic orientation, and surface termination (H, O) are the main factors. For their characterization a wide scale of methods is being used: The Raman spectroscopy is quite sensitive to the presence of non-diamond carbon impurities. Scanning electron microscopy and scanning tunneling and atomic force microscopies are used to evaluate the film morphology and probe the local electronic properties. Powder X-ray diffraction analysis is used to investigate the preferential crystallite orientation of the films. Surface elemental composition is determined by Auger electron and X-ray photoelectron spectroscopies. Secondary ion mass spectrometry is used to quantify the boron dopant concentration and probe the spatial distribution of the dopant species over the surface and within the bulk.

Nevertheless, the linkage of the properties of the BDD film to its electrochemical characteristics is not fully understood. Crucial role plays the termination of BDD surface. While the freshly prepared BDD film contains hydrogenated aliphatic structural moieties (sp^3 hybridized, H-terminated surface), anodic oxidation of BDD electrodes in aqueous solvents leads to O-termination, i.e., to the introduction of different functionalities such as alcoholic, ketonic, and carboxylic groups into the carbon skeleton. Nevertheless, sp^2 impurities are also present after the CVD process and the electrochemical reactions are linked to both sp^2 active sites and BDD.¹¹ For some organic compounds, the cathodic pretreatment of the surface is advantageous.¹²

In electroanalysis, BDD electrodes are preferably used for electrooxidation, rather than reduction. There are three basic mechanisms of electrooxidation at BDD electrodes: (1) direct electrochemical oxidation on the BDD surface; (2) indirect electrooxidation mediated by hydroxyl radicals produced at the BDD surface as a result of water decomposition; and (3) indirect electrooxidation mediated by electrogenerated oxidants, such as peroxodisulfates (in the presence of SO_4^-) and active chlorine (in the presence of Cl^-). The (2) oxidation pathway is unique for BDD surfaces, because analytes capable to be oxidized by hydroxyl radicals and not directly oxidizable at other electrode materials can be oxidized within the potential window of BDD.

The aspects and applications concerning the redox reactions of organic compounds at BDD electrodes were reviewed recently,^{13–18} and also by our group.^{14,18–20} Further, reviews on general electrochemical properties²¹ and surface modifications,^{22–24} electrosynthesis and anodic waste treatment,^{25–28} and electroanalytical applications including BDD-based biosensors^{24,29} appeared in last 5 years together with compact reviews^{30–32} and books devoted to diamond electrochemistry, physics, and applications.^{7,33}

11.1.2 Applicability

In this chapter, the electrochemical approaches for determination of redox-active environmental pollutants by means of BDD-based sensors and BDD electrodes using batch-experimental setup are presented. Mostly model samples prepared by

spiking of analyzed matrices by the studied substances were used for verification of the practical applicability of the developed methods.

In Table 11.1, there are selected examples of organic contaminants of water, soil, and atmosphere investigated so far for any purpose by batch voltammetric methods

Table 11.1 Selected applications of BDD-based sensors in environmental analysis

Analyte	BDD electrode, pretreatment ^a	Method	Matrix	L_D^b ($\mu\text{mol L}^{-1}$),	Refs.
Phenolic compounds					
4-Chlorophenol 4-Chlorophenol ^c	HFCVD BDD, AT at +3.0 V followed by CT at -3.0 V, 30 min of each	SWV SWV	Bulk solution River water	0.16 ^d 0.31	47,51
4-Chlorophenol	Commercial polished BDD, ¹¹² 60 s of ultrasound or AT at +5.0 V followed by CT at -5.0 V, 10 s of each in 0.1 M HNO ₃	Sono-CV	Bulk solution	1 ^e	48
Pentachlorophenol	HFCVD BDD, AT + CT as in reference (51), polarized at -3.0 V for 30 s between scans	SWV	Bulk solution River water Soil	0.020 0.056 ^d Not given	50,53
Methylparaben, ethylparaben, propylparaben	Commercial polished BDD, ¹¹³ oxidation by CV between large potential limits in neutral media	CV ChrA	Bulk solution Bulk solution	1.5, 1.97, 3.6 0.7, 1.03, 0.97 ^f	65
Bisphenol A	Commercial BDD, ¹¹⁴ CT at -250 mA cm ⁻² for 180 s	DPV	Bulk solution Tap and lake water	0.21 ^e Not given	67
Phenol Hydroquinone 4-Nitrophenol	MPCVD BDD ^g	CV DPV	Bulk solution	CV ^{h,i} , DPV ^{h,i} 8.2, 1.82 12, 1.67 11, 1.44	60,61
4-Nitrophenol	HFCVD BDD, pretreatment as in reference (69)	SWV	Bulk solution River water	0.068 ^j , 0.101 ^k 0.382 ^j , 0.441 ^{d,k}	56-58
4-Nitrophenol	Commercial BDD, ¹¹⁴ AT at +3.0 (5 s) followed by CT at -3.0 V (30 s) in 0.5 M H ₂ SO ₄	Sono-SWV	Bulk solution	0.093 ^j 0.062 ^{d,k}	55

(continued)

Table 11.1 (continued)

Analyte	BDD electrode, pretreatment ^a	Method	Matrix	L_D^b ($\mu\text{mol L}^{-1}$),	Refs.
4-Nitrophenol 2,4-Dinitrophenol 2-Nitrophenol	Commercial BDD, ¹¹³ oxidation by repeated cycling between -2.5 V and $+2.5$ V in 1 M HNO_3	DPV ^{j,k}	Deionized water Drinking water River water Deionized water Drinking water River water Deionized water Drinking water River water	direct/after SPE ^f $0.5^j, 0.1^k/0.03^k$ $1^j, 0.1^k/0.04^k$ $1^j, 0.1^k/0.2^k$ $0.3^j, 0.1^k/0.02^k$ $0.5^j, 0.1^k/0.02^k$ $0.3^j, 0.6^k/0.2^k$ $0.3^k/0.02^k$ $0.2^k/0.02^k$ $0.1^k/0.2^k$	⁴²
Monocyclic and polycyclic aromatic hydrocarbons					
Pyrene	Commercial BDD, ¹¹³ AT in phosphoric acid/ acetonitrile at $+2.5$ V for 10 min	Amperometry at rotating BDD	Bulk solution	0.0005	⁷⁸
Benzene	HFCVD BDD, AT + CT as in reference (51)	CV	Bulk solution	Not given	⁸¹
Benzo(<i>a</i>)pyrene	Commercial polished BDD, ¹¹³ manual polishing by Al_2O_3 slurry followed by AT at $+1.3$ V for 30 s	AdS-SWV	Blank solution Tap water	0.00286 0.0102	⁸⁰
Amino-, nitro-, and hydroxy derivatives of polycyclic aromatic hydrocarbons					
3-Amino-fluoranthene	Si(100), MPCVD nanocrystalline BDD	DPV	Bulk solution	0.2^1	⁹¹
1-AN, 2-AN	Si(100), MPCVD microcrystalline BDD, AT at $+2.4$ V for 60 s	DPV	Bulk solution	$0.89, 0.44^f$	⁹⁰
2-AB, 3-AB 4-AB	Si(100), MPCVD nanocrystalline BDD	DPV	Bulk solution	$0.12, 0.13/0.25^1$	⁸⁹

(continued)

Table 11.1 (continued)

Analyte	BDD electrode, pretreatment ^a	Method	Matrix	L_D^b ($\mu\text{mol L}^{-1}$),	Refs.
1-Aminopyrene 1-Nitropyrene 1-Hydroxypyrene	Commercial polished BDD ¹¹³	DPV	Bulk solution	0.06 0.3 0.1	⁹²
3-Nitro-fluoranthene	Si(100), MPCVD nanocrystalline BDD	DPV	Bulk solution	0.03 ^m	⁹¹
Agrochemicals					
Carbaryl	HFCVD BDD, AT + CT as in reference (51)	SWV	Bulk solution River water	0.14 ^d 0.16	⁵⁴
Carbendazime fenamiphos ⁿ	Commercial BDD, ¹¹⁴ AT at +3.0 (10 min) followed by CT at -3.0 V (10 min) in 0.5 M H ₂ SO ₄	SWV	Bulk solution River water	0.12, 0.10 ^d 0.41, 0.10	⁹⁵
Methyl parathion	Commercial BDD, ¹¹⁴ AT at +3.0 (1 s) followed by CT at -3.0 V (30 s) in 0.5 M H ₂ SO ₄	Sono-SWV	Bulk solution	0.019 ^{d,k}	⁹⁷
Parathion	HFCVD BDD, AT + CT as in reference (51)	SWV	Bulk solution River water	0.030 ^m 0.132	⁹⁶
Other compounds					
Oxalic acid in the presence of 4-CP	Commercial polished BDD, ¹¹³ oxidation by three repetitive cycling between -0.5 V to +1.75 V in 0.1 M Na ₂ SO ₄	ChrA, DPV	Bulk solution	Not given	⁶²
<i>Escherichia coli</i> (detection of 2-NP) ^o	Commercial BDD, ¹¹³ cleaning when passivated by 40 cycles from +1.0 V to -1.7 V range	Amperometry	Foodstuffs Tap water	400 cells mL ^{-1h}	¹¹⁵

^aIf no details are given, as deposited polycrystalline H-terminated electrodes and undefined silica support used. AT — anodic treatment; CT — cathodic treatment

^bIn the presence of 2,4-DCP+2,4,6-TCP

^cno intentional AT, nevertheless BDD presumably oxygen-terminated due to experiments at high anodic potentials

^dSimultaneous voltammetric determination; e oxidative determination;

^eExperimental L_D — the first appearance of a limiting-current wave

Table 11.1 (continued)

^fLD = $3\sigma/m$, LQ = $10\sigma/m$ where σ is the standard deviation of the signal measured for the lowest analyte concentration corresponding to calibration plot

^gNo intentional AT, nevertheless BDD presumably oxygen-terminated due to experiments at high anodic potentials

^hdetection of 2-NP released from *o*-nitrophenyl- β -D-galactopyranose as catalyzed by β -galactosidase, a tetramer of *Escherichia coli*; A LD for $S/N = 3$, if not otherwise specified; B LD = $3sb/m$, LQ = $10sb/m$ where sb is the standard deviation of the mean of the current of the blank in amperometric detection or current at the peak potential for repeated voltammograms of the blank solution, m is slope of the analytical curve; C experimental LD – the first appearance of a limiting-current wave; D LD = $3\sigma/m$, LQ = $10\sigma/m$ where σ is the standard deviation of the signal measured for the lowest analyte concentration corresponding to calibration plot, E no details on calculation given; F LQ calculated using statistic software ADSTAT version 2.0 (Trilobyte, Czech Republic). This software uses confidence bands ($\alpha = 0.05$) for calculation of the LOQ. It corresponds to the lowest signal for which relative standard deviation RSD is equal 0.1; G LQ = $y_b + 10sb$, where intercept value y_b and standard deviation of the slope sb are calculated from the analytical curve

ⁱSimultaneous voltammetric determination

^jOxidative determination

^kReductive determination

^lL_Q calculated using statistic software ADSTAT version 2.0 (Trilobyte, Czech Republic). This software uses confidence bands ($\alpha = 0.05$) for calculation of the LOQ. It corresponds to the lowest signal for which relative standard deviation RSD is equal 0.1

^mL_Q = $y_b + 10s_b$, where intercept value y_b and standard deviation of the slope s_b are calculated from the analytical curve

ⁿSimultaneous determination possible

^oDetection of 2-NP released from *o*-nitrophenyl- β -D-galactopyranose as catalyzed by β -galactosidase, a tetramer of *Escherichia coli*

using BDD electrodes. These contaminants include phenolic compounds including chlorinated phenols (CPs) and nitrophenols (NPs), several pesticides, and monocyclic and polycyclic aromatic hydrocarbons and their derivatives. The table contains for each analyte methods and conditions used, further characterization of used BDD electrode, matrix, and achieved limit of detection (L_D). The electrochemistry of other biological active compounds not considered as environmental pollutants is not included in detail and more on these studies on BDD electrodes can be found in several reviews and monographs published recently.^{7,14,17}

11.2 Detection at BDD-Based Sensors in Bulk Measurements

11.2.1 Phenolic Compounds

Phenolic type compounds are among the most frequent environmental pollutants, especially when considering water pollution. Many of these compounds were included in the US Environmental Protection Agency (US EPA) list of priority pollutants.³⁴ The

most important class includes chlorophenols (CPs) with 2-chlorophenol (2-CP), 2,4-dichlorophenol (2,4-DCP), 2,4,6-trichlorophenol (2,4,6-TCP), pentachlorophenol (PCP), and parachlorometacresol on the list. Non-chlorinated phenols are represented by nitrophenols (2-nitrophenols, 4-nitrophenol, 2,4-dinitrophenol, 4,6-dinitro-*o*-cresol), phenol, and 2,4-dimethylphenol on the list.

Chlorinated phenols enter the aquatic environment as by-products of industrial processes, such as the production of antioxidants, dyes, and drugs. In drinking water they occur as a result of the chlorination of phenols, as by-products of reactions with phenolic acids, as biocides, or as degradation products of phenoxy herbicides and chlorinated bleaching of paper.^{35–37} CP concentration in drinking water usually does not exceed $1 \mu\text{g L}^{-1}$, which is the US EPA's maximum allowable contaminant level (MCL) for drinking water for pentachlorophenol, the only listed CP.³⁸

Nitrophenols are present in numerous food-processing wastewaters such as those from wine distilleries, olive oil factories, boiling cork process, as well as other industrial synthetic effluents. Further, they originate from oxidation of many pesticides including parathion and other organophosphorus pesticides^{39–41} or as reactants or intermediates in pesticide production and thus are important soil, agricultural, industrial, and municipal water pollutants. Many national health agencies set their own limits for them in these matrices. The US EPA has restricted the concentration of 2-nitrophenol, 4-nitrophenol, and 2,4-dinitrophenol to $10 \mu\text{g L}^{-1}$ in natural water (corresponds to $5 \times 10^{-8} \text{ mol L}^{-1}$ for 2,4-DNP and $7 \times 10^{-8} \text{ mol L}^{-1}$ for 2-NP and 4-NP).⁴²

Electroanalysis of phenol derivatives including CPs is commonly problematic at most solid electrodes mainly due to the electrode passivation resulting from oxidation products. The studies on reaction mechanism of electrooxidation of phenol^{5,43,44} and CPs^{45,46} in acidic media at BDD electrodes revealed that in the potential region of water stability direct electron transfer can occur on BDD surface at the potential of +800 to +1,400 mV forming phenoxy radical species with possible electrode fouling due to the formation of a polymeric film on its surface. The formation of *o*- and *p*-benzoquinone as the main products of phenol oxidation at BDD electrodes was confirmed by Terashima et al.⁴⁶ The comparative studies on the electrooxidation of selected chlorophenols on glassy carbon and BDD electrodes reported similar⁴⁶ or slightly higher¹¹ oxidation potential on the latter one.

To prevent the passivation, the successful strategy for BDD electrodes includes the oxidation at highly anodic potential in the region of water decomposition. Hydroxyl radicals produced by the high applied potential are believed to be responsible for the oxidation of the passivating layer. This concept was successfully applied also for selected dichloro- and trichlorophenols,^{11,46} which are presumably more prone to inactivation of electrode surface than mono-substituted CPs.¹⁸ For them the detection at BDD electrodes is possible even without any electrochemical remediation of the electrode surface as demonstrated for phenol, 2-chlorophenol (2-CP), and 4-chlorophenol (4-CP).^{45,47}

The other three approaches to overcome the fouling problems include the use of power ultrasound during the electrooxidation, which enhances also the oxidation current signal due to more efficient mass transport as demonstrated for 4-CP⁴⁸ and

other substituted phenols,⁴⁹ the use of acidic methanol supporting electrolyte as it provides reasonable solubility of the intermediates and reaction product, or the use of media with microemulsion-containing surfactants that increase the solubility of phenolic compounds.¹¹

The several studies aiming at determination of CPs in natural waters were published by Avaca et al.^{47,50,51}: Direct determination of 4-CP using square-wave voltammetry (SWV) at BDD electrode in Britton–Robinson (BR) buffer, pH 6 without any electrode pretreatment was reported with L_Q $6.4 \mu\text{g L}^{-1}$ for pure and $21.5 \mu\text{g L}^{-1}$ for polluted river water. These achieved detection limits are satisfactory for the US EPA's concentration limit of $100 \mu\text{g L}^{-1}$ for surface waters⁵² and show that the technique is analytically useful over a concentration range where aquatic 4-CP pollution is known to occur. In the next study the same authors focused on the use of SWV for simultaneous determination of 4-CP, 2,4-DCP, and 2,4,6-TCP⁵¹ using mathematical deconvolution procedure to separate the unique voltammetric peak of each compound. The limit of quantitation (L_Q) for 4-CP in the presence of the other analytes of $0.072 \mu\text{mol L}^{-1}$ ($9.2 \mu\text{g L}^{-1}$) for pure water and $0.329 \mu\text{mol L}^{-1}$ ($42.2 \mu\text{g L}^{-1}$) for river water was achieved. Specialized methods were developed for direct determination of PCP in natural waters, as this persistent pesticide is widely used for wood preservation and can be used as model compound for the development of new analytical techniques. When using BR buffer, pH 5.5 as the supporting electrolyte and SWV, PCP oxidation occurs at $+0.80 \text{ V}$ vs. Ag/AgCl in a two-electron process controlled by adsorption of the species.⁵⁰ The SWV signal reproducibility (relative standard deviation (RSD) 1.3 % for $c(\text{PCP}) = 5 \times 10^{-5} \text{ mol L}^{-1}$, $n = 5$) was achieved by rinsing of the electrode surface with water and polarization at -3.0 V for 30 s after each measurement. The detection limits obtained were $0.02 \mu\text{mol L}^{-1}$ ($5.5 \mu\text{g L}^{-1}$) in pure water and $0.056 \mu\text{mol L}^{-1}$ ($15.5 \mu\text{g L}^{-1}$) for contaminated river water which is just about the guideline value recommended by World Health Organization (WHO) for drinking water ($9 \mu\text{g L}^{-1}$, i.e., $0.033 \mu\text{mol L}^{-1}$). However, extraction and preconcentration of PCP from this matrix followed by analogous determination at BDD electrode should be easily feasible. In the next study, the same authors focused on the determination of PCP in contaminated soil from a chemical plant.⁵³ The soil samples were extracted with hexane for 3 h in Soxhlet apparatus. The organic extract was evaporated and reconstituted in 1.5 mL of acetonitrile, which was analyzed by SWV at BDD or Au microelectrode as well as by HPLC/UV or GC/MS for validation of the results and identification of other soil components. For SWV at BDD, 0.25 mL of the acetonitrile fraction was simply added to 20 mL of BR buffer, pH 5 and analyzed using standard addition method. In addition to the PCP, the peak of its degradation product *o*-tetrachlorobenzoquinone (*o*-chloranil) was identified. Recovering experiments for PCP quantitation in soil showed good agreement of results obtained by electroanalytical determinations (27.5 mg kg^{-1}) and HPLC/UV analysis (26.8 mg kg^{-1}). This application reveals that a simple voltammetric method can represent useful alternative to officially approved, but more expensive and time-demanding method.

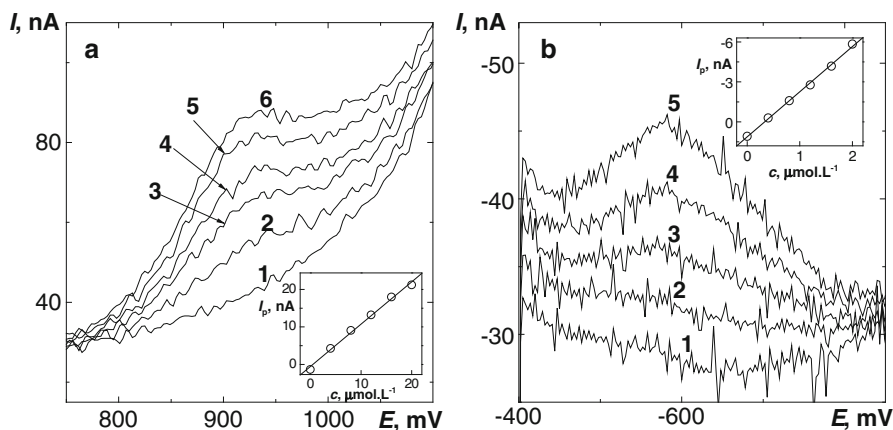


Fig. 11.1 Anodic (a) and cathodic (b) DP voltammograms and calibration dependences (in *insert*) for 4-NP at BDD film electrode in river water. (a) Base electrolyte BR buffer pH 11, concentration of 4-NP in river water: 0 (1), 4 (2), 8 (3), 12 (4), 16 (5), 20 (6) $\mu\text{mol L}^{-1}$; (b) base electrolyte BR buffer pH 6, c (4-NP) in river water: 0 (1), 0.8 (2), 1.2 (3), 1.6 (4), 2 (5) $\mu\text{mol L}^{-1}$. Adapted from reference (42)

Further voltammetric studies were devoted to nitrophenols^{42,54–58} and aminonitrophenols⁵⁹ which may be determined at BDD electrodes by both the hydroxyl, respective amino group oxidation and nitro group reduction. This was clearly demonstrated for 2-nitrophenol (2-NP), 4-nitrophenol (4-NP), and 2,4-dinitrophenol (2,4-DNP), at anodically oxidized BDD electrode.⁴² Using differential pulse voltammetry (DPV), the electrochemical reduction was more sensitive than the oxidation (for 4-NP demonstrated in Fig. 11.1). Direct reductive determination of these analytes in drinking and river water resulted in L_Q s of 0.1–0.6 $\mu\text{mol L}^{-1}$, and preconcentration step using solid-phase extraction lowered L_Q s to 0.02–0.04 $\mu\text{mol L}^{-1}$ for drinking and 0.2 $\mu\text{mol L}^{-1}$ for river water. These detection limits are about the US EPA limits mentioned above. Comparable L_Q s were reported for SWV determination of 4-NP,^{56–58} when the L_Q s varied between 9.4 and 53.1 $\mu\text{g L}^{-1}$ (i.e., 0.067 and 0.38 $\mu\text{mol L}^{-1}$) for the oxidation process and between 14.1 and 61.3 $\mu\text{g L}^{-1}$ (i.e., 0.10 and 0.44 $\mu\text{mol L}^{-1}$) for the reduction process, depending on water sample (either deionized or river water), which was comparable to results achieved by SWV at HMDE. Lower quantitation limits 12.9 and 8.6 $\mu\text{g L}^{-1}$ (i.e., 0.092 and 0.061 $\mu\text{mol L}^{-1}$) for oxidative, respective reductive determination were obtained when sonication was employed due to enhanced transport of 4-NP towards the electrode surface.⁵⁵ Codognoto et al.⁵⁴ demonstrated that using SWV, the oxidation peak of 4-NP does not coincide with signals of some organophosphorus or carbamate pesticides. This is an important issue, because 4-NP is their common degradation product. All mentioned methods are promising regarding the water analysis, as they are simple, convenient, and inexpensive.

Further studies were devoted to detection of phenolic compounds and their degradation products during anodic treatment of wastewaters. Lei and

Zhao^{60,61} developed a DPV method for the simultaneous direct determination of hydroquinone, phenol, and 4-NP potentially applicable for wastewater analysis. These environmental pollutants gave consecutive oxidation peaks at the potentials of +0.76 V, +1.24 V, and +1.52 V and detection limits of phenol, hydroquinone, and 4-NP were estimated to be $1.82 \mu\text{mol L}^{-1}$ ($184 \mu\text{g L}^{-1}$), $1.67 \mu\text{mol L}^{-1}$ ($171 \mu\text{g L}^{-1}$), and $1.44 \mu\text{mol L}^{-1}$ ($200 \mu\text{g L}^{-1}$), respectively. A DPV and chronoamperometric method was suggested for the simultaneous determination of 4-CP and oxalic acid, which is a common intermediate or end product of advanced oxidation procedures using indirect treatment of wastewater at BDD and other anodes. As the oxidation of oxalic acid proceeds very close to the potential limit of oxygen evolution at BDD electrodes, i.e., more positive than the electrooxidation of CPs, their simultaneous, as well as individual determination in treated wastewater is possible.⁶² Gallic acid, as a common representative of phenolic type compounds present in numerous food-processing wastewaters, was also investigated by means of BDD electrodes for the purpose of its quantitative mineralization and characterization of electrochemical behavior.⁶³ Its anodic peak appears at similar potential of structurally similar phenolic compounds (e.g., caffeic acid, chlorogenic acid) occurring in food-processing wastewaters⁶⁴; thus a preliminary separation would have to be employed to determine particular contaminants.

Among phenolic compounds are further suspect endocrine disrupting compounds (EDC) – parabens and bisphenol A. The paraben preservatives, acting simultaneously as antimicrobial agents and antioxidants, improve the stability of the food and pharmaceutical products and prevent rancidness in products containing lipids or fats.⁶⁵ Since 2004, when they have been found in biopsies from breast tumors,⁶⁶ the results of intensive research on their toxicity indicate that parabens are linked to cancer, reproductive toxicity, immunotoxicity, neurotoxicity, and skin irritation, and are suspected EDC. Similarly, bisphenol A, used as plasticizer, act as xenoestrogen and its use in baby bottles has been recently banned in the European Union, Canada, and the USA. These personal care products and plasticizers have the potential to enter the water supply through treated and untreated sewage. Bisphenol A was determined at cathodically pretreated BDD at submicromolar concentration and it was demonstrated that the recovery of known concentration of bisphenol A in tap and lake water determined by DPV is close to 100%.⁶⁷ The alkyl parabens are often used in combination. Nevertheless, based on their similar susceptibility to anodic oxidation at BDD electrode, an “overall paraben index” was defined especially by chronoamperometric data. Further, the assessment of the stability and the saturation solubility in both double-distilled and tap water of the relatively slightly water-soluble alkyl parabens was easily carried out using the electrochemical alternatives. This is an important environmental aspect due to the presence of alkyl parabens in municipal wastewater and their accidental occurrence in natural river or even tap water.⁶⁵ Otherwise, an HPLC method was developed for the determination of alkyl parabens in shampoo with BDD electrode serving as indicator electrode in an amperometric thin-layer detection cell. This is a desirable approach for analysis of all complex matrices, because the electrooxidation of phenolic compounds occurs usually in a narrow potential

range and only compounds of the hydroquinone type or derivatives possessing groups with distinct negative or positive inductive effect at the aromatic skeleton can alter the oxidation potential of a phenol-type compound so that the simultaneous determination of more phenols is possible, as, e.g., in the abovementioned study on hydroquinone, phenol, and 4-NP.^{60,61} Otherwise, batch voltammetric methods can offer determination of total phenol content⁶⁸ or separation step using HPLC or electrophoretic methods has to be employed.

Increased selectivity and prevention of passivation of the BDD surface may be also achieved by its modification. An enzyme-based amperometric sensor was proposed for detection of phenolic compounds by Notsu et al.⁶⁹: BDD was anodically polarized for the introduction of hydroxyl groups onto its surface, then treated with (3-aminopropyl)triethoxysilane (APTES), and finally coated with a tyrosinase film cross-linked with glutaraldehyde. Tyrosinase catalyzes oxidation of phenol and various phenol derivatives to *o*-benzoquinone derivatives via catechol derivatives and thus the quinones generated are ready to be reduced electrochemically at an appropriate potential and obtained reduction currents serve as good analytical signals for the determination of the phenol derivatives. Bisphenol A and 17- β -estradiol were detected at -0.3 V vs. Ag/AgCl with the detection limit of $1 \mu\text{mol L}^{-1}$ in FIA. However, the biosensor retained its activity only for a few days due to weak bonding of APTES to BDD surface.

Improved stability of tyrosinase-based BDD biosensor was reported by Zhi's group.^{70,71} They combined chemical and electrochemical modifications of BDD film with 4-nitrobenzenediazonium tetrafluoroborate to produce aminophenyl-modified BDD, followed by immobilizing tyrosinase covalently at the BDD surface via carbodiimide coupling. They used this sensor for detection of phenol, *p*-cresol, and 4-CP and reported 90 % of its original activity after intermittent use for 5 weeks. In all mentioned studies on tyrosinase-based BDD aminosensor no applications on analysis of model or real matrices are presented.

11.2.2 Monocyclic and Polycyclic Aromatic Hydrocarbons

Monocyclic and polycyclic aromatic hydrocarbons (PAHs) constitute a group of priority pollutants which are widespread and found in air, water, and terrestrial and biological systems and may transfer between these resources, typically from a soil resource into groundwater, or by transport of particulate soil PAH in the atmosphere.⁷²

The simple aromatics are usually used as solvents, chemical reactants, or intermediates and for blending of petrol, so they enter the environment usually from industrial effluents or atmospheric pollution. The humans' exposure to them may be increased due to smoking or heavy traffic. WHO recommends guideline values for drinking water for benzene, toluene, xylenes, and styrene. The lowest limit ($10 \mu\text{g L}^{-1}$, i.e., $0.13 \mu\text{mol L}^{-1}$) is set for benzene, a proved human carcinogen (International Agency for Research on Cancer (IARC) group 1, reference (73)). The

common concentrations of these compounds in drinking and surface water are a few $\mu\text{g L}^{-1}$; higher concentrations were found due to point emissions.⁷⁴

PAHs enter the environment via the atmosphere from a variety of combustion processes and pyrolysis sources (see WHO review⁷⁵). In contrary to simple aromatics, they are owing to their low water solubility and high affinity for particulate matter usually not found in natural water in notable concentrations; their levels are usually in the range of 0–5 ng L^{-1} . Nevertheless, in contaminated groundwater their concentration may exceed 10 $\mu\text{g L}^{-1}$.⁷⁶ This value also represents the limit for the sum of selected PAHs of some national agencies.⁷⁷ Besides the sum of PAHs, the limits for individual PAHs may be enforceable. WHO recommends the guideline values for drinking water for benzo[*a*]pyrene (IARC group 1, reference (73)). The US EPA priority list of pollutants registers 16 PAHs (naphthalene, acenaphthylene, acenaphthene, fluorene, phenanthrene, anthracene, fluoranthene, pyrene, benz(*a*)anthracene, chrysene, benzo(*b*)fluoranthene, benzo(*k*)fluoranthene, benzo(*a*)pyrene, dibenz(*a,h*)anthracene, benzo(*g,h,i*)perylene, indeno(*1,2,3-c,d*)pyrene). All of them were investigated on oxidized BDD electrode.⁷⁸ While naphthalene, acenaphthene, fluorene, phenanthrene, and anthracene displayed oxidation peaks in the region of +1.16 to +1.75 V, the other PAHs investigated were oxidized nearer to the onset of background current caused by oxygen evolution reaction and thus displayed more positive onset of the current compared to the background current. Nevertheless, the difference of both currents at +1.8 to +1.9 V vs. Ag/AgCl was utilized for batch amperometric determination of pyrene at rotating BDD (L_D 0.5 nmol L^{-1}) or amperometric detection in HPLC-ED after separation of all analytes with detection limits in the 10^{-8} mol L^{-1} (i.e., units of $\mu\text{g L}^{-1}$) concentration range. These limits meet or exceed those specified in HPLC methods using UV or laser-induced fluorescence or the official US EPA Method 550 (liquid-liquid extraction and HPLC with coupled UV and fluorescence detection⁷⁹), even for PAHs displaying no clear oxidation peak in cyclic voltammetry (CV) experiments. This study undoubtedly represents a promise for the determination of PAHs in various environmental matrices and is an excellent example of the extraordinary versatile use of BDD electrodes in electroanalysis, as PAHs are hardly detectable at other carbon-based electrodes.⁸⁰

First attempts were also made to the use of adsorptive stripping voltammetry together with a medium exchange procedure in aqueous and aqueous/surfactant solutions for the determination of benzo(*a*)pyrene.⁸⁰ In the presence of sodium dodecyl sulfate (SDS), cetyl trimethylammonium bromide (CTAB), and Tween 80, the oxidation signal of benzo(*a*)pyrene is increased by the factor 10–18 compared to surfactant-free media, because the lipophilic analyte interacts with the hydrophobic moiety of the surfactant accumulated on electrode surface. The transfer eliminates the problem with potential interferents that are electrochemically active but do not adsorb or adsorb slightly at the electrode surface. The use of surfactant also lowers the problems with hazardous organic solvents potentially used either for extraction purposes or in subsequent separation and detection step when using liquid flow or other methods. The applicability of the proposed methodology was tested on spiked tap water samples in the presence of selected cations

and anions and other PAHs as possible interferents. The detection limit for tap water – 10.2 nmol L^{-1} (2.57 ng mL^{-1}) – is higher than the maximum contaminant level set at 0.2 ng mL^{-1} by the US EPA; nevertheless, it is lower than maximum amount of benzo(a)pyrene allowed in wastewater (61 ng mL^{-1}) revealing the promising outlooks of this method in environmental analysis.

The other scare reports on the use of BDD for oxidation of simple aromatics and PAHs include the pioneering study on benzene oxidation published by Oliveira et al.⁸¹ They used anodically oxidized electrodes (removal of the hydrophobic film) consecutively polarized at high negative potential (-3.0 V) for surface conditioning. This cathodic polarization enhances and stabilizes the electrochemical response, as shown previously on the example of PCP and 4-CP.^{12,50,51} The CV studies indicate that benzene is irreversibly oxidized in acidic medium ($0.5 \text{ mol L}^{-1} \text{ H}_2\text{SO}_4$) on BDD at $+2.0 \text{ V}$ vs. Ag/AgCl in a diffusion-controlled process, presumably caused by indirect oxidation of benzene by OH radicals produced by water electrolysis on the BDD electrode. This reaction way can be foreseen also for electrooxidation of 1,3,5-trimethylbenzene.⁸² In general, for the electroanalysis of monocyclic and polycyclic aromatic hydrocarbons and other compounds oxidizable at far positive potentials in acidic media or mixed aqueous acidic-acetonitrile media are recommendable, because they offer the largest potential window in anodic region. Additions of other organic solvents, e.g., aliphatic alcohols, lower substantially the potential window as these themselves undergo electrooxidation mediated by OH radicals at BDD electrodes.⁸³

The last interesting example on the use of BDD determination of aromatic hydrocarbons is a BDD microelectronic gas sensor constructed by Gurbuz et al.,⁸⁴ who proposed it to detect volatile organics, i.e., benzene and toluene in soil/subsoil, and so locate potential oil reservoirs or environmental pollution. This seems usable with regard to protection of drinking water, as these compounds may also penetrate from contaminated soil through plastic pipes into it. The sensor consists of three important layers – catalytic metal (Pd), intrinsic-diamond, and BDD layer – and registries changes of transient characteristics after analyte adsorption at the Pd/i-diamond interface.

11.2.3 Derivatives of Monocyclic and Polycyclic Aromatic Hydrocarbons

Substituted PAHs belong among important environmental pollutants as reviewed by IARC⁸⁵ and WHO⁸⁶ and may have higher toxicity than the parent PAHs. Amino-, hydroxy-, and nitro-derivatives of PAHs are formed by atmospheric photochemical PAH reactions and are distributed between the gas and particulate phase depending on their physicochemical properties. Thus, they can be detected in atmosphere, soil, and water as well as in various consumable products. The problem for the analysis consists in the complexity of the matrices, myriad of interfering substances, and low analyte concentration as highlighted recently in a review on the analysis of amines in the environment.⁸⁷

The easily reducible nitro- and oxidizable amino and hydroxy derivatives of PAHs have been extensively studied in our group and the results obtained for BDD electrodes were summarized in several recent reviews.^{14,19,20,88} The amino derivatives of biphenyl,⁸⁹ naphthalene,⁹⁰ fluoranthene,⁹¹ and pyrene⁹² were investigated by batch voltammetric methods in aqueous or mixed aqueous-organic media and they are oxidized in the potential range of 0 to +0.7 V with drop of the peak potential with increasing pH. The first, one-electron oxidation step corresponds to the formation of nitrene cation radicals that are susceptible to subsequent reactions forming polymeric films fouling the electrode surface at other electrode materials. Nevertheless, they do not cause any serious problems at bare BDD electrodes and rinsing of their surface by an organic solvent or mixing of the analyzed solution between the individual scans usually assures repeatable results. Under optimized conditions, simultaneous determination of some amino derivatives using DPV is possible, when the difference of the peak potentials is higher than 150 mV as demonstrated on the example of biphenyl amino derivatives.⁹⁰ The detection limits for DPV methods are in the concentration ranges 10^{-7} to 10^{-8} mol L⁻¹; slightly lower limits are usually achieved when the BDD electrode is employed for amperometric detection in FIA or HPLC. Naturally, the latter method is more convenient for analysis of complex matrices and the analysis of model drinking and river water samples containing aminobiphenyls revealed that after off-line solid-phase extraction leading to 100-fold preconcentration of the analytes the detection limits can be lowered down to the 10^{-8} mol L⁻¹ concentration range.⁹³

Further, it was demonstrated that simultaneous determination of 1-amino- and 1-hydroxypyrene is not possible due to close oxidation potentials; nevertheless, the wide potential window of BDD electrodes enables simultaneous determination of these oxidizable compounds with the nitro analog and their precursor in the atmosphere – I-nitropyrene.⁹²

11.2.4 Chemicals from Agricultural Activities

Chemicals from agricultural activities include chemicals used in agriculture and in animal husbandry. Most chemicals that may arise from agriculture are pesticides. The content of pesticides in surface, ground, and wastewater, soil, sludge, sediments, feed, or foodstuffs may be under control of national health agencies. Contamination of drinking water can result from their application and subsequent movement following rainfall or from inappropriate disposal method.⁹⁴

The few pesticides investigated so far on BDD electrodes using voltammetric methods include some carbamate pesticides (carbaryl,⁵⁴ carbendazim⁹⁵), and organophosphorus pesticides (parathion,⁹⁶ methyl parathion,⁹⁷ and fenamiphos⁹⁵). Determination of the latter group is based on the reduction of the nitro group and thus these pesticides are among the few examples on utilization of BDD electrodes for electroreduction. Carbamate pesticides, the *N*-substituted esters of carbamic

acid with general formula $R^1NH-CO-OR^2$, where R^2 is an aromatic or aliphatic moiety and R^1 is a methyl group, aromatic moiety, or benzimidazole moiety, are oxidizable on the amide nitrogen in the carbamate molecule. Further, the phenolic derivatives produced by alkaline hydrolysis of some carbamate pesticides can be utilized for electroanalysis. Both approaches were used by Rao et al.⁹⁸ in their pioneering work dealing with voltammetric characterization and HPLC/ED determination of carbamate pesticides at BDD electrodes. CV experiments in 0.1 mol L^{-1} phosphate buffer, pH 7.2 were performed with the *N*-methylcarbamate carbaryl. The relatively well-defined CVs were obtained at BDD electrode due to direct oxidation of carbaryl observable at potentials higher than +1.2 V (vs. saturated calomel electrode). No electrode fouling was observed, when stirring the solution between each CV cycle. The signal-to-background ratio was found to be five to ten times higher than that of glassy carbon electrode, where in this potential region the oxygen evolution reactions coincide with carbaryl oxidation. After alkaline hydrolysis of carbaryl to 1-naphthol, its oxidation peak appeared at +0.7 V and fouling of the electrode was observed under repetitive cycling due to the formation of polynaphthol film. It seems that this film adsorbs more strongly at the BDD surface than polyphenol films, observed by the same authors when oxidizing CPs.⁴⁶ However, the electrode could be perfectly cleaned by treating it at the anodic potential of +2.5 V for 10 min.

Direct voltammetric determination of carbaryl in polluted urban creek with L_D of $9.3 \text{ } \mu\text{g L}^{-1}$ ($L_Q = 31.2 \text{ } \mu\text{g L}^{-1}$) succeeded in a study by Codognoto et al.⁵⁴ Spiked samples were analyzed using SWV at BDD without any previous extraction, cleanup, or preconcentration steps that could impede in situ and real-time determinations. This simple approach was tested also for other electroactive pesticides by these Brazilian researchers. The *N*-benzimidazole carbamate fungicide carbendazim was determined together with the organophosphorus pesticide fenamiphos based on their electrooxidation. Despite the fact that the sensitivity of the determination is for both compounds influenced by the presence of other organic compounds in the matrix (river water), both compounds can be detected in the mixture with excellent recovery.⁹⁵ The other organophosphorus pesticides parathion and methyl parathion were studied based on electroreduction of the aromatic nitro group in the skeleton. Because these very potent insecticides and acaricides are relatively persistent and one of the most dangerous pesticides with high acute toxicity to wildlife and humans and suspected carcinogenicity, numerous environmental organizations propose their general and global ban.⁹⁹ SWV in BR buffer was selected for the determination of parathion in pure and polluted river waters at BDD by Pedrosa et al.⁹⁶ The comparison of reduction signals obtained using a hanging mercury drop electrode (HMDE) and BDD electrode favored slightly the latter one – detection limit of $7.9 \text{ } \mu\text{g L}^{-1}$ for river water was obtained. For methyl parathion lower L_D of $4.9 \text{ } \mu\text{g L}^{-1}$ was obtained, this time using sonovoltammetry to enhance the sensitivity.⁹⁷ These values are sufficient with respect to the hazardous level of $10 \text{ } \mu\text{g L}^{-1}$ set by WHO for drinking water.¹⁰⁰ Nevertheless, parathion concentration is likely to be far under this limit because parathion disappears from surface water in about 1 week; the main source of

exposure is generally food. The studies aimed at the degradation products of organophosphorus pesticides – nitrophenols are discussed in Sect. 11.2.1.

The last group of pesticides so far investigated at BDD electrodes are chlorophenoxy herbicides. They are derived from CPs and these compounds are often their degradation products in environment. As a group, chlorophenoxy herbicides have been classified in Group 2B (possibly carcinogenic to humans) by IARC.⁷³ Among them, 2(2-methyl-4-chlorophenoxy)propionic acid (MCP, mecoprop) was reported to be the most often found herbicide in drinking water, where the guideline value $10 \mu\text{g L}^{-1}$ ($0.046 \mu\text{mol L}^{-1}$) is recommended by WHO, and can achieve concentrations up to 0.4 mg L^{-1} in natural waters.^{101–103} Basic voltammetric and chronoamperometric studies were performed by Boye et al.¹⁰² for 4-chloro-2-methylphenoxyacetic acid (MCPA), MCP, and structurally related clofibric acid in $1 \text{ mol L}^{-1} \text{ HClO}_4$. They realized that these compounds display one diffusion-controlled oxidation peak at about $+1.6 \text{ V}$ (vs. standard hydrogen electrode (SHE)). A fast electrode fouling was observed under repetitive cycling. However, the formed film can be easily removed by applying a positive potential ($+2.6 \text{ V}$ vs. SHE) in the region of water oxidation (generation of OH^\bullet). The film seems to be formed by polymerization of a phenoxy-type radical and/or its products. This radical is formed in the first one-electron reaction step, leading to the formation of herbicides' radical cation, and its consecutive hydrolysis to corresponding phenoxy radical and 2-hydroxycarboxylic acid. As mentioned above, the phenoxy radicals may be responsible for BDD passivation also when oxidizing chlorophenols, and the number of methods for their determination using BDD electrodes reveals that this should be no serious obstacle when developing similar applications for chlorophenoxy herbicides. Thus, other studies on the use of BDD electrodes for quantitation of chlorophenoxy herbicides can be expected in the near future.

11.2.5 Other Organic Pollutants

There exists a myriad of other compounds representing serious risk to environment. This is valid especially for genotoxic compounds, where the exposure limits are questionable, as sometimes a minimal amount of the compound can initiate processes leading to unavoidable health damage. In this chapter, a brief overview on the use of BDD electrodes for determinations of other important environmental pollutants than mentioned above is given.

Many dyes and dye-related compounds belong to the most recalcitrant and durable pollutants and due to their water solubility present the risk especially for the aquatic life. The anthraquinone dyes Alizarin Red S¹⁰⁴ and quinizarin,¹⁰⁵ the triphenylmethane dye malachite green, and its reduced form leucomalachite green¹⁰⁶ are oxidizable at BDD electrodes.

For *N*-nitrosoamines, formed due to the presence of nitrite and amines in the water supply and thus potentially occurring in drinking water, an SWV method for

determination of their total content was proposed with detection limit $6 \times 10^{-8} \text{ mol L}^{-1}$.¹⁰⁷

An interesting method has been exploited for the detection of contamination in foodstuffs and tap water by *Escherichia coli*. It is based on detection of 2-NP that is released from hydrolysis of *o*-nitrophenyl- β -D-galactopyranose as catalyzed by β -galactosidase, an enzyme present in most strains of *E. coli*. Maximum enzyme activity was observed in phosphate buffer with addition of sodium dodecyl sulfate; released 2-NP was detected at bare BDD electrode. The detection limit was 4×10^4 cells mL^{-1} with a total analysis time of <1.5 h.

Other studies concern the electrochemical behavior of derivatives of simple aromatic compounds. Different voltammetric behavior of aniline,¹⁰⁸ benzoic, and salicylic acids and phthalic anhydride,¹⁰⁹ and of hydroquinone, resorcinol, and catechol¹¹⁰ was reported at BDD electrode. Nevertheless, bulk electrolysis of these pollutants at BDD electrode leads to their complete mineralization with exception of aniline with about 80 % conversion. Other study was devoted to the determination of residues of selected sulfonamides in egg samples by HPLC with amperometric detection at BDD electrode.¹¹¹

11.3 Detection of Aromatic Hydrocarbons and Their Derivatives Using Carbon Paste Electrodes

11.3.1 Methods Based on Anodic Oxidation

Anodic oxidation of aromatic hydrocarbons proceeds frequently by one-electron transfer leading to monocation radical. This electron-deficient species can be stable enough during the time interval of particular electrochemical reaction in particular medium. The relative stability of monocation radical could be ensured by high degree of charge delocalization in radical, by blocking the reactive sites in the radical or by stabilization of the radical by specific functional moieties. The instability of the monocation radical usually comes from chemical follow-up reactions by well-known EC and ECE mechanism or further processes involving another direct electron transfer without chemical reaction. Direct oxidation of aromatic hydrocarbons usually proceeds at potentials above 1 V (vs. SCE or Ag/AgCl reference electrodes, and depending on pH of the medium used) so that easily oxidizable hydroxy and amino derivatives of aromatic hydrocarbons or heterocyclic aromatic compounds are frequently determined using CPE not only due to their relative ease of oxidation, but also due to their widespread utilization in many industrial processes and connected occurrence in various environmental matrices. Great attention was paid to the determination of detrimental substances in drinking (and surface) water,¹¹⁶ among them to amino derivatives of aromatic hydrocarbons. Some amino derivatives of aromatic hydrocarbons are proven carcinogens¹¹⁷; therefore, they are frequently monitored in the environment utilizing mainly powerful separation methods like GC, HPLC, or electrophoresis with MS or

other types of detection. High sensitivity of electrochemical methods could be utilized usually only in connection with a preliminary analyte separation from the matrices using either solid-phase extraction or liquid-liquid extraction. The easier oxidation of amino and hydroxy derivatives of aromatic hydrocarbons which is reflected in their lower oxidation potentials in comparison with their parent aromatic hydrocarbons is on the other hand compromised by rapid follow-up reactions giving dimeric or polymeric products which often block the electroactive surface of the CPE or carbon paste sensors. Hydroxy derivatives of aromatic hydrocarbons belong often among antioxidants which are oxidized quite easily, however, usually highly irreversibly with the formation of either quinone-like or phenoxide species with low stability in the analytical media used for their determinations. Therefore, either mechanical or electrochemical cleaning of the CPE is needed after each measurement which complicates or at least slows down the analytical process. On the other hand, the prevailing hydrophobic character of both parent or amino or hydroxy derivatives of aromatic hydrocarbons enables the utilization of the analyte accumulation on the electrode surface in mixed organic solvent-aqueous media giving rise to very low limits of detection of these analytes, sometimes even in sub-nanomolar concentration range. The determination of 2-, 3-, and 4-aminobiphenyls using DPV at CPE with limits of determination in submicromolar range¹¹⁸ can serve as an example. The selectivity of the method was improved by preliminary separation using liquid-liquid and solid-phase extraction. Cyclodextrin-modified carbon paste electrodes enable the determination of carcinogenic polycyclic aromatic amines, namely 1- and 2-aminonaphthalene and 2-aminobiphenyl¹¹⁹ with nanomolar limits of determination. Beta-cyclodextrin is the most successful modifier of CPE which enabled the most efficient accumulation of tested analytes on the surface of the paste, in comparison to alfa- and gamma-cyclodextrin. Square-wave voltammetry and differential pulse voltammetry have been used for the determination of 2-acetamidofluorene and fluoren-9-ol at CPE,¹²⁰ following the study of the influence of the carbon paste composition on the voltammetric signals of the analytes. The methods are based on the oxidation of the above compounds and they include adsorptive accumulation of the analyte on the surface of the working electrode. The oxidation peak potentials vs. saturated Ag/AgCl electrode of +1.54 V for naphthalene, +1.61 V for fluorene, and +1.21 V for anthracene were utilized for the voltammetric determination of these analytes using their adsorptive accumulation on CPE.¹²¹ The results of the determination of anthracene and fluorene in spiked environmental samples were also presented.

Hydroxy derivatives or phenolics are frequent target for method development using carbon paste electrodes based either on direct oxidation of hydroxy group on an aromatic ring or on enzyme-based reactions with the final determination of the product of the enzymatic reaction involved. The reason lies both in their usual ease of oxidation and in their relatively frequent occurrence as hydroxy derivatives of aromatic hydrocarbons form the base of various biologically active organic compounds used as disinfectants, pharmaceuticals, herbicides, and pesticides. CPE and CPE modified with humic acids were used for the determination of pentachlorophenol.¹²² With modified electrode lower determination limit was reached due to better accumulation of the analyte. Formation of a quinone-like compound during

the oxidation is suggested. Laccase-based biosensor¹²³ was used for the determination of acetaminophen in environmental (and pharmaceutical) samples. Laccase uses dissolved oxygen as the cofactor, and oligomers and polymers are formed during the reaction according to the extent of the reaction. This laccase-mediated oxidative coupling system enabled to reach micromolar limits of determination for acetaminophen. A flow system method for continuous determination of phenolic compounds in environmental matrices¹²⁴ utilizing laccase- and tyrosinase-based biosensors as detectors was described with a dialysis membrane sampler. The laccase-based biosensor showed high sensitivity to guaiacol and chloroguaiacol, while the tyrosinase-based biosensor was more sensitive to phenol and chlorophenol. The authors claim high sensitivity of the determination with limits of determination below micromolar concentration range. The method worked well even in real paper mill effluent sample. Amperometric determination of phenol concentration using a tyrosinase modified carbon paste electrode by the developed immunoelectrochemical method in a flow injection analysis system¹²⁵ is an example of rapid detection of *Salmonella typhimurium* in chicken carcass wash water. Within 2.5 h, *Salmonella typhimurium* bacteria in chicken carcass wash water could be identified and quantified with a detection limit of 5×10^3 colony forming unit (CFU)/mL. The iridium-polyphenol oxidase-modified carbon paste electrode is a base for amperometric biosensor for phenols and catechols.¹²⁶ The polyphenol oxidase catalyzes the hydroxylation and oxidation of phenols to quinones, and iridium doping of carbon paste electrode ensures excellent electrocatalytic activity towards the reduction of the enzymatically formed quinone species, so that the quantification of the micromolar/submicromolar levels of phenols and catechols can be performed at potentials lower than in the case of bare CPE. Modification of CPE by the incorporation of polyphenol oxidase into a composite matrix¹²⁷ was used for the determination of 4-methyl-5-nitrocatechol and 2,4,5-trihydroxytoluene, the two compounds obtained from the 2,4-dinitrotoluene biodegradation. Around micromolar detection limits enabled the determination of the above biodegradation products even in the presence of large excess of 2,4-dinitrotoluene. The formation of molecularly imprinted microgel for electrochemical sensing of 2,4,6-trichlorophenol (TCP) based on dehalogenative function of the microgel substituting the function of natural chloroperoxidase for *p*-halophenols was used for the determination of TCP.¹²⁸ The sensor was developed for environmental waste screening. The determination of released *p*-nitrophenol from *p*-nitrophenyl-substituted organophosphate nerve agent is the basis of selective amperometric microbial biosensor for organophosphates. This whole-cell sensor has reportedly the service life of 5 days when stored in the operating buffer at 4 °C.¹²⁹

The growing interest in monitoring of estrogenic compounds, which are known endocrine disruptors, in the environment and especially in waters, is reflected in the use of CPE for their determination, as their steroid skeleton contains hydroxy group on benzene ring, thus making it relatively easily oxidizable. Highly sensitive electrocatalytic oxidation and determination of estradiol using carbon paste electrode modified with carbon nanotubes and ionic liquid were reported.¹³⁰ Electrocatalytic properties enabled to reach the limit of detection 5 nM of estradiol and the developed method was applied to the direct determination of estradiol in rabbit blood serum

and in environmental waters. Five phenolic xenoestrogens (pentachlorophenol, bisphenol A, 2,4-dichlorophenol, 4-*tert*-octylphenol, and 4-nonylphenol) were determined by pressurized CEC (capillary electrokinetic chromatography) with amperometric detection in spiked chicken eggs and milk powder samples.¹³¹ Diethylstilbestrol was determined at carbon black paste electrode (simultaneously with malachite green)¹³² and the method developed was used for the determination of diethylstilbestrol in real fishery water samples.

Highly sensitive simultaneous determination of strychnine and brucine in *Strychnos nux-vomica* seeds using CPE modified with multi-walled carbon nanotubes¹³³ was also reported although it is not based on direct oxidation of the aromatic ring of both analytes. The electrocatalytic oxidation of dipyrone was utilized for the determination using cobalt phthalocyanine-modified carbon paste as an amperometric detector in FIA system.¹³⁴ The method was used for the determination of this pharmaceutical both in pharmaceutical and environmental water samples. Restricted-use pesticide linuron was monitored on the basis of the oxidation of its secondary amino group at CPE with tricresyl phosphate as liquid binder.¹³⁵ The method was verified by determining linuron in spiked river water sample and a commercial product. The results obtained agreed well with those obtained by the reference HPLC/UV determination of linuron.

Phenylhydrazine was determined using DPV at carbon nanotubes and ferrocene-modified CPE utilizing catalytic wave at phenylhydrazine around +0.3 V.¹³⁶ The shift of about 0.31 V in DPV peak potential of hydrazine towards more positive values enabled the determination of both compounds in synthetic water samples during one measurement. Cobalt phthalocyanine-modified carbon paste was used also for phenylhydrazine determination (plus hydrazine and 1,1-dimethylhydrazine) in microchip capillary electrophoresis.¹³⁷ The miniaturized microsystem could be used for field monitoring in the environment with reasonable sensitivity. While in the two above papers phenylhydrazine was determined as environmental pollutant, plant growth regulator maleic hydrazide (a nitrogen-containing non-saturated cyclic compound) was determined¹³⁸ using palladium-modified CPE with remarkably low detection limit of 14 nM for flow injection analysis with amperometric detection. Palladium was used to enhance the electrochemical oxidation of the analyte giving rise to an oxidation signal at ca +0.7 V in a buffered neutral medium.

There are many other methods using CPE for the determination of either heterocyclic hydrocarbons, as, e.g., multi-walled carbon nanotube paste electrode used for AdS SWV determination of insecticide cyromazine,¹³⁹ or methods for the determination of aromatic hydrocarbons containing compounds, e.g., reference (140) but they are based on reactions of nonaromatic components (as thiocholine) which is out of the scope of this chapter.

The basic parameters of published methods for the determination of some environmental pollutants using various forms and modifications of CPE are summarized in Table 11.2.

Table 11.2 Selected examples of detection of various derivatives of aromatic and heterocyclic compounds using CPE

Analyte	Working electrode	Medium	Method	Matrix	LOD	Ref.
Phenylhydrazine, hydrazine	Ferrocene +CNT CPE	0.1 M PB pH 7.0	DPV	Water, urine samples	0.6 and 14 μM	136
Cyromazine	CNT CPE	0.1 M H ₂ SO ₄	SW ASV	Tap water	0.12 g mL ⁻¹	139
Pentachlorophenol	Humic acid in CPE		CV			122
Clofibrac acid, diclofenac, ofloxacin, propranolol	CNT CPE	0.2 M NaClO ₄	CV, DPV, NPV	Spiked river water, SPE enrichment	To 0.5 nM	141
APAH	CPE		DPV, HPLC-ED	Water samples, SPE, or LL extraction pre-concentration		118
Strychnine, brucine	CNT CPE	BRB pH 5.5	CV, CHC, DPV	Milk, saltwater, seeds	0.4 and 0.3 nM	133
Dipyrene	CoPC CPE	0.1 M phosphate buffer pH 7	FIA, 0.3 V	Pharm., environm. samples	ca 5 μM	134
Acetaminophen			Amp	Pharm., environm. samples	ca 2 μM	123
Phenolics	Laccase CPE	Weakly acidic	Amp	Pharm., environm. samples	2.4 μM	124
2,4,6-Trichlorophenol	Polymer CPE	0.1 M AcB pH 5.0, 0.001 M H ₂ O ₂	DPV, CV, oxidative dehalogenation	Environm. wastes	25 μM	128
Linuron	TCP CPE	BR buffer pH 2	DPV	River water	ca 5 μM	135
Phenols	Laccase, tyrosinase CPE	pH 5	Potent. sensor	Mill effluents	ca 10 nM	119
Naphthalene, fluorene, anthracene	CPE	0.1 M H ₂ SO ₄ , MeOH or AcN	VA	Environmental samples	0.2 nM	121
Fluorene deriv.	CPE	0.1 M H ₂ SO ₄ or BRB pH 7	SWV, DPV	Water samples	To 1 nM	120
Phenol (<i>Salmonella t.</i>)	Tyrosinase CPE	pH 7.0	FIA	Carcass wash water	5 $\times 10^5$ CFU mL ⁻¹	125

(continued)

Table 11.2 (continued)

Analyte	Working electrode	Medium	Method	Matrix	LOD	Ref.
OP pesticides	Whole cells MCPE	50 mM citrate-phosphate buffer pH 7.5, 50 μ M CoCl ₂	AmB	Waters	0.3 ppb	¹²⁹
MCPA	MnO ₂ M CPE	0.1 M KCl	Amperometry	Waters	0.20 ppm	¹⁴⁴
Diethylstilbestrol, malachite green	CBPE	BRB pH 6.5	VA	Fishery water samples	8 and 6 nM	¹³²
Methylparathion, monocrotophos	ACHe CPE	0.1 M phosphate buffer and 0.1 M KCl pH 7.0	CVA	Water, fruit samples	0.04 and 0.14	¹⁴⁰
4MSNC, 2,4,5-THT	PPO CPE	0.05 M PB pH 7.4	Amp	Biosensor environmental 2,4-DNT	4.7 μ M, 0.2 μ M	¹²⁷
Phenol, catechol	Ir PPO CPE	0.05 M PB pH 7.4	Amp, -0.1 V	Intended for environmental samples	To 0.1 μ M	¹²⁶
Maleic hydrazide	Pd CPE	0.05 M phosphate buffer pH 7.0	FIA, 700 mV	Drinking water	14 nM	¹³⁸
Aromatic hydrazines	CoPc CPE	10 mM phosphate run buffer pH 6.5	CZE, Am 0.5 V (Ag/AgCl)	Environmental water samples	0.5 μ M	¹³⁷
Chlorpyrifos	Sep CPE	BRB pH 2.0	AdS DPV	Tap water, soil samples, juices	0.08 ppb	¹⁴⁵
inoseb, dinoterb	CPE, Sep CPE	BRB pH 4.0	AdS DPV	Tap water, soil samples, juices	0.1 μ M, 0.5 nM	¹⁴⁶
Estradiol	CNT CPE	0.1 M PB pH 7.0	CVA	Environmental samples, rabbit blood serum	5 nM	¹³⁰
Estrogens	CPE	60 % ACN + 40 % v/v Tris (5 mmol L ⁻¹ , pH 8.0)	CEC-Amp	Chicken eggs, milk samples	2–50 ng mL ⁻¹	¹³¹
Nitrophenols	PVP CPE	25 mmol L ⁻¹ Tris-2.85 mmol L ⁻¹ citric acid-10 mmol L ⁻¹ beta-CD-10 % ethanol	CE-Amp	Environmental samples		¹⁴⁷

ACHe acetylcholinesterase, APAAH amino derivatives of polycyclic aromatic hydrocarbons, BRB Britton – Robinson buffer, CBPE carbon black paste electrode, CNT carbon nanotubes, CoPc cobalt phthalocyanine, OP organophosphates, PB phosphate buffer, PPO polyphenol oxidase, PVP polyvinylpyrrolidone, SEP sepiolite, TCP tricresyl phosphate, MnO₂ M CPE CPE modified with MnO₂

11.3.2 *Methods Based on Cathodic Reduction*

Methods utilizing reduction reactions at carbon paste electrodes are not so frequent due to the fact that it is practically impossible to get rid of oxygen which is adsorbed on carbon particles. Therefore, the oxygen waves or peaks often interfere with the signals of analytes so that other materials than carbon pastes are preferred. During the above-cited period just several papers appeared which dealt with the utilization of carbon paste electrodes for cathodic determination of derivatives of aromatic hydrocarbons and their application for environmental samples. Carbon nanotube paste and bare carbon paste were used for the determination of neutral pharmaceuticals clofibrac acid and ofloxacin¹⁴¹ in spiked water samples. To increase the sensitivity solid phase extraction (SPE) was used; nevertheless, relatively highly negative peak (wave) potentials did not allow reaching necessary detection limits to apply the method for analysis of real environmental samples. Cyanazine and propazine¹⁴² (heterocyclic hydrocarbons) were simultaneously determined on carbon paste electrode modified by a molecularly imprinted polymer, utilizing accumulation of the analytes at about -0.45 V and chemometric treatment with partial least squares method of the resulting cathodic stripping voltammograms. Both pesticides were successfully determined in food and environmental samples in micromolar concentrations. Herbicide aziprotryne¹⁴³ was determined by FIA using amperometric detection at -0.13 V on phthalocyanine-modified CPE. When utilizing preliminary solid-phase extraction step, aziprotryne concentrations lower than 0.2 ng/mL could be measured. MnO_2 -modified carbon paste electrode was used for catalytic reduction of herbicide monochlorophenoxyacetic acid (MCPA).¹⁴⁴ Amperometric determination of MCPA resulted in quite low detection limit of 0.2 ppm and was developed to monitor the environment on farmlands with MCPA control of broadleaf weeds. Quite high sensitivity was claimed for the determination of herbicide chlorpyrifos using adsorptive accumulation preceding the DP voltammetric measurement,¹⁴⁵ in spite of relatively negative potential for analyte reduction. The modification of paste composition by sepiolite enabled reaching the limit of detection of 0.008 ppb. Similarly, sepiolite-modified CPE was used for the determination of dinitrophenolic herbicides dinoseb and dinoterb.¹⁴⁶ The reduction of nitro groups proceeds at low negative potentials with remarkably low influence of oxygen reduction in the paste. This enabled to reach very low detection limits of 1×10^{-10} M and 5.4×10^{-10} M for dinoseb and dinoterb, respectively, with the adsorptive accumulation time of 10 s. A dual electrode and a dual channel determination of four nitrophenols at polyvinylpyrrolidone-modified CPE is described,¹⁴⁷ with oxidative ($+0.5$ V) and reductive (-1.4 V) detection potentials for hydroxy groups and nitro groups. This capillary electrophoretic method with dual electrochemical detection was successfully used for environmental samples where the separation power of electrophoresis is essential and high sensitivity of electrochemical detection is advantageous.

11.4 Conclusions

BDD thin films as an electrode and electrochemical sensor material have gained deserved attention since its introduction in early 1990s. Thanks to its hardness, stability, relative fouling resistance, and last but not least commercial availability it has been proven as a versatile electrode material for detection of a myriad of organic compounds with low detection limits, high sensitivity, and excellent stability. Among them, environmentally important organic compounds with widespread occurrence are undoubtedly in the focus of interest and common electroanalytical techniques succeeded in their detection. For bare BDD electrodes, these include mainly differential pulse and square-wave voltammetry among batch voltammetric techniques and amperometric detection modes in HPLC, FIA, or electrophoretic methods including analysis on the chips. The analysis is preferably performed in aqueous or mixed aqueous-organic acidic and neutral media, because in basic media BDD thin films undergo slow degradation. Construction of BDD-based sensors after modification of the BDD surface represents a fast-growing field of interest in last years; nevertheless up to now only few sensors were aimed at environmental pollutants. At bare H- or O-terminated BDD electrodes basic voltammetric studies were performed for chlorophenols, nitrophenol-based pesticides, monocyclic and polycyclic aromatic hydrocarbons and their derivatives, dye-related compounds, and others demonstrating the possibility of their oxidation or less frequently reduction at BDD thin films, the latter relying almost exclusively on the reduction of the nitro group on the aromatic skeleton. Although only few voltammetric or liquid flow methods with amperometric detection at BDD electrodes so far were developed exactly for the determination of these analytes or group of analytes in environmental matrices, under optimized conditions in pure solvents in many cases notable reproducibility, high sensitivity, and linear dynamic range over three orders of magnitude were reported without any previous preconcentration of the analytes. The potential of the usage of BDD is great even for pollutants passivating other solid electrode materials (phenolic compounds, aromatic amines, and others). The achieved detection limits usually meet or are below the enforceable or recommended concentration limits of WHO or national health agencies.

The actual challenges in environmental electroanalysis may be seen in (1) development of new voltammetric and amperometric methods using BDD electrodes and their validation so that they can be routinely used in environmental, biochemical, and other laboratories; (2) search on reasonable ways for construction of BDD-based sensors and extension of their applications in environmental analysis; and (3) construction of field-deployable analytical devices based on BDD sensors for *on-site* monitoring of environmental pollutants.

Thus, it can be concluded that the properties and results concerning electroanalysis of environmental pollutants indicate great promise for environmental applications of BDD electrodes and BDD-based sensors and more novel and inspirational results can be expected in the near future.

It is obvious from examples given in Sect. 11.2 and from Table 11.2 that carbon paste electrodes can play very useful role in the field of detection of various

electrochemically active derivatives of aromatic and heterocyclic compounds in various environmental matrices. Most applications are based on anodic oxidation. However, cathodic reductions were successfully employed as well. Further important development can be expected in connection with their modification with various nanoparticles and/or biological molecules. Moreover, combination with a suitable method for preliminary separation and preconcentration can substantially increase both the selectivity and sensitivity of aforementioned determinations.

Acknowledgements This research was supported by the Grant Agency of the Czech Republic (Project P206/12/G151).

References

1. Patel K, Hashimoto K, Fujishima A (1992) Application of boron-doped CVD-diamond film to photoelectrode. *Denki Kagaku* 60:659–661
2. Iniesta J, Michaud PA, Panizza M et al (2001) Electrochemical oxidation of 3-methylpyridine at a boron-doped diamond electrode: application to electroorganic synthesis and wastewater treatment. *Electrochem Commun* 3:346–351
3. Malkowsky IM, Griesbach U, Putter H et al (2006) Unexpected highly chemselective anodic ortho-coupling reaction of 2,4-dimethylphenol on boron-doped diamond electrodes. *Eur J Org Chem* 2006:4569–4572
4. Marselli B, Garcia-Gomez J, Michaud PA et al (2003) Electrogeneration of hydroxyl radicals on boron-doped diamond electrodes. *J Electrochem Soc* 150:D79–D83
5. Panizza M, Michaud PA, Iniesta J et al (2002) Electrochemical oxidation of phenol at boron-doped diamond electrode. Application to electro-organic synthesis and wastewater treatment. *Ann Chim* 92:995–1006
6. Fischer AE, Show Y, Swain GM (2004) Electrochemical performance of diamond thin-film electrodes from different commercial sources. *Anal Chem* 76:2553–2560
7. Fujishima A, Einaga Y, Rao TN (eds) (2005) *Diamond electrochemistry*. Elsevier, Amsterdam
8. McCreery RL (1999) Nonmetallic and semiconductor electrodes. In: Wieckowski A (ed) *Interfacial electrochemistry*. Dekker, New York, pp 627–631
9. Xu J, Granger MC, Chen Q et al (1997) Boron-doped diamond thin-film electrodes. *Anal Chem News Features* 1997:591A–597A
10. Ivandini TA, Einaga Y, Honda K et al (2005) Preparation and characterization of polycrystalline chemical vapor deposited boron-doped diamond thin films. In: Fujishima A, Einaga Y, Rao TN, Tryk DA (eds) *Diamond electrochemistry*. Elsevier, Amsterdam, pp 11–25
11. Narmadha M, Noel M, Suryanarayanan V (2011) Relative deactivation of boron-doped diamond (BDD) and glassy carbon (GC) electrodes in different electrolyte media containing substituted phenols – voltammetric and surface morphologic studies. *J Electroanal Chem* 655:103–110
12. Suffredini HB, Pedrosa VA, Codognoto L et al (2004) Enhanced electrochemical response of boron-doped diamond electrodes brought on by a cathodic surface pre-treatment. *Electrochim Acta* 49:4021–4026
13. Bairu SG, Stefan RI, van Staden JF (2003) Polycrystalline diamond-based electrochemical sensors and their applications in inorganic and organic analysis. *Crit Rev Anal Chem* 33:145–153
14. Barek J, Fischer J, Navratil T et al (2007) Nontraditional electrode materials in environmental analysis of biologically active organic compounds. *Electroanalysis* 19:2003–2014

15. Compton RG, Foord JS, Marken F (2003) Electroanalysis at diamond-like and doped-diamond electrodes. *Electroanalysis* 15:1349–1363
16. Hupert M, Muck A, Wang R et al (2003) Conductive diamond thin-films in electrochemistry. *Diam Relat Mater* 12:1940–1949
17. Chailapakul O, Siangproh W, Tryk DA (2006) Boron-doped diamond-based sensors: a review. *Sens Lett* 4:99–119
18. Peckova K, Musilova J, Berek J et al (2008) Voltammetric and amperometric determination of organic pollutants in drinking water using boron doped diamond film electrodes. In: Lefebvre MH, Roux MM (eds) *Progress on drinking water research*. Nova, New York, pp 103–142
19. Peckova K, Berek J (2011) Boron doped diamond microelectrodes and microelectrode arrays in organic electrochemistry. *Curr Org Chem* 15:3014–3028
20. Peckova K, Musilova J, Berek J (2009) Boron-doped diamond film electrodes – new tool for voltammetric determination of organic substances. *Crit Rev Anal Chem* 39:148–172
21. de Barros RDM, Ribeiro MC, An-Sumodjo PT et al (2005) Boron-doped CVD diamond films. Part I. History, production and characterization. *Quim Nova* 28:317–325 (in Portuguese)
22. Szunerits S, Boukherroub R (2008) Investigation of the electrocatalytic activity of boron-doped diamond electrodes modified with palladium or gold nanoparticles for oxygen reduction reaction in basic medium. *C R Chim* 11:1004–1009
23. Tryk DA, Kondo T, Fujishima A (2005) Chemical, photochemical and electrochemical modifications of diamond. In: Fujishima A, Einaga Y, Rao TN, Tryk DA (eds) *Diamond electrochemistry*. Elsevier, Amsterdam, pp 174–217
24. Yu Y, Zhou Y, Wu L et al (2012) Electrochemical biosensor based on boron-doped diamond electrodes with modified surface. *Int J Electrochem*. 567171. doi:10.1155/2012/567171
25. Alfaro MAQ, Ferro S, Martinez-Huitle CA et al (2006) Boron doped diamond electrode for the wastewater treatment. *J Braz Chem Soc* 17:227–236
26. Canizares P, Saez C, Lobato J et al (2006) Electrochemical technology and conductive-diamond electrodes. Part II: Applications of the electric conductive-diamond electrodes. *Afinidad* 63:121–129 (in Spanish)
27. Martinez-Huitle CA, Ferro S (2006) Electrochemical oxidation of organic pollutants for the wastewater treatment: direct and indirect processes. *Chem Soc Rev* 35:1324–1340
28. Panizza M, Cerisola G (2005) Application of diamond electrodes to electrochemical processes. *Electrochim Acta* 51:191–199
29. Zhou YL, Zhi JF (2009) The application of boron-doped diamond electrodes in amperometric biosensors. *Talanta* 79:1189–1196
30. Kraft A (2007) Doped diamond: a compact review on a new, versatile electrode material. *Int J Electrochem Sci* 2:355–385
31. Luong JHT, Male KB, Glennon JD (2009) Boron-doped diamond electrode: synthesis, characterization, functionalization and analytical applications. *Analyst* 134:1965–1979
32. McCreery RL (2008) Advanced carbon electrode materials for molecular electrochemistry. *Chem Rev* 108:2646–2687
33. Koizumi S, Nebel C, Nesladek M (2008) *Physics and applications of CVD diamond*. Wiley-VCH, Weinheim
34. US EPA (2013) US EPA list of priority pollutants. <http://water.epa.gov/scitech/methods/cwa/pollutants.cfm>. Accessed 21 Aug 2013
35. Gilman A, Douglas U, Arbuckle-Sholtz T et al (1982) Chlorophenols and their impurities: a health hazard evaluation. Bureau of Chemical Hazards, Environmental Health Directorate, National Health and Welfare, Ottawa
36. Kristiansen NK, Froshaug M, Aune KT et al (1994) Identification of halogenated compounds in chlorinated seawater and drinking-water produced offshore using n-pentane extraction and open-loop stripping technique. *Environ Sci Technol* 28:1669–1673
37. WHO (2006) Chlorophenols. In: *Guidelines for drinking-water quality: first addendum to third edition*. WHO, Geneva, pp 329–331
38. US EPA (2013). <http://water.epa.gov/drink/contaminants/index.cfm#List>. Accessed 22 Aug 2013

39. Castillo M, Domingues R, Alpendurada MF et al (1997) Persistence of selected pesticides and their phenolic transformation products in natural waters using off-line liquid solid extraction followed by liquid chromatographic techniques. *Anal Chim Acta* 353:133–142
40. Dzyadevych SV, Chovelon JM (2002) A comparative photodegradation studies of methyl parathion by using lumistox test and conductometric biosensor technique. *Mater Sci Eng C Mater Biol Appl* 21:55–60
41. US EPA (1980) Ambient water quality criteria for nitrophenols. <http://www.epa.gov/waterscience/criteria/library/ambientwqc/nitrophenols80.pdf>. Accessed 22 Aug 2013
42. Musilova J, Berek J, Peckova K (2011) Determination of nitrophenols in drinking and river water by differential pulse voltammetry at boron-doped diamond film electrode. *Electroanalysis* 23:1236–1244
43. Polcaro AM, Vacca A, Palmas S et al (2003) Electrochemical treatment of wastewater containing phenolic compounds: oxidation at boron-doped diamond electrodes. *J Appl Electrochem* 33:885–892
44. Zhi JF, Wang HB, Nakashima T et al (2003) Electrochemical incineration of organic pollutants on boron-doped diamond electrode. Evidence for direct electrochemical oxidation pathway. *J Phys Chem B* 107:13389–13395
45. Muna GW, Tasheva N, Swain GM (2004) Electro-oxidation and amperometric detection of chlorinated phenols at boron-doped diamond electrodes: a comparison of microcrystalline and nanocrystalline thin films. *Environ Sci Technol* 38:3674–3682
46. Terashima C, Rao TN, Sarada BV et al (2002) Electrochemical oxidation of chlorophenols at a boron-doped diamond electrode and their determination by high-performance liquid chromatography with amperometric detection. *Anal Chem* 74:895–902
47. Pedrosa VD, Codognoto L, Avaca LA (2003) Electroanalytical determination of 4-chlorophenol by square wave voltammetry on boron-doped diamond electrodes. *Quim Nova* 26:844–849 (in Portuguese)
48. Saterlay AJ, Foord JS, Compton RG (2001) An ultrasonically facilitated boron-doped diamond voltammetric sensor for analysis of the priority pollutant 4-chlorophenol. *Electroanalysis* 13:1065–1070
49. Zhu XP, Ni JR, Li HN et al (2010) Effects of ultrasound on electrochemical oxidation mechanisms of p-substituted phenols at BDD and PbO₂ anodes. *Electrochim Acta* 55:5569–5575
50. Codognoto L, Machado SAS, Avaca LA (2002) Square wave voltammetry on boron-doped diamond electrodes for analytical determinations. *Diam Relat Mater* 11:1670–1675
51. Pedrosa VA, Machado SAS, Avaca LA (2006) Application of a deconvolutive procedure to analyze several chlorophenol species in natural waters by square-wave voltammetry on the boron-doped diamond electrode. *Anal Lett* 39:1955–1965
52. US EPA (2013). <http://www.epa.gov/waterscience/criteria/wqcriteria.html>. Accessed 22 Aug 2013
53. Codognoto L, Zuin V, de Souza D et al (2004) Electroanalytical and chromatographic determination of pentachlorophenol and related molecules in a contaminated soil: a real case example. *Microchem J* 77:177–184
54. Codognoto L, Tanimoto ST, Pedrosa VA et al (2006) Electroanalytical determination of carbaryl in natural waters on boron doped diamond electrode. *Electroanalysis* 18:253–258
55. Garbellini GS, Salazar-Banda GR, Avaca LA (2007) Sonovoltammetric determination of 4-nitrophenol on diamond electrodes. *J Braz Chem Soc* 18:1095–1099
56. Pedrosa VA, Codognoto L, Machado SAS et al (2004) Is the boron-doped diamond electrode a suitable substitute for mercury in pesticide analyses? A comparative study of 4-nitrophenol quantification in pure and natural waters. *J Electroanal Chem* 573:11–18
57. Pedrosa VA, Suffredini HB, Codognoto L et al (2005) Carbon surfaces for electroanalytical applications: a comparative study. *Anal Lett* 38:1115–1125

58. Pedrosa VD, Codognoto L, Avaca LA (2003) Electroanalytical determination of 4-nitrophenol by square wave voltammetry on diamond electrodes. *J Braz Chem Soc* 14:530–535
59. Dejmekova H, Berek J, Zima J (2011) Determination of aminonitrophenols in hair dyes using a carbon paste electrode and a boron-doped diamond film electrode – a comparative study. *Int J Electrochem Sci* 6:3550–3563
60. Lei YZ, Zhao GH, Liu MC et al (2007) Simple and feasible simultaneous determination of three phenolic pollutants on boron-doped diamond film electrode. *Electroanalysis* 19:1933–1938
61. Zhao GH, Tang YT, Liu MC et al (2007) Direct and simultaneous determination of phenol, hydroquinone and nitrophenol at boron-doped diamond film electrode. *Chin J Chem* 25:1445–1450
62. Pop A, Ilinoiu E, Manea F et al (2011) Determination of organic pollutants from water by electrochemical methods. *Environ Eng Manag J* 10:75–80
63. Panizza M, Cerisola G (2009) Electrochemical degradation of gallic acid on a BDD anode. *Chemosphere* 77:1060–1064
64. Yardim Y (2012) Electrochemical behavior of chlorogenic acid at a boron-doped diamond electrode and estimation of the antioxidant capacity in the coffee samples based on its oxidation peak. *J Food Sci* 77:C408–C413
65. Radovan C, Cinghita D, Manea F et al (2008) Electrochemical sensing and assessment of parabens in hydro-alcoholic solutions and water using a boron-doped diamond electrode. *Sensors* 8:4330–4349
66. Darbre PD, Aljarrah A, Miller WR et al (2004) Concentrations of parabens in human breast tumours. *J Appl Toxicol* 24:5–13
67. Pereira GF, Andrade LS, Rocha RC et al (2012) Electrochemical determination of bisphenol A using a boron-doped diamond electrode. *Electrochim Acta* 82:3–8
68. Dejmekova H, Scampicchio M, Zima J et al (2009) Determination of total phenols in foods by boron doped diamond electrode. *Electroanalysis* 21:1014–1018
69. Notsu H, Tatsuma T, Fujishima A (2002) Tyrosinase-modified boron-doped diamond electrodes for the determination of phenol derivatives. *J Electroanal Chem* 523:86–92
70. Zhou YL, Tian RH, Zhi JF (2007) Amperometric biosensor based on tyrosinase immobilized on a boron-doped diamond electrode. *Biosens Bioelectron* 22:822–828
71. Zhou YL, Zhi JF (2006) Development of an amperometric biosensor based on covalent immobilization of tyrosinase on a boron-doped diamond electrode. *Electrochem Commun* 8:1811–1816
72. Wick AF, Haus NW, Sukkariyah BF et al (2011) Remediation of PAH-contaminated soils and sediments: a literature review. Virginia Polytechnic Institute and State University, Blacksburg. <http://landrehab.org/userfiles/files/Dredge/Virginia%20Tech%20PAH%20Remediation%20Lit%20Review%202011.pdf>. Accessed 23 Aug 2013
73. IARC (1987) Overall evaluations of carcinogenicity: an updating of IARC monographs volumes 1 to 42. IARC monographs on the evaluation of carcinogenic risks to humans, supplement 7. IARC, Geneva. <http://monographs.iarc.fr/ENG/Monographs/suppl7/index.php>. Accessed 23 Aug 2013
74. WHO (2006) Chemical fact sheets. In: Guidelines for drinking-water quality: first addendum to third edition. WHO, Geneva, pp 296–460
75. WHO (1998) Selected non-heterocyclic polycyclic aromatic hydrocarbons, vol 202, Environmental health criteria. WHO, Geneva
76. WHO (2006) Polynuclear aromatic hydrocarbons. In: Guidelines for drinking-water quality: first addendum to third edition. WHO, Geneva, pp 428–430
77. The Council of the European Union (1998) Council directive 98/83/ec. Official Journal of the European Union, 32–54

78. Bouvrette P, Hrapovic S, Male KB et al (2006) Analysis of the 16 Environmental Protection Agency priority polycyclic aromatic hydrocarbons by high performance liquid chromatography-oxidized diamond film electrodes. *J Chromatogr A* 1103:248–256
79. US EPA-NERL (1990) Method 550 Determination of polycyclic aromatic hydrocarbons in drinking water by liquid-liquid and HPLC with coupled ultraviolet and fluorescence detection. https://www.nemi.gov/methods/method_summary/4782/. Accessed 22 Aug 2013
80. Yardim Y, Levent A, Keskin E et al (2011) Voltammetric behavior of benzo(a)pyrene at boron-doped diamond electrode: a study of its determination by adsorptive transfer stripping voltammetry based on the enhancement effect of anionic surfactant, sodium dodecylsulfate. *Talanta* 85:441–448
81. Oliveira RTS, Salazar-Banda GR, Santos MC et al (2007) Electrochemical oxidation of benzene on boron-doped diamond electrodes. *Chemosphere* 66:2152–2158
82. Suryanarayanan V, Noel M (2010) A comparative evaluation on the voltammetric behavior of boron-doped diamond (BDD) and glassy carbon (GC) electrodes in different electrolyte media. *J Electroanal Chem* 642:69–74
83. Kapalka A, Foti G, Comninellis C (2009) The importance of electrode material in environmental electrochemistry. Formation and reactivity of free hydroxyl radicals on boron-doped diamond electrodes. *Electrochim Acta* 54:2018–2023
84. Gurbuz Y, Kang WP, Davidson JL et al (2004) Diamond microelectronic gas sensor for detection of benzene and toluene. *Sens Actuators B Chem* 99:207–215
85. IARC (2010) Some aromatic amines, organic dyes, and related exposures. IARC monographs on the evaluation of carcinogenic risks to humans, vol 99. IARC, Lyon. <http://monographs.iarc.fr/ENG/Monographs/PDFs/index.php>. Accessed 23 Aug 2013
86. WHO (2003) Selected nitro- and nitro-oxy-polycyclic aromatic hydrocarbons, vol 229, Environmental health criteria. WHO, Geneva
87. Fekete A, Malik AK, Kumar A et al (2010) Amines in the environment. *Crit Rev Anal Chem* 40:102–121
88. Vyskocil V, Barek J (2011) Electroanalysis of nitro and amino derivatives of polycyclic aromatic hydrocarbons. *Curr Org Chem* 15:3059–3076
89. Barek J, Jandova K, Peckova K et al (2007) Voltammetric determination of aminobiphenyls at a boron-doped nanocrystalline diamond film electrode. *Talanta* 74:421–426
90. Zavazalova J, Dejmkova H, Barek J et al (2013) Voltammetric and amperometric determination of mixtures of aminobiphenyls and aminonaphthalenes using boron doped diamond electrode. *Electroanalysis* 25:253–262
91. Cizek K, Barek J, Fischer J et al (2007) Voltammetric determination of 3-nitrofluoranthene and 3-aminofluoranthene at boron doped diamond thin-film electrode. *Electroanalysis* 19:1295–1299
92. Yosypchuk O, Barek J, Vyskocil V (2012) Voltammetric determination of carcinogenic derivatives of pyrene using a boron-doped diamond film electrode. *Anal Lett* 45:449–459
93. Peckova K, Jandova K, Maixnerova L et al (2009) Amperometric determination of aminobiphenyls using HPLC-ED with boron-doped diamond electrode. *Electroanalysis* 21:316–324
94. WHO (2006) Chemicals from agricultural activities. In: Guidelines for drinking-water quality: first addendum to third edition. WHO, Geneva, pp 187–188
95. Franca RF, de Oliveira HPM, Pedrosa VA et al (2012) Electroanalytical determination of carbendazim and fenamiphos in natural waters using a diamond electrode. *Diam Relat Mater* 27–28:54–59
96. Pedrosa VA, Miwa D, Machado SAS et al (2006) On the utilization of boron doped diamond electrode as a sensor for parathion and as an anode for electrochemical combustion of parathion. *Electroanalysis* 18:1590–1597
97. Garbellini GS, Salazar-Banda GR, Avaca LA (2009) Sonovoltammetric determination of toxic compounds in vegetables and fruits using diamond electrodes. *Food Chem* 116:1029–1035

98. Rao TN, Loo BH, Sarada BV et al (2002) Electrochemical detection of carbamate pesticides at conductive diamond electrodes. *Anal Chem* 74:1578–1583
99. Kegley S, Hill B, Orme S, Choi AH (2011) PAN pesticide database. Pesticide Action Network, San Francisco. <http://www.pesticideinfo.org>. Accessed 23 Aug 2013
100. WHO (2006) Parathion. In: Guidelines for drinking-water quality: first addendum to third edition. WHO, Geneva, pp 421–422
101. Albrechtsen HJ, Mills MS, Aamand J et al (2001) Degradation of herbicides in shallow Danish aquifers: an integrated laboratory and field study. *Pest Manag Sci* 57:341–350
102. Boye B, Brillas E, Marselli B et al (2006) Electrochemical incineration of chloromethylphenoxy herbicides in acid medium by anodic oxidation with boron-doped diamond electrode. *Electrochim Acta* 51:2872–2880
103. Reffstrup TK, Sorensen H, Helweg A (1998) Degradation of mecoprop at different concentrations in surface and sub-surface soil. *Pestic Sci* 52:126–132
104. Sun JR, Lu HY, Du LL et al (2011) Anodic oxidation of anthraquinone dye alizarin red S at Ti/BDD electrodes. *Appl Surf Sci* 257:6667–6671
105. Dimov IB, Batchelor-McAuley C, Aldous L et al (2012) The adsorption of quinzarin on boron-doped diamond. *Phys Chem Chem Phys* 14:2375–2380
106. Ngamukot P, Charoenraks T, Chailapakul O et al (2006) Cost-effective flow cell for the determination of malachite green and leucomalachite green at a boron-doped diamond thin-film electrode. *Anal Sci* 22:111–116
107. de Oliveira RTS, Salazar-Banda GR, Machado SAS et al (2008) Electroanalytical determination of N-nitrosamines in aqueous solution using a boron-doped diamond electrode. *Electroanalysis* 20:396–401
108. Mitadera M, Spataru N, Fujishima A (2004) Electrochemical oxidation of aniline at boron-doped diamond electrodes. *J Appl Electrochem* 34:249–254
109. Louhichi B, Bensalash N, Gadi A (2006) Electrochemical oxidation of benzoic acid derivatives on boron doped diamond: voltammetric study and galvanostatic electrolyses. *Chem Eng Technol* 29:944–950
110. Nasr B, Abdellatif G, Canizares P et al (2005) Electrochemical oxidation of hydroquinone, resorcinol, and catechol on boron-doped diamond anodes. *Environ Sci Technol* 39:7234–7239
111. Preechaworapun A, Chuanuwatanakul S, Einaga Y et al (2006) Electroanalysis of sulfonamides by flow injection system/high-performance liquid chromatography coupled with amperometric detection using boron-doped diamond electrode. *Talanta* 68:1726–1731
112. ElementSix (2013). <http://www.e6.com/en/>. Accessed 21 Aug 2013
113. WindsorScientific (2013). <http://www.windsorscientific.co.uk/>. Accessed 23 Aug 2013
114. NeoCoat (2013). <http://neocoat.ch/en>. Accessed 23 Aug 2013
115. Majid E, Male KB, Luong JHT (2008) Boron doped diamond biosensor for detection of *Escherichia coli*. *J Agric Food Chem* 56:7691–7695
116. Zima J, Švancara I, Peckova K, Barek J (2008) Carbon paste electrodes for the determination of detrimental substances in drinking water. In: LeFebvre MH, Roux MM (eds) Progress on drinking water research. Nova Science Publishers, Inc., New York
117. International Agency for Research on Cancer. <http://monographs.iarc.fr/ENG/Classification/index.php>
118. Barek J, Cvacka J, Muck A, Quaiserova V, Zima J (2001) Polarographic and voltammetric determination of carcinogenic nitro and amino derivatives of polycyclic aromatic hydrocarbons. *Electroanalysis* 13:799–803
119. Ferancova A, Korgova E, Labuda J, Zima J, Barek J (2002) Cyclodextrin modified carbon paste based electrodes as sensors for the determination of carcinogenic polycyclic aromatic amines. *Electroanalysis* 14:1668–1673
120. German N, Armalis S, Zima J, Barek J (2005) Voltammetric determination of fluoren-9-ol and 2-acetamidofluorene using carbon paste electrodes. *Collect Czech Chem Commun* 70:292–304

121. German N, Armalis S (2012) Voltammetric determination of naphthalene, fluorene and anthracene using mixed water-organic solvent media. *Chemija* 23:86–90
122. Airoidi FPS, Da Silva WTL, Crespilho FN, Rezende MOO (2007) Evaluation of the electrochemical behavior of pentachlorophenol by cyclic voltammetry on carbon paste electrode modified by humic acids. *Water Environ Res* 79:63–67
123. Cordeiro DD, Gil ED (2011) Laccase-based biosensor for determination of acetaminophen. *Lat Am J Pharm* 30:599–603
124. Freire RS, Duran N, Kubota LT (2002) Electrochemical biosensor-based devices for continuous phenols monitoring in environmental matrices. *J Braz Chem Soc* 13:456–462
125. Che YH, Li YB, Slavik M, Paul D (2000) Rapid detection of *Salmonella typhimurium* chicken carcass wash water using an immunoelectrochemical method. *J Food Prot* 63:1043–1048
126. Rubianes MD, Rivas GA (2000) Amperometric biosensor for phenols and catechols based on iridium-polyphenol oxidase-modified carbon paste. *Electroanalysis* 12:1159–1162
127. Rodriguez MC, Monti MR, Argarana CE, Rivas GA (2006) Enzymatic biosensor for the electrochemical detection of 2,4-dinitrotoluene biodegradation derivatives. *Talanta* 68:1671–1676
128. Diaz-Diaz G, Blanco-Lopez MC, Lobo-Castanon MJ, Miranda-Ordieres AJ, Tunon-Blanco P (2011) Preparation and characterization of a molecularly imprinted microgel for electrochemical sensing of 2,4,6-trichlorophenol. *Electroanalysis* 23:201–208
129. Lei Y, Mulchandani P, Wang J, Chen W, Mulchandani A (2005) Highly sensitive and selective amperometric microbial biosensor for direct determination of p-nitrophenyl-substituted organophosphate nerve agents. *Environ Sci Technol* 39:8853–8857
130. Tao H, Wei WZ, Zeng XD, Liu XY, Zhang XJ, Zhang YM (2009) Electrocatalytic oxidation and determination of estradiol using an electrode modified with carbon nanotubes and an ionic liquid. *Microchim Acta* 166:53–59
131. Wu WM, Yuan XM, Wu XP, Lin XC, Xie ZH (2010) Analysis of phenolic xenoestrogens by pressurized CEC with amperometric detection. *Electrophoresis* 31:1011–1018
132. Qu KM, Zhang XZ, Lv ZL, Li M, Cui ZG, Zhang Y, Chen BJ, Ma SS, Kong Q (2012) Simultaneous detection of diethylstilbestrol and malachite green using conductive carbon black paste electrode. *Int J Electrochem Sci* 7:1827–1839
133. Behpour M, Ghoreishi SM, Khayatkashani M, Motaghedifard M (2012) A new method for the simultaneous analysis of strychnine and brucine in *Strychnos nux-vomica* unprocessed and processed seeds using a carbon-paste electrode modified with multi-walled carbon nanotubes. *Phytochem Anal* 23:95–102
134. Boni AC, Wong A, Dutra RAF, Sotomayor MDT (2011) Cobalt phthalocyanine as a biomimetic catalyst in the amperometric quantification of dipyrone using FIA. *Talanta* 85:2067–2073
135. Dordevic J, Papp Z, Guzsvany V, Svancara I, Trtic-Petrovic T, Purenovic M, Vytras K (2012) Voltammetric determination of the herbicide linuron using a tricresyl phosphate-based carbon paste electrode. *Sensors* 12:148–161
136. Afzali D, Karimi-Maleh H, Khalilzadeh MA (2011) Sensitive and selective determination of phenylhydrazine in the presence of hydrazine at a ferrocene-modified carbon nanotube paste electrode. *Environ Chem Lett* 9:375–381
137. Siangproh W, Chailapakul O, Laocharoensuk R, Wang J (2005) Microchip capillary electrophoresis/electrochemical detection of hydrazine compounds at a cobalt phthalocyanine modified electrochemical detector. *Talanta* 67:903–907
138. Sanchez A, Zapardiel A, de Prado FL, Bermejo E, Moreno M, Perez-Lopez JA, Chicharro M (2007) Flow injection analysis of maleic hydrazide using an electrochemical sensor based on palladium-dispersed carbon paste electrode. *Electroanalysis* 19:1683–1688
139. Mercan H, Inam R, Aboul-Enein HY (2011) Square wave adsorptive stripping voltammetric determination of cyromazine insecticide with multi-walled carbon nanotube paste electrode. *Anal Lett* 44:1392–1404

140. Raghu P, Reddy TM, Swamy BEK, Chandrashekar BN, Reddaiah K, Sreedhar M (2012) Development of AChE biosensor for the determination of methyl parathion and monocrotophos in water and fruit samples: a cyclic voltammetric study. *J Electroanal Chem* 665:76–82
141. Ambrosi A, Antiochia R, Campanella L, Dragone R, Lavagnini I (2005) Electrochemical determination of pharmaceuticals in spiked water samples. *J Hazard Mater* 122:219–225
142. Gholivand MB, Shariati-Rad M, Karimian N, Torkashvand M (2012) A chemometrics approach for simultaneous determination of cyanazine and propazine based on a carbon paste electrode modified by a molecularly imprinted polymer. *Analyst* 137:1190–1198
143. Chicharro M, Zapardiel A, Bermejo E, Madrid E, Rodriguez C (2002) Flow injection analysis of aziprotryne using an electrochemical sensor based on cobalt phthalocyanine modified carbon paste electrode. *Electroanalysis* 14:892–898
144. Priyantha N, Navaratne A, Weliwegamage S, Ekanayake CB (2007) Determination of MCPA through electrocatalysis by manganese species. *Int J Electrochem Sci* 2:433–443
145. Sirisha K, Mallipattu S, Reddy SRJ (2007) Differential pulse adsorptive stripping voltammetric determination of chlorpyrifos at a sepiolite modified carbon paste electrode. *Anal Lett* 40:1939–1950
146. Sreedhar M, Reddy LM, Sirisha KR, Reddy SRJ (2003) Differential pulse adsorptive stripping voltammetric determination of dinoseb and dinoterb at a modified electrode. *Anal Sci* 19:511–516
147. Yang BY, Mo JY, Lai R (2005) Determination of nitrophenols of environment by dual-electrode and dual-channel electrochemical detection of capillary electrophoresis with polyvinylpyrrolidone modified carbon paste electrode. *Chem J Chin Univ Chin* 26:227–230

Chapter 12

Explosives

Jiri Barek, Jan Fischer, and Joseph Wang

List of Abbreviations

CFME	Carbon fiber microelectrode
CRP	Cathode ray polarography
C-SPE	Carbon ink screen-printed electrode
CV	Cyclic voltammetry
DCP	Direct current polarography
DME	Dropping mercury electrode
DMSO	Dimethylsulfoxide
DPV	Differential pulse voltammetry
GCE	Glassy carbon electrode
gm-GCE	Graphene oxide-modified glassy carbon electrode
HMDE	Hanging mercury drop electrode
MIP-E	Molecularly imprinted polymer-modified electrode
pTTP-GCE	Poly[<i>meso</i> -tetrakis(2-thienyl)porphyrin]-modified glassy carbon electrode
SWV	Square wave voltammetry
THFA	Tetrahydrofurfuryl alcohol

J. Barek (✉) • J. Fischer

Faculty of Science, Department of Analytical Chemistry, UNESCO Laboratory of Environmental Electrochemistry, University Research Centre UNCE “Supramolecular Chemistry”, Charles University in Prague, Albertov 6, 128 43 Prague 2, Czech Republic
e-mail: barekj096@seznam.cz

J. Wang

Department of Nanoengineering, University of California San Diego
9500 Gilman Drive, La Jolla 92093-0448, CA, USA

© Springer Science+Business Media New York 2015

L.M. Moretto, K. Kalcher (eds.), *Environmental Analysis by Electrochemical Sensors and Biosensors*, DOI 10.1007/978-1-4939-1301-5_12

965

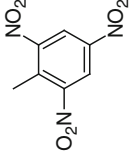
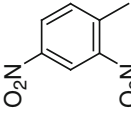
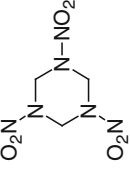
12.1 Introduction

Explosives produced both for military and civilian use^{1,2} are important pollutants of soils and aquatic systems in the vicinity of places where they are produced, stored, or used.³ Many of them are classified as toxic by the US EPA and other environmental agencies. Therefore, there is an ever-increasing demand for sensitive and selective analytical methods suitable for their determination in various environmental matrices. There are many review articles available on the detection of explosives utilizing a multitude of different analytical techniques.⁴⁻⁷ The most common current techniques for detection of trace explosives include ion mobility spectrometry (IMS), mass spectrometry (MS), and gas chromatography (GC); however, most of these devices are bulky, expensive, and require time-consuming procedures.⁸ There are several hundreds of explosive materials officially listed,⁹ most of them being based on nitrated organic compounds (see Table 12.1). Because of easy electrochemical reducibility of nitro group, voltammetric and amperometric methods are frequently used for their determination.¹⁰ Differential pulse voltammetry,¹¹ square wave voltammetry,¹² and adsorptive stripping voltammetry¹³ are most frequently used for the determination of nitrated explosives. Voltammetric and amperometric detection of explosives has received considerable attention for security screening and other defense applications.¹⁴ Terrorist threats resulted in increasing demand for on-site detection of explosives and the low-cost, portable, highly sensitive, and specific electrochemical sensors can be viable tools for these purposes.¹⁵ Moreover, electrochemical detection of nitrated explosives is extremely sensitive and necessary instrumentation can be easily miniaturized and integrated on microchip platform.

Nitro group can be relatively easily reduced via nitroso group and hydroxylamino group to amino group, each step being accompanied with the exchange of two electrons. Mechanism of reduction of polynitrocompounds depends on number and relative position of nitro groups, nature of aromatic rings and possible presence of other substituents, and especially on pH of the solution. Trinitro compounds are usually reduced more readily than dinitro or mononitro compounds. Methyl substituent position has an influence on redox properties of nitroaromatics related to 2,4,6-trinitrotoluene.¹⁶ Detail information on reduction pathways of 2,4,6-trinitrotoluene can be found in paper.¹⁷ Reduction of nitrobenzenes and nitrotoluenes usually occurs in one single four-electron step to form arylhydroxylamines, which is followed by two-electron step leading to arylamines. Two-electron reduction of aromatic nitro group to a nitroso group never occurs because of relatively higher reduction potential of the nitroso group in comparison with corresponding nitro group. Reduction potentials of nitro groups depend on electrode material; for example, they are usually more negative on glassy carbon than on mercury.

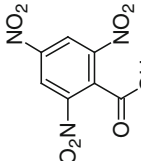
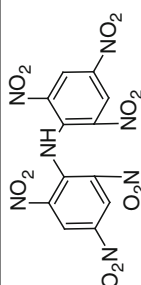
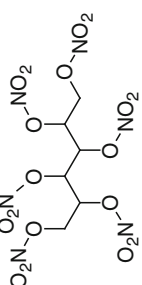
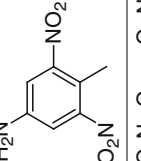
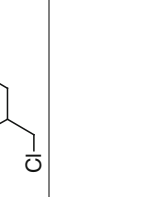
Several portable, low-cost electrochemical sensors for detection of nitrated explosives were developed.¹⁴ These include Hg-film electrodes,¹⁸⁻²⁰ glassy carbon electrodes,^{21,22} carbon fiber electrodes,²³⁻²⁵ and screen-printed carbon

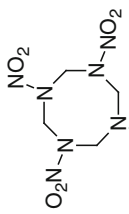
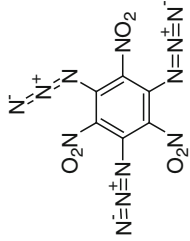
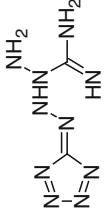
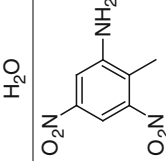
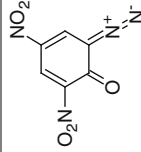
Table 12.1 Selected methods for voltammetric determination of explosives

Structure	CAS #	Common name	CAS name	Technique	Electrode	Detection potential vs. Ag/AgCl (mV)	Medium	LOQ ($\mu\text{mol L}^{-1}$)	Reference
	118-96-7	Tritrotoluene	Benzene, 2-methyl-1,3,5-trinitro-	DCP SWV SWV CV SVW DPV DPV	DME HMDE CFME C-SPE C-SPE pTTP-GCE gm-GCE	-360; -580; -790 -60; -180 -375; -517; -620 -1,170; +500 -1,080; +15 -410; -555; -680 -400; -510; -600	LiClO ₄ , 20 % ethanol, 10 % pyridine Acetate buffer, acetonitrile Phosphate buffer (pH 7.0), acetonitrile Phosphate buffer (pH 6.5), acetonitrile Phosphate buffer (pH 6.5), acetonitrile Phosphate buffer (pH 7.0), acetonitrile 20 mM borate buffer, pH 9.3	30 0.005 1 - 30 0.1 60	65 66 3 14 14 67 68
	121-14-2	DNT, 2,4-dinitrotoluene	Benzene, 1-methyl-2,4-dinitro-	CV SVW DPV	C-SPE C-SPE gm-GCE	-1,090; -110 -840; -90; +670 -580; -710	Phosphate buffer (pH 6.5), acetonitrile Phosphate buffer (pH 6.5), acetonitrile 20 mM borate buffer, pH 9.3	- 40 70	14 14 68
	121-82-4	RDX, hexogen	1,3,5-Triazine, hexahydro-1,3,5-trinitro	DCP SWV CV SVW DPV	DME HMDE C-SPE C-SPE pTTP-GCE	-920; -1,110; -1,380 -101; -286 -1,220; +780 -1,190; +870 -830	KNO ₃ , 10 % Pyridine Acetate buffer, acetonitrile Phosphate buffer (pH 6.5), acetonitrile Phosphate buffer (pH 6.5), acetonitrile Phosphate buffer (pH 7.0), acetonitrile	30 0.2 - 30 1	65 66 14 14 67

(continued)

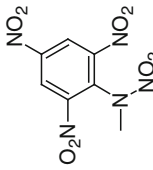
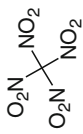
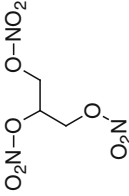
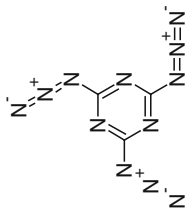
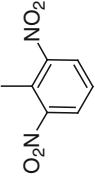
Table 12.1 (continued)

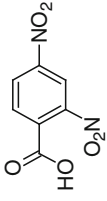
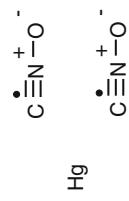

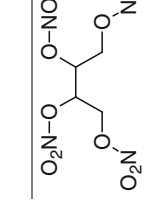
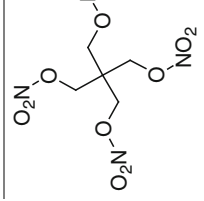
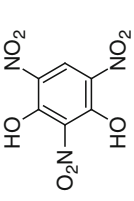
Structure	CAS #	Common name	CAS name	Technique	Electrode	Detection potential vs. Ag/AgCl (mV)	Medium	LOQ ($\mu\text{mol L}^{-1}$)	Reference
	129-66-8	TNBA, 2,4,6-trinitrobenzoic acid	Benzoic acid, 2,4,6-trinitro-	SWV DPV	HMDE MIP-E	-65; -161; -238 -450	Acetate buffer, acetonitrile 0.03 M HClO ₄	0.001 -	66 69
	131-73-7	Hexanitrodi(phenyl)amine, HEXIL	Benzenamine, 2,4,6-trinitro-N-(2,4,6-trinitrophenyl)-	DCP SWV	DME HMDE	-460; -580; -690, -760 -47; -232, -339	LiClO ₄ , 20 % ethanol, 10 % pyridine Acetate buffer, acetonitrile	40 0.01	65 66
	15825-70-4	Mannitol hexanitrate	D-Mannitol, 1,2,3,4,5,6-hexanitrate	CRP CV	DME GCE	-310 -830	NH ₄ NO ₃ , KNO ₃ , 30 % THFA Phosphate buffer (pH 7.0), DMSO	40 -	65 70
	19406-51-0	4-Amino-2,6-dinitrotoluene	Benzenamine, 4-methyl-3,5-dinitro-	SWV CV	HMDE GCE	-190; -321 -537; -623	Acetate buffer, acetonitrile Phosphate buffer (pH 8.0), acetonitrile	0.03 -	66 17
	2612-33-1	Dinitrochlorhydrin	1,2-Propanediol, 3-chloro-, 1,2-dinitrate	DCP	DME	-560	NH ₄ Cl, KCl, 10 % pyridine	80	65

	2691-41-0	HMX, octogen	1,3,5,7-Tetrazocine, octahydro-1,3,5,7-tetranitro-	DCP SWV SVW	DME HMDE C-SPE	-1,110; -1,380 -101; -286; -452 -1,170; +800	KNO ₃ , 10 % pyridine Acetate buffer, acetonitrile Phosphate buffer (pH 6.5), acetonitrile	20 0.3 20	65 66 14
	29306-57-8	Trinitrotriazidobenzene	Benzene, 1,3,5-triazido-2,4,6-trinitro-	DCP	DME	-560; -760	LiClO ₄ , 20 % ethanol, 10 % pyridine	50	65
	31330-63-9	Tetrazene	3-Tetrazene-2-carboximidamide, 4-(2H-tetrazol-5-yl)-, hydrate (1:1)	DCP	DME	-530	LiClO ₄ , 20 % ethanol, 20 % formic acid	40	65
	35572-78-2	2-Amino-4,6-dinitrotoluene	Benzenamine, 2-methyl-3,5-dinitro-	SWV SWV	HMDE CFME	-202; -309 -519; -632	Acetate buffer, acetonitrile Phosphate buffer (pH 7.0), acetonitrile	0.02 3	66 3
	4682-03-5	DINOL, diazodinitrophenol	2,4-Cyclohexadien-1-one, 6-diazo-2,4-dinitro-	DCP	DME	-160	LiClO ₄ , HCl, pH 1, 20 % ethanol	80	65

(continued)

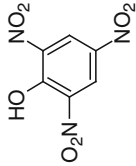
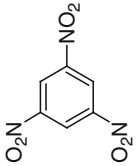
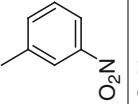
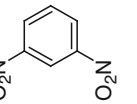
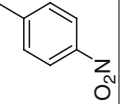
Table 12.1 (continued)

Structure	CAS #	Common name	CAS name	Technique	Electrode	Detection potential vs. Ag/AgCl (mV)	Medium	LOQ ($\mu\text{mol L}^{-1}$)	Reference
	479-45-8	Tetryl	Benzenamine, N-methyl-N,2,4,6-trinitro-	CRP DPV	DME pTTP-GCE	-240; -430; -630 -445; -590	LiClO ₄ , 20 % ethanol Phosphate buffer (pH 7.0), acetonitrile	2 0.1	65 67
	509-14-8	Teranitromethane	Methane, tetranitro-	DCP	DME	-560; -60	LiClO ₄ , 20 % ethanol, 10 % pyridine	90	65
	55-63-0	Glyceroltrinitrate	1,2,3-Propanetriol, 1,2,3-trinitrate	DCP CV SVW	DME C-SPE C-SPE	-230 -1,060; +720 -1,230; +780	NH ₄ Cl, KCl, 10 % pyridine Phosphate buffer (pH 6.5), methanol Phosphate buffer (pH 6.5), methanol	70 - 30	65 14 14
	5637-83-2	Cyanuric triazide	1,3,5-Triazine, 2,4,6-triazido-	DCP	DME	-560; -760	KNO ₃ , 10 % pyridine	30	65
	606-20-2	2,6-Dinitrotoluene	Benzene, 2-methyl-1,3-dinitro-	SWV SWV	HMDE CFME	-190; -321 -524; -637	Acetate buffer, acetonitrile Phosphate buffer (pH 7.0), acetonitrile	0.04 2	66 3

	610-30-0	2,4-Dinitrobenzoic acid	Benzoic acid, 2,4-dinitro-	SWV	HMDE	-140; -238	Acetate buffer, acetonitrile	0.009	66
	628-86-4	Mercury fulminate	Mercury, bis (fulminate-κC)-	DCP	DME	-140	KNO ₃ , 10 % pyridine	1	65
	628-96-6	Ethylene glycol dinitrate	1,2-Ethanediol, 1,2-dinitrate	DCP CV	DME GCE	-410; -580 -634	LiClO ₄ , 20 % ethanol Phosphate buffer (pH 7.0), DMSO	100 -	65 70
	7297-25-8	Erythritol tetranitrate	1,2,3,4-Butanetetrol, 1,2,3,4-tetranitrate, (2 <i>R</i> ,3 <i>S</i>)-rel-	DCP CV	DME GCE	-410 -847	NH ₄ NO ₃ , KNO ₃ , 30 % THFA Phosphate buffer (pH 7.0), DMSO	60 -	65 70
	78-11-5	PENT, penthit	1,3-Propanediol, 2,2-bis[(nitro-oxy)methyl]-, 1,3-dinitrate	DCP CV SVW	DME GCE C-SPE	-280 -770 -1,130; +800	LiClO ₄ , 20 % ethanol, 20 % formic acid Phosphate buffer (pH 7.0), DMSO Phosphate buffer (pH 6.5), acetonitrile	50 - 2	65 70 14
	82-71-3	Styphnic acid	1,3-Benzenediol, 2,4,6-trinitro-	DCP	DME	-410; -760; -1,060	LiClO ₄ , 20 % ethanol	10	65

(continued)

Table 12.1 (continued)

Structure	CAS #	Common name	CAS name	Technique	Electrode	Detection potential vs. Ag/AgCl (mV)	Medium	LOQ ($\mu\text{mol L}^{-1}$)	Reference
	88-89-1	Picric acid	Phenol, 2,4,6-trinitro-	DCP SWV	DME HMDE	-340; -530; -860; -1060 -131; -244; -339	LiClO ₄ , 20 % ethanol Acetate buffer, acetonitrile	30 0.003	65 66
	99-35-4	TNB, trinitrobenzene	Benzene, 1,3,5-trinitro-	DCP CV	DME GCE	-460; -640; -780 -456; -614; -754	LiClO ₄ , 20 % ethanol, 10 % pyridine Borate buffer (pH 9.2), acetonitrile	30 -	65 16
	99-08-1	3-NT, 3-nitrotoluene	Benzene, 1-methyl-3-nitro-	CV SWV	C-SPE C-SPE	-960; -110 -970; -118	Phosphate buffer (pH 6.5), acetonitrile Phosphate buffer (pH 6.5), acetonitrile	- 50	14 14
	99-65-0	1,3-Dinitrobenzene	Benzene, 1,3-dinitro-	SWV CV SWV	HMDE C-SPE C-SPE	-149; -262 -990; +90 -820; -10	Acetate buffer, acetonitrile Phosphate buffer (pH 6.5), acetonitrile Phosphate buffer (pH 6.5), acetonitrile	0.03 - 40	66 14 14
	99-99-0	4-Nitrotoluene	Benzene, 1-methyl-4-nitro-	SWV CV	HMDE GCE	-238 -705	Acetate buffer, acetonitrile Borate buffer (pH 9.2), acetonitrile	0.2 -	66 16

electrodes.^{12,14,21,26–28} The need for detection of nanomolar levels of explosives has led to the development of nano-material-based sensors which provide control over the local microenvironment.

Electrochemical (amperometric) detection is also the method of choice for the analysis of nitroaromatic explosives on microchip devices since it offers up to three orders of magnitude higher sensitivity than indirect laser-induced fluorescence.^{29,30} Microfluidic device for detection of five TNT-related explosive compounds with exchangeable carbon thick-film screen-printed amperometric detector can be mentioned in this context.³¹

12.2 Voltammetric Detection of Nitrated Explosives

The most suitable electrode for these purposes is the hanging mercury drop electrode³² because of its atomically smooth and easily renewable surface and broad cathodic potential windows. However, fears of mercury toxicity initiated an intensive search for more environmentally friendly and less toxic electrode materials, e.g., based on solid silver amalgams.^{32–34} Amalgam electrodes have similar potential window and similar sensitivity as the hanging mercury drop electrode³⁴ and thus can be used for the determination of explosive agents and for development of electrochemical sensors for these purposes. Good example of their applicability is the sensitive voltammetric determination of 4-nitrophenol³⁵ and of picric acid¹⁰ using a silver amalgam paste electrode.

Another possibility is to use bismuth-film-modified electrodes which were used, e.g., for detection of picric acid.³⁶ Different types of bismuth-based electrodes (bismuth-film electrodes, bismuth bulk electrodes, bismuth-nanoparticle-modified electrodes) and their applications for determination of (among others) various nitro-compounds were reviewed.³⁷

Boron-doped diamond presents another attractive material with low and stable background current and noise over a wide potential range, corrosion resistance, high thermal conductivity, and high current densities. Usually no mechanical or electrochemical pretreatment of BDD film electrode is needed. Therefore, BDD film electrodes find use also in the area of environmental analysis for organic explosive determinations. BDD-based electrochemical detector allowed, e.g., amperometric detection of 2,4,6-trinitrotoluene, 1,3-dinitrobenzene, and 2,4-dinitrotoluene over the 200–1,400 ppb range, with detection limits at the 100 ppb level.³⁸

Disposable screen-printed electrodes are useful single-use sensors for routine analysis. Method of screen printing allows one to construct the whole-electrode systems. Screen-printed carbon thick-film electrodes were used to measure 2,4,6-trinitrotoluene by square wave voltammetry in as little as 50 μ L sample volume.³⁹ This assay was coupled with a solid-phase extraction and the preconcentration factor of 1:500 yielded a 100-fold higher sensitivity resulting in a calibration range of 2 ppb to 2 ppm for 2,4,6-trinitrotoluene. A polyphenol-coated

screen-printed carbon electrode was used for highly sensitive voltammetric measurements of 2,4,6-trinitrotoluene in the presence of surface-active substances⁴⁰ with detection limit around 1 ppm. Measurement in single 20 μL sample droplet was proposed for three-electrode screen-printed system based on preanodized carbon electrode²⁷ and used for square wave voltammetric determination of 2,4,6-trinitrotoluene in lake water at the micromolar level.

Voltammetric determination of explosives in gas phase was realized by coating of screen-printed three-electrode system by hydrogel based on 0.5 mol L^{-1} potassium chloride in agarose.¹² The thermally desorbed 2,4,6-trinitrotoluene from a preconcentration device was moved by gas to detection system and concentration was measured using rapid square wave voltammetry.

The application of graphene for the electrochemical detection of trace levels of nitroaromatic explosives is based on their strong adsorption on this electrode material; see, e.g., detection of 2,4,6-trinitrotoluene.⁴¹ Graphene oxide was successfully used for determination of dinitrotoluene, dinitrobenzene, trinitrobenzene, and 2,4,6-trinitrotoluene.⁴² Further information on the use of graphene for detection of nitroaromatic explosives can be found in reviews.^{43–45} Square wave voltammetry on carbon nanotube-modified glassy carbon electrode was successfully used for the detection of 2,4,6-trinitrotoluene in seawater.⁴⁶ Multiwall carbon nanotube-modified glassy carbon electrode is suitable for detection of cyclotrimethylenetrinitramine in spiked ground and tap water.⁴⁷ Sensors based on TiO_2 electrode modified with Pt or Au nanoparticles,⁴⁸ on functionalized Au nanoparticles⁴⁹ and on poly(guanine)-functionalized Si nanoparticles,⁵⁰ were used for detection of 2,4,6-trinitrotoluene. Silica- and carbon-based porous nanomaterials⁵¹ and mesoporous SiO_2 and poly(diallyldimethylammonium chloride) adsorbed on glassy carbon electrode were used to detect ultratrace nitroaromatic compounds.⁵² Nanoporous organosilicas were used as preconcentration materials for the electrochemical detection of 2,4,6-trinitrotoluene⁵³ and nanosensor based on core-shell-structured mesoporous silica microspheres with SiO_2 particle core which was functionalized with 3-aminopropyltriethoxysilane was used for 2,4,6-trinitrotoluene detection.⁵⁴ Glassy carbon electrode modified with ordered mesoporous carbon was used for detection of ultratrace trinitrotoluene, dinitrotoluene, and dinitrobenzene.^{55,56} Pt nanoparticle ensemble-on-graphene hybrid nanosheet was reported for detection of 2,4,6-trinitrotoluene.⁵⁷ An ionic liquid-graphene composite prepared by combining ionic liquid and three-dimensional graphene material with a large specific area and pronounced mesoporosity was used for detection of ultratrace 2,4,6-trinitrotoluene⁵⁸ and porphyrin-functionalized graphene for sensitive electrochemical detection of dinitrotoluene, trinitrotoluene, dinitrobenzene, and trinitrobenzene.⁵⁹ Hybrids of carbon nanotubes and metallic nanoparticles (single-wall and multi-wall nanotube composites with Pt, Au, and Cu nanoparticles) were used for determination of 2,4,6-trinitrotoluene.⁶⁰ Detection of ultratrace 2,4,6-trinitrotoluene can be based on electrodes functionalized with multi-wall carbon nanotubes modified with triphenylene.⁶¹ The combination of voltammetry and chemometric treatment for detection of nitroaromatics has been examined⁶² through multivariate analysis of

square wave voltammetric data of 2,4,6-trinitrotoluene, 2,6-dinitrotoluene, 2,4-dinitrotoluene, and 2-nitrotoluene at bare and modified glassy carbon electrodes.

Selected voltammetric methods for the determination of nitrated explosives are summarized in Table 12.1, showing broad scope of explosives, techniques, electrodes, and matrices investigated for those purposes.

12.3 Amperometric Detection of Nitrated Explosives

Amperometric detection is useful for fast flow injection analysis or HPLC of explosives in complicated environmental matrices which can be demonstrated by the analysis of the mixture of 14 standard explosives with detection limit around $0.2 \mu\text{g mL}^{-1}$.⁶³

“Lab-on-a-chip” technology, particularly micromachined capillary electrophoresis system, was used, e.g., for flow-injection/amperometric determination of 2,4,6-trinitrotoluene²⁰ using simple crossing of four channels with an amalgam mercury/gold disc electrode at a fixed potential of -600 mV . Detection limit of about $7.0 \mu\text{g L}^{-1}$ with sample volume $3 \mu\text{L}$ was obtained. Similar arrangement was also used for electrophoretic separation of neutral nitroaromatic explosives and nerve agent compounds in the microchip channel.⁶⁴

12.4 Conclusions

Growing requirements for safety and environmental controls has led to the development of voltammetric and amperometric methods for determination of explosives described in this chapter. Further development can be envisaged, especially in the field of nano-material-based electrochemical devices for detection of explosives,¹⁵ namely at graphene, carbon nanotubes, nanoparticles, and nanoporous materials, and composites of these materials. Electrochemical sensors offer rapid, sensitive, inexpensive, and reliable detection of explosive materials in any conceivable scenario. Coupling these attractive properties with the portable nature of electrochemical devices facilitates a wide range of decentralized applications.

Acknowledgements This research was supported by the Ministry of Education, Youth and Sports of the Czech Republic (project LH 13002 Program KONTAKT II).

References

1. Agrawal JP, Hodgson RD (2007) *Organic chemistry of explosives*. Wiley, Chichester
2. Akhavan J (2004) *The chemistry of explosives*, 2nd edn. Royal Society of Chemistry, Cambridge
3. Ageui L, Vega-Montenegro D, Yanez-Sedeno P et al (2005) Rapid voltammetric determination of nitroaromatic explosives at electrochemically activated carbon-fiber electrodes. *Anal Bioanal Chem* 382:381–387
4. Wang J (2007) Electrochemical sensing of explosives. *Electroanalysis* 19:415–423
5. Caygill JS, Davis F, Higson SPJ (2012) Current trends in explosive detection techniques. *Talanta* 88:14–29
6. Singh S (2007) Sensors—an effective approach for the detection of explosives. *J Hazard Mater* 144:15–28
7. Yinon J (2002) Field detection and monitoring of explosives. *Trends Anal Chem* 21:292–301
8. Senesac L, Thundat TG (2008) Nanosensors for trace explosive detection. *Mater Today* 11:28–36
9. Bureau of Alcohol, Tobacco, Firearms, and Explosives (2013) *Commerce in explosives; list of explosives materials*. Fed Reg 78:64246–64247
10. Barek J, Fischer J, Wang J (2011) Voltammetric and amperometric detection of nitrated explosives (a review). In: Kalcher K, Metelka R, Svancara I et al (eds) *Sensing in electroanalysis*, vol 6. University Press Centre, Pardubice, pp 139–147
11. Vyskocil V, Barek J (2011) Electroanalysis of nitro and amino derivatives of polycyclic aromatic hydrocarbons. *Curr Org Chem* 15:3059–3076
12. Cizek K, Prior C, Thammakhet C et al (2010) Integrated explosive preconcentrator and electrochemical detection system for 2,4,6-trinitrotoluene (TNT) vapor. *Anal Chim Acta* 661:117–121
13. Barek J, Peckova K, Vyskocil V (2008) Adsorptive stripping voltammetry of environmental carcinogens. *Curr Anal Chem* 4:242–249
14. Galik M, O'Mahony AM, Wang J (2011) Cyclic and square-wave voltammetric signatures of nitro-containing explosives. *Electroanalysis* 23:1193–1204
15. O'Mahony AM, Wang J (2013) Nanomaterial-based electrochemical detection of explosives: a review of recent developments. *Anal Methods* 5:4296–4309
16. Chua CK, Pumera M (2011) Influence of methyl substituent position on redox properties of nitroaromatics related to 2,4,6-trinitrotoluene. *Electroanalysis* 23:2350–2356
17. Chua CK, Pumera M, Rulisek L (2012) Reduction pathways of 2,4,6-trinitrotoluene: an electrochemical and theoretical study. *J Phys Chem C* 116:4243–4251
18. Bratin K, Kissinger PT, Briner RC et al (1981) Determination of nitro aromatic, nitramine, and nitrate ester explosive compounds in explosive mixtures and gunshot residue by liquid-chromatography and reductive electrochemical detection. *Anal Chim Acta* 130:295–311
19. Ly SY, Kim DH, Kim MH (2002) Square-wave cathodic stripping voltammetric analysis of RDX using mercury-film plated glassy carbon electrode. *Talanta* 58:919–926
20. Wang J, Pumera M (2006) Microchip flow-injection analysis of trace 2,4,6-trinitrotoluene (TNT) using mercury-amalgam electrochemical detector. *Talanta* 69:984–987
21. O'Mahony AM, Valdes-Ramirez G, Windmiller JR et al (2012) Orthogonal detection of nitroaromatic explosives via direct voltammetry coupled to enzyme-mediated biocatalysis. *Electroanalysis* 24:1811–1816
22. Saravanan NP, Venugopalan S, Senthilkumar N et al (2006) Voltammetric determination of nitroaromatic and nitramine explosives contamination in soil. *Talanta* 69:656–662
23. Wang J, Thongngamdee S (2003) On-line electrochemical monitoring of (TNT) 2,4,6-trinitrotoluene in natural waters. *Anal Chim Acta* 485:139–144
24. Wang J, Thongngamdee S, Lu D (2006) Sensitive voltammetric sensing of the 2,3-dimethyl-2,3-dinitrobutane (DMNB) explosive taggant. *Electroanalysis* 18:971–975

25. Fu X, Benson RF, Wang J et al (2005) Remote underwater electrochemical sensing system for detecting explosive residues in the field. *Sens Actuators B* 106:296–301
26. Honeychurch KC, Hart JP, Pritchard PRJ et al (2003) Development of an electrochemical assay for 2,6-dinitrotoluene, based on a screen-printed carbon electrode, and its potential application in bioanalysis, occupational and public health. *Biosens Bioelectron* 19:305–312
27. Chen J-C, Shih J-L, Liu C-H et al (2006) Disposable electrochemical sensor for determination of nitroaromatic compounds by a single-run approach. *Anal Chem* 78:3752–3757
28. Wang J, Lu F, MacDonald D et al (1998) Screen-printed voltammetric sensor for TNT. *Talanta* 46:1405–1412
29. Pumera M (2006) Analysis of explosives via microchip electrophoresis and conventional capillary electrophoresis: a review. *Electrophoresis* 27:244–256
30. Pumera M (2008) Trends in analysis of explosives by microchip electrophoresis and conventional CE. *Electrophoresis* 29:269–273
31. Wang J, Tian BM, Sahlin E (1999) Micromachined electrophoresis chips with thick-film electrochemical detectors. *Anal Chem* 71:5436–5440
32. Vyskocil V, Barek J (2009) Mercury electrodes—possibilities and limitations in environmental electroanalysis. *Crit Rev Anal Chem* 39:173–188
33. Danhel A, Barek J (2011) Amalgam electrodes in organic electrochemistry. *Curr Org Chem* 15:2957–2969
34. Yosypchuk B, Barek J (2009) Analytical applications of solid and paste amalgam electrodes. *Crit Rev Anal Chem* 39:189–203
35. Niaz A, Fischer J, Barek J et al (2009) Voltammetric determination of 4-nitrophenol using novel type of silver amalgam paste electrode. *Electroanalysis* 21:1786–1791
36. Jacobsen M, Duwensee H, Wachholz F et al (2010) Directly heated bismuth film electrodes based on gold microwires. *Electroanalysis* 22:1483–1488
37. Lezi N, Vyskocil V, Economou A et al (2012) Electroanalysis of organic compounds at bismuth electrodes: a short review. In: Kalcher K, Metelka R, Svancara I et al (eds) *Sensing in electroanalysis*, vol 7. University Press Centre, Pardubice, pp 71–78
38. Wang J, Chen G, Chatrathi MP et al (2003) Microchip capillary electrophoresis coupled with a boron-doped diamond electrode-based electrochemical detector. *Anal Chem* 75:935–939
39. Pearson R, Rogers K (2000) Electrochemical technique for detection of TNT using disposable screen-printed electrodes. Paper present on environmental chemistry: emphasis on EPA and EPA supported research, American Chemical Society, Division of Environmental Chemistry, Washington, DC, 20–24 Aug 2000
40. Wang J, Thongngamdee S, Kumar A (2004) Highly stable voltammetric detection of nitroaromatic explosives in the presence of organic surfactants at a polyphenol-coated carbon electrode. *Electroanalysis* 16:1232–1235
41. Tang L, Feng H, Cheng J et al (2010) Uniform and rich-wrinkled electrophoretic deposited graphene film: a robust electrochemical platform for TNT sensing. *Chem Commun* 46:5882–5884
42. Chen T-W, Sheng Z-H, Wang K et al (2011) Determination of explosives using electrochemically reduced graphene. *Chem Asian J* 6:1210–1216
43. Pumera M (2010) Graphene-based nanomaterials and their electrochemistry. *Chem Soc Rev* 39:4146–4157
44. Pumera M (2009) Electrochemistry of graphene: new horizons for sensing and energy storage. *Chem Rec* 9:211–223
45. Pumera M (2011) Graphene-based nanomaterials for energy storage. *Energy Environ Sci* 4:668–674
46. Wang J, Hocevar SB, Ogorevc B (2004) Carbon nanotube-modified glassy carbon electrode for adsorptive stripping voltammetric detection of ultratrace levels of 2,4,6-trinitrotoluene. *Electrochem Commun* 6:176–179
47. Rezaei B, Damiri S (2010) Using of multi-walled carbon nanotubes electrode for adsorptive stripping voltammetric determination of ultratrace levels of RDX explosive in the environmental samples. *J Hazard Mater* 183:138–144

48. Filanovsky B, Markovsky B, Bourenko T et al (2007) Carbon electrodes modified with TiO₂/metal nanoparticles and their application to the detection of trinitrotoluene. *Adv Funct Mater* 17:1487–1492
49. Riskin M, Tel-Vered R, Bourenko T et al (2008) Imprinting of molecular recognition sites through electropolymerization of functionalized Au nanoparticles: development of an electrochemical TNT sensor based on π -donor-acceptor interactions. *J Am Chem Soc* 130:9726–9733
50. Wang J, Liu G, Wu H et al (2008) Sensitive electrochemical immunoassay for 2,4,6-trinitrotoluene based on functionalized silica nanoparticle labels. *Anal Chim Acta* 610:112–118
51. Zhang H-X, Cao A-M, Hu J-S et al (2006) Electrochemical sensor for detecting ultratrace nitroaromatic compounds using mesoporous SiO₂-modified electrode. *Anal Chem* 78:1967–1971
52. Shi G, Qu Y, Zhai Y et al (2007) {MSU/PDDA}_n layer-by-layer assembled modified sensor for electrochemical detection of ultratrace explosive nitroaromatic compounds. *Electrochem Commun* 9:1719–1724
53. Trammell SA, Zeinali M, Melde BJ et al (2008) Nanoporous organosilicas as preconcentration materials for the electrochemical detection of trinitrotoluene. *Anal Chem* 80:4627–4633
54. Fu X-C, Chen X, Wang J et al (2010) Amino functionalized mesoporous silica microspheres with perpendicularly aligned mesopore channels for electrochemical detection of trace 2,4,6-trinitrotoluene. *Electrochim Acta* 56:102–107
55. Zang J, Guo CX, Hu F et al (2011) Electrochemical detection of ultratrace nitroaromatic explosives using ordered mesoporous carbon. *Anal Chim Acta* 683:187–191
56. Poh HL, Pumera M (2012) Nanoporous carbon materials for electrochemical sensing. *Chem Asian J* 7:412–416
57. Guo SJ, Wen D, Zhai YM et al (2010) Platinum nanoparticle ensemble-on-graphene hybrid nanosheet: one-pot, rapid synthesis, and used as new electrode material for electrochemical sensing. *ACS Nano* 4:3959–3968
58. Guo CX, Lu ZS, Lei Y et al (2010) Ionic liquid-graphene composite for ultratrace explosive trinitrotoluene detection. *Electrochem Commun* 12:1237–1240
59. Guo S, Wen D, Zhai Y et al (2011) Ionic liquid-graphene hybrid nanosheets as an enhanced material for electrochemical determination of trinitrotoluene. *Biosens Bioelectron* 26:3475–3481
60. Hrapovic S, Majid E, Liu Y et al (2006) Metallic nanoparticle-carbon nanotube composites for electrochemical determination of explosive nitroaromatic compounds. *Anal Chem* 78:5504–5512
61. Zhang H-X, Hu J-S, Yan C-J et al (2006) Functionalized carbon nanotubes as sensitive materials for electrochemical detection of ultra-trace 2,4,6-trinitrotoluene. *Phys Chem Chem Phys* 8:3567–3572
62. Polsky R, Stork CL, Wheeler DR et al (2009) Multivariate analysis for the electrochemical discrimination and quantitation of nitroaromatic explosives. *Electroanalysis* 21:550–556
63. Marple RL, LaCourse WR (2005) Application of photoassisted electrochemical detection to explosive-containing environmental samples. *Anal Chem* 77:6709–6714
64. Wang J, Pumera M, Chatrathi MP et al (2002) Single-channel microchip for fast screening and detailed identification of nitroaromatic explosives or organophosphate nerve agents. *Anal Chem* 74:1187–1191
65. Hetman JS (1973) Polarography of explosives. *Fresenius J Anal Chem* 264:159–164
66. Zimmermann Y, Broekaert JAC (2005) Determination of TNT and its metabolites in water samples by voltammetric techniques. *Anal Bioanal Chem* 383:998–1002
67. Chen W, Wang Y, Brueckner C et al (2010) Poly[meso-tetrakis(2-thienyl)porphyrin] for the sensitive electrochemical detection of explosives. *Sens Actuators B* 147:191–197
68. Ong BK, Poh HL, Chua CK et al (2012) Graphenes prepared by hummers, Staudenmaier and Hofmann methods for analysis of TNT-based nitroaromatic explosives in seawater. *Electroanalysis* 24:2085–2093

69. Pesavento M, D'Agostino G, Alberti G et al (2013) Voltammetric platform for detection of 2,4,6-trinitrotoluene based on a molecularly imprinted polymer. *Anal Bioanal Chem* 405:3559–3570
70. Sarlauskas J, Krikstopaitis K, Miliukiene V et al (2011) Investigation on the electrochemistry and cytotoxicity of organic nitrates and nitroamines. *Cent Eur J Energ Mater* 8:15–24

Chapter 13

Pesticides

Elmorsy Khaled and Hassan Y. Aboul-Enein

13.1 Introduction

The term “pesticide” refers to a variety of products which are intended for destroying or controlling any pest. The term pesticides may also include substances intended for use as plant-growth regulators, defoliants, agents for preventing the premature fall of fruit, and chemicals applied to crops either before or after harvest to inhibit deterioration during storage or transport. Pesticides have been used to a limited degree since ancient times (1550 BC); but, in the last decades, not only the number of pesticides and their tonnage have increased, but also the number and variety of their uses.^{1–3} Nowadays, approximately 1,000 pesticide active ingredients are recognized worldwide.⁴ Common subclasses of pesticides are insecticides, fungicides, herbicides, molluscicides, rodenticides, and plant growth regulators which have become important in agriculture, mainly in the developed countries, but also progressively more in developing countries. Modern developed and developing countries utilize millions of synthetic organic compounds in their civilian, commercial, and defense sectors for an ever-expanding diversity of uses.⁵

Pesticides are sprayed in large amounts, also because only 1 % reaches the intended target. Some of these contaminants have long half-lives and thus persist to varying degrees in the environment. They migrate through large regions of soil until to reach water resources, where they may present an ecological or human-health threat.⁶ Organisms, vegetation, animals, and humans are affected by various chemicals through absorption, inhalation, or ingestion. These contaminants pose

E. Khaled (✉)

Microanalysis Laboratory, National Research Centre, Dokki, Giza 12262, Egypt
e-mail: elmorsykhaled@yahoo.com

H.Y. Aboul-Enein

Pharmaceutical and Medicinal Chemistry Department, National Research Centre,
Dokki, Giza 12262, Egypt

serious fatal health hazards to humans, such as asthma, birth defects, and deaths. However, the presence of pesticide residues in food, water, and soil has become a major issue in environmental chemistry.^{2,7} Pesticides are recommended for use with a minimum of 14 days before harvesting. Nevertheless, residues can be detected in the crops even a month after their application.⁸ Moreover, some procedures for food processing, i.e., oil refinery, can result in additional accumulation of pesticides and formation of products that are more toxic than the parent compound.⁹

Among pesticides, organophosphorus (OP) and carbamate insecticides form an important class of toxic compounds. These neurotoxic substances, which are structurally similar to the nerve gases soman and sarin, irreversibly inhibit the enzyme acetylcholinesterase (AChE). This enzyme hydrolyzes the neurotransmitter acetylcholine (ACh) in the synaptic membrane in order to avoid its accumulation. AChE inhibition and subsequent ACh accumulation cause a marked dysfunction of many autonomic and behavioral systems, eventually leading to respiratory paralysis and death.^{10–16} Exposure to low levels of some organophosphates also results in long-term (chronic) neurotoxic effects, related to the inhibition of neuropathy target esterase (delayed polyneuropathy).¹⁷ In addition, anticholinesterase pesticides cause frequent poisoning of agricultural workers mainly in developing countries.¹⁸ Furthermore, the continuous exposure to organophosphorus compounds has been linked to chronic fatigue syndrome.¹⁹ The ability of pesticides to interact with estrogen receptors, androgen receptors, thyroid receptors, and other types of endocrine-disrupting effects have been researched to a limited extent and many long-term effects are still unknown.^{20–24} The toxicity of organophosphate and carbamate pesticides varies considerably depending on the chemical structure of the pesticide.^{16,25}

13.2 Pesticide Analysis

Their toxicity justifies the crucial need of accurate and reliable methods to monitor the level of pesticides for safety considerations. Moreover, the area of biodefense is also interesting in this field of research, since several organophosphate compounds can be used as nerve agents (i.e., sarin and soman). The development and continual improvement of analytical methods for the determination of this large group of compounds, mostly at trace level, is a great challenge for analysts, and constitutes the subject of research and development for contemporary analytical chemistry.^{26–28}

Colorimetry,²⁹ capillary electrophoresis (CE),³⁰ mass spectrometry (MS),³¹ gas chromatography (GC),³² high-performance liquid chromatography (HPLC),^{33,34} thin-layer chromatography³⁵ coupled with different detectors, and spectral techniques are the most commonly employed methods for trace environmental analysis of pesticides and also are part of regulations in monitoring the environmental pollutants.

In spite of the advantages of chromatographic techniques, these methods do not easily allow continuous on-site monitoring and usually require previous pretreatments. Assay procedures with complex and expensive equipment, and demand of a

qualified and experienced staff, prohibit its use for rapid analyses under field conditions.³⁶ In addition, chromatographic techniques usually generate waste containing organic solvents, which require their treatment after analysis. Gas chromatography is undoubtedly the most common method and when coupled to an FTIR or mass spectrometer it has the unique ability to “fingerprint” pesticides. However, because of their thermal lability, low volatility, and high polarity some pesticides can be missed in any surveillance analysis by this technique.³⁷ Furthermore, immunoassays require long analysis time (1–2 h), fastidious sample handlings (numerous washing steps), and a considerable quantity of plastic well kits which are expensive; additionally, these techniques are not suitable for continuous monitoring.

The current tendency to carry out field monitoring has driven the development of biosensors as new analytical tools able to provide fast, reliable, and sensitive measurements with lower cost; many of them aimed at on-site analysis. In this sense, biosensors would not compete with official analytical methods, but they can be used both by regulatory authorities and by industry to provide enough information for routine testing and screening of samples. On the other hand, biosensors offer the possibility of determining not only specific chemicals, but also their biological effects, such as toxicity or endocrine-disrupting effects, which is an information of great interest. Thus, they are suitable as a screening tool providing a rapid response and signalling the existence of contaminated samples.

Biosensors are generally defined as analytical devices, incorporating a biological or biologically derived sensing element (e.g., enzymes, antibodies, microorganisms, or DNA), either intimately associated with or integrated within a physicochemical transducer (e.g., electrochemical, optical, or piezoelectric transducers^{38–41}). Biosensors, because of their biological base, can represent an ideal sensing systems to monitor the effects of pollution on both flora and fauna, e.g., toxicity sensors, while on the other hand, the exquisite specificity of some enzymes can even distinguish between stereoisomers of the same compound.

As many pesticides are designed to inhibit various enzymes in insects and other pests, utilizing these enzymes for detection purposes seemed a logical route. In this manner, enzymes such as acetylcholinesterase, butyrylcholinesterase, alkaline and acid phosphatase, tyrosinase, organophosphorus hydrolase, aldehyde dehydrogenase, and others were investigated for their ability to detect pesticides in water and other matrices such as soil, food, and beverages. In the initial stages of the development of analytical biosensors, in the early 1960s, research was focused only on clinical applications. Isolated from various organisms, acetylcholinesterase (AChE) was already used in the early 1950s for the determination of pesticides in measuring systems with potentiometric detection.^{42,43} In the middle 1980s it was used for the construction of the first integrated amperometric and potentiometric biosensors for the detection of pesticides based on inhibition of this enzyme.^{44,45} Rapid progress in the development of biosensors was observed in the recent decade where the design of biosensors for the determination of pesticides with other enzymes had been applied. Enzymatic determinations of pesticides are usually based on inhibition. The methodology involves the measurement of the uninhibited

activity of the enzyme, followed by an incubation period for the reaction between enzyme and inhibitor, and measurement of the enzyme activity after the inhibition. Several books and review articles are already published about the achievements in this field.^{26,27,38–41,46–66} One of the advantages of biosensors over other analytical techniques is the fact that because they are biologically based biosensors can measure toxicity, whereas analytical techniques measure only concentration. The magnitude of response from biosensor correlated directly with the acute toxicity of the pesticide in question is expressed as LD₅₀ (oral) for rats.

13.3 Biosensors for Pesticide Analysis

13.3.1 *Biosensors Based on Enzymatic Inhibition*

A huge number of methods based on enzyme inhibition-based biosensors can be found in the literature.⁶⁷ Most times (57.6 %) acetylcholinesterase, butyrylcholinesterase, or cholinesterase are used followed by tyrosinase (13 %) mainly combined with electrochemical procedures (44.5 % amperometric, 35.8 % potentiometric, frequently based on oxygen and pH measurements, and, to a very less extent, piezoelectrical).

13.3.2 *Cholinesterase Biosensors*

Acetylcholinesterases (AChE) are a class of enzymes that catalyze the hydrolysis of acetylcholine, an ester which is a neurotransmitter.^{13,15} AChE is present in mammals, birds, fish, reptiles, and insects.¹⁵ Cholinesterase inhibition occurs because pesticide molecules have a shape that resembles the shape of the substrate, thus blocking the active esteric center of the enzyme inhibiting its activity. The inhibition of AChE by organophosphates takes place as a result of the phosphorylation of the serine residue in the active site of the enzyme. The hydroxyl group on the serine residue acts as an electrophile which attacks the nucleophilic phosphorus. The phosphorylated enzyme is highly stable and hydrolysis of acetylcholine is blocked.¹⁵ In some cases, depending on the chemical structure of the pesticide, phosphorylation, and thus inhibition, may be irreversible. The inhibition of the enzyme causes a buildup of acetylcholine in the neural synapses. The free enzyme may be restored by a nucleophilic attack of water on the bond between phosphorus and enzyme.¹³ If this takes place, the enzyme can be restored to its active state. If the pesticide is a phosphorothionate ester with a P = S moiety rather than a P = O, it generally acts as a poor cholinesterase inhibitor, due to the low reactivity of the compound.¹³ However, they display a high level of toxicity towards insects as a result of the oxidation of the P = S to a P = O moiety through the metabolic action

of a set of enzymes termed mixed function oxidases (MFOs). Oxidation activates the compound *in vivo* which increases its reactivity and toxicity. The principle of cholinesterase inhibition in a biosensor may be inadequate or fail to detect phosphorothionate esters. This can be overcome by chemically oxidizing the phosphorothionate ester into its more active form prior to detection.⁶⁸ Carbamate pesticides are cholinesterase inhibitors with a similar mechanism of action as organophosphate pesticides.¹⁵ Analogously, the hydroxyl of the serine residue within the active site of the enzyme is carbamylated.

AChE has been used extensively for the enzymatic detection of organophosphates as well as carbamate pesticides, nerve agents, several natural toxins,^{69,70} and some drugs.⁷¹ Hence, AChE is widely used as a potent recognition element for the construction of biosensors for pesticide detection.^{72,73} Biosensors based on AChE as well as butyrylcholinesterase were first reported during the 1980s. Since then, there has been a continuous improvement of cholinesterase-based biosensors due to the gradual improvement of transducer devices and the availability of pure enzymes.⁷³

Most of the biosensors constructed for the determination of OPs are based on an electrochemical transducer, which is usually incorporated in a single unit with the biological recognition element. Both amperometric and potentiometric cholinesterase biosensors were developed and demonstrated comparable analytical parameters. It was pointed out previously^{60,74} that potentiometric biosensors are preferable for inhibitor measurement than amperometric ones, due to their higher inhibitor sensitivity and in general their much easier preparation technique and measurement procedure. Furthermore, the potentiometric working principle fits better to *in-field* measurements. Many configurations can be found in literature as described in the following.

13.3.2.1 Single-Enzyme System

When using acetylcholine (ACh) or butyrylcholine (BCh) as a substrate, the reaction products are choline (Ch) and the corresponding organic acid (Fig. 13.1).

Since choline is not electrochemically active, the change of enzyme activity is detected by the pH variation due to the acid production at the surface of the biosensor. In this case the electrochemical method of choice is a potentiometric one.

There are no natural substrates producing electroactive species; therefore, with amperometric measurements, artificial substrates such as butyrylthiocholine (BTCh) or acetylthiocholine (ATCh) are used. The products of the reaction are thiocholine (TCh) and an organic acid that can be oxidized anodically using platinum electrodes, but chemically modified carbon electrodes are a better option (Fig. 13.2).

13.3.2.2 Bi-enzyme System

In this system cholinesterase (ChE) is coupled to a second enzyme to transform one of the products of the hydrolysis reaction into another product that can be detected

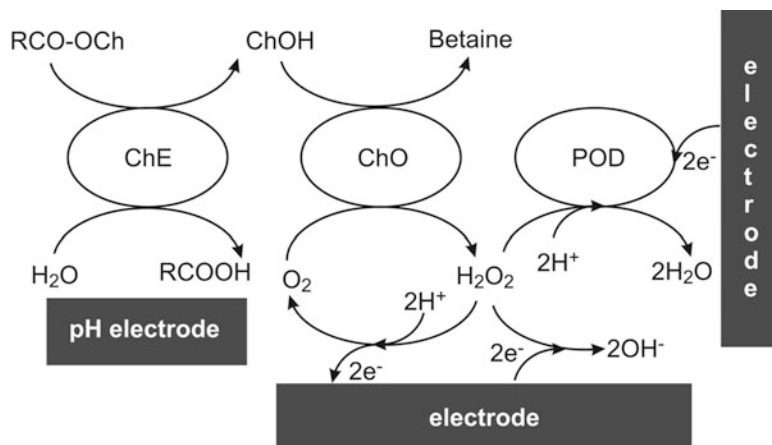


Fig. 13.1 Measurement principle of choline esterase (ChE) activity using R-choline (RCO-OCh) as substrate. According to the enzymes used in the recognition process, transduction may be potentiometric or amperometric; adapted from reference ⁽⁵²⁾ and modified; ChO—choline oxidase, POD—peroxidase, RCOOH—organic acid, ChOH—choline

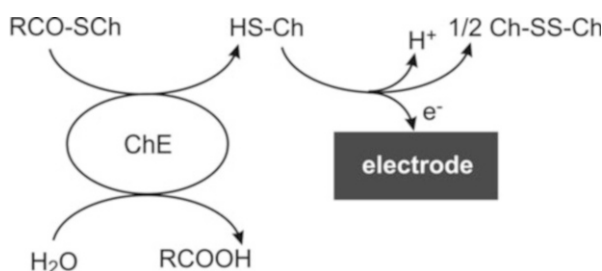


Fig. 13.2 Measurement principle of the choline esterase (ChE) activity using R-thiocholine (RCO-SCh) as substrate using an amperometric transducer, adapted from reference ⁽⁵²⁾ and modified; RTCh—thiocholine ester, RH—organic acid

amperometrically. When butyrylcholinesterase (BChE) or acetylcholinesterase (AChE) are used with choline oxidase (ChO), the enzyme system can be coupled to amperometric H_2O_2 or O_2 devices. Normally, the detection of O_2 is achieved with Clark electrodes and H_2O_2 with platinum, graphite, or screen-printed electrodes polarized to a fixed potential.

13.3.2.3 Tri-Enzyme System

Peroxidase (POD) may be added to the bi-enzyme system to build a tri-enzyme device. Multienzyme systems pose greater challenges than mono-enzyme ones. However, they produce biosensors that are more specific and less prone to

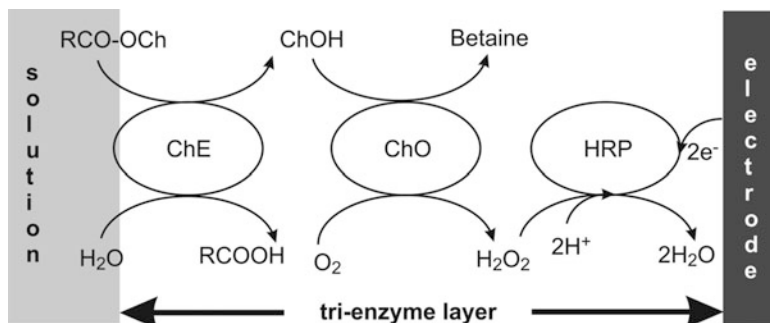


Fig. 13.3 Consequence of the enzymatic reaction at tri-enzymatic electrode surface adapted and modified from reference ⁽⁷⁶⁾

interferences.⁷⁵ The most frequently used electrochemical transducers are hydrogen peroxide electrodes (usually platinum is used as the working electrode material). The amperometric signal in this case is due to electrooxidation of hydrogen peroxide, which is the coproduct of the enzymatic choline oxidation (Fig. 13.3).

13.3.2.4 Cholinesterase Potentiometric Sensors

Potentiometric devices have a relatively high sensitivity and selectivity and a broad response range. They are also simple, reliable, and inexpensive and use commonly available instrumentation. Potentiometric enzyme-based biosensor systems have been recently reviewed.^{51,52,56,62} The most general approach for the determination of OP compounds (OPCs) is based on their inhibition of the activity of choline esterase enzymes. The presence of low concentrations of inhibitors strongly and specifically affects the enzyme activity. Therefore, by measuring the enzyme activity, the concentration of the OPCs can be assayed. Different enzymes, such as acetylcholine (ACh), BuCh, and, most often, pH sensors, were used as transducers in potentiometric biosensors.

pH-Based Potentiometric Sensors

Potentiometric biosensors for OPCs have been designed based on the measurement of pH change. Most of them are based on the determination of the H^+ liberated during the hydrolysis of acetylcholine by using different H^+ -sensitive electrodes.

Tran-Minh et al.⁷⁷ have used glass pH electrodes coated with an AChE, acrylamide/methacrylamide polymer membrane as the internal detector for the pH change. After incubating the electrodes for 1 h in the presence of paraoxon or malathion, the reduced steady-state potentials in buffered aqueous solutions containing ACh could be measured within 8–10 min with low limits of detection of 10^{-10} M and 10^{-9} M for malathion and paraoxon, respectively. The enzyme

could be fully reactivated with 1 mM 2-pyridine aldoxime (2-PAM), suggesting that this biosensor could be used repeatedly. More recently, Kumaran and Morita⁷⁸ have measured OP pesticides in soil extracts using butyrylcholinesterase immobilized on commercially available, pre-activated nylon-polyamide membranes held in place at the surface of a pH electrode by a nylon mesh. The response to the addition of substrate (BuCh) before and after inhibition by OP compounds was measured after a set time interval. The stated detection limit for ethyl parathion was 3.9 ppm in the soil. Although the biosensor lost 65–85 % of its original activity after 3–7 days in buffer, the dried enzyme membranes retained their original activity even after 3-year storage at 4 °C. The advantages of this system are its low cost and the ease of preparing and replacing the enzyme membrane. Thus, there is no need to reactivate and reuse the membranes after enzyme inhibition; they may be disposed of after each use. It was demonstrated that the oxidation of the organophosphorus compounds to their oxon forms by bromine, prior to analysis, enhances the sensitivity of the pH measurement and decreases the detection limit.⁶⁸

A new potentiometric enzymatic membrane biosensor for the detection of organophosphorus pesticides (OPs) was recently constructed.⁷⁹ The basic element of this biosensor was a glass pH electrode modified with an immobilized acetylcholinesterase layer formed by entrapment with methylcellulose, *N,N*-dimethylformamide, and bovine serum albumin. It was shown that there is a good linear relationship between the inhibition rate and the negative logarithm of OP concentration in the range from 10^{-7} to 10^{-5} mol L⁻¹ with detection limits of 10^{-7} mol L⁻¹ for five pesticides. Measurement results obtained by the biosensor method were in good agreement with those obtained by gas chromatography. This method was successfully applied to detect OPs that remained in potted lettuce. In this study, chlorpyrifos was also determined by the conventional analytical method (i.e., GC).

A simple and convenient method was proposed for the preparation of fast response potentiometric acetylcholine (ACh) biosensors based on pH detection.⁸⁰ As signal transducer antimony pH electrodes with a flat, easily renewable surface were used. Among different techniques tested, immobilization of acetylcholinesterase (AChE) onto the antimony disk electrode surface by intermolecular cross-linkage of AChE and bovine serum albumin (BSA) via glutaraldehyde vapor in vacuum proved to be most advantageous with respect to the analytical parameters of the biosensor. The biosensor was tested for the determination of an organophosphorus insecticide, trichlorfon. After each inhibition measurement cycle the biosensor was reactivated in pyridin-2-aldoxime methiodide for prolonged lifetime. For a biosensor with an antimony electrode, a very fast response was reported (10 s) with a limit of detection for trichlorfon equal to 0.12 ppb (10 % of inhibition with 50-min incubation time). Satisfactory results have also been obtained using pH-sensitive oxide electrodes such as Pd/PdO or Ir/IrO₂.^{77,81}

A comparison of two solid-state biosensors for organophosphorus pesticide analysis was presented by Campanella et al.⁸² The indicating sensor was either a graphite electrode or a field-effect transistor (FET), coated with an ion-selective polymeric membrane sensitive to pH containing tridodecylamine. Liu et al.⁸³ proposed a potentiometric acetylcholinesterase biosensor based on a pH-sensitive PVC membrane

with plasma-polymerized ethylenediamine. Glow discharge plasma technique was utilized to deposit a film containing amino groups on the surface of the membrane. Such an approach made it possible to fabricate a very simple self-mounted acetylcholinesterase membrane directly attached to the PVC pH-sensing electrode surface. Two neutral carriers, dioctyloctadecylamine (DOODA) and *N,N*-didecylamino-methylbenzene (DAMAB), were compared, and the biosensor based on DAMAB showed better response characteristics. The biosensor was employed more than 200 times in 20 days, with the maximum response span of biosensor retaining 90 %.

Ion-sensitive field-effect transistors (ISFETs) were also used to fabricate potentiometric biosensors for OP compounds. Nyamsi-Hendji et al.⁸⁴ have constructed a differential ISFET-based system. Acetyl or butyryl cholinesterase with BSA was fixed from solution to the surface of one pH-FET by glutaraldehyde treatment. Inhibition by solutions of diisopropyl fluorophosphate (10^{-7} – 10^{-13} M) was almost complete in about 30 min. However, reactivation of the inhibited enzyme with 1 mM 2-PAM was insufficient (30–40 %), making the system of limited usefulness for repeated analyses. Stripping off the used enzyme membrane and recoating the FET is a time-consuming process.

Rapid detection of anticholinesterase insecticides was also reported by a reversible light addressable potentiometric sensor (LAPS) with an additional enzymatic step. LAPSs belong to the group of field-effect transistors where detection is based on potential difference between gate insulator and electrolyte solution.⁸⁵ In such biosensors for determination of pesticides, biotinylated AChE was immobilized on the biotinylated nitrocellulose membrane via a streptavidin bridge. The sensors were used for the detection of fluorophosphates (DFP), echothiophate,⁸⁶ and also numerous other insecticides.⁸⁷ Important features of LAPSs for the detection of AChE inhibitors are fastness (eight samples assayed simultaneously), precision, and reversibility.

Each type of transducer has its own advantage, e.g., small size and easy way of mass production for ISFETs, reference electrode free-action of the LAPSs, and general availability and simplicity in the case of pH electrodes. The analytical performance of biosensors based on pH detection depends, in general, much more on the origin of the enzyme, the way of its immobilization, and the measurement methodology rather than the type of transducer.

Generally, biosensors with pH detection offer a simple and well-adapted method for in-field analysis for the determination of OPs. Although potentiometric methods are fast and accurate, they show quite high detection limits. Furthermore, the detection of H^+ ions lacks sensitivity due to the consumption of protons by the buffer following proton liberation during the enzyme reaction. The disadvantage of this approach consists in the necessity to use a low buffer capacity of the sample. Thus, changes in pH could cause also changes in the enzyme activity. Commonly, the response time of these sensors was found to exceed 5 min. In order to perform inhibition measurements in a reliable way, before each measurement the components entered or generated in the reaction layer of the biosensor in the previous step should be washed out carefully. Thus, if a biosensor has a response time of 5 min (due to thick membranes or membranes of poor permeability) the time needed to wash out the membrane before each analysis step can be as long as 20 min;

therefore, the real analysis time is considerably increased. Although the relevant results published are convincing, a rather complicated sensor fabrication method requiring a large quantity of expensive, high specific activity enzyme is employed.

Substrate-Based Potentiometric Sensors

Membrane electrodes which are sensitive to choline esters can be applied for monitoring the AChE activity and their inhibition by pesticides. These potentiometric sensors are usually designed on the basis of ion pair formation between acetylcholine with different ion-pairing agents such as tetraphenylborate or dipicrylamine. Both liquid-state membrane electrodes and PVC-based polymeric types of sensors have been developed.

Baum and Ward reported the potentiometric determination of a pesticide using an acetylcholine-sensitive liquid membrane electrode.⁸⁸ They achieved detection limits in the useful concentration ranges of 10–100 ng/mL for paraoxon and 50–300 ng/mL for tetram. The detection limit of their method seemed to be determined by interference from choline, a product of the enzyme reaction, and the detection limit of the acetylcholine electrode itself.

A potentiometric acetylcholine biosensor with selective membranes consisting of two layers was also reported⁸⁹; one membrane was a choline- and H⁺-selective membrane with the choline-phosphotungstate ion pair in PVC as an electroactive compound, and the second layer was loaded with AChE. A highly sensitive potentiometric butyrylcholine (BuCh) sensor based on plasticized poly(vinyl chloride) membrane was fabricated using tetrakis (3,5-bis[2-methoxy-hexafluoro-methyl] phenyl) borate (HFPB) as a cation exchanger.⁹⁰ The sensor showed a Nernstian response from 10⁻¹ to 10⁻⁶ M for BuCh with high selectivity (6.3×10^{-3}) towards BuCh against the reaction product (Ch). Determinations of organophosphate pesticides, 2,2-dichlorovinyl-dimethylphosphate and *o*-(4-bromo-2-chlorophenyl)*o*-ethyl *S*-propylphosphothiolate, were conducted by measuring inhibition of the enzyme activity. The enzyme reaction rate was related to the concentration of pesticides. Pesticides were successfully determined between micromole and sub-nanomole levels by the BuCh sensor. A butyrylcholine-selective polymeric membrane electrode using *o*- β -cyclodextrin as ionophore was described as a reagent controlled-release system for reagentless detection of butyrylcholinesterase.⁹¹ BuCh released across the membrane from the inner filling solution of the ion-selective electrode was consumed by the reaction of the enzyme in the sample solution, and the concentration of BuCh at the membrane surface could be sensed potentiometrically. The electrode with 0.01 M butyrylcholine in the inner solution yielded a potential that varied linearly with a butyrylcholinesterase concentration over the range of 0.0075–0.15 U mL⁻¹ in sodium phosphate buffer solution. This approach could also be used to analyze organophosphate pesticides (parathion) in the concentration range 0.05–0.5 ng mL⁻¹ with a detection limit of 0.03 ng mL⁻¹.

β -Cyclodextrin (β -CD)-based polyvinylchloride (PVC) and carbon paste electrodes (CPEs) were fabricated and applied for the potentiometric determination of

different acetylcholine (ACh) derivatives, namely butyrylcholine (BCh), acetylmethylcholine (AmCh), and acetylthiocholine (AtCh).⁹² Matrix composition optimization was done with respect to type and content of the sensing material, anionic sites, and plasticizer. Electrodes incorporated with heptakis (2,3,6-tri-*o*-methyl)- β -CD as sensing ionophore, potassium tetrakis (4-fluorophenyl) borate (KTFPB) as anionic site, and *o*-nitrophenyloctyl ether (*o*-NPOE) as electrode plasticizer showed the best electroanalytical performances. The fabricated electrodes worked satisfactorily in the concentration range from 10^{-6} to 10^{-2} mol L⁻¹. The developed sensors possessed improved selectivity towards various acetylcholine derivatives rather than choline. The sensors have been successfully applied for the potentiometric determination of ACh and its derivatives under flow injection analysis (FIA) and potentiometric titration conditions. The same authors⁹³ developed a highly sensitive disposable screen-printed butyrylcholine (BuCh) potentiometric sensor, based on heptakis (2,3,6-tri-*o*-methyl)- β -cyclodextrin for butyrylcholinesterase (BuChE) activity monitoring. Improved selectivity towards BuCh with minimal interference from choline (Ch) was achieved and the sensor was used for the determination of 0.06–1.25 U mL⁻¹ BuChE. The developed disposable sensors were successfully applied for real-time intoxication monitoring through assaying cholinesterase (ChE) activity in human serum. Determination of organophosphate pesticide was conducted by measuring their inhibition of BuChE, a successful assay for malathion in insecticide samples with high accuracy and precision.

More recently,⁹⁴ a rapid and sensitive disposable potentiometric sensor for the determination of the organophosphorus pesticide ethion and its degradation residues was fabricated. This study demonstrated the application of a screen-printed potentiometric sensor with multi-walled carbon nanotube (MWCNT)-modified polyvinylchloride (MWNT-PVC) based on α -cyclodextrin (α -CD) as ionophore for butyrylcholine (BuCh). The fabricated electrodes were used for measuring butyrylcholinesterase (BuChE) activity through monitoring of the BuCh hydrolysis. The electrode potential varied linearly with the BuChE concentration over a range from 0.04 to 0.4 U mL⁻¹ in phosphate buffer solution (pH 7.0). This approach could also be used to determine BuChE ethion in the concentration range from 0 to 330 ng mL⁻¹, by measuring the relative inhibition percentage of BuChE. From different ethion degradation products, inhibition by dioxon and monooxon was more potent than from the parent pesticide. The proposed method was applied to the determination of ethion in different samples with good accuracy and precision. The relative simple fabrication protocol of the biosensor, high sensitivity, and stability represented a promising approach for the determination of environmental pollutants under field conditions.

13.3.2.5 Cholinesterase Amperometric Sensors

The response of amperometric biosensors to various inhibitors is often considered to be a linear function of the enzyme activity, and calculations of kinetic parameters

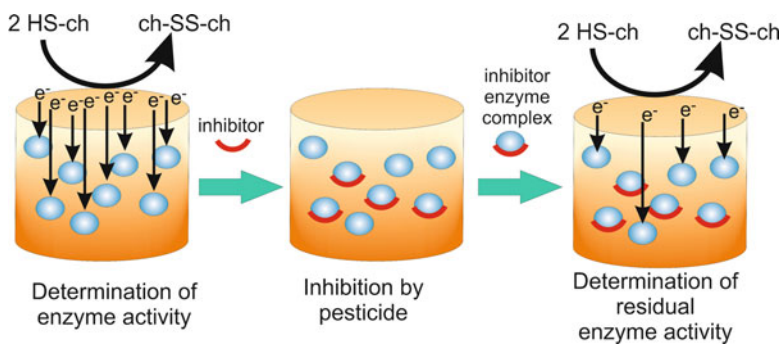


Fig. 13.4 Inhibitory effect of pesticides on cholinesterase amperometric sensor; arranged and modified from reference ⁽⁴⁹⁾

based on this assumption are in a good agreement with the results obtained with traditional measurements of the specific activity of the immobilized enzyme.⁹⁵

Three basic ways of amperometric monitoring of the inhibition of hydrolysis of choline esters have been used. Direct anodic measurement of choline or thiocholine using a biosensor either with or without a suitable mediator of the electron transfer was found in literature. Most often, indirect determination of choline is performed via amperometric measurement of hydrogen peroxide formed using a choline biosensor, either immobilized ChOD alone or with esterases. The third amperometric method which has been applied is monitoring of choline through the measurement of the concentration of oxygen consumed.

Single-Enzyme System

A number of papers describe techniques for the determination of choline esterase activity based on amperometric measurement of the product formed as a result of enzymatic hydrolysis. The oxidation potential of choline is too high to be electrochemically oxidized directly. In this case, artificial (nonnative) choline esterase substrates are used. Thus, butyryl or acetyl thiocholine forms thiocholine as a result of choline esterase hydrolysis. When the analyte is not present in the solution, the substrate acetylthiocholine is converted into thiocholine and acetic acid. Thiocholine is oxidized by the applied voltage. In the presence of an inhibitor, conversion of acetylthiocholine is decreased or even null.⁹⁶ Furthermore, the anodic oxidation current is inversely proportional to the concentration of pesticides in samples and the exposed time as well. The procedure of the preparation of an AChE biosensor and pesticide detection is shown in Fig. 13.4.

Thiol-containing compounds are known to undergo electrochemical oxidation processes at solid electrodes, but oxidations occur at relatively high potentials (ca. 0.7 V). The easiest way to solve the overpotential problem seems to be the use of an electron mediator, which facilitates the electron transfer. In this case, the

working potential of the enzyme electrode is determined by the oxidation potential of the mediator.

For example, Carlo and co-workers⁹⁷ modified the surface of a screen-printed carbon electrode with a thin layer of perfluorinated ion-exchanger films containing 7,7,8,8-tetracyanoquinodimethane (TCNQ) as mediator. It was found that the reduced form of TCNQ was oxidized at 0.4 V vs. the pseudo-reference electrode (Ag wire). The TCNQ-based biosensors were applied to a recovery test using egg, bovine meat, milk, and honey as food matrices. No false-negative or false-positive samples were detected in the assay.

The direct anodic detection of thiocholine formed using graphite electrodes modified with cobalt phthalocyanine was described.⁹⁸ For a BChE-containing biosensor, with a 10-min incubation time, the limit of detection for paraoxon was estimated as 1.5 ppb. The lifetime of membranes with immobilized esterases was 3 months. The disposable sensing electrode described by Skladal⁹⁹ comprised a layer of glutaraldehyde cross-linked cholinesterase over a cobalt phthalocyanine-modified carbon composite electrode formed on a plastic strip. With butyrylthiocholine as substrate the current due to the oxidation of the product, thiocholine, reached a steady state within a minute. Inhibition of cholinesterase by organophosphates over a period of 10 min resulted in a proportional decrease in current. For paraoxon the lower limit of detection was 0.3 nM. Skladal and Mascini¹⁰⁰ described an amperometric biosensor for organophosphate and carbamate pesticides which could detect nanogram levels of paraoxon and heptenophos within 3 min. AChE or BuChE was immobilized on a nylon net together with their relevant substrates. The inhibition of either acetylcholinesterase or butyrylcholinesterase by pesticides was measured by the decrease of the cleavage product of acetylthiocholine or butylthiocholine, i.e., thiocholine, which was monitored by direct electrochemical oxidation at 0.300 V (vs. Ag/AgCl). The use of a cobalt phthalocyanine-modified composite electrode overcame the problem of a high operation potential as would be required for a platinum electrode. Rippeth et al.¹⁰¹ avoided the problems related to electrode fouling by using cobalt phthalocyanine (CoPC)-modified SPEs, which allowed working at 0 V vs. Ag/AgCl, thus improving the selectivity. Furthermore, the replacement of the electrode after each measurement eliminated the need for enzyme regeneration. Another work using CoPC-modified SPEs was done by Bucur et al.¹⁰² The authors used AChE extracted from different sources as well as genetically modified mutants.

Neufeld et al.¹⁰³ developed a disposable micro-flow injection electrochemical biosensor, based on an AChE-modified nylon membrane attached to an SPE with hexacyanoferrate (III) in solution. The presence of this mediator allowed the determination of dichlorvos at +0.3 V vs. Ag/AgCl. Since the electrode was continuously washed by the flow stream, it was not necessary to clean it between repetitive measurements. This simplified the procedure and reduced analysis time.

Khayyami et al. used Meldola blue (MB) as electron mediator.¹⁰⁴ Although MB allows working at -0.1 V vs. Ag/AgCl, they applied a working potential of +0.25 V in order to accelerate the oxidation rate. At this potential, the background interference was higher, but the utility of the mediator was proved, since unwanted contributions to the signal from other electroactive compounds were minimized.

Another possibility in the development of amperometric biosensors is the use of *p*-aminophenyl acetate (PAPA) as AChE substrate, since the enzymatic product, *p*-aminophenol (PAP), can be detected by anodic oxidation at +0.25 V vs. Ag/AgCl.¹⁰⁵ The authors used a rapidly responding and sensitive amperometric biosensor in a flow injection system to estimate pesticide contaminants in spring water. The sensor was based on a glassy carbon electrode covered by a nylon membrane to which an acetylcholinesterase-BSA mixture was immobilized using glutaraldehyde. The determination of carbaryl and paraoxon was carried out in lagoon water and kiwi fruits. The lowest concentration of the pesticides determined in lagoon water was 1.0×10^{-7} M for paraoxon and 4.0×10^{-7} M for carbaryl.

Bi-enzyme Systems

Amperometric determination of pesticides based on inhibition of cholinesterases can be also carried out in bi-enzymatic systems with an additional enzymatic step involving choline oxidase. During the oxidation of choline by this enzyme oxygen is consumed and hydrogen peroxide is produced (see Figs. 13.1 and 13.3); hence, the change of the concentration of one of these species can be the basis for the amperometric response.

Bi-enzymatic determinations are carried out using biosensors either with only ChO or with both enzymes AChE and ChO immobilized. In the first case hydrogen peroxide can be measured with a Pt electrode at anodic polarization with the oxidase immobilized in a membrane.¹⁰⁶ Marty et al.¹⁰⁷ co-immobilized the two enzymes on a cellulose nitrate membrane. Acetylcholinesterase activity was proportional to the production of H₂O₂, which was measured at a Pt electrode. Decreases in current due to inhibition of acetylcholinesterase activity by as little as 10 nM paraoxon could be determined with a stability under wet storing conditions at 4 °C being of months. Trichlorfon was determined in water samples using AChE–ChOx biosensors, which were constructed by a layer-by-layer deposition of the enzymes on the surface of a platinum disk electrode.¹⁰⁸ The response of the sensor to trichlorfon was evaluated by a successive addition of trichlorfon to a solution of 2 mM ACh. The output current of the sensor decreased with increasing concentration of trichlorfon over the concentration range of 1×10^{-8} – 2×10^{-5} g mL⁻¹. A key point for constructing high-performance OP sensors in bi-enzyme systems may be to suitably control the ratio of the catalytic activity of AChE and ChOx in the sensor. The catalytic activity of ChOx should be higher than that of AChE—the overall rate of the reactions is determined by the rate of AChE-catalyzed reaction because OP compounds disturb this step. Therefore, usually excess amounts of ChOx are mixed with AChE and the ChOx–AChE mixture is immobilized on the surface of the electrode to make the AChE-catalyzed reaction a rate-limiting step.

A choline amperometric biosensor based on screen-printed configuration, immobilized by adsorption from aqueous solution on the surface of ruthenium-activated carbon electrodes, was assembled and used to assess the inhibitory effect of organophosphorus and carbamic pesticides on acetylcholinesterase activity both

in standard solutions and environmental samples.¹⁰⁹ An inhibition calibration curve was obtained using carbofuran with the lowest detectable standard solution $2 \mu\text{g L}^{-1}$ following an incubation time of 10 min. The method was then applied to samples of fruits and vegetables showing its suitability as a rapid screening assay (12 min per test) for the assessment of anticholinesterase pesticides. The biosensor results were compared with a standard analytical technique (gas chromatography with a nitrogen phosphorus detector, GC-NPD).

Oxygen amperometric sensors (Clark-type electrodes) have been also used as basic transducers for the construction of choline electrodes.¹¹⁰ The signal in this case is based on the reduction of molecular oxygen which is the co-reactant for the oxidation of choline. Free acetylcholinesterase was more sensitive to paraoxon than immobilized acetylcholinesterase, depending on the nature and concentration of solvent (500-fold in the presence of 5 % cyclohexane). Under these conditions, as low as 10^{-9} M paraoxon could be detected. The sensitivity of paraoxon detection with free acetylcholinesterase in the presence of 5 % cyclohexane corresponded to 0.2 ppb paraoxon, tenfold below the limit admitted in the European Economic Community.

Similar other sensors were also reported.¹¹¹ In this case one or two enzymes were immobilized on a cellulose triacetate membrane. It was shown that better results were obtained for the determination of pesticides when BChE was used instead of AChE, and a better detection limit was achieved with the esterase present in solution rather than immobilized together with ChOx on the membrane. The fabricated sensor was sensitive to malathion.

Low-molecular-weight redox mediators have been used in the construction of choline electrodes for hydrogen peroxide detection. A sensor for choline and acetylcholine was described using anodic detection of hexacyanoferrate (III) in solution.¹¹² Ferrocene¹¹³ and tetracyanoquinodimethane¹¹⁴ were also used in the construction of choline electrodes. The use of redox mediators facilitates the electron transfer but leads to the system complications.

Tri-Enzyme Systems

In order to facilitate the detection of hydrogen peroxide, a third enzyme, horseradish peroxidase, can be employed as a catalyst for the hydrogen peroxide reduction with the enzymatic oxidation of an electron donor substance (Fig. 13.3).

Redox mediators have been used in this case for cathodic detection. An amperometric sensor for choline based on electron transfer between horseradish peroxidase and a redox polymer was described.¹¹⁵ Amperometric biosensors based on acetylcholinesterase or butyrylcholinesterase were used for the kinetic determination of organophosphate and carbamate pesticides.

Biosensors for carbamates in vegetables based on five different cholinesterase as biorecognition elements and a screen-printed electrode system as an amperometric transducer were developed by Skladal et al.¹¹⁶ The biosensor was used for the direct analysis of vegetable juices without any pretreatment steps. In this case, $10 \mu\text{g L}^{-1}$

levels of added carbofuran and propoxur were reliably identified. The whole procedure took less than 20 min including 10-min incubation with samples.

13.3.2.6 General Considerations for Cholinesterase Biosensors

Source of Enzyme

Although sensitive, biosensors based on AChE inhibition are not selective (since AChE is inhibited by neurotoxins, which include organophosphorous pesticides (OPs), carbamate pesticides, many other compounds, and heavy metals) and cannot, therefore, be used for quantification of either an individual or a class of pesticides. One approach to solve the lack of specificity of AChE involves genetic engineering of the cholinesterase enzyme to obtain new specific enzymes for desired analytes or families of compounds. Different expression systems for the production of recombinant AChEs for biosensor applications were reviewed by Schulze et al.¹¹⁷ The enzyme source has a drastic effect on the biosensor performance; enzymes from different sources give different inhibition constants for the same pesticide. Generally, cholinesterases isolated from insects are more sensitive to insecticides than those extracted from other sources. Additionally, the use of mutant enzymes with improved sensitivity and selectivity produced by genetic engineering techniques contributes to a decrease in the limits of detection of the developed biosensors. Marques et al. compared various wild-type AChEs as well as some genetically modified enzymes.¹¹⁸ Of the wild-type enzymes, AChE from electric eel (*Electrophorus electricus*) was more sensitive than AChE from bovine and human erythrocytes.¹¹⁸ Genetically engineered acetylcholinesterase (AChE) variants from *Drosophila melanogaster* showed inhibition constants for the insecticide methamidophos that were up to three orders of magnitude higher than those from commercially available AChE from *Electrophorus electricus*. In another report, a biosensor constructed from a genetically modified AChE variant from *D. melanogaster* was inhibited by the insecticide omethoate with a limit of detection (LOD) of 10^{-17} M.¹⁰² This finding was of particular significance in that the AChE from the eel was not inhibited by omethoate, suggesting that it may be possible to select an array of variants that would respond to specific insecticides.

Enzyme Immobilization

The most important step in the development of an enzyme sensor is the firm attachment of the enzyme onto the surface of the working electrode. This process is governed by various interactions between the enzyme and the electrode material, and strongly affects the performance of the biosensor in terms of sensitivity, stability, response time, and reproducibility. This immobilization should be sufficiently strong to provide good mechanical stability of the sensor, but also sufficiently soft to provide optimal conformation freedom of the enzymes that is crucial

for reaching sufficient enzymatic activity. There are a variety of methods by which enzymes can be immobilized, ranging from physical adsorption and entrapment to covalent chemical bonding.¹¹⁹

Physical methods such as adsorption generally consist of a simple deposition of AChE on the surface of the working electrode and attachment of AChE through weak bonds such as van der Waals forces and electrostatic interactions between the AChE and the transducer. This simple and inexpensive way of immobilization involves no damage of the enzyme, no chemical change of the support, and reversibility to allow regeneration of free enzyme. Leakage of enzyme, nonspecific binding, overloading of the enzyme on the support, poor operational and storage stability, and sensitivity to changes in pH, temperature, and ionic strength are the major disadvantages of this method.¹²⁰

Entrapment in sol-gel matrices and lattice of a polymer matrix or membrane was also used for AChE electrodes. It was done in such a way as to retain the protein while allowing penetration of the substrate. This one-step procedure at ambient or low temperature allows no damage of the enzyme and no chemical change of the support, and is suitable for a large variety of bio-receptors. Advantages for this strategy also include thermal stability, pH buffering, and physical ruggedness typically required for environmental applications. On the other hand leakage of the enzyme, nonspecific unstable immobilization, and problems of reproducibility and control of the pore size and diffusion barriers are the most frequently occurring problems.¹²¹

Covalent attachment of AChE is the most widely used procedure. AChE can be linked to the surfaces of a transducer through formation of a stable covalent bond between functional groups of the enzyme and the transducer. The absence of diffusion barriers and enzyme leakage improves the sensor performance although with the disadvantage of using of high amounts of enzyme with possible denaturation.^{122,123} High-affinity binding of the enzyme (AChE) to a concanavalin A (Con A)-activated screen-printed carbon ink electrode yielded highly sensitive response for chlorpyrifos and good operational stability.¹²⁴ Both covalent and non-covalent immobilization of AChE to a polyethyleneimine-modified screen-printed electrode resulted in the maintenance of the enzyme activity on a dried electrode up to 1 year.¹²⁵

A self-assembled monolayer (SAM) is an organized layer of amphiphilic molecules in which one end of the molecule, the "head group," shows a specific reversible affinity for a substrate. SAMs may also consist of molecules with a terminal functional group on the tail for enzyme coupling (see Chap. 16 of Vol. 1). Du and co-workers reported an immobilization method of AChE on a cysteamine SAM-modified Au electrode for carbaryl detection.¹²⁶ High degree of structural order, nanometer size, molecular recognition properties, ease of preparation, and diversity of terminal functionalities are the most promising features.

New trends focus on the development of protocols for the oriented immobilization of AChE through specific functional groups located at their surface. In this way, active sites may be faced towards the target analytes present in the sample, and substrates and products may freely diffuse in the biological layer.¹²⁷

Enzyme Reactivation

Inhibition of AChE by organophosphorus pesticides occurs by binding the phosphoryl group of the pesticide molecule to the serine group present in the active site of enzyme. The free enzyme may be restored by a nucleophilic attack of water on the bond between phosphorus and the enzyme.¹³ If this takes place, the enzyme can be restored to its active state. However, this is considered a rate-limiting step. Should an alkyl group be removed from the phosphorylated enzyme, it cannot be restored at all. Stronger nucleophiles, such as the *N*-methylpyridinium-2-aldoxime (MPA) ion, can be used to restore enzymes to their active state.¹³ This is often used for reactivation of a biosensor using acetylcholinesterase.^{77,84,110} For a BChE biosensor with the esterase immobilized in a cellulose triacetate layer, incomplete reactivation with MPA was observed. This type of sensor was therefore suggested for use as a relatively low-cost disposable probe.⁸¹

13.3.2.7 Future Perspectives of Cholinesterase Biosensors

Flow Injection Analysis

The combination of biosensors with flow injection analysis (FIA) techniques offers the possibility to control the whole procedure, simplifying the sequence of steps and allowing an easier optimization of the reaction conditions with reducing the measurement time by a three- to fourfold.^{128–131} The use in such systems of enzymatic biosensors for the determination of pesticides may provide a device competitive to immunoassay kits, or single-use disposable biosensors, due to mechanization leading to more objective measurements and elimination of operations of transfer of solutions and their volumetric measurements.

Several systems combining cholinesterases and flow systems were described.¹³² Among the different detection methods able to be integrated into flow injection analysis (FIA) systems the electrochemical ones offer high sensitivity, simple sample pretreatment, easy operational procedures, and real-time detection. There are three basic types of FIA systems designed for the determination of pesticides with electrochemical detection via inhibition of enzymes: flow systems with flow-through enzymatic reactors or with the enzyme immobilized on magnetic particles and separate electrochemical detection, systems with enzymatic flow-through electrochemical detector of particular design, and systems with integrated electrochemical biosensor placed in flow-through detection cell.¹³⁰

A flow system with an enzymatic reactor with AChE on porous glass beads, and conductivity detection of the released acetic acid, was reported for the semiquantitative determination of paraoxon with a detection limit of 10 mM and a sampling rate of 10 samples h⁻¹.¹³³ A more complex FIA system with three enzymatic reactors, a flow-through pH detector, and an amperometric detector for oxygen was developed for the discrimination between organophosphorus and carbamate pesticides.¹³⁴ The reported system contained reactors with AChE, ChO, and

organophosphate hydrolase (OPH) immobilized on activated silica gel. Because OPH specifically hydrolyzes organophosphorus pesticides they could be removed from the mixture with carbamate pesticides prior to the inhibition of AChE.

A flow injection system not requiring the regeneration of the enzyme in the measuring system was based on the use of AChE immobilized on magnetic particles.¹³⁵ Detection of thiocholine was carried out amperometrically with the use of a flow cell with platinum electrodes produced by screen-printed technology. In 40 min the procedures achieved detection limits for carbofuran, paraoxon-ethyl and -methyl, and also malaoxon in the range from 3 to 7 ppm using AChE from erythrocytes. Good recovery tests were reported for drinking and brook waters.

In a computer-controlled system the incubation time used was from 1 to 16 min and several minute regeneration with 2-PAM.¹³⁶ A system with electric eel AChE was employed for the determination of chlorpyrifos and its metabolites obtaining a detection limit of 24 ppb. The use in the same system of immobilized AChE allows one to improve the detection limit for chlorpyrifos oxon down to 1.1 ppb. In the same system paraoxon and malaoxon were quantified and also determinations of three analytes in spiked river water were carried out. The whole measuring cycle for a single sample with three injections of the substrate prior to inhibition and two after it, incubation and reactivation, took about 40 min.

In another report biosensors with cholinesterases immobilized on membranes were used in a FIA system. Paraoxon and carbaryl were determined with a detection limit of 0.1 M with 4-aminophenyl acetate as the substrate.¹⁰⁵ A commercial Metrohm flow-through cell with a glassy carbon electrode was used. In such a system determinations in extracts from kiwi fruits treated with carbaryl were carried out. For a concentration of 3 ppm of the analyte in the extract a good agreement with the UV determinations was obtained.

Especially outstanding low detectability was reported for a FIA system with a flow-cell, which housed a screen-printed biosensor with immobilized AChE.¹⁰¹ For 20-min incubation time and one unit of enzyme loading the detection limits for dichlorvos and paraoxon were 6 nM and 0.04 nM, respectively. Some initial evaluations were made for river water samples.

Disposable Sensors

There is an increasing end-user demand for the use of rapid, reliable, and low-cost field-based methods for the determination of toxic compounds in environmental samples, further fuelled by public concerns with respect to environmental pollution and safe-guarding of global ecosystems. Because the inhibition of AChE by OP compounds is irreversible, an inexpensive disposable biosensor which would eliminate the enzyme reactivation maneuver is highly desirable.⁵² The wide application of disposable strip test in clinical analysis suggests that electrochemical biosensors could also find wide acceptance for the determination and monitoring of pesticides. Such sensors could serve as alternatives to chromatographic methods which, although more versatile in providing information about numerous species from

one run, are much more expensive, require well-trained personnel, and cannot be readily used in the field.

In the last decades, many studies have focused on the development of low-cost screen-printed biosensors, well suited for mass production and portable devices. They have the additional advantage of allowing both real-time and in situ monitoring. Depending on the biosensor properties, which include the use of electrochemical mediators and the enzyme immobilization procedure, the electrochemical response can be suitable to detect low levels of several organic contaminants, such as pesticides.

Numerous studies on the construction of screen-printed electrodes (SPEs) have been published.^{137–140} The first disposable biosensors with immobilized cholinesterases were produced manually employing copper-covered plastic sheets used commonly for producing electronic circuits.^{99,141} For the determination of carbofuran and propoxur in spiked vegetable juices without any pretreatment, satisfactory results were reported for carbofuran at concentration levels from 10 to 125 ppb with 10-min incubation. A screen-printed enzyme electrode developed for the determination of organophosphorus pesticides was fabricated by co-immobilization of acetylcholinesterase with choline oxidase and peroxidase.⁷⁶ The electroreduction of hydrogen peroxide proceeded at a decreased overvoltage. The electrodes allowed rapid quantitative assay of cholinesterase inhibitors, such as organophosphate pesticides, with a low detection limit in submicromolar concentration ranges with an overall assay time of 20 min.

A sensitive screen-printed amperometric multielectrode biosensor for the rapid discrimination of the insecticides paraoxon and carbofuran in mixtures was developed.¹⁴² It was based on the principle of acetylcholinesterase (AChE) inhibition and chemometric data analysis using artificial neural networks (ANNs). Four types of native or recombinant AChEs (electric eel, bovine erythrocytes, rat brain, *Drosophila melanogaster*) were immobilized by screen printing on four thick-film sensors, each containing an AChE. The multisensors were used for quantitative inhibition analysis of binary reagent mixtures combining the AChE-multisensor with feed-forward ANNs. The sensors registered a detection range for both analytes of 0.2–20 mg L⁻¹ with an overall assay time of less than 60 min. The individual inhibition pattern of each AChE–analyte combination enabled the discrimination of both analytes by the use of neural network data processing.

Collier et al.¹⁴³ incorporated AChE and BChE into the carbon-based ink used for printing electrodes. The SPEs were used for the determination of chlorfenvinphos and diazinon, organophosphate pesticides employed for the control of insect pests in wool. The BChE-based biosensor was shown to be very sensitive towards a mixture of chlorfenvinphos and diazinon, with a limit of detection equal to 0.5 µg g⁻¹.

Modification of SPEs with different mediators including TCNQ mediator [7,7,8,8-tetracyanoquinonedimethane] in the graphite electrode,¹⁴⁴ cobalt(II) phthalocyanine (CoPC),¹⁴⁵ and *o*-phenylenediamine onto carbon/CoPC¹⁴⁶ can be found in the literature. In 1994 Hart and Hartley studied the electrochemical mechanism of a CoPC-modified screen-printed device using cyclic voltammetry.¹⁴⁷ The voltammograms

showed that with dissolved AChE it is possible to determine pesticides at lower potentials (0.100 V), hence lowering interferences. In a later report the same authors immobilized AChE cross-linking it on a CoPC-modified planar device.

SPEs offer a number of advantages over conventional electrodes such as they are suitable for working with microvolumes and easy to prepare and modify. They are reusable and inexpensive and have excellent specificity and selectivity. SPEs have important advantages such as the elimination of memory effects for analysis at trace levels, and they appear to be particularly attractive for in situ determinations. The construction of SPEs involves the printing of different inks on planar ceramic or plastic supports. The great flexibility of SPEs resides in their large number of possible modifications. In fact, the composition of the inks used in the printing process can be modified by adding substances of a very different nature such as metals, enzymes, polymers, and complexing agents.

Nanosized Materials

In recent years, with high mechanical strength, good conductivity, large surface area, and extremely small size, nanomaterials have been widely employed in electrode modification and electrochemical sensor development (see Chap. 17 of Vol. 1). The nanomaterials and their applications have been the subject of many reviews. Pumera et al. reported the major techniques and methods employed in the construction of electrochemical biosensors using nanoscale materials.¹⁴⁸ Nanoparticle (NP)-based AChE biosensors have many advantages both in terms of stability and in terms of promoting the catalytic reduction of redox species. The accuracy, efficiency, and detection limit of biosensors can be enhanced with the use of nanomaterials. In this regard, carbon nanotubes (CNTs) have attracted considerable attention due to their high electrical conductivity, strong adsorptive ability, good mechanical strength, and excellent biocompatibility.^{149–151} In recent years, AChE has been immobilized onto various nanomaterial surfaces in order to improve the response and stability in trace pesticide detection.¹⁵²

Liu et al. reported a highly sensitive flow injection amperometric biosensor based on self-assembling acetylcholinesterase on carbon nanotubes for paraoxon detection.¹⁵³ Cyclic voltammetric results showed that electrooxidation of thiocholine occurred at much lower oxidation potential (+0.55 V) at MWCNT-modified glassy carbon electrodes (GCE). The amperometric results further revealed that the response of thiocholine at an MWCNT/GCE was 200 times higher than that of bare GCE. This significant enhancement could be attributed to the fast electron transfer and big working surface area of CNTs. Under optimal conditions, the biosensor was used to measure as low as 0.4 pM paraoxon with a 6-min inhibition time. The biosensor had excellent operational lifetime stability with no decrease in the activity of enzymes for more than 20 repeated measurements over a period of 1 week. The developed biosensor system was an ideal tool for online monitoring of organophosphate pesticides and nerve agents.

Incorporation of an AChE-multiwall-carbon nanotube biosensor into a flow system was recently reported by Kandimalla and Ju.¹⁵⁴ The sensor was able to detect concentrations of insecticides ranging from 1.5 to 80 μM , and was reproducible and renewable by reactivation with 2-MPA. Du et al.¹⁵⁵ proposed a simple method for immobilization of AChE on multiwall carbon nanotube-chitosan (MC) composites (AChE—MC/GCE) and thus a sensitive, fast, and stable amperometric sensor for detection of organophosphorus insecticide was obtained. The homogeneously netlike matrix prevented the enzyme from leaking from the electrode. The inhibition of the enzymatic activity of AChE by the insecticide was evaluated from cyclic voltammograms. It was found that the inhibition of triazophos was proportional to its concentration range from 0.03 to 7.8 μM and 7.8 to 32 μM with a detection limit of 0.01 μM . A 95 % reactivation of the inhibited AChE could be regenerated for using pralidoxime iodide within 8 min.¹⁵⁵

A disposable CNT-based biosensor was successfully developed and applied to the detection of organophosphorus pesticides and nerve agents. The biosensors using bi-enzyme modification with AChE and CHO provided high sensitivity, wide linear ranges, and low detection limits for the determination of OP compounds. Such characteristics may be attributed to the catalytic activity of carbon nanotubes to promote the redox reaction of hydrogen peroxide produced during enzymatic reactions, as well as the large surface area of carbon nanotube materials.¹⁵⁶

Apart from CNTs several nanomaterials were used to modify electrode surfaces. Fan and co-workers¹⁵⁷ improved the enzyme-modified electrode through Au nanoparticles/silicon nanowires (AuNPs/Si-NWs) coated on glassy carbon electrodes. This sensor showed a rapid response towards the substrate acetylcholine in the concentration range of 1.0 μM to 1.0 mM. This electrode could detect as low as 8 ng L^{-1} dichlorvos.

Norouzi et al.¹⁵⁸ used gold nanoparticles and multiwalled carbon nanotubes to promote the electron transfer and catalyze the electro-oxidation of thiocholine in an amperometric biosensor for the detection of monocrotophos (LOD 10 nM). Their flow-based system used glassy carbon electrodes modified with gold nanoparticles and multiwalled carbon nanotubes. The nanotubes contained chitosan to increase the immobilization level and improve the stability of AChE.

A novel amperometric biosensor based on immobilizing acetylcholinesterase on and electrode modified with 3-carboxyphenyl boronic acid/reduced graphene oxide–gold nanocomposites was developed for the detection of organophosphorus and carbamate pesticides.¹⁵⁹ Acetylcholinesterase was successfully immobilized on the electrode with relatively high activity by the specific binding between the boronic acid group of 3-carboxyphenylboronic acid and the glycosyl group of acetylcholinesterase. The biosensor presented good sensitivity owing to the excellent properties of gold nanoparticles and reduced graphene oxide, which promoted the electron transfer reaction and enhanced the electrochemical response. Based on the inhibition of the enzymatic activity of AChE, organophosphorus and carbamate pesticides were determined with satisfactory results in the presence of acetylthiocholine chloride as a substrate. Moreover, the fabricated biosensor had good repeatability and high stability.

Chitosan–Prussian blue–multiwall carbon nanotube–hollow gold nanosphere (Chit–PB–MWNT–HGN) films were fabricated to be employed in AChE biosensors.¹⁶⁰ Incorporating MWNTs and HGNs into a Chit–PB hybrid film promoted the electron transfer reaction, enhanced the electrochemical response, and improved the microarchitecture of the electrode surface. Based on the inhibition of the AChE activity by the pesticides malathion, chlorpyrifos, monocrotophos, and carbofuran as model compounds, the biosensor showed a wide dynamic range, low detection limit, good reproducibility, and high stability. Moreover, the AChE/Chit–PB–MWNT–HGN/Au biosensor could also be used for the direct analysis of a practical samples, which would be a new promising tool for pesticide analysis.¹⁶⁰

13.3.3 Other Enzymatic Systems for Pesticide Analysis

13.3.3.1 Alkaline and Acid Phosphatase

Alkaline phosphatase (ALP, EC 3.1.3.1) catalyzes the transfer of a phosphate group to water (hydrolysis) or alcohol (transphosphorylation).¹⁶¹ The enzyme is characterized by a high pH and a broad substrate specificity and uses a wide variety of phosphomonoesters. It can be observed in the literature reports that ALP is suitable for the detection of organochlorine, organophosphate, and carbamate pesticides, although only a limited number of compounds were tested. The inhibition of alkaline phosphatase was successfully exploited by Su et al.¹⁶² Three electrodes, a ruthenized carbon working electrode, an Ag/AgCl reference electrode, and a silver counter electrode, were screen-printed on a polyester substrate. The enzyme reaction employed glucose oxidase (GOD) adsorbed on the working electrode, and alkaline phosphatase in solution. The sensors were immersed in a solution containing the pesticide and ALP and incubated for 10 min. Then the substrate, glucose-6-phosphate, was added and the current arising from the oxidation of hydrogen peroxide (applied +0.7 V) was recorded after a further 1 min of incubation. The percentage of inhibition was calculated as a function of the concentration of the pesticide dichlorvos.

One of the most regrettable characteristics of enzyme inhibition-based biosensors is the different inhibition degree caused by different inhibitors. An example of this behavior is an amperometric acid phosphatase inhibition-based biosensor proposed by Mazzei et al.,¹⁶³ which shows different inhibition efficiency towards organophosphorus and carbamate compounds (the latter with a weaker inhibition efficacy and higher detection limits, as a result).

Acid phosphatases (Aps) are enzymes with a low pH that catalyze the hydrolysis of orthophosphoric monoester to alcohol and H_3PO_4 . This enzyme has been utilized to a limited extent for the detection of pesticides through inhibition of the enzyme. AP was used with another enzyme, glucose oxidase (GOD), in a bi-enzymatic biosensor¹⁶³ for the determination of malathion, methyl parathion, and paraoxon. Biocatalytic hydrolysis of glucose-6-phosphate in the presence of acid phosphatase was reversibly

inhibited by organophosphorus and carbamate pesticides. The amperometric detection of this inhibition required a bi-enzymatic system with glucose oxidase (GOD) and resulted in a final measurement of hydrogen peroxide on a Pt electrode.

13.3.3.2 Tyrosinase

Tyrosinase (Tyr) is a type of catechol oxidase and a binuclear copper-containing metalloprotein, which oxidizes monophenols and *o*-diphenols into their corresponding *o*-quinones at the expense of oxygen reduction to water. The conversion of monophenols by Tyr proceeds in two consecutive steps; that is, in the first step the monophenol is oxidatively hydroxylated to its corresponding *o*-diphenol (hydroxylase activity), which in a second step is further oxidized to its corresponding *o*-quinone, whereby the enzyme is oxidized by molecular oxygen back to its native form (catecholase activity).¹⁶⁴

Tyrosinase is inhibited by many different compounds such as carbamate and dithiocarbamate pesticides, atrazines, chlorophenols, and thioureas and this characteristic has been used to develop biosensors for the enzymatic detection of many pesticides. In several published articles it was demonstrated that reversible inhibition of Tyr can be followed by amperometric measurement of the reaction product (*o*-quinone). Inhibition by atrazine and chloroisopropylphenylcarbamate (CIPC) at micromolar level was shown with the use of an amperometric biosensor with glassy carbon electrode and a pyrrole amphiphilic monomer-tyrosinase coating.¹⁶⁵ Three other carbamate pesticides inhibited Tyr in an amperometric biosensor in a medium of reversed micelles.¹⁶⁶ With phenol as a substrate for ziram, diram, and zinc diethyldithiocarbamate the detection limits were evaluated. Detection limits at the micromolar level of concentrations were reported through inhibition of Tyr incorporated into graphite paste in a screen-printed amperometric biosensor.¹⁶⁷ A tyrosinase (Tyr) screen-printed biosensor based on the electroreduction of enzymatically generated quinoid products was electrochemically characterized and optimized for the determination of carbamates and OP.¹⁶⁸ A composite electrode prepared by screen-printing a CoPc modified cellulose-graphite composite. Inhibition studies on the *o*-quinone steady-state current (at -0.20 V vs. Ag/AgCl) were performed to investigate the inhibition kinetics of the pesticides on the enzymatic activity of mushroom tyrosinase. The results showed that methyl parathion and carbofuran could lead to competitive inhibition processes of the enzyme, while diazinon and carbaryl acted as mixed inhibitors. Analysis of natural river water samples spiked with 30 ppb of each pesticide showed recoveries between 92.5 and 98.5 % and relative standard deviations of 2 %.

Andreescu et al.¹⁴⁴ indicated that Tyr biosensors suffer from poor specificity and many substrates and inhibitors interfere with the enzyme ability to detect the target compounds. The enzyme is further inherently unstable, reducing the lifetime and usability of the Tyr-based biosensors.¹⁶⁹ However, Sole et al.⁵² have pointed out that Tyr detectors have some advantages over other types of enzymes such as tolerance for

high temperatures and organic solvents.¹⁷⁰ A Tyr biosensor can also be operated faster than, for instance, an AChE sensor as it does not require preincubation.¹⁶⁷

13.3.3.3 Aldehyde Dehydrogenase

Aldehyde dehydrogenase (ADH) catalyzes the oxidation of various aldehydes using β -nicotinamide adenine dinucleotide (NAD^+) as a cofactor.¹⁷¹ The enzyme is inhibited by dithiocarbamate fungicides and this can be utilized to detect these pesticides in the environment.¹⁷²

Dithiocarbamate fungicides inhibit aldehyde dehydrogenase. In order to produce an amperometric biosensor with this enzyme also a bi-enzymatic system was designed with the enzyme diaphorase. Reaction of propionaldehyde and NAD^+ in the presence of ADH produced NADH which could be detected via its reaction with hexacyanoferrate(III) by diaphorase. The changes of hexacyanoferrate (II) concentrations were monitored amperometrically with a Pt electrode¹⁸² or bi-amperometrically with two platinum electrodes.¹⁷¹ A bi-amperometric biosensor was also developed in screen-printed configuration with Pt-sputtered carbon paste¹⁷³ In all these biosensors both enzymes were immobilized in a poly(vinyl alcohol)–styrylpyridinium (PVA-SbQ) layer.

13.3.3.4 Organophosphorus Hydrolase

Although being sensitive and useful sensors for environmental monitoring, biosensors based on enzyme inhibition have some limitations. They have a long and tedious protocol that requires long incubation with inhibitors prior to analysis for good sensitivity and require reactivation of the enzyme which is inhibited irreversibly by OPs. Since AChE is inhibited by neurotoxins, which include not only OP pesticides but also carbamate pesticides and many other compounds, these analytical tools are not selective and cannot be used for quantification of either an individual or a class of pesticides that may be required for monitoring detoxification processes.

Organophosphorus hydrolase (OPH), a biological catalyst, was shown to effectively hydrolyze a range of organophosphate esters; pesticides such as parathion, coumaphos, and acephate; and chemical warfare agents such as soman, sarin, VX, and tabun.^{174,175} The enzyme was first discovered in soil microorganisms, i.e., *Pseudomonas diminuta* and *Flavobacterium* spp.⁵⁵

The catalytic hydrolysis of each molecule of these compounds releases two protons, the measurement and correlation of which to the OP concentration forms the basis of a potentiometric enzyme electrode. The basic element of this very simple enzyme potentiometric electrode is a pH electrode modified with an immobilized purified organophosphorus hydrolase (OPH) layer formed by cross-linking OPH with bovine serum albumin and glutaraldehyde. Thus, potentiometric OP biosensors were prepared by coupling OPH and a glass pH electrode. The sensors were constructed by immobilizing OPH on the surface of a pH-sensitive

layer of a commercially available pH electrode by cross-linking with bovine serum albumin (BSA) to form a thin film.¹⁷⁶ The sensor could detect OPs including paraoxon, ethyl parathion, and methyl parathion.

In a similar mechanism of signal transduction, one can use a pH-sensitive field-effect transistor (FET) for developing enzyme-modified FETs. The use of a FET provides superiority in miniaturization of the sensor body because a FET is usually produced through mass production on semiconductor materials.¹⁷⁷

A potentiometric disposable enzyme sensor for the direct and fast determination of OP insecticides was developed by using an OPH immobilized on screen-printed electrodes. The potentiometric device consisted of *N,N*-dioctadecylmethylamine as H^+ -sensitive ionophore electrode with an integrated Ag/AgCl reference electrode.¹⁷⁸ The sensor performance was investigated with regard to enzyme load, concentration, pH, and temperature of the measuring buffer using paraoxon as analyte. Response times to reach 95 % of maximum change in potential did not exceed 5 min. Sensors stored under dry conditions at 4 °C still showed 60 % of their initial hydrolytic rate after 70 days. A range of putative interfering substances did not influence the sensor response, and the suitability of measuring OPs in soil extracts was ascertained.

OPH can be integrated with an amperometric transducer to monitor the oxidation or reduction current of the hydrolysis products such as 4-nitrophenol and 2-(diisopropylamino) ethanethiol. An improvement of the detection limit more than one order of magnitude for paraoxon and methyl parathion was achieved when OPH was employed in an amperometric screen-printed biosensor.^{179,180} The measurement was based on the rapid anodic signal of *p*-nitrophenol at the OPH/Nafion layer immobilized on the printed carbon surface. An OPH-based amperometric biosensor was also made by enzyme modification of carbon paste, which was operated in a chronoamperometric mode.⁵⁵ It selectively hydrolyzed the P–F bond of fluorine-containing organophosphates, making it suitable for discriminative detection of fluorine-containing organophosphates. Taking advantage of this simplified procedure, the same author¹⁸¹ carried out analysis under flow analysis with a sample throughput of 30 measurements per hour. This system provided highly reproducible and stable responses and excellent storage stability, making it possible to do repeated measurements without regular calibration. Furthermore, broader linear range, higher sensitivity, and lower detection limits were achieved compared to potentiometric or optical results. Wang et al.¹⁸² immobilized OPH onto thin-film gold electrodes rather than inside a reactor. The application of +0.75 V vs. Ag/AgCl and the already known problems of surface passivation due to the oxidation of phenolic compounds led the authors to examine the reproducibility of the anodic detection. The results showed that low-volume flow injections apparently contributed to a negligible fouling of the electrode surface. V-type nerve agent biosensors based on immobilized OPH on the surface of a CNT-modified carbon electrode were reported.¹⁸³ The OP biosensors thus prepared exhibited an electrochemical response to demeton-S at 0.4 V. This biosensor was successfully applied to analyze lake water spiked with demeton-S.

Simonian et al.¹³⁴ combined a potentiometric and an amperometric detector in order to discriminate between organophosphorus and carbamate pesticides. Three enzyme reactors were used with AChE, ChO, and OPH immobilized on activated silica gel. First, the OPH-based reactor hydrolyzed only organophosphorus pesticides. Then, the subsequent AChE/ChO-based system was inhibited by the remaining pesticides in the solution. The potentiometric measurement gave the concentration of organophosphorus pesticides, while the amperometric measurement indicated the concentration of carbamate pesticides. Although this approach allowed the discrimination between both types of neurotoxins, it was not possible to quantify the concentrations of each pesticide. Hence, the biosensor had to be used as a tool to screen the toxicity of the sample, prior to the analysis with a conventional chromatographic technique. Similarly, a dual-potentiometric/amperometric biosensor system was proposed^{184,185} based on (1) the potentiometric detection of protons liberated by organophosphorus pesticides upon OPH hydrolysis and (2) the amperometric detection of *p*-nitrophenol produced by some pesticides, such as paraoxon and parathion. The combination of both transducers makes it possible to distinguish some organophosphorus pesticides in samples. It is important to notice that short response times (less than 1 min) were obtained, even though no mutual influence of the sensor signals was observed, opening the possibility to design powerful cross-reactive biosensor arrays. Nevertheless, the discrimination was still not high enough to give more details than a screening assay.

Generally, the detection scheme based on monitoring OPH-catalyzed hydrolysis products of OPs offers the advantages of simpler, more direct, and quicker measurements of only the OP class of nerve agents over that based on the inhibition of AChE activity that responds to all types of nerve agents. Additionally, the OPH-based biosensor has the potential of quantifying individual organophosphate pesticides when used as a detector in conjunction with high-pressure liquid chromatography (HPLC) for chromatographic separations. The OPH enzyme electrode, however, will be suitable for online monitoring of detoxification processes for the treatment of wastewater generated during the production and consumption of the organophosphate-based pesticides and insecticides and disposal of organophosphate-based nerve agents.

13.3.3.5 Cells and Tissues

Immobilized whole cells or tissues from various organisms can be utilized alternatively to isolated enzymes for the design of electrochemical biosensors. They function as renewable sources of specific enzymes, which additionally operate in their natural biological surrounding (cell or tissue) that may provide often optimum conditions for long-term stability. In the design of these biosensors both cells hydrolyzing directly organophosphorus pesticides and tissues rich in enzymes that can be inhibited by pesticides are employed. An easy-to-construct and inexpensive potentiometric microbial biosensor for the direct measurement of organophosphate (OP) nerve agents was developed by Mulchandani et al.¹⁸⁶

The biological sensing element of this biosensor was recombinant *Escherichia coli* cells containing the plasmid pJK33 that expressed organophosphorus hydrolase (OPH) intracellularly. The cells were immobilized by entrapment behind a microporous polycarbonate membrane on the top of the hydrogen ion-sensing glass membrane pH electrode. OPH catalyzed the hydrolysis of organophosphorus pesticides to release protons, the concentration of which was proportional to the amount of hydrolyzed substrate. The biosensor was applied for the determination of paraoxon, ethyl parathion, methyl parathion, and diazinon.

Also other potentiometric studies were based on the use of the OPH enzyme. For example, Rainina et al.¹⁸⁷ entrapped recombinant *E. coli* onto gel spheres retained inside a reactor by using poly(vinylalcohol) (PVA) and cryo-immobilization. Paraoxon could be detected in the concentration range from 0.25 to 250 ppm, with a response time of 10 min for the batch mode and 20 min in the flow-through system. One of the major advantages of the use of PVA-cryo-immobilized cells was the increased stability during use and storage of up to 60 days.

An acid phosphatase (AP) hybrid biosensor was developed using a thin layer of potato tissue coupled to an amperometric GOD-based biosensor based on internal sensing of H_2O_2 .¹⁶³ The reversible inhibition of AP was utilized for the determination of malathion, paraoxon methyl, paraoxon, and aldicarb with limits of detection of 0.5 ppb for paraoxon methyl, and 40 ppb for aldicarb. The tissue-based biosensor exhibited a longer shelf life and a better reliability on the amperometric results than a bi-enzymatic sensor with purified AP and GOD. A similar biosensor was also developed using a potato layer with a Clark-type dissolved oxygen electrode.¹⁸⁸

13.3.4 Limitations of Enzymatic Pesticide Assay

In analysis of natural samples with complex matrices several different factors may affect the result of the determination depending on the enzyme used, the method of its immobilization, the pH of sample solution, its ionic strength, or content of dissolved oxygen. Due to the complexity of biocatalytic processes, numerous additional species besides analytes may inhibit the used enzyme.⁴⁶ Inhibition-based methods suffer from the serious interference that enzymes can be inhibited by a large number of different compounds, including metal cations, other inorganic species, and organic compounds different to the target analyte.¹⁸⁹ Evident responses of a biosensor were observed for nicotine, lead, and fluoride. In addition, some surfactants (dodecylbenzyl-sulfonate and sodium dodecylsulfate) and also chromium (VI) interfere with enzymatic reactions of AChE.¹⁹⁰ Strong inhibition of AChE was also found for As(III) while As(V) did not interfere.¹⁹¹ As many pesticides inhibit AChE and BuChE, specificity is poor and identification of compounds in real samples is regarded by some authors as an unsolved problem.¹⁹²

Among enzymes used for inhibitive determination of pesticides only the activity of the less often used enzymes acetolactate synthase, acid phosphatase, and tyrosinase is inhibited reversibly. Regeneration of an inhibited enzyme is a crucial

problem to solve for multiple use of biosensors which are irreversibly inhibited by the determined analyte. Much attention was paid to the regeneration of the activity of cholinesterases which is usually performed using 2-pyridine aldoxime methochloride (2-PAM).^{68,77}

There are two main characteristics of performance of the OPC assay based on the inhibition of choline esterase activity: detection limit and assay time. The assay time involves the stage of incubation of choline esterase (solubilized or immobilized) with an OPC-containing solution. This step is usually the longest of the assay. Obviously, the longer incubation time leads to a higher degree of enzyme inhibition and results in a lower detection limit. However, practical analytical application requires rapid analysis. Therefore, there is a trade-off between rapidity of the assay and the detection limit. The detection limits for different OPCs are different because of the difference in the ability of various OPCs to inhibit choline esterase. The detection limits for different OPCs can differ by three orders of magnitude.¹⁹³ In general, very toxic OPCs have a greater inhibiting effect on choline esterase than less toxic ones and the detection limit for more toxic OPCs is lower than that of the less toxic OPCs.

13.3.5 Advantages and Future Prospects of Pesticide Biosensors

In many cases, the biosensor assays based on inhibitory effects of pesticides or other chemical contaminants show high sensitivity and could be the basis for relatively simple and cost-effective procedures. A particular advantage of these biosensing systems is that they offer the possibility of analysis in both batch and flow mode, allowing the use of these sensors for analysis of a large number of samples in a reasonable time interval. These methods can also be recommended for the development of single-use test strips, especially with screen-printed electrodes, to avoid problems related to fouling of the electrode which generally involves a chemical or electrochemical deactivation of the working electrode surface. SPEs offer several additional advantages including low fabrication cost, simple handling, and being amenable to both mass production and instrument miniaturization for field analysis. Current research studies involve numerous efforts at improving the analytical performance of the biosensing systems in order to be able to monitor a wide range of pollutants in environmental and food samples.⁴⁹⁻⁶⁷

The use of genetically modified enzymes for the design of biosensors can be an effective way to improve the sensor sensitivity. Indeed, the combination of such engineered enzymes (double and triple mutants) with microporous-activated carbon technology could improve the efficiency of enzyme-based biosensors. Furthermore, engineered variants of enzymes could be another approach in the biosensor design for discrimination and detection of various enzyme-inhibiting compounds when used in combination with chemometric data analysis using artificial neural networks.

Analytical applications of biosensors based on enzyme inhibition are still limited since these sensor technologies are not usually able to discriminate various toxic compounds in the same sample. A strategy for the detection and discrimination of neurotoxins was investigated.¹⁹⁴ It was possible to separate the effects of different inhibitors, using a combined recognition/discrimination strategy based on the joint action of acetylcholinesterase and organophosphorus-hydrolase enzymes. The feasibility of eliminating the organophosphate neurotoxins from the different multicomponent inhibitor combination via sample pretreatment with immobilized forms of OPH was demonstrated. Because of such manipulation, the inhibiting influence of non-OP neurotoxins on AChE can be separated and their true concentration may be determined. In another study, engineered variants of *Drosophila melanogaster* acetylcholinesterase (AChE) were used as biological receptors (AChE-multisensors) for the simultaneous detection and discrimination of binary mixtures of cholinesterase-inhibiting insecticides.¹⁹⁵ In this method the system was based on a combination of amperometric multi-electrode biosensors with chemometric data analysis of sensor outputs using artificial neural networks (ANN). The AChE mutants were selected on the basis of displaying an individual sensitivity pattern towards the target analytes. The multisensor was capable of simultaneously detecting and discriminating paraoxon and carbofuran.

In general, biosensors based on AChE inhibition are not capable of distinguishing among specific pesticides, but one of their major advantages over other analytical techniques is that, owing to the biological origin of their active sites, they are sensitive to general toxicity, whereas other analytical techniques measure only concentration data. Thus the biosensor response is believed to correlate closely to the acute toxicity of a particular pesticide, expressed as LD₅₀ (oral) for rats.⁵⁰

Most previous studies have been carried out on aqueous samples, whereas these pesticides and their metabolites, which are very often more toxic than their parental compounds, are generally poorly soluble in water. The extraction of these compounds from solid matrices or their concentration from aqueous media requires the use of organic solvents. Biocatalysis in nonaqueous media has opened opportunities for the development of biosensors which work in nonaqueous solvents. In this way, it has been shown by various researchers that enzymes can function in organic solvents, in a mixed aqueous-organic phase, as they do in aqueous solvents. Preliminary results on the detection of organophosphorus insecticides with an enzymatic sensor in an organic medium seem promising.¹⁹⁶ For this purpose, 4-aminophenyl acetate was used as the substrate of AChE in place of acetylthiocholine because of its high solubility in organic solvents and the redox-active nature of 4-aminophenol produced by the enzymatic reaction. Marty and co-workers prepared an AChE-modified carbon electrode by coating an AChE-containing polymer film on the electrode.¹⁴⁴ The enzyme in the film retained ca. 80 % of its catalytic activity even if the aqueous solution contained 1–5 % acetonitrile or ethanol, though more than 20 % organic solvent induced nearly complete deactivation of the enzyme, suggesting a possible use of the sensor in the presence of a small amount of a water-miscible organic solvent in aqueous media. A disposable cholinesterase biosensor based on screen-printed electrodes was

assembled¹⁹⁷ and used to assess the effect of miscible organic solvents on the acetylcholinesterase activity and on the inhibitory effect of organophosphorus pesticides on acetylcholinesterase activity. With 5 % acetonitrile and 10 % ethanol, an increase of the recorded current was observed. The addition of 0.2 % polyethylenimine to the enzyme preparation, before immobilization, allowed the utilization of 15 % acetonitrile without any negative effect on the enzyme activity.

The future integration of wireless communication systems will generate huge interest as this will inevitably lead to the emergence of extensive networked multiple autonomous analytical stations in rivers, lakes, wells, or even water treatment plants. These units will provide high-quality information about key chemical parameters that determine the quality of our environment.¹⁹⁸ By means of this network system and by an intelligent remote surveillance, an active response will be possible. To accomplish this, there is a need for robust and unattended working analytical instrumentation. Each unit will be portable, plug and playable, user friendly, and fully automated with little need for maintenance. The emergence of these compact, self-sustaining, networked instruments will have enormous impact on all field-based environmental measurements including biosensors. Gu et al.¹⁹⁹ have recently applied a novel early warning protocol to monitor the toxicity of the effluents of a water treatment plant.

The acceptance of biosensors is dependent upon several factors as they should be comparable to conventional analytical systems in terms of reliability, sensitivity, selectivity, specificity, and robustness.²⁰⁰ Therefore, biosensor measurements have to be verified by comparing them with the results of chemical analysis²⁰¹ which is known as validation. The overall commercial status and general acceptance of the technology will depend on the performance characteristics, sample throughput, associated costs, and acceptance by regulatory authorities, based on independent validation data generated using internationally recognized procedures (e.g., AOAC, ISO, and IDF).²⁰²

References

1. Hayes WJ, Laws ER (1991) Handbook of pesticide toxicology. Academic Press Limited, San Diego, California, USA
2. Aspelin L (1994) Pesticides industry sales and usage, 1992 and 1993 market estimates. USEPA, Washington, DC
3. Sherma J (1989) Analytical methods for pesticides and plant growth regulators. Academic, San Diego, CA
4. Fintschenko Y, Krynitsky AJ, Wong JW (2010) Emerging pesticide residue issues and analytical approaches. *J Agric Food Chem* 58:5859–5861
5. Ariese F, Ernst WHO, Sijm DTHM (2001) Natural and synthetic organic compounds in the environment—a symposium report. *Environ Toxicol Pharmacol* 10:65–80
6. Karr JR, Dudley DR (1981) Ecological perspective on water quality goals. *Environ Manage* 5:55–68
7. FAO (2010) Agriculture: towards 2010 document. In: Proceedings of the C 93/94 Document of 27th Session of the FAO Conference, Rome, Italy, 1993

8. Basanta R, Nunez A, Lopez E, Fernandez M, Diaz-Fierros F (1995) Measurement of cholinesterase activity inhibition for the detection of organophosphorus and carbamate pesticides in water. *Int J Environ Stu* 48:211–219
9. Sinclair CJ, Boxall AB (2003) Assessing the ecotoxicity of pesticide transformation products. *Environ Sci Technol* 37:4617–4625
10. Hassal KA (1983) *The chemistry of pesticides: their metabolism, mode of action and uses in crop protection*. Macmillan, New York, NY
11. Corbett JR, Wright K, Baillie AC (1984) *The biochemical mode of action of pesticides*, 2nd edn. Academic, New York, NY
12. Baron RL (1991) Carbamate insecticides. In: Hayes WJ Jr, Laws ER Jr (eds) *Handbook of pesticide toxicology*. Academic, New York, NY
13. Stenersen J (2004) *Chemical pesticides. Mode of action and toxicology*. CRC Press, Boca Raton, FL
14. Compton JA (1988) *Military chemical and biological agents*. Telford Press, Caldwell, NJ, p 135
15. Fukuto TR (1990) Mechanism of action of organophosphorus and carbamate insecticides. *Environ Health Perspect* 87:245–254
16. Chapalamadugu S, Chaudhry GR (1992) Microbiological and biotechnological aspects of metabolism of carbamates and organophosphates. *Crit Rev Biotechnol* 12:357–389
17. Oehme DS, Oehme FW (1985) A review of organophosphorus ester-induced delayed neurotoxicity. *Vet Human Toxicol* 27:22–37
18. Coye MJ, Barnett P, Midtling MJ, Velasco AR, Clements CL, O'Malley MA, Tobin MW (1986) Clinical confirmation of organophosphate poisoning of agricultural workers. *Am J Ind Med* 10:399–409
19. Corrigan FM, Macdonald S, Brown A, Armstrong K, Armstrong EM (1994) Neurasthenic fatigue, chemical sensitivity and GABA_A receptor toxins. *Med Hypotheses* 43:195–200
20. Klotz DM, Arnold SF, McLachlan JA (1997) Inhibition of 17 beta-estradiol and progesterone activity in human breast and endometrial cancer cells by carbamate insecticides. *Life Sci* 60:1467–1475
21. Jaeger JW, Carlson IH, Porter WP (1999) Endocrine, immune, and behavioral effects of aldicarb (carbamate), atrazine (triazine) and nitrate (fertilizer) mixtures at groundwater concentrations. *Toxicol Ind Health* 15:133–151
22. Andersen HR, Vinggaard AM, Rasmussen TH, Gjermansen IM, Bonefeld-Jorgensen EC (2002) Effects of currently used pesticides in assays for estrogenicity, androgenicity, and aromatase activity in vitro. *Toxicol Appl Pharm* 179:1–12
23. Kojima H, Katsura E, Takeuchi S, Niiyama K, Kobayashi K (2004) Screening for estrogen and androgen receptor activities in 200 pesticides by in vitro reporter gene assays using Chinese hamster ovary cells. *Environ Health Perspect* 112:524–531
24. Li J, Li N, Ma M, Giesy JP, Wang Z (2008) In vitro profiling of the endocrine disrupting potency of organochlorine pesticides. *Toxicol Lett* 183:65–71
25. Dikshith TSSS (1991) Pesticides. In: Dikshith TSS (ed) *Toxicology of pesticides in animals*. CRC Press, Boston, MA
26. Barcelo D, Hennion MC (1997) *Trace determination of pesticides and their degradation products in water*. Elsevier, Amsterdam
27. Martin-Esteban A, Fernandez P, Fernandez-Alba A, Camara C (1998) Analysis of polar pesticides in environmental water. *Quim Analytica* 17:51–66
28. Aprea C, Colosio C, Mammone T, Minoia C, Maroni M (2002) Biological monitoring of pesticide exposure: a review of analytical methods. *J Chromatogr B* 769:191–219
29. Ellman GL, Courtney KD, Andres V, Featherstone RM (1961) A new and rapid colorimetric determination of acetylcholinesterase activity. *Biochem Pharmacol* 7:88–95
30. Lu WJ, Chen YL, Zhu JH, Chen XG (2009) The combination of flow injection with electrophoresis using capillaries and chips. *Electrophoresis* 30:83–91
31. Hernandez F, Sancho JV, Pozo O, Lara A, Pitarch E (2001) Rapid direct determination of pesticides and metabolites in environmental water samples at sub-mg/L level by on-line solid-

- phase extraction–liquid chromatography–electrospray tandem mass spectrometry. *J Chromatogr A* 939:1–11
32. Hoff GR, Van Zoonen P (1999) Trace analysis of pesticides by gas chromatography. *J Chromatogr A* 843:301–322
 33. Sherma J (1993) Pesticides. *Anal Chem* 65:R40–R54
 34. Mitobe H, Ibaraki T, Tanabe A, Kawata K, Yasuhara A (2001) High performance liquid chromatographic determination of pesticides in soluble phase and suspended phase in river water. *Toxicol Environ Chem* 81:97–110
 35. Sherma J (2005) Thin-layer chromatography of pesticides: a review of applications for 2002–2004. *Acta Chromatogr* 15:5–30
 36. Beltran J, Lopez FJ, Hernandez F (2000) Solid-phase microextraction in pesticide residue analysis. *J Chromatogr A* 885:389–404
 37. Vasilescu MN, Medvedovici AV (2005) Pesticides. In: Poole CF, Worsfold PJ, Townshend A (eds) *Encyclopedia of analytical science*, vol 2, 2nd edn. Elsevier, Oxford
 38. Turner APF, Karube I, Wilson GS (1989) *Biosensors: fundamentals and applications*. Oxford University Press, New York, NY
 39. Wise DL (1991) *Bioinstrumentation and biosensors*. Marcel Dekker, New York, NY
 40. Coulet PR (1991) What is a biosensor? In: Blum LJ, Coulet PR (eds) *Biosensor principles and applications*. Marcel Dekker, New York, NY
 41. Blum LJ, Coulet PR (1992) *Biosensor principles and applications*. Marcel Dekker, New York, NY
 42. Giang P, Hall S (1951) Enzymatic determination of organic phosphorus insecticides. *Anal Chem* 23:1830–1834
 43. Mascini M, Moscone D (1986) Amperometric acetylcholine and choline sensors with immobilized enzymes. *Anal Chim Acta* 179:439–444
 44. Tor R, Freeman A (1986) New enzyme membrane for enzyme electrodes. *Anal Chem* 58:1042–1046
 45. Guilbault GG, Kramar DN, Cannon JL Jr (1962) Electrical determination of organophosphorous compounds. *Anal Chem* 34:1437–1439
 46. Jain MJ (1982) *Handbook of enzyme inhibitors*. Wiley, New York, NY
 47. Wittmann C, Reidel K, Schmid RD (1997) Microbial and enzyme sensors for environmental monitoring. In: Kress-Rogers E (ed) *Handbook of biosensors and electronic noses: medicine, food and the environment*. CRC Press, Boca Raton, FL
 48. Vanloon GW, Duffy J (2001) *Environmental chemistry—a global perspective*. Oxford University Press, New York, NY
 49. Pundir CS, Chauhan N (2012) Acetylcholinesterase inhibition-based biosensors for pesticide determination: a review. *Anal Biochem* 429:19–31
 50. Dennison MJ, Turner APF (1995) Biosensors for environmental mentoring. *Biotechnol Adv* 13:1–12
 51. Trojanowicz M (2002) Determination of pesticides using electrochemical enzymatic biosensors. *Electroanalysis* 14:1311–1329
 52. Solé S, Merkoçi A, Alegret S (2003) Determination of toxic substances based on enzyme inhibition. Part I. electrochemical biosensors for the determination of pesticides using batch procedures. *Crit Rev Anal Chem* 33:89–126
 53. Jimenez-Jorquera C, Orozco J, Baldi A (2010) ISFET based microsensors for environmental monitoring. *Sensors* 10:61–83
 54. Rodriguez-Mozaz S, Marco M, Lopez de Alda MJ, Barceló D (2004) Biosensors for environmental applications: future development trends. *Pure Appl Chem* 76:723–752
 55. Mulchandani A, Chen W, Mulchandani P, Wang J, Rogers KR (2001) Biosensors for direct determination of organophosphate pesticides. *Biosens Bioelectron* 16:225–230
 56. Rekha K, Thakur MS, Karanth NG (2000) Biosensors for the detection of organophosphorous pesticides. *Crit Rev Biotechnol* 20:213–235

57. Marty JL, Leca B, Noguer T (1998) Biosensors for the detection of pesticides. *Anal Mag* 26: M144–M149
58. McGrath TF, Elliott CT, Fodey TL (2012) Biosensors for the analysis of microbiological and chemical contaminants in food. *Anal Bioanal Chem* 403:75–92
59. Van Dyk JS, Pletschke B (2011) Review on the use of enzymes for the detection of organochlorine, organophosphate and carbamate pesticides in the environment. *Chemosphere* 82:291–307
60. Evtugyn GA, Budnikov HC, Nikolskaya EB (1998) Sensitivity and selectivity of electrochemical enzyme sensors for inhibitor determination. *Talanta* 46:465–484
61. Trojanowicz M, Hitchman ML (1996) Determination of pesticides using electrochemical biosensors. *Trends Anal Chem* 15:38–45
62. Marty JL, Garcia D, Rouillon R (1995) Biosensors: potential in pesticide detection. *Trends Anal Chem* 14:329–333
63. Marco MP, Barcelo D (1996) Environmental applications of analytical biosensors. *Meas Sci Technol* 7:1547–1562
64. Everett WR, Redmitz GA (1999) Enzyme-based electrochemical biosensors for determination of organophosphorous and carbamate pesticides. *Anal Lett* 32:1–10
65. Rogers KR (2006) Recent advances in biosensor techniques for environmental monitoring. *Anal Chim Acta* 568:222–231
66. Bilitewski U, Turner AFP (2000) *Biosensors for environmental monitoring*. Harwood Academic Publishers, Amsterdam, The Netherlands
67. Luque de Castro MD, Herrera MC (2003) Enzyme inhibition-based biosensors and biosensing systems, questionable analytical devices. *Biosens Bioelectron* 18:279–294
68. Lee HS, Kim YA, Cho YA, Lee YT (2002) Oxidation of organophosphorus pesticides for the sensitive detection by a cholinesterase-based biosensor. *Chemosphere* 46:571–576
69. Wang M, Gu X, Zhang G, Zhang D, Zhu D (2009) Continuous colorimetric assay for acetylcholinesterase and inhibitor screening with gold nanoparticles. *Langmuir* 25:2504–2507
70. Weinbroum AA (2005) Pathophysiological and clinical aspects of combat anticholinesterase poisoning. *Br Med Bull* 72:119–133
71. Pepeu G, Giovannini MG (2009) Cholinesterase inhibitors and beyond. *Curr Alzheimer Res* 6:86–96
72. Pohanka M, Musilek K, Kuca K (2009) Progress of biosensors based on cholinesterase inhibition. *Curr Med Chem* 16:790–1798
73. Andreescu S, Marty JL (2006) Twenty years research in cholinesterase biosensors: from basic research to practical applications. *Biomol Anger* 23:1–15
74. Budnikov GK, Evtugyn GA (1996) Electrochemical biosensors for inhibitor determination: selectivity and sensitivity control. *Electroanalysis* 8:817–820
75. Campanella L, De Luca S, Sammartino MP, Tomassetti M (1999) A new organic phase enzyme electrode for the analysis of organophosphorus pesticides and carbamates. *Anal Chim Acta* 385:59–71
76. Espinosa M, Atanasov P, Wilkins E (1999) Development of a disposable organophosphate biosensor. *Electroanalysis* 11:1055–1062
77. Tran-Minh C, Pandey PC, Kumaran S (1990) Studies on acetylcholine sensor and its analytical application based on the inhibition of cholinesterase. *Biosens Bioelectron* 5:461–471
78. Kumaran S, Morita M (1995) Application of a cholinesterase biosensor to screen for organophosphorus pesticides extracted from soil. *Talanta* 42:649–655
79. Zhang J, Luo A, Liu P, Wei S, Wang G, Wei S (2009) Detection of organophosphorus pesticides using potentiometric enzymatic membrane biosensor based on methylcellulose immobilization. *Anal Sci* 25:511–515
80. Gyurcsanyi RE, Vagfoldi Z, Toth K, Nagy G (1999) Fast response potentiometric acetylcholine biosensor. *Electroanalysis* 11:712–718
81. Hitchman ML, Trojanowicz M (1995) A simple disposable potentiometric biosensor for pesticides. *Chem Anal (Warsaw)* 40:609–617

82. Campanella L, Colapicchioni C, Favero G, Sammartino MP, Tomassetti M (1996) Organophosphorus pesticide (Paraoxon) analysis using solid state sensors. *Sensor Actuat B Chem* 33:25–33
83. Liu B, Yang Y, Wu Z, Wang H, Shen G, Yu R (2005) A potentiometric acetylcholinesterase biosensor based on plasma-polymerized film. *Sensor Actuat B Chem* 104:186–190
84. Hendji N, Jaffrezic-Renault AM, Martelet N, Clechet C, Shulga P, Strikha AA, Netchiporuk LI, Soldatkin AP, Wlodarski WB (1993) Sensitive detection of pesticides using a differential ISFET-based system with immobilized cholinesterases. *Anal Chim Acta* 281:3–11
85. Panasyuk-Delaney T, Mirsky VM, Ulbricht M, Wolfbeis OS (2001) Impedimetric herbicide chemosensors based on molecularly imprinted polymers. *Anal Chim Acta* 435:157–162
86. Rogers KR, Foley M, Alter S, Koga P, Eldefrani M (1991) Light addressable potentiometric biosensor for the detection of anticholinesterases. *Anal Lett* 24:191–198
87. Fernando JC, Rogers KR, Anis NA, Valdes JJ, Thomson RG, Eldefarni AT, Eldefrawi ME (1993) Rapid detection of anticholinesterase insecticides by a reusable light addressable potentiometric biosensor. *J Agric Food Chem* 41:511–516
88. Baum G, Ward FB (1971) Ion-selective electrode procedure for organophosphate pesticide analysis. *Anal Chem* 43:947–948
89. Eppelsheim C, Hampp N (1994) Potentiometric thick-film sensor for the determination of the neurotransmitter acetylcholine. *Analyst* 119:2167–2171
90. Imato T, Ishibashi N (1995) Potentiometric butyrylcholine sensor for organophosphate pesticides. *Biosens Bioelectron* 10:435–441
91. Ding J, Qina W (2009) Polymeric membrane ion-selective electrode for butyrylcholinesterase based on controlled release of substrate. *Electroanalysis* 21:2030–2035
92. Khaled E, Hassan HNA, Mohamed GG, Ragab FA, Seleim AA (2010) β -Cyclodextrin-based potentiometric sensors for flow-injection, determination of acetylcholines. *Int J Electrochem Sci* 5:448–458
93. Khaled E, Hassan HNA, Mohamed GG, Ragab FA, Seleim AA (2010) Disposable potentiometric sensors for monitoring cholinesterase activity. *Talanta* 83:357–363
94. Khaled E, Kamel MS, Hassan HNA, Abdel-Gawad H, Aboul-Enein HY (2014) Performance of a portable biosensor for the analysis of ethion residues. *Talanta* 119:467–472
95. Amine A, Alafandy M, Kauffmann J, Pekli MN (1995) Cyanide determination using an amperometric biosensor based on cytochrome oxidase inhibition. *Anal Chem* 67:2822–2827
96. Jha N, Ramaprabhu S (2009) Development of MWNT based disposable biosensor on glassy carbon electrode for the detection of organophosphorus nerve agents. *J Nanosci Nanotech* 9:5676–5680
97. Carlo MD, Mascini M, Pepe A, Diletti G, Compagnone D (2004) Screening of food for carbamate and organophosphate pesticides using an electrochemical bioassay. *Food Chem* 84:651–656
98. Skladal P (1991) Determination of organophosphate and carbamate pesticides using a cobalt phthalocyanine-modified carbon paste electrode and a cholinesterase enzyme membrane. *Anal Chim Acta* 252:11–15
99. Skladal P (1992) Detection of organophosphate and carbamate pesticides using disposable biosensors based on chemically modified electrodes and immobilized cholinesterase. *Anal Chim Acta* 269:281–287
100. Skladal P, Mascini M (1992) Sensitive detection of pesticides using amperometric sensors based on cobalt phthalocyanine-modified composite electrodes and immobilised cholinesterases. *Biosens Bioelectron* 7:335–343
101. Rippeth JJ, Gibson TD, Hart JP, Hartley IC, Nelson G (1997) Flow-injection detector incorporating a screen-printed disposable amperometric biosensor for monitoring organophosphate pesticides. *Analyst* 122:1425–1429
102. Bucur B, Dondoi M, Danet A, Marty JL (2005) Insecticide identification using a flow injection analysis system with biosensors based on various cholinesterases. *Anal Chim Acta* 539:195–201
103. Neufeld T, Eshkenazi I, Cohen E, Rishpon J (2000) A micro flow injection electrochemical biosensor for organophosphorus pesticides. *Biosens Bioelectron* 15:323–329

104. Khayyami M, Pérez Pita MT, Pena Garcia N, Johansson G, Danielsson B, Larsson P (1998) Development of an amperometric biosensor based on acetylcholine esterase covalently bound to a new support material. *Talanta* 45:557–563
105. La Rosa C, Pariente F, Hernández L, Lorenzo E (1995) Amperometric flow-through biosensor for the determination of pesticides. *Anal Chim Acta* 308:129–136
106. Bernabei M, Chiavarini S, Cremsini C, Palleschi G (1993) Anticholinesterase activity measurement by a choline biosensor: application in water analysis. *Biosens Bioelectron* 8:265–271
107. Marty JL, Sode K, Karube I (1992) Biosensor for detection of organophosphate and carbamate insecticides. *Electroanalysis* 4:249–252
108. Shi H, Zhao Z, Song Z, Huang J, Yang Y, Anzai J, Osa T, Chen Q (2005) Fabricating of acetylcholine biosensor by a layer-by-layer deposition technique for determining Trichlorfon. *Electroanalysis* 17:1285–1290
109. Palchetti P, Cagnini A, Del Carlo M, Coppi C, Mascini M, Turner PF (1997) Determination of anticholinesterase pesticides in real samples using a disposable biosensor. *Anal Chim Acta* 337:315–321
110. Fennouh S, Casimiri V, Burstein C (1997) Increased paraoxon detection with solvents using acetylcholinesterase inactivation measured with a choline oxidase biosensor. *Biosens Bioelectron* 12:97–104
111. Campanella L, Achili M, Sammartino MP, Tomasetti M (1991) Butyrylcholine enzyme sensor for determining organophosphorus inhibitors. *Bioelectrochem Bioenerg* 26:237–249
112. Lopez Riuz B, Dempsey E, Hua C, Smyth MR, Wang J (1993) Development of amperometric sensors for choline, acetylcholine and arsenocholine. *Anal Chim Acta* 273:425–430
113. Yabuki S, Mizutani F, Katsura T (1994) Choline-sensing electrode based on polyethylene glycol-modified enzyme and mediator. *Sensor Actuat B Chem* 20:159–162
114. Martorell D, Cespedes F, Martinez-Fabregas E, Alegret S (1997) Determination of organophosphorus and carbamate pesticides using a biosensor based on a polishable, 7,7,8,8-tetracyanoquino-dimethane-modified, graphite—epoxy biocomposite. *Anal Chim Acta* 337:305–313
115. Skladal P, Fiala M, Krejci J (1996) Detection of pesticides in the environment using biosensors based on cholinesterases. *Int J Environ Anal Chem* 65:139–148
116. Skladal P, Nunes GS, Yamanaka H, Ribeiro ML (1997) Detection of carbamate pesticides in vegetable samples using cholinesterase-based biosensors. *Electroanalysis* 9:1083–1087
117. Schulze H, Vorlova S, Villatte F, Bachmann TT, Schmid RD (2003) Design of acetylcholinesterase for biosensor applications. *Biosens Bioelectron* 18:201–209
118. Marques PR, Nunes GS, dos Santos TC, Andreescu S, Marty JL (2004) Comparative investigation between acetylcholinesterase obtained from commercial sources and genetically modified *Drosophila melanogaster*. Application in amperometric biosensors for methamidophos pesticide detection. *Biosens Bioelectron* 20:825–832
119. Stein K, Schwedt G (1993) Comparison of immobilization methods for the development of an acetylcholinesterase biosensor. *Anal Chim Acta* 272:73–81
120. Bonnet C, Andreescu S, Andreescu JL (2003) Adsorption: an easy and efficient immobilisation of acetylcholinesterase on screen-printed electrodes. *Anal Chim Acta* 481:209–211
121. Andreescu S, Avramescu A, Bala C, Magearu V, Marty JL (2002) Detection of organophosphorus insecticides with immobilized acetylcholinesterase: comparative study between two enzyme sensors. *Anal Bioanal Chem* 74:39–45
122. Gabrovska K, Nedelcheva T, Godjevargova T, Stoilova O, Manolova N, Rashkov I (2008) Immobilization of acetylcholinesterase on new modified acrylonitrile copolymer membranes. *J Mol Catal B* 55:169–176
123. Upadhyay S, Rao GR, Sharma MK, Bhattacharya BK, Rao VK, Vijayaraghavan R (2009) Immobilization of acetylcholinesterase–choline oxidase on a gold–platinum bimetallic nanoparticles modified glassy carbon electrode for the sensitive detection of organophosphate pesticides, carbamates, and nerve agents. *Biosens Bioelectron* 25:832–838

124. Bucur B, Danet AF, Marty JL (2004) Versatile method of cholinesterase immobilisation via affinity bonds using Concanavalin A applied to the construction of a screen-printed biosensor. *Biosens Bioelectron* 20:217–225
125. Vakurov A, Simpson CE, Daly CL, Gibson TD, Millner PA (2005) Acetylcholinesterase-based biosensor electrodes for organophosphate pesticide detection: II. Immobilization and stabilization of acetylcholinesterase. *Biosens Bioelectron* 20:2324–2329
126. Du D, Chen W, Cai J, Zhang J, Qu F, Li H (2008) Development of acetylcholinesterase biosensor based on CdTe quantum dots modified cysteamine self-assembled monolayers. *J Electroanal Chem* 623:81–85
127. Campàs M, Prieto-Simon P, Marty JL (2009) A review of the use of genetically engineered enzymes in electrochemical biosensor. *Semin Cell Dev Biol* 20:3–9
128. Trojanowicz M (2000) Flow injection analysis. Instrumentation and applications. World Scientific Publishing, Singapore
129. Schmidt HL (1993) Biosensors and flow injection analysis in bioprocess control. *J Biotechnol* 31:v–vi
130. Trojanowicz M, Alexander PW (1997) Portable flow-injection systems for field testing Present development and perspectives. In: Nikolelis DP, Krull UJ, Wang J, Mascini M (eds) *Biosensors for direct monitoring of environmental pollutants in field*. Kluwer Academic Publishers, Dordrecht
131. Diehl-Faxon J, Ghindlis AL, Atanasov P, Wilkins E (1996) Direct electron transfer based tri-enzyme electrode for monitoring of organophosphorus pesticides. *Sensor Actuat B Chem* 36:448–457
132. Prieto-Simón B, Campàs M, Andreescu S, Marty JL (2006) Trends in flow-based biosensing systems for pesticide assessment. *Sensors* 6:1161–1186
133. Rodrigues TC, Tubino M, Godinho OES, de Oliveira Neto G (1997) An immobilized acetylcholinesterase flow-injection conductometric system for the determination of Paraoxon. *Anal Sci* 13:423–428
134. Simonian AL, Rainina EI, Wild JR (1997) A new approach for discriminative detection for organophosphate neurotoxins in the presence of other cholinesterase inhibitors. *Anal Lett* 30:2453–2468
135. Gunther A, Bilitewski U (1995) Characterization of inhibitors of acetylcholinesterase by an automated amperometric flow-injection system. *Anal Chim Acta* 300:117–125
136. Jeanty G, Ghommidh C, Marty JL (2001) Automated detection of chlorpyrifos and its metabolites by a continuous flow system-based enzyme sensor. *Anal Chim Acta* 436:119–128
137. Hart JP, Wring SA (1997) Recent developments in the design and application of screen-printed electrochemical sensors for biomedical, environmental and industrial analyses. *Trends Anal Chem* 16:89–103
138. Hart JP, Crew A, Crouch E, Honeychurch KC, Pemberton RM (2004) Some recent designs and developments of screen-printed carbon electrochemical sensors/biosensors for biomedical, environmental and industrial analyses (review). *Anal Lett* 37:789–830
139. Renedo OD, Alonso-Lomillo MA, Martinez MJ (2007) Recent developments in the field of screen-printed electrodes and their related applications. *Talanta* 73:202–219
140. Li M, Li Y, Li D, Long Y (2012) Recent developments and applications of screen-printed electrodes in environmental assays—a review. *Anal Chim Acta* 743:31–44
141. Skladal P, Parlik M, Fiala M (1994) Pesticide biosensor based on coimmobilized acetylcholinesterase and butyrylcholinesterase. *Anal Lett* 27:29–40
142. Bachmann TT, Schmid RD (1999) A disposable multielectrode biosensor for rapid simultaneous detection of the insecticides paraoxon and carbofuran at high resolution. *Anal Chim Acta* 401:95–103
143. Collier WA, Clear MA, Hart AL (2002) Convenient and rapid detection of pesticides of extracts of sheep wool. *Biosens Bioelectron* 17:815–819
144. Andreescu S, Noguer T, Magearu V, Marty JL (2002) Screen-printed electrode based on AChE for the detection of pesticides in presence of organic solvents. *Talanta* 57:169–176

145. Laschi S, Ogonczyk D, Palchetti I, Mascini M (2007) Evaluation of pesticide induced acetylcholinesterase inhibition by means of disposable carbon modified electrochemical biosensors. *Enzym Microbiol Technol* 40:485–489
146. Law KA, Higson SPJ (2005) Sonochemically fabricated acetylcholinesterase micro-electrode arrays within a flow injection analyser for the determination of organophosphate pesticides. *Biosens Bioelectron* 20:1914–1924
147. Hart JP, Hartley IC (1994) Voltammetric and amperometric studies of thiocholine at a screen-printed carbon electrode chemically modified with cobalt phthalocyanine: studies towards a pesticide sensor. *Analyst* 119:259–263
148. Pumera M, Sanchez S, Ichinose I, Tang J (2007) Electrochemical nanobiosensors. *Sensor Actuat B Chem* 123:1195–1205
149. Agui L, Sedenó PL, Pingarrón JM (2008) Role of carbon nanotubes in electroanalytical chemistry A review. *Anal Chim Acta* 622:11–47
150. Ji X, Kadara RO, Krussma J, Chen Q, Banks CE (2010) Understanding the physicoelectrochemical properties of carbon nanotubes: current state of the Art. *Electroanalysis* 22:7–19
151. Vashist SK, Zheng D, Al-Rubeaan K, Luong JHT, Sheu FS (2011) Advances in carbon nanotube based electrochemical sensors for bioanalytical applications. *Biotechnol Adv* 29:169–188
152. Periasamy AP, Umasankar Y, Chen S (2009) Nanomaterials - acetylcholinesterase enzyme matrices for organophosphorus pesticides electrochemical sensors: a review. *Sensors* 9:4034–4055
153. Liu G, Lin Y (2006) Biosensor based on self-assembling acetylcholinesterase on carbon nanotubes for flow injection/amperometric detection of organophosphate pesticides and nerve agents. *Anal Chem* 78:835–843
154. Kandimalla VB, Ju HX (2006) Binding of acetylcholinesterase to multiwall carbon nanotube-crosslinked chitosan composite for flow-injection amperometric detection of an organophosphorous insecticide. *Chem Eur J* 12:1074–1080
155. Du D, Huang X, Cai J, Zhang A (2007) Amperometric detection of triazophos pesticide using acetylcholinesterase biosensor based on multiwall carbon nanotube–chitosan matrix. *Sensor Actuat B Chem* 127:531–535
156. Lin Y, Lu F, Wang J (2004) Disposable carbon nanotube modified screen-printed biosensor for amperometric detection of organophosphorus pesticides and nerve agents. *Electroanalysis* 16:145–149
157. Su S, He Y, Zhang M, Yang K, Song S, Zhang X, Fan C, Lee S (2008) High-sensitivity pesticide detection via silicon nanowires-supported acetylcholinesterase-based electrochemical sensors. *Appl Phys Lett* 93:023113
158. Norouzi P, Pirali-Hamedani M, Ganjali MR, Faridbod F (2010) A Novel acetylcholinesterase biosensor based on chitosan-gold nanoparticles film for determination of monocrotophos using FFT continuous cyclic voltammetry. *Int J Electrochem Sci* 5:1434–1446
159. Liu T, Su H, Qu X, Ju P, Cui L, Ai S (2011) Acetylcholinesterase biosensor based on 3-carboxyphenylboronic acid/reduced graphene oxide–gold nanocomposites modified electrode for amperometric detection of organophosphorus and carbamate pesticides. *Sensor Actuat B Chem* 160:1255–1261
160. Zhai C, Sun X, Zhao W, Gong Z, Wang X (2013) Acetylcholinesterase biosensor based on chitosan/Prussian blue/multiwall carbon nanotubes/hollow gold nanospheres nanocomposite film by one-step electrodeposition. *Biosens Bioelectron* 42:124–130
161. Chen QX, Zheng WZ, Lin JY, Shi Y, Xie WZ, Zhou HM (2000) Effect of metal ions on the activity of green crab (*Scylla serrata*) alkaline phosphatase. *Int J Biochem Cell Biol* 32:879–885
162. Su Y, Cagnini A, Mascini M (1995) Screen-printed biosensor alkaline phosphatase-based for environmental applications. *Chem Anal (Warsaw)* 40:579–585
163. Mazzei F, Botre F, Botre C (1996) Acid phosphatase/glucose oxidase-based biosensors for the determination of pesticides. *Anal Chim Acta* 336:67–75
164. Hedenmo M, Narvaez A, Dominguez E, Katakin I (1997) Improved mediated tyrosinase amperometric enzyme electrodes. *J Electroanal Chem* 425:1–11

165. Besombes JL, Cosnier S, Labbe P, Reverdy G (1995) A biosensor as warning device for the detection of cyanide, chlorophenols, atrazine and carbamate pesticides. *Anal Chim Acta* 311:255–263
166. Perez Pita T, Reviejo AJ, Manuel de Villena FJ, Pingarron JM (1997) Amperometric selective biosensing of dimethyl- and diethyldithiocarbamates based on inhibition processes in a medium of reversed micelles. *Anal Chim Acta* 340:89–97
167. Wang J, Nascimento VB, Kane SA, Rogers K, Smyth MR, Angnes L (1996) Screen-printed tyrosinase-containing electrodes for the biosensing of enzyme inhibitors. *Talanta* 43:1903–1907
168. Tanimoto de Albuquerque YD, Ferreira LF (2000) Amperometric biosensing of carbamate and organophosphate pesticides utilizing screen-printed tyrosinase-modified electrodes. *Anal Chim Acta* 596:210–221
169. Carralero V, Mena ML, Gonzalez-Cortes A, Yanez-Sedeno P, Pingarron JM (2006) Development of a high analytical performance-tyrosinase biosensor based on a composite graphite–Teflon electrode modified with gold nanoparticles. *Biosens Bioelectron* 22:730–736
170. Wang J, Dempsey E, Eremenko A (1993) Organic-phase biosensing of enzyme inhibitors. *Anal Chim Acta* 279:203–208
171. Noguer T, Marty JL (1997) High sensitive bienzymic sensor for the detection of dithiocarbamate fungicides. *Anal Chim Acta* 347:63–70
172. Marty JL, Mionetto N, Noguer T, Ortega F, Roux C (1993) Enzyme sensors for the detection of pesticides. *Biosens Bioelectron* 8:273–280
173. Noguer T, Gradinaru A, Cincu A, Marty J (1999) A new disposable biosensor for the accurate and sensitive detection of ethylenebis-(Dithiocarbamate) fungicides. *Anal Lett* 32:1723–1738
174. Munnecke DM (1980) Enzymatic detoxification of waste organophosphate pesticides. *J Agric Food Chem* 28:105–111
175. Dumas DP, Durst HD, Landis WG, Raushel FM, Wild JR (1990) Inactivation of organophosphorus nerve agents by the phosphotriesterase from *Pseudomonas diminuta*. *Arch Biochem Biophys* 227:155–159
176. Mulchandani P, Mulchandani A, Kaneva I, Chen W (1999) Biosensor for direct determination of organophosphate nerve agents. Potentiometric enzyme electrodes. *Biosens Bioelectron* 14:77–85
177. Simonian AL, Flounders AW, Wild JR (2004) FET-based biosensors for the direct detection of organophosphate nerve toxins. *Electroanalysis* 16:1896–1906
178. Gaberlein S, Knoll M, Spener F, Zaborosch C (2000) Disposable potentiometric enzyme sensor for direct determination of organophosphorus insecticides. *Analyst* 125:2274–2279
179. Mulchandani A, Mulchandani P, Chen W, Wang J, Chen L (1999) Amperometric thick-film strip electrodes for monitoring organophosphate nerve agents based on immobilized organophosphorus hydrolase. *Anal Chem* 71:2246–2249
180. Eshkenazi I, Sacks V, Neufeld T, Rishpon J (2000) Amperometric biosensors based on micro flow injection system. *Appl Biochem Biotechnol* 89:217–230
181. Mulchandani P, Chen W, Mulchandani A (2001) Flow injection amperometric enzyme biosensor for direct determination of organophosphate nerve agents. *Environ Sci Technol* 35:2562–2565
182. Wang J, Krause R, Block K, Musameh M, Mulchandani A, Schöning MJ (2003) Flow injection amperometric detection of OP nerve agents based on an organophosphorus-hydrolase biosensor detector. *Biosens Bioelectron* 18:255–260
183. Joshi KA, Prouza M, Kum M, Wang J, Tang J, Haddon R, Chen W, Mulchandani A (2006) V-type nerve agent detection using a carbon nanotube-based amperometric enzyme electrode. *Anal Chem* 78:331–336
184. Wang J, Krause R, Block K, Musameh M, Mulchandani A, Mulchandani P, Chen W, Schöning MJ (2002) Dual amperometric-potentiometric biosensor detection system for monitoring organophosphorus neurotoxins. *Anal Chim Acta* 469:197–203
185. Schöning MJ, Rause R, Block K, Musahmeh M, Mulchandani A, Wang J (2003) A dual amperometric/potentiometric FIA-based biosensor for the distinctive detection of organophosphorus pesticides. *Sensor Actuat B Chem* 95:291–296

186. Mulchandani A, Mulchandani P, Chauhan S, Kaneva I, Chen W (1998) A potentiometric microbial biosensor for direct determination of organophosphate nerve agents. *Electroanalysis* 10:733–737
187. Rainina EI, Efremenco EN, Varfolomeyev SD, Simonian AL, Wild JR (1996) The development of a new biosensor based on recombinant *E. coli* for the direct detection of organophosphorus neurotoxins. *Biosens Bioelectron* 11:991–1000
188. Gouda MD, Thakur MS, Karanth NG (1997) A dual enzyme amperometric biosensor for monitoring organophosphate pesticide. *Biotech Tech* 11:653–655
189. Campanella L, Cocco R, Sammartino MP, Tomassetti M (1992) A new enzyme inhibition sensor for organophosphorus pesticides analysis. *Sci Tot Environ* 123(124):1–16
190. Guilhermino L, Barros P, Silva MC, Soares AM (1998) Should the use of inhibition of cholinesterases as a specific biomarker for organophosphate and carbamate pesticides be questioned? *Biomarkers* 3:157–163
191. Stoytcheva M, Sharkova V, Panayotova M (1998) Electrochemical approach in studying the inhibition of acetylcholinesterase by arsenate(III): analytical characterisation and application for arsenic determination. *Anal Chim Acta* 364:195–201
192. Simonian AL, Good TA, Wang SS, Wild JR (2005) Nanoparticle-based optical biosensors for the direct detection of organophosphate chemical warfare agents and pesticides. *Anal Chim Acta* 534:69–77
193. Dumschat C, Müller H, Stein K, Schwedt G (1991) Pesticide-sensitive ISFET based on enzyme inhibition. *Anal Chim Acta* 252:7–9
194. Simonian AL, Efremenko EN, Wild JR (2001) Discriminative detection of neurotoxins in multi-component samples. *Anal Chim Acta* 444:179–186
195. Bachmann TT, Leaca B, Vilatte F, Marty JL, Fournier D, Schmid DR (2000) Improved multianalyte detection of organophosphates and carbamates with disposable multielectrode biosensors using recombinant mutants of *Drosophila* acetylcholinesterase and artificial neural networks. *Biosens Bioelectron* 15:193–201
196. Marty JL, Mionetto N, Lacorte S, Barcelo D (1995) Validation of an enzymatic biosensor with various liquid chromatographic techniques for determining organophosphorus pesticides and carbaryl in freeze-dried waters. *Anal Chim Acta* 311:265–271
197. Montesinos T, Pérez-Munguia S, Valdez F, Marty JL (2001) Disposable cholinesterase biosensor for the detection of pesticides in water-miscible organic solvents. *Anal Chim Acta* 431:231–237
198. Sequeira M, Bowden M, Minogue E, Diamond D (2002) Towards autonomous environmental monitoring systems. *Talanta* 56:355–363
199. Gu MB, Kim EJ, Cho J, Hansen PD (2001) The continuous monitoring of field water samples with a novel multi-channel two-stage mini-bioreactor system. *Environ Monitor Assess* 70:71–81
200. Thevenot DR, Toth K, Durst RA, Wilson GS (2001) Electrochemical biosensors: recommended definitions and classification. *Biosens Bioelectron* 16:121–131
201. Sticher PM, Jaspers C, Stemmler K, Harms H, Zehnder AJ, van der Meer YR (1997) Development and characterization of a whole-cell bioluminescent sensor for bioavailable middle-chain alkanes in contaminated groundwater samples. *Appl Environ Microbiol* 63:4053–4060
202. Patel PD (2002) (Bio)sensors for measurement of analytes implicated in food safety: a review. *Trends Anal Chem* 21:96–115

Part IV
Electrochemical Sensors for Gases
of Environmental Importance

Chapter 14

Volatile Organic Compounds

Tapan Sarkar and Ashok Mulchandani

14.1 Introduction

Volatile organic compounds (VOCs) are numerous, varied, and ubiquitous. In nature, VOCs are both biogenic and anthropogenic. Plants are the primary biogenic source of VOCs as evident by the strong plant odors. The anthropogenic sources of VOCs include hydrocarbons from crude oil production and processing, solvents such as ketones (acetone and methylethyl ketone), alkanes (hexane), alcohols (ethanol, isopropanol), and aromatics (benzene and toluene) that are widely used in chemical processing industries, household products, etc. While most VOCs are not toxic, health problems, such as acute headache, allergy, respiratory problem, nausea, and immunity in children/infants, may arise upon long-term exposure to some of these VOCs even at low concentrations. VOCs such as formaldehyde, acrylonitrile, benzene, toluene, ethylbenzene, and xylenes are highly toxic and/or carcinogenic. Formaldehyde and acrylonitrile are used as base raw material in the resin industry. Benzene, toluene, ethylbenzene, and xylenes (commonly known as BTEX) are released as automobile exhaust. Other synthetic products, such as paints and wax, can also release toxic vapors when stored. Further, despite being present at extremely low concentrations, some VOCs like organic amines can catalyze the oxidative atmospheric photochemistry and facilitate smog formation through nucleation of aerosol formation, which has a potential impact on environmental condition deterioration, in particular climate change. Hence, accurate and real-time detection of VOCs is necessary to protect/monitor the indoor and outdoor air quality and to provide occupational health safety at workplace. To ensure safe environment in the workplace, various regulatory bodies such as occupational

T. Sarkar • A. Mulchandani (✉)

Department of Chemical and Environmental Engineering, University
of California Riverside, Riverside, CA 92521, USA

e-mail: adani@engr.ucr.edu

Table 14.1 Permissible exposure limits for VOCs in the workplace

Analyte	OSHA PEL (ppm)	NIOSH REL (ppm)	ACGIH TLV (ppm)	Health factors
<i>n</i> -Hexane	500	50	50	A narcotic agent; a neurotoxin; and an eye, upper respiratory tract, and skin irritant.
Formaldehyde	0.75	–	0.3	Potential occupational carcinogen.
Acetone	1,000	250	500–750	An eye and respiratory irritant. May cause headache, dizziness.
Methyl ethyl ketone	200	200–300	200–300	Eyes, nose, and throat irritant.
Methanol	200	200–250	200–250	Visual disturbances and respiratory irritant. May cause headache, drowsiness.
Ethanol	1000	1000	1000	An eye and upper respiratory tract irritant. May cause headache, fatigue.
<i>Iso</i> -propanol	400	400	400	Eye, nose, and throat irritant.
Benzene	1	1	10	Potential occupational carcinogen.
Toluene	200	100	20	May cause central nervous system depression, causing fatigue, and muscular incoordination.
Ethylbenzene	100	100	100	An eye, mucous membrane, and skin irritant.
Xylenes	100	100	100	May cause central nervous system depression and irritation of the eyes and skin.

OSHA Occupational Safety and Health Administration, *PEL* Permissible Exposure Limit, *NIOSH* National Institute for Occupational Safety and Health, *REL* Recommended Exposure Limit, *ACGIH* American Conference of Governmental Industrial Hygienists, *TLV* Threshold Limit Value www.osha.gov

safety and health administration (OSHA), national institute for occupational safety and health (NIOSH), and American conference of governmental industrial hygienists (ACGIH) have set limits of the VOCs in the environment. Table 14.1 provides data of the permissible exposure limit for select VOCs. Further, some VOCs like nitroaromatic and organophosphorus compounds are serious threat to the homeland security due to their mass destruction capability. For example, nitroaromatic compounds such as trinitrotoluene (TNT) and cyclotrimethylenetrinitramine (commonly known as RDX) are used as explosive while organophosphates such as sarin are used as lethal chemical warfare agents. Recently, VOCs in exhaled breath have also been identified as potential biomarkers of diseases—for example alkanes and benzene derivatives for lung cancer and acetone for diabetes. Hence an accurate quantitative detection of VOCs at trace level is also important for disease diagnosis in the healthcare sector and for homeland security.

In spite of recent advances, the task of identification and quantification of pollutants in a complex environment containing thousands of interfering species using an inexpensive, reliable device remains a serious challenge. The most commonly practiced analytical methods for pollutant/contaminant detection are

separation-based techniques along with suitable detector. The current state of the art for VOC detection typically utilizes gas chromatograph (GC) for separation in combination with various schemes including flame ionization (GC-FID), photoionization (GC-PID), or mass spectrometry (GC-MS). GC-PID is an advantageous technique for simultaneous detection of simple aromatic molecules such as BTEX; however, selectivity may be compromised if alkanes are present in the sample. This drawback could be overcome partially by performing the separation process simultaneously on two columns with different polarity. GC-FID provides unambiguous identification of VOCs with a large linear dynamic range. GC-MS combination provides high sensitivity and accuracy. However, these instruments are expensive, do not provide real-time measurements, require trained personnel to operate, are not easily field deployable due to bulky size, and do not currently exhibit the potential for full miniaturization in the form of wearable badges. Alternative quick and easy methods for pollutant identification employ a target-specific chemical sensor or an electronic nose/tongue.

Conventional strategies for target-specific chemical sensor development have largely depended on the traditional “lock-and-key” design, where the sensor selectivity and sensitivity depend on the binding specificity/affinity between the analyte of interest and the specific receptor. This strategy can lead to highly selective and sensitive detection if the analyte binding is strong enough and specific to the recognition element. Another related strategy involves exploiting a physicochemical change selectively towards a target analyte, where selectivity is achieved through the transduction mechanism in which the method of detection indicates which species are identified. Such strategies are reliable when a specific target analyte is to be detected within controlled backgrounds and interferences. However, this strategy demands the synthesis of separate, highly selective, and target-responsive sensor elements for each analyte to be detected. Another alternative for sensitive and real-time detection of target analyte would be to employ a highly sensitive sensor in combination with a suitable micro-separation unit. However, design, fabrication, and integration of such micro-separation unit within the sensor module are complex and challenging.

On the other hand, in the electronic nose/tongue architecture, an array of different nonselective sensors is used, with every element in the array responding to a number of different chemicals and generating a nonspecific response pattern or chemical signature of the tested toxins/pollutants which is then analyzed with a suitable statistical based chemometric method, pattern recognition algorithm, neural network, or some combination for identification of the pollutants. In practice, most chemical sensors provide cross-reactivity due to the interaction or response of the sensor towards interfering chemicals that are structurally and chemically similar to the desired analyte. Moreover, most VOCs are chemically inert and bind weakly with the recognition element that limits the realization of target-specific sensor development. Hence, use of an electronic nose/tongue is the most practical option for the reliable identification and quantification of VOCs.

Chemical sensor can be developed based on the interaction of VOCs with recognition element in conjugation with transducer such as optical,^{1,8,9,10,11}

surface plasmon resonance (SPR),² quartz crystal microbalance (QCM),^{3,12} surface acoustic waves (SAW),⁴ microcantilever,⁵ thermistor,⁶ and field-effect transistor.⁷ The response of the sensor based on optical, SPR, QCM/SAW/microcantilever, and thermistor can be measured in the resulting absorbance/reflectance/fluorescence/chemiluminescence, refractive index, mass, and temperature, respectively. Table 14.2 summarizes different types of optical and mass transduction-based sensors reported for detection of VOCs. Although, sensitive detection of VOCs is possible using these sensors, however, they are difficult to miniaturize limiting their application as a point-of-use/field-deployable device and building a sensor arrays/e-nose for reliable detection in a complex environment. On the other hand, solid-state electrochemical sensors, i.e., chemiresistor/field-effect transistor (FET) sensors based on electrical transduction mechanism, are an attractive alternative because of low power consumption, low cost, possibilities for miniaturization to make high-density sensor array, and multiplexing capabilities.

14.2 Scope and Overview of the Chapter

In light of the above discussion, in this chapter we provide a comprehensive review of electrochemical sensors for VOCs. We start with a brief description of sensor configuration followed by materials used as recognition element in these sensors. While discussing the various methods used for device fabrication using different sensing materials, we discuss the success and limitation of the methods used and possible solutions to those problems. Further, we discuss the functionalization strategy and demonstrate their importance for the improvement of device sensitivity. Finally, we conclude by highlighting some challenges in the field of electrochemical sensor development/research for VOCs and also predict the direction towards which future of this area might be directed.

14.3 Electrochemical Sensors

Figure 14.1 shows the schematic of a basic chemiresistor/FET-based electrochemical sensor. It consists of two metal microelectrodes on a dielectric separated by a gap which is bridged by a semiconductor material. The interaction of chemical species of VOCs with semiconductor material bridging the gap causes changes in the physicochemical properties of the chemically interactive layers or changes in the surface morphology or charge transfer between the interacting components that result in a change in the resistance/conductance of the semiconductor. Chemiresistor/FET device can be developed using two kinds of sensing platforms: (1) planar or two-dimensional (2-D) thick/thin film (Fig. 14.1a) and (2) - one-dimensional (1-D) nanostructures like nanotubes, nanowires, nanoribbons, and nanobelts (Fig. 14.1b), as the conduction channel bridging the source and

Table 14.2 Summary for optical and mass transduction-based sensors for VOCs

Transduction mechanism	Detection technique	Sensor configuration	Analyte	Lowest concentration	Reference
Optical	UV-Vis absorbance	A composite thin film of zinc(II) tetra-4-(2,4-di- <i>tert</i> -amylphenoxy) phthalocyanine and copper(II) tetrakis (<i>p</i> - <i>tert</i> -butylphenyl) porphyrin prepared via spin coating on quartz substrate	Alcohols Amines Ketones Alkanes	Saturated vapors	1
	Color	An array of sensor prepared by using different dyes (Lewis acid/base dye, Bronsted acidic or basic dye and dye with large permanent dipoles) entrapped into a hydrophobic organic sol-gel matrix	Alcohols Carboxylic acids Amines Aldehyde Ketones	OSHA PEL concentration	8
Mass	Surface-enhanced Raman scattering (SERS)	2,6-Dimethylphenylisocyanide (2,6-DMPI)-capped Au nanoparticle aggregate thin film on glass substrate	CCl ₄ MeOH Butylamine	6.5 ppm	9
	Diffuse reflectance infrared Fourier transform (DRIFT)	Graphene decorated with ZnO nanoparticle	Formaldehyde	25 ppm	10
	Fluorescence	TiO ₂ nanoparticle coated with porphyrin dye	Alcohols Acetone		11
	QCM	Array of piezoelectric sensor modified with MWNTs	Alcohols Aromatic organics	Saturated vapors	3
	SAW	Piezoelectric sensor modified with poly(isobutylene) (PIB) gel	BTEX		12
	Microcantilever	ZnO piezoelectric films by reactive sputtering on Si/SiO ₂ substrate	Toluene	25 ppm	4
		Si resonator modified with polyglycolic acid	Toluene	5 ppm	5

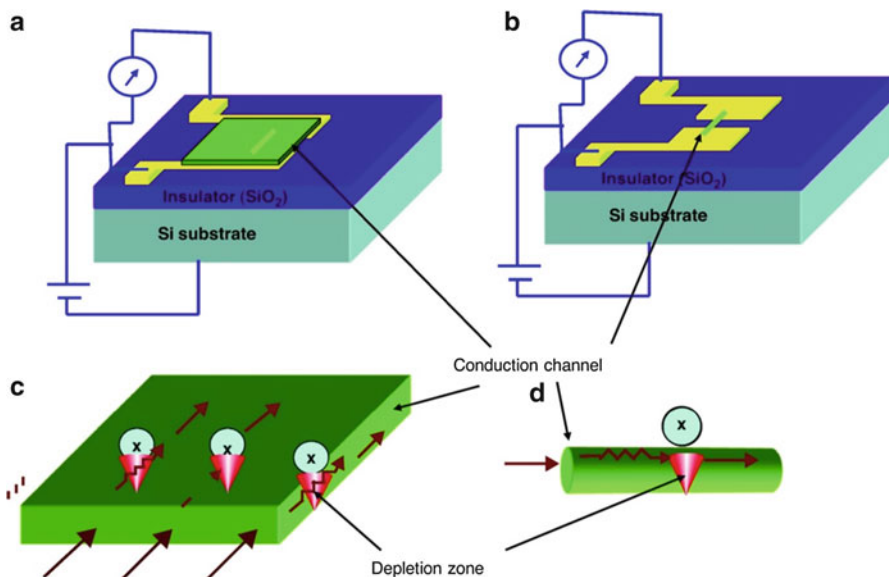


Fig. 14.1 The major advantage of 1-D nanostructures (b) over 2-D thin films (a). Binding of a charged analyte (letter *x* within a circle) to a 1-D nanowire leads to depletion or accumulation zone in the “body” of the nanowire (d) as opposed to only the surface in a 2-D thin-film case (c)¹³

drain electrodes. In a thick/thin-film-based sensor only a fraction of the total cross-sectional area is affected by the modulation in the number of charge carriers. As a result, the current can shunt across such regions of modified conductance and leads to depletion in the sensing signal (Fig. 14.1c). On the other hand, one-dimensional nanostructures like nanowires/nanotubes show modification in the electrical properties across its entire cross section due to their small sizes and allow surface chemistry to play a role as compared to in bulk state (Fig. 14.1d). This ballistic conduction of current through the nanostructures leads to increase in the signal and thus makes them more sensitive than the thin-film sensors. Additional benefits of 1-D nanostructures include the following:

- (a) A large surface-to-volume ratio means that a significant fraction of the atoms (or molecules) in such systems are surface atoms that can participate in surface reactions.
- (b) The Debye length λ_D (a measure of the field penetration into the bulk) for most nanowires and nanotubes is comparable to their radius, which causes their electronic properties to be strongly influenced by processes at their surface. This could result in better sensitivity and selectivity.
- (c) Finally, nanowires and nanotubes can be easily configured as field-effect transistors (FETs) and can be potentially integrated with conventional devices and device fabrication techniques.

Table 14.3 Summary of electrochemical sensors for VOCs

Material	Sensor configuration	Analyte	Lowest concentration	Remarks	Reference
Metal oxides	Screen-printed SnO ₂ thick film doped with various metal/metal oxide on alumina substrate	Ethanol	100 ppm (sensitivity: 10–80 %)	Temperature: 200–400 °C	14
		Benzene			
		Toluene	50 ppm (sensitivity: 5–50 %)		
		Acetone	500 ppm (sensitivity: 10–80 %)		
			3,000 ppm (sensitivity: 50–90 %)		
			59,000 ppm		
			126,000 ppm		
			285,000 ppm		
			43,000 ppm		
			13,000 ppm		
			5 ppm (sensitivity: 40–70 %)		
			2.5 ppm (sensitivity: 50–80 %)		
			1 ppm (sensitivity: 60–100 %)		
	0.1 ppm (sensitivity: 15–25 %)				
	Screen-printed SnO ₂ thick film on alumina substrate	Ethanol		Potential applied: 5 V	15
		Benzene			
		Acetone			
		Isopropanol			
		Xylenes			
	Printed thick-film SnO ₂ ; Metal oxide (ZnO ₂ , InO ₂ , NbO ₂) (50:50) composite on prefabricated interdigitated electrode	Ethanol		Temperature: 350 °C	16
		Propanol			
		Butanol			
		Ethylbenzene			

(continued)

Table 14.3 (continued)

Material	Sensor configuration	Analyte	Lowest concentration	Remarks	Reference		
Conducting polymers	Monodispersed SnO ₂ nanocrystal prepared by heating tin(IV) acetylacetonate in dibenzyl ether in the presence of oleic acid and oleylamine. Sensor fabricated on a interdigitated electrode by solvent-casting technique	Toluene	20 ppm	Temperature: 350 °C	120		
		Formaldehyde	5 ppm				
		Ethanol	5 ppm				
	Indium tin oxide (ITO)	Thin film (~150 nm) grown by CVD method on glass substrate	Methanol	2,500 ppm	Temperature: 620–675 °C	18	
			Ethanol	2,500 ppm			
			Butanol	2,500 ppm			
			Acetone	200 ppm			
	ZnO	Ce-doped ZnO thin film fabricated by dip-coating process on alumina substrate	Alcohol	50 ppm (sensitivity: 5 %)	Temperature: 370 °C	19	
			Benzene	100 ppm			
			Acetone	100 ppm			
WO ₃	Silicon-doped WO ₃ nanoparticle assembled on an interdigitated electrode by spray-coating process	Acetone	100 ppb (LOD: 20 ppb)	Temperature: 400 °C	20		
		Ethanol	100 ppb				
		Benzene	20 ppb				
		Toluene	5 ppb				
		<i>m</i> -Xylenes	5 ppb				
Polythiophene	Sensor/array of sensor based on block copolymers of polythiophenes nanostructures fabricated through ink-jet printing on prefabricated electrode	Ethanol	10 ppm for all analytes		22–24		
		Acetone					
		Benzene					
		(7 other VOCs)					
		Methanol				50 ppm	25

Carbon-based materials	Polyaniline/carbon nanotube hybrid	Chemically synthesized size control polypyrrole nanoparticles assembled on prefabricated electrode through drop-casting/spin-coating techniques	Acetonitrile	100 ppm	26
			Acetic acid	100 ppm	
Carbon-based materials	Carbon nanotubes	Sensor was prepared on prefabricated interdigitated electrode by spray layer by layer (LBL) assembly using polyaniline nanoparticle-MWNT solution	Methanol	Saturated vapors	27
			Toluene		
			Chloroform		
			Aliphatic hydrocarbons	130–14,500 ppm	
				1250–80,000 ppm	
				350–90,000 ppm	
	Carbon nanotubes	An array of sensors having random network of covalently modified MWNTs	An array of sensors having random network of MWNTs	Aromatic hydrocarbons	80–65,000 ppm
				Ketones	
				Alcohols	
				Ethanol	33 ppm
				Acetone	285 ppm
				TMA	29 ppm
Carbon-based materials	Carbon nanotubes	MWNT network	Methanol	Functionalized with porphyrin	28
			Toluene		
			Chloroform		
			Hexane	10 ppb	
			Octane	10 ppb	
			Trimethyl benzene	10 ppb	
Carbon-based materials	Carbon nanotubes	An array of sensors having random network of SWNTs	Methanol	Functionalized with poly/lactic acid	29
			Toluene		
			Chloroform		
			Hexane	10 ppb	
			Octane	10 ppb	
			Trimethyl benzene	10 ppb	
Carbon-based materials	Carbon nanotubes	An array of sensors having random network of SWNTs	Methanol	Functionalized with porphyrin	30
			Toluene		
			Chloroform		
			Hexane	10 ppb	
			Octane	10 ppb	
			Trimethyl benzene	10 ppb	

(continued)

Table 14.3 (continued)

Material	Sensor configuration	Analyte	Lowest concentration	Remarks	Reference
	An array of sensors having single semiconducting single-walled carbon nanotube	Methanol	1 ppm	Functionalized with DNA oligomers	31
		TMA	0.05 ppm		
		DMMP			
		Propanoic acid			
Graphene/ZnO hybrid	Sensor fabricated on prefabricated gold electrode through drop-casting technique using graphene/ZnO composite solution	Formaldehyde	25 ppm		10

Three types of materials, metal oxide semiconductors such as ZnO and SnO₂, conducting polymers such as polyaniline and polypyrrole, and carbon-based materials such as carbon nanotubes (CNTs) and graphene, have shown significant performance benefit for the development of 1-D- and 2-D-based sensors for VOCs (Table 14.3). Until recently, the development of 1-D nanostructure-based VOC sensor using the abovementioned materials was slow because of challenges in the synthesis and fabrication of these nanostructures with controlled dimensions, morphology, and purity.

14.3.1 Metal Oxide-Based VOC Sensors

Chemical and physical properties of metal oxide semiconductors such as In₂O₃, ZnO, and SnO₂ have been extensively studied for the last few decades. Metal oxide thin-film-based solid-state chemical sensors have been developed and successfully commercialized by exploiting the change in their properties caused by the surface adsorption process. The detection principle mainly relies on the conductance change of the material based on the interaction between the analyte and the oxygen vacancy sites available on the oxide surface. The oxygen vacancies, created due to the molecular adsorption on the oxide surfaces, are chemically and electrically active. When vacancies are created they tend to bind with more atoms or molecules and the electrons that are left behind form a space charge region (SCR) closer to the oxide surface.^{32,36,37} As a result, when charged molecules bind to the surface, they either donate or accept electrons to or from the SCR depending on their charge types and change the conductivity of the oxides.

The limited sensitivity and high operating temperature are major drawbacks for the available metal oxide-based commercial sensors. The issue of sensitivity can be overcome by using one-dimensional nanostructures because of their comparable diameters with respect to the width of the SCR.

Several physical and chemical methods have been developed for synthesizing one-dimensional oxide nanostructures. Solution-phase growth,³³ chemical vapor deposition (CVD),^{34,39} laser ablation,³⁵ and electrochemical methods followed by annealing^{32,36} are the most common routes for the synthesis of single-crystal and polycrystalline oxide nanowires,^{32,35,38} nanotubes,^{34,36} and nanobelts.⁴⁰ Using these nanostructures, sensitive detection of a number of analytes such as NO₂,³⁸ NH₃,^{38,41} and H₂⁴² has been demonstrated. Further, sensitivity enhancements by doping the nanostructures and functionalizing with catalytic metals have also been reported.^{33,42}

Detection of VOCs such as alcohols, ketones, and aromatic hydrocarbons has been demonstrated using metal oxides such as SnO₂,^{14,16,18,45,120,94,47} ZnO,^{19,95} WO₃,²⁰ and Co₃O₄⁴³ (Table 14.3). In most of the cases, these sensors were prepared by screen-printing a thick film of metal oxide on pre-patterned electrodes. However, electrodes have also been written after making the film on a substrate. Screen-printed SnO₂ thick film detected alcohols and aromatics.¹⁵ However, device

sensitivity was improved enormously upon doping with metals¹⁴ such as Pt, Cu, and metal oxides¹⁶ such as ZnO₂, InO₂, and NbO₂. A further enhancement in device sensitivity was observed using SnO₂ nanoparticles due to the enhancement of active surface-to-volume ratio.⁴⁴ A similar improvement in sensitivity towards alcohols and other VOCs was observed for ZnO- and WO₃-based sensors, when doped with a suitable dopant.^{19,20} Metal oxides have also been used as functional material to decorate conducting polymers,^{45,46} carbon nanotubes,^{47,48} and graphene¹⁰ to improve the sensor sensitivity as well as response/recovery time. The synthesis of controlled one-dimensional nanostructure such as meso- and macroporous Co₃O₄ nanorods⁴³ and TiO₂ nanotubes has been reported which provides superior sensing performance in terms of sensitivity, selectivity, response time, and relative humidity. A sub-ppb-level detection of VOCs is possible when a metal oxide sensor is coupled with a pre-concentration unit.²¹

14.3.2 Conducting Polymer-Based Sensors

Conducting polymers (CPs) such as polypyrrole (PPy), polyaniline (PANI), polythiophene (PTH), and poly (3,4-ethylenedioxythiophene) (PEDOT) are an attractive class of organic materials which exhibit unique electronic, magnetic, and optical properties of metal and semiconductors while retaining the mechanical properties and ease of processing advantages of polymers.^{49,50,59} These polymers can be synthesized and doped or dedoped through chemical and electrochemical processes to alter their conductivities from a near metallic (1 S/cm) to an insulating (10^{-10} S/cm) regime by varying the dopant type and concentration to tune charge transport.⁵⁰ This prominent feature of tunable charge transport combined with high chemical sensitivity at ambient temperature and stability makes them ideal for the use as transducing materials in chemical sensors.^{51,96}

CPs can be synthesized through oxidative polymerization of the monomers by (1) chemical routes, where an oxidizing agent is used to facilitate the polymerization process, and (2) electrochemical routes, where a positive potential is employed to perform the polymerization process.

Thick/thin-film sensor can be fabricated on prefabricated electrodes by dip/spray-coating chemically synthesized polymer solution or by electropolymerization of monomer on the electrode from a solution in the presence of the dopant. The dip/spray-coating process results in a 2-D structure without control over the thickness, morphology, and porosity, and also does not provide the process flexibility to tune the material properties. On the other hand, electropolymerization processes such as cyclic voltammetry and chronoamperometry provide in situ fabrication on the electrode pads and also allow manipulating material properties by changing the process conditions. However, the film thickness in these methods cannot be controlled as there is no direct indication of the completion of the device fabrication process. Additionally, the contact between the gold electrode pad and the CP film and adhesion of the film to the substrate are issues for fabrication of CP-based

sensors. The film thickness of the CP film can be controlled by performing the electropolymerization in bipotentiostatic mode where the bifurcation of the chronoamperogram indicates the successful completion of device fabrication.⁵² Further, use of a hydrophobic substrate, which could be done through chemical treatment, facilitates to reduce the film thickness and also improve the adhesion of the film with the substrate. For example, an ultrathin film of polyaniline was synthesized through electropolymerization of aniline on a SiO₂ substrate treated with octadecyltrichlorosilane to make it hydrophobic and using bipotentiostatic mode.⁵²

One-dimensional (1-D) CP nanowires (NWs) can be synthesized by template-directed and template-free methods.^{53,60,97,98,99} In the template-directed method, a nanoporous membrane (anodized alumina or track-etched polycarbonate) with uniform cylindrical pores is used as scaffold and the conducting polymer is polymerized chemically or electrochemically within the pores of the membrane to form nanowires or nanotubes followed by etching of the template to release the NWs in the solution.^{54,100} The NW diameter and length can be manipulated by controlling the diameter of the pores and the current density and charge, respectively. The use of a strong etchant, for example strong acid/base for alumina and organic solvent for polycarbonate, may affect the morphology and chemical and electronic properties of the NWs/NTs.

Template-free methods include electrospinning, dip-pen lithography, and aqueous/organic interfacial polymerization. Among the template-free methods, electrospinning is most widely used due to its simplicity, versatility, and capability to produce extremely long CP NWs. The method requires an application of high-voltage electrostatic field to charge the CP solution droplet and passing through the liquid injection nozzle. By adjusting the distance between the source and the collecting surface, which acts as a counter electrode, oriented nanofibers can be deposited. The morphology of the nanostructure can be manipulated by changing the solution concentration, applied electrical field, and feeding rate of the precursor solution.^{51,55}

Dip-pen nanolithography (DPN) is a scanning probe nanopatterning technique. In the DPN process, an AFM tip is used to deliver polymerized conducting polymer molecules as ink to a surface via a solvent meniscus to form the nanostructure. This technique provides a precise positioning of nanostructure and also has good control over the dimension. However, this method is expensive and requires post-synthesis processing for writing the electrodes.^{56,101}

The solution-phase nanowire synthesis was developed by the Kaner group using aqueous/organic phase interfacial polymerization. This method is suitable for bulk synthesis of CP NWs and can produce 30–50 nm diameter and 500 nm to several microns long NWs having a yield of 6–10 %.^{57,102,103}

For making of a FET device, the NWs synthesized by any of the above methods have to be immobilized within a prefabricated source-drain electrode because of the incompatibility of the CP NWs with the chemicals and conditions used for lithography process. The easiest method of immobilization of NWs is solvent-casting process where a drop of NWs containing solution is dispensed over the

prefabricated electrode followed by evaporation for the attachment of NWs on the electrode surface. However, this method results in random orientation and number of NWs connecting the electrodes, making it an inconsistent and unreliable method of device making. A better control on alignment of the NWs could be achieved by dielectrophoretic, fluidic, or magnetic alignment.⁵⁸ However, fabricating high-density large area conducting polymer nanostructure device using these techniques is still a technological challenge. A high-density sensor array using CP NWs can be achieved by lithographically patterned nanowire electrodeposition (LPNE) or nanoimprint lithography (NIL).

Over the past few years, CP-based (CPs/CP composites) thin/thick-film sensors for the detection of a wide variety of analytes ranging from biomolecules to VOCs have been demonstrated (Table 14.3).^{22,23,24,25,26,59,60} However, in recent times, focus has shifted to the use of one-dimensional CP nanostructures as a sensory element due to the advantages mentioned earlier. Kaner and co-workers fabricated PANI nanofiber network-based sensors using PANI nanofibers synthesized by chemical polymerization and demonstrated performance enhancement over the conventional PANI thin-film sensors.^{57,61} The higher surface area, porosity, and nanometer diameter PANI nanofibers contributed towards the sensor signal enhancement. Liu et al. demonstrated single PANI nanowire-based chemical sensor, fabricated using a nanolithographic deposition process, which showed a rapid and reversible resistance change upon exposure to NH₃ at concentrations as low as 0.5 ppm.⁵¹ Hangarter et al. reported template-directed synthesis of PPy nanowires, their integration on a prefabricated microelectrode by drop casting/electrophoretic alignment, and successful demonstration towards NH₃ detection.⁶²

Yaping et al. used the template-directed method to fabricate Au-PEDOT/PSS-Au nanowires, assembled on a prefabricated gold electrode by dielectrophoretic alignment method, and demonstrated the effectiveness as a sensor towards VOCs (methanol, ethanol, and acetone).⁶³ Cao et al. reported the performance enhancement of the sensors towards methanol by replacing the PEDOT/PSS nanowire with PEDOT/CIO₄ nanowires.⁶⁴ The possible reason for the enhanced performance of PEDOT/CIO₄ over PEDOT/PSS nanowire sensor is attributed to domination of the partial charge transfer between the polymer and the absorbed analyte as opposed to the increase in hopping distance due to swelling of polymer.

Although CP nanostructure-based gas sensors show an excellent sensing performance in terms of sensitivity and quick response at room-temperature operation, the long-term stability of the polymers for practical applications and the scalability issues due to complex fabrication process still remain a challenge.

14.3.3 Carbon Nanotube-Based Sensors

Carbon nanotubes are sp²-bonded carbon-based materials consisting of a single- or multiple-graphene sheet seamlessly wrapped up into a cylindrical tube. Carbon nanotubes could be single-walled or multi-walled. Multi-walled carbon nanotubes

(MWNTs) are metallic in nature. Single-walled carbon nanotubes (SWNTs) are one-dimensional nanostructures that are approximately 0.4–3 nm in diameter and few hundred microns long. The structure of SWNTs provides them with inherently unique electrical, physical, and chemical properties.^{65,104,105,106,107} Mechanically, SWNTs are the strongest fibers among the known materials due to the C–C bond.⁶⁶ Thermally, they have high thermal stability in both vacuum and air.⁶⁶ Electronically, they can be either metallic or semiconducting in nature depending on their diameter and helicity of the graphitic ring arrangement in their wall.^{67,108} The nanometer diameter and high electrical transport property make SWNTs potential candidates for many microelectronic applications. Their superior electrical conductivity as compared to other semiconducting materials facilitates the development of low-power electronic devices and their smaller size facilitates the miniaturization process to build high-density nanosensor array in small footprint.

The SWNTs consist solely of surface atoms such that every single carbon atom is in direct contact with the environment and this makes them highly sensitive to any surface adsorption event. SWNTs thus could be ideal building blocks for making gas sensors. The sensing behavior arises from the fact that changes in their local chemical environment have a direct impact on their electronic structure and hence provide unambiguous path for detecting interacting molecules that initiate the change.

SWNT-based FET/chemiresistor sensors have been typically based on single SWNT or a network of SWNTs bridging the source and drain electrodes. The techniques used to make single SWNT device included lithographically patterned catalyst as carbon nanotube nucleation site followed by writing of source and drain electrodes by e-beam lithography or manipulating carbon nanotubes on pre-patterned electrodes by atomic force microscope. These methods while adequate for laboratory demonstration have limited controllability and throughput and therefore not feasible for scaling to production level. On the other hand, sensors based on SWNT network because of their simplicity, low cost, and scalability are attractive alternative. Such SWNT network devices can be fabricated by simple drop casting or spin coating of an SWNT suspension in either dimethyl formamide (DMF) or a surfactant (sodium cholate or sodium dodecyl sulfate) in water. While drop casting is simple and easy to perform, the inability to control position and bundling of SWNTs is a major limitation of this method as this reduces the sensor sensitivity and increases the response and recovery times (Fig. 14.2a). The bundling of nanotubes can be reduced or eliminated by spin coating or dielectrophoresis. The density/numbers of SWNTs within the electrode can be controlled by manipulating the SWNT concentration and/or rotational speed and time. Spin coating process provides an opportunity for wafer-level device fabrication. However, when spin coating is performed, the SWNTs aligned in the radial direction along the lines of centrifugal force requiring patterning the electrode radially and cause complications in chip dicing (Fig. 14.2b). On the other hand, in the dielectrophoretic (DEP) method, the nanotubes align perpendicularly to the electrodes. However, a wafer-level device fabrication is still impractical right at this moment (Fig. 14.2c).

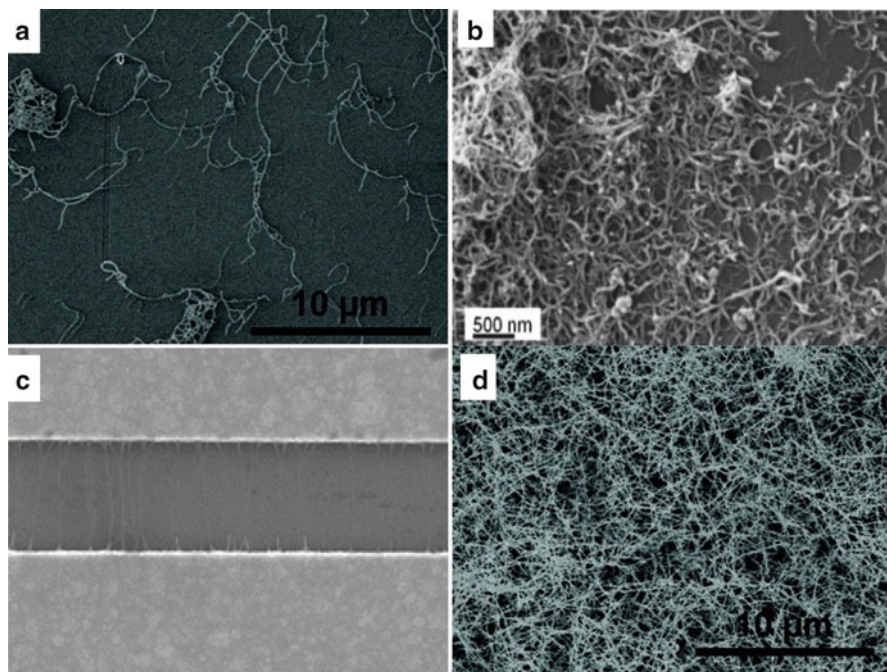


Fig. 14.2 SEM images of (a) drop-casted SWNTs,⁶⁸ (b) spin-coated SWNTs,⁶⁹ (c) dielectrophoretically aligned SWNTs between two Au electrodes,⁷⁰ and (d) aminosilane functionalization of Si/SiO₂⁶⁸

Recently, a modified drop casting method for FET fabrication was reported. In this method, the Si/SiO₂ wafer was modified with a monolayer of aminosilane, a chemical known for its affinity to the CNTs, by treating with aminopropyltriethoxy silane (APTES) followed by assembly of SWNTs from a dilute solution of SWNTs.⁶⁸ This method resulted in uniformly distributed high-density SWNT network when compared to surface without APTES (Fig. 14.2d). The process enables a wafer-level fabrication that can be used on both pre- and post-patterned electrodes and possesses flexibility with regard to controlling SWNT density in the network by manipulating SWNT concentration and deposition time.

In the year 2000, Kong et al. first established the proof of concept for the development of semiconducting SWNT-based chemiresistor as a sensor and predicted the potential of SWNTs as a sensing material.⁷¹ Since then various groups have demonstrated the use of SWNTs for detection of gases such as NH₃, NO₂, and O₂ and metal ions such as Hg²⁺, establishing SWNTs as promising sensing material.^{72,109} The range of molecules that can be detected by SWNT-based sensors, however, is limited by their binding energies and thereby the charge transfer with SWNTs. Gases such as carbon monoxide and most VOCs can be hardly detected due to their low binding energy with SWNTs or almost negligible adsorption to SWNT surface.⁶⁶ However, this limitation can be alleviated by either modifying the

electronic and chemical properties of the SWNTs through substitutional doping³⁰ of impurity atoms (boron and nitrogen) into intrinsic SWNTs or functionalizing SWNTs with a suitable recognition molecule that has greater affinity to the target molecule.^{73,74} SWNT surface can be functionalized through covalent or non-covalent binding. Significant improvement in sensing performance was observed for NH₃ detection when SWNTs were functionalized covalently with poly(*m*-aminobenzene sulfonic acid) (PABS).⁷⁴ Similarly, enhancement in sensitivity was observed for H₂ detection on functionalizing SWNTs with palladium nanoparticles that catalyzed the surface adsorption process.⁷⁵ Additional examples of improved sensitivity for a range of chemicals upon functionalizing SWNTs with metal and metal oxide nanoparticles and conducting polymers by electrochemical deposition have also been reported.^{73,76}

Pristine SWNTs are inert to most VOCs. However, when chemically modified by certain functional groups through covalent attachment they become active and respond to VOCs as well as other chemicals (Table 14.3).²⁷ Alternatively, coating or decorating the nanotube surface with molecules chemically active to VOCs can enhance the sensitivity. For example, inorganic molecules (TiO₂, SnO₂ nanoparticles, etc.),⁷⁷ polymers (polymethyl methacrylate, polypyrrole, etc.),^{17,29,110} organic macromolecules (porphyrin, phthalocyanine, polycyclic aromatic hydrocarbons, etc.),^{78,28} and biomolecules (DNA)³¹ with higher affinity to VOCs can be used as functional material. Various groups have demonstrated a wide range of aliphatic and aromatic hydrocarbons. Surface modification of nanotubes with porphyrins and polylactic acid imparts the device sensitivity as well as selectivity.^{29,78} A sensitive and discriminative sensor for detection of alcohols, acids, and other VOCs has been developed by the Johnson group through functionalization of the nanotube with oligonucleotides (short DNAs). A sub-ppm level of VOC detection and identification have also been reported using an array of carbon nanotube network modified with nonpolymeric organic materials.^{79,111,112}

14.3.4 Graphene-Based Sensors

Graphene is an allotrope of carbon having one-atom-thick sp² carbon atoms tightly packed into a two-dimensional (2-D) hexagonal honeycomb networks.⁸⁰ In the graphene lattice, two sub-lattices of carbon atoms couple together through strong covalent bonds/ σ -bonds and π -electron of each carbon atom in the lattice to form a delocalized π -electron system.

Graphene possesses several interesting thermal, mechanical, optical, and electronic properties. It is thermally stable, mechanically strong, and optically transparent. Graphene exhibits ambipolar electric field-effect behavior with huge mobilities of charge carrier (15,000–200,000 cm²/V s), which is limited only by the defects/impurity scattering.^{81,113,114} The high mobility facilitates the ballistic transport of electron on submicron scale. Further, the dependency of electronic properties to the adsorption when exposed to various analyte molecules, total

exposure of all its surface carbon atoms for analyte adsorption, higher surface-to-volume ration, possibilities to synthesize large-scale quality graphene sheet without any impurities, and inertness towards the chemical used for conventional lithographic process for making the sensor devices make graphene the next-generation material for sensor applications.

Currently, there are four primary processes, epitaxial, mechanical exfoliation, reduced graphene oxide, and chemical vapor deposition (CVD), which have been employed to produce pristine graphene.

In the epitaxial method, graphene formation is initiated by the sublimation of Si atoms and the formation of carbon-segregated surface containing mobile carbon atoms, during the annealing at $>1,300$ °C either in ultrahigh vacuum or atmospheric pressure. Diffusion of those carbon atoms on the surface at that high temperature produces a monolayer of epitaxial graphene film on top of the solid support.^{82,115,116} The size of the graphene here depends on the size of the SiC substrate used; hence a large-area graphene synthesis is possible with the help of this process.

In the mechanical exfoliation process, mono/few layers of graphene flake/sheet is isolated from highly oriented pyrolytic graphite (HOPG) by repeated peeling/exfoliation using scotch tape,⁸¹ ultrasonication,⁸³ etc., followed by transferring to SiO₂/Si or any suitable substrate for the device fabrication. This is the cheapest technique to produce a high-quality single-layer graphene flake. However, the size of the graphene produced by this method is very small, few microns to millimetre range, and hence not practical for commercial applications.

Reduced graphene oxide (RGO) platelets can be synthesized by dispersing the graphene oxide (GO) in aqueous medium followed by reduction of GO by a reducing agent. In general GO is synthesized using modified Brodie, Staudenmaier, or Hummers methods where a strong oxidizer is used to oxidize the graphite. First two methods involve a combination of potassium chlorate (KClO₃) with nitric acid (HNO₃) to oxidize graphite, while the latter involves a combination of potassium permanganate (KMnO₄) and sulfuric acid (H₂SO₄) treatment to oxidize graphite. The reduction of GO into graphene sheets can be done by reducing agents such as hydrazine,⁸⁴ hydroquinone,⁸⁵ sodium borohydride (NaBH₄),^{86,117} and ascorbic acid.⁸⁷

In the CVD process, graphene is grown on metal surfaces by hydrocarbon decomposition at elevated temperature (~ 800 – $1,100$ °C). Large-area graphene synthesis is possible using this process because of the availability of large metallic substrate in the form of metallic films or foils. CVD growth of graphene has been performed on several metallic substrates, but commonly used ones are copper (Cu)^{88,118} and nickel (Ni).^{89,119}

In 2007, Novoselov and co-workers first demonstrated the application of pristine graphene as a sensor for room-temperature detection of NH₃, NO₂, and CO.⁹⁰ Subsequently, Kern and co-workers functionalized graphene with palladium nanoparticles to impart sensitivity towards hydrogen.⁹¹ Currently, there are not many reports in the literature for detection of VOCs by pristine graphene. However, graphene functionalized with ZnO¹⁰ and SnO₂⁹² nanoparticles and GO functionalized with polypyrene⁹³ have been reported for rapid and sensitive detection of formaldehyde, propanal, and toluene, respectively (Table 14.3).

14.4 Conclusions

Recent advances in the rapidly developing field of electrochemical sensor technology using engineered materials such as functionalized carbon nanostructure have shown a great potential for VOC detection. However, in most cases the devised sensor was tested in a control environment to estimate its sensing potential. Hence, their effectiveness in real environment is questionable for real application.

Researchers around the world have achieved tremendous improvements in lithographic techniques to fabricate FETs/chemiresistors; however, there are still several challenges associated with bulk-scale fabrication of these devices with reproducibility and reliability. Improvement in the lithographic methods/strategies to make a high-density electrode along with the site-specific functionalization strategy and/or engineered novel material synthesis for making an individually addressable sensors array is required for the realization of sensor array for simultaneous multiple analyte identification and quantification in real environment. Low-cost, low-power, reliable, robust, and portable electrochemical sensors that are manufactured in industry are expected in near future.

References

1. Spadavecchia J, Ciccarella G et al (2004) Variation in the optical sensing responses toward vapors of a porphyrin/phthalocyanine hybrid thin film. *Chem Mater* 16(11):2083–2090
2. Sen S, Capan R et al (2010) p-Phthalimidobenzoic thin film for volatile organic vapor detection. *J Optoelectron Adv Mater* 12(7):1534–1538
3. Shogenov YK, Kuchmenko TA et al (2012) Quartz crystal microbalance determination of vapors of volatile organic compounds on carbon nanotubes under batch conditions. *J Anal Chem* 67(1):21–27
4. Horrillo MC, Fernandez MJ et al (2006) Optimization of SAW sensors with a structure ZnO-SiO₂-Si to detect volatile organic compounds. *Sens Actuators B-Chem* 118(1–2):356–361
5. Hajjam A, Pourkamali S (2012) Fabrication and characterization of MEMS-based resonant organic gas sensors. *IEEE Sens J* 12(6):1958–1964
6. Ramanathan K, Danielsson B (2001) Principles and applications of thermal biosensors. *Biosens Bioelectron* 16(6):417–423
7. Ibanez FJ, Zamborini FP (2008) Chemiresistive sensing of volatile organic compounds with films of surfactant-stabilized gold and gold-silver alloy nanoparticles. *ACS Nano* 2(8):1543–1552
8. Suslick KS, Bailey DP et al (2007) Seeing smells: development of an optoelectronic nose. *Quim Nova* 30(3):677–681
9. Kim K, Lee JW et al (2012) Organic isocyanide-adsorbed gold nanostructure: a SERS sensory device for indirect peak-shift detection of volatile organic compounds. *Analyst* 137(8):1930–1936
10. Huang Q, Zeng D et al (2012) Room temperature formaldehyde sensors with enhanced performance, fast response and recovery based on zinc oxide quantum dots/graphene nanocomposites. *Nanoscale* 4(18):5651–5658
11. Yusoff N-H, Salleh MM et al (2008) TiO₂ nanoparticles coated with porphyrin dye thin film as fluorescence gas sensor. *Sains Malaysiana* 37(3):249–253

12. Hwang M-J, Shim WG et al (2012) Low-pressure adsorption isotherms of aromatic compounds on polyisobutylene gel measured on a quartz crystal microbalance. *J Chem Eng Data* 57(3):701–707
13. Mulchandani A, Myung NV (2011) Conducting polymer nanowires-based label-free biosensors. *Curr Opin Biotechnol* 22(4):502–508
14. Lee DS, Kim YT et al (2002) Fabrication and characteristics of SnO₂ gas sensor array for volatile organic compounds recognition. *Thin Solid Films* 416(1–2):271–278
15. Skubal LR, Meshkov NK et al (2002) Detection and identification of gaseous organics using a TiO₂ sensor. *J Photochem Photobiol A* 148(1–3):103–108
16. Costello BPD, Ewen RJ et al (2003) Thick film organic vapour sensors based on binary mixtures of metal oxides. *Sens Actuators B-Chem* 92(1–2):159–166
17. Feller JF, Lu J et al (2011) Novel architecture of carbon nanotube decorated poly(ethyl methacrylate) microbead vapour sensors assembled by spray layer by layer. *J Mater Chem* 21(12):4142–4149
18. Vaishnav VS, Patel PD et al (2006) Indium tin oxide thin-film sensor for detection of volatile organic compounds (VOCs). *Mater Manuf Process* 21(3):257–261
19. Ge C, Xie C et al (2007) Preparation and gas-sensing properties of Ce-doped ZnO thin-film sensors by dip-coating. *Mat Sci Eng B Solid-State Mater Adv Technol* 137(1–3):53–58
20. Righettoni M, Tricoli A et al (2010) Si:WO₃ sensors for highly selective detection of acetone for easy diagnosis of diabetes by breath analysis. *Anal Chem* 82(9):3581–3587
21. Zampolli S, Betti P et al (2007) A supramolecular approach to sub-ppb aromatic VOC detection in air. *Chem Commun* 27:2790–2792
22. Li B, Lambeth DN (2008) Chemical sensing using nanostructured polythiophene transistors. *Nano Lett* 8(11):3563–3567
23. Li B, Sauv e G et al (2006) Volatile organic compound detection using nanostructured copolymers. *Nano Lett* 6(8):1598–1602
24. Li B, Santhanam S et al (2007) Inkjet printed chemical sensor array based on polythiophene conductive polymers. *Sens Actuators B-Chem* 123(2):651–660
25. Kwon OS, Hong J-Y et al (2010) Resistive gas sensors based on precisely size-controlled polypyrrole nanoparticles: effects of particle size and deposition method. *J Phys Chem C* 114(44):18874–18879
26. Lu J, Park BJ et al (2010) Polyaniline nanoparticle-carbon nanotube hybrid network vapour sensors with switchable chemo-electrical polarity. *Nanotechnology* 21:255501–11
27. Wang F, Swager TM (2011) Diverse chemiresistors based upon covalently modified multiwalled carbon nanotubes. *J Am Chem Soc* 133(29):11181–11193
28. Penza M, Rossi R et al (2010) Metalloporphyrins-modified carbon nanotubes networked films-based chemical sensors for enhanced gas sensitivity. *Sens Actuators B* 144(2):387–394
29. Kumar B, Castro M et al (2012) Poly(lactic acid)-multi-wall carbon nanotube conductive biopolymer nanocomposite vapour sensors. *Sens Actuators B-Chem* 161(1):621–628
30. Peng S, Cho K (2003) Ab initio study of doped carbon nanotube sensors. *Nano Lett* 3(4):513–517
31. Johnson ATC, Khamis SM et al (2010) DNA-coated nanosensors for breath analysis. *IEEE Sens J* 10(1):159–166
32. Zhang Y, Kolmakov A et al (2004) Control of catalytic reactions at the surface of a metal oxide nanowire by manipulating electron density inside it. *Nano Lett* 4(3):403–407
33. Sivalingam Y, Martinelli E et al (2012) Gas-sensitive photoconductivity of porphyrin-functionalized ZnO nanorods. *J Phys Chem C* 116(16):9151–9157
34. Liu Y, Liu M (2005) Growth of aligned square-shaped SnO₂ tube arrays. *Adv Funct Mater* 15(1):57–62
35. Li C, Zhang D et al (2003) Surface treatment and doping dependence of In₂O₃ nanowires as ammonia sensors. *J Phys Chem B* 107(45):12451–12455

36. Zhao J, Lee CW et al (2009) Solution-processable semiconducting thin-film transistors using single-walled carbon nanotubes chemically modified by organic radical initiators. *Chem Commun (Camb, UK)* 46:7182–7184
37. Kohl D (2001) Function and applications of gas sensors. *J Phys D Appl Phys* 34(19):R125–R149
38. Li C, Zhang D et al (2003) In₂O₃ nanowires as chemical sensors. *Appl Phys Lett* 82(10):1613–1615
39. Mathur S, Barth S et al (2005) Size-dependent photoconductance in SnO₂ nanowires. *Small* 1(7):713–717
40. Pan ZW, Dai ZR et al (2001) Nanobelts of semiconducting oxides. *Science* 291(5510):1947–1949
41. Zhang D, Li C et al (2003) Doping dependent NH₃ sensing of indium oxide nanowires. *Appl Phys Lett* 83(9):1845–1847
42. Kolmakov A, Klenov DO et al (2005) Enhanced gas sensing by individual SnO₂ nanowires and nanobelts functionalized with Pd catalyst particles. *Nano Lett* 5(4):667–673
43. Nguyen H, El-Safty SA (2011) Meso- and macroporous Co₃O₄ nanorods for effective VOC gas sensors. *J Phys Chem C* 115(17):8466–8474
44. Dattoli EN, Davydov AV et al (2012) Tin oxide nanowire sensor with integrated temperature and gate control for multi-gas recognition. *Nanoscale* 4(5):1760–1769
45. Li-Na G (2009) Gas sensitivity of polyaniline/SnO₂ hybrids to volatile organic compounds. *Trans Nonferr Metal Soc* 19:S678–S683
46. Huang J, Yang T et al (2011) Gas sensing performance of polyaniline/ZnO organic-inorganic hybrids for detecting VOCs at low temperature. *J Nat Gas Chem* 20(5):515–519
47. Ahmadnia-Feyzabad S, Khodadadi AA et al (2012) Highly sensitive and selective sensors to volatile organic compounds using MWCNTs/SnO₂. *Sens Actuators B-Chem* 166:150–155
48. Wongchoosuk C, Wisitsoraat A et al (2010) Portable electronic nose based on carbon nanotube-SnO₂ gas sensors and its application for detection of methanol contamination in whiskeys. *Sens Actuators B-Chem* 147(2):392–399
49. Heeger AJ (2001) Semiconducting and metallic polymers: the fourth generation of polymeric materials. *J Phys Chem B* 105(36):8475–8491
50. MacDiarmid AG (2001) Synthetic metals: a novel role for organic polymers. *Synth Met* 125(1):11–22
51. Liu H, Kameoka J et al (2004) Polymeric nanowire chemical sensor. *Nano Lett* 4(4):671–675
52. Srinives S, Sarkar T et al (2013) Nanothin polyaniline film for highly sensitive chemiresistive gas sensing. *Electroanalysis* 25:1439–1445
53. Kauffman DR, Star A (2008) Electronically monitoring biological interactions with carbon nanotube field-effect transistors. *Chem Soc Rev* 37(6):1197–1206
54. Martin CR (1994) Nanomaterials: a membrane-based synthetic approach. *Science* 266(5193):1961–1966
55. Kameoka J, Craighead HG (2003) Fabrication of oriented polymeric nanofibers on planar surfaces by electrospinning. *Appl Phys Lett* 83(2):371–373
56. Lim JH, Mirkin CA (2002) Electrostatically driven dip-pen nanolithography of conducting polymers. *Adv Mater* 14(20):1474–1477
57. Huang J, Virji S et al (2003) Polyaniline nanofibers: facile synthesis and chemical sensors. *J Am Chem Soc* 125(2):314–315
58. Lahav M, Weiss EA et al (2006) Core-shell and segmented polymer-metal composite nanostructures. *Nano Lett* 6(9):2166–2171
59. McQuade DT, Pullen AE et al (2000) Conjugated polymer-based chemical sensors. *Chem Rev* 100(7):2537–2574
60. Hangarter CM, Bangar M et al (2010) Conducting polymer nanowires for chemiresistive and FET-based bio/chemical sensors. *J Mater Chem* 20(16):3131–3140
61. Virji S, Huang J et al (2004) Polyaniline nanofiber gas sensors: examination of response mechanisms. *Nano Lett* 4(3):491–496

62. Hangarter CM, Bangar M et al (2008) Maskless electrodeposited contact for conducting polymer nanowires. *Appl Phys Lett* 92(7):073104
63. Dan Y, Cao Y et al (2009) Gas sensing properties of single conducting polymer nanowires and the effect of temperature. *Nanotechnology* 20:434014–18
64. Cao Y, Kovalev AE et al (2008) Electrical transport and chemical sensing properties of individual conducting polymer nanowires. *Nano Lett* 8(12):4653–4658
65. Iijima S (1991) Helical microtubules of graphitic carbon. *Nature* 354(6348):56–58
66. Wang Y, Yeow JTW (2009) A review of carbon nanotubes-based gas sensors. *J Sens* 2009:1–24
67. Odom TW, Huang J-L et al (1998) Atomic structure and electronic properties of single-walled carbon nanotubes. *Nature* 391(6662):62–64
68. Wang C, Zhang J et al (2009) Wafer-scale fabrication of separated carbon nanotube thin-film transistors for display applications. *Nano Lett* 9(12):4285–4291
69. Wei G, Zhang J et al (2011) Biomimetic growth of hydroxyapatite on super water-soluble carbon nanotube-protein hybrid nanofibers. *Carbon* 49(7):2216–2226
70. Tili C, Cella LN et al (2010) Single-walled carbon nanotube chemoresistive label-free immunosensor for salivary stress biomarkers. *Analyst* 135(10):2637–2642
71. Kong J, Franklin NR et al (2000) Nanotube molecular wires as chemical sensors. *Science* 287(5453):622–625
72. Collins PG, Bradley K et al (2000) Extreme oxygen sensitivity of electronic properties of carbon nanotubes. *Science* 287(5459):1801–1804
73. Hernández SC, Kakoullis J et al (2012) Hybrid ZnO/SWNT nanostructures based gas sensor. *Electroanalysis* 24(7):1613–1620
74. Bekyarova E, Davis M et al (2004) Chemically functionalized single-walled carbon nanotubes as ammonia sensors. *J Phys Chem B* 108(51):19717–19720
75. Kong J, Chapline MG et al (2001) Functionalized carbon nanotubes for molecular hydrogen sensors. *Adv Mater* 13(18):1384–1386
76. Zhang T, Nix MB et al (2006) Electrochemically functionalized single-walled carbon nanotube gas sensor. *Electroanalysis* 18(12):1153–1158
77. Zeng W, Liu T et al (2010) Sensitivity improvement of TiO₂-doped SnO₂ to volatile organic compounds. *Physica E* 43(2):633–638
78. Shirsat MD, Sarkar T et al (2012) Porphyrin-functionalized single-walled carbon nanotube chemiresistive sensor arrays for VOCs. *J Phys Chem C* 116(5):3845–3850
79. Haick H, Hakim M et al (2009) Sniffing chronic renal failure in rat model by an array of random networks of single-walled carbon nanotubes. *ACS Nano* 3(5):1258–1266
80. Geim AK, Novoselov KS (2007) The rise of graphene. *Nat Mater* 6(3):183–191
81. Novoselov KS, Geim AK et al (2004) Electric field effect in atomically thin carbon films. *Science* 306(5696):666–669
82. Berger C, Song Z et al (2004) Ultrathin epitaxial graphite: 2D electron gas properties and a route toward graphene-based nanoelectronics. *J Phys Chem B* 108(52):19912–19916
83. Emtsev KV, Bostwick A et al (2009) Towards wafer-size graphene layers by atmospheric pressure graphitization of silicon carbide. *Nat Mater* 8(3):203–207
84. Stankovich S, Dikin DA et al (2007) Synthesis of graphene-based nanosheets via chemical reduction of exfoliated graphite oxide. *Carbon* 45(7):1558–1565
85. Wang G, Yang J et al (2008) Facile synthesis and characterization of graphene nanosheets. *J Phys Chem C* 112(22):8192–8195
86. Si Y, Samulski ET (2008) Synthesis of water soluble graphene. *Nano Lett* 8(6):1679–1682
87. Dua V, Surwade SP et al (2010) All-organic vapor sensor using inkjet-printed reduced graphene oxide. *Angew Chem Int Ed Engl* 49(12):2154–2157
88. Li X, Cai W et al (2009) Large-area synthesis of high-quality and uniform graphene films on copper foils. *Science* 324(5932):1312–1314
89. Reina A, Jia X et al (2009) Large area, few-layer graphene films on arbitrary substrates by chemical vapor deposition. *Nano Lett* 9(1):30–35

90. Schedin F, Geim AK et al (2007) Detection of individual gas molecules adsorbed on graphene. *Nat Mater* 6(9):652–655
91. Sundaram RS, Gómez-Navarro C et al (2008) Electrochemical modification of graphene. *Adv Mater* 20(16):3050–3053
92. Song H, Zhang L et al (2011) Graphene sheets decorated with SnO₂ nanoparticles: in situ synthesis and highly efficient materials for cataluminescence gas sensors. *J Mater Chem* 21(16):5972–5977
93. Zhang L, Li C et al (2012) Electrosynthesis of graphene oxide/polypyrrene composite films and their applications for sensing organic vapors. *J Mater Chem* 22(17):8438–8443
94. Wen Z, Tian-mo L (2010) Gas-sensing properties of SnO₂-TiO₂-based sensor for volatile organic compound gas and its sensing mechanism. *Physica B* 405(5):1345–1348
95. Calestani D, Mosca R et al (2011) Aldehyde detection by ZnO tetrapod-based gas sensors. *J Mater Chem* 21(39):15532–15536
96. Dong B, Lu N et al (2006) Fabrication of high-density, large-area conducting-polymer nanostructures. *Adv Funct Mater* 16(15):1937–1942
97. Bangar MA, Chen W et al (2010) Conducting polymer 1-dimensional nanostructures for FET sensors. *Thin Solid Films* 519(3):964–973
98. Ramanathan K, Bangar M et al (2004) Individually addressable conducting polymer nanowires array. *Nano Lett* 4:1237–1239
99. Ramanathan K, Bangar M et al (2005) Bioaffinity sensing using biologically-functionalized conducting polymer nanowire. *J Am Chem Soc* 125:496–497
100. Jackowska K, Bieguński AT et al (2008) Hard template synthesis of conducting polymers: a route to achieve nanostructures. *J Solid State Electrochem* 12(4):437–443
101. Maynor BW, Filocamo SF et al (2002) Direct-writing of polymer nanostructures: poly (thiophene) nanowires on semiconducting and insulating surfaces. *J Am Chem Soc* 124(4):522–523
102. Blair R, Shepherd H et al (2008) Construction of a polyaniline nanofiber gas sensor. *J Chem Educ* 85:1102–1104
103. Li D, Huang J et al (2009) Polyaniline nanofibers: a unique polymer nanostructure for versatile applications. *Acc Chem Res* 42(1):135–145
104. Mintmire JW, Dunlap BI et al (1992) Are fullerene tubules metallic? *Phys Rev Lett* 68(5):631–634
105. Buongiorno Nardelli M, Fattbert JL et al (2000) Mechanical properties, defects and electronic behavior of carbon nanotubes. *Carbon* 38(11–12):1703–1711
106. Rinzler AG, Liu J et al (1998) Large-scale purification of single-wall carbon nanotubes: process, product, and characterization. *Appl Phys A Mater Sci Process* 67(1):29–37
107. Wong EW, Sheehan PE et al (1997) Nanobeam mechanics: elasticity, strength, and toughness of nanorods and nanotubes. *Science* 277(5334):1971–1975
108. Saito R, Fujita M et al (1992) Electronic structure of chiral graphene tubules. *Appl Phys Lett* 60(18):2204–2206
109. Kim TH, Lee J et al (2009) Highly selective environmental nanosensors based on anomalous response of carbon nanotube conductance to mercury ions. *J Phys Chem C* 113(45):19393–19396
110. Fan Q, Qin Z et al (2011) Vapor sensing properties of thermoplastic polyurethane multifilament covered with carbon nanotube networks. *Sens Actuators B-Chem* 156(1):63–70
111. Zilberman Y, Tisch U et al (2009) Spongelike Structures of hexa-peri-hexabenzocoronene derivatives enhance the sensitivity of chemiresistive carbon nanotubes to nonpolar volatile organic compounds of cancer. *Langmuir* 25(9):5411–5416
112. Zilberman Y, Tisch U et al (2010) Carbon nanotube/hexa-peri-hexabenzocoronene bilayers for discrimination between nonpolar volatile organic compounds of cancer and humid atmospheres. *Adv Mater* 22(38):4317–4320
113. Morozov SV, Novoselov KS et al (2008) Giant intrinsic carrier mobilities in graphene and its bilayer. *Phys Rev Lett* 100(1)

114. Dean CR, Young AF et al (2010) Boron nitride substrates for high-quality graphene electronics. *Nat Nanotechnol* 5(10):722–726
115. Berger C, Song Z et al (2006) Electronic confinement and coherence in patterned epitaxial graphene. *Science (New York, NY)* 312(5777):1191–1196
116. de Heer WA, Berger C et al (2007) Epitaxial graphene. *Solid State Commun* 143(1–2):92–100
117. Shin H-J, Kim KK et al (2009) Efficient reduction of graphite oxide by sodium borohydride and its effect on electrical conductance. *Adv Func Mater* 19(12):1987–1992
118. Wei D, Liu Y et al (2009) Synthesis of N-doped graphene by chemical vapor deposition and its electrical properties. *Nano Lett* 9(5):1752–1758
119. Kim KS, Zhao Y et al (2009) Large-scale pattern growth of graphene films for stretchable transparent electrodes. *Nature* 457(7230):706–710
120. Kida T, Doi T et al (2010) Synthesis of monodispersed SnO₂ nanocrystals and their remarkably high sensitivity to volatile organic compounds. *Chem Mater* 22(8):2662–2667

Chapter 15

Sulphur Compounds

Tjarda J. Roberts

This chapter presents a review of electrochemical sensors applied to the detection of sulphur compounds in the atmosphere, with a focus on environmental analysis of volcanic emissions of H₂S and SO₂. It describes the application to environmental monitoring of low-cost, low-power, miniature electrochemical sensors, originally developed for use in gas leak alarm systems within industry and for occupational health and safety monitoring systems. Over the last decade, such miniature electrochemical sensors have begun to be applied to real-time environmental monitoring of pollutants, including the characterisation of volcanic sulphurous emissions. This review outlines the principles of electrochemical sensor detection of volcanic gases, and highlights recent advances made in volcano hazard monitoring by using electrochemical sensors within multi-gas in situ measurement systems. A critical view on sources of measurement error in the characterisation of pollution plumes by electrochemical (and other) in situ sensors is presented, including the challenges imposed by sensor cross-sensitivities and finite sensor response within complex plume environments. Finally, future directions in this field are outlined, including the application of miniature electrochemical sensors to the monitoring of urban pollution, and sensor deployment on novel platforms such as balloon or unmanned aerial vehicle.

T.J. Roberts (✉)

LPC2E, UMR 7328, CNRS-Université d'Orléans, 3A avenue de la Recherche Scientifique,
45071 Orléans, Cedex 2, France

e-mail: Tjarda.Roberts@cnrs-orleans.fr; TjardaRoberts@gmail.com

© Springer Science+Business Media New York 2015

L.M. Moretto, K. Kalcher (eds.), *Environmental Analysis by Electrochemical Sensors and Biosensors*, DOI 10.1007/978-1-4939-1301-5_15

1047

15.1 Introduction

15.1.1 Sources of Sulphur to the Atmosphere

Sulphur is found in the atmosphere predominantly in the form SO_2 , at typical abundances of pptv to ppbv. Elevated concentrations may occur near source emissions, or in cities where SO_2 contributes to photochemical smog pollution: a public health concern. SO_2 becomes oxidised to sulphuric acid (sulphate) aerosols in the atmosphere, with significant effects on regional and global climate, as well as ecosystems through sulphuric acid deposition. Atmospheric sulphur originates from both anthropogenic and natural sources, with anthropogenic emissions ($60\text{--}100 \text{ Mt (S) year}^{-1}$) estimated to represent about 70 % of present-day global sulphur emissions⁽¹⁾ and references therein). A major anthropogenic source is the burning of fossil fuels (as coal and crude oil deposits commonly contain 1–2 % sulphur by weight), in power stations, and from ship and road transport.² Smelting of metal sulphur ores can also be a strong localised source of atmospheric sulphur. Natural sources contribute the remaining 30 % of global sulphur emissions. These include an oceanic source ($13\text{--}36 \text{ Mt(S) year}^{-1}$), volcanoes ($6\text{--}20 \text{ Mt(S) year}^{-1}$), biomass burning ($1\text{--}6 \text{ Mt(S) year}^{-1}$) and land biota and soils ($0.4\text{--}5.6 \text{ Mt(S) year}^{-1}$). The oceanic source consists of oceanic plankton that release dimethyl sulphide (CH_3SCH_3) to the marine boundary layer, and sea spray which is a source of sulphate aerosol. The volcanic source consists principally of SO_2 and H_2S (as well as smaller quantities of OCS and H_2SO_4), which become oxidised to SO_2 and sulphate aerosol in the atmosphere. Wildfires (arguably both a natural and anthropogenic phenomenon) are also a source of SO_2 , whilst decomposition of biological matter in soils, especially through anaerobic decomposition, leads to the emission of H_2S , which becomes oxidised to SO_2 in the atmosphere.

The balance between anthropogenic and natural sources has changed over time. Anthropogenic emissions from Europe and North America have declined in recent years following legislative action and the introduction of new technologies such as flue gas desulphurisation (FGD). Mareckova et al.³ estimate that over the period 1990–2010, annual SO_x emissions declined from 21 to 15 Tg for the USA, and from 25 to 5 Tg for the European Union. Declining trends are also evident in the occurrence of acid rain, and in records of sulphur (but not reactive nitrogen) pollution that undergoes long-range transport followed by deposition in the Arctic^{4,5}. Conversely, annual SO_2 emissions from China were relatively stable or declining during the 1990s but increased by 50 % over 2000–2006 to reach 33 Tg due to rapid economic growth and energy consumption.⁶ Since 2006, legislative and industry pollution reduction measures such as FGS have successfully reduced SO_2 emissions in China.

15.1.2 Health Impacts and Exposure Limits to Sulphurous Gases

Both SO₂ and H₂S are highly toxic to health, and exposure to their oxidation product, sulphuric acid aerosol—particularly fine particles (PM_{2.5}, having diameter of 2.5 µm or less)—is also associated with adverse health impacts. SO₂ and sulphate aerosol exposure causes increased airway resistance, with asthma sufferers being particularly susceptible. WHO (World Health Organisation) guidelines recommend short-term SO₂ exposure should not exceed 500 µg/m³ over 10 min whilst the long-term average exposure limit has recently been revised downwards from 125 to 20 µg/m³ over 24 h.⁷ H₂S affects the nervous system, causing eye irritation at 15 mg/m³ (9 ppmv) and serious eye damage at 70 mg/m³ (43 ppmv), and concentrations above 400 mg/m³ (250 ppmv) can cause unconsciousness and death. The WHO-recommended average exposure limit for H₂S is 0.15 mg/m³ over 24 h, with a recommended 30-min 7 µg/m³ maximum to avoid odour annoyance in the general population, noting its characteristic ‘rotten egg’ odour.

Exposure to sulphurous and other toxic gases at high concentrations is of particular concern within industry, where accidental gas release can present a significant occupational exposure hazard. For example, hydrogen sulphide is formed as a by-product whenever sulphur-containing compounds come into contact with organic materials at high temperatures, such as in wastewater treatment, in wood pulp production (using the sulphate method), during coke production, in the manufacture of viscose rayon and in the tanning industry.⁸ H₂S exposure is also a significant hazard in the oil and gas industry; natural gas deposits can contain up to 40 % hydrogen sulphide, and in work related to the treatment of sewage and farm slurry. An accident at a natural gas-treatment plant in Poza Rica, Mexico, in 1950 resulted in a major hydrogen sulphide gas leak (likely several thousands of ppmv), with 22 killed and 320 hospitalized (WHO air quality guidelines for Europe⁷ and references therein). Such very large gas releases are rare, but occasional H₂S exposure to industry workers is not uncommon. In the UK, there is potential H₂S exposure to an estimated 125,000 workers in the treatment of sewage, effluent waste and farm slurry, and 3,000 workers in the offshore oil and gas industries. Industry H₂S exposure limits of 5 ppm (8 h average) and 10 ppm (short-term 15-min exposure limit) are currently recommended in the UK.⁸

15.1.3 Electrochemical Detection of Toxic Gases Within Industry

To improve industry safety, a range of electrochemical sensors that detect toxic gases have been developed. Such sensors can be used for flue gas emission testing. They are integrated into industry sites as part of gas leak alarm systems, which trigger an alarm if gas is detected above a particular threshold, enabling rapid

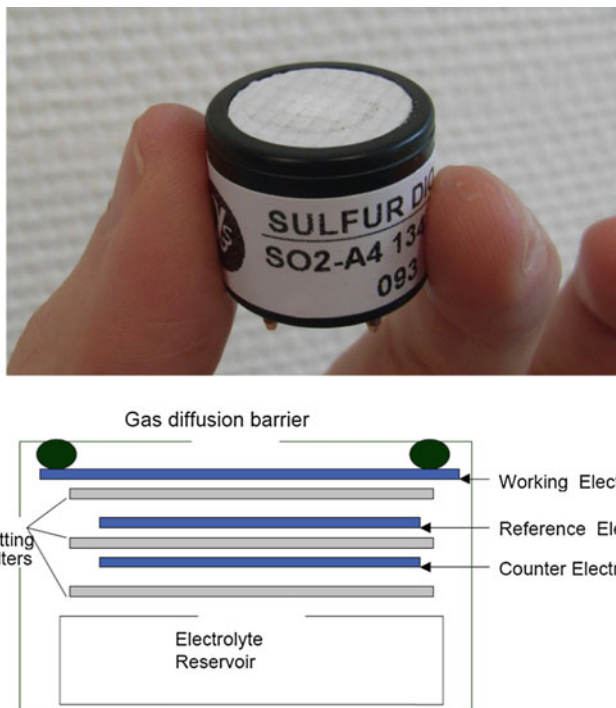


Fig. 15.1 Photograph of miniature (cm-sized) electrochemical sensor, and sensor diagram (image supplied by *Alphasense Ltd*)

evacuation following a gas leak, and a toxic hazard safety team to be directly dispatched to the polluted area. Output from such electrochemical sensors can also be monitored over time to assess variations in on-site gas exposure. A range of electrochemical sensors are commercially available to detect gases such as CO, H₂, HCl, NH₃ as well as H₂S and SO₂. Sensor company Interscan has developed portable (2 kg) electrochemical-sensor-based instruments with integrated sample-draw pump, capable of detecting ppmv and sub-ppmv concentrations of H₂S or SO₂. Sensor technology companies such as Alphasense Ltd, CityTech and Membrapor have developed miniature electrochemical sensors to detect toxic gases (including SO₂ and H₂S). The small size of these sensors—just a few cm and less than 10 g—enables such sensor alarm systems to be worn by the industry workers, thus providing industry exposure estimates on an individual level. Figure 15.1 illustrates the miniature size of these electrochemical sensors. The sensor's three electrodes are separated by wetting filters that allow capillary transport of the electrolyte (typically H₂SO_{4(aq)}). Gas diffusion into the cell leads to reactions at the working and counter electrodes. A general review is given by Stetter and Li,⁹ highlighting the key working electrode reactions for SO₂ and H₂S electrochemical sensors: $\text{SO}_2 + 2\text{H}_2\text{O} \rightarrow \text{SO}_4^{2-} + 4\text{H}^+ + 2\text{e}^-$ and $\text{H}_2\text{S} + 4\text{H}_2\text{O} \rightarrow \text{SO}_4^{2-} + 10\text{H}^+ + 8\text{e}^-$, respectively. The electrochemical current thereby generated is proportional to the rate of gas

diffusion, hence gas mixing ratio abundance in the ambient atmosphere. For more details see manufacturers' websites (www.alphasense.com, www.citytech.com, www.membrapor.com).

15.1.4 Sulphur Gas Detection for Volcano Monitoring and Impact Assessment

During the last decade, the abovementioned portable electrochemical instrument and miniature electrochemical sensors have also been applied to environmental pollution monitoring within a research context. The low cost, low power and small size of the electrochemical sensors present advantages for the monitoring of gases in remote, challenging-to-access regions, where power supply is limited. In particular, the sensors have been applied to quantify sulphurous emissions from the remote summits of volcanoes. Volcanoes release a range of gases and aerosols, including H₂O, CO₂, SO₂, HCl, H₂S, SO₄²⁻, OCS, HBr, HI, Hg and trace metals (in decreasing order of abundance). The major volcanic sulphurous emissions, SO₂ and H₂S, typically reach several to tens or hundreds of ppmv at the volcano crater rim, and thus are readily detectable by electrochemical sensor in the near-source or downwind plume.

The technological advance such electrochemical sensors bring to the monitoring, characterisation and quantification of volcano gas emissions is of interest to both volcanology and environmental science. Volcanologists monitor the composition and flux of volcano gas emissions in order to understand the subsurface process; a review for volcanic sulphur is provided by Oppenheimer et al.¹⁰ Temporal changes in the observed volcanic sulphur emissions—both in terms of gas flux and gas composition—can provide predictive indications of changes in volcanic eruptive activity. Thus, monitoring of the volcanic gas emissions facilitates understanding of the subsurface magmatic conditions and can contribute to early-warning systems for volcanic unrest.

Observations of volcanic emissions are also integral to the assessment of plume atmospheric and ecological impacts, on local to global scales. Approximately 40 % of volcanic emissions are continuously released from persistently degassing volcanoes, into the lower-mid troposphere.¹¹ At low altitudes, such emissions impact local air quality (e.g. resulting in sulphurous volcanic smog, or VOG episodes of poor air quality¹²) and cause ecological damage (e.g. impacting a 22 km² zone downwind of Masaya volcano, Nicaragua, according to reference¹³). For volcanoes that have high altitude summits (e.g. Mt Etna, 3,300 m a.s.l.), the emission enters directly into the free troposphere, which limits the extent of a local impact but results in a prolonged atmospheric lifetime of the emission. Approximately 60 % of global volcanic emissions are released during explosive eruptions (such as Mt Pinatubo, 15 June 1991) that inject gases directly into the mid-upper troposphere or stratosphere. At stratospheric altitudes, inter-hemispheric dispersion and

oxidation of volcanic SO₂ to sunlight-scattering sulphate aerosol can lead to significant climate impacts.¹⁴

Thus, there is a strong interest in incorporating new low-cost, low-power electrochemical gas-sensing techniques to volcanic gas detection. Within volcano-monitoring networks, electrochemical sensors offer the potential for automated in situ monitoring of gas concentrations at the volcano summit, with wireless data transfer to the observatory in real time. This contrasts to traditional more labour-intensive methods for in situ gas sampling, involving sample collection by alkaline bottle or filter trap,¹⁵ followed by laboratory analysis. Electrochemical sensors deployed on airborne platforms can also be used to detect the composition of the volcanic emission, and also map the plume dispersion^{16,17} and study in-plume chemical processing,¹⁸ thereby contributing observational data to support plume impact assessment.

15.2 Electrochemical Sensing of Volcanic Gas Emissions

15.2.1 Development of “Multi-Gas” in Situ Volcanic Gas Measurement Systems

The first application of a commercial (*Interscan*) H₂S instrument to volcanic gas detection was demonstrated by McGee et al.,¹⁶ and was followed by further ground-based and airborne applications of this portable (2 kg) instrument to measure H₂S and SO₂ at a range of volcanoes.^{17–21} In particular, these studies have demonstrated the capability of airborne plume mapping using electrochemical sensor instruments alongside other in situ sensors. Of growing interest is the application of miniature electrochemical sensors to detect volcanic gases, due to their small size (few cm and ~10 g), low cost and low power requirements. Such miniature electrochemical sensors have been integrated alongside other small sensors into backpack-sized portable sensing systems. The first so-called multi-gas system was developed by Shinohara²² followed by numerous further volcanic applications.^{23–42}

Table 15.1 summarizes notable developments in multi-gas instrumentation and volcanic electrochemical sensor deployments over the past decade. The first multi-gas system contained an electrochemical sensor for SO₂ and a CO₂ sensor based on infra-red spectroscopy.²² Subsequent multi-gas instrument developments include the incorporation of an additional electrochemical sensor for H₂S,^{28,37} and infra-red spectroscopic detection of H₂O alongside CO₂.^{23,25,32} Recently, electrochemical sensor detection of volcanic H₂ has been demonstrated,³³ as well as CO and HCl.⁴² The multi-gas systems have also been deployed alongside other in situ sensors, e.g. references^(36, 37) and instrument miniaturisation has recently allowed deployment on novel platforms.^{25,39,40,43}

Deployment of a multi-gas system to analyse gas emissions from the fumaroles of La Fossa crater, Vulcano, Italy, is illustrated in Fig. 15.2a. To make in situ

Table 15.1 Overview of multi-gas instruments that incorporate electrochemical sensors for in situ detection of volcanic gases as portable “backpack” and fixed-installation instruments, as well as commercial instruments based on electrochemical sensing techniques

Gases detected	Method	Comments	
SO ₂	Commercial electrochemical instrument	Airborne, in the plume of Mt. Baker (USA)	16
SO ₂	As above	Heliborne, alongside CO ₂ instrument (prototype sensor deployed), plume of Miyakejima (Japan)	19
SO ₂	As above	Ground based, alongside CO ₂ instrument, plume of Kilauea (Hawaii, USA)	20
SO ₂	As above	Airborne, alongside CO ₂ and H ₂ S sensors, plume of White Island volcano, New Zealand	21
H ₂ S, SO ₂	As above	All measurements integrated in single data acquisition system, in the eruption plume of Mt. Redoubt	17
H ₂ S, SO ₂	As above	Simultaneous measurements of in-plume ozone depletion, in eruption plume of Mt. Redoubt	18
SO ₂ CO ₂ Humidity (H ₂ O)	Electrochemical Infra-red Capacitance	First portable multi-gas system, deployed at Tarumae, Tokachi and Meakan volcanoes (Japan)	22
As above + H ₂ O	Infra-red	In plume of Villarrica (Chile)	23
As above		In Mt. Etna (Italy) plume	25
As above + H ₂	Semi-conductor	Plumes of Meakandake and Kuchinoerabujima (Japan)	44,45
As above		Portable, deployed on UAV in plume of Shinmoedake (Japan)	25
SO ₂ , H ₂ S	Electrochemical	Direct-to-vent detection of Nisyros fumaroles (Greece)	26
CO ₂	Infra-red	Long-term installation with data telemetry and remote operation	27
SO ₂ , H ₂ S CO ₂ Humidity (H ₂ O)	Electrochemical Infra-red Capacitance	Portable system, chemical mapping of fumarolic emissions from Vulcano and Mt. Etna (Italy)	28,29
As above		Simultaneous Hg instrument in fumaroles at Vulcano (Italy)	30
As above + H ₂ O	H ₂ O infra-red	In plume of Mt. Etna (Italy)	31
As above		Long-term automated system with data telemetry at Stromboli (Italy)	32,34,35
As above + H ₂	Electrochemical	In plume of Mt. Etna	33

(continued)

Table 15.1 (continued)

Gases detected	Method	Comments	
SO ₂ , H ₂ S	Electrochemical	Portable and simultaneous with Hg instrument, in plume of Masaya and Telica volcanoes, Nicaragua	36
CO ₂ Humidity (H ₂ O)	Infra-red Capacitance	In the Tatun fumarole field (Taiwan)	37
SO ₂ , H ₂ S, CO	Electrochemical	Portable, Solfatar crater (Italy)	38
SO ₂	Electrochemical	Deployed on UAV in fumarole plume from Vulcano (Italy)	39
CO ₂	Infra-red		
SO ₂	Electrochemical	Deployed on CMET Balloon in Kilauea plume (Hawaii)	40
Humidity (H ₂ O)	Capacitance		
SO ₂ , H ₂ S, CO, H ₂ , HCl	Electrochemical	Portable, deployed in plumes of Villarrica (Chile)	41
As above		In plume of Mt. Aso (Japan)	42
SO ₂	Electrochemical	Portable, deployed on UAV in plume of Turrialba Volcano (Costa Rica)	43

measurements in such a polluted environment requires a gas mask to be worn, as plume sulphur gas concentrations that can reach several hundreds of ppmv. In fact, H₂S and SO₂ concentrations are sufficiently high to react and form a yellow sulphur deposit around the fumarole vents as seen in Fig. 15.2a. Details of the instrument design are shown in Fig. 15.2b. This multi-gas system contains a suite of electrochemical sensors (capable of detecting H₂S, SO₂, CO, H₂ and HCl) with the air flow drawn over the sensors (contained in small housing) by a miniature pump. The electrochemical sensors generate a current output (nA) that is stored every second using a handheld computer. A filter on the inlet removes particles in order to prolong the sensor and pump lifetime. The system is approximately ‘shoe-box’ sized and is powered by a 12 V battery. See reference ⁽⁴²⁾ for further information.

An example of data obtained using this instrument at the crater rim of Aso volcano (also detecting fumarolic emissions) is shown in Fig. 15.3. The sensor current outputs show co-varying variations with time (all sensor currents are positive except for HCl which also exhibits a larger baseline drift). These variations reflect the exposure of the instrument to fluctuating plume concentrations, due to the complex wind fields at the volcano summit. Gas mixing ratio time series derived from the sensor current outputs are shown in Fig. 15.3 and show similar co-varying variations with time that reflects the temporal plume exposure. Scatter plots of these gases relative to plume tracer SO₂ are shown in Fig. 15.4, with linear regression used to identify the characteristic molar gas ratio, finding H₂/SO₂ = 0.2,

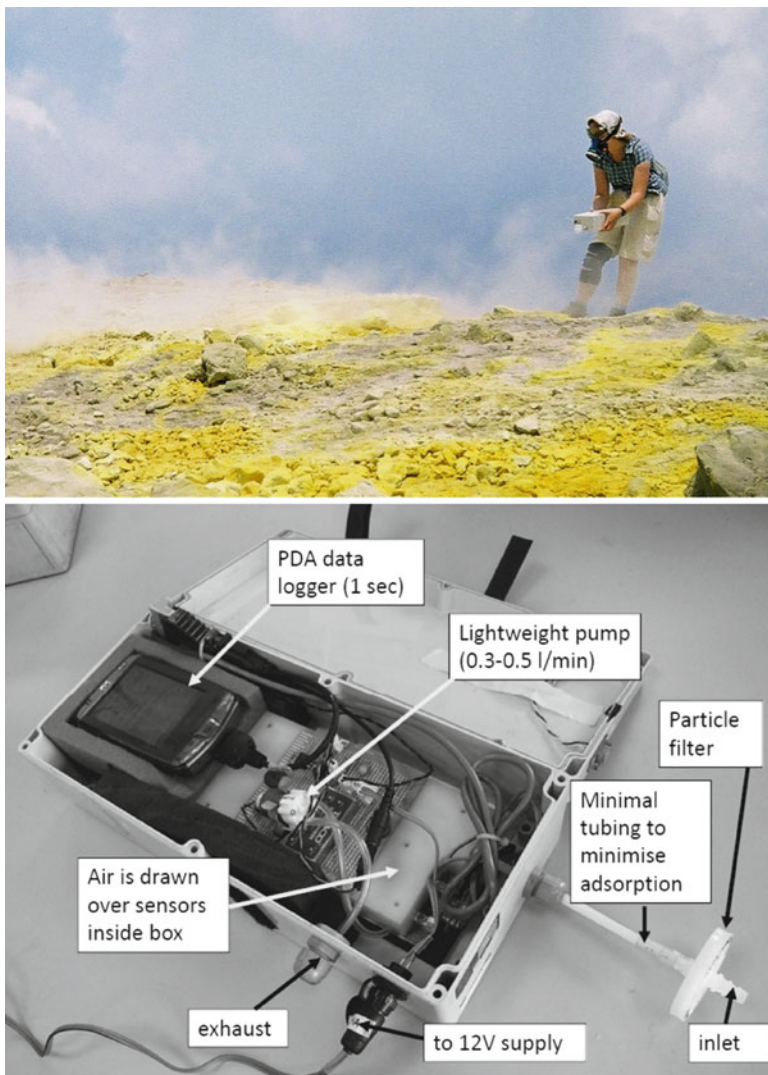


Fig. 15.2 *Upper:* Deployment of multi-gas instruments in fumaroles at Vulcano (Italy). *Lower:* Diagram of multi-gas instrument that includes six electrochemical sensors, as described by Roberts et al.⁴²

$\text{CO}/\text{SO}_2 = 0.02$, for $\text{H}_2\text{S}/\text{SO}_2 = 0.15$, with estimated error of ± 0.01 . These measurements show that under the reduced magmatic conditions of this fumarolic emission, reduced gases (such as H_2 , H_2S and CO) are relatively abundant so as to be detectable. The general correlation with plume tracer SO_2 suggests limited in-plume chemistry of these species between their emission and detection (\sim minutes). Details of electrochemical sensor data analysis methodology are now discussed.

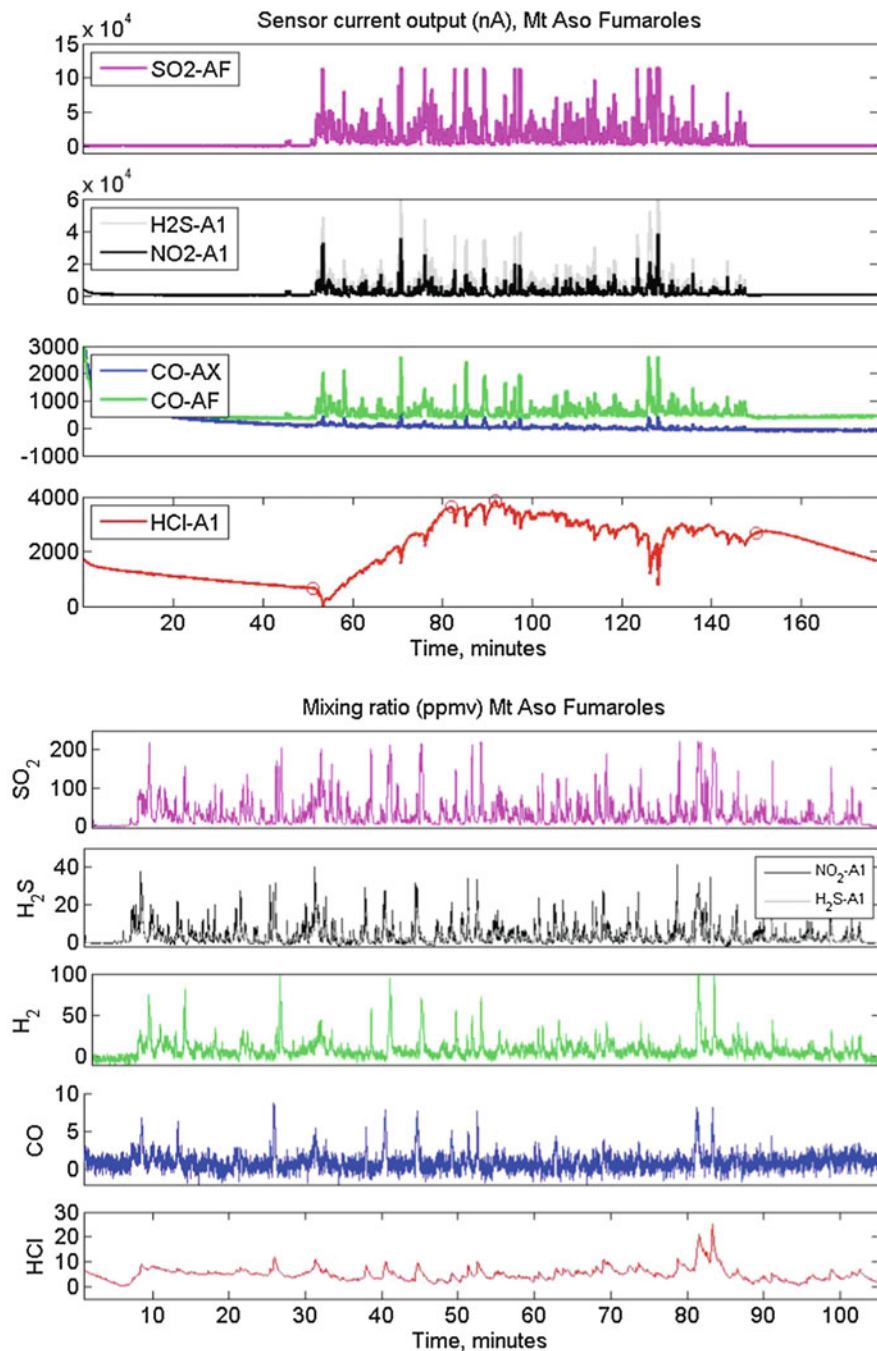


Fig. 15.3 Upper figure: Raw data showing 1 Hz time series of instrument output for electrochemical sensors SO₂-AF, H₂S-A1, NO₂-A1, CO-AX, CO-AF and HCl-A1 at Aso volcano⁽⁴²⁾ for details). Lower figure: Processed data showing SO₂, H₂S, H₂, CO and HCl gas ppmv mixing ratio time series determined from analysis of the 1 Hz sensor signal

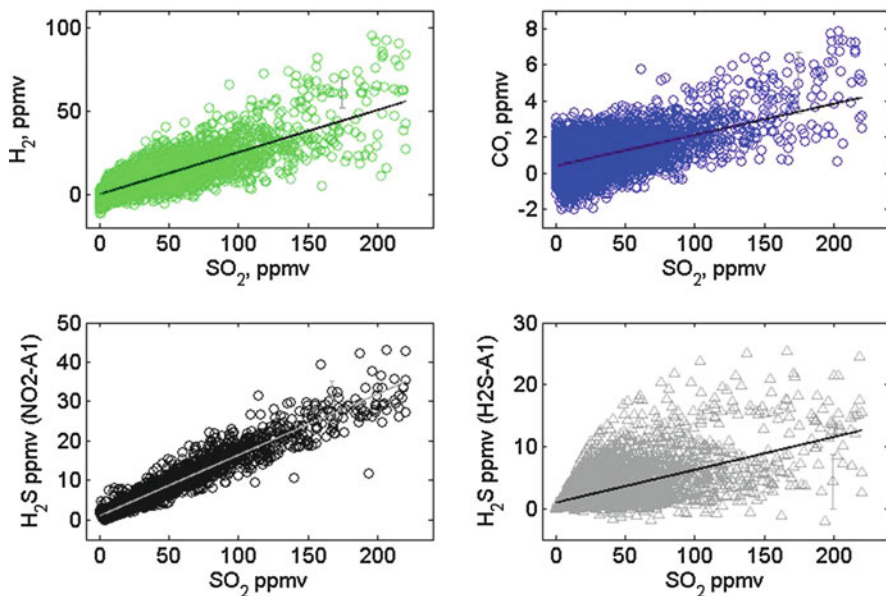


Fig. 15.4 Scatter plots of the gas mixing ratios derived from the electrochemical sensor data of Fig. 15.3, shown as X versus SO_2 where X is H_2 , CO or H_2S . The estimate of H_2S from NO2-A1 sensor is preferred over that of H2S-A1 sensor which exhibits enhanced scatter: see text for explanation. Linear regression is used to determine the characteristic gas ratios in the Aso volcano fumarole emission

15.2.2 Data Analysis and the Importance of Sensor Cross-Sensitivities

Volcanic gas abundances encountered at the crater rim are sufficiently high (few to hundreds of ppmv) so as to be readily detected by electrochemical sensors, with the sensor current proportional to the gas abundance. However, the plume environment consists of a complex cocktail of volcanic gases that can cause interferences in the gas detection, and which must be removed during data post-processing. Electrochemical sensors for SO_2 typically do not exhibit significant cross-sensitivities to other volcanic gases (an integrated filter on the sensor prevents interferences from H_2S). Thus, Eq. (15.1) shows that the sensor output current, I_{SO_2} (in nA), is related to the SO_2 mixing ratio, $[\text{SO}_2]$, by the sensor sensitivity, c_{SO_2} (in nA/ppmv), a constant determined from laboratory calibration. The baseline current, B_{SO_2} , may also need to be removed during data analysis, but can be readily determined during periods when the volcano plume is absent:

$$I_{\text{SO}_2} = B_{\text{SO}_2} + c_{\text{SO}_2} \cdot [\text{SO}_2] \quad (15.1)$$

$$I_{\text{H}_2\text{S}} = B_{\text{H}_2\text{S}} + s_{\text{H}_2\text{S}} \cdot [\text{H}_2\text{S}] + c_{\text{SO}_2} \cdot [\text{SO}_2] \quad (15.2)$$

However, electrochemical sensors for H₂S do tend to exhibit a cross-sensitivity to SO₂, of around 10–20 %. Thus the H₂S sensor current, Eq. (15.2), is a function of the baseline, B_{H₂S}, the H₂S mixing ratio, [H₂S], according to the sensor sensitivity, c_{H₂S}, and also the SO₂ mixing ratio, [SO₂], according to the sensor cross-sensitivity, c_{SO₂}. The interference from SO₂ can be removed during data post-processing, provided both the H₂S sensor sensitivity and cross-sensitivity are known, and by using the concurrent SO₂ mixing ratio determined from the SO₂ sensor. It is important that sensor cross-sensitivities are properly taken into account for accurate determination of plume gas ratios. For example, in a plume with H₂S/SO₂ = 0.05 gas ratio, failure to remove a 10 % cross-sensitivity of an H₂S sensor to SO₂ would lead to a measured gas ratio of 0.15, i.e. an error of 300 %. Alternatively, a filter may be applied to the specific sensor inlet to remove SO₂, e.g. references ^(44, 45); however care must be taken that it does not co-remove H₂S.

Nevertheless, sensor cross-sensitivities can also bring new opportunities for gas measurement. Roberts et al.⁴² deployed an NO₂ sensor in the plumes of Japanese volcanoes Aso and Miyakejima, and, noting that NO₂ concentrations were much less than H₂S, used the sensor's cross-sensitivity to measure H₂S abundance. The sensor presented advantages over traditional H₂S sensors because it did not exhibit a cross-sensitivity to SO₂, and also because the time-response of the NO₂ sensor (to H₂S) is more similar to the SO₂ sensor (see further discussion of measurement uncertainties below). In the same study⁴² Roberts et al. also co-deployed two CO sensors, both of which exhibited cross-sensitivities to H₂. By co-analysing the two sensor outputs (which contrasted in their degree of cross-sensitivity), both CO and H₂ abundances could be determined in the volcanic plume.

15.2.3 Critical View on Sources of Multi-Gas Measurement Error

The accuracy of plume gas ratios reported from multi-gas systems depends on a number of factors influencing the sensor measurement error. These include sensor calibration, linearity and possible calibration drift, the sensor baseline and possible temperature, humidity and pressure dependences of the sensor output, as outlined below.

Of key importance is the sensitivity of the sensor current or voltage output, expressed as nA/ppmv or mV/ppmv of target gas, and any cross-sensitivity to nontarget gases, as mentioned above. These sensitivities are usually quantified by pre- and/or post-fieldwork laboratory calibrations where the sensor is exposed to a fixed concentration of gas. Such point calibrations assume linearity of the sensor responses to the target gases, which is generally a valid assumption; see, e.g., reference⁽⁴²⁾. In order to reduce adverse effects from possible sensitivity drift, calibrations should be performed immediately prior to or after the fieldwork. Further, the laboratory calibrations performed at room temperature (~20–25 °C) and ambient pressure (~1 atm) do not necessarily reflect sensor properties at the

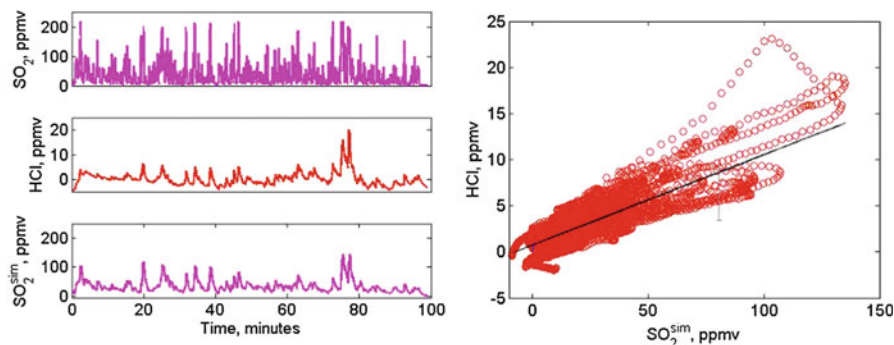


Fig. 15.5 The importance of sensor response time illustrated for HCl and SO₂ sensor pair. *Left*: SO₂ and HCl ppmv time series illustrated alongside a simulated *slow* SO₂ time series using E3, SO₂^{sim}. The latter has an improved correlation to HCl compared to the standard SO₂ time series. *Right*: Scatter plot of HCl versus simulated *slow* SO₂ time series used to derive an estimate for HCl/SO₂ ratio

temperature and pressure of the field measurements at the volcano summit (typically between a few hundred metres and 4 km altitude a.s.l.). Both atmospheric pressure and temperature decrease with altitude in the troposphere, the latter also varying diurnally and with season and latitude. Few studies have considered these effects on multi-gas measurements.

In addition to the above, it has recently been shown that the finite response time of the sensors is also a source of multi-gas measurement error, particularly in plumes with fluctuating gas abundance.⁴⁶ Direct comparison of output from sensors with contrasting response times can result in enhanced scatter and also bias in the derived volcanic gas ratios, and hence lead to inaccurate estimations of plume composition. Such errors are enhanced when interferences are removed in post-processing (e.g. for H₂S from the H₂S-A1 sensor in Fig. 15.2). Both data integration techniques⁴⁶ and sensor response modelling approaches⁴² have been proposed to combat these measurement uncertainties. Sensors with vastly contrasting response times exhibit non-identical responses to fluctuating plume gas concentrations and thus cannot be compared directly. An example is the determination of HCl/SO₂ ratios from a fast SO₂ (~12 s response time) and slow HCl (approximately few minutes response time) sensor; Fig. 15.3⁴² proposes the following sensor response modelling approach to analyse the data. A slower response SO₂ signal, SO₂^{SIM}, is first simulated from the fast response SO₂ output, SO₂^{FAST}, using Eq. (15.3) that is iteratively applied (beyond the starting value of SO₂^{SIM}_(t=1) that is set to SO₂^{FAST}_(t=1)). The slowness factor, *F*, takes a value between 0 and 1, and can either be determined from laboratory measurements of sensor response time or inferred by optimising the correlation between the HCl sensor and SO₂^{SIM}. Figure 15.5 shows how the slow response SO₂ signal, SO₂^{SIM}, exhibits much greater similarity to the HCl sensor signal than the fast SO₂ measurement. Once the slow response SO₂ signal, SO₂^{SIM}, has been generated, it can be directly compared to the HCl sensor output, and a

scatter plot of HCl versus SO_2^{SIM} used to estimate the HCl/ SO_2 ratio. For the fumaroles of Aso volcano, it was estimated that $HCl/SO_2 = 0.1 \pm 0.02$:

$$SO_2^{SIM}(t) = F \cdot SO_2^{SIM}(t-1) + (1 - F) \cdot SO_2^{FAST}(t) \quad (15.3)$$

Further sensor response modelling approaches are in development for other multi-gas sensor pairs. In summary, it is emphasized that accurate determination of plume gas ratios from co-deployed in situ electrochemical (and other) sensors requires a consideration of sensor response times. Non-identical sensor response times can result in scatter and bias in the derived gas ratios, particularly in cases where cross-sensitivities need to be removed. Reported plume gas ratios from multi-gas instruments may need to be revisited in this context, and the effect is likely also important in the monitoring of other environments, such as urban pollution.

15.2.4 Insights Gained from Electrochemical Sensing of Volcanic Emissions

The growing application of electrochemical sensors to volcanic gas monitoring is bringing a wealth of new data on gas composition. Notwithstanding the abovementioned issues concerning measurement uncertainties, it is clear that electrochemical sensors bring new and valuable insights into volcanology, as highlighted by the examples below.

The volcanic plume composition, as quantified by the observed volcanic gas ratios, reflects the subsurface volcanic conditions. Partitioning between reduced and oxidised gases leads to characteristic H_2S/SO_2 , CO/CO_2 and H_2/H_2O in the volcanic emission.⁴⁷ These gas ratios are dependent on the magmatic redox state, temperature and pressure, and thus can be used to infer subsurface magmatic plumbing scenarios. For example, Edmonds et al.⁴⁸ deployed a multi-gas electrochemical sensor system (including an electrochemical sensor for SO_2 alongside a separate in situ CO_2 (infrared sensor)) during the 2008–2010 summit eruption of Kilauea volcano, Hawaii. Analysis of the CO_2/SO_2 ratio was used to infer sub-surface magmatic plumbing during the eruption. The CO_2/SO_2 ratio in the main summit crater plume was lower than expected based on the previous eruptive history, yet during periods when the plume was absent (e.g. due to wind direction that advected it away from the sensors) CO_2 -enriched (but SO_2 poor) air masses were occasionally observed. It was inferred that CO_2 accumulation at the magma chamber roof followed by diffuse degassing through permeable rock was likely responsible for this separation of volcanic sulphur and carbon emissions to the atmosphere.

Moreover, repeated or continuous monitoring of the volcanic emission chemical composition over time can provide useful insights into temporal changes in the subsurface magmatic processes. For example, Aiuppa et al.^{34,35} used three fully automated multi-gas instruments at the summit of Mt. Stromboli, to measure CO_2 and SO_2 gas concentrations over several years. The observations were analysed to

yield CO_2/SO_2 time series as well as CO_2 fluxes. It was shown that major explosions at Stromboli are systematically preceded by a phase of increasing CO_2 degassing, with CO_2/SO_2 increasing from ~ 5 to >20 . This finding is in agreement to conceptual models of volcanic degassing at Stromboli, indicating a subsurface separation and accumulation of CO_2 -rich gas bubbles, whose episodic release results in an explosive event. This demonstrated capability of automated multi-gas monitoring systems to detect temporal changes in the plume gas ratio opens new promising perspectives for in situ electrochemical sensor methods in the forecasting of explosive volcanic events in future.

15.3 Future Directions for Miniature Electrochemical Sensors

15.3.1 *Electrochemical Sensor Deployments on Novel Platforms*

The lightweight, low-cost and low-power properties of miniature electrochemical sensors make the sensors very suitable for deployment on novel platforms such as unmanned aerial vehicle (UAV). Such platforms can be advantageous if deployment of in situ sensors is impractical due to a high risk of an imminent explosive volcanic eruption, or where the region of volcanic degassing cannot practically be accessed using a handheld instrument. Some recent volcanological applications are outlined below.

McGonigle et al.³⁹ presented the first study to use an in situ electrochemical sensor deployed on an unmanned aerial vehicle alongside an infra-red spectrometer to characterise CO_2 and SO_2 in the plume ≤ 200 m downwind of La Fossa, Vulcano, Italy. This study demonstrated the advantages of UAV-based sensing not only from a safety perspective (obtaining plume measurements with minimal personal gas exposure), but also to quantify the bulk plume emission arising from individual fumarole sources.

Shinohara²⁵ performed a UAV-based characterisation of the plume from Shinmoedake, Kirishima volcano, Japan, using electrochemical and other in situ sensors. Due to ongoing explosive eruptive activity, access to the volcano summit area 4 km around the volcano was restricted (even for manned aircraft). Therefore this study demonstrates UAVs as a viable method to obtain plume gas measurements under hazardous summit conditions. Several molar gas ratios were determined during a period with Vulcanian eruptions in May 2011, including $\text{CO}_2/\text{SO}_2 = 8$, $\text{H}_2\text{O}/\text{CO}_2 = 70$ and $\text{H}_2/\text{SO}_2 = 0.03$. It was found that plume $\text{SO}_2/\text{H}_2\text{S}$ showed a decrease over March to May 2011 from 8 to 0.8, which is interpreted as resulting from an increase in degassing pressure of the volcano.

Pieri et al.⁴³ present measurements of SO_2 in the plume of Turrialba Volcano in Costa Rica for UAV flights that reach up to 3.5 km. This study demonstrates the first

routine (monthly deployments since 2013) UAV-based SO₂ data acquisition and are being used for validation of satellite SO₂ retrievals during ASTER (Advanced Spaceborne Thermal Emission and Reflection Radiometer, ASTER) overpasses. Pieri et al.⁴³ also provide an overview of reported UAV approaches to volcanic plume detection as well as tethered and meteorological balloon applications.

UAVs can also be used to explore the temporal evolution of the volcano plume chemistry. A novel CMET (controlled meteorological) balloon system⁴⁹ has been used to follow the trajectory of the Kilauea (Hawaii) plume to perform quasi-Lagrangian studies of the plume evolution. Observations from the payload that included an electrochemical SO₂ sensor as well temperature, pressure and humidity sensors⁴⁰ demonstrated correlation between SO₂ and humidity in the near-source plume, but appear to show anti-correlation further downwind, potentially due to in-plume processing.

Finally, the potential of in situ sensors upon airborne platforms to perform detailed plume characterisation and chemical mapping and to trace the chemical evolution of the plume with time is shown by Kelly et al.¹⁸ who deployed an electrochemical SO₂ sensor alongside an ozone sensor based on UV spectroscopy on an instrumented aircraft. Through repeated transects across the plume, the dispersion of SO₂ downwind of the volcano could be mapped. Moreover, the ozone sensor identified rapid ozone depletion within the plume. This ozone depletion was attributed to rapid in-plume reactive halogen chemistry: numerical simulations using the *PlumeChem* model⁵⁰ were able to spatially reproduce the observed ozone depletion for the reported SO₂ flux and dispersion rate. It is anticipated that further advances in instrumented balloon and UAV technologies will allow airborne chemical mapping studies to become more frequent in future in order to probe the plume impact on downwind atmospheric chemistry, as well as quantify the emissions near source.

15.3.2 Improved Accuracy and Detection Limit: Applications Beyond Volcanoes

Improvements to the sensitivity and stability specifications of commercially available miniature electrochemical sensors have also brought the possibility to measure gases at ever lower concentrations, and the capability to detect pollutants in new environments. To improve resolution and detection limits, the miniature electrochemical sensors should be deployed using low noise electronics. Figure 15.6 (upper) illustrates the detection of SO₂ in the relatively dilute grounding plume from Mt. Etna, using high- and low-sensitivity electrochemical sensors logging at 1 Hz and 0.1 Hz, respectively, and low-noise electronics. The two sensors show very similar response to the plume gases, and are capable of observing sub-ppmv (tens to hundreds of ppbv) variations in SO₂ gas abundance. Baseline noise is lowest for the high-sensitivity sensor.

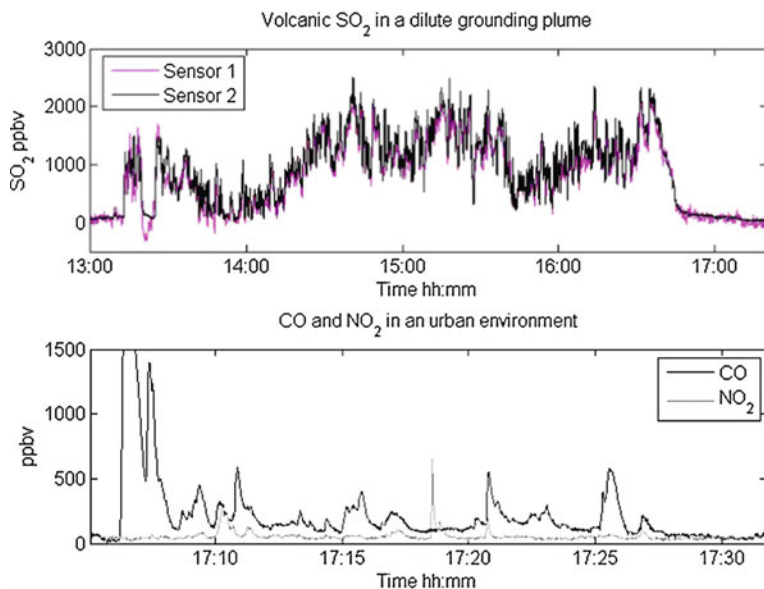


Fig. 15.6 *Upper:* SO_2 mixing ratio time series obtained in a dilute downwind volcanic plume using low-noise electronics, logging output from two non-identical miniature electrochemical SO_2 sensors with high sensitivity (black) and lower sensitivity (purple), at 1 Hz and 0.1 Hz, respectively. *Lower:* Mixing ratio abundances of excess (plume peaks - background) CO and NO_2 at a cross-roads in an urban environment (Orleans, France), measured at 1 Hz using low-noise electronics, with the high-sensitivity SO_2 sensor used to detect NO_2 (cross-sensitivity $\sim 120\%$) alongside a high-sensitivity sensor for CO

Similar miniature electrochemical sensors have recently been applied to quantifying ozone, CO, NO and NO_2 pollution in an urban environment^{51–53} in stationary networks as well as on moving (tramway, pedestrian, bicyclist) platforms. This potential for urban monitoring is demonstrated here through a short instrument deployment at urban cross-roads in Orleans (France). Figure 15.6 (lower) shows the electrochemical sensor response to emissions from passing traffic, where ‘excess’ CO and NO_2 are calculated by subtracting the constant background abundance. The SO_2 (high sensitivity) sensor is used here to detect NO_2 by means of its $\sim 120\%$ cross-sensitivity to this gas, whilst a CO sensor is used to detect CO. Note that in urban environments the SO_2 electrochemical sensor signal due to NO_2 greatly exceeds that due to volcanic sulphurous gases, in contrast to volcanic plumes. The measurements of Fig. 15.6 show fluctuations in excess NO_2 and CO abundance that exhibit a degree of independence, with the CO traffic signal generally exceeding NO_2 . These observations are similar to the study of Mead et al.⁵³

At low concentrations (e.g. towards background levels), the zero-gas baseline exerts a more significant influence on the sensor output current, and needs careful correction.⁵³ Issues of sensor cross-sensitivity also need to be considered, for example, the interferences of H_2 on the detection of CO. Future urban sensor networks may co-deploy additional sensors in order to extract these interferences,

in analogous manner to the approach demonstrated by Roberts et al.⁴² regarding CO and H₂ in volcanic plumes. Measurement errors caused by finite sensor response to fluctuating gas abundances, as highlighted above, are also likely of quantitative importance in electrochemical sensing of urban pollution. Whilst these measurement uncertainties require further careful consideration, miniature electrochemical sensor technology appears a promising low-cost method for urban pollutant and personal health (as well as volcano) monitoring in future.

References

1. Stevenson DS, Johnson CE, Collins WJ, Derwent RG (2003) The tropospheric sulphur cycle and the role of volcanic SO₂. In: Clive O, David M, Pyle-Jenni B (eds) *Volcanic degassing*. Geological Society of London, London, ISBN 186239136X, 9781862391369
2. Smith SJ, van Aardenne J, Klimont Z, Andres RJ, Volke A, Delgado AS (2011) Anthropogenic sulphur dioxide emissions 1850–2005. *Atmos Chem Phys* 11:1101–1116. doi:10.5194/acp-11:1101-2011
3. Mareckova K, Wankmueller R, Whiting R, Pinterits M (2012) Review of emission data reported under the LRTAP Convention and NEC Directive. EMEP Inventory Review. <http://www.ceip.at/review-results/>
4. Hole LR, Christensen JH, Ruoho-Airola T, Torseth K, Ginzburg V, Glowacki P (2009) Past and future trends in concentrations of sulphur and nitrogen compounds in the Arctic. *Atmos Environ* 43:928–939
5. Kühnel R, Roberts TJ, Bjorkman MP, Isaksson E, Aas W, Holmen K, Strom J (2011) 20-year climatology of NO₃⁻ and NH₄⁺ wet deposition at Ny-Alesund, Svalbard, *Adv Meteorol*. doi:10.1155/2011/406508, Article ID 406508
6. Lu Z, Streets DG, Zhang Q, Wang S, Carmichael GR, Cheng YF, Wei C, Chin M, Diehl T (2000) Tan Q (2010) Sulphur dioxide emissions in China and sulphur trends in East Asia since. *Atmos Chem Phys* 10:6311–6331
7. Krzyzanowski M, Cohen A (2008) Update of WHO air quality guidelines. *Air Qual Atmos Health* 1:7–13. doi 10.1007/s11869-008-0008-9. See also: WHO air quality guidelines for Europe, 2nd ed. WHO Regional Publications, European Series, No. 91 (2000). ISBN 92 890 1358 3. Ch 6.6: Hydrogen sulphide. Ch 7.4: Sulphur dioxide. WHO air quality guidelines for particulate matter, ozone, nitrogen dioxide and sulphur dioxide, Global update 2005. Summary of risk assessment. http://whqlibdoc.who.int/hq/2006/WHO_SDE_PHE_OEH_06.02_eng.pdf
8. Costigan MG (2003) Hydrogen sulphide: UK occupational exposure limits. *Occup Environ Med* 60:308–312
9. Stetter JR, Li J (2008) Amperometric gas sensors: a review. *Chem Rev* 108:352–366
10. Oppenheimer C, Scaillet B, Martin RS (2011) Sulphur degassing from volcanoes: source conditions, surveillance, plume chemistry and impacts. *Rev Miner Geochem* 73:363–421. doi:10.2138/rmg.2011.73.13
11. Halmer MM, Schmincke HU, Graf HF (2002) The annual volcanic gas input into the atmosphere, in particular into the stratosphere: a global data set for the past 100 years. *J Volcanol Geotherm Res* 115(3–4):511–528
12. Michaud JP, Krupitsky D, Grove JS, Anderson BS (2005) Volcano related atmospheric toxicants in Hilo and Hawaii volcanoes national park: implications for human health. *Neurotoxicology* 26(4):555–563
13. Delmelle P, Stix J, Baxter PJ, Garcia-Alvarez J, Barquero J (2002) Atmospheric dispersion, environmental effects and potential health hazard associated with the low-altitude gas plume of Masaya volcano, Nicaragua. *Bull Volcanol* 64(6):423–434

14. Robock A (2000) Volcanic eruptions and climate. *Rev Geophys* 38(2):191–219
15. Gigenbach WF (1975) A simple method for the collection and analysis of volcanic gas samples. *Bull Volcanol* 39:15–27
16. McGee KA, Doukas MP, Gerlach TM (2001) Quiescent hydrogen sulphide and carbon dioxide degassing from Mount Baker, Washington. *Geophys Res Lett* 28(23):4479–4482
17. Werner C, Kellu PJ, Doukas M, Lopez T, Pfeffer M, McGimsey R, Neal C (2013) Degassing of CO₂, SO₂, and H₂S associated with the 2009 eruption of Redoubt Volcano, Alaska. *J Volcanol Geotherm Res* 259:270–284
18. Kelly PJ, Kern C, Roberts TJ, Lopez T, Werner C, Aiuppa A (2013) Rapid chemical evolution of tropospheric volcanic emissions from Redoubt Volcano, Alaska, based on observations of ozone and halogen-containing gases. *J Volcanol Geotherm Res* 259:317–333
19. Shinohara H, Kazahaya K, Saito G, Fukui K, Odai M (2003) Variation of CO₂/SO₂ ratio in volcanic plumes of Miyakejima: stable degassing deduced from heliborne measurements. *Geophys Res Lett* 30(5):1208. doi:[10.1029/2002GL016105](https://doi.org/10.1029/2002GL016105)
20. Hager SA, Gerlach TM, Wallace PJ (2008) Summit CO₂ emission rates by the CO₂/SO₂ ratio method at Kilauea Volcano, Hawaii, during a period of sustained inflation. *J Volcanol Geotherm Res* 177(4):875–882
21. Werner C, Hurst T, Scott B, Sherburn S, Christenson BW, Britten K, Cole-Baker J, Mullan B (2008) Variability of passive gas emissions, seismicity, and deformation during crater lake growth at White Island Volcano, New Zealand, 2002–2006. *J Geophys Res* 113, B01204. doi:[10.1029/2007JB005094](https://doi.org/10.1029/2007JB005094)
22. Shinohara H (2005) A new technique to estimate volcanic gas composition: plume measurements with a portable multi-sensor system. *J Volcanol Geotherm Res* 143(4):319–333
23. Shinohara H, Witter JB (2005) Volcanic gases emitted during mild strombolian activity of Villarrica volcano, Chile. *Geophys Res Lett* 32:L20308. doi:[10.1029/2005GL024131](https://doi.org/10.1029/2005GL024131)
24. Shinohara H, Aiuppa A, Giudice G, Gurrieri G, Liuzzo M (2008) Variation of H₂O/CO₂ and CO₂/SO₂ ratios of volcanic gases discharged by continuous degassing of Mount Etna volcano, Italy. *J Geophys Res* 113, B09203
25. Shinohara H (2013) Composition of volcanic gases emitted during repeating Vulcanian eruption stage of Shinmoedake, Kirishima volcano, Japan. *Earth Planets Space* 65:667–675
26. Teschner M, Vougioukalakis GE, Faber E, Poggenburg J, Hatziyannis G (2005) Real time monitoring of gas-geochemical parameters in Nisyros fumaroles. *Dev Volcanol* 7:247–254
27. Teschner M, Faber E, Poggenburg J, Vougioukalakis GE, Hatziyannis G (2007) Continuous, direct gas-geochemical monitoring in hydrothermal vents: installation and long-term operation on Nisyros Island (Greece). *Pure Appl Geophys* 164(12):2549–2571
28. Aiuppa A, Federico C, Giudice G, Gurrieri S (2005). Chemical mapping of a fumarolic field: La Fossa Crater, Vulcano Island (Aeolian Islands, Italy). *Geophys Res Lett* 32: L13309. doi:[10.1029/2005GL023207](https://doi.org/10.1029/2005GL023207)
29. Aiuppa A, Federico C, Giudice G, Gurrieri S, Liuzzo M, Shinohara H, Favara, R, Valenza M (2006) Rates of carbon dioxide plume degassing from Mt Etna volcano. *J Geophys Res* 111: B09207. doi:[10.1029/2006JB004307](https://doi.org/10.1029/2006JB004307)
30. Aiuppa A, Bagnato BE, Witt MJ, Mather TA, Parello F, Pyle DM, Martin RS (2007) Real-time simultaneous detection of volcanic Hg and SO₂ at La Fossa Crater, volcano (Aeolian Islands, Sicily). *Geophys Res Lett* 34(21), L21307
31. Aiuppa A, Giudice G, Gurrieri S, Liuzzo M, Burton M, Caltabiano T, McGonigle AJS, Salerno G, Shinohara H, Valenza M (2008) Total volatile flux from Mount Etna. *Geophys Res Lett* 35, L24302
32. Aiuppa A, Federico C, Giudice G, Giuffrida G, Guida R, Gurrieri S, Liuzzo M, Moretti R, Papale P (2009) The 2007 eruption of Stromboli volcano: Insights from real-time measurement of the volcanic gas plume CO₂/SO₂ ratio. *J Volcanol Geotherm Res* 182:221–230. doi:[10.1016/j.jvolgeores.2008.09.013](https://doi.org/10.1016/j.jvolgeores.2008.09.013)

33. Aiuppa A, Shinohara H, Tamburello G, Giudice G, Liuzzo M, Moretti R (2011a). Hydrogen in the gas plume of an open vent volcano, Mount Etna, Italy. *J Geophys Res* 116: B10204. doi:10.1029/2011JB008461
34. Aiuppa A, Burton M, Allard P, Caltabiano T, Guidice G, Gurrieri S, Liuzzo M, Salerno G (2011) First observational evidence for CO₂ driven origin of Stromboli's major explosions. *Solid Earth* 2:135–142
35. Aiuppa A, Bertagnini A, Métrich A, Di Muro A, Liuzzo M, Tamburello G (2010) A model of degassing for Stromboli volcano. *Earth Planet Sci Lett* 295(1–2):195–204
36. Witt MLI, Mather TA, Pyle DM, Aiuppa A, Bagnato E, Tsanev VI (2008) Mercury and halogen emissions from Masaya and Telica volcanoes, Nicaragua. *J Geophys Res Solid Earth* 113, B06203
37. Witt M, Fischer TP, Pyle DM, Yang TF, Zellmer GF (2008) Fumarole compositions and mercury emissions from the Tatun Volcanic Field, Taiwan: results from multi-component gas analyser, portable mercury spectrometer and direct sampling techniques. *J Volcanol Geotherm Res* 178(4):636–643
38. De Vito S, Massera E, Quercia L, Di Francia G (2007) Analysis of volcanic gases by means of electronic nose. *Sensor Actuat B Chem* 127(1):36–41
39. McGonigle AJS, Aiuppa A, Giudice G, Tamburello G, Hodson AJ, Gurrieri S (2008) Unmanned aerial vehicle measurements of volcanic carbon dioxide fluxes. *Geophys Res Lett* 35, L06303
40. Durant A, Voss P, Watson M, Roberts TJ, Thomas H, Prate F, Sutton J, Mather T, Witt M, Patrick M (2010) Real-time in situ measurements of volcanic plume physico-chemical properties using controlled METeorological balloons. EGU General Assembly 2010. 2–7 May 2010, Vienna, Austria, p. 4937
41. Sawyer GM, Salerno GG, Le Blond JS, Martin RS, Spampinato L, Roberts TJ, Mather TA, Witt MLI, Tsanev VI, Oppenheimer C (2011) Gas and aerosol emissions from Villarrica volcano, Chile. *J Volcanol Geotherm Res* 203:62–75
42. Roberts TJ, Braban CF, Oppenheimer C, Martin RS, Freshwater RA, Dawson DH, Griffiths PT, Cox RA, Saffell JR, Jones RL (2012) Electrochemical sensing of volcanic gases. *Chem Geol* 332–333:74–91
43. Pieri DD, Diaz JA, Bland G, Fladeland M, Madrigal Y, Corrales E, Alan A, Realmuto V, Miles T, Abtahi A (2013) In situ observations and sampling of volcanic emissions with Nasa and Ucr unmanned aircraft including a case study at Turrialba volcano, Costa Rica. In: Pyle DM, Mather TA, Biggs J (eds). *Remote-sensing of volcanoes and volcanic processes: integrating observation and modelling*. Geological Society, London. Geological Society Special Publication 380
44. Shinohara H, Matsushima N, Kazahaya K, Ohwada M (2011) Magma-hydrothermal system interaction inferred from volcanic gas measurements obtained during 2003–2008 at Meakandake volcano, Hokkaido, Japan. *Bull Volcanol* 73(4):409–421
45. Shinohara H, Hirabayashi J, Nogami K, Iguchi M (2011) Evolution of volcanic gas composition during repeated culmination of volcanic activity at Kuchinoerabujima volcano, Japan. *J Volcanol Geotherm Res* 202(1–2):107–116
46. Roberts TJ, Saffell JR, Oppenheimer C, Lurton T (2014). Electrochemical sensors applied to pollution monitoring: measurement error and gas ratio bias—a volcano plume case study. *J Volcanol Geotherm Res* 281:85–96
47. Gerlach TM, Nordlie BE (1975) The CO₂/H₂S gaseous system, part II: temperature, atomic composition, and molecular equilibria in volcanic gases. *Am J Sci* 275:377–394
48. Edmonds M, Sides IR, Swanson D, Werner C, Martin RS, Mather TA, Herd RA, Jones RL, Mead MI, Sawyer G, Roberts TJ, Sutton AJ, Elias T (2013) Magma storage, transport and degassing during the 2008–10 summit eruption at Kilauea Volcano, Hawaii. *Geochim Cosmochim Acta* 123:284–301. doi:10.1016/j.gca.2013.05.038

49. Voss PB, Hole LR, Helbling EF, Roberts TJ (2013) Continuous in-situ soundings in the arctic boundary layer: a new atmospheric measurement technique using controlled meteorological balloons. *J Intell Robot Syst* 70(1–4):609–617. doi:[10.1007/s10846-012-9758-6](https://doi.org/10.1007/s10846-012-9758-6)
50. Roberts TJ, Braban CF, Martin RS, Oppenheimer C, Adams JW, Cox RA, Jones RL, Griffiths PT (2009) Modelling reactive halogen formation and ozone depletion in volcanic plumes. *Chem Geol* 263(1–4):151–163. doi:[10.1016/j.chemgeo.2008.11.012](https://doi.org/10.1016/j.chemgeo.2008.11.012)
51. Hasenfratz D, Saukh O, Thiele L (2012) On-the-fly calibration of low-cost gas sensors. *Wireless sensor networks*. Springer, Berlin. pp. 228–244
52. Li JJ, Faltings B, Saukh O, Hasenfratz D, Beutel J (2012) Sensing the air we breathe—the OpenSense Zurich dataset. In: *Proc. 26th int'l conf. on the advancement of artificial intelligence (AAAI '12)*. pp. 323–325
53. Mead IM, Popoola OAM, Stewart GB, Landshoff P, Calleja M, Hayes M, Baldovi JJ, McLeod MW, Hodgson TF, Dicks J, Lewis A, Cohen J, Baron R, Saffell JR, Jones RL (2013) The use of electrochemical sensors for monitoring urban air quality in low-cost, high-density networks. *Atmos Environ* 70:186–203

Chapter 16

Nitrogen Compounds: Ammonia, Amines and NO_x

Jonathan P. Metters and Craig E. Banks

This chapter provides an overview of the utilisation of electrochemistry to measure ammonia, amines and *N*-oxides (NO_x) compounds which have potential application in being the basis of electrochemical gas sensors.

The analytical sensing of ammonia is of significant and wide importance due to its high toxicity and a plethora of applications where the gas is utilised or generated. Such applications include environmental protection, such as in the monitoring of water systems, industrial processes, food processing, power plants, fuel cells and medical diagnostics such as within breath/exhaled/expressed air.¹ In this latter case ammonia can provide clinical information via breath such as haemodialysis monitoring, *helicobacter pylori*, halitosis and asthma assessment,² with many more constantly being diagnosed.³

It is abundantly clear that there is a whole diversity of applications where the detection and monitoring of ammonia is required and as such sensors have been extensively applied.¹ Timmer et al.¹ provide a thorough overview of ammonia sensors highlighting the pros and cons of each; particularly they highlight the diverse range of applications where ammonia is encountered but also show that this dictates the required analytical parameters (concentration range etc.) and consequently which sensors are useful or not.¹ One particular sensor of merit is electrochemically based which is mainly due to electrochemical processes being relatively easily transferred from the lab to the field and due to the potential for their miniaturisation and low cost; as such these clear advantages have made them indispensable as analytical tools over traditionally employed analytical sensing approaches which include: Selected Ion Flow Tube-Mass Spectrometry (SIFT-MS),⁴ Gas Chromatography-Ion Mobility Spectrometry (GC-IMS),⁵ Laser Induced

J.P. Metters • C.E. Banks (✉)

Faculty of Science and Engineering, Division of Chemistry and Environmental Science,
School of Chemistry and the Environment, Manchester Metropolitan University, Chester
Street, Manchester M15GD, Lancs, UK

e-mail: c.banks@mmu.ac.uk

Fluorescence (LIF),⁶ Cavity Ring Down Spectroscopy (CRDS),⁷ Photoacoustic Spectroscopy (PAS)⁸ and Quartz Crystal Microbalance (QCM),⁸ which do not have all the advantages possessed by electrochemical methodologies. In this chapter we consider those applying dynamic electrochemistry rather than potentiometric⁹ or those similarly related using resistivity.

The electrochemical sensing of ammonia can be divided into four main areas; the first is the direct electrochemical oxidation using unmodified electrodes; the second involves the use of chemical mediators such as a chemical reagent reacting with ammonia to form a product which is electroactive and is thus monitored; the third involves polymers where the ammonia interacts with the polymeric layers with the physical change monitored electrically and fourth, the use of metal electrocatalysts and their incorporation into composites such as using carbon nanotubes or graphene. Table 16.1 provides a thorough overview of these reports detailing the electrochemical system described and the resulting analytical performance and applications/matrix determined within.

In this chapter we explore each of the four main areas identified above. In the first case, that is the electrochemical oxidation of ammonia at bare unmodified electrodes. Ji et al.²¹ reported for the first time the electrochemical sensing of ammonia at Boron-Doped Diamond electrodes which was compared to other commercially available electrodes including that of glassy carbon, edge-plane pyrolytic graphite and HOPG electrodes. Figure 16.1 displays the observed voltammetric signatures where it is clear that a large quantifiable response is evident at the Boron-Doped Diamond electrode surface which occurs at lower overpotentials over that at the other reported electrode materials. Typically in electroanalysis it is well reported that an edge-plane pyrolytic graphite electrode, which has a large global % coverage of edge-plane sites, usually gives rise to fast heterogeneous electron transfer over the other electrodes explored. However in this example it is not the case. Indeed it is thought that ammonia intercalates graphite and hence no response is observed at the edge-plane pyrolytic graphite electrode the severity of which depends upon the electrode morphology/structure.

Thus due to the unique structure of Boron-Doped Diamond (that is, diamond doped with boron) intercalation is greatly reduced/alleviated all together.²¹ Proof-of-concept was shown for the sensitive and direct detection of ammonia gas bubbled into aqueous solutions²¹ which has clear applications in gas sensing. Other work has focused upon the application of the Boron-Doped Diamond electrodes as anodes for the electro-oxidation of ammonia within wastewater^{22,23} where in comparison to metal oxide-based sensors, Boron-Doped Diamond was able to decrease the total ammonia and nitrogen as well as chemical oxygen demand with greater current efficiencies; such work provides a basis for wastewater *treatment* but also can potentially be used in *sensing*. Michels et al.²² diligently explored the mechanism of the electrochemical oxidation of ammonia on Boron-Doped Diamond in aerated solutions finding that the oxygen evolution reaction is hindered which in turn enhances the main reaction.²²

Table 16.1 A summary of the various electrochemical approaches for the sensing of ammonia

Materials/electrodes	Sensitivity	Detection limit	Linear range	Comments	Ref.
Hexagonal-shaped ZnO nanopencils	26.5822 $\mu\text{A cm}^{-2} \text{mM}^{-1}$	5.0 mM	50 nM–0.5 mM	–	10
Polyurethane acrylate	8.5254 $\mu\text{A cm}^{-2} \text{mM}^{-1}$	0.018 μM	0.05 μM –0.05 M	–	11
β -Fe ₂ O ₃ nanoparticles	0.5305 $\mu\text{A cm}^{-2} \text{mM}^{-1}$	21.8 μM	77 μM –0.7 M	–	12
CuP co-doped ZnO nanorods	1.549 $\mu\text{A cm}^{-2} \text{mM}^{-1}$	8.9 μM	–	–	13
Inkjet polyanaline nanoparticle	–	6.2 ppbv	40–2,175 ppbv	Determination in gaseous simulated human breaths	3
Pt electrode in [C ₄ mim][OTf]	–	49 ppm	200–1,000 ppm	–	14
Pt electrode in [C ₂ mim][NTf ₂]	–	48 ppm	200–1,000 ppm	–	14
Pt electrode in [C ₄ mim][BF ₄]	–	56 ppm	200–1,000 ppm	–	14
Glassy carbon spheres with anthraquinone moieties	–	9×10^{-9} M	5×10^{-8} – 3×10^{-5} M	Determination of ammonia in urine and soil samples also explored	15
Glassy carbon electrode in the presence of fluorescamine	–	0.71 μM	0–60 μM	LOD determined through measurement of the reduction in peak height observed for fluorescamine	16
Glassy carbon electrode in the presence of fluorescamine	–	3.17 μM	0–60 μM	LOD determined through measurement of the reaction product with ammonia	16
Glassy carbon electrode in the presence of <i>N,N'</i> -diphenyl-1,4-phenylenediamine in propylene carbonate	9.62×10^{-8} A ppm^{-1}	8 ppm	40–600 ppm	Mediated electrochemical determination of ammonia where ammonia reversibly removes protons from oxidised DPPD; facilitating the oxidative process with a new peak occurring at lower potentials	17

(continued)

Table 16.1 (continued)

Materials/electrodes	Sensitivity	Detection limit	Linear range	Comments	Ref.
Glassy carbon electrode in a propylene carbonate solution containing 0.5 mM hydroquinone with 0.1 M TBAP	1.29×10^{-7} A ppm ⁻¹	4.91 ppm	10–100 ppm	–	18
Electrochemiluminescence with (phenylquinoline) ₂ Ir(acetylacetonone)		4×10^{-8} M	1.0×10^{-7} – 1.0×10^{-3} M	–	19
Inkjet printed polyaniline nanoparticles	–	–	1–100 ppm	Found to be stable at high temperatures with heating of the sensors allowing for improved recovery times and control over the analytical profile	20

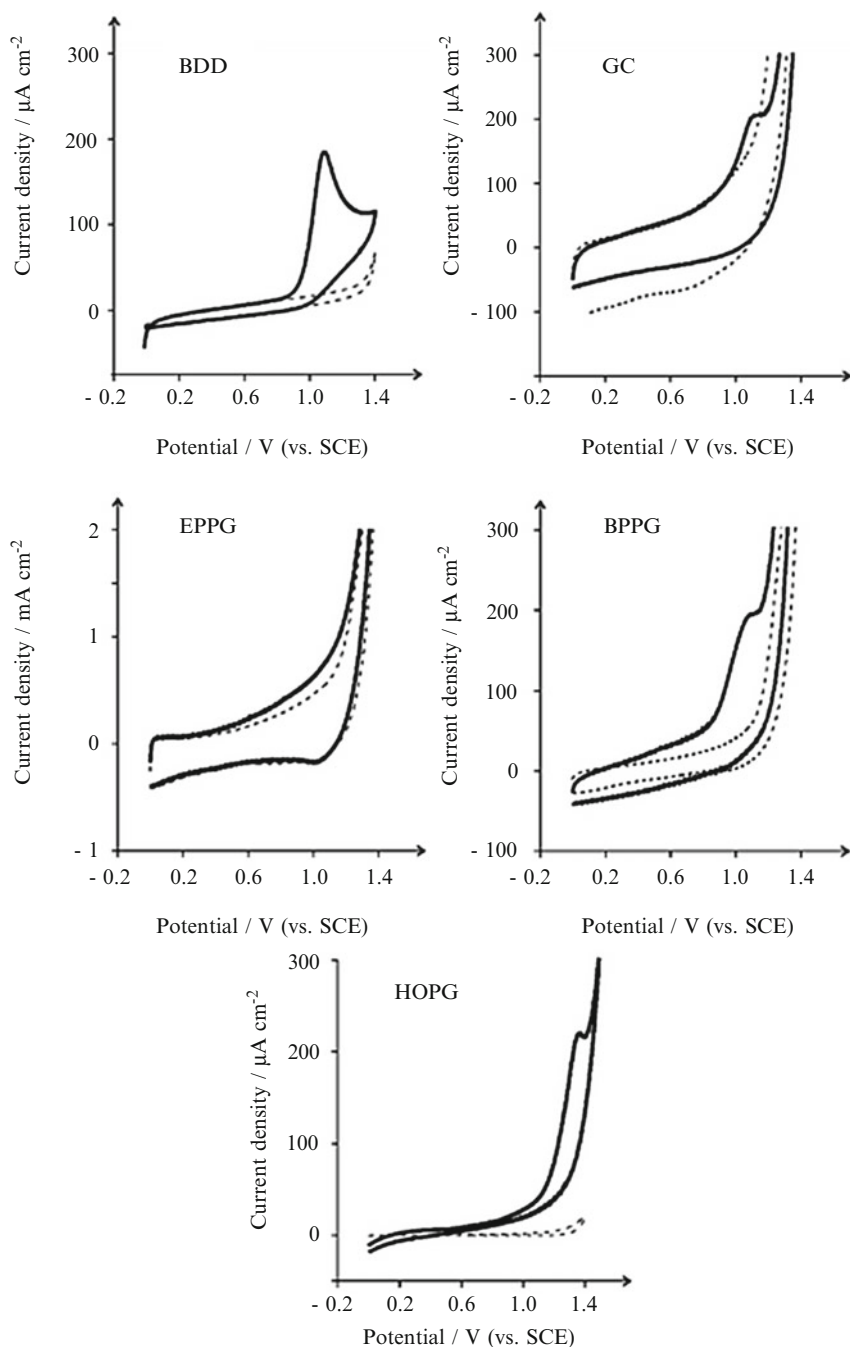


Fig. 16.1 Cyclic voltammetric response of Boron-Doped Diamond (BDD), glassy carbon (GC), edge plane pyrolytic graphite (EPPG), basal plane pyrolytic graphite (BPPG) and highly ordered pyrolytic graphite (HOPG) electrodes in a 0.1 M KCl aqueous solution which has had 0.1 % ammonia bubbled through it for 4 min. The *dashed line* is the response of the electrode in the absence of ammonia. The scan rate in all cases was 100 mV s⁻¹. Reproduced from reference (21) with permission from the Royal Society of Chemistry

Note however that a key consideration is also the electrolyte/solution media which not only affects the electrochemical sensing of ammonia through the solubility of ammonia within the electrolyte so as not to be rate limiting, the solvent can itself intercalate detrimentally with graphite. Generally gas sensor designs, and as is the case for ammonia, the electrolyte employed is aqueous based. The appreciable water vapour pressure inevitably means that the sensor will dry out over time so limiting the lifetime at typical operating temperatures and restricting the sensor reliability; the volatility of the water can be reduced by the use of high concentrations of sulphuric acid (~5 M) as an electrolyte but this places significant constraints on the voltammetry possible. In the context of ammonia sensing, the ammonia will be converted into the electro-inactive NH_4^+ ion; alternatives are clearly desirable.²⁴ Consequently propylene carbonate has been reported to be a useful alternative to aqueous electrolytes since additionally it offers large anodic potential window limits: 5.9 V for glassy carbon electrode, 6.3 V for Boron-Doped Diamond electrode, 2.9 V for edge-plane pyrolytic graphite electrode and 3.7 V for basal-plane pyrolytic graphite electrode. Further and most notably, the vapour pressure of propylene carbonate is 0.03 mmHg (at 20 °C) in contrast to the vapour pressure of water which is 17.5 mmHg (at 20 °C).

Ji et al. have reported the direct electrochemical oxidation of ammonia at glassy carbon electrodes in propylene carbonate (with 0.1 M TBAP) and in comparison to Boron-Doped Diamond, edge-plane pyrolytic and basal-plane pyrolytic graphite electrodes, glassy carbon electrodes exhibits the most analytically useful signal for the electrochemical oxidation of ammonia. Additionally results obtained using glassy carbon spheres supported on a BPPG electrode were demonstrated for potential scale-up but added confidence that glassy carbon is a near optimal choice as electrode substrate in amperometric electrochemical ammonia sensors where propylene carbonate is utilised as an electrolyte.²⁴

Following this theme, the use of room temperature ionic liquids (RTILs) as useful and new gas sensor designs was proposed by Buzzeo and co-workers.²⁵ Early gas sensor models involved macroelectrodes while later designs incorporate electrodes on the micrometre scale. A gas-permeable membrane is usually employed to separate the sample from electrolyte, and the properties of this layer have significant implications on the rate of transport of analyte to the electrode surface. The original design was proposed by Clark in 1956 comprising a container that houses both the electrodes and electrolyte, with a gas-permeable membrane separating the electrolyte from the gaseous sample (see Fig. 16.2a).^{25,26} This membrane frequently consists of poly(tetrafluoroethylene) (PTFE, Teflon) or polyethylene and typically ranges from 1 to 20 μm in thickness. In this arrangement, the diffusion layer of the electrode completely overlaps the membrane and significant concentration gradients exist in both the membrane and the electrolyte. The second sensor, as shown in Fig. 16.2b, consists of a similar arrangement, but the working electrode is now of micrometre dimensions, resulting in a partial overlap of the diffusion layer with the membrane. The third design, Fig. 16.2c, contains a microelectrode situated inside a thin-layer chamber, with reference and counter electrodes in adjacent compartments and a flow path for delivery of the target gas. The size of

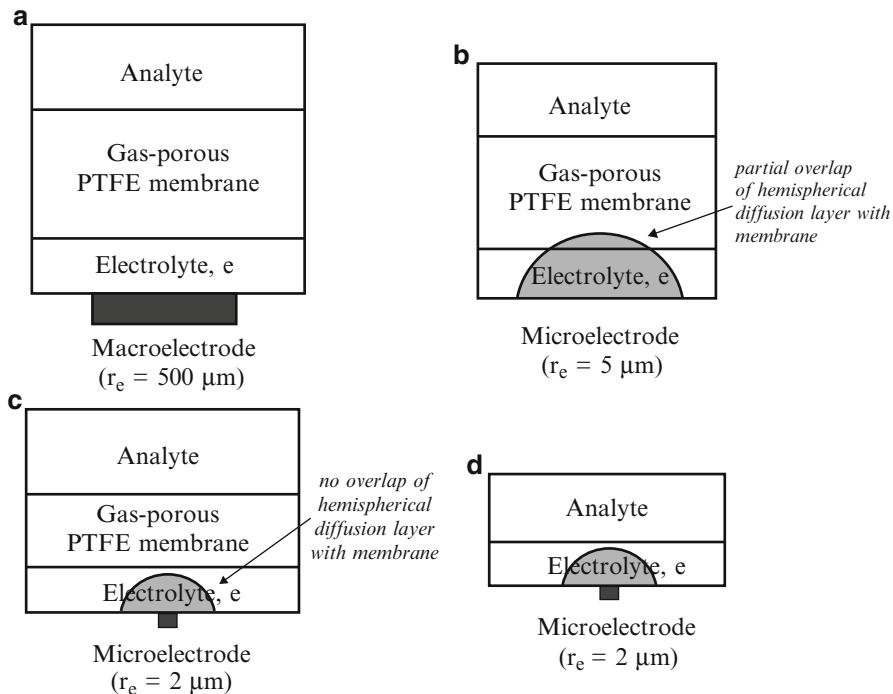


Fig. 16.2 Diagram of the four different types of amperometric gas sensors. Copyright (2004) The American Chemical Society²⁵

the microelectrode employed must be sufficiently small so that its diffusion layer does not encroach on the membrane. As such, the signal observed only reflects the transport of the electroactive species within the thin layer of electrolyte, not the membrane. Buzzeo et al. reported on the use of RTILs as an electrolyte which eliminates the requirement of a membrane which is presented in Fig. 16.2d.²⁵

In this configuration a two-electrode cell design is realised where the surface of a macroelectrode is modified with a thin layer of RTIL which serves as the non-volatile electrolyte excluding the requirement of a membrane. RTILs have been proven to be electrochemically useful since they exhibit wide potential windows, resulting from the robustness of the cations and anions often employed in their composition.²⁷ For example a window in excess of 5 V is not atypical for an ionic liquid,^{28,29} which surpasses that accessible in any aqueous system and is, in many cases, a substantial improvement over that observed in common supporting electrolyte/organic solvent systems, such as acetonitrile (MeCN).^{15,30,31} Additionally RTILs possess low volatility and high thermal stability which render them potentially advantageous media for the detection of gases and thus they are useful for the development of robust gas sensors. Clearly there are advantages to using

RTILs in gas sensing designs and the vast number of RTILs available gives rise to a wide choice for those designing sensors incorporating RTILs.

RTILs have been useful for the sensing of ammonia and the mechanism of the electrochemical oxidation of ammonia has been extensively explored due to the potential benefits of the RTILs.¹⁴ Critically however, Ji et al.¹⁴ have compared propylene carbonate with several RTILs. These were: 1-butyl-3-methylimidazolium tetrafluoroborate ($[\text{C}_4\text{mim}][\text{BF}_4]$), 1-butyl-3-methylimidazolium trifluoromethylsulfonate ($[\text{C}_4\text{mim}][\text{OTf}]$), 1-Ethyl-3-methylimidazolium bis(trifluoromethylsulfonyl)imide ($[\text{C}_2\text{mim}][\text{NTf}_2]$), 1-butyl-3-methylimidazolium bis(tri-fluoromethylsulfonyl)imide ($[\text{C}_4\text{mim}][\text{NTf}_2]$) and 1-butyl-3-methylimidazolium hexafluorophosphate ($[\text{C}_4\text{mim}][\text{PF}_6]$) using a 10 μm diameter Pt microdisc electrode. In four of the RTILs studied, the cyclic voltammetric analysis suggested that ammonia is initially oxidised to nitrogen, N_2 , and protons, which are transferred to an ammonia molecule, forming NH_4^+ via the protonation of the anion(s) (A^-). However, in $[\text{C}_4\text{mim}][\text{PF}_6]$, the protonated anion was formed first, followed by NH_4^+ . In all five RTILs, both HA and NH_4^+ are reduced at the electrode surface, forming hydrogen gas, which is then oxidised.¹⁴ The analytical ability of this work has also been explored further, giving a limit of detection close to 50 ppm in $[\text{C}_2\text{mim}][\text{NTf}_2]$, $[\text{C}_4\text{mim}][\text{OTf}]$, $[\text{C}_4\text{mim}][\text{BF}_4]$, with a sensitivity of ca. $6 \times 10^{-7} \text{ A ppm}^{-1}$ ($R^2 = 0.999$) for all three ionic liquids, showing that the limit of detection was ca. ten times larger than that in propylene carbonate since ammonia in propylene carbonate might be more soluble in comparison with RTILs when considering the higher viscosity of RTILs.¹⁴ Clearly, the factors that need to be considered with RTILs are solubility of the target gas and also the diffusion coefficient of the analyte *within* the sample matrix which are extensively different in RTILs; typically one or two orders of magnitude less than in conventional aprotic solvents due to their higher viscosity; consequently such factors can significantly limit the electroanalytical sensing of ammonia and other key target gases and need to be diligently explored and considered. As we can observe from this section, the direct electrochemical oxidation occurs at high oxidation potentials and is generally not selective towards other species which could be electrochemically oxidised. Hence, researchers have generally turned to reducing the overpotential of the electrochemical oxidation of ammonia through the mediated reaction of ammonia with chlorine³²; it is this we next consider.

In order to reduce the high overpotential typically observed for ammonia detection indirect electrochemical approaches utilising a range of mediators have been reported.^{16,19,33–35} The main tactic is to employ a chemical moiety that chemically reacts, usually instantaneously or fast enough over the experimental timescale with the target analyte, in this case ammonia. Following this there are two scenarios. The first is that the product formed between the chemical reaction of the chemical moiety and ammonia is electrochemically active—as such a new voltammetric peak/signal might be observed but the usefulness of this will depend upon its electrochemical properties. The second is that the loss of chemical moiety might be utilised if again this is electroactive. Last, in a superb situation, *both* may occur. Note that chemical selectivity can be towards the target analyte and reduced

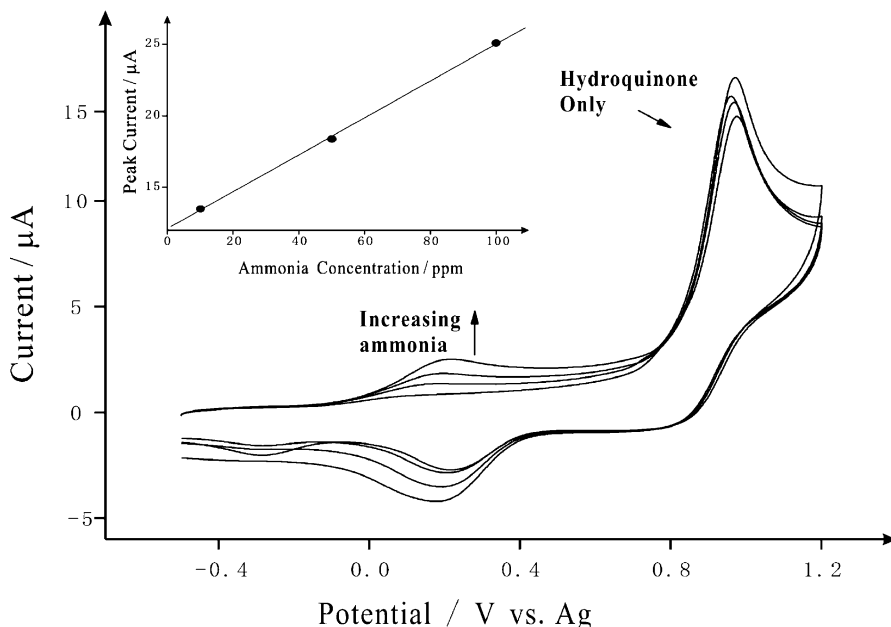


Fig. 16.3 Cyclic voltammetric responses of 0.5 mM hydroquinone to increasing ammonia concentration (10, 59 and 100 ppm) in PC (0.1 M TBAP) at GC. *Insert graph:* A plot of the anodic peak current at +0.15 V against the concentration of ammonia (ppm). Copyright (2007) The American Chemical Society¹⁴

interferents reactivity can be potentially addressed, such as adding electron donating/withdrawing groups for example. Recently the above indirect approach has been utilised using the additional benefits of incorporation of a non-aqueous solution, namely propylene carbonate (see above).^{14,17} In this application the electrochemically active redox system—hydroquinone/benzoquinone in propylene carbonate—has been successfully utilised. Figure 16.3 shows the typically observed voltammetric response where a new peak is observed upon the increasing concentration of ammonia. Scheme 16.1 shows the proposed mechanism. An analytical selectivity of $\sim 1.3 \times 10^{-7} \text{ A ppm}^{-1}$ over the range (0–100 ppm) and a limit of detection of 4.9 ppm is reported to be possible.¹⁴

A different tact for the sensing of ammonia is the use of an electro-catalyst; Table 16.2 overviews the various approaches which utilise metallic (and alloys and oxides thereof) micro- and nano-particles of various shapes and geometries. Platinum is the most commonly explored electro-catalyst for the electrochemical oxidation of ammonia and through its utilisation the slow kinetic rates and large overpotentials of the electrochemical oxidation are overcome. Ideally an effective electro-catalyst should satisfy a number of requirements, such as reasonable cost, high activity, minimum Ohmic loss and long-term stability; which may of course

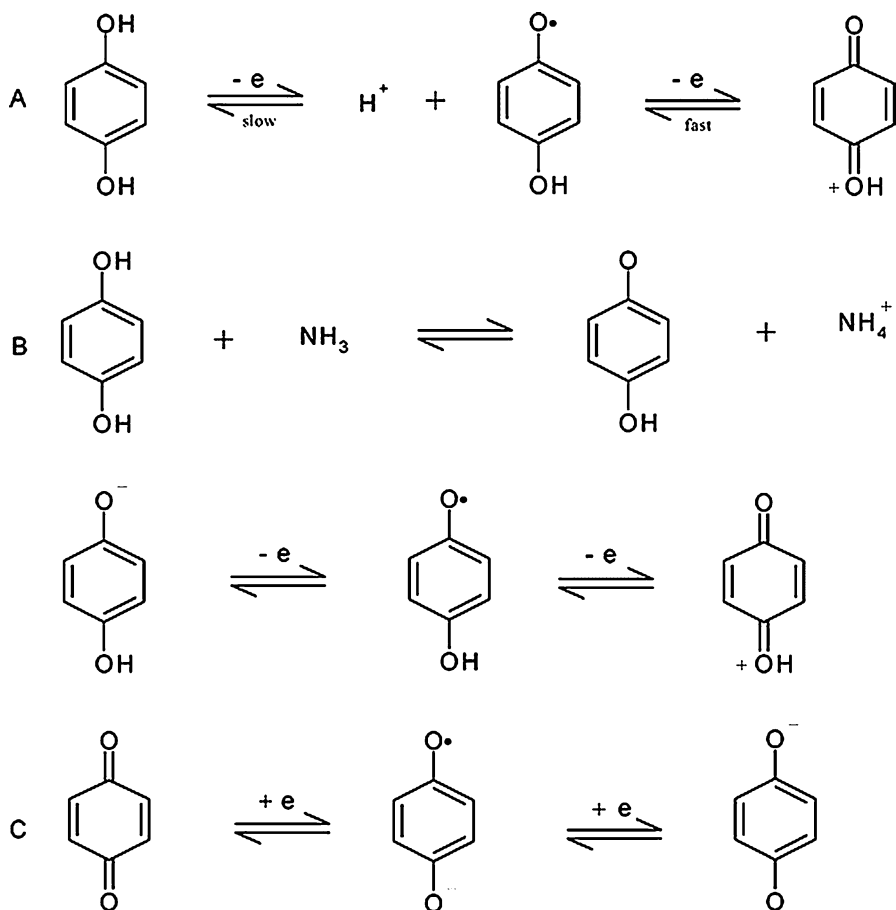
conflict with each other. Platinum is, due to its cost, utilised in alloys but a high loading is still required to achieve appreciable electroanalysis and consequently limits its application. Zhong et al.³⁶ have overviewed the recent efforts reported to reduce the platinum loading in electro-catalysts. These are (1) alloying of platinum with other cheaper metals that have been a potential synergistic effect with platinum for ammonia electro-oxidation (e.g. Ir, Ru and Rh); (2) enhancing the mass activity of the platinum-based electro-catalysts for ammonia electro-oxidation via increasing the electrochemically active sites and/or controlling the surface structure of the electro-catalysts (preferential orientation, shape, morphology, etc.); (3) developing well-performing platinum-free electro-catalysts for ammonia electro-oxidation and; (4) exploring appropriate support strategies which have a positive effect on improving the performance of the electro-catalysts. Zhong and colleagues go further and provide a rigorous overview of the electro-catalysts available for the electroanalytical oxidation of ammonia; the approaches described are (1) pure metal electrocatalysis; (2) platinum-based electro-catalysts that are alloyed by other metals such as Ir, Ru and Rh and; (3) non-platinum electrocatalysts. It has been noted that the performance of the electro-catalysts is dependent not only on the type of the electro-catalysts, but also on the preparation method. Table 16.2 provides an overview of typical electro-catalysts prepared for the electrocatalytic oxidation of ammonia which is taken from and expanded upon the elegant overview provided by Zhong.³⁶

Clearly the majority of the electro-catalysts explored in Table 16.2 lend themselves to fuel cell applications. A key parameter to the success of the electrocatalytic sensing of ammonia involves the design of the catalyst. That is, a surface which gives rise to a large active surface area which also stabilises active intermediates and is of a composition to induce changes in the activation energy. The performance of the electro-catalyst³⁶ is characterised by the mass activity (MA; activity mass⁻¹) which is the current density (at a specific potential) normalised by the mass of the electro-catalyst which is related to the specific electrochemically active area (SSA; area mass⁻¹) and the specific activity (SA; activity area⁻¹) which is the current density normalised by the electrochemically active surface area (ECSA) of the electro-catalyst. As such, the mass activity is the key parameter given by:

$$\text{MA}(\text{activity mass}^{-1}) = \text{SSA}(\text{area mass}^{-1}) \times \text{SA}(\text{activity area}^{-1}) \quad (16.1)$$

Last, the durability that is the long-term performance of the electro-catalyst to resist permanent changes to its morphology is a key concern/parameter; this is clearly more evident in the case of all applications where constant potential cyclability is required which in the case of a sensor, where a one-shot electro-catalyst modified screen-printed sensor might be beneficially utilised, this is obviously less of a constraint.

As previously discussed, platinum and platinum-based materials are still the most effective electro-catalysts for ammonia electro-oxidation. In order to



Scheme 16.1 Mechanisms for the electrochemical processes of Hydroquinone-Benzoquinone and the reaction between Hydroquinone and Ammonia

maximise the platinum utilisation, novel platinum and platinum-based electro-catalysts with improved SSA and/or SA have been developed. Although these electro-catalysts can have both high SSA and SA, they can be simply grouped in two classes, as shown in Fig. 16.4. The first group lies in improving the electrochemically active surface area of the electro-catalysts where MA can be increased (and thus the platinum loading can be lowered) by increasing the SSA of the catalyst. This can be achieved by reducing the particle size so as to increase the surface to volume ratio and thus to increase catalytically active sites per mass. Other studies have reported that particle size is a critical parameter such as in the electrochemical reduction of oxygen and the oxidation of methanol, but the size-dependent catalyst activity for the electrochemical oxidation of ammonia is not well defined³⁶; clearly such an area is ripe for further exploration. From this wealth of electro-catalysts explored fundamentally and in fuel cell applications, some of

Table 16.2 Comparison of typical electro-catalysts for ammonia electro-oxidation prepared by different methodologies. Reproduced from reference (36) with permission from the Royal Society of Chemistry

Electro-catalyst type/substrate or support	Preparation method	Structural characteristics	Noble metal loading (mg cm ⁻²)	Test protocol	Performance	Ref.
Pt–Rh/carbon fibre	Galvanostatic electrodeposition	Continuous Pt–Rh layer on carbon fibres	5.2 mg cm ⁻²	Cyclic voltammetry at 25 °C in 1.03 mM NH ₃ + 0.1 M KOH	Peak current density 15 mA cm ⁻² (scan rate n = 10 mV s ⁻¹)	37
Pt deposited on Rh/RANEY [®] Ni	Galvanostatic electrodeposition	Amorphous, boulder-like Pt deposits	10 mg cm ⁻² Pt + 1 mg cm ⁻² Ru	Cyclic voltammetry at 25 °C in 1 M NH ₃ + 1 M KOH	Peak current density ca. 200 mA cm ⁻² ($\nu = 10$ mV s ⁻¹)	38
Pt or Pt–M alloys/carbon fibre paper (M = Ir, Rh, Ru)	Potentiostatic electrodeposition	Continuous noble metal layer on carbon fibres	20.0 ± 0.1 mg cm ⁻²	Cyclic voltammetry at 25 °C in 5 M KOH	Peak current density ca. 130 mA cm ⁻² ($\nu = 5$ mV s ⁻¹) on pure Pt; ca. 110 mA cm ⁻² ($\nu = 5$ mV s ⁻¹) on Pt–Ir; ca. 90 mA cm ⁻² ($\nu = 5$ mV s ⁻¹) on Pt–Ru	39
Pt, Pt–Ir or Pt–Ru/Pt	Galvanostatic electrodeposition	Film with rough surface for pure Pt and Pt–Ru, while with smoother surface for Pt–Ir	2.5 mg cm ⁻²	Potentiostatic polarisation at 60 °C in 1 M NH ₃ + 5 M KOH	Current density (3 min after potentiostatic step) ca. 70 mA cm ⁻² on Pt–Ir at an overpotential of ca. 0.36 V compared to that of ca. 0.42 V on Pt–Ru and ca. 0.82 V on Pt black	40
Pt–Ir/Au	Potentiostatic electrodeposition	fcc Pt ₇₀ Ir ₃₀ alloy	–	Cyclic voltammetry at room temperature in 2–50 mM NH ₃ + 0.1 M KOH solution	Peak current density increased linearly from ca. 0.12 to ca. 0.25 mA cm ⁻² ($\nu = 10$ mV s ⁻¹) with	41

Pt/Au	–	–	–	Cyclic voltammetry at room temperature in 2–50 mM NH ₃ + 0.1 M KOH solution	increasing NH ₃ concentration from 2 to 10 mM Peak current density increased linearly from ca. 0.04 to ca. 0.20 mA cm ⁻² ($\nu = 10$ mV s ⁻¹) with increasing NH ₃ concentration from 2 to 10 mM	41
Ir/glassy carbon	Potentiostatic electrodeposition	–	–	Cyclic voltammetry at 30 °C in 5–20 mM NH ₃ + 0.4 M NaClO ₄	Peak current density increased linearly from 1.77 to 7.38 mA cm ⁻² ($\nu = 100$ mV s ⁻¹) with increasing NH ₃ concentration from 5 to 20 mM	42
Pt/graphite	Pulsed potentiostatic electrodeposition	Pt layer consisting of aggregates	–	Cyclic voltammetry at room temperature in 0.1 M NH ₃ + 0.2 M NaOH	Peak current density varied from ca. 15 mA to ca. 32 mA ($\nu = 20$ mV s ⁻¹), depending on the deposition potential	43
Pt black	Potentiostatic electrodeposition	Pt film with rough surface	–	Cyclic voltammetry at room temperature in 0.1 M NH ₃ + 1 M KOH	Peak current density 22.5 mA cm ⁻² ($\nu = 5$ mV s ⁻¹)	44
Pt/Ni	Galvanostatic electrodeposition	Submicron-sized Pt particles	1.0–2.0 mg cm ⁻²	Cyclic voltammetry at room temperature in 0.1 M NH ₃ + 1 M KOH	Peak current density increased from 0.4 to 1 mA cm ⁻² ($\nu = 5$ mV s ⁻¹) with increasing Pt loading from 1.0 to 2.0 mg cm ⁻²	45

(continued)

Table 16.2 (continued)

Electro-catalyst type/substrate or support	Preparation method	Structural characteristics	Noble metal loading (mg cm ⁻²)	Test protocol	Performance	Ref.
Pt/ITO	Galvanostatic electrodeposition	Dispersed Pt particles, particle size 700–800 nm	0.12 mg cm ⁻²	Cyclic voltammetry at 25 °C in 0.2 M NH ₃ + 1 M KOH	Peak current density 0.7 mA cm ⁻² ($\nu = 5$ mV s ⁻¹)	46
Pt/ITO	Galvanostatic electrodeposition	3D porous flower-like Pt particles assembled by nanosheets	0.065 mg cm ⁻²	Cyclic voltammetry at 25 °C in 0.1 M NH ₃ + 1 M KOH	Peak current density 3.5 mA cm ⁻² ($\nu = 10$ mV s ⁻¹)	47
Pt/ITO	Cyclic voltammetric electrodeposition	Hierarchical Pt nanoparticles with various morphologies including sheet-, flower-, prickly sphere- and cauliflower-like shapes	0.055–0.095 mg cm ⁻²	Cyclic voltammetry at 25 °C in 0.1 M NH ₃ + 1 M KOH	Peak current density increased from 2.5 to 4.3 mA cm ⁻² ($\nu = 10$ mV s ⁻¹) with the increasing Pt loading from 0.055 to 0.095 mg cm ⁻²	48
Pt/glassy carbon	Galvanostatic electrodeposition	Pt nanoparticles with size of several nm to tens of nm within a short deposition time, or Pt nanosheets at a longer deposition time	0.007–0.055 mg cm ⁻²	Cyclic voltammetry at 25 °C in 0.1 M NH ₃ + 1 M KOH	Peak current density increased from 0.8 to 4.6 mA cm ⁻² ($\nu = 10$ mV s ⁻¹) with increasing Pt loading from 0.007 to 0.055 mg cm ⁻²	49
Pt–Ir/Pt or Au	Potentiostatic electrodeposition	fcc Pt ₇₀ Ir ₃₀ alloy	–	Chronoamperometry at room temperature in 0.075–1.5 mM NH ₃ + 1 M KOH	Current density increased linearly from ca. 1 to 5 mA cm ⁻² (E = 0.65 V vs. RHE) with increasing NH ₃ concentration from 0.075 to 0.9 mM	50
	Mixture of Pt and Ir black powder	Unalloyed Pt–Ir mixture powder	–	Chronoamperometry at room temperature in	Current density increased linearly from ca. 0.02 to 0.12 mA cm ⁻² (E = 0.6 V)	50

Unsupported Pt	Microemulsion method with N ₂ H ₄ as the reducing agent	Pt nanoparticles with size 4.5 ± 0.8 nm	—	0.075–1.5 mM NH ₃ + 1 M KOH	vs. RHE) with increasing NH ₃ concentration from 0.3 to 1.5 mM, Pt: Ir = 75:25	51
Unsupported Pt	Microemulsion method with NaBH ₄ as the reducing agent	Pt nanoparticles with size 4.2 ± 0.7 nm	—	Cyclic voltammetry at room temperature in 0.1 M NH ₃ + 0.2 M NaOH	Peak current density ca. 0.2 mA cm ⁻² (ν = 10 mV s ⁻¹)	51
Unsupported Pt	Reduction of Pt precursor by H ₂ in the presence of sodium polyacrylate	Cubic Pt nanoparticles with dominant (100) face, particle size 10 ± 3 nm	—	Cyclic voltammetry at room temperature in 0.1 M NH ₃ + 0.2 M NaOH	Peak current density ca. 0.3 mA cm ⁻² (ν = 10 mV s ⁻¹)	51
Unsupported Pt _x M _{1-x} (M = Ir, Rh, Pd and Ru, x = 20–80 %)	Microemulsion method with NaBH ₄ as the reducing agent	PtM alloy nanoparticles with size ca. 4 nm	—	Cyclic voltammetry at room temperature in 0.1 M NH ₃ + 0.2 M NaOH	Peak current density ca. 1.3 mA cm ⁻² (ν = 10 mV s ⁻¹)	52
Pt/C	Modified polyol method	Carbon black supported highly dispersed Pt nanoparticles with size 2.5 ± 0.5 nm	20 wt% of metal loading	Cyclic voltammetry at room temperature in 0.5 M NH ₃ + 1 M KOH	Peak current density ca. 6 mA cm ⁻² (ν = 30 mV s ⁻¹)	53

(continued)

Table 16.2 (continued)

Electro-catalyst type/substrate or support	Preparation method	Structural characteristics	Noble metal loading (mg cm ⁻²)	Test protocol	Performance	Ref.
Pt-M/C (M = Pd and Ir)	Modified polyol method	Carbon black supported highly dispersed Pt alloy nanoparticles with size 2.0–4.7 nm	20 wt% of metal loading	Cyclic voltammetry at room temperature in 0.5 M NH ₃ + 1 M KOH	Peak current density ca. 1.5 mA cm ⁻² ($\nu = 30$ mV s ⁻¹) on Pt ₅ Pd ₅ ; ca. 4 mA cm ⁻² ($\nu = 30$ mV s ⁻¹) on Pt ₇ Pd ₃ ; ca. 4 mA cm ⁻² ($\nu = 30$ mV s ⁻¹) on Pt ₇ Ir ₃	53
Pt-SnO _x /C	Modified polyol method	Carbon supported highly dispersed unalloyed Pt ₇ (SnO _x) ₃ nanoparticles with size 3.5 ± 0.5 nm	20 wt% of metal loading	Cyclic voltammetry at room temperature in 0.5 M NH ₃ + 1 M KOH	Peak current density ca. 4 mA cm ⁻² ($\nu = 30$ mV s ⁻¹)	53
Pt-M/glassy carbon (M = Ir, Ru and Ni)	Thermal decomposition	Film with nominal thickness ca. 0.3 μm	–	Cyclic voltammetry at 25 °C in 1 M NH ₃ + 1 M KOH	Peak current density ca. 0.9 mA cm ⁻² ($\nu = 10$ mV s ⁻¹) on pure Pt; ca. 0.5 mA cm ⁻² ($\nu = 10$ mV s ⁻¹) on Pt ₂₀ Ir ₈₀ ; ca. 0.2 mA cm ⁻² ($\nu = 10$ mV s ⁻¹) on Pt ₈₀ Ru ₂₀ ; ca. 0.1 mA cm ⁻² ($\nu = 10$ mV s ⁻¹) on Pt ₈₀ Ni ₂₀	54
				Potentiostatic polarisation at 25 °C in 1 M NH ₃ + 5 M KOH, potential –0.5 V (vs. Ag/AgCl)	Current density (1 min after potentiostatic step) ca. 0.025 mA cm ⁻² on Pt ₂₀ Ir ₈₀ ; ca. 0.01 mA cm ⁻² on Pt ₈₀ Ru ₂₀ , which were higher than that on the pure Pt	54

Pt-Ir/graphite	Thermal decomposition	Supported Pt-Ir alloy on graphite, Ir content 20 or 50 %	6-7 mg cm ⁻²	Test in a fuel cell operation at 100-120 °C with 30 mL min ⁻¹ NH ₃ /O ₂ , electrolyte 54 % KOH	Anode voltage decreased by more than 0.1 V compared to pure Pt up to 200 mA cm ⁻² on 5.5 mg Pt-50 % Ir	55
Unsupported Pt-Ir	Modified Adams procedure	Unsupported Pt-Ir alloy powder, Ir content 21.3 or 51 %	34 mg cm ⁻²	Test in a fuel cell operation at 100-120 °C with 30 mL min ⁻¹ NH ₃ /O ₂ , electrolyte 54 % KOH	Anode voltage decreased by 0.1-0.12 V compared to pure Pt black up to 300 mA cm ⁻²	55
Pt-Pd-Rh/glassy carbon	Coprecipitation method	Pt:Pd:Rh = 4:3:1 (weight ratio)	-	Cyclic voltammetry at room temperature in 0.1 M NH ₃ + 0.5 M H ₂ SO ₄	Peak current density ca. 0.3 mA cm ⁻² (ν = 50 mV s ⁻¹)	55

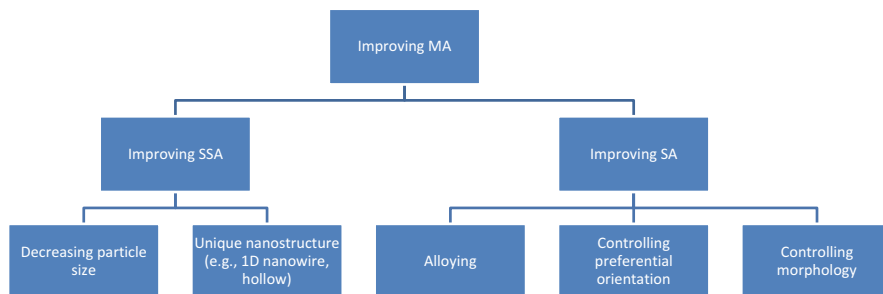


Fig. 16.4 Scheme of the general approaches to improve the mass activity of the electro-catalysts for ammonia electro-oxidation. Adapted from reference (36) with permission from the Royal Society of Chemistry

course will make excellent sensors. Other electro-catalysts of note are ZnO nanopencils have been reported fabricated via a low temperature facile hydrothermal technique.¹⁰ Figure 16.5 shows the unique structure which gives rise to the unique nanopencil name. These unique materials were immobilised onto a supporting glassy carbon electrode and found to exhibit a highly sensitive analytical response with a detection limit of 5 nM and a sensitivity of $\sim 26.58 \mu\text{A cm}^{-2} \text{mM}^{-1}$ with a response time of less than 10 seconds. In comparison of this work against other previously reported modified sensors, as shown in Table 16.1, favourable analytical performances are observed.

Another approach in order to overcome the problematic direct sensing of ammonia via its electrochemical oxidation is through the use of polymeric-based sensors, such as polypyrrole and the more widely explored polyaniline and composites thereof. In such approaches, the target analyte reduces the oxidised form of the conducting polymer polypyrrole where this change can be used as the basis of a sensor due to the changes in conductivity as a function of ammonia concentrations^{56,57} which was extended to operate amperometrically.⁵⁸ Lähdesmäki et al.⁵⁹ reported upon an ammonia sensor comprising a membrane (which is a thin layer of oxidised polypyrrole) upon a platinum substrate for the amperometric measurement of ammonia in aqueous solutions in the potential range of +0.2 to +0.4 V (vs. Ag/AgCl), where contact with ammonia causes a current to flow through the electrode which is proportional to the concentration of free ammonia in the solution. Note that ammonium ions do not contribute to the measured signal.⁵⁹ The analytical signal is due to reduction of polypyrrole by ammonia with subsequent oxidation of polypyrrole by the external voltage source. The sensor is reported to be able to detect ammonia reproducibly at the μM level. The main interference is the doping effect of small anions such as Cl^- and NO_3^- , also giving a response on polypyrrole at the μM level. Apparently this anionic response can, to a certain degree, be reduced by covering the polymer surface with dodecyl sulphate; however this can be a limitation depending on the application. However, the sensor

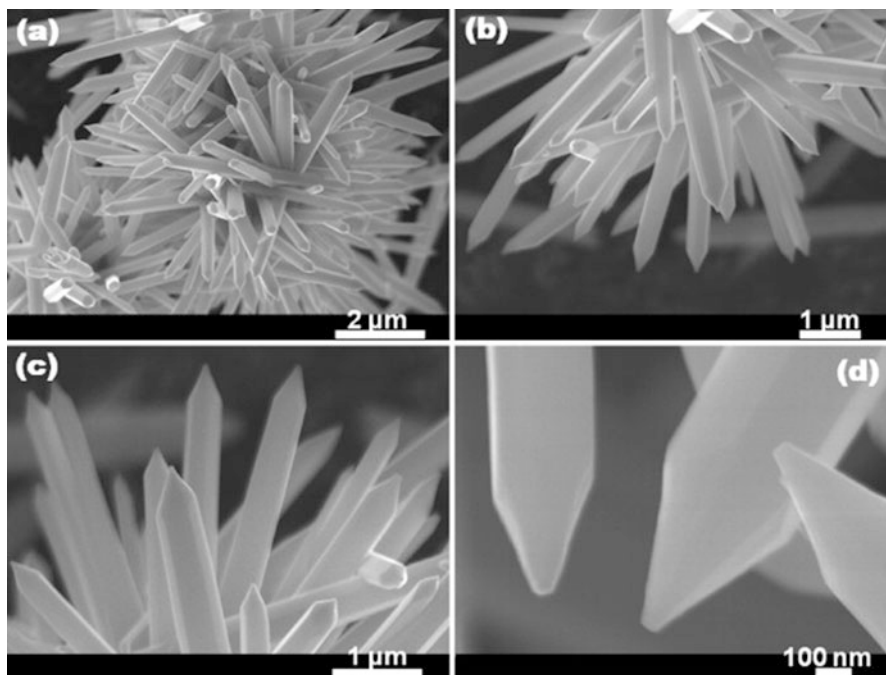


Fig. 16.5 Low magnification (a and b) and high-resolution (c and d) FESEM micrographs of as-synthesised ZnO nanopencils. Reproduced from reference (10) with permission from Elsevier

gradually loses its activity when exposed to ammonia concentrations greater than 1 mM.⁵⁹ Such work has been extended to nanoribbons of polypyrrole (>1 cm in length) where the unique morphology being of one-dimension exhibits a high surface to volume ratio which have reported to enhance responses to surface processes with the overall response producing more sensitive and fast responding sensors; a detection limit in the sub-ppm range using the polypyrrole nanoribbons has been reported.⁶⁰ Massafra⁶¹ reported the synthesis of polypyrrole nanowires via normal pulse voltammetry and a constant potential methodology. The low µM levels of ammonia were reported to be achieved with different analytical characteristics obtained due to the fabrication approach and parameters that were altered; using normal pulse voltammetry a more sensitive response to ammonia was observed over the constant potential method, since the latter approach produced longer and less conductive nanowires; clearly such work is fundamental to producing optimal geometries.

The above two examples demonstrate how the conducting polymer was incorporated into a sensor: the first was immobilised upon an electrode material and the second was a technique which grew them upon gold electrodes. Related to polypyrrole is the conducting polymer polyaniline which is widely studied since its properties can be “tuneable” that is, its structure can be modified to give

favourable changes in performance. However, as identified above for polypyrrole, *how does one exploit such characteristics for use within electrochemical devices?* Polyaniline is insoluble in a range of common solvents, substantially hindering its processability. Note that the monomer, aniline, is a carcinogen which thus potentially has implications when applied into medical diagnostics and additionally it must be distilled prior to use and stored under nitrogen; giving rise to handling problems. Finally, acidic conditions are required for the formation of the most highly conductive form of PANI. Recent breakthroughs in the synthesis and fabrication of conducting polymers with nanodimensional control have managed to overcome the issue of processability. A stable nanodispersion has been reported and can be handled more easily and applied in a similar fashion.⁶² In addition, enhanced properties of conducting polymer materials become apparent at the nanodimension such as higher conductivity and more rapid, discrete, electrochemical switching processes which are useful in electrode devices.⁶³ To date, several techniques have been employed in the fabrication of polymer thin films, such as thermal evaporation, electropolymerization,⁶⁴ spin-coating,⁶⁵ dipping,⁶⁵ electrophoretic patterning⁶¹ and printing.²⁰ Printing is one of the more successful methods for achieving patterning at speed in recent years. Among the printing techniques available, screen printing, micro-contact printing, dip-pen printing, inkjet printing, offset and thermal-line patterning have been used for the deposition of numerous materials including conducting polymers.⁶⁶

As such inkjet printing for the deposition of conducting polymer solutions is a well-developed field which has been used in a range of ammonia sensing applications such as refrigerant wastewater and medical diagnostics in breath.^{64–68}

16.1 Composites

Following on from the use of conducting polymers, researchers have turned to their composites. For example Li et al.⁶⁹ reported a polyaniline/titanium dioxide composite where $\text{Mn}_3\text{O}_4/\text{TiO}_2$ nanotubes were prepared by electrospinning where the Mn_3O_4 results in the polymerisation of the incorporated aniline where the former is consumed to leave simply the PANI/ TiO_2 composite nanotubes. The sensing of ammonia was found to be possible over the range of 25–200 ppb and was determined to exhibit a response improved over that obtained at a pure PANI sensor. Interestingly the ratio of PANI to TiO_2 is critical and can dramatically alter the sensitivity of the PANI/ TiO_2 composite.⁶⁹ Clearly such composites take benefits from the main sensing strategies towards the detection of ammonia; for example, the above example utilises an electro-catalyst (TiO_2) with an already proven sensing strategy of using conducting polymers (PANI). In the same direction Chang et al. reported gold/polyaniline/multi-walled nanotubes.⁷⁰

Figure 16.6 shows the fabrication approach and a TEM image of the final composite. It is thought that the presence of the π - π^* electron interaction, as well as the hydrogen bond interaction between the carboxyl groups of MWNTs and the

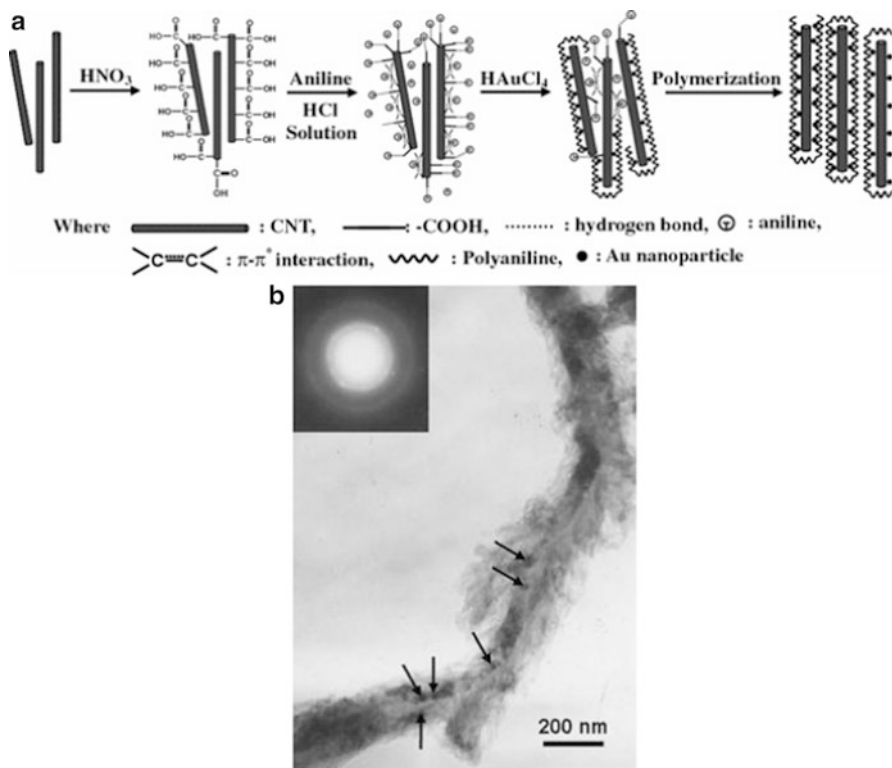
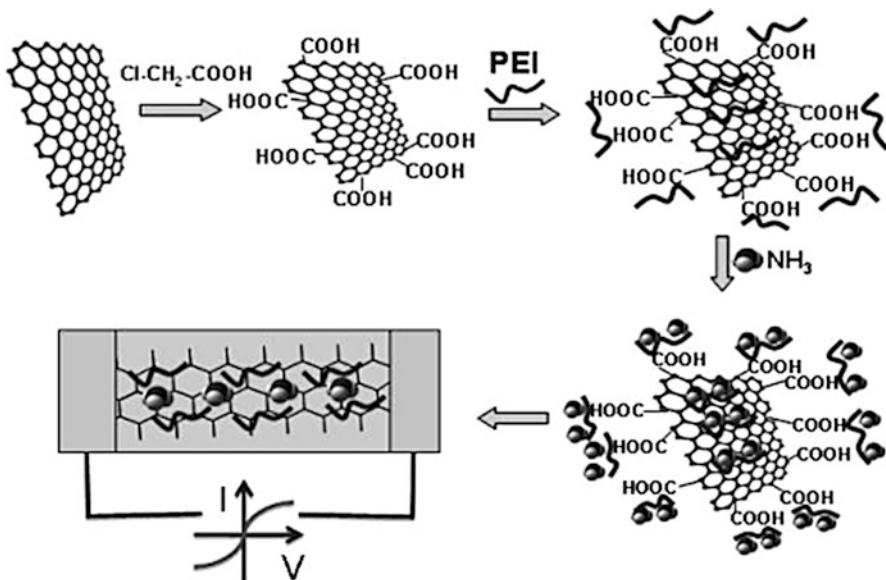


Fig. 16.6 (a) Schematic drawing of the mechanism governing the formation of Au/PANI/MWNT nanocomposites. (b) TEM images of the Au/PANI/MWNT nanocomposites (*inset*: an ED pattern of the nanocomposites). Reproduced from reference (70) with permission from Springer

amino groups of the aniline monomer provide a strong adsorption. The composite was found to provide a wide linear range from 200 ppb to 10 ppm.⁷⁰ Other work has extended to graphene oxide composites⁷¹ with polyethylenimine where it is thought that the composite increases the surface area and provides conducting bridges for electron transfer. The graphene oxide sheet was obtained by chemical conversion of graphite oxide. Then the graphene oxide sheet was used as substrate to synthesise carboxylic acid functionalized graphene (GO-COOH). Branched PEI, which contains a large amount of electron rich amine groups, was covalently linked to GO-COO to form the GO-COOH/PEI composites as is depicted in Scheme 16.2. To evaluate the dependence of the electrocatalytic current on the concentration of NH₃, cyclic voltammograms of the GO-COOH/PEI composites-modified GCE in NaClO₄ solution containing a series of ammonia concentrations have been obtained (Fig. 16.7). The authors went onto show that a limit of detection of 9.5×10^{-7} M was possible with a sensitivity of 2.3×10^{-5} A μM^{-1} which is competitive when compared to alternative configurations such as propylene carbonate solution



Scheme 16.2 Schematic representation of the construction procedure for the PEI functionalized GO-COOH sheets and the electrochemical oxide of ammonia on the surface of the relative electrode. Reproduced from reference (71) with permission from Wiley

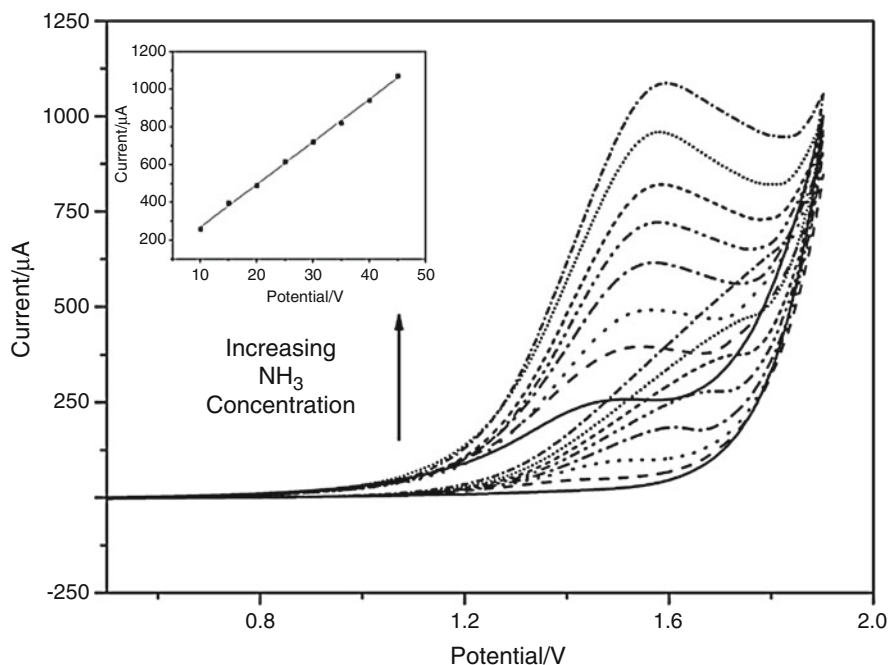


Fig. 16.7 Cyclic voltammograms of GO-COOH/PEI composites modified GCE with different NH₄OH concentrations of 2.7×10^{-5} , 4.0×10^{-5} , 5.3×10^{-5} , 6.7×10^{-5} , 8.0×10^{-5} , 9.3×10^{-5} , 1.1×10^{-4} , 1.2×10^{-4} M (from bottom to up) in the NaClO₄ solution at scan rates 50 mV s^{-1} . The inset shows the linear calibration plot of the catalytic peak current to the NH₄OH concentration. Reproduced from reference (71) with permission from Wiley

containing hydroquinone,¹⁴ multi-walled nanotube/copper nanoparticle paste electrodes,⁷² polyaniline-based sensor⁷³ and Ir/nanotube composites.⁷¹⁻⁷⁴

Of course this theme has been extended to the utilisation of graphene and electro-catalysts such as a graphene-gold composite,⁷⁵ single-walled nanotube-PANI composite,⁷⁶ reduced graphene oxide-PANI composites,⁷⁷ graphene supported on platinum, Ir and platinum-Ir,⁷⁸ lead (IV) oxide-graphite composites⁷⁹ and anthraquinone-carbon composites.³⁵ As such all of these configurations discussed utilise the combined effect of different materials in order to impart significant improvements in sensing. However, composites can be difficult to make reproducibly especially when scaled-up and additionally there is an undeniable cost element to their fabrication; such considerations should not be overlooked.

We now consider the case of organic amines and *N*-oxides (NO_x) which are important analytes to measure in the context of gas sensors. NO_x of course is a generic term for mono-nitrogen oxides NO and NO₂ (nitric oxide and nitrogen dioxide). The quantification of odorous amine compounds is of importance in many areas of human activities such as environmental and industrial monitoring applications but also and as an indicator of food quality or spoilages and in medical diagnostics.^{1,80-87}

In order to electrochemically measure amine-type compounds the first starting point is the direct detection based on a variety of electrode substrates examined such as graphite,⁸⁸ gold,⁸⁹ nickel,^{90,91} boron-doped diamond⁹² and Ag-Pb alloy electrodes⁹³ or on modified electrodes such as polymer and DNA layers.^{94,95} Other approaches involve amperometric biosensors for amines with immobilised amine oxidases or amine dehydrogenases have been reported based on either a direct or a mediated electron-transfer pathway.⁹⁶⁻⁹⁹

Amine vapours are of interest since both aliphatic and aromatic amines can induce toxicological responses with the former found in a multitude of wastewater effluents with volatile organic amines among the important air pollutants which are emitted into the atmosphere from anthropogenic sources such as cattle feedlot operations, waste incineration, sewage treatment and car exhausts to name just a few.¹⁰⁰⁻¹⁰³

Most alkylamines/aliphatic amines are toxic and can irritate the skin, mucous membrane and respiratory tract, through all routes of exposure, i.e. inhalation, ingestion and direct contact make their detection and determination of the compounds an on-going challenging area. Electrochemical approaches are thus favoured as they can provide portable and analytical useful measurements. Aliphatic amines, such as methylamine, ethylamine, *n*-propylamine, iso-propylamine and butylamine, are well known to adsorb onto gold, platinum, silver and mercury electrode surfaces,¹⁰⁴⁻¹⁰⁹ thus generally indirect approaches are favoured but direct have been reported such as methylamine electro-oxidation at gold electrodes,¹¹⁰ the electro-oxidation of methylamine and ethylamine on Pt single crystal electrodes in acid medium.¹¹¹ Other approaches have reported on the use of gold and platinum electrodes with Pulsed Amperometric Detection (PAD) in order to produce surfaces with the requisite oxides and to clean the surfaces fouled by the accumulation of reaction products.¹¹²

Tsuda et al.¹¹³ first reported the anodic oxidations of 17 aliphatic amines have been examined by cyclic voltammetry at a glassy-carbon electrode in aqueous alkaline solution. Until this point, there were not many studies exploring the anodic oxidation of aliphatic amines in aqueous solution and rather studies explored non-aqueous electrochemistry since it was difficult to obtain reproducible oxidation of most aliphatic amines with a platinum electrode which has a limited potential range and due to adsorption (see above). Tsuda elegantly reported that out of the aliphatic amines studied all were irreversibly oxidised where primary amines showed no wave while secondary amines showed one wave and last most tertiary amines exhibited two waves and the peak potentials of their first waves are less positive than those of secondary amines. The peak potentials of the first wave of substituted tertiary amines were observed to shift to more positive values with increasing electronegativity of the substituent, and some amines with a strongly electron-withdrawing group give one wave or no wave. A linear relationship was obtained between pKa values and peak potentials of the first waves for tertiary amines. The postulated reaction mechanism for tertiary amines was reported to involve the loss of two electrons, followed by reaction with water to form a secondary amine and an aldehyde.¹¹³

Lomba and co-workers reported on the electrochemistry of methylamine, propylamine, *n*-butylamine and iso-butylamine at glassy carbon electrode substrates by derivatising the target analytes with phenylisothiocyanate finding that they can be oxidised through two one-electron steps at acidic pH values, presumably involving the intermediacy of proton transfers. The approach was coupled with liquid chromatography with amperometric oxidative detection providing a sensitive method of determination with detection limits in the lower μgL^{-1} range. Other work has focussed generally on specific analytes rather than a total analysis of aliphatic amines. For example, *n*-butylamine has been reported to be possible at a nickel oxide Carbon Nanotube Composite utilising the well-known $\text{Ni}(\text{OH})_2/\text{NiO}(\text{OH})$ redox couple which exists in basic (e.g. from ca. pH 8 upwards) aqueous hydroxide solutions which acts as the electro-catalyst and was found to have no reactivity to ammonia.⁹¹ Note that at bare carbon/carbon nanotube surface no voltammetry was observed justifying the need for the nickel composite. Other authors have also explored redox mediators such as tris(*p*-bromophenyl)amine for the sensing of *n*-butylamine. In other approaches glassy carbon electrodes coated with thin films of Nafion[®] metalized with silver and lead species have been explored towards the oxidation of ethylamine and tert-butylamine.¹¹⁴

More general work by Porter et al.¹¹⁵ report a novel and generic methodology for the modification of glassy carbon electrodes with amine-containing compounds for the development of electro-catalytic and biosensor applications. The method utilises the electro-oxidation of amines to their analogous cation radical forming a chemically stable covalent linkage between the nitrogen atom of the amine and the edge plane sites residing at the glassy carbon surface. A dopamine modified glassy carbon electrode has been fabricated to facilitate the oxidation of NADH via a surface EC mechanism and additionally the ability to create a biotinylated glassy carbon surface capable of binding the protein avidin which is useful for fabricating

anchored enzymes for biosensor applications. Such an approach is reported to dramatically simplify the fabrication of modified electrodes, a process which often involves an extended series of pre-treatment, activation and functionalisation steps. Additionally the extent of immobilisation is reported to be strongly dependent on the degree of substitution at the amine functionality, whereby the electro-oxidation of primary amines yields the largest relative surface coverage and tertiary amines show no detectable surface coverage. Such work is an important fundamental contribution to fabricating electro-catalytic amine sensors and has been extensively extended.^{115,116}

In terms of monitoring amines in food samples, biogenic amines are the class of amine compounds that are relevant and can be used as a monitor of food quality or spoilages.¹¹⁷ Of note, histamine is an important biogenic amines present in a plethora of food products where the former is produced by the bacterial decarboxylation of histidine, the corresponding amino acid, which is present particularly in fish tissues of the Scomberiscida and Scombridae families, e.g. tuna fish, mackerel, sardine, anchovy.¹¹⁸ It is reported that a histamine intake of 70–1,000 mg per single meal can cause the so-called “sgombroide poisoning” that generally reveals itself in a slight form and evolves in a short time but may cause death.¹¹⁸ Consequently histamine is therefore used as an indicator of the good manufacturing practice and of the preservation state of some food, for instance tuna fish in oil.^{118–122}

Note however that histamine is a non-volatile amine and hence recourse is to explore in solution and apply an extraction protocol (such as liquid-liquid extraction) from the sample matrix. Electrochemical approaches have involved the use of boron-doped diamond electrodes which are reported to be superior to GC electrodes due to diamond’s higher sensitivity, stability and reproducibility.¹²³ Diamond is demonstrated to be the best electrode material for the detection of histamine, possessing high sensitivity, even at high oxidation potentials, and for the detection of serotonin, which fouls other electrodes such as GC after oxidation. High stability and remarkable detection limits for the determination of histamine (with serotonin also explored) via amperometry are reported to be possible.¹²³ Table 16.3 provides a thorough overview of the electrochemical approaches for sensing histamine.

Other related work has reported the development of an inexpensive, sensitive and reliable method for histamine at gold disc electrodes via chronopotentiometry which involves an indirect catalytic approach involving electrogenerated chlorine which facilitates charge transfer between histamine and the gold electrode resulting in enhancement of sensitivity. Under optimal experimental conditions, linear response of histamine was observed in the range 2–100 µg/L with achieved limit of detection for 0.27 µg/L of histamine with the protocol applied for histamine determination in fermented sausages.¹²⁹ Other work has reported the determination of histamine in cheese by chronopotentiometry on a thin film mercury electrode.¹³⁰

Other work on the topic of the spoilage of food, particularly fish quality and freshness, the volatile compound trimethylamine (TMA) is used as a marker. In fact, the odour of fish and the relevant chemicals is shown in Fig. 16.8.¹³¹ Traditionally headspace analysis is utilised and as pointed out by Nilsen et al.¹³¹; while such instruments with a high degree of automation are available for the trapping and

Table 16.3 An overview and analysis of the literature using electrochemical approaches for sensing histamine and the report analytical performances and applications; clearly a diverse range exists giving researchers a broad spectrum of configurations to utilise

Electrode	Linear range	Limit of detection	Comments	Reference
Thin film nickel electrode	0.5–110 mg L ⁻¹	0.11 mg L ⁻¹	Offers a short analysis time, appreciable sensitivity and good reproducibility of the results	124
Polycrystalline, boron-doped diamond thin-film electrodes	0.5–100 μM	0.5 μM	Overcome the problems of glassy carbon electrode, which is known to be vulnerable to deactivation and fouling due to strong adsorption of this oxidation product	123
Carbon fibre microelectrode	Δ	1.4 μM	Determination of histamine and 5-hydroxytryptamine in isolated mast cells	125
Methylamine dehydrogenase immobilised in a polypyrrole (PPy) film deposited upon a gold microelectrode	25 μM–4 mM	Δ	Four amino-containing compounds, which are present in blood and other biological samples, were tested for potential interference: glutamine, creatine, creatinine and urea with no interference noted	99
Quinoprotein dehydrogenase enzyme modified carbon electrode	0–200 μM	4.8 μM	The sensor correlates well with elevated histamine levels prevalent in patients with chronic myelogenous leukaemia	126
Gold nanocrystal-modified glassy carbon electrodes	Δ	0.6 μM	Flow injection and high performance liquid chromatography using pulsed amperometric detection. Proof of concept demonstrated through determination of histamine in sardine samples	127
Histamine dehydrogenase modified glassy carbon electrode	20 μM–0.6 mM	100 pM	Noted interfering response caused from ascorbate was fully removed by using continuous flow column electrolytic method. Proof of concept demonstrated through determination of histamine in fish samples	128

Δ = Information not provided

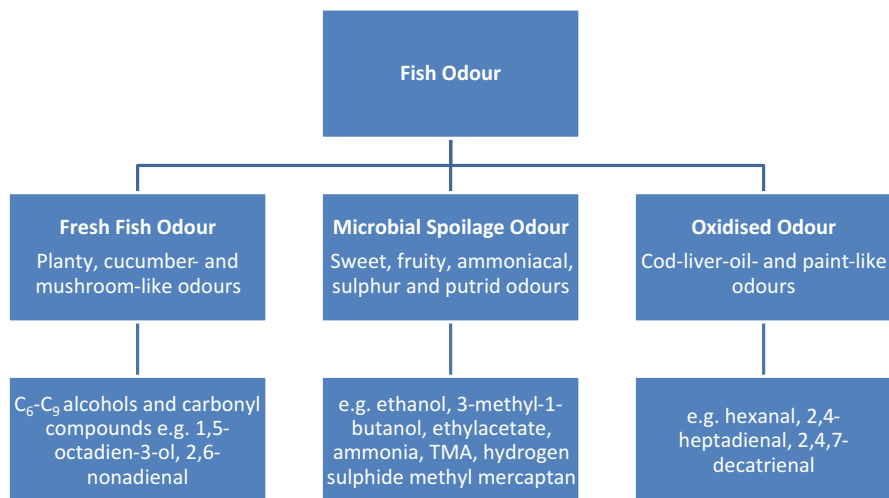


Fig. 16.8 Categorisation of fish odours and the volatile compounds that contribute to the characteristic odour of fresh, spoiled and oxidised fish. TMA, trimethylamine. Adapted from reference (133) with permission from Elsevier

chromatography steps, the complexity, cost and lengthiness of the volatile analysis protocols make them suitable only for specialised research and analytical laboratories. Note that the quality evaluation of raw material for fish meal production is based on a chemical measurement of total volatile bases (TVB) rather than single compounds which form during spoilage of fish and as such, the fish meal industry classifies the raw material according to TVB values. The rapid assessment of volatile compounds is required and gas sensors¹³² and electrochemical-based sensors fit this accordingly. For example, Jonsson and co-workers¹³³ utilised a range of commercially available electrochemical gas sensors: CO, H₂S, NO, NO₂ and SO₂ (Dräger) CO, SO₂ and NH₃ (City Technology, Portsmouth, Britain) and designed a sensing chamber which effectively measures the analysing direct headspace of the fish Capelin caught in Iceland. Their work concluded that the responses of the three sensors (CO, NH₃ and SO₂) were found to increase with capelin headspace at different stages of spoilage, and it is suggested to use only these three selective gas sensors to simplify the data handling. The responses of the CO and NH₃ sensors correlated well with the classical TVB measurements (TVB as mg of N/100 g of whole fish) which were measured with a Struer automatic distillation unit. Such work elegantly highlights that the development of electrochemical gas sensors can be advantageously utilised in real life applications.¹³³

In a different approach, three enzyme-based amperometric biosensors for biogenic amines were applied for meat spoilage monitoring.¹³⁴ The enzyme diamine oxidase (EC 1.4.3.6) was used to monitor the total biogenic amine content (cadaverine, histamine, tyramine, tryptamine, phenylethylamine and spermidine) while Monoamine oxidase A (EC 1.4.3.4) was used for determination of tyramine,

tryptamine and phenylethylamine content. Putrescine was selectively detected with putrescine oxidase (EC 1.4.3.10). The enzymes were separately co-immobilised on graphite electrodes with peroxidase and an Osmium mediator and applied in the analysis of pork and fish samples with the results found to correlate with the total biogenic amine content measured by HPLC. In other work electrochemical biosensors have arisen such as the use of trimethylamine dehydrogenase in an enzyme linked amperometric electrode with TMA determined in different fish samples with a detection limit of 2 mg TMA per 100 g wet fish muscle.¹³⁵

Related to food spoilage and food monitoring, Matysik and co-workers proposed a method for the efficient extraction and determination of volatile aliphatic amines by means of single-drop microextraction (SDME) in combination with microchip electrophoresis and contactless conductivity detection. The method consists of an optimised protocol for extraction via ultrasound assisted headspace SDME and the separation and determination of the target analytes methylamine, dimethylamine, trimethylamine, diethylamine and triethylamine with a novel microfluidic device. Limits of detection were reported to be well below 400 ng/mL and successfully applied into the sensing of the target analytes in shrimp and fish to provide a methodology for monitoring decay of these food products. The proposed method by Matysik et al. is simple, quick, presents low levels of waste, works with small sample quantities and is suitable for quantification of aliphatic amines in seafood samples like shrimp or fish from where they are naturally developing upon biodegradation. In the present study the accelerated decay of shrimp tissue due to improper storage was monitored.¹³⁶

Thus in summary, electrochemical approaches are ripe for sensing amines and due to the possibility of miniaturisation and the low detection limits that are possible, such approaches are better than the typical mammalian sense of smell for example, in the case of fish spoilage/decomposition, before the fish would begin to smell rancid.

We last consider the electrochemical sensing of (NO)_x compounds. The detection of nitric oxide (NO) is an active area of research in fields as diverse as high temperature combustion through to clinical analysis.¹³⁷ NO plays a vital role in the normal vascular biology and pathophysiology and is a neuronal signalling molecule in the central and peripheral nervous system that is synthesised by mammalian cells and acts as a physiological messenger and cytotoxic agent.^{138,139} It is very unstable with a half-life of 2–30 s and rapidly reacts with molecular oxygen to form NO_x.¹⁴⁰ Therefore, sensitive and accurate methods for the determination of NO_x are required.

There are many sensing strategies for detection of NO, including optical spectroscopy, mass spectrometry, chemiluminescence and electrochemistry.^{141–144} Each approach of course has its advantages and disadvantages, depending on the intended application. In a clinical setting, chemiluminescence analysers perform very well, but would not be optimised at all for monitoring NO for mobile diesel vehicle exhaust for example. Also, the extent to which the sensing devices can be miniaturised varies, with electrochemical sensors enjoying a clear advantage;

Table 16.4 provides a thorough overview of the reported electrochemical-based sensors for this target analyte.

Recently a thorough overview of NO sensing using electrochemical sensor arrays has been provided by Griveau and Bedioui¹⁶⁰ along with a thorough general overview offered by the same authors.¹⁶¹ Sensors based on detection of NO via its reduction generally suffer from interference from dioxygen, so detection by electro-oxidation is preferred. However, electro-oxidation of NO at conventional electrode materials (carbon, gold, platinum) necessitates high overpotential oxidation of NO typically occurs at 0.9–1 V (vs. SCE). This high oxidation potential is critical to achieve selective measurement of NO by inducing its electro-oxidation. Indeed, several biological compounds are oxidizable (nitrite, ascorbic acid, hydrogen peroxide, etc.) at potentials lower than or equal to the oxidation potential of NO. So, making an amperometric measurement at this potential will produce a faradic current corresponding to the sum of oxidation currents of all the species oxidizable at potentials ≤ 0.9 V, leading to limited selectivity for NO. This problem of low selectivity can be partly resolved by modification or functionalisation of the electrode surface. Two main strategies have been developed: (1) use of permselective membranes and/or (2) use of electro-catalysts. Table 16.4 provides a thorough overview of sensing NO_x.

As we have discussed above in terms of ammonia where ionic liquids were able to provide membrane-less gas sensors, this has been extended by Toniolo et al. for the monitoring NO₂ and NO. At room temperature, excellent repeatable (± 3.9 %) was observed and linearly dependent current signals were recorded, reporting a detection limit of 0.96 ppb v/v while at higher temperatures (100 °C) a lower detection limit of 0.55 ppb v/v could be instead estimated.¹⁶²

Other work has reported Yttria-stabilised zirconia (YSZ)-based amperometric NO₂ sensors comprised of an In₂O₃ sensing electrode (SE), a Pt counter electrode (CE) and a Mn₂O₃ reference electrode (RE) in both tubular and rod geometries were fabricated and their sensing characteristics were examined. Furthermore, both sensors (tubular or rod geometry) exhibited a linear response to increasing NO₂ concentration in the range of 20–200 ppm at 550 °C.^{163,164}

A different approach has reported on the incorporation of hemin on a ZnO–PPy nanocomposite modified Pt electrode; Fig. 16.9 shows the steps required to produce the sensor.

It was reported that the hemin–ZnO–PPy–Pt electrode exhibited threefold enhanced electro-catalytic activity towards NO_x compared to the hemin–PPy–Pt electrode. The electrocatalytic response of the sensor was proportional to the NO_x concentration in the range of 0.8–2,000 μM ($r^2 = 0.9974$) with a sensitivity of 0.04 $\mu\text{A } \mu\text{M}^{-1} \text{ cm}^{-2}$ and detection limit of 0.8 μM for the hemin–ZnO–PPy–Pt electrode.¹⁶⁶

Other work has reported on a biomimetic microsensor for measuring nitric oxide (NO) in the brain in vivo consisting of hemin and functionalized multi-wall carbon nanotubes covalently attached to chitosan via the carbodiimide crosslinker EDC followed by chitosan electrodeposition on the surface of carbon fibre microelectrodes.¹⁶⁷ An impressive analytical performance was reported with a sensitivity of

Table 16.4 An overview of key literature reports for different electrode configurations employed for the determination of NO_x

Electrode	Linear range	Limit of detection	Comments	Reference
Hb/gold nanoparticles/graphene-modified basal plane graphite electrode	0.72–7.92 μM	12 nM		145
Glassy carbon modified with (PMePy ₂ FeHPA)/Nafion	7–25 μM	0.25 μM		146
Glassy carbon modified with CuPtBr ₆	50 nM–100 μM	20 nM		147,148
Glassy carbon modified with CoTPPCL in Nafion	5–150 nM	1.2 nM		149
Pyrolytic graphite modified with Hb in phosphatidylcholine	0.1–300 μM	0.1 μM		150
Platinum disc modified with Ni(ABED)/Nafion	10 nM–1 μM	5 nM		151
Hemoglobin entrapped in a dimethyldidodecylammonium bromide film modified glassy carbon electrode	0.8–68 μM	0.063 μM		152
Pt/NiTSPc	2–40 μM	Δ	Six electrode array utilised	153
Pt/Nafion	0.03–5 μM	10 nM	Potential interference from nitrite, ascorbic acid, uric acid, dopamine, norepinephrine, epinephrine, 5-hydroxytryptamine, 3,4-dihydroxyindole-3-acetic acid, 3,4-dihydroxyphenylacetic acid explored	154
C/WPI membrane electrode	0–0.4 μM	0.3 nM		155
C/NiTSPc/hydrogel electrode	0.1–10 μM	0.01 μM		155
Multi-walled carbon nanotube/Nafion modified glassy carbon electrode	0.2–150 μM	80 nM	Due to the Nafion layer, interference effects of NO ₂ ⁻ and some biological substances are virtually eliminated	156

<i>o</i> -phenylenediamine and Nafion to modified carbon fibre electrodes	0–6 μM	35 nM	Potentially time-consuming and laborious preparation with the optimal modification of this electrode found to require the application of three coats of Nafion at 200 °C, followed by electropolymerization of <i>o</i> -phenylenediamine for 15 min	157
Pt/Ir alloy coated with a three-layered membrane	Δ	0.2 nM–1 μM	Nitric oxide-selective electrode was found to be applicable to real-time nitric oxide assay in biological systems	158
Manganese tetrakis(1-methyl-4-pyridyl)porphyrin (MnTMPyP) in ZnO-polypyrrole (PPy) nanocomposite on Pt electrode	0.8 μM	0.8–2,000 μM	The electrode exhibited stability over a period of 1 month	159

Δ = Information not provided

PMePy = poly(*N*-methylpyrrole)

FeHPA = iron substituted Keggin-type heteropolyanion

CoTPPC = tetraphenylporphyrin cobalt(III) chloride

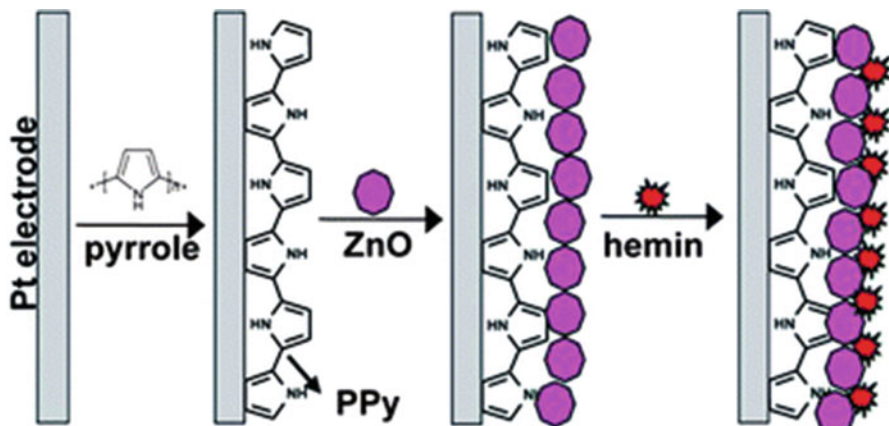


Fig. 16.9 The steps involved in producing a hemin modified ZnO–PPy nanocomposite supported upon a platinum electrode. Reproduced from reference (165) with permission from the Royal Society of Chemistry

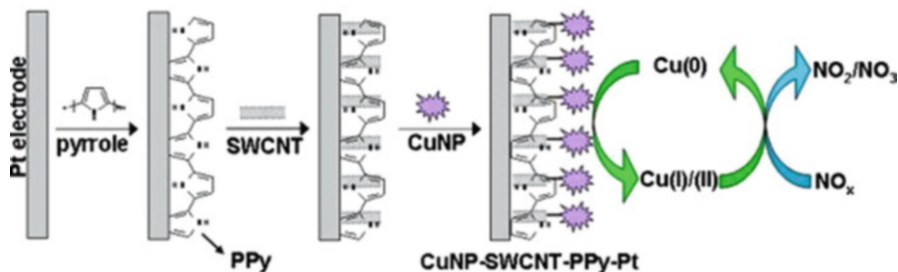


Fig. 16.10 Schematic stepwise preparation of the CuNP-SWCNT-PPy-Pt electrode and illustration of the reaction processes occurring at the surface of the sensor during the determination of NO_x . Reproduced from reference (165) with permission from Elsevier

1.72 $\text{nA}/\mu\text{M}$ and the limit of detection was 25 nM. The microsensor was successfully applied to the measurement of exogenously applied NO in the rat brain *in vivo*.¹⁶⁷

Prakash et al. who pioneered the studies utilising hemin modified sensors¹⁶⁵ have also reported on the use of nanomaterials, namely copper nanoparticle modified SWCNTs-polypyrrole (PPy) nanocomposite modified Pt electrode; Fig. 16.10 shows a schematic of how the electrode is produced. The sensor utilises the electrocatalytic activity of the copper nanoparticle electrode towards NO_x which is fourfold times more than the just CuNP-PPy-Pt electrode. A linear dependence towards NO_x concentrations ranging from 0.7 to 2,000 μM , with a sensitivity of $0.22 \pm 0.002 \mu\text{A} \mu\text{M}^{-1} \text{cm}^{-2}$ and detection limit of 0.7 μM , was reported.¹⁶⁵

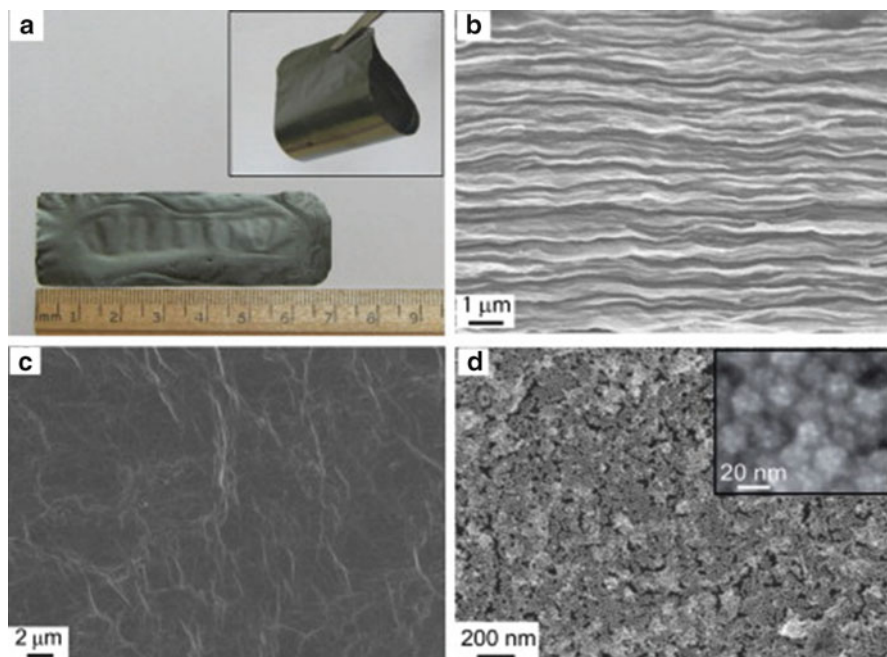


Fig. 16.11 Schematic illustration (*top image*) of the fabrication of the freestanding hybrid electrode from 2D-assembly of Au@Pt nanoparticles and graphene paper. Also shown (*bottom image*, Panel **a**) is an optical photograph of rGO paper. Cross-sectional (**b**) and top (**c**) view of rGO paper. (**d**) SEM image of Au@Pt-rGO paper. Reproduced from reference (168) with permission from Elsevier

In a similar vein of using nanomaterials, graphene has also been used as a support material in the form of a flexible graphene paper loaded with Au@Pt core-shell nanoparticles; the fabrication approach is shown in Fig. 16.11 where the hybrid electrode was fabricated through a modular approach in which the nanoparticle assembly was transferred onto graphene paper through dip-coating.¹⁶⁸

A high electro-catalytic activity is reported for the detection of nitric oxide with a high sensitivity, wide linear range and low detection limit. The graphene composite was used in the real-time monitoring of nitric oxide secretion by human endothelial vein cells grown on the electrode. Such results demonstrate a modular approach for designing high-performance flexible electrodes with tailored surface properties. Other work using graphene modified electrodes can also be found within the literature^{169,170} which will likely continue to be an extensively explored area given the reported beneficial properties of graphene within electrochemical sensors.

Other work to impart improvements in the electrochemical response towards NO detection includes platinisation with platinum black (Pt-black) with a limit of detection using a Pt-black/Nafion-coated glassy carbon electrode reported to be as low as 9 nM. These electrodes were embedded in a polystyrene substrate, with the applicability of these sensitive and selective electrodes being demonstrated by

monitoring the adenosine triphosphate-mediated release of NO from endothelial cells immobilised in a microfluidic network.¹⁷¹

In summary we have overviewed the recent approaches to the electrochemical sensing of ammonia, amines and NO_x and strategies employed in order to give rise to improvements in sensitivities and limits of detection. Clearly there are unique benefits to using electrochemical-based sensors with different strategies needed for different sensing applications; due to the wide range of applications where ammonia and related amine and NO_x compounds need to be monitored, and over the wide analytical range needed, there is still a need to develop new electrochemically based sensors.

References

1. Timmer B, Olthuis W, van den Berg A (2005) Ammonia sensors and their applications - a review. *Sensor Actuat B Chem* 107:666–677
2. Hibbard T, Killard A (2011) Breath ammonia analysis: clinical application and measurement. *Crit Rev Anal Chem* 41:21–35
3. Hibbard T, Crowley K, Killard AJ (2013) Direct measurement of ammonia in simulated human breath using an inkjet-printed polyaniline nanoparticle sensor. *Anal Chim Acta* 779:56–63
4. Davies S, Spanel P (1997) Quantitative analysis of ammonia on the breath of patients in end-stage renal failure. *Kidney Int* 52:223–228
5. Ruzsanyi V (2005) Detection of human metabolites using multi-capillary columns coupled to ion mobility spectrometers. *J Chromatogr A* 1084:145–151
6. Westblom U, Alden M (1990) Laser-induced fluorescence detection of NH₃ in flames with the use of two-photon excitation. *Appl Spectr* 44:881–886
7. Manne J (2006) Pulsed quantum cascade laser-based cavity ring-down spectroscopy for ammonia detection in breath. *Appl Optics* 45:9230–9237
8. Ishida H (2008) The breath ammonia measurement of the hemodialysis with a QCM-NH₃ sensor. *Bio Med Mater Eng* 18:99–106
9. Lopez ME, Rechnitz GA (1982) Selectivity of the potentiometric ammonia gas sensing electrode. *Anal Chem* 54:2085–2089
10. Dar GN, Umar A, Zaidi SA, Baskoutas S, Hwang SW, Abaker M, Al-Hajry A, Al-Sayari SA (2012) Ultra-high sensitive ammonia chemical sensor based on ZnO nanopencils. *Talanta* 89:155–161
11. Khan SB, Rahman MM, Jang ES, Akhtar K, Han H (2011) Special susceptible aqueous ammonia chemi-sensor: extended applications of novel UV-curable polyurethane-clay nanohybrid. *Talanta* 84:1005–1010
12. Jamal A, Rahman MM, Faisal M, Khan SB (2011) Studies on photocatalytic degradation of acridine orange and chloroform sensing using As-grown antimony oxide microstructures. *Mater Sci Appl* 2:676–683
13. Rahman MM, Jamal A, Faisal M (2011) CuO codoped ZnO based nanostructured materials for sensitive chemical sensor applications. *App Mater Interf* 3:1346–1353
14. Ji X, Banks CE, Silvester DS, Aldous L, Hardacre C, Compton RG (2007) Electrochemical ammonia gas sensing in nonaqueous systems: a comparison of propylene carbonate with room temperature ionic liquids. *Electroanalysis* 19:2194–2201
15. Buzzeo MC, Hardacre C, Compton RG (2006) Extended electrochemical windows made accessible by room temperature ionic liquid/organic solvent electrolyte systems. *Chem Phys Chem* 7:176–180

16. Panchompoo J, Compton RG (2012) Electrochemical detection of ammonia in aqueous solutions using fluorescamine: a comparison of fluorometric versus voltammetric analysis. *J Electrochem* 18:437–449
17. Ji X, Compton RG (2007) Determination of ammonia based on the electrochemical oxidation of N, N'-diphenyl-1,4-phenylenediamine in propylene carbonate. *Anal Sci* 23:1317–1320
18. Ji X, Banks CE, Silvester DS, Wain AJ, Compton RG (2007) Electrode kinetic studies of the hydroquinone-benzoquinone system and the reaction between hydroquinone and ammonia in propylene carbonate: application to the indirect electroanalytical sensing of ammonia. *J Phys Chem C* 111:1496–1504
19. Li C, Zhu S, Ding Y, Song Q (2012) Electrochemiluminescence of iridium complexes with ammonia in dimethylformamide and its analytical application for ammonia detection. *J Electroanal Chem* 682:136–140
20. Crowley K, Morrin A, Hernandez A, O'Malley E, Whitten PG, Wallace GG, Smyth MR, Killard AJ (2008) Fabrication of an ammonia gas sensors using inkjet-printed polyaniline nanoparticles. *Talanta* 77:710–717
21. Ji X, Banks CE, Compton RG (2005) The electrochemical oxidation of ammonia at boron-doped diamond electrodes exhibits analytically useful signals in aqueous solutions. *Analyst* 130:1345–1347
22. Michels NL, Kapalka A, Abd-El-Latif AA, Baltruschat H, Comninellis C (2010) Enhanced ammonia oxidation on BDD induced by inhibition of oxygen evolution reaction. *Electrochem Commun* 12:1199–1202
23. Hege KV, Verhaege M, Verstraete W (2004) Electro-oxidative abatement of low-salinity reverse osmosis membrane concentrates. *Water Res* 38:1550–1558
24. Ji X, Banks CE, Compton RG (2006) The direct electrochemical oxidation of ammonia in propylene carbonate: a generic approach to amperometric gas sensors. *Electroanalysis* 18:449–455
25. Buzzeo MC, Hardacre C, Compton RG (2004) Use of room temperature ionic liquids in gas sensor design. *Anal Chem* 76:4583–4588
26. Clark LC (1956) Monitor and control of blood and tissue O₂ tensions. *Trans Am Soc Artif Intern Organ* 2:41–48
27. Hultgren VM, Mariotti AWM, Bond AM, Wedd AG (2002) 2002, Reference potential calibration and voltammetry at macrodisk electrodes of metallocene derivatives in the ionic liquid [bmim][PF₆]. *Anal Chem* 74:3151–3154
28. Wasserschild P, Welton T (2003) *Ionic liquids in synthesis*. Wiley-VCH, Weinheim
29. Compton DL, Laszlo JA (2002) Direct electrochemical reduction of hemin in imidazolium-based ionic liquids. *J Electroanal Chem* 520:71–78
30. Kosmulski M, Osteryoung RA, Ciszlowska M (2000) Diffusion coefficients of ferrocene in composite materials containing ambient temperature ionic liquids. *J Electrochem Soc* 147:1454–1458
31. Evans RG, Klymenko OV, Wadhawan JD, Hardacre C (2003) Oxidation of N, N, N', N'-tetraalkyl-para-phenylenediamines in a series of room temperature ionic liquids incorporating the bis(trifluoromethylsulfonyl)imide anion. *J Electroanal Chem* 556:179–188
32. Kapalka A, Joss L, Anglada A, Comninellis C, Udert KM (2010) Direct and mediated electrochemical oxidation of ammonia on boron-doped diamond electrode. *Electrochem Commun* 12:1714–1717
33. Ji X, Buzzeo MC, Banks CE, Compton RG (2006) Electrochemical response of cobalt (II) in the presence of ammonia. *Electroanalysis* 18:44–52
34. Sizun T, Bouvet M, Suisse J-M (2012) Humidity effect on ammonia sensing properties of substituted and unsubstituted cobalt phthalocyanines. *Talanta* 97:318–324
35. Ramakrishnappa T, Pandurangappa M, Nagaraju DH (2011) Anthraquinone functionalized carbon composite electrode: application to ammonia sensing. *Sensor Actuat B* 155:626–631
36. Zhong C, Hu WB, Cheng YF (2013) Recent advances in electrocatalysts for electro-oxidation of ammonia. *J Mater Chem A* 1:3216–3238

37. Bonnin EP, Biddinger EJ, Botte GG (2008) Effect of catalyst on electrolysis of ammonia effluents. *J Power Sources* 182:284–290
38. Cooper M, Botte GG (2006) Hydrogen production from the electro-oxidation of ammonia catalyzed by platinum and rhodium on rane nickel substrate. *J Electrochem Soc* 153: A1894–A1901
39. Boggs BK, Botte GG (2010) Optimization of Pt-Ir on carbon fiber paper for the electro-oxidation of ammonia in alkaline media. *Electrochim Acta* 55:5287–5293
40. Vitse F, Cooper M, Botte GG (2005) On the use of ammonia electrolysis for hydrogen production. *J Power Sources* 142:18–26
41. Moran E, Cattaneo C, Mishima H, Mishima BAL, Silvette SP, Rodriguez JL, Pastor E (2008) Ammonia oxidation on electrodeposited Pt–Ir alloys. *J Solid State Electrochem* 12:583–589
42. Han YP, Luo P, Cai CX, Xie L, Lu TH (2008) Electrochemical oxidation of ammonia on Ir anode in potential fixed electrochemical sensor. *Chem Res Chin Univ* 24:782–785
43. Vot SL, Reyter D, Roue L, Belanger D (2012) Electrochemical oxidation of NH₃ on platinum electrodeposited onto graphite electrode physical and analytical electrochemistry. *J Electrochem Soc* 159:F91–F96
44. Zhou L, Cheng YF, Amrein M (2008) Fabrication by electrolytic deposition of platinum black electrocatalyst for oxidation of ammonia in alkaline solution. *J Power Sources* 177:50–55
45. Yao K, Cheng YF (2007) Electrodeposited Ni–Pt binary alloys as electrocatalysts for oxidation of ammonia. *J Power Sources* 173:96–101
46. Deng XH, Wu YT, He MF, Dan CY, Chen YJ, Deng YD, Jiang DH, Zhong C (2011) Electrochemical deposition of Pt particles on indium tin oxide electrode and their electrocatalytic applications in ammonia oxidation. *Acta Chim Sin* 69:1041–1046
47. Liu J, Zhong C, Yang Y, Wu YT, Jiang AK, Deng D, Zhang Z, Hu WB (2012) Electrochemical preparation and characterization of Pt particles on ITO substrate: morphological effect on ammonia oxidation. *Int J Hydr Energy* 37:8981–8987
48. Liu J, Hu WB, Zhong C, Cheng Y (2013) Surfactant-free electrochemical synthesis of hierarchical platinum particle electrocatalysts for oxidation of ammonia. *J Power Sources* 223:165–174
49. Zhong C, Hu WB, Cheng YF (2011) On the essential role of current density in electrocatalytic activity of the electrodeposited platinum for oxidation of ammonia. *J Power Sources* 196:8064–8072
50. Lopez de Ishima BA, Lescano D, Holgado TM, Mishima HT (1998) Electrochemical oxidation of ammonia in alkaline solutions: its application to an amperometric sensor. *Electrochim Acta* 43:395–404
51. Vidal-Iglesias FJ, Solla-Gullon J, Rodriguez O, Herrero E, Montiel V, Feliu JM, Aldaz A (2004) Shape-dependent electrocatalysis: ammonia oxidation on platinum nanoparticles with preferential (1 0 0) surfaces. *Electrochem Commun* 6:1080–1084
52. Vidal-Iglesias FJ, Solla-Gullon J, Montiel V, Feliu JM, Aldaz A (2007) Screening of electrocatalysts for direct ammonia fuel cell: ammonia oxidation on PtMe (Me: Ir, Rh, Pd, Ru) and preferentially oriented Pt (1 0 0) nanoparticles. *J Power Sources* 171:448–456
53. Lomosco TL, Baranova EA (2011) Electrochemical oxidation of ammonia on carbon-supported bi-metallic PtM (M=Ir, Pd, SnOx) nanoparticles. *Electrochim Acta* 56:8551–8558
54. Endo K, Nakamura K, Katayama Y, Miura T (2004) Pt–Me (Me = Ir, Ru, Ni) binary alloys as an ammonia oxidation anode. *Electrochim Acta* 49:2503–2509
55. McKee DW, Scarpellino AJ Jr, Danzig IF, Pak MS (1969) Improved electrocatalysts for ammonia fuel cell anodes. *J Electrochem Soc* 116:562–568
56. Kanazawa KK, Diaz AF, Geiss RH, Gill WD, Kwak JF, Logan JA, Rabolt JF, Street GB (1979) Organic metals-polypyrrole, a stable synthetic metallic polymer. *J Chem Soc Chem Commun* 19:854–855

57. Josowicz M, Janata J (1986) Suspended gate field effect transistors modified with polypyrrole as alcohol sensor. *Anal Chem* 58:514–517
58. Trojanowicz M, Matuszewski W, Szczepanczyk B, Lewenstam A (1993) In: Guibault GG, Mascini M (eds) *Uses of immobilized biological compounds*. Kluwer, Dordrecht
59. Lahdesmaki I, Lewenstam A, Ivaska A (1996) A polypyrrole-based amperometric ammonia sensor. *Talanta* 43:125–134
60. Chartuprayoon N, Hangarter CM, Rheem Y, Jung H, Myung NV (2010) Wafer-scale fabrication of single polypyrrole nanoribbon-based ammonia sensor. *J Phys Chem C* 114:11103–11108
61. Massafera MP, de Torressi SIC (2012) Evaluating the performance of polypyrrole nanowires on the electrochemical sensing of ammonia. *J Electroanal Chem* 669:90–94
62. Li G, Martinez C, Semancik S (2005) Controlled electrophoretic patterning of polyaniline from a colloidal suspension. *J Am Chem Soc* 127:4903–4909
63. Innis PC, Wallace GG (2002) Inherently conducting polymer nanostructures. *J Nanosci Nanotechnol* 2:441–451
64. Crowley K, O'Malley E, Morrin A, Smyth MR, Killard AJ (2008) An aqueous ammonia sensor based on an inkjet-printed nanoparticle-modified electrode. *Analyst* 133:391–399
65. Crowley KH, Morrin A, Smyth MR, Killard AJ, Shepherd R (2008) Fabrication of chemical sensors using inkjet printing and application to gas detection. *UEEE Sensors Conference Proceedings, Lecce, Italy*
66. Morrin A, Ngamna O, O'Malley E, Kent N, Moulton SE, Wallace GG, Smyth MR, Killard AJ (2008) The fabrication and characterisation of inkjet-printed polyaniline nanoparticle films. *Electrochim Acta* 53:5092–5099
67. Subramanian R, Crowley K, Morrin A, Killard AJ (2013) A sensor probe for the continuous in situ monitoring of ammonia leakage in secondary refrigerant systems. *Anal Meth* 5:134–140
68. Aguilar AD, Forzani ES, Nagahara LA, Amlani I, Tsui R, Tao NJ (2008) A breath ammonia sensor based on conducting polymer nanojunctions. *IEEE Sensors J* 8:269–273
69. Li Y, Gong J, He G, Deng Y (2011) Fabrication of polyaniline/titanium dioxide composite nanofibers for gas sensing application. *Mater Chem Phys* 129:477–482
70. Chang Q, Zhao K, Chen X, Li M, Liu J (2008) Preparation of gold/polyaniline/multiwall carbon nanotube nanocomposites and application in ammonia gas detection. *J Mater Sci* 43:5861–5866
71. Song M, Xu J (2013) Preparation of polyethylenimine-functionalized graphene oxide composite and its application in electrochemical ammonia sensors. *Electroanalysis* 25:523–530
72. Valentini F, Biagiotti V, Lete C, Palleschi G, Wang J (2007) The electrochemical detection of ammonia in drinking water based on multi-walled carbon nanotube/copper nanoparticle composite paste electrodes. *Sens Actuators B* 128:326–333
73. Jin Z, Su Y, Duan Y (2001) Development of a polyaniline-based optical ammonia sensor. *Sensor Actuat B* 72:75–79
74. Kong QM, Jiang YZ, Chen C, Zhou YM, Lu TH, Chen Y, Tang YW (2010) Preparation of Ir/CNTs catalyst and its electrocatalytic performance for ammonia oxidation. *Chem J Chin Univ* 31:2260–2263
75. Song M, Xu J (2013) Electrochemical oxidation of ammonia on graphene-gold composites. *ECS Solid State Lett* 2:M24–M27
76. Zhang T, Nix MB, Yoo B-Y, Deshusses MA, Myung NV (2006) Electrochemically functionalized single-walled carbon nanotube gas sensor. *Electroanalysis* 18:1153–1158
77. Huang X, Hu N, Gao R, Yu Y, Wang Y, Yang Z, Kong ES-W, Wei H, Zhang Y (2012) Reduced graphene oxide-polyaniline hybrid: preparation, characterization and its applications for ammonia gas sensing. *J Mater Chem* 22:22488–22495
78. Cunci L, Rao CV, Velez C, Ishikawa Y, Cabrera CR (2013) Graphene-supported Pt, Ir and Pt-Ir nanoparticles as electrocatalysts for the oxidation of ammonia. *Electrocatalysis* 4:61–69

79. Sljukic B, Banks CE, Crossley A, Compton RG (2007) Lead (IV) oxide-graphite composite electrodes: application to sensing of ammonia, nitrite phenols. *Anal Chim Acta* 587:240–246
80. Bjorkqvist M, Salonen J, Tuura J, Jalkanen T, Lehto V-P (2009) Detecting amine vapours with thermally carbonized porous silicon gas sensor. *Phys Status Solidi C* 6:1769–1772
81. Pacquitt A, Lau KT, McLaughlin H, Frisby J, Quilty B, Diamond D (2006) Development of a volatile amine sensor for the monitoring of fish spoilage. *Talanta* 69:515–520
82. Olafsdottir G, Nesvadba P, Natale CD, Careche M, Oehlenschlager J, Tryggvadottir SV, Schubring R, Kroeger M, Heia K, Esaiassen M, Macagnano A, Jorgensen BM (2004) Multisensor for fish quality determination. *Trends Food Sci Technol* 5:86–93
83. Belitz HD, Grosch W (1987) Food chemistry. Springer, Berlin
84. Landete JM, de las Rivas B, Marcobal A, Munoz R (2007) Molecular methods for the detection of biogenic amine-producing bacteria on foods. *Int J Food Microbiol* 117:258–269
85. Chen S, Mahadevan V, Zieve L (1970) Volatile fatty acids in the breath of patients with cirrhosis of the liver. *J Lab Clin Med* 75:622–627
86. Preti G, Labows JN, Kostelc JG, Aldinger S, Daniele R (1988) Analysis of lung air from patients with bronchogenic carcinoma and controls using gas chromatography-mass spectrometry. *J Chromatogr Biomed Appl* 432:1–11
87. Simenhoff ML, Burker JF, Saukkonen JJ, Ordinario AT, Doty RN (1977) Biochemical profile or uremic breath. *N Engl J Med* 297:132–135
88. Surmann P, Peter B (1996) Carbon electrodes in amine analysis: effect of chemically modified carbon surfaces on signal quality and reproducibility. *Electroanalysis* 8:685–691
89. Jackson WA, Lacourse WR, Dobberpuhl DA, Johnson DC (1991) The voltammetric response of ethanolamine at gold electrodes in alkaline media. *Electroanalysis* 3:607–616
90. Casella IG, Rosa S, Deimoni E (1998) Electrooxidation of aliphatic amines and their amperometric detection in flow injection and liquid chromatography at a nickel-based glassy carbon electrode. *Electroanalysis* 10:1005–1009
91. Panchompoo J, Aldous L, Xiao L, Compton RG (2010) Electroanalytical detection of n-butylamine at a nickel/carbon nanotube composite. *Electroanalysis* 22:912–917
92. Koppang MD, Witek M, Blau J, Swain GM (1999) Electrochemical oxidation of polyamines at diamond thin-film electrodes. *Anal Chem* 71:1188–1195
93. Ge JS, Johnson DC (1995) Electrocatalysis of anodic oxygen-transfer reactions: oxidation of ammonia at anodized Ag-Pb eutectic alloy electrodes. *J Electrochem Soc* 142:3420–3423
94. Wang J, Rivas G, Luo DB, Cai XH, Valerra FS, Dontha N (1996) DNA-modified electrode for the detection of aromatic amines. *Anal Chem* 68:4365–4369
95. Collyer SD, Butler AJ, Higson SPJ (1997) The electrochemical determination of N-nitrosamines at polymer modified electrodes via an adsorptive stripping voltammetric regime. *Electroanalysis* 9:985–989
96. Niculescu M, Nistor C, Pec IF, Mattiasson B, Csoregi E (2000) Redox hydrogel-based amperometric bienzyme electrodes for fish freshness monitoring. *Anal Chem* 72:1591–1597
97. Niculescu M, Ruzgas T, Nistor C, Frebort I, Sebelas M, Pec IF, Csoregi E (2000) Electrooxidation mechanism of biogenic amines at amine oxidase modified graphite electrode. *Anal Chem* 72:5988–5993
98. Tsugawa W, Ogawa K, Ishimura F, Sode K (2001) Fructosyl amine sensing based on Prussian blue modified enzyme electrode. *Electrochemistry* 69:973–975
99. Zeng K, Tachikawa H, Zhu ZY, Davidson VL (2000) Amperometric detection of histamine with a methylamine dehydrogenase polypyrrole-based sensor. *Anal Chem* 72:2211–2215
100. Mnahan SE (1990) Environmental chemistry, 4th edn. Chelsea, Lewis, p 442
101. Finlayson-Pitts BJ, Pitts JN (1986) Atmospheric chemistry. Wiley, New York, NY, p 561
102. Fuselli S, Cerquiglini S, Chiacchierini E (1978) Air pollution by methylamines, Sampling and gas chromatographic determination. *Chim Ind* 60:711–714
103. Cadle SH, Mulava PA (1980) Low-molecular-weight aliphatic amines in exhaust from catalyst-equipped cars. *Environ Sci Technol* 14:718–723
104. Luczak T (2005) A comparative study of adsorption of aliphatic amines at a gold electrode. *Collect Czech Chem Commun* 70:2027–2037

105. Horanyi G, Rizmayer EM (1989) Radiotracer study of the adsorption of butylamine at a platinumized platinum-electrode. *J Electroanal Chem* 264:273–279
106. Dyatkina SL, Rott GM, Damaskin BB (1977) Joint adsorption of thiourea and butyl alcohol or butylamine on mercury-electrode surface. *Sov Electrochem* 13:807
107. Hampson NA, Lee JB, Morley JR, Scanlon B (1970) Adsorption of normal-butylamine at polycrystalline silver electrodes in aqueous solutions. *J Electroanal Chem* 24:229–230
108. Luczak T (2006) Adsorption of methylamine at a polycrystalline gold/solution interface. *Colloids Surf A* 280:125–129
109. Luczak T (2006) The effect of gold oxide on electrooxidation of aliphatic amines. *Collect Czech Chem Commun* 71:1371–1382
110. Luczak T (2007) Activity of gold towards methylamine electrooxidation. *J Appl Electrochem* 37:461–466
111. Huerta F, Morallon E, Perez JM (1999) Oxidation of methylamine and ethylamine on Pt single crystal electrodes in acid medium. *J Electroanal Chem* 469:159–169
112. Johnson DC, LaCourse WR (1990) Anal Chem Liquid chromatography with pulsed electrochemical detection at gold and platinum electrodes. *Anal Chem* 62:589A–597A
113. Masui M, Sayo H, Tsuda Y (1968) Anodic oxidation of amines. Part I. Cyclic voltammetry of aliphatic amines at a stationary glassy-carbon electrode. *J Chem Soc B* 1968:973–976
114. Casella IG (2001) An electrochemical and XPS study of Ag–Pb binary alloys incorporated in nafion® coatings. *J Appl Electrochem* 31:481–488
115. Deinhammer SR, Ho M, Anderegg JW, Porter MD (1994) Electrochemical oxidation of amine-containing compounds: a route to the surface modification of glassy carbon electrodes. *Langmuir* 10:1306–1313
116. Kado Y, Atobe M, Nonaka T (2000) Ultrasonic effects on electroorganic processes. XVIII. A limiting current study on indirect electrooxidation of n-butylamine with a triarylamine redox mediator. *Electrochemistry* 68:262
117. Kivirand K, Rincken T (2011) Biosensors for biogenic amine: the present state of art mini-review. *Anal Lett* 44:2821–2833
118. Frattini V, Lionetti C (1988) Histamine and histidine determination in tuna fish samples using high-performance liquid chromatography: derivatization with o-phthalaldehyde and fluorescence detection or UV detection of “free” species. *J Chromatogr A* 809:241–245
119. Cinquina AL, Longo F, Cali A, Santis LD, Baccelliere R, Cozzani R (2004) Validation and comparison of analytical methods for the determination of histamine in tuna fish samples. *J Chromatogr A* 1032:79–85
120. Tahmouzi S, Khaksar R, Ghasemlou M (2011) Development and validation of an HPLC-FLD method for rapid determination of histamine in skipjack tuna fish (*Katsuwonus pelamis*). *Food Chem* 126:756–761
121. Hwang D-F, Chang S-H, Shiua C-Y, Chai T-J (1997) *J Chromatogr B* 693:23–30
122. Patange SB, Mukundan MK, Kumar KA (2005) A simple and rapid method for colorimetric determination of histamine in fish flesh. *Food Control* 16:465–472
123. Sarada BV, Rao TN, Tryk DA, Fujishima A (2000) Electrochemical oxidation of histamine and serotonin at highly boron-doped diamond electrodes. *Anal Chem* 72:1632–1638
124. Svarc-Gajic J, Stojanovic Z (2010) Electrocatalytic determination of histamine on a nickel-film glassy carbon electrode. *Electroanalysis* 22:2931–2939
125. Pihel K, Hsieh S, Jorgenson JW, Wightman RM (1995) Electrochemical detection of histamine and 5-hydroxytryptamine at isolated mast cells. *Anal Chem* 67:4514–4521
126. Loughran MG, Hall JM, Turner APF (1995) Amperometric detection of histamine at a quinoprotein dehydrogenase enzyme electrode. *Biosens Bioelectron* 10:569–576
127. Carralero V, Gonzalez-Cortes A, Yanez-Sedeno P, Pingarron JM (2005) Pulsed amperometric detection of histamine at glassy carbon electrodes modified with gold nanoparticles. *Electroanalysis* 17:289–297
128. Takagi K, Shikata S (2004) Flow injection determination of histamine with a histamine dehydrogenase-based electrode. *Anal Chim Acta* 505:189–193

129. Stojanovic ZS, Svarc-Gajic JV (2011) A simple and rapid method for histamine determination in fermented sausages by mediated chronopotentiometry. *Food Control* 22:2013–2019
130. Svarc-Gajic JV, Stojanovic ZS (2011) Determination of histamine in cheese by chronopotentiometry on a thin film mercury electrode. *Food Chem* 124:1172–1176
131. Martinsdottir OO, Oehlenschlager J, Dalgaard P, Jensen B, Undeland I, Mackie IM, Henehan G, Nielsen J, Nilsen H (1997) Methods to evaluate fish freshness in research and industry. *Trends Food Sci Technol* 8:258–265
132. Mielle P (1996) “Electronic noses”: towards the objective instrumental characterization of food aroma. *Trends Food Sci Technol* 7:432–438
133. Olafsdottir G, Martinsdottir E, Jonsson EH (1997) Rapid gas sensor measurements to determine spoilage of capelin (*mallothus villosus*). *J Agric Food Chem* 45:2654–2659
134. Boka B, Adanyi N, Virag D, Sebela M, Kiss A (2012) Spoilage detection with biogenic amine biosensors, comparison of different enzyme electrodes. *Electroanalysis* 24:181–186
135. Loechel C, Basram A, Basram J, Scrutton NS, Hall EAH (2003) Using trimethylamine dehydrogenase in an enzyme linked amperometric electrode Part 1. Wild-type enzyme redox mediation. *Analyst* 128:166–172
136. Mark JJP, Kumar A, Demattio H, Hoffmann W, Malik A, Matysik FM (2011) Combination of headspace single-drop microextraction, microchip electrophoresis and contactless conductivity detection for the determination of aliphatic amines in the biodegradation process of seafood samples. *Electroanalysis* 23:161–168
137. Kharitonov SA, Barnes PJ (2001) Exhaled markers of pulmonary disease. *Am J Respir Crit Care Med* 163:1693–1722
138. Koshland DE (1992) The molecule of the year. *Science* 258:1861
139. Lei JP, Ju HX, Ikeda O (2004) Catalytic oxidation of nitric oxide and nitrite mediated by water-soluble high-valent iron porphyrins at an ITO electrode. *J Electroanal Chem* 567:331–338
140. Ignarro LJ, Fukuto JM, Griscavage JM, Rogers NE, Byrns RE (1993) Oxidation of nitric oxide in aqueous solution to nitrite but not nitrate: comparison with enzymatically formed nitric oxide from L-arginine. *Proc Natl Acad Sci* 90:8103–8107
141. Fontijn A, Sabadell AJ, Ronco RJ (1970) Homogeneous chemiluminescent measurement of nitric oxide with ozone. Implications for continuous selective monitoring of gaseous air pollutants. *Anal Chem* 42:575–579
142. Kipping PJ, Jeffery PG (1963) Detection of nitric oxide by gas-chromatography. *Nature* 200:1314
143. Malinski T, Mesáros S, Tomboulían P (1996) Nitric oxide measurement using electrochemical methods. *Methods Enzymol* 268:58–69
144. Kosterev AA, Malinovsky AL, Tittel FK, Gmachl C, Capasso F, Sivo DL, Baillargeon JN, Hutchinson AL, Cho AY (2001) Cavity ringdown spectroscopic detection of nitric oxide with a continuous-wave quantum-cascade laser. *Appl Opt* 40:5522–5529
145. Xu M-Q, Wu J-F, Zhao G-C (2013) Direct electrochemistry of hemoglobin at a graphene gold nanoparticle composite film for nitric oxide biosensing. *Sensors* 13:7492–7504
146. Trevin S, Bedoui F, Gomez Villegas MG, Bied-Charreton VC (1997) Electropolymerized nickel macrocyclic complex-based films: design and electrocatalytic application. *J Mater Chem* 7:923–928
147. Pei J, Li X-Y (2000) Preparation, characterization, and application of electrodes modified with electropolymerized one-dimensional Magnus’ green salts: Pt(NH₃)₄ • PtCl₄ and Pt(NH₃)₄ • PtCl₆. *J Solid State Electrochem* 4:131–140
148. Pei J, Li XY, Buffle J (2000) Preparation, characterization and application of an electrode modified with electropolymerized CuPtBr₆ film. *Electrochim Acta* 45:1581–1593
149. Kashevski AV, Safronov AY, Ikeda O (2001) Behaviors of H₂TPP and CoTPPCL in Nafion® film and the catalytic activity for nitric oxide oxidation. *J Electroanal Chem* 510:86–95
150. Fan C, Pang J, Shen P, Li G, Zhu D (2002) Nitric oxide biosensors based on Hb/phosphatidylcholine films. *Anal Sci* 18:129–132
151. Tu H, Mao L, Cao X, Jin L (1999) A novel electrochemical microsensor for nitric oxide based on electropolymerized film of o-aminobenzaldehyde-ethylene-diamine nickel. *Electroanalysis* 11:70–74

152. Wu H, Fan S, Zhu W, Dai Z, Zou X (2013) Investigation of electrocatalytic pathway for hemoglobin toward nitric oxide by electrochemical approach based on protein controllable unfolding and in-situ reaction. *Biosens Bioelectron* 41:589–594
153. Pereira-Rodrigues N, Albin V, Koudelka-Hep M, Auger V, Pailleret A, Bedioui F (2002) Nickel tetrasulfonated phthalocyanine based platinum microelectrode array for nitric oxide oxidation. *Electrochem Commun* 4:922–927
154. Xian Y, Liu M, Cai Q, Li H, Lu J, Jin L (2001) Preparation of microporous aluminium anodic oxide film modified Pt nano array electrode and application in direct measurement of nitric oxide release from myocardial cells. *Analyst* 126:871–876
155. Wartelle C, Schuhmann W, Blockl A, Bedioui F (2005) Integrated compact biocompatible hydrogel-based amperometric sensing device for easy screening of drugs involved in nitric oxide production by adherent cultured cells. *Electrochim Acta* 50:4988–4994
156. Wu F-H, Zhao G-C, Wei X-W (2002) Electrocatalytic oxidation of nitric oxide at multi-walled carbon nanotubes modified electrode. *Electrochem Commun* 4:690–694
157. Friedemann MN, Robinson SW, Gerhardt GA (1996) o-Phenylenediamine-modified carbon fiber electrodes for the detection of nitric oxide. *Anal Chem* 68:2621–2628
158. Ichimori K, Ishida H, Fukahori M, Nakazawa H, Murakami E (1994) Practical nitric oxide measurement employing a nitric oxide-selective electrode. *Rev Sci Instrum* 65:2714–2718
159. Prakash S, Rajesh S, Singh SK, Bhargava K, Llavazhagan G, Vasu V, Karunakaran C (2011) Electrochemical incorporation of manganese(III) tetrakis(1-methyl-4-pyridyl)porphyrin in ZnO-polyppyrole nanocomposite on Pt electrode as NO_x sensor. *Sens Lett* 9:1623–1628
160. Griveau S, Bedioui F (2013) Overview of significant examples of electrochemical sensor arrays designed for detection of nitric oxide and relevant species in a biological environment. *Anal Bioanal Chem* 405:3475–3488
161. Bedioui F, Griveau S (2013) Electrochemical detection of nitric oxide: assessment of twenty years of strategies. *Electroanalysis* 25:587–600
162. Toniolo R, Dossi N, Pizzariello A (2012) A membrane free amperometric gas sensor based on room temperature ionic liquids for the selective monitoring of NO_x. *Electroanalysis* 24:865–871
163. Werchmeister RML (2012) Electrochemical testing of composite electrodes of (La_{1-x}Sr_x)₂MnO₃ and doped ceria in NO-containing atmosphere. *J Solid State Electrochem* 16:703–714
164. Jeun JH, Kin DH, Hong SE (2012) Synthesis of porous SnO₂ foams on SiO₂/Si substrate by electrochemical deposition and their gas sensing properties. *Sensor Actuat B* 161:784–790
165. Prakash S, Rajesh S, Singh SK, Bhargava K, Llavazhagan G, Vasu V, Karunakaran C (2011) Copper nanoparticles entrapped in SWCNT-PPy nanocomposite on Pt electrode as NO_x electrochemical sensor. *Talanta* 85:964–969
166. Prakash S, Rajesh S, Singh SR (2012) Electrochemical incorporation of hemin in a ZnO-PPy nanocomposite on a Pt electrode as NO_x sensor. *Analyst* 137:5874–5880
167. Santos RM, Rodrigues MS, Laranjinha J (2013) Biomimetic sensor based on hemin/carbon nanotubes/chitosan modified microelectrode for nitric oxide measurement in the brain. *Biosens Bioelectron* 44:152–159
168. Zan X, Fang Z, Wu J, Xiao F, Huo F, Duan H (2013) Freestanding graphene paper decorated with 2D-assembly of Au@Pt nanoparticles as flexible biosensors to monitor live cell secretion of nitric oxide. *Biosens Bioelectron* 49:71–78
169. Shao Y, Wang J, Wu H, Liu J, Aksay IA, Lin Y (2010) Graphene based electrochemical sensors and biosensors: a review. *Electroanalysis* 22:1027–1036
170. Pumera M, Ambrosi A, Bonanni A, Chng ELK, Poh HL (2010) Graphene for electrochemical sensing and biosensing. *TrAC Trends Anal Chem* 29:954–965
171. Selimovic A, Martin SR (2013) Encapsulated electrodes for microchip devices: microarrays and platinumized electrodes for signal enhancement. *Electrophoresis* 34:2092–2100

Chapter 17

Carbon Oxides

Nobuhito Imanaka and Shinji Tamura

17.1 Carbon Dioxide

In the late twentieth century, the generation of oxide gases such as CO₂, NO_x, and SO₂ through human activities became recognized as an extremely serious environmental problem. In 1997, at COP3, carbon dioxide (CO₂) was also identified as a major greenhouse effect gas and the goal of reducing CO₂ emissions was declared an international priority. The development of smart gas-sensing tools is an important step in effectively suppressing CO₂ emissions into the atmosphere. Up to now, however, although many different CO₂ sensors have been extensively studied, most have not been commercialized, with the exception of devices incorporating IR detection. Even these are expensive and bulky and require pretreatment of the sample gas, and so are difficult to install at the various sites where CO₂ gas may be emitted. As a result, it is necessary to develop a compact CO₂ gas sensor which can readily be positioned for on-site monitoring.

To allow commercial applications of sensors at various potential emission sites, the construction of these sensors from solid materials is desirable, so as to minimize the size of the sensors and simplify the manufacturing process. To date, a number of small CO₂ gas sensors have been developed, and these may be categorized by their sensing mechanism, whether based on optical cells, resistance/capacitance of semiconductors, or electromotive force (EMF)/current measurements based on solid electrolytes. However, such sensors continue to exhibit deficits, including low selectivity, poor chemical and physical stability, or high cost, and these problems must be mitigated to improve their usefulness.

N. Imanaka (✉) • S. Tamura

Division of Applied Chemistry, Graduate School of Engineering, Osaka University,
2-1 Yamadaoka, Suita, Osaka 565-0871, Japan
e-mail: imanaka@chem.eng.osaka-u.ac.jp

In this section, we discuss compact CO₂ sensors applying the detection methods noted above. These devices, following future modifications, are anticipated to represent the next generation of practical CO₂-sensing tools.

17.1.1 Solid Electrolyte Sensors

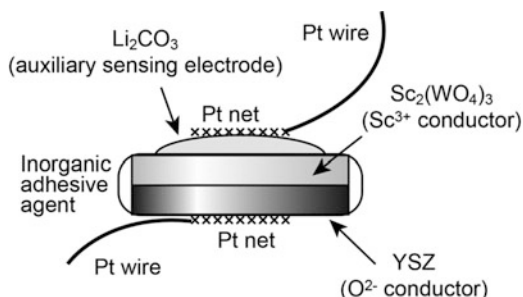
A solid electrolyte is a functional material in which single ions migrate through a solid structure, and these materials are expected to be applied as components of compact gas sensors. There are two sensing mechanisms which may be exploited in solid electrolyte sensors: potentiometric and amperometric. Potentiometric sensors may be further divided into equilibrium and non-equilibrium potential (mixed potential) types, although typically only the equilibrium potential type has been investigated for use in CO₂ sensors.

The equilibrium potential sensors are further classified into three categories based on their specific construction, as summarized in Table 17.1. Although the type I sensors will work for simple gas species such as O₂ and H₂ when using appropriate solid electrolytes which are O²⁻ and H⁺ ion conductors, it is not possible to apply these devices to the sensing of oxide gases like CO₂, since such gases do not generate interface reactions. Type II sensors capable of detecting oxide gases have been proposed by Gauthier et al.^{1,2} An important breakthrough in this regard was the application of alkali metal or alkaline earth metal salts as the solid electrolyte for the detection of oxide gas species. As an example, K₂CO₃ has been applied as the solid electrolyte in a CO₂ sensor. Although sensors using alkali metal or alkaline earth metal carbonates as the solid electrolyte are able to detect CO₂, such salts would not be acceptable for practical applications because of their high solubility in water as well as their poor mechanical strength. A type III sensor using the Na⁺ ion-conducting material NASICON (Na⁺ super ionic conductor: Na₃Zr₂Si₂PO₁₂) and Na₂CO₃ as the solid electrolyte and auxiliary sensing electrode, respectively, was proposed by Saito and Maruyama in 1984.³ In this CO₂ sensor, the solid electrolyte (NASICON) and the auxiliary sensing electrode (Na₂CO₃) have a common mobile ion species (Na⁺). Although NASICON is a superior solid electrolyte exhibiting high ion conductivity, Na₂CO₃ shows measurable solubility in water and also reacts with water vapor at elevated temperatures, which disallows the commercial application of the sensor. In order to overcome this problem, various mixed carbonates such as a Na₂CO₃-BaCO₃ mixture^{4,5} have been proposed for use as the auxiliary sensing electrode. CO₂ sensors employing mixed carbonates as the auxiliary sensing electrode have shown good sensing performance over a wide CO₂ concentration range (between 4 ppm and 40 %), but they still suffer from the problem of high water solubility. Following the development of the above type III CO₂ sensor, many different type III CO₂ sensors have been reported with the aim of developing a commercially marketable device. Most of the solid electrolytes, however, have been limited to Na⁺ and Li⁺ ion-conducting solids such as NASICON, Na⁺-β/β''-alumina, and LISICON, so as to ensure high ion

Table 17.1 Classes of equilibrium potential gas sensors based on solid electrolytes

Type	Relationship between the conducting ion species in solid electrolyte and the ion which electrochemically derived from gas phase	Sensing electrode	Reference electrode
I	Same	Unnecessary	Unnecessary
II	Different	Unnecessary	Unnecessary
III	Different	Necessary	Necessary

Fig. 17.1 Schematic illustration of a CO₂ sensor combining Sc³⁺- and O²⁻-conducting solid electrolytes with a Li₂CO₃-sensing auxiliary electrode



conductivity and thus sufficient sensing performance. Although sensors made with Na⁺ and Li⁺ ion-conducting solid electrolytes of this type offer high sensitivity, the associated compounds which form other parts of the CO₂-sensing mechanism (such as oxides and carbonates containing conducting ion species) are not inert and readily react with ambient gas species. As a result, the output of these sensors constantly undergoes interference in the presence of ambient species such as water vapor.

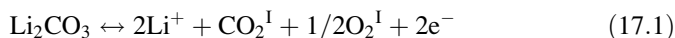
Based on optimizing both the chemical stability and the long-term stability of the sensor, multivalent cation-conducting solid electrolytes are considered to be preferable as sensor components. However, since reasonably high ion conductivity is required for the solid electrolyte in order to obtain desired performance parameters such as fast responsiveness, it is necessary to develop multivalent cation conductors with high ionic conductivity.

In 1999, a potentiometric CO₂ sensor employing a trivalent Sc³⁺ ion conductor, based on the structure of CO₂-air, Pt^I|Li₂CO₃|Sc₂(WO₄)₃⁶|YSZ||Pt, and CO₂-air, was reported.^{7,8} A schematic illustration of the sensor cell is presented in Fig. 17.1. The design of this sensor incorporates a number of important aspects. Firstly, yttria-stabilized zirconia (YSZ) is used as one of the components of the sensor cell as an O²⁻ ion-conducting solid. By incorporating YSZ, the oxide which forms at the interface between the cation-conducting solid electrolyte and the YSZ does not have contact with the ambient atmosphere, limiting the influence of other gas species such as O₂, H₂O, and NO_x even if the entire sensor cell is exposed to the ambient atmosphere. In addition, a Sc³⁺ ion-conducting Sc₂(WO₄)₃ solid is applied as the solid electrolyte. The stability of the oxide which forms at the interface of this material is a key factor in its sensing performances. When an M⁺ ion conductor

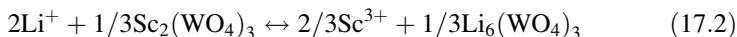
(M = Na or Li) is applied as a sensor component, the M_2O oxide formed at the interface readily reacts with permeated CO_2 and/or H_2O gas species to form M_2CO_3 and/or MOH , respectively, and the formation of such compounds results in deterioration of the sensing performance. It is therefore essential that a thermodynamically stable oxide forms at the interface to ensure reliable sensor output. When the Sc^{3+} cation-conducting solid electrolyte is used, the oxide formed at the interface is Sc_2O_3 , a compound which is extraordinarily stable. $Sc_2(WO_4)_3$ also exhibits high trivalent ion conductivity ($6.5 \times 10^{-5} \text{ S cm}^{-1}$ at 600°C),⁹ which allows quick sensor response based on the electrochemical reactions described below.

The proposed operating mechanism of a CO_2 sensor based on solid $Sc_2(WO_4)_3$ and YSZ together with an auxiliary Li_2CO_3 -sensing electrode is as follows.

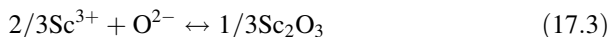
(Auxiliary sensing electrode)



(Interface between Li_2CO_3 and Sc^{3+} ion-conducting solid electrolyte)



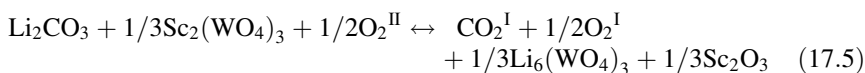
(Interface between the two solid electrolytes)



(Reference electrode: YSZ)



Overall, the chemical reaction may be written as below:

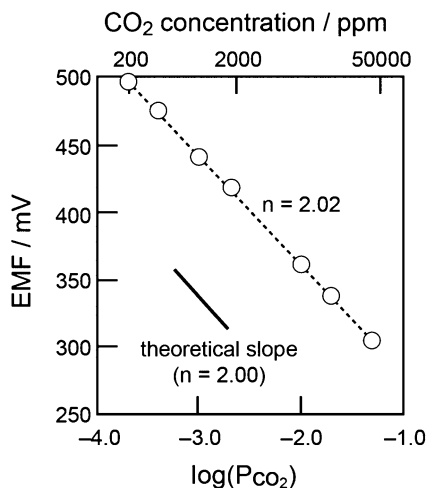


Based on the above, the following Nernst equation is derived:

$$E = E_0 - \frac{RT}{2F} \ln \left\{ \frac{(p_{CO_2^I}) (a_{Li_6(WO_4)_3})^{1/3} (p_{O_2^I})^{1/2} (a_{Sc_2O_3})^{1/3}}{(a_{Li_2CO_3}) (a_{Sc_2(WO_4)_3})^{1/3} (p_{O_2^{II}})^{1/2}} \right\} \quad (17.6)$$

Since $Sc_2(WO_4)_3$ and Li_2CO_3 are the base electrolyte and auxiliary sensing electrode and $Li_6(WO_4)_3$ is formed between the Li_2CO_3 and the Sc^{3+} ion-conducting solid electrolyte, the activities (a) of these solids should be unity. In addition, as the entire sensor cell is exposed to the same atmosphere (as shown in Fig. 17.1), O_2^I is exactly equal to O_2^{II} . Based on this, the Nernst equation (17.6) is simplified as follows:

Fig. 17.2 Relationship between sensor output (EMF) and $\log(P_{\text{CO}_2})$ at 550 °C for a sensor incorporating Sc^{3+} -conducting $\text{Sc}_2(\text{WO}_4)_3$. The solid line represents the theoretical slope obtained from Eq. (17.8) ($n = 2.00$)



$$E = C_1(\text{const.}) - \frac{RT}{2F} \ln \{ (p_{\text{CO}_2}) (a_{\text{Sc}_2\text{O}_3}) \} \quad (17.7)$$

Here, because Sc_2O_3 formed between the two solid electrolytes is very stable at the operating temperature, $a(\text{Sc}_2\text{O}_3)$ is constant and the following equation can be obtained from Eq. (17.7):

$$E = C_2(\text{const.}) - \frac{RT}{2F} \ln (p_{\text{CO}_2}) \quad (17.8)$$

The CO_2 concentration dependence of the sensor output is presented in Fig. 17.2. 1:1 theoretical linear Nernst relationship was obtained over the CO_2 concentration range between 200 ppm and 5 %, with a response time less than several minutes. The quantity of electrons (n) calculated from the slope was 2.02, which is in good agreement with the theoretical value of 2.00 obtained from Eq. (17.8).

One of the most remarkable advantages of this sensor is its highly stable sensor output (measured as EMF). Figure 17.3 shows the variation over time in the sensor output EMF when exposed to 1 % CO_2 . Compared to a sensor containing the Li^+ ion-conducting $\text{LiTi}_2(\text{PO}_4)_3 + 0.2\text{Li}_3\text{PO}_4$, the sensor with $\text{Sc}_2(\text{WO}_4)_3$ exhibits a highly stable EMF from the beginning of the CO_2 measurements, while significant deviations as high as 100 mV are observed in the case of the Li^+ ion conductor. This difference between the two sensors occurs because the solid formed at the interface between the two solid electrolytes for the sensor with Sc^{3+} ion conductor is the chemically stable compound Sc_2O_3 , while reactive Li_2O is generated at the interface in the case of the Li^+ ion conductor and, therefore, the EMF of this device undergoes gradual drift and several days are required to obtain a stable reading. These contrasting behaviors clearly indicate the merit of employing a trivalent

Fig. 17.3 Deviation of sensor output (Δ EMF) in response to 1 % CO_2 at 550°C over time for a CO_2 sensor incorporating $\text{Sc}_2(\text{WO}_4)_3$. The corresponding data for a sensor based on a Li^+ ion-conducting $\text{LiTi}_2(\text{PO}_4)_3 + 0.2\text{Li}_3\text{PO}_4$ solid is shown as a *dashed line*

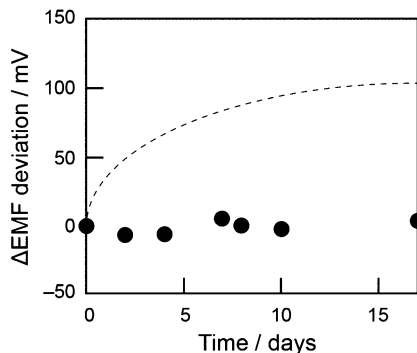
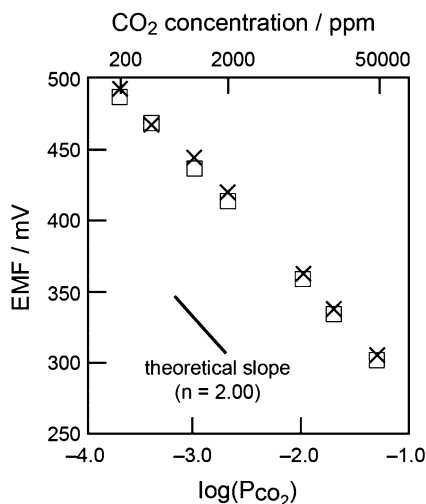


Fig. 17.4 Variations in sensor EMF with the logarithm of CO_2 concentration in dry (*open square*) and humid (water vapor content: 3.0 vol%) (\times) atmospheres at 550°C . The *solid line* represents the theoretical slope estimated from Eq. (17.8) ($n = 2.00$)



cation conductor as a sensor component. In addition, the sensor using $\text{Sc}_2(\text{WO}_4)_3$ has demonstrated extraordinary stable sensor EMF outputs over a prolonged test period spanning 150 days.

Figure 17.4 depicts the sensor output EMFs in both dry and humid atmospheres at 550°C . Even in an atmosphere containing 3.0 vol% water vapor (saturated water vapor at 25°C), the EMF values are essentially identical to those obtained in a dry atmosphere, suggesting that there is no interference by water vapor with regard to the sensing performance. Furthermore, the sensor responds only to CO_2 without any interference due to the presence of O_2 (tested concentration range: 5–40 %), NO (100–500 ppm), or NO_2 (100–500 ppm). These results also support the contention that multivalent cation conductors are one of the promising candidates for sensor components.

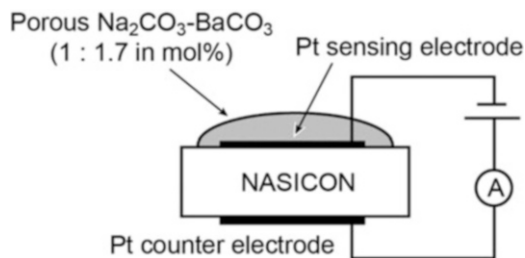
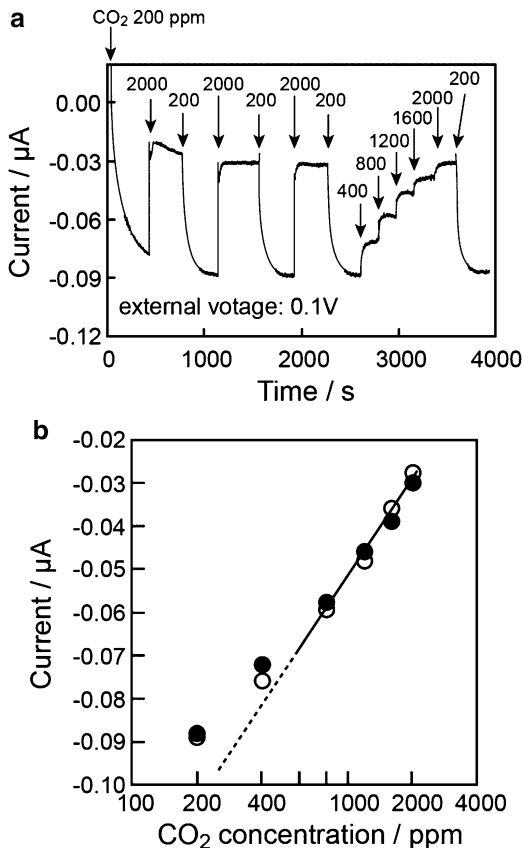


Fig. 17.5 Schematic illustration of an amperometric type CO_2 sensor cell with a combination of NASICON and $\text{Na}_2\text{CO}_3\text{-BaCO}_3$

Although lithium carbonate is the most promising simple carbonate material for the construction of an auxiliary sensing electrode, due to its high durability in the presence of water vapor as well as its high sensitivity for CO_2 , Li_2CO_3 does dissolve in water ($1.29 \text{ g}/100 \text{ g H}_2\text{O}$ at 25°C) and so it is regarded as not sufficiently stable for commercial use. Beginning in 2001, the rare earth oxycarbonate ($\text{R}_2\text{O}_2\text{CO}_3$; R: rare earths)-based material $(\text{Nd}_{0.47}\text{Ba}_{0.12}\text{Li}_{0.29})_2\text{O}_{0.94}\text{CO}_3$ was proposed as a new component of a novel CO_2 auxiliary sensing electrode.^{10–13} The base material of $\text{Nd}_2\text{O}_2\text{CO}_3$ has extremely low solubility in water ($3.2 \times 10^{-4} \text{ g}/100 \text{ g H}_2\text{O}$) as well as reasonably high thermal stability up to 600°C . While the solubility in water of $(\text{Nd}_{2/3}\text{Li}_{1/3})_2\text{O}_{4/3}\text{CO}_3$ is $6.0 \times 10^{-3} \text{ g}/100 \text{ g H}_2\text{O}$, the solid solution containing both BaCO_3 and Li_2CO_3 has an extraordinarily low solubility of $1.1 \times 10^{-4} \text{ g}/100 \text{ g H}_2\text{O}$. All CO_2 sensors manufactured with multivalent cation-conducting solid electrolytes using the $(\text{Nd}_{0.47}\text{Ba}_{0.12}\text{Li}_{0.29})_2\text{O}_{0.94}\text{CO}_3$ sensing auxiliary electrode^{13–15} demonstrated superior sensing performance similar to that of the $\text{Sc}_2(\text{WO}_4)_3$ device described above.

Amperometric sensors are generally more applicable when linear and reliable sensing is required over a narrow concentration range, compared to potentiometric sensors. Lee et al. reported an amperometric CO_2 sensor using $\text{Na}^{+16,17}$ or Li^+ ion conductors¹⁸ in 2003. The construction of the sensor incorporating NASICON, as shown in Fig. 17.5, was similar to that of the potentiometric sensor: CO_2 , carbonate, Pt|NASICON|Pt, and CO_2 . The response curve of a sensor with $\text{Na}_2\text{CO}_3\text{-BaCO}_3$ during the applications of a 0.1 V external voltage at 400°C is depicted in Fig. 17.6a. While the current decayed during the initial stage, stable CO_2 -sensing behavior was observed with a 90 % response time of 16 s. The current change of this sensor is linear with the logarithm of the CO_2 concentration, even in a humid atmosphere (Fig. 17.6b), although the sensor output currents at low CO_2 concentrations deviate slightly from the linear relationship. This sensor requires 20 min to obtain a stable current at every stage of operation since the carbonate reacts with NASICON and, as a result, Na^+ activity in the sensor cell continually changes during the current passage. These deficits make it difficult to find practical applications for such a device.

Fig. 17.6 (a)
Representative response curve for a sensor based on $\text{Na}_2\text{CO}_3\text{-BaCO}_3$ at $400\text{ }^\circ\text{C}$.
(b) Sensor signals for CO_2 in dry (*open circle*) and humid (ca. 2.3 vol% H_2O) atmospheres (*filled circle*)



17.1.2 CO₂ Sensors Using Semiconductors

Semiconductors are widely used as gas sensor elements, since they are capable of detecting combustible gases. The sensing mechanism of a device incorporating a semiconductor is based on the resistivity change of the semiconductor following gas adsorption on its surface. These sensors, however, have difficulty detecting CO_2 gas, since the semiconductor resistance undergoes little change with the adsorption of CO_2 molecules. Thus far, only SnO_2 -, In_2O_3 -, and BaTiO_3 -based metal oxides have been reported to show CO_2 sensing characteristics.

In 1990, Tamaki et al. first reported the possibility of using SnO_2 for CO_2 sensing.¹⁹ SnO_2 undergoes a resistance change when CO_2 is adsorbed on its surface, although a meaningful change is observed only in dry atmospheres. In a humid atmosphere, the resistivity of SnO_2 does not vary due to interference by the surface adsorption of water vapor. In order to improve the CO_2 -sensing properties of SnO_2 , a variety of metal oxides were loaded onto the material by a sintering method and the resulting sensing properties were investigated.^{20,21} Table 17.2 summarizes the

Table 17.2 CO₂-sensing performance^a of metal oxide-loaded SnO₂ at 400 °C

Metal oxide	Amount of metal oxide (wt%)	R _{air} /R _{CO₂}	Response time ^b (min)
Pure SnO ₂		1.02	2.4
Li ₂ O	0.6	1.41	0.7
Na ₂ O	5.9	1.02	0.3
K ₂ O	2.8	0.82	
MgO	0.6	1.24	7.8
CaO	1.3	1.53	4.3
SrO	1.1	1.53	4.2
BaO	0.5	1.68	4.5
V ₂ O ₅	0.4	1.04	
Cr ₂ O ₃	1.2	1.33	2.6
Fe ₂ O ₃	0.5	1.34	1.4
Co ₃ O ₄	2.6	1.17	2.7
NiO	1.4	1.32	3.4
CuO	1.8	1.16	1.4
ZnO	2.9	0.97	
ZrO ₂	0.4	1.04	3.2
MoO ₃	0.4	1.27	7.2
La ₂ O ₃	4.2	1.79	0.4
Pr ₂ O ₃	3.4	1.54	0.5
Nd ₂ O ₃	4.2	1.76	0.4

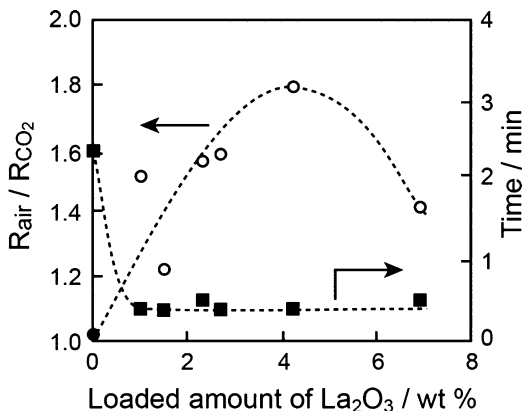
^aCO₂ concentration: 2,080 ppm

^b90 % response time for the increase of CO₂ concentration

sensitivities ($R_{\text{air}}/R_{\text{CO}_2}$) and 90 % response times measured at 400 °C for the metal oxide-loaded SnO₂. The sensitivity was increased by loading with metal oxide in the following order: pure SnO₂ \approx alkaline metal oxides \leq transition metal oxides \leq alkaline earth oxides \leq rare earth oxides. Among the various metal oxides tested, La₂O₃ showed the highest sensitivity along with a rapid response to CO₂. In addition, sensitivity was found to depend on the amount of metal oxide loaded, although the response time does not change with La₂O₃ loadings over 1.0 wt% (0.375 at.%), as shown in Fig. 17.7. These sensors, as prepared by the sintering method, still have deficits associated with their inability to detect CO₂ at the ppm level and are also hampered by their significant sensitivity to the presence of water vapor.

To enhance the CO₂ sensitivity and durability in the presence of water vapor of sensors incorporating La₂O₃-loaded SnO₂, Sakama et al. developed an improved sensor element based on the application of a sputtering technique.²² They succeeded in loading increased amounts of La₂O₃ onto the SnO₂ as compared to samples prepared by sintering. In the case of samples fabricated with the sputtering method, the optimum La concentration was 5 at.% which is considerably higher than that required for devices processed with the sintering method (0.375 at.%). Furthermore, it was shown that La₂O₃-loaded SnO₂ prepared by calcination

Fig. 17.7 La_2O_3 content dependencies of the sensitivity (*open circle*) and 90 % response time (*filled square*) at 400 °C of a La_2O_3 -loaded SnO_2 sensor

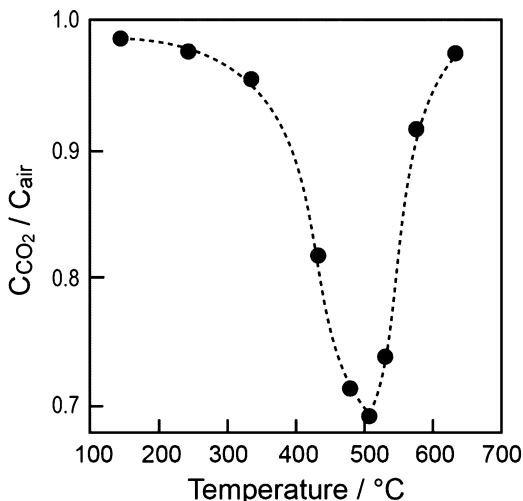


contained a considerable concentration of impurities and that the La in the material tended to form a hydroxide. As a result, the sensor degenerated after several days of exposure to humid air due to reaction with water,²³ and additional additives such as Y, Gd, and Mg were required to stabilize the sensor by preventing the aggregation of La. In contrast, additives are not necessary when employing films prepared by the sputtering method. In addition, the operating temperature of the sensor produced by sputtering was reduced to 200 °C. These enhancements are primarily attributed to the loading of higher amounts La_2O_3 onto the SnO_2 .

Similar to manner in which the SnO_2 -based sensors were investigated, the effects of In_2O_3 on the CO_2 sensor element have also been examined.²⁴ Pure In_2O_3 has been shown to respond to CO_2 with a sensitivity factor ($R_{\text{air}}/R_{\text{CO}_2}$) of 7.8, although its 90 % response time is overly long (ca. 64 min). Both the sensitivity and the 90 % response time, however, are improved dramatically by the loading of a metal oxide, just as was observed with SnO_2 . In case of In_2O_3 , CaO (5.5 wt%) is the most appropriate choice of metal oxide and a sensor with 5.5 wt% CaO loaded onto In_2O_3 exhibited high sensitivity (12.9) with a 90 % response time of 40 min. Even though the sample was prepared using the sintering method, it was able to detect CO_2 gas in a humid atmosphere. Interestingly, the 90 % response time of the sensor in humid atmospheres (1.8 vol% H_2O) decreased to 12 min, although the reason for the acceleration of the response in humid atmospheres was not determined.

An equimolar complex oxide of BaTiO_3 -PbO has been shown to function as a capacitive-type CO_2 sensor.²⁵ While the capacitance of pure BaTiO_3 does not change in response to CO_2 , the capacitance of a BaTiO_3 -PbO mixture is significantly decreased in an atmosphere of 2 % CO_2 in dry air. Since BaTiO_3 does not react with PbO during the measurement process, BaTiO_3 behaves as a semiconductor at the operating temperature of 500 °C and the capacitance of the mixed oxide is greatly increased by mixing PbO and BaTiO_3 . The sensitivity of BaTiO_3 -PbO to CO_2 drastically changes with temperature and the highest sensitivity is obtained at ca. 500 °C, as shown in Fig. 17.8. The CO_2 -sensing mechanism of this device is based on an initial reaction involving the carbonation of PbO. While the

Fig. 17.8 Temperature dependence of the sensitivity of BaTiO₃-PbO to 2 % CO₂ at an operation frequency of 50 kHz



carbonation proceeds readily at elevated temperatures, the PbCO₃ formed in this reaction will decompose when heated above its decomposition temperature of 315 °C. Unfortunately, the temperature at which maximum sensitivity is obtained is higher than this decomposition temperature. Because the reaction rate between solids and gases is generally reduced at lower temperatures, the rate of PbO carbonation should increase significantly with heating, but these higher temperatures will also decrease the equilibrium yield of PbCO₃. As a result, the maximum sensitivity of these devices is attained at ca. 500 °C. Other mixed oxide capacitors based on BaTiO₃ were also tested²⁶ and the CO₂-sensing characteristics of the resulting mixed oxide capacitors are listed in Table 17.3. The optimum operating temperature of all the sensors is ca. 150–200 °C above the decomposition temperature of the carbonates of the compounds combined with BaTiO₃, and it is clear that the optimum operating temperature strongly depends on the thermal stability of the corresponding carbonate, similar to the case of PbO as described above. This relationship between the operating temperature and the decomposition temperature of the carbonate suggests that the capacitance change of the mixed oxides is caused by the carbonation of the oxides combined with BaTiO₃. Therefore, no capacitance change was observed when SiO₂, Al₂O₃, and V₂O₅ were applied, since these compounds do not form carbonates under relatively mild conditions.

The selectivity of the BaTiO₃-CuO-based sensor which showed the highest sensitivity to CO₂ among the various different BaTiO₃-M_xO_y compounds was subsequently investigated. Figure 17.9 displays the time dependence of the capacitance of an equimolar mixture of BaTiO₃-CuO during exposure to 2 % CO, H₂, CH₄, CO₂, and C₂H₅OH as well as 2.8 % H₂O at 456 °C. While neither CH₄ nor H₂ produces a response in the sensor, CO, H₂O, and C₂H₅OH all affect the capacitance of the sensor element. This response occurs as a result of the oxidation of both CO and C₂H₅OH to CO₂ by CuO, which is a well-known oxidation catalyst. Conversely,

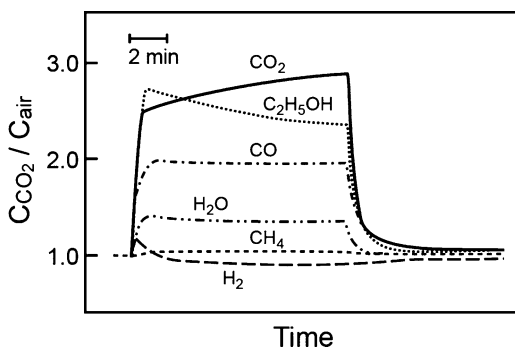
Table 17.3 CO₂-sensing properties of the equimolar mixed oxide M_xO_y-BaTiO₃

M _x O _y	Operating temperature ^a (°C)	Sensitivity ^b , C _{CO₂} /C _{air}	Upper limit for detection (%)
CaO	>900	0.891	8
MgO	867	0.329	10
La ₂ O ₃	766	0.451	8
Nd ₂ O ₃	550	0.641	6
Y ₂ O ₃	759	0.794	10
CeO ₂	661	0.410	8
PbO	501	0.711	6
NiO	555	0.441	20
CuO	456	2.892	6
ZrO ₂	642	0.740	10
Co ₃ O ₄	528	0.362	6
Fe ₂ O ₃	341	0.678	2
Bi ₂ O ₃	445	0.824	2
V ₂ O ₅		1.000	0
Nb ₂ O ₅		1.000	0
SiO ₂		1.000	0
Al ₂ O ₃		1.000	0
SnO ₂		1.000	0

^aOptimum temperature for CO₂ detection

^bSensitivity to 2 % CO₂

Fig. 17.9 Time dependence of the capacitance of an equimolar mixture of BaTiO₃-CuO on exposure to 2 % CO, H₂, CH₄, CO₂, and C₂H₅OH, and 2.8 % H₂O at 456 °C (frequency 50 kHz)



adsorption of H₂O on the sensor element increases the capacitance due to its large dielectric constant, such that the capacitance change varies with the amount of adsorbed water vapor. Since the sensitivity for CO₂ is affected by the presence of other gases such as CO and C₂H₅OH, it is thought that CO₂ sensors based on semiconductors will be difficult to utilize for practical applications. Although Ishihara et al. theorized that the CO₂-sensing mechanism was based on the carbonate reaction of the metal oxide in the equimolar mixed oxide, Liao and co-workers proposed a different mechanism.^{27,28} Their calculations of the Gibbs free energy based on the thermodynamic theory of chemical reaction processes suggested that a

chemical carbonation reaction does not occur between CuO or BaTiO₃ and CO₂ gas. Furthermore, XPS analysis of oxide samples did not show any evidence of carbonation and, as a result, they concluded that the temperature sensitivity characteristics of the sensor (for example, Fig. 17.8) are simply due to typical surface adsorption processes, similar to those which most oxide-based gas sensors exhibit. The adsorption of a gas can be divided into physical and chemical processes, with physical adsorption predominant at lower temperatures and chemical adsorption increasingly important at higher temperatures. Sensitivity will therefore initially increase with temperature but, at a certain value of temperature, disadsorption of CO₂ will occur and both chemical and physical adsorptions will thus decrease. As a result, the sensitivity of these sensing devices will increase with temperature, reach a maximum value, and then decrease with increasing temperatures.

17.1.3 Other Sensor Types

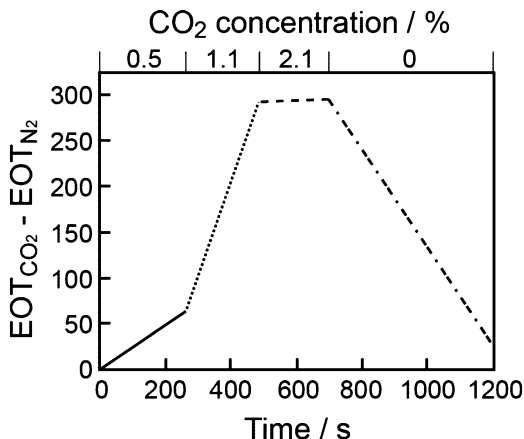
In 1995, an amine-based, surface-bonded silica gel was reported to be useful as a scrubber for CO₂ produced in industrial gaseous streams.²⁹ In this silica gel, CO₂ interacts reversibly with the amine, forming carbamate species, and the adsorbed CO₂ is subsequently liberated by heating above 40 °C. Since this characteristic may have applications to CO₂ sensing, Rocchia et al. have studied a CO₂ sensor based on a porous silicon (PS) film modified on its surface by the application of an amine.³⁰

The porous silicon used in this manner was modified in two steps, consisting of oxidation with ozone and chemical modification with 3-amino-1-propanol. The samples prepared in this manner were found to have been successfully modified by the amine based on their FT-IR spectra. The resulting PS layer is sufficiently smooth so as to produce a Fabry-Perot pattern, described by

$$EOT = 2nd - m\lambda \quad (17.9)$$

where EOT , n , d , and m are the effective optical thickness, the refractive index, the sample thickness, and the fringe order, respectively. The sensing mechanism is based on tracking wavelength shifts in the fringe pattern in response to CO₂ adsorption. The interaction between the modified PS surface and CO₂ causes a change in the refractive index, resulting in a shift of the fringe pattern as a function of the CO₂ partial pressure. The shift of the interference pattern at different CO₂ concentrations is depicted in Fig. 17.10. Low concentrations of CO₂ (5,000 ppm to 1.1 %) cause a red shift of the fringe pattern which plateaus when the CO₂ concentration reaches 2.1 %. The red shift is presumably caused by an increase of the refractive index due to the formation of new species as a consequence of the interaction between CO₂ and PS-NH₂ functional groups, and the sensor behavior at very high CO₂ concentrations is attributed to saturation of the accessible amine groups. The initial spectral fringe pattern is recovered by removing CO₂ from the carrier gas (dash-dot line in Fig. 17.10), although the rate of recovery is slow.

Fig. 17.10 Shift of the fringe pattern with increasing CO₂ partial pressures (carrier gas: dry N₂): 5,000 ppm CO₂ (solid line); 1.1 % CO₂ (dotted line); 2.1 % CO₂ (dashed line); 0 ppm CO₂ (dash-dot line)



Furthermore, since the interference of other gas species on CO₂ sensing has not yet been investigated, the selectivity of this type of sensor is uncertain at present.

Optical CO₂ sensors may be classified into two types: those based on the colorimetric change of a pH indicator dye such as phenolsulfonphthalein (phenol red)^{31–35} and those based on the CO₂-induced fluorescence change in a luminescent dye such as 1-hydroxypyrene trisulfonate.^{36–39} Although fluorescent phenol-based sensors are capable of measuring CO₂ gas concentrations, the number of compounds which will work in such sensors is extremely limited. In 2003, Nakamura et al. reported an optical CO₂ sensor fabricated by combining the colorimetric change of a pH indicator dye, such as thymol blue, phenol red, or cresol red, with a luminescent dye consisting of a tris(thenoyltrifluoroacetate) europium(III) hydrate complex [Eu(tta)₃].^{40,41} In this sensor configuration, emission from the luminescent dye is decreased in the absence of CO₂ due to absorption by the pH indicator dye, while the emission intensity increases with the ambient CO₂ concentration since the attendant colorimetric change of the pH indicator dye leads to a successive decrease in its absorbance of the luminescence. In this manner, the CO₂ concentration is determined by measuring the luminescence intensity from the luminescent dye which is able to transmit through the pH indicator. Among the various pH indicators investigated in conjunction with an internal reference luminescent dye composed of a Eu(III) complex, α -naphtholphthalein was found to exhibit a large A_0/A_{100} value, where A_0 and A_{100} are absorbance in 100 % Ar and 100 % CO₂, respectively.

Although the luminescence intensity is dependent of the particular luminescent dye applied, the most important component of this sensor is the pH indicator. The CO₂-sensing properties of a film composed of a combination of α -naphtholphthalein with tetraphenylporphyrin (TPP) as the pH indicator and internal reference dyes may be used as an example.⁴² The exact constitution of this sensing film is α -naphtholphthalein/tetraoctyl ammonium hydroxide/cellulose/tributyl phosphate/non-luminescent glass slide/TPP/polystyrene.

Fig. 17.11 (a) Reaction scheme of α -naphtholphthalein with CO_2 . (b) Molecular structures of deprotonated (N^-) and protonated (NH) α -naphtholphthalein

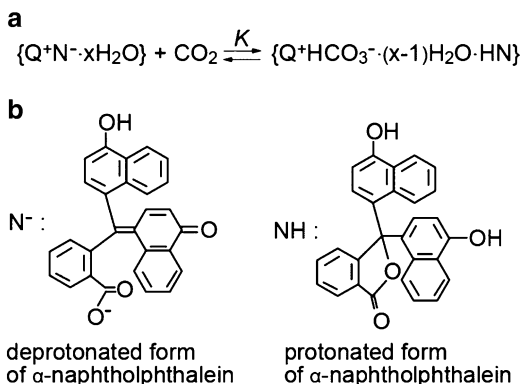


Fig. 17.12 I/I_0 values of CO_2 -sensing films consisting of 2.8 mM α -naphtholphthalein in an ethyl cellulose layer and TPP in a polystyrene layer at various CO_2 concentrations. The excitation and emission wavelengths were 350 nm and 655 nm, respectively

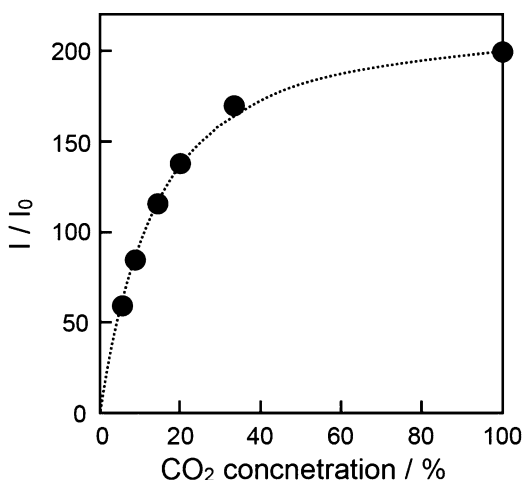


Figure 17.11 shows the reaction between α -naphtholphthalein and CO_2 . $\{\text{Q}^+\text{N}^- \cdot x\text{H}_2\text{O}\}$ is the ion pair formed from the tetraoctyl ammonium cation (Q^+) and the deprotonated form of α -naphtholphthalein (N^-) and K is the equilibrium constant. In this sensor, the relationship between observed luminescence intensity and the CO_2 concentration may be described as (based on the derivation in reference (42))

$$I/I_0 = 10^{\{-C(1/K+[\text{CO}_2])\}+1+K} \quad (17.10)$$

where I_0 and I are the luminescence intensities at 655 nm when the film is exposed to 100% N_2 and various concentration of CO_2 , respectively, and C is a constant.

When an excitation light source (350 nm) is introduced from the α -naphtholphthalein side under various CO_2 concentrations at room temperature, the absorption band of α -naphtholphthalein at approximately 655 nm decreases with increasing CO_2 concentration and, as a result, the luminescence intensity of the TPP measured at 655 nm is enhanced with increasing CO_2 concentrations, as depicted in Fig. 17.12. The 90% response and recovery times of a film containing

2.8 mM α -naphtholphthalein and TPP are 5.4 and 4.5 s, respectively, when the CO₂ concentration changes between 0 and 100 %. While the luminescence intensity is not affected by the presence of either O₂ or CO, the intensity is increased when the film is exposed to acidic gas such as HCl. Furthermore, since the CO₂-sensing properties of this device have not been examined in humid atmospheres nor in the presence of gases such as NO_x, further investigation is necessary.

17.2 Carbon Monoxide

Carbon monoxide is one of the most well-known toxic gases, notorious as the “invisible silent killer” due to its colorless, tasteless, and odorless nature, and so sensors capable of detecting CO gas have been in demand as a means of ensuring human safety. Until now, various types of CO sensors such as semiconductor, catalytic, electrochemical, optical, and solid electrolyte variations have been investigated. Among these, the catalytic and electrochemical types have been commercialized since these sensors offer reliable sensing performance along with long-term stability, high sensitivity, and low cost, although some problems such as selectivity, thermal stability, and safety still remain. Due to their advantages with regard to long-term stability and sensitivity, the electrochemical sensors are most commonly employed as commercial CO gas-monitoring devices.

17.2.1 Catalytic Combustion CO Sensors

In the catalytic-type sensor, otherwise known as the catalytic combustion sensor, the sensing mechanism is based on resistance changes in a Pt wire (generally present as a coil to allow an increased surface contact area with the catalyst) resulting from the heat generated by oxidation of CO on a catalyst. Pt-loaded Al₂O₃ (Pt/Al₂O₃) is commonly used as the CO oxidation catalyst in these devices. Since the Pt/Al₂O₃ requires temperatures above 400 °C to fully oxidize CO to CO₂, other gases (such as H₂) are also oxidized and therefore the selectivity of these devices for CO is often compromised. Much effort has gone into finding other metal oxides which can be added to Pt/Al₂O₃ to improve the performance of these sensors, but high selectivity for CO has not yet been obtained. It is therefore important to lower the operational temperature of these sensors to improve their CO selectivity, by incorporating new CO oxidation catalysts that work at relatively low temperatures at which gases other than CO are not oxidized.

In 2013, a new, low-temperature catalytic combustion CO sensor was reported,⁴³ using a CeO₂-ZrO₂-SnO₂-based oxide as the catalyst. Since 10 wt% Pt-loaded Ce_{0.68}Zr_{0.17}Sn_{0.15}O_{2.0} (10 wt% Pt/Ce_{0.68}Zr_{0.17}Sn_{0.15}O_{2.0}) shows superior CO-oxidizing performance at 65 °C (Fig. 17.13), a sensor with 10 wt% Pt/Ce_{0.68}Zr_{0.17}Sn_{0.15}O_{2.0} as the catalyst exhibited CO detection at temperatures as

Fig. 17.13 CO conversion properties of the 10 wt% Pt/Ce_{0.68}Zr_{0.17}Sn_{0.15}O_{2.0} catalyst as a function of temperature

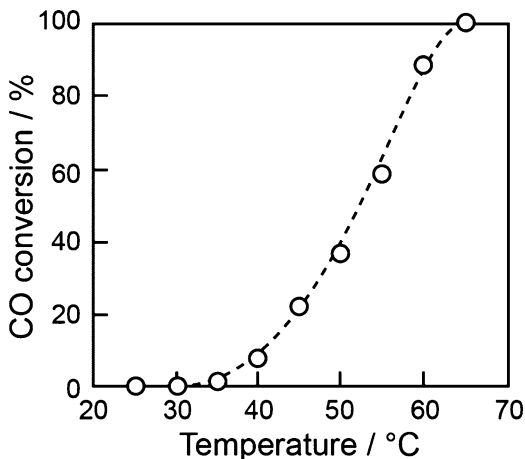
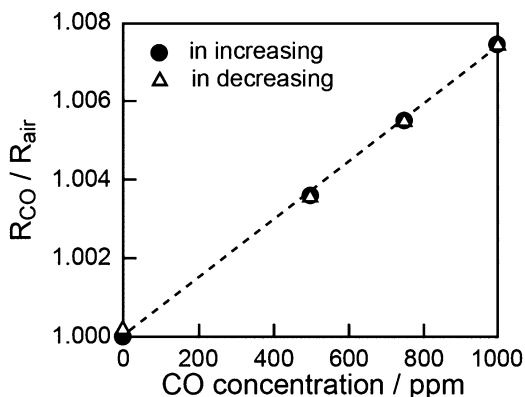


Fig. 17.14 Sensor signals (as the ratio of resistance in CO to that in air: R_{CO}/R_{air}) at various CO concentrations of a catalytic combustion-type sensor incorporating 10 wt% Pt/Ce_{0.68}Zr_{0.17}Sn_{0.15}O_{2.0} catalyst at 70 °C



low as 70 °C (Fig. 17.14). Although this catalyst can fully oxidize CO at 65 °C, a temperature of 70 °C is required in order to compensate for the very small amount of catalyst used in the sensor. The development of this sensor, capable of detecting CO gas at temperatures below 100 °C, should contribute to the future commercialization of catalytic combustion-type CO sensors.

17.2.2 Semiconductor Type

As noted above, gas sensing with semiconductors is based on the resistance change of the semiconductor in response to gas adsorption onto the semiconductor surface. Therefore, n-type semiconductors such as SnO₂ have been widely used for the

detection of electron-donating CO gas. Similar to the catalytic combustion sensor described earlier, sensors incorporating semiconductors are generally lacking in selectivity and so efforts have been made to improve their properties by adding metal or metal oxides to the base semiconductor. A reliable and selective semiconductor-based CO sensor, however, has not yet been realized by this technique.

More recently, nanomaterials have been widely studied in various fields due to their unique properties, which are often significantly different from those of the bulk material, and there are some reports on CO sensing using nanomaterials. Among the various studies on practically applicable CO sensors incorporating semiconductors, room temperature operation was reported for sensors based on carbon nanotubes (CNTs) in 2013.⁴⁴ Although pristine carbon nanotubes are insensitive to CO due to the small adsorption energy of CO on the CNT surface, a response to CO has been obtained by coating single-wall nanotubes (SWCNTs) with SnO₂ nanoparticles. The resulting sensor is able to detect CO gas concentrations above 1 ppm with a response time of ca. 2 s (63.2 % response of the overall resistance change) at room temperature. Difficulties with cross-sensitivity for H₂ still remain, although the interference effects of H₂ are minimal compared to those experienced by conventional semiconductor-type sensors. Even so, further improvements are necessary before these new sensors can be considered for everyday use.

Although other nanostructured materials (NiO nanotubes,⁴⁵ ZnO nanowires,⁴⁶ WO₃ nanoparticles,⁴⁷ and SnO₂ nanorods⁴⁸) have been intensively studied as promising candidates for use in CO sensors operable at room temperature, their sensitivity is also insufficient to allow their use in practical application, similar to the status of sensors incorporating CNTs.

17.2.3 Solid Electrolyte-Type Sensors

With regard to the solid electrolyte CO₂ sensors described in Sect. 17.1, there have been no reports of auxiliary sensing electrode materials which undergo equilibrium reactions solely with CO, and therefore it is difficult to develop solid electrolyte CO sensors which detect gas based on equilibrium potentials. A significant number of studies concerning solid electrolyte sensors have, however, identified another approach which makes use of the non-equilibrium potential, in other words, mixed potential. Sensors based on this approach can be expected to detect various gases which are not detected by the conventional equilibrium potential method. If both O₂ and CO are present, these gases will react according to Eq. (17.11) until the three gases are in equilibrium:



Table 17.4 Typical examples of mixed potential CO gas sensors reported in the 1980s and 1990s

Sensor structure ^a Air, (cat), RE electrolyte SE, (cat), target gas	Sensing property		Ref.
	Operating temp. (°C)	Gas conc.	
Air, Pt YSZ Pt(Pd), CO(+air)	500–700	0–1.5 %	49
CO(+air), (Pt-Al ₂ O ₃), Pt YSZ Pt, CO(+air)	260–350	0–100 ppm	50
CO(+air), (Pt-Al ₂ O ₃), Pt YSZ Pt, (SnO ₂ +KCl), CO(+air)	360	100–3,000 ppm	51
Air, Pt YSZ Pt, (CuO-ZnO/Al ₂ O ₃), CO(+air)	450	0–10,000 ppm	52
Air, Pt YSZ Pt, CO(+air)	500	32–800 ppm	53
CO(+air), LaMnO ₃ YSZ LaMnO ₃ , (Pt-Al ₂ O ₃), CO(+air)	350–450	0–7,000 ppm	54
CO(+air), Pt, SnO ₂ YSZ CdO, Pt, CO(+air)	600	20–4,000 ppm	55

^aRE reference electrode, SE sensing electrode, cat catalyst

At the electrolyte–electrode interface, however, O₂ and CO can establish a mixed potential by reduction of O₂ and oxidation of CO as shown in reactions (17.12) and (17.13), before reaching equilibrium concentrations:



At the sensing electrode, the electrochemical oxidation (Eq. 17.13) and reduction (Eq. 17.12) occur simultaneously and establish a local cell. When the rates of these reactions are equal to one another, the potential of the sensing electrode is a mixed potential.

Throughout the 1980s and 1990s, a large number of mixed potential-type CO sensors were reported. Most of these reports concerned sensors employing YSZ as a solid electrolyte,^{49–55} as listed in Table 17.4, due to its high O²⁻ ion conductivity. During the preliminary investigation of mixed potential CO sensors with YSZ, the noble metal Pt was widely used as a sensing electrode, in a manner similar to its use in conventional equilibrium potentiometric sensors. Sensors using Pt electrodes, however, exhibited low EMF responses to the target gas at elevated temperatures above 500 °C and poor gas selectivity below 400 °C if the catalytic layer was not covered by the Pt electrode. As a result, there were efforts to improve the CO-sensing performance of these devices. One approach used a Pt-based alloy electrode, while another applied a metal oxide as the sensing electrode. Vogel et al. reported that sensor EMF responses were improved by using Pt-based alloy electrodes.⁵⁶ Among the Pt-based alloys, Pt-Au alloy electrodes exhibited the highest response to CO, although such sensors also responded to H₂. The increased sensitivity of sensors incorporating alloy electrodes was considered to be due to the reduced catalytic activity for the gas-phase oxidation of CO resulting from alloying Pt with Au. Although the adoption of the Pt-based alloy electrodes was effective at improving the sensitivity at high

Table 17.5 EMF responses to CO and H₂ of YSZ-based sensors incorporating various metal oxides as the sensing electrode at 600 °C

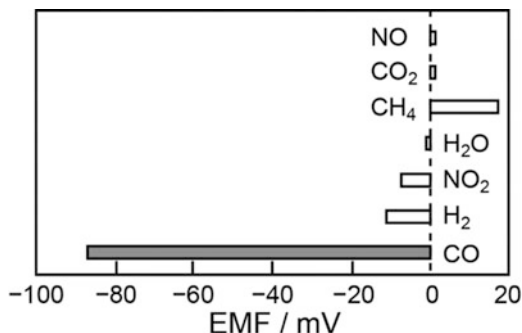
Metal oxide	EMF (mV)	
	200 ppm H ₂	200 ppm CO
TiO ₂	-7	0
Cr ₂ O ₃	0	0
Mn ₂ O ₃	0	0
Fe ₂ O ₃	-4	-2
Co ₃ O ₄	0	0
NiO	0	0
CuO	-1	0
ZnO	-125	-44
MoO ₃	-5	-1
CdO	-104	-126
In ₂ O ₃	-70	-47
SnO ₂	-92	-50
Sb ₂ O ₃	-15	-7
WO ₃	-2	-1
PbO ₂	0	0
Pt only	-3	-1

temperatures, there was still the problem of poor selectivity. As a result, various different metal oxides were studied as potential candidates for the sensing electrode.

Miura et al. intensively investigated mixed potential CO sensors with various kinds of metal oxide electrodes in 1998. To evaluate the efficiency of metal oxide electrodes for selective CO detection, 15 different metal oxides were used as the sensing electrodes in a YSZ-based sensor (reference electrode: Pt). Table 17.5 summarizes the observed sensitivities to 200 ppm CO and 200 ppm H₂ at 600 °C. Although the sensitivities to CO and H₂ were low when Pt metal was used as the sensing electrode, as described above, remarkable increases in the sensitivity to CO were obtained with sensors using ZnO, CdO, In₂O₃, and SnO₂, suggesting that some metal oxides can improve the sensitivity to CO when applied as the sensing electrode. Although these metal oxides do exhibit high sensitivity to H₂, their sensitivity to H₂ is almost equal to that of sensors fabricated with CdO or SnO₂. Miura et al. produced a sensor using two kinds of metal oxides CdO and SnO₂ as the sensing electrode and investigated the CO-sensing performance by measuring the EMF response between CdO and SnO₂ electrodes. Figure 17.15 displays the cross-sensitivity of the YSZ sensor with CdO and SnO₂ electrodes at 600 °C. By combining CdO and SnO₂, selectivity to CO is greatly improved, although there still remains the issue of sensitivity to H₂, NO₂, and CH₄.

Mixed potential CO sensors incorporating oxide ion conductors other than YSZ have been investigated, but superior sensing performance offering both high selectivity and sensitivity has not yet been realized. The primary factor in improving these mixed potential sensors to the point where they can be marketed will be the discovery of new sensing electrode materials which provide both high selectivity and sensitivity.

Fig. 17.15 Cross-sensitivity to various gases of a YSZ sensor with CdO and SnO₂ electrodes at 600 °C.



References

- Gauthier M, Chamberland A (1977) Solid-state detectors for the potentiometric determination of gaseous oxides: I. measurement in air. *J Electrochem Soc* 124:1579–1583
- Côté R, Bale CW, Gauthier M (1984) K₂CO₃ solid electrolyte as a CO₂ probe: decomposition measurements of CaCO₃. *J Electrochem Soc* 131:63–67
- Saito Y, Maruyama T, Matsumoto Y, Kobayashi K, Yano Y (1984) Applicability of sodium sulfate as a solid electrolyte for a sulfur oxides sensor. *Solid State Ion* 14:273–281
- Miura N, Yao S, Shimizu Y, Yamazoe N (1992) Carbon dioxide sensor using sodium ion conductor and binary carbonate auxiliary electrode. *J Electrochem Soc* 139:1384–1388
- Miura N, Yao S, Shimizu Y, Yamazoe N (1992) High-performance solid-electrolyte carbon dioxide sensor with a binary carbonate electrode. *Sensor Actuat B* 9:165–170
- Köhler J, Imanaka N, Adachi G (1998) Multivalent cationic conduction in solids. *Chem Mater* 10:3790–3812
- Imanaka N, Kamikawa M, Tamura S, Adachi G (1999) Carbon dioxide gas sensor based on trivalent Sc³⁺ ion conducting Sc₂(WO₄)₃ solid electrolyte. *Electrochem Solid-State Lett* 2:602–604
- Imanaka N, Kamikawa M, Tamura S, Adachi G (2001) Carbon dioxide gas sensor with multivalent cation conducting solid electrolytes. *Sensor Actuat B* 77:301–306
- Imanaka N, Kobayashi Y, Fujiwara K, Asano T, Okazaki Y, Adachi G (1998) Trivalent rare earth ion conduction in the rare earth tungstates with the Sc₂(WO₄)₃-type structure. *Chem Mater* 10:2006–2012
- Imanaka N, Kamikawa M, Adachi G (2001) A carbon dioxide gas sensing with the combination of divalent magnesium cation and divalent oxide anion conducting solid electrolytes with neodymium oxycarbonate based auxiliary electrode. *Electroanalysis* 13:1291–1294
- Imanaka N, Ogura A, Kamikawa M, Adachi G (2001) High performance CO₂ gas sensing with the combination of multivalent ion conducting solid electrolytes with water-insoluble auxiliary electrode. *Chem Lett* 30:718–719
- Imanaka N, Kamikawa M, Adachi G (2002) A carbon dioxide gas sensing with the combination of multivalent cation and anion conductors with water insoluble oxycarbonate based auxiliary electrode. *Anal Chem* 74:4800–4804
- Imanaka N, Ogura A, Adachi G (2003) Practical smart CO₂ gas sensor applicable for in-situ real time monitoring at every emitting site. *Electrochemistry* 71:14–18
- Tamura S, Imanaka N, Kamikawa M, Adachi G (2000) A CO₂ sensor based on a trivalent ion conducting Sc_{1/3}Zr₂(PO₄)₃ solid electrolyte. *Adv Mater* 12:898–901
- Imanaka N, Ogura A, Kamikawa M, Adachi G (2001) CO₂ gas sensor with the combination of tetravalent zirconium cation and divalent oxide anion conducting solids with water-insoluble oxycarbonate electrode. *Electrochem Commun* 3:451–454

16. Lee JS, Lee JH, Hong SH (2003) Solid-state amperometric CO₂ sensor using a lithium-ion conductor. *Sensor Actuat B* 89:311–314
17. Lee JS, Lee JH, Hong SH (2003) NASICON-based amperometric CO₂ sensor using Na₂CO₃–BaCO₃ auxiliary phase. *Sensor Actuat B* 96:663–668
18. Lee JS, Lee JH, Hong SH (2003) Solid-state amperometric CO₂ sensor using a sodium ion conductor. *J Eur Ceram Soc* 24:1431–1434
19. Tamaki J, Akiyama M, Xu C, Miura N, Yamazoe N (1990) Conductivity change of SnO₂ with CO₂ adsorption. *Chem Lett* 19:1243–1246
20. Yoshioka T, Mizuno N, Iwamoto M (1991) La₂O₃-loaded SnO₂ element as a CO₂ gas sensor. *Chem Lett* 20:1249–1252
21. Mizuno N, Yoshioka T, Kato K, Iwamoto M (1993) CO₂-sensing characteristics of SnO₂ element modified by La₂O₃. *Sensor Actuat B* 13:473–475
22. Sakama H, Saeki S, Ono A, Ichikawa N, Tanokura A, Uetsuka H, Onishi H (2004) CO₂ sensing properties of La-loaded SnO₂ thin films prepared by sputtering. *Chem Lett* 33:1080–1081
23. Hanada M, Onaga K, Nishiguchi M, Onouchi T (1999) Development of CO₂ gas sensor using La³⁺ and Y³⁺ doped SnO₂ semiconductor. *Chem Sensors* 15(Suppl B):130–132
24. Mizuno N, Kato K, Yoshioka T, Iwamoto M (1992) A remarkable sensitivity of CaO-loaded In₂O₃ element to CO₂ gas in the presence of water vapor. *Chem Lett* 21:1683–1684
25. Ishihara T, Kometani K, Hashida M, Takita Y (1990) Mixed oxide capacitor of BaTiO₃–PbO as a new type CO₂ gas sensor. *Chem Lett* 19:1163–1166
26. Ishihara T, Kometani K, Mizuhara Y, Takita Y (1992) Mixed oxide capacitor of CuO–BaTiO₃ as a new type CO₂ gas sensor. *J Am Ceram Soc* 75:613–618
27. Liao B, Wei Q, Wang K, Liu Y (2001) Study on CuO–BaTiO₃ semiconductor CO₂ sensor. *Sensor Actuat B* 80:208–214
28. Wei Q, Luo WD, Liao B, Liu Y, Wang G (2000) Giant capacitance effect and physical model of nano crystalline CuO–BaTiO₃ semiconductor as a CO₂ gas sensor. *J Appl Phys* 88:4818–4824
29. Leal O, Bolívar C, Ovalles C, García JJ, Sepidel Y (1995) Reversible adsorption of carbon dioxide on amine surface-bonded silica gel. *Inorg Chim Acta* 240:183–189
30. Rocchia M, Garrone E, Geobaldo F, Boarino L, Sailor MJ (2003) Sensing CO₂ in a chemically modified porous silicon film. *Phys Stat Sol (a)* 197:365–369
31. Mills A, Monaf L (1996) Thin plastic film colorimetric sensors for carbon dioxide: effect of plasticizer on response. *Analyst* 121:535–540
32. Mills A, Chang Q, McMurray HM (1992) Equilibrium studies on colorimetric plastic film sensors for carbon dioxide. *Anal Chem* 64:1383–1389
33. Mills A, Lepre A, Wild L (1997) Breath-by-breath measurement of carbon dioxide using a plastic film optical sensor. *Sensor Actuat B* 39:419–425
34. Kawabata Y, Kamichika T, Imasaka T, Ishibashi N (1989) Fiber-optic sensor for carbon dioxide with a pH indicator dispersed in a poly(ethylene glycol) membrane. *Anal Chim Acta* 219:223–229
35. Cooney CG, Towe BC, Eyster CR (2000) Optical pH, oxygen and carbon dioxide monitoring using a microdialysis approach. *Sensor Actuat B* 69:183–188
36. Marazuela MD, Moleno-Bondi MC, Orellana G (1995) Enhanced performance of a fibre-optic luminescence CO₂ sensor using carbonic anhydrase. *Sensor Actuat B* 29:126–131
37. Zhujun Z, Seitz WR (1984) A carbon dioxide sensor based on fluorescence. *Anal Chim Acta* 160:305–309
38. Wolfbeis OS, Weis LJ, Leiner MJP, Ziegler WE (1988) Fiber-optic fluorosensor for oxygen and carbon dioxide. *Anal Chem* 60:2028–2030
39. Mills A, Chang Q (1993) Fluorescence plastic thin-film sensor for carbon dioxide. *Analyst* 118:839–843
40. Nakamura N, Amao Y (2003) An optical sensor for CO₂ using thymol blue and europium(III) complex composite film. *Sensor Actuat B* 92:98–101

41. Nakamura N, Amao Y (2003) Optical CO₂ sensor with the combination of colorimetric change of pH indicator and internal reference luminescent dye. *Bull Chem Soc Jpn* 76:1459–1462
42. Amao Y, Nakamura N (2004) Optical CO₂ sensor with the combination of colorimetric change of α -naphtholphthalein and internal reference fluorescent porphyrin dye. *Sensor Actuat B* 100:347–351
43. Hosoya A, Tamura S, Imanaka N (2013) Low-temperature-operative carbon monoxide gas sensor with novel CO oxidizing catalyst. *Chem Lett* 42:441–443
44. Zhang Y, Cui S, Chang J, Ocola LE, Chen J (2013) Highly sensitive room temperature carbon monoxide detection using SnO₂ nanoparticle-decorated semiconducting single-walled carbon nanotubes. *Nanotechnology* 24:025503
45. Cho NG, Woo HS, Lee JH, Kim ID (2011) Thin-walled NiO tubes functionalized with catalytic Pt for highly selective C₂H₅OH sensors using electrospun fibers as a sacrificial template. *Chem Commun* 47:11300–11302
46. Zhang Y, Xu J, Xu P, Zhu Y, Yu W (2010) Decoration of ZnO nanowires with Pt nanoparticles and their improved gas sensing and photocatalytic performance. *Nanotechnology* 21:285501
47. Zhang J, Liu X, Xu M, Guo X, Wu S, Zhang S, Wang S (2010) Pt clusters supported on WO₃ for ethanol detection. *Sensor Actuat B* 147:185–190
48. Lee YC, Huang H, Tan OK, Tse MS (2008) Semiconductor gas sensor based on Pd-doped SnO₂ nanorod thin films. *Sensor Actuat B* 132:239–242
49. Shimizu F, Yamazoe N, Seiyama T (1978) Detection of combustible gases with stabilized zirconia sensor. *Chem Lett* 7:299–300
50. Okamoto H, Obayashi H, Kudo T (1980) Carbon monoxide gas sensor made of stabilized zirconia. *Solid State Ion* 1:319–326
51. Katsumoto M, Okamoto H, Kobayashi M (1985) *Denki Kagaku* 53:577–581
52. Li N, Tan TC, Zeng HC (1993) High-temperature carbon monoxide potentiometric sensor. *J Electrochem Soc* 140:1068–1073
53. Zhang ZY, Narita H, Mizusaki J, Tagawa H (1995) Detection of carbon monoxide by using zirconia oxygen sensor. *Solid State Ion* 79:344–348
54. Sorita R, Kawano T (1997) A highly selective CO sensor using LaMnO₃ electrode-attached zirconia galvanic cell. *Sensor Actuat B* 40:29–32
55. Miura N, Lu G, Yamazoe N (1997) Zirconia-based potentiometric sensor using a pair of oxide electrodes for selective detection of carbon monoxide. *J Electrochem Soc* 144:L198–L200
56. Voge A, Baier G, Schüle V (1993) Non-Nernstian potentiometric zirconia sensors: screening of potential working electrode materials. *Sensor Actuat B* 15:147–150

Part V
Data Treatment of Electrochemical
Sensors and Biosensors

Chapter 18

Data Treatment of Electrochemical Sensors and Biosensors

Elio Desimoni and Barbara Brunetti

18.1 Introduction

The ultimate aim of developing electrochemical sensors or biosensors, EBs, is proposing to the scientific community devices suitable for real sample analysis. It follows that sensor performances should be concretized by proper figures of merit, FM, estimated according to agreed protocols, and reported according to unambiguous formats. As far as we know the most frequently reported FM are those usually estimated in validation studies, e.g., linear range, limits of detection and quantification, precision, trueness, uncertainty, selectivity, and recovery (see for example reference (1)). Of course, developing and testing new EBs seldom need a complete validation study. Most frequently, papers are mainly aimed at reporting details of the method used to prepare the sensor, of experiments used for characterizing its chemical/biochemical/electrochemical/morphological features, and of its potential applications. But, if some analytical performances of the proposed sensor are presented to the reader, then they should be estimated by reliable approaches and allow a reasonably appropriate interpretation. However, while preparing a recent review paper dealing with glassy carbon electrode surface modified by acidic functionalities,² it was noticed that quite often some of the reported FM were ill defined or reported in an inadequate format.^{2,3} In such a situation, reconsidering how to estimate and to report them might be valuable to any experimentalist involved in developing EBs.

Based on many well-known books and guidelines,^{1,4–12} the matter here below is aimed at suggesting the simplest ways for estimating the selected FM, avoiding incorrect/unreasonable statements. Additional information is also given for eventual in-depth insights.

E. Desimoni (✉) • B. Brunetti

Department of Food, Environmental and Nutritional Sciences, University of Milan,
Via Celoria 2, 20133 Milan, Italy

e-mail: elio.desimoni@unimi.it; Barbara.brunetti@unimi.it

18.2 Linear Range and Regression Relationship

Almost any paper dealing with EBs reports a calibration curve. The calibration curve is the graphical representation of the measured signal as a function of the concentration (or sometimes of the quantity) of analyte, and the linearity defines the ability of the method to obtain test results proportional to the analyte concentration.¹ The calibration function is most frequently estimated by applying a regression technique in the linear range. When reporting a linear range, it is mandatory detailing how it was estimated. Sometimes, a “good” (may be larger than 0.9) correlation coefficient, r , is assumed as a proof of linearity. This is not correct.^{13–16} The correlation coefficient is an indicator of correlation, not of linearity. According to the Analytical Methods Committee of the Royal Chemical Society, choosing r as an indicator of linearity could be accepted only for $r > 0.9991$.¹³

A simple way to check the “absence of nonlinearity” (linearity can never be proved) is the visual inspection of residuals.^{5,9–12,17–19} These are the differences between any experimental signal and the relevant signal value predicted by the regression line. Residuals must be properly scaled to facilitate their inspection. Figure 18.1 shows few examples of residual plots to be used in regression diagnostic.

Ideally, residuals should be randomly distributed around zero, thus evidencing the absence of a clear nonlinearity (see Fig. 18.1a). Moreover, residuals should not increase on increasing concentration (see Fig. 18.1c). As far as we know, the residuals window is quite rarely reported in the published papers. Figure 18.2 shows an example of calibration completed by the residual window. Of course, less qualitative evaluations of linearity are possible (see Sect. 18.2.1).

Sometimes, when describing the analytical performances of the proposed sensor, authors state that the explored analytical range is characterized by two (or even

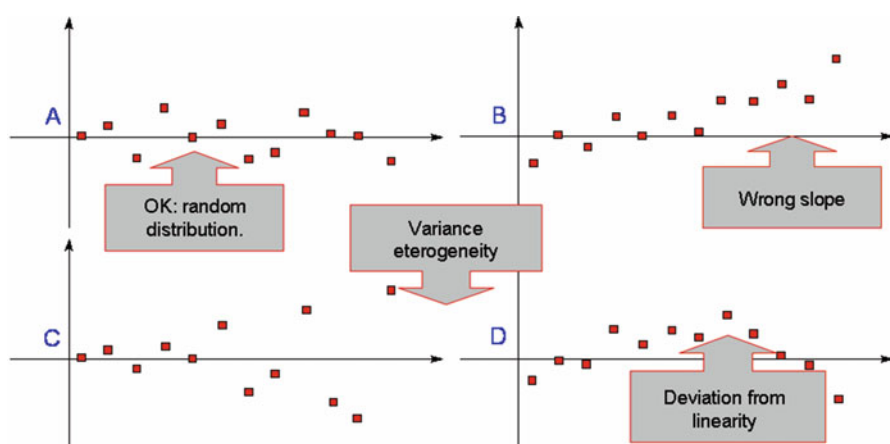


Fig. 18.1 Distributions of regression residuals. (a) Satisfactory distribution (absence of nonlinearity); (b) wrong slope; (c) probable heteroscedasticity; (d) evidence of nonlinearity

Fig. 18.2 Calibration of caffeine at a Nafion-modified glassy carbon electrode showing the regression line and the relevant residuals

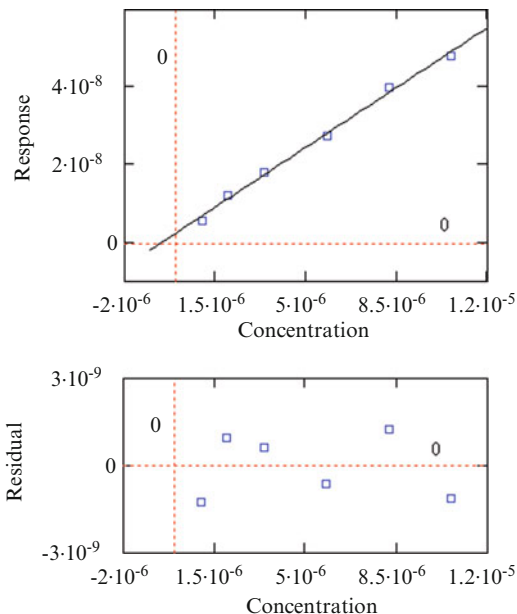
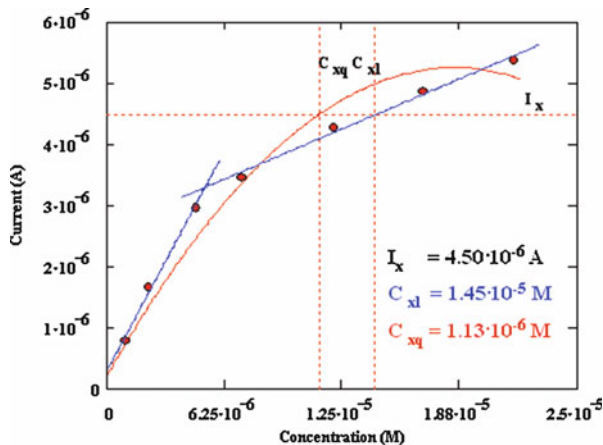


Fig. 18.3 Calibration plot relevant to the analysis of uric acid at a taurine-modified glassy carbon electrode. Experimental point can be fitted by nonlinear least-square regression. The two additional lines show the fitting of the curvilinear dynamic range by two subsequent linear ranges



three) subsequent linear portions. This is frequently observed in the case of adsorption mechanisms since linear ranges could have different slopes due to the different amounts of analyte adsorbed on the modified electrode surface: the analyte could be directly adsorbed as a monolayer onto the modifier at low concentrations, and as a multilayer at higher concentrations. This causes the calibration curve to break. But reporting two/three linear ranges for stating a larger than real linear range should be avoided, since it actually means that the functional relationship is not linear at all.³

Figure 18.3 shows an example highlighting possible systematic errors resulting from such a practice. The explored data are displayed in Table 18.1. The dispersion

Table 18.1 Experimental data used in Fig. 18.3

C/M	S/A
9.9800×10^{-7}	8.08×10^{-7}
2.2399×10^{-6}	1.66×10^{-6}
4.7053×10^{-6}	2.97×10^{-6}
7.1474×10^{-6}	3.47×10^{-6}
1.2016×10^{-5}	4.29×10^{-6}
1.6837×10^{-5}	4.86×10^{-6}
2.1612×10^{-5}	5.39×10^{-6}

plot is clearly not linear. The regression relationship, RR, obtained by nonlinear least-square regression is

$$y(x) = -1.4806 \cdot 10^4 \cdot x^2 + 0.5471 \cdot x + 2.0089 \cdot 10^{-7} \quad (18.1)$$

In the same Fig. 18.3, experimental data are also fitted by ordinary linear least-square regression, OLS, over two linear ranges. The two RRs are

$$y(x) = 0.5759 \cdot x + 2.8795 \cdot 10^{-7} \quad (\text{lowest 3 calibration points}) \quad (18.2)$$

and

$$y(x) = 0.1313 \cdot x + 2.6109 \cdot 10^{-6} \quad (\text{highest 4 calibration points}) \quad (18.3)$$

Let us consider, for example, a signal $I_x = 4.5 \times 10^{-6}$ A (see Fig. 18.3). The interpolation of the quadratic (Eq. 18.1) and linear (Eq. 18.3) RRs returns $C_{xq} = 1.13 \times 10^{-5}$ M and $C_{xl} = 1.43 \times 10^{-5}$ M, respectively. The obvious conclusion is that using RRs estimated by choosing two or more linear ranges, in place of the nonlinear RR, can return more or less biased interpolated concentrations. When the dispersion plot is clearly not linear, using data transformations,^{9,11,18} reducing the concentration range or (why not?) using a nonlinear regression would certainly be more correct.

18.2.1 About Ordinary Least-Square Regression

The estimation of RRs is usually performed by ordinary least-square linear regression. This should be done by preferably testing at least six different concentration levels within the linear range plus the blank (if this last exists or it is measurable).¹ To minimize eventual experimental drifts, test samples should be examined in random order (not in order of increasing concentration values). Possibly, standard or test samples should be analyzed in duplicate (or more), especially when it is not possible to analyze at least six standards. If repeating the analysis of some

standards, independent values must be used. Of course, calibrations should be performed in a matrix having a composition as close as possible to that of real samples. If this is not possible, the method of standard additions is mandatory.

It should be also remembered that OLS relies on some mandatory assumptions^{11,18,19}:

1. Experimental errors associated with the independent variable (concentration) should be negligible compared to those associated with the dependent variable (signal).
2. Errors associated with the dependent variable must be normally distributed.
3. The analytical system must be homoscedastic; for example, precision must not significantly change on changing concentration.
4. Signals must be a linear function of concentration (whatever the scatter diagram, OLS always return a linear function).

Even when papers describing new EBs are not involved in complete validation studies, nevertheless some information about the above points should significantly improve their quality.

Assumption (1) is usually satisfied when working with signal/concentration RRs. This is because concentrations are assumed error free. Such a kind of regression is known as Model I regression.²⁰ On the contrary, when both the dependent and independent variables are affected by experimental uncertainty, a Model II regression analysis is mandatory. This is usually the case when dealing with method comparison (see for example references^(9, 20–23)).

Few tests are available for checking assumption (2). However, this task is not always meaningful since the available tests always need a consistent number of repetitions of the analysis of the examined concentration level, a condition rarely verified when developing EBs. The Shapiro-Wilk test can be performed by using at least three replicates,^{24,25} but the result obtained by using such a low number of data is hardly significant.

Assumption (3) can be easily checked by Bartlett or Cochran tests.^{9–11} But also these tests require performing some replicates of the analysis of the standard samples used in the calibration. The Cochran test is simpler, but all variances associated to the different concentration levels must have the same degrees of freedom. The Bartlett test does not suffer of this limitation, but it is a little more complicated.

When precision significantly changes with concentration, the analytical system is heteroscedastic and a weighted least-square regression is mandatory.^{10,11,18,25,26} The literature reports examples of in-house-developed worksheets that allow performing weighted regression along with all (or many of) the abovementioned tests.^{27,28}

Assumption (4) can be easily checked by examining the residuals window, as above mentioned. But more suitable statistical tests, like lack-of-fit or Mandel test, are available.^{12,17,26}

18.2.2 About Rounding Results

When reporting the results of a calibration, it should be mandatory reporting also the uncertainty intervals of slope and intercept. The raw RR estimated in the case of Fig. 18.2 is the following:

$$y(x) = (4.4059 \pm 0.23126) \cdot 10^{-3} \cdot x + (2.5398 \pm 1.85825) \cdot 10^{-9} \quad (P : 95\%; n = 6) \quad (18.4)$$

Slope and intercept are reported with their uncertainties, estimated as the product of relevant standard deviations by the Student *t*-value (two-tails, $n - 2$ degrees of freedom, $P = 95\%$). In this equation, n is the number of data points and P the confidence level. Reporting the bare standard deviations of slope and intercept as a sort of uncertainty of the relevant parameters should be avoided, since uncertainties must be quoted at a certain confidence level. Moreover, according to the *Guide to the expression of uncertainty in measurement*, it is rarely necessary reporting the uncertainty at more than two significant digits.⁴ By rounding at the second significant digit of uncertainty, Eq. (18.4) changes to

$$y(x) = (4.41 \pm 0.23) \cdot 10^{-3} \cdot x + (2.5 \pm 1.9) \cdot 10^{-9} \quad (P : 95\%; n = 6) \quad (18.5)$$

Slope and intercept are rounded to the same decimal place as their uncertainty. Hopefully, as done in Eqs. (18.4) and (18.5), the number of data points, n , or the degrees of freedom, ν , and the confidence level should complete the information. Stating that the proposed sensor is characterized by a linear RR without the information above specified is almost meaningless.

The same rounding format should be used when reporting interpolated/extrapolated concentrations of the analyte.

18.3 Limit of Detection

The limit of detection, *LOD*, is the lowest analyte concentration that can be measured with reasonable statistical certainty.¹ A lively debate is still open about how *LOD* can be estimated.^{6-8,29-42} According to a renowned expert, at the end of 1990s the current meanings attached to the expression *detection limit* led to numerical values spanning three orders of magnitude.^{29,37} Even today, the meaning/quality of *LOD* estimates is often unsatisfactory.

A first observation concerns the use of estimating *LOD* as the signal-to-noise (S/N) ratio. Even nowadays, the S/N approach is frequently adopted by many researchers, as recently underlined.³ It can be easily estimated, being based on a more or less subjective evaluation of the noise (the stochastic component of any experimental signal) and explicitly recognizing only false-positive errors while

accepting a 50 % probability of false-negative errors.³⁷ This explains why this approach was enclosed in the Prehistory section of the Historical Background part of the cited review.³⁷

This practice can be dismissed by choosing few equally simple approaches. In particular, the S/N approach can be replaced by those represented by the following equations^{1,11,18,30,31,37}:

$$LOD = \frac{3.0 \cdot \sigma_B}{b} \quad (18.6)$$

and

$$LOD = \frac{2 \cdot 1.645 \cdot \sigma_B}{b} = \frac{3.29 \cdot \sigma_B}{b} \quad (18.7)$$

in which σ_B is the standard deviation of the population of blank signals and b is the slope of the regression line. In practice, σ_B is often substituted by s_B , the sample standard deviation. The 3.29 multiplier is usually rounded to 3.3. Of course these approaches imply some more work, since the blank must be analyzed by performing a consistent number of replicates (at least ten¹), but relies on more statistical bases than the S/N one. The two equations are quite different, since Eq. (18.6) is used for controlling false-positive error at about 0,135 % and false-negative errors at 50 %, while Eq. (18.7) is chosen when controlling both errors at 5 % (see for example references^(11, 29–31)). Equations (18.6) and (18.7) are based on several severe assumptions which can hardly be satisfied:

1. Random errors must be normally distributed (but very likely the distribution of signals close to a physical limit—absence of the analyte—is not Gaussian).
2. Systematic errors must be absent.
3. The blank must be a sample in which the analyte concentration is equal to zero.
4. The analytical system in the explored concentration range is homoscedastic.
5. The blank is the same matrix to all the samples.

Nevertheless Eqs. (18.6) and (18.7) are widely accepted since they allow reasonable, and above all simple, estimations of the limit of detection.

Using the S/N approach in place of those represented by Eqs. (18.6) and (18.7) is often justified in terms of an unacceptable increase of time and cost of the measurements, of the unavailability of the real blank, or of the impossibility to measure the signal of the blank. This last problem can usually happen when using instrumentations which automatically subtract the background from the signal of any test sample. In these cases it is possible spiking the blank with the lowest analyte concentration allowing the measurement of the minimum signal different from zero. However, spiking of the blank with the analyte can significantly reduce the value of the standard deviation of the signal with respect to the true σ_B . In fact, it is well known that experimental precision exponentially decreases on decreasing the concentration (see Sect. 18.4.1). It follows that even a limited spiking of the blank

with the analyte can significantly reduce the value of the standard deviation of the measured signal with respect to the true σ_B , so as to obtain a somewhat optimistic *LOD*.

Alternatively, it is possible replacing σ_B by the residual standard deviation of the regression, $s_{y/x}$, also known as standard error of the regression. This because a fundamental assumption of OLS is that each point of the regression line, including the point representing the blank, has a normally distributed y variation with a standard deviation estimated by $s_{y/x}$.¹¹ This is a convenient approach because $s_{y/x}$ is already estimated in OLS calculations necessary to obtain the RR and, in this way, no additional work is necessary.

All the abovementioned approaches cannot be applied in the case of heteroscedastic systems.¹¹ A paper was aimed at evaluating some approaches useful for estimating *LOD* when data are characterized by a significant change of precision with concentration.³⁸

Of course, much reliable and/or less approximated approaches exist (see for example references (6–8) and (30–38, 40–42)), but those above mentioned can be more easily accepted by experimentalists, since they require very simple calculations.

18.3.1 About the Limit of Detection

The real meaning of the *LOD* needs some clarifying. It is quite evident that repeating the measurements necessary for estimating an *LOD* would undoubtedly return a more or less different value. This because any *LOD* is simply a point estimate test statistic for the true *LOD* composite population parameter.³¹ Moreover, it is very probable that the real *LOD* distribution be skewed or abnormal,³⁹ so that estimating the *LOD* on the basis of a hypothetical normal distribution is questionable. This potential limited reliability of *LOD* estimates justifies the use of the abovementioned, heavily approximated approaches.

Because of these limitations, *LOD* estimates should always be completed by detailed information about the relevant experimental condition (number of measurements, matrix, selected approach, analytical method). This raises the question of the comparability of *LOD* estimates with other values from different authors (may be relevant to different sensors and/or experimental techniques/and or matrices, approach, etc.). A really meaningful comparison should accurately take into account any difference between experimental conditions and approaches.

The *LOD* allows only a binary decision, since it can state the presence/absence of the analyte. Reasonably, a quantitative measurement can only be performed at concentration levels somewhat higher than the *LOD*. The limit of quantification, *LOQ*, is calculated as an arbitrary multiple of *LOD*. The most frequent choices are those in which the multiplier of σ_B (or s_B , $s_{y/x}$) in Eqs. (18.6) and (18.7) is chosen equal to 5, 6, or 10.¹ Choosing the multiplier and reporting the *LOQ* is crucial, since *LOQ* is the real lower limit of the linear range.

18.4 Precision

Precision is the closeness of agreement between independent test results obtained under stipulated conditions.¹ Repeatability is the precision estimated by a single analyst using a given equipment over a short time scale. Reproducibility is the precision estimated by elaborating the results obtained by a number of laboratories (for example in among-laboratories comparison). A third type of precision is sometimes known as intermediate precision. In this last case, it is estimated in a single laboratory but by different analysts, or over extended time scales.

Repeatability and reproducibility can be estimated by analyzing standards, reference material, or fortified sample blanks at different concentration levels across the working range. A minimum of ten independent repeats is necessary.¹ Repeatability and reproducibility are usually presented as absolute standard deviations (σ_R in the case of reproducibility and σ_r of repeatability) or relative standard deviations (RSD_R and RSD_r) possibly evaluated at different concentration levels. When reporting the relevant information, data should be accompanied by the relevant concentration levels and number of repeats.

Reproducibility or repeatability can also be reported as repeatability or reproducibility limits, r or R , respectively.^{1,43} They can be then obtained by the equations

$$r = 2 \cdot \sqrt{2} \cdot \sigma_r = 2.8 \cdot \sigma_r \quad (18.8)$$

and

$$R = 2 \cdot \sqrt{2} \cdot \sigma_R = 2.8 \cdot \sigma_R \quad (18.9)$$

R and r enable the experimentalist to decide whether the difference between duplicate determinations of a test sample, under reproducibility or repeatability conditions, is significant.¹

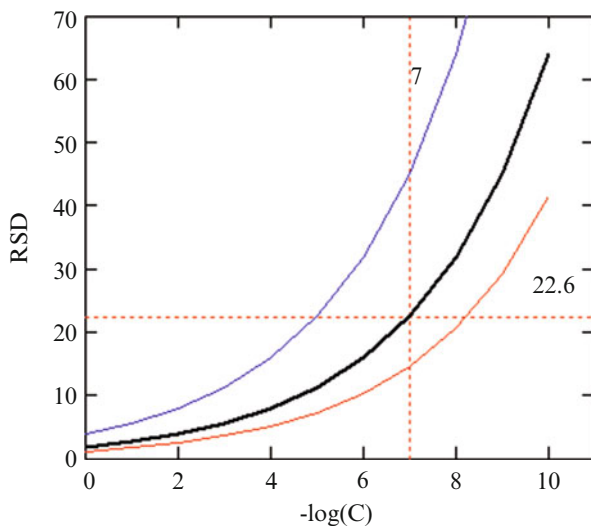
18.4.1 Horwitz Equation

The reliability of repeatability and reproducibility RSD estimates can be tested against values obtained by the Horwitz empirical equation.⁴⁴⁻⁴⁶ The equation allows an a priori estimation of the RSD as a function of the analyte concentration expressed as mass/mass units (e.g., as mass fraction: $1 \text{ mg/kg} = 10^{-6}$, $1 \text{ }\mu\text{g/kg} = 10^{-9}$) whatever analyte, matrix, and method of measurement:

$$RSD = \pm 2^{(1-0.5 \cdot \log(C))} \quad (18.10)$$

Among-laboratories RSD (RSD_R) values are expected to range within one-half to twice the value predicted by Eq. (18.10). Within-laboratory RSD (RSD_r) is expected

Fig. 18.4 Horwitz curves: RSD (—); $RSD_R = 2 \times RSD$ (—); $RSD_r = 0.65 \times RSD$ (—). At 10^{-7} concentration levels (100 ppb level) RSD and RSD_r values are about 22.63 and 14.7 %



to range within one-half to two-thirds of RSD_R . The so-called Horwitz curves are reported in Fig. 18.4. Owing to the technological progress in analytical measurements, some corrections of the Horwitz equation may be convenient.⁴⁷ Nevertheless, Eq. (18.10) it is still used, especially in the food analysis field, as a good predictor of RSD_R within the 10^{-8} to 10^{-1} mass fraction.⁴⁷

In routine measurements, the Horwitz equation can be used to evaluate the reliability of experimental standard deviations. Authors must never use the values obtained by Eq. (18.10) in place of their experimental ones.

18.5 Trueness

This figure of merit is less frequently mentioned in papers relevant to the development of EBs. Trueness is the closeness of agreement between the average value obtained from a large set of test results and an accepted reference value.¹ In the simplest way, it can be estimated by analyzing suitable Certified Reference Materials, *CRMs*. In such a case, one can carry out an adequate series of measurements of the *CRM* and then perform a simple *t*-test for the comparison of the experimental mean with the certified value (see for example reference¹¹):

$$t_{\text{exp}} = \frac{|x_{\text{mean}} - C_{\text{CRM}}| \cdot \sqrt{N}}{s} \quad (18.11)$$

where x_{mean} and C_{CRM} are the experimental mean relevant to the analysis of the CRM and the certified value, respectively, N is the sample size, and s is the sample standard deviation. If t_{exp} exceeds the critical two-tail t-value for $N - 1$ degrees of freedom and the selected confidence level, P , then one can reject the hypothesis of the absence of a difference between x_{mean} and C_{CRM} . Of course, tested CRM should mimic as much as possible analyte concentration and matrix composition of the real samples to be analyzed by the sensor.

An alternative way to estimate trueness is to analyze a series of test samples by the method based on the developed sensor and by another method (preferably a reference/validated method) based on different physical/chemical principles. This because it is quite unlikely that the second method can suffer from the same systematic errors. Method comparison must be performed by specific regression techniques since, in its case, assumption (1) of the OLS method is not valid anymore: both variables are affected by experimental errors (see Sect. 18.2.1) and Model II regression methods are mandatory. The relevant literature information is unexpectedly plentiful, since disciplines interested in such a kind of comparison span from statistics to astronomy, geology, physics, chemistry, biology, allometry, industrial pharmacology, and medicine (references ^(21–23) and ^(48–50) allow a first overview on method comparison).

18.6 Uncertainty

Uncertainty of measurements, UOM , is rarely estimated when developing EBs. The Guide to the Expression of Uncertainty in Measurements, GUM, defines uncertainty as a parameter associated with the result of a measurement that characterizes the dispersion of the values that could reasonably be attributed to the measurand.⁴ The GUM, accepted as the master reference on UOM throughout the testing community, reports general rules for evaluating and expressing this figure of merit. The most detailed guideline for UOM estimation according to the GUM is the EURACHEM/CITAC Guide.⁵¹

According to the abovementioned references, UOM can be estimated, by the so-called modelling approach or bottom-up approach as expanded uncertainty, U . By a comprehensive mathematical model of the measurement procedure

1. Every uncertainty contribution identified along the whole analytical procedure is associated with a dedicated input quantity, an uncertainty component, $u(y)$.
2. All components evaluated individually are combined as variances. The result of the calculation is the combined standard uncertainty, $u_c(y)$.
3. At last, the expanded uncertainty, U , is obtained by multiplying the total uncertainty, estimated as combined standard uncertainty, $u_c(y)$, by the coverage factor k :

$$U = k \cdot u_c(y) \quad (18.12)$$

Multiplying $u_c(y)$ by k allows associating a level of confidence to U .

Usually, k is set to 2 for providing the interval within which the value of the measurand is believed to lie with a 95 % level of confidence. Such an approach can be quite challenging since some contributions can be erroneously ignored or unnecessarily duplicated.

Alternative approaches to uncertainty evaluation are currently considered, since the GUM approach is often criticized as inapplicable to chemical systems.⁵² This explains why alternative “empirical” approaches have recently raised attention. They are based on whole-method performance investigations designed and conducted so as to comprise the effects from as many relevant uncertainty sources as possible. Such alternative approaches are fully compliant with the GUM, provided that the GUM principles are observed. Whatever approach is chosen, uncertainty evaluation is a difficult task, prone to mistakes. Several studies have shown that measurement uncertainty is often significantly underestimated.

Even a base introduction to the existing approaches is outside the aim of this chapter. Interested reader can find all the necessary information in the abovementioned references.

18.7 Selectivity

Selectivity is reported in almost any paper dealing with EBs. Selectivity is the ability of a method to accurately determine the analyte of interest in the presence of other components in a sample matrix under the stated conditions of the test.¹ Attention is called at the difference between selectivity and specificity. In the opinion of many, specificity indicates an absolute, ultimate selectivity (a quite rare case).^{53,54} But agreement is not universal.

Selectivity can be estimated by analyzing test samples spiked with the suspected interferents alongside with an unspiked portion of a test sample. The comparison of the results allows evidencing if the presence of a given interferent enhances or inhibits the detection and quantification of the analyte. When testing only one interfering species, one could use the known t -test for comparing two experimental means.^{9–11,19} When testing the influence of a larger number of interferents, so that it is necessary comparing some means, the analysis of variance is more suitable.

When evaluating the performances of EBs, suspected interferents should be added at concentration levels as close as possible to those in which they are present in test samples. The evaluation of the effects of their presence should be done after waiting for a suitable time, in order to allow their equilibration with the test sample. Interferents potentially present in sample matrix, their concentration level, and the chosen equilibration time should be properly mentioned within the selectivity information.

18.8 Recovery

Recovery is another figure of merit largely reported when describing the analytical performances of EBs. Recovery is the proportion of the amount of analyte, present in or added to the analytical portion of the test sample, which is extracted and presented for measurement.^{1,55} When developing electrochemical sensors or biosensors, recovery is usually estimated by spiking. This means that known amounts of the analyte are added to the blank or to suitable CRM or, most frequently, to ordinary test samples. Spiked samples are analyzed alongside an unspiked portion of the test sample. The difference between these two results allows estimating the recovered part of the added analyte, which can be compared with the known amount added. This type of recovery estimate is called the “surrogate recovery.”⁵⁵

In the most simple case, the percentage recovery, % R, is calculated as follows¹:

$$\%R = \frac{C_F - C_U}{C_A} \cdot 100 \quad (18.13)$$

where C_F is the analyte concentration in the fortified sample, C_U is the analyte concentration in the unfortified sample, and C_A is the analyte concentration (known, not determined by method) added in the unfortified sample.

A main drawback of recovery tests is that the added analyte may not be in the same physical/chemical status of that present in the unspiked test sample. If so, the estimated recovery will tend to be higher than that of the native analyte (that present in the test sample before spiking).¹ This will lead to a negative bias in a corrected analytical result.⁵⁵

When examining the performances of a sensor, any recovery test should be repeated at different times in order to ascertain if eventual time-dependent results suggest that spikes are still equilibrating with the sample. So, when reporting this figure of merit, it should be necessary reporting some information about the chosen equilibration time.

Acceptable recovery estimates are a function of the analyte concentration and of the purpose of the analysis. So recoveries more or less different from 100 % can also be accepted (see for example reference ⁽⁵⁶⁾).

The use of recovery information to evaluate the reliability of analytical results is controversial.⁵⁵ In studies aimed at presenting new electrochemical sensors, recovery is usually reported as an indicator of trueness. But recovery studies evidence eventual bias due to factors affecting the detection of the added analyte, and these factors do not necessarily affect to the same degree the analyte present in the unspiked sample. It follows that while a good recovery is not a guarantee of trueness, a poor recovery is certainly an indication of lack of trueness.

Acknowledgement Financial support by COFIN 2010-2011 (Programmi di Ricerca Scientifica di Rilevante Interesse Nazionale, MIUR, 2010AXENJ8_002) is acknowledged.

References

1. EURACHEM (1998) The fitness for purpose of analytical methods. 1st internet version. Available at <http://www.eurachem.org/images/stories/Guides/pdf/valid.pdf>. Accessed 15 Oct 2013
2. Desimoni E, Brunetti B (2012) Glassy carbon electrodes film-modified with acidic functionalities. *Rev Electroanal* 24:1481–1500
3. Desimoni E, Brunetti B (2013) Presenting analytical performances of electrochemical sensors. Some suggestions. *Accred Qual Assur* 25:1645–1651
4. ISO (1995) Guide to the expression of uncertainty in measurement
5. VAM (2003) Preparation of calibration curves. A guide to best practice. http://www.nmschembio.org/dm_documents/lgcvam2003032_xsjpgl.pdf. Accessed 15 Oct 2013
6. ISO (1997) Capability of detection—part 1: terms and definition
7. ISO (2000) Capability of detection—part 2: methodology in the linear calibration case
8. ISO (2003) Capability of detection—part 3: methodology for determination of the critical value for the response variable when no calibration data are used
9. Anderson RL (1987) *Practical statistics for analytical chemists*. Van Nostrand Reinhold, New York
10. Massart DL, Vandeginste BGM, Deming SL et al (2003) *Chemometrics: a textbook*, 5th edn. Elsevier, Amsterdam
11. Miller JN, Miller JN (2005) *Statistics and chemometrics for analytical chemistry*, 5th edn. Pearson Prentice Hall, Edinburgh
12. Funk W, Dammann V, Donnevert G (2007) *Quality assurance in analytical chemistry*, 2nd edn. Wiley-VCH, Weinheim
13. Analytical Method Committee (1988) Uses (proper and improper) of correlation coefficients. *Analyst* 113:1469–1471
14. Van Loco J, Elskens M, Croux C, Beernaert H (2002) Linearity of calibration curves: use and misuse of the correlation coefficient. *Accred Qual Assur* 7:281–285
15. Huber W (2004) On the use of the correlation coefficient r for testing the linearity of calibration functions. *Accred Qual Assur* 9:726
16. Hibbert DB (2005) Further comments on the (miss-)use of r for testing the linearity of calibration functions. *Accred Qual Assur* 10:300–301
17. Analytical Method Committee (1994) Is my calibration linear? *Analyst* 119:2363–2366
18. Müller JN (1991) Basic statistical methods for analytical chemistry. Part 2. Calibration and regression methods. A review. *Analyst* 116:3–14
19. Alfassi ZB, Boger Z, Ronen Y (2005) *Statistical treatment of analytical data*. Blackwell Science Ltd, Oxford
20. Otto M (2007) *Chemometrics*. Wiley-VCH, Weinheim
21. Ludbrook J (1997) Comparing methods of measurement. *Clin Exp Pharmacol Physiol* 24:193–203
22. Ludbrook J (2002) Statistical techniques for comparing measurers and methods of measurement: a critical review. *Clin Exp Pharmacol Physiol* 29:527–536
23. Warton DJ, Wright IJ, Falster DS et al (2006) Bivariate line-fitting methods for allometry. *Biol Rev* 81:259–291
24. Shapiro SS (1990) *How to test normality and other distributional assumptions*. ASCQ Quality Press, Milwaukee
25. Sen A, Srivastava M (1990) *Regression analysis theory. Methods and applications*. Springer, New York
26. Danzer K, Currie LA (1988) Guidelines for calibration in analytical chemistry. *Pure Appl Chem* 70:993–1014
27. Gort SM, Hoogerbrugger R (1995) A user-friendly spreadsheet program for calibration using weighted regression. *Chemometr Intell Lab Syst* 28:193–199
28. Desimoni E (1999) A program for the weighted linear least-squares regression of unbalanced response arrays. *Analyst* 124:1191–1196

29. Currie LA (1968) Limits for qualitative detection and quantitative determination. *Anal Chem* 40:586–593
30. Vial J, Jardy A (1999) Experimental comparison of the different approaches to estimate LOD and LOQ of an HPLC method. *Anal Chem* 71:2672–2677
31. Montville D, Voightman E (2003) Statistical properties of limit of detection test statistics. *Talanta* 59:461–476
32. Currie LA (2004) Detection and quantification limits; basic concepts, international harmonization, and outstanding (“low level”) issues. *Appl Radiat Isotop* 61:145–149
33. Voigtman E (2008) Limits of detection and decision. Part 1. *Spectrochim Acta B* 63:115–128
34. Voigtman E (2008) Limits of detection and decision. Part 2. *Spectrochim Acta B* 63:129–141
35. Voigtman E (2008) Limits of detection and decision. Part 3. *Spectrochim Acta B* 63:142–153
36. Voigtman E (2008) Limits of detection and decision. Part 4. *Spectrochim Acta B* 63:154–165
37. Currie LA (1997) Detection: International update, and some emerging di-lemmas involving calibration, the blank, and multiple detection decisions. *Chemometr Intell Lab Syst* 37:151–181
38. Desimoni E, Brunetti B (2009) About estimating the limit of detection of heteroscedastic analytical systems. *Anal Chim Acta* 655:30–37
39. Currie LA (2001) Some case studies of skewed (and other ab-normal) data distributions arising in low-level environmental research. *Fresenius J Anal Chem* 370:705–718
40. Huber W (2003) Basic calculations about the limit of detection and its optimal determination. *Accred Qual Assur* 8:213–217
41. Justino CIL, Rocha-Santos TA, Duarte AC (2010) Review of analytical figures of merit of sensors and biosensors in clinical applications. *Trends Anal Chem* 29:1172–1183
42. Loock H-P, Wenzell PD (2012) Detection limits of chemical sensors: applications and mis-applications. *Sens Actuators B* 173:157–163
43. ISO 5725 (1994) Accuracy (trueness and precision) of measurement methods and results. ISO
44. Horwitz W (1983) Today’s chemical realities. *J Assoc Off Anal Chem* 66:1295–1301
45. Albert R, Horwitz W (1997) A heuristic derivation of the Horwitz curve. *Anal Chem* 69:789–790
46. Horwitz H, Albert R (1997) The concept of uncertainty as applied to chemical measurements. *Analyst* 122:615–617
47. Thompson M (2007) Limitations of the application of the Horwitz equation: a rebuttal. *Trends Anal Chem* 26:659–661
48. Cheng CL, Riu J (2006) On estimating linear relationships when both variables are subject to heteroscedastic measurement errors. *Technometrics* 48:511–519
49. Alanen E (2012) Everything all right in method comparison studies? *Stat Methods Med Res* 21:297–309
50. Nawarathna RLS, Choundhary PK (2013) Measuring agreement in method comparison studies with heteroscedastic measurements. *Statist Med*. doi:10.1002/sim.5955
51. EURACHEM/CITAC Guide (2012) Quantifying uncertainty in analytical measurement, 3rd ed. Laboratory of Government Chemist, London. <http://www.eurachem.org/index.php/publications/guides/quam>. Accessed 15 Oct 2013
52. Measurement uncertainty revisited: alternative approaches to uncertainty evaluation. Eurolab Technical Report No. 1/2007, Paris
53. Den Boef G, Hulanicki A (1983) Recommendations for the usage of selective, selectivity and related terms in analytical chemistry. *Pure Appl Chem* 55:553–556
54. Vessman J, Stefan RI, Van Staden JF et al (2001) Selectivity in analytical chemistry. *Pure Appl Chem* 73:1381–1386
55. Thompson M, Ellison SLR, Fajgeli A et al (1999) Harmonized guidelines for the use of recovery information in analytical measurement. *Pure Appl Chem* 71:337–348
56. EC document SANCO/3030/99 rev.4 11/07/00. Technical material and preparations; guidance for generating and reporting methods of analysis in support of pre- and post registration data requirements for Annex II (part A, Section 4) and Annex III (part A, Section 5) of Directive 91/414. http://ec.europa.eu/food/plant/pesticides/approval_active_substances/docs/wrkd0c13_en.pdf. Accessed 15 Oct 2013

Index

A

- Acaricides, 736
- Accumulation, 764, 781, 782, 785, 788–794, 798, 802–805, 808, 809, 811–817, 832, 834, 885, 888, 892, 949, 954, 982, 1028, 1060, 1061, 1091
extractive, 804, 815–816
- Acenaphthene, 943
- Acenaphthylene, 943
- Acephate, 1005
- 2-Acetamidofluorene, 949
- Acetolactate synthase, 1008
- Acetone, 1023, 1024, 1027, 1029–1031, 1036, 1072
- Acetylcholine (ACh), 913, 982, 984, 985, 987, 988, 990, 991, 1002
- Acetylcholine esterase (AChE), 953, 982–990, 992–1003, 1005, 1007, 1008, 1010
- Acetyl salicylic acid, 887–889
- Acetylthiocholine (AtCh), 985, 991–993, 1002, 1010
- Achromobacter* spp., 923
- Acid phosphatase (APs), 983, 1003–1004, 1008
- Acid rain, 836, 1048
- Acoustic sensors, 1026
- Acrylamide, 893
- Acrylonitrile, 1023
- Activity coefficient, 751
- Acyclovir, 891
- Adams, R.N., 889, 918
- Adenine, 1005
- Adenosine triphosphate (ATP), 1102
- Adsorption, 721, 731, 739, 743, 757, 761, 765, 768, 770, 789, 798, 801–807, 811, 813–815, 829, 831, 833, 843, 850, 889, 890, 893, 895, 939, 944, 974, 994, 997, 1033, 1037–1040, 1089, 1092, 1094, 1118, 1122, 1123, 1127, 1128, 1139
physical, 731, 997, 1123
- Adsorptive stripping analysis, 803, 885
- Adsorptive stripping voltammetry (AdSV), 799–803, 807, 812, 813, 817, 849, 922, 943, 966
- Advanced Spaceborne Thermal Emission and Reflection Radiometer (ASTER), 1062
- Aerobic, 729, 730, 732, 733, 735, 736, 906, 1048
- Aerosol, 1023, 1048, 1049, 1051, 1052
- Affinity binding, 997
- AFM. *See* Atomic force microscopy (AFM)
- Ag-amalgam, 807
- Agglomeration, 859, 865, 866
- Aggregates, 868, 1027, 1081
- Alcohols, 795, 906, 944, 1003, 1023, 1027, 1030, 1031, 1033, 1034, 1039
- Aldehyde dehydrogenase, 1005
- Alginate, 910
- Alginic acid, 846
- Aliphatic amines, 1091, 1092, 1096
- Alizarine, 807
- Alizarin red S, 947
- Alkaline earth metals, 808, 1112, 1119
- Alkaline error, 753, 754
- Alkaline metals, 804, 808, 1119
- Alkaline phosphatase (ALP), 1003
- Alkalinity, 753

- Alkanes (hexane), 1023
Alkane sulfonate, 912
Alkylbenzene sulfonate, 906, 923
Alkyl parabens, 941
Alkyl-sulphonic acids, 805
ALP. *See* Alkaline phosphatase (ALP)
Alphasense Ltd, 1050
Aluminium, 797, 807, 862, 914, 915
Aluminum chlorohydrate, 895
Amalgam, 789, 802, 807, 893, 896, 973, 975
Amalgam electrode, 973
Amine, A., 1123
Amines, 770, 858, 906, 944, 947, 949, 955, 1023, 1027, 1069–1102, 1123
Amines aliphatic, 1091, 1092, 1096
2-Aminobiphenyl, 949
Aminobiphenyls, 945
1-Aminonaphthalene, 949
2-Aminonaphthalene, 949
Aminonitrophenols, 940
4-Aminophenol, 1010
4-Aminophenyl acetate (PAPA), 994, 999, 1010
3-(Aminopropyl)trimethoxysilane, 730
1-Aminopyrene, 936
Amlodipine besylate, 888
Ammonia, 792, 799, 830, 1069–1102
Ammonium, 784, 805, 831, 832, 906, 916, 922, 1086, 1124, 1125
Amperometric gas sensor, 1075
Amperometric measurements, 746, 887, 985, 992, 1004, 1086, 1097
Amperometric sensors, 722, 906, 907, 921, 922, 991–996, 1117
 chronoamperometry, 831
 electrode with periodical renewal of the diffusion layer, 860
Amperometry, 830, 888, 889, 891, 935, 936, 953, 1093
Anaerobic, 733, 896, 906, 1048
Androgen receptor, 982
Aniline, 915, 948, 1035, 1088, 1089
ANN. *See* Artificial neural network (ANN)
Anodic particle coulometry (APC), 864–873
Anodic stripping voltammetry (ASV), 783, 785, 788, 794, 798, 804, 813, 831, 843, 849, 850, 873, 874, 886, 922, 952
Antarox, 910
Anthracene, 831, 943, 949, 952
Anthraquinones, 744
Antibiotics, 881, 883, 885
Antibody(ies), 896, 983
Antimony, 755, 769–770, 795, 808, 817, 846, 988
 electrode, 988
 film electrode (SbFEs), 795
 nanowires, 769–770
Antioxidants, 856, 938, 941, 949
Antiperspirant, 896
APCVD. *See* Chemical vapor deposition, atmospheric pressure (APCVD)
Aptamers, 896
Aquatic environment, 882, 883, 906, 938
Aromatic amines, 949, 955, 1091
Aromatic hydrocarbons, 931–956, 1031, 1033, 1039
 derivatives, 931–956
 monocyclic, 935–937, 942–944
 polycyclic, 935–937, 942–944
Array, 746, 759, 791, 798, 828, 886, 896, 897, 916, 919, 996, 1007, 1025–1027, 1030–1032, 1036, 1037, 1039, 1041, 1097, 1098
Arrays of microelectrodes, 886
Arsenic, 755, 781, 791, 846, 849, 856
Arthroconidia, 731
Artificial neural network (ANN), 916, 1000, 1009, 1010
Arylhydroxyamines, 966
Ascorbate, 771, 1094
Ascorbic acid, 787, 886, 890, 1040, 1097, 1098
Aso volcano, 1054, 1056, 1057
Associated measurements, 866
ASTER. *See* Advanced Spaceborne Thermal Emission and Reflection Radiometer (ASTER)
ASV. *See* Anodic stripping voltammetry (ASV)
Atmosphere, 763, 881, 934, 942–945, 1047, 1048, 1051, 1060, 1091, 1111, 1113, 1114, 1116–1118, 1120, 1126
Atmospheric aerosol, 1023
Atmospheric photochemistry, 1023
Atomic force microscopy (AFM), 725, 857
ATP. *See* Adenosine triphosphate (ATP)
Atrazine, 896, 1004
Atura innoxia, 816
AuFE. *See* Gold film electrode (AuFE)
Auger electron spectroscopy, 933
Au nanoparticles, 857, 974, 1027
Auxiliary electrode, 919, 1015, 1117
Avidin, 1092
Azide, 832, 834, 835
Aziprotryne, 954

B

Band, 764, 937
BAS. *See* Bioactivity sensor (BAS)
Basal plane pyrolytic graphite (BPPG), 831, 860, 1073, 1074
Batch injection analysis (BIA), 887, 888
BDD. *See* Boron doped diamond (BDD)
BDDE. *See* Boron-doped diamond electrode (BDDE)
Behavior, Nernstian, 913, 915, 916
Benz(*a*)anthracene, 943
Benzene, 942, 944, 950, 1023, 1024, 1029–1031
Benzo(*b*)fluoranthene, 943
Benzo(*k*)fluoranthene, 943
Benzo(*g,h,i*)perylene, 943
Benzo(*a*)pyrene, 935, 943, 944
Benzoquinone, 938, 1077
Benzyltrimethylcetylammmonium cholate (BSCAC), 917
Benzyltrimethylhexadecylammmonium-reineckate, 911, 917
17 Beta (β)-estradiol, 895, 942
BEWS. *See* Biological early warning system (BEWS)
BIA. *See* Batch injection analysis (BIA)
BiFE. *See* Bismuth film electrode (BiFE)
Bioaccumulation, 781, 789, 790, 816
Bioactivity sensor (BAS), 733
Bioavailability, 841
Bioavailable fraction, 841
Biochemical cycle, 781
Biochemical oxygen demand (BOD), 729–733
Biofilms, 731, 732, 746
Biofuel cell, 733
Biogeochemical, 896
Biological fluids, 885, 891
Biological receptors, 1010
Biomimetic microsensor, 1097
Biosensor(s)
 based on enzymes, 984, 1010
 DNA, 983
 DNA-modified, 816
 whole-cell, 950
Bis-(ethylenediamine)-diaqua-copper(II) cation, 922
Bismuth, 755, 789, 795, 802, 808, 809, 813, 817
 bulk electrode, 795
 electrode, 789
Bismuth film electrode (BiFE), 784, 785, 788, 789, 795, 802, 807, 817, 831, 887, 973
Bisphenol A, 766, 895, 934, 941, 942, 951

Bis(2-ethylhexyl) sebacate (BEHS), 913
BOD. *See* Biochemical oxygen demand (BOD)
Boron, 932, 933
Boron doped diamond (BDD), 722, 782, 788, 802, 831, 835, 860, 890, 932–933, 973, 1074, 1091
Boron-doped diamond electrode (BDDE), 722–723, 800, 860, 890–891, 1070, 1093
Boron-doped diamond thin-film, 932–937
Boron nitride, 932
Bovine serum albumin (BSA), 988, 989, 994, 1005, 1006
Breast tumor, 941
BTEX, 1023, 1025, 1027
BuChE. *See* Butrylcholinesterase (BChE)
Buffering, 796, 829, 834, 997
Butrylcholine (BCh/BuCh), 983, 985, 987, 988, 990, 991
Butrylcholinesterase (BChE), 983, 985, 986, 988, 990, 991, 993, 995, 1008
Butrylthiocholine (BTCh), 985, 993

C

Cadmium (Cd), 781, 792, 795
Caffeic acid, 941
Caffeine, 888, 889, 1139
Calibration, 746, 783, 784, 792, 814, 861, 870, 910, 915, 921, 922, 937, 940, 973, 995, 1006, 1057, 1058, 1090, 1138–1142
 curve, 995, 1138, 1139
Calixarenes, 913
Cancer, 809, 882, 941, 1024
Capacitive sensors, 768
Capacitive-type CO₂ sensor, 1120
Capillary electrokinetic chromatography (CEC), 951
Capillary electrophoresis, 851, 905, 932, 951, 954, 975, 982
Carbamate pesticides, 940, 945, 946, 982, 985, 995, 996, 999, 1003–1005, 1007
Carbamates, 995, 1004, 1123
Carbamazepine, 891, 894
Carbaryl, 936, 945, 946, 994, 997, 999, 1004
Carbendazim, 936, 945, 946
Carbidopa, 888
Carbofuran, 995, 996, 999, 1000, 1003, 1004, 1010
Carbon
 based material, 1033, 1036
 black, 951, 953, 1083, 1084

- Carbon (*cont.*)
 electrodes, 831, 849, 863, 872, 887–895,
 918, 923, 974, 985, 993, 1006, 1010
 fiber electrode, 770, 771, 966
 fibers, 770–772, 893
 mesoporous, 974
 nanostructures, 1041
 paste, 736, 737, 784, 788, 797, 802, 804,
 805, 808, 809, 813, 844, 889, 918, 919,
 931, 948–954, 1006
- Carbon dioxide (CO₂), 720, 836, 1111–1126
- Carbon dioxide sensor, 1052, 1111–1114,
 1116–1126, 1128
- Carbon monoxide, 735, 836, 1038, 1126–1128
- Carbon nanotubes (CNTs)
 multi-walled, 766, 784, 788, 802, 894, 895,
 991, 1001
 single walled, 765, 912, 1100, 1128
- Carbon oxide, 1111–1131
- Carbon paste electrodes (CPE), 788, 794, 797,
 802, 813, 814, 835, 889–890, 893, 908,
 918, 922, 931, 948–955
- 3-Carboxyphenylboronic acid, 1002
- Carcinogens, 942, 946–949, 1023, 1024, 1088
- Carrageenan, 910
- Casting, 916, 1030–1032, 1035–1038
- Catalyst, 743, 806, 808, 834, 995, 1005, 1037,
 1078, 1079, 1121, 1126, 1127, 1129
- Catalytic combustion sensors, 1126, 1128
- Catechol, 799, 801, 894, 942, 948, 950,
 953, 1004
- Catecholamines, 771
- Cat-floc, 910
- Cathodic particle coulometry (CPC), 866–869,
 899, 911, 918–922
- Cathodic stripping voltammetry (CSV), 788,
 802, 813, 831, 843, 849
- Cation exchanger, 990
- CCSA. *See* Constant current stripping analysis
(CCSA)
- CCT. *See* Colloidal crystal templating (CCT)
- Cefoperazone, 885
- Cells, 720, 730–733, 735, 746, 752, 789, 799,
 857, 886, 891, 897, 998, 999, 1007,
 1075, 1078, 1079, 1085, 1113, 1114,
 1117, 1129
 electrochemical, 720
- Cellulose, 908, 994, 995, 998, 1004, 1124
- Ceramic, 738, 755, 758, 759, 889, 1001
- Cerium, 797
- Certified reference materials (CRMs),
 786, 788, 802, 812, 813, 1146,
 1147, 1149
- Cetylpyridinium chloride (CPC), 866–869,
 911, 912, 918–922
- Cetyl trimethylammonium bromide (CTAB),
 800–802, 805, 811, 813, 885, 895, 911,
 912, 916, 919, 921, 943
- CFA. *See* Continuous flow analysis (CFA)
- Channel, 768, 954, 1026
- Charge transfer resistance, 1026
- ChE. *See* Cholinesterase (ChE)
- Chelate, 792, 801, 802, 814
- Chemical equilibrium, 810, 836, 842, 846
- Chemically modified carbon electrode, 985
- Chemically modified electrode (CME), 782,
 803–806, 834, 844, 846, 850, 913,
 1054, 1062
- Chemical mediators, 1070
- Chemical oxygen demand (COD),
 719–725, 1095
- Chemical sensor, 756, 1025, 1033, 1036
- Chemical speciation, 841–851
- Chemical vapor deposition (CVD), 722, 890,
 891, 932, 1030, 1033, 1040
 atmospheric pressure (APCVD), 1040
 microwave plasma assisted, 722, 932
 ultrahigh vacuum, 1040
- Chemical warfare agents, 1005, 1024
- Chemiresistor/FET, 1026, 1037, 1041
- Chemiresistors, 1038
- Chemisorption, 800, 803, 804
- Chicken carcass wash water, 950
- Chitosan, 910, 1002, 1003, 1097
- Chlorella pyrenoidosa, 816
- Chlorfenvinphos, 1000
- Chlorinated phenols (CPs), 937–939, 941, 946,
 947, 1034, 1036
- Chlorine, 933, 1093
- Chlorogenic acid, 941
- Chloroguaiacol, 950
- Chloroisopropylphenylcarbamate
(CIPC), 1004
- 4-Chloro-2-methylphenoxyacetic acid, 947
- Chloroperoxidase, 950
- 2-Chlorophenol, 938
- 4-Chlorophenol, 934, 938
- Chlorophenols (CPs), 938, 947, 950, 955, 1004
- Chlorophenoxy herbicides, 947
- (4-Chlorophenyl)borate, 915
- Chlorotetracycline, 886
- Chlorpyrifos, 953, 954, 988, 997, 999, 1003
- Choline (Ch), 985, 987, 990–992, 994, 995,
 1000, 1009
- Cholinesterase (ChE), 923, 984–1003, 1010
- Chromate, 800, 846, 849

- Chromatography (CG), 849, 857, 883, 894, 895, 905, 951, 966, 982, 983, 988, 995, 1070, 1092, 1094, 1095
- Chromium, 796, 807, 846, 849, 1008
- Chronoamperometric, 746, 870, 941, 947, 1006
- Chronoamperometry, 741, 831, 1034, 1082
- Chronopotentiometry (CP), 1093
- Chrysene, 831, 943
- Cis*-platinum, 809
- CityTech, 1050
- Clark electrode, 736, 986
- Clark, L., 736–737, 741, 745, 986, 995, 1008, 1074
- Clay, 850, 862, 893
- Clay colloids, 862
- Clofibrac acid, 947, 952, 954
- CMC. *See* Critical micelle concentration (CMC)
- CME. *See* Chemically modified electrode (CME)
- CNTs. *See* Carbon nanotubes (CNTs)
- Coated wire electrode (CWE), 914, 915
- Coating, 720, 732, 752, 765–766, 795, 804, 906, 974, 989, 1004, 1010, 1027, 1030, 1031, 1034, 1037, 1039, 1101, 1128
- Cobalt oxide, 724
- Cobalt phthalocyanine, 831, 951, 993
- COD. *See* Chemical oxygen demand (COD)
- Colloidal, 844, 849, 857, 859, 861, 869, 874
- Colorimetry, 982
- Combination pH electrodes, 752
- Combustibles, 1118
- Combustion, 726, 1096, 1126–1128
- Complex, 722, 757, 758, 772, 781, 793, 795, 796, 798–802, 804, 807, 811–813, 815–817, 841, 843–846, 850, 856, 883, 889, 894, 896, 907, 909, 911, 912, 914, 918, 922, 941, 945, 982, 998, 1008, 1024, 1025, 1036, 1047, 1054, 1057, 1120
- labile, 845
- non-labile, 845
- Complexation, 787, 803, 843, 910
- Composites, 892, 894, 896, 974, 975, 1002, 1036, 1070, 1088–1102
- Concanavalin A (Con A), 997
- Concentration profile, 859
- Conducting polymer (CP), 896, 1030, 1033–1036, 1039, 1086–1088
- Conductivity, 742, 754, 757, 766, 767, 829, 856, 862, 887, 888, 917, 932, 973, 998, 1001, 1033, 1037, 1086, 1088, 1096, 1112–1114, 1129
- Conductometric sensors, 767
- Conductometry, 831
- Confocal laser scanning microscopy (CLSM), 731
- Constant current stripping analysis (CCSA), 782, 784, 787, 788, 799, 802, 803, 807, 810, 812, 813, 830, 831, 843
- Constant phase element (CPE), 785, 786, 788, 802, 805, 807, 810, 811, 813, 831, 834, 835, 844, 849, 889, 890, 893, 922, 948–954
- Continuous flow analysis (CFA), 723
- Conventional electrode, 1001, 1097
- Copper, 723, 725, 755, 757, 763, 781, 790–793, 856, 862, 864, 873, 886, 1000, 1004, 1040, 1091, 1100
- Copper metallic nanoparticles, 856
- Copper oxide (CuO), 757, 762, 763, 1119, 1121–1123, 1129, 1130
- Copper oxide nanowire, 763
- CoTSPc. *See* Cobalt tetrasulphonate phthalocyanine (CoTSPc)
- Coulometry, 726, 864, 865
- Coumaphos, 1005
- Counter electrode, 745, 746, 1003, 1035, 1050, 1097
- Covalent
- attachment, 740, 997, 1039
- binding, 1039
- CP. *See* Chronopotentiometry (CP)
- CPE. *See* Carbon paste electrodes (CPE)
- Cremer, M., 752
- Critical micelle concentration (CMC), 912
- CRMs. *See* Certified reference materials (CRMs)
- Crosslinking, 731, 942, 988, 993, 1001, 1006
- Crown ethers, 913
- Crystal violet, 909
- CSV. *See* Cathodic stripping voltammetry (CSV)
- CTAB. *See* Cetyltrimethylammonium bromide (CTAB)
- Cupferron, 800, 807, 813
- CVD. *See* Chemical vapor deposition (CVD)
- CWE. *See* Coated wire electrode (CWE)
- Cyanazine, 954
- Cyanide, 808, 832, 836
- Cyclam, 914
- Cyclic voltammetry, 725, 831, 943, 965, 1000, 1034, 1080–1084, 1092
- Cyclodextrins (CDs), 857, 886, 892, 913, 949
- Cyclones, 886

- Cyclotrimethylenetrinitramine (RDX), 967, 974, 1024
- Cylindrical, 1035, 1036
- Cysteamine, 997
- Cysteine, 788, 791, 849, 874, 892, 922
- D**
- DBS. *See* Dodecylbenzene sulphonate (DBS)
- Deconvolution, 868, 939
- Decylbenzene sulfonate, 910, 911, 915–917, 921
- Defects, 756, 757, 759, 829, 882, 933, 982, 1039
- Demeton-S, 1006
- Deodorants, 896
- Deoxyribonucleic acid (DNA), 857
damage, 882
- Deposition
electrochemical, 723, 724, 843, 1039
electrolytic, 782, 787, 788, 790, 798, 800, 809, 812, 817
- Detection
amperometric, 808, 831, 937, 943, 948, 951, 954, 955, 966, 973, 975, 1007, 1091, 1094
limit, 815, 885–896, 910, 913, 914, 916, 917, 939–946, 948, 950, 951, 954, 955, 973–975, 988–990, 995, 998–1001, 1003, 1004, 1006, 1009, 1049, 1062–1064, 1086, 1087, 1092, 1093, 1096, 1097, 1100, 1101, 1142
- Detergents, 905, 906, 911, 912, 915, 917, 921, 923
- DGT. *See* Diffusive gradients in thin films (DGT)
- Di-alkyl sulfosuccinate, 906
- Diamond, 722–723, 782, 788, 802, 831, 835, 860, 882, 890–891, 931–937, 973, 1070, 1073, 1074, 1091, 1093, 1094
- Diaphorase, 1005
- Diazinon, 1000, 1004, 1008
- Diazonium salt, 771
- Dibutylphthalate, 911
- Dichlorophenol, 938, 951, 965, 967–972
- 2,4-Dichlorophenols (2,4-DCP), 938, 939, 951
- 2,2-Dichlorovinyl-dimethylphosphate, 990
- Dichlorvos, 993, 999, 1002, 1003
- Dichromate, 719
- Diclofenac, 889, 952
- Dielectrophoresis, 1037
- Diethylstilbestrol, 951, 953
- Differential pulse voltammetry (DPV), 741, 782, 786, 788, 800, 802, 813, 828, 829, 831, 857, 858, 887–891, 895, 896, 922, 934–936, 940, 945, 949, 951–953, 967, 968, 970
- Diffusion, 736, 743, 744, 758, 761, 764, 860, 869–873, 944, 947, 997, 1040, 1050, 1051, 1074–1076
coefficient, 869–871, 1076
layer, 860, 1074, 1075
layer thicknesses, 1074
- Diffusive gradients in thin films (DGT), 850
- Digestion, wet, 793, 796
- Dihydroxybenzene, 894
- Diisobutylphenoxyethoxyethyl-(dimethyl) benzylammonium chloride (DIPEBC), 921
- Diisooctyl phthalate, 913
- 2-(Diisopropylamino) ethanethiol, 1006
- Diisopropyl fluorophosphates, 989
- Dimensionally stable anode (DSA), 722
- Dimethylglyoxime, 797, 802, 921
- Dimethylglyoxime, nickel complex, 921
- 1,1-Dimethylhydrazine, 951
- 2,4-Dimethylphenol, 938
- Dinitrobenzene, 972, 973
- 4,6-Dinitro-o-cresol, 938
- 2,4-Dinitrophenol, 935, 938, 940
- 2,4-Dinitrophenyloctyl ether, 915
- Dinitrotoluene, 974
- 2,4-Dinitrotoluene, 950, 967, 973, 975
- Dinonylnaphthalene sulfonic acid, 915
- Dinoseb, 954
- Dinoterb, 953, 954
- Dioclyloctadecylamine, 989
- Dioclylphthalate (DOP), 910, 911, 916
- Dioxon, 991
- Dip-coating, 1030, 1101
- Dipicrylamine, 990
- Dip-pen lithography, 1035
- Dipyron, 886, 951, 952
- Direct potentiometry, 790
- Disc electrode, 720–721, 723, 788, 791, 793, 813, 833, 863, 869, 975, 1093
- Disinfectant, 808, 869, 870, 874, 911, 912, 922, 949
- Disinfection, electrochemical, 932
- Dispersant, 906
- Disposable electrodes, 919
- Disposable sensor, 919, 991, 999–1001
- Dissociation constant, 846
- Dissolved oxygen (DO), 735–746, 830, 890, 923, 950, 1008

DL-alpha-tocopherol, 893
DME. *See* Dropping mercury electrode (DME)
DNA. *See* Deoxyribonucleic acid (DNA)
DO. *See* Dissolved oxygen (DO)
Dodecylbenzene sulphate (DBS), 910, 911,
915–917, 921, 1008
Dodecyl sulphate (DS), 1086
Dodecyltrimethylammonium-reineckate
(DTA-RN), 917
Domperidone, 895
Dopamine, 772, 886, 890, 893, 1092, 1098
Doping, 721, 757, 760, 765, 768, 892, 932, 933,
1031, 1033, 1034, 1039, 1086
Doxazosin, 893
DPV. *See* Differential pulse voltammetry
(DPV)
Drain-source current, 738
Drinking water, 810, 828, 830, 856, 884, 886,
935, 938, 939, 942–947, 953
Dropping mercury electrode (DME), 782, 789,
918, 921, 965
Drosophila melanogaster, 770, 996
Drugs, 735, 881, 883, 885, 886, 889–892, 897,
938, 985
DS. *See* Dodecyl sulphate (DS)
DSA. *See* Dimensionally stable anode (DSA)
Dynamic electrochemistry, 1070
Dynamic light scattering (DLS), 857, 868

E

ECE mechanism, 948
Echothiophate, 989
ECL. *See* Electrochemiluminescence (ECL)
EC mechanism, 1092
Edge plane pyrolytic graphite (EPPG), 888,
889, 892, 1070, 1073, 1074
EDTA, 786, 792, 810, 811
EGFET. *See* Field-effect transistor extended
gate (EGFET)
EIS. *See* Electrochemical impedance
spectroscopy (EIS)
Electrical conductivity, 742, 856, 888,
1001, 1037
Electric eel, 996, 999, 1000
Electroanalysis, 782, 789, 792–796,
805–807, 834–836, 841–851, 884,
887, 890, 932, 933, 938, 943, 944,
946, 955, 1070, 1078
Electrocatalysis, 790, 806, 815, 892, 1078
Electro-catalysts, 1077–1080, 1082, 1084,
1086, 1088, 1091, 1092, 1097

Electrochemical
cell, 720
methods, 807–808, 832, 836, 856, 857, 874,
949, 950, 985, 1033, 1070
sensing, 742, 950, 1052–1060, 1069,
1070, 1074
sensors, 733, 742, 752, 889, 905, 923, 932,
955, 966, 973, 975, 1001, 1026, 1029,
1041, 1047, 1049–1057, 1060–1064,
1096, 1097, 1101, 1126, 1137–1149
Electrochemical detection (ED), 721, 782,
789, 803, 954, 966, 974, 998,
1049–1051, 1089
Electrochemical gas sensors, 1069, 1095
Electrochemical stripping analysis (ESA), 789,
790, 792, 793, 803, 815, 849
Electrochemiluminescence (ECL), 836, 1072
Electrode
chemically modified, 782, 803, 844, 846,
850, 913, 1054, 1062
liquid membrane, 908–910, 990
macroporous, 1034
metallic, 755, 770, 789, 793, 846,
886–887, 893
modified, 721–723, 725, 739–745, 761,
782, 803, 805, 844, 884, 890, 892, 913,
949, 965, 973, 1002, 1070, 1091, 1093,
1101, 1139
position, 886, 1036, 1080–1082, 1097
potential, 752, 753, 858–860, 917, 991
solid contact, 908, 914–918
Electrokinetic chromatography (EKC), 951
Electrolytical deposition, 782
Electromotive force (EMF), 1111
Electron
transfer, 730, 733, 739, 740, 743, 744, 771,
789, 832, 860, 872, 873, 887, 938, 948,
992, 995, 1001–1003, 1070, 1089, 1091
transfer kinetic, 873, 887
Electronic noses, 1025
Electronic tongue, 916
Electrooxidation, 933, 938, 941, 944, 987, 1001
Electrophoretic, 942, 954, 955, 975,
1036–1038
Electrophorus electricus. *See* electric eel
Electropolymerization, 723, 739, 742, 743,
895, 1034, 1035, 1088, 1099
Electrospinning, 1035, 1088
Embryonary defects, 882
Emerging contaminants, 855–874, 882, 883,
894, 897
Emerging pollutants, 894

- EMF. *See* Electromotive force (EMF)
- Endocrine disrupting
effect, 982, 983
estrogens, 894
- Endocrine disrupting compounds (EDCs), 895,
941, 1097
- Endocrine disruptors, 894, 895, 941, 950,
982, 983
- Ensemble, 974
- Entrapment, 730, 804, 988, 997, 1008
- Environment, 735, 736, 738, 743, 752, 765,
766, 770, 772, 796, 797, 809, 827, 832,
836, 841, 855–856, 869, 881–883, 905,
906, 938, 942–944, 947–951, 954, 981,
1005, 1011, 1023, 1024, 1026, 1037,
1041, 1057, 1063, 1079
- Environmental
nanoparticles, 855–857, 874
protection, 856, 937, 1069
specimen bank, 845
- Enzyme, 730, 790, 829, 834, 844, 896, 923,
942, 948, 949, 982–990, 992–1011,
1094–1096
activity, 948, 984, 985, 987, 989–991,
997, 1011
immobilization, 996–997, 1000
- Enzyme-based biosensor, 987, 1009
- Epinephrine, 886, 1098
- ESA. *See* Electrochemical stripping
analysis (ESA)
- Escherichia coli*, 923, 936, 937, 948, 1008
- Estradiol, 895, 950, 953
- Estrogen receptor, 982
- Estrogens, 883, 894, 895, 941, 950, 953, 982
- Etchants, 1035
- Ethanol, 922, 953, 967–972, 1010, 1011, 1023,
1024, 1029–1031, 1036, 1095
- Ethinyle-estradiol, 885
- Ethylbenzene, 1023, 1024, 1029
- Ethylene oxide, 906, 907
- 4-Ethylnitrobenzene, 908
- Explosives, 832, 834, 965–975
nitrated, 966, 973–975
- Extraction
liquid-liquid, 883, 949, 1093
solid phase, 940, 973
Soxhlet, 939
- F**
- Fast Blue RR (FBRR), 771, 772
- Fatty acid, 906
- Fenamiphos, 936, 945, 946
- Ferricyanide, 730, 923
- Ferrocene, 922, 951, 995
- 11-Ferrocenyltrimethylundecyl ammonium
ion, 922
- FET. *See* Field effect transistor (FET)
- FIA. *See* Flow injection analysis (FIA)
- Field effect transistor (FET)
extended gate (EGFET), 765
metal insulator semiconductor (MISFET),
737, 738
sensors, 1026
- Field-effect transistor extended gate
(EGFET), 765
- Film electrode, 788, 789, 792, 793, 795,
802, 973
- Films, 722, 731, 737, 755, 782, 788, 843,
887, 906, 931, 966, 989, 1026,
1080, 1120
- Filtration, 845, 849, 897
- Fingerprint, 857, 861, 983
- Flame ionization, 1025
- Flow injection analysis (FIA), 721–723,
787, 791, 799, 802, 807, 810,
812, 813, 830, 831, 884, 886,
889, 891, 911, 916, 917, 932, 942,
945, 950–955, 975, 991, 998–999,
1094
- Flow system, 732, 905, 921, 950, 998
- Fluoranthene, 943, 945
- Fluoren-9-ol, 949
- Fluoride, 721, 832, 836, 1008
- Fluorine, 1006
- Fluoroborate, 918, 921
- Fluorophosphates, 989
- Flutamide, 889
- Flux, 870, 871, 897, 1051, 1062
- Foaming agent, 906
- Folic acid, 887, 893
- Food, 827, 832, 881, 886, 897, 906, 941,
947, 954, 982, 983, 1009, 1069,
1091, 1093, 1096, 1146
- Food-processing, 938, 941, 982, 1069
- Formaldehyde, 815, 1023, 1024, 1027,
1030, 1032, 1040
- Fouling, 891, 932, 938, 945–947, 955, 993,
1006, 1009, 1094
- Fresh water, 801
- Fuel cell, 732, 1069, 1078, 1079, 1085
- Fullerenes, 856, 891–892, 894, 895
- Fulvic acids (FA), 843, 846
- Fumaroles, 1052–1055, 1057, 1060, 1061
- Fumarolic emission, 1053–1055
- Fungicides, 946, 981, 1005

G

- β-Galactosidase, 937, 948
- Gallic acid, 941
- Gallium, 755
- Galvanostatic electrodeposition, 1080–1082
- Gas chromatography (GC), 883, 895, 966, 988, 995
- Gas-permeable membrane, 1074
- Gas sensing, 1052, 1070, 1076, 1111, 1127, 1129
- Gas sensor, amperometric, 1075
- Gas sensors, 944, 1036, 1037, 1060, 1069, 1074, 1075, 1091, 1095, 1097, 1111–1113, 1118, 1123, 1129
- GC. *See* Gas chromatography (GC)
- GCE. *See* Glassy carbon electrode (GCE)
- Gel, 730, 731, 754, 756, 850, 997, 999, 1007, 1008, 1027, 1123
- Geochemical cycle, 796
- Gibb's free energy, 1122
- Glass
 - electrodes, 752–754, 763, 770, 858
 - membrane, 752, 754
- Glassy carbon (GC), 723, 740, 783, 785, 788, 802, 809, 883, 891, 894, 895, 938, 946, 982, 988, 1025, 1070, 1073, 1077, 1093
- Glassy carbon electrode (GCE), 723, 731, 783, 784, 787, 799, 800, 802, 807, 811–813, 829, 888, 891, 892, 965, 968, 970–972, 1001, 1002, 1089, 1090
- Glassy carbon electrode, activated, 723–724
- Glucose, 913
- Glucose oxidase (GOD), 1003, 1004, 1008
- Glucose-6-phosphate, 1003
- Glutaraldehyde, 942, 988, 989, 993, 994, 1005
- Gold
 - nanoparticles, 856, 865, 866, 872, 892, 902, 1098
 - nanospheres, 1003
- Graphene, 768–769, 891, 892, 895, 975, 1002, 1027, 1032, 1034, 1039–1040, 1070, 1089, 1091, 1098, 1101
- Graphene oxide (GO), 892, 974, 1002, 1040, 1089, 1091
- Graphite, 733, 740, 766, 860, 889, 892, 894, 914, 916, 918, 919, 986, 988, 1004, 1040, 1070, 1081, 1085, 1089, 1091, 1098
- Graphite electrode, 740, 860, 888, 892, 922, 990, 993, 1070, 1074, 1096, 1098
- Graphite, pyrolytic, 809, 831, 860, 888, 889, 892, 1040, 1070, 1073, 1074, 1098
- Green element, 809

Greenhouse effect, 1111

Griseofulvin, 885

Guaiacol, 950

Guanine, 974

H

- Haber, F., 752
- Haloperidol, 885
- Hanging mercury drop electrode (HMDE),
 - 782, 783, 788, 789, 793, 798–804, 807, 811–813, 829, 831, 843, 849, 885, 886, 921, 940, 965, 967–973
- Heavy metals, 781–796, 798, 803, 808–817, 845, 846, 883, 996
- Helmholtz double layer, 756
- Heptenophos, 993
- Herbicide, 938, 947, 949, 954, 981
- Heterogeneous electrode, 889
- Hexacyanoferrate, 731, 921, 993, 995, 1005
- Hexadecylpyridinium chloride (HDPC), 921
- Hexadecylpyridinium-phosphotungstate (HDP-PT), 912, 917
- Hexadecyltrioctadecylammonium-tetraphenylborate (HDTA-TPB), 912
- Heyrovsk, J., 831, 843, 861, 862, 866, 872, 885
- Highly ordered pyrolytic graphite (HOPG), 1040, 1070, 1073
- High performance liquid chromatography (HPLC), 791, 816, 851, 916, 932, 939, 941–943, 945, 948, 951, 955, 975, 982, 1007, 1094, 1096
- High pressure ashing (HPA), 793
- Hindered diffusion, 871
- Histamine, 1093–1095
- Histidine, 1093
- HMDE. *See* Hanging mercury drop electrode (HMDE)
- Hormones, 897
- Horseradish peroxidase (HRP), 995
- Horwitz equation, 1145–1146
- HPLC. *See* High performance liquid chromatography (HPLC)
- HRP. *See* Horse radish peroxidase (HRP)
- Human serum, 885, 891, 893, 991
- Humic acid, 844, 949, 952
- Humics (HA), 1076
- Humic substance, 844
- Humidity, 1034, 1053, 1054, 1058, 1062
- Hyamine, 912, 913, 915, 916
- Hybrid film, organic-inorganic, 730, 732
- Hybrid materials, 730–732

Hydrazine, 951, 952, 1040
 Hydraziniumion, 815
 Hydrocarbons, 931–956, 1023, 1031, 1033, 1039
 Hydrocortisone, 889
 Hydrogel, 731, 773, 974, 1098
 Hydrogen, 753, 754, 756, 758, 815, 885, 913, 932, 994, 1040, 1076, 1088, 1097
 Hydrogen peroxide (H₂O₂), 740, 741, 745, 832, 987, 992, 994, 995, 1000, 1002–1004
 Hydrogen sulphide (H₂S), 1049, 1095
 Hydroquinone, 767, 894, 922, 941, 942, 948, 1040, 1072, 1077, 1079, 1091
 Hydroquinone-Benzoquinone, 1079
 Hydroxylamine, 767
 Hydroxyl radical, 720–723, 733, 738
 1-Hydroxypyrene, 936, 945, 1124
 8-Hydroxyquinoline, 783, 800

I

IARC. *See* International Agency for Research on Cancer (IARC)
 Ibuprofen, 894
 IgG. *See* Immunoglobulin G (IgG)
 IgM. *See* Immunoglobulin M (IgM)
 Immobilization, 731, 742, 988, 989, 996–997, 1000, 1002, 1008, 1011, 1035
 Immobilization methods, 997
 Immunoassay, 983, 998
 direct, 983
 Immunosensor, 896
 Immunotoxicity, 941
 Impedance, 773
 Incidental nanoparticles, 856
 Indeno(1,2,3-c,d)pyrene, 973
 Indium, 768, 808, 809, 817, 858, 1033
 Indium-tin oxide (ITO), 768, 858, 1030
 Individually addressable electrodes, 1041
 Indolamines, 771
 Induction, 722
 Industrial waste, 720
 Inhibition, 723, 829, 834, 922, 923, 982–985, 987–996, 998–1004, 1009, 1010
 Ink, 889, 919, 1000, 1030, 1035
 Inkjet printing, 1088
 Inorganic compounds, 720
 Insecticides, 886, 946, 951, 981, 982, 988, 989, 991, 996, 1000, 1002, 1006, 1007, 1010
 In-situ, 720, 793, 795, 798, 800, 801, 805, 811, 814, 850, 873, 896, 905, 946, 1000, 1001, 1034, 1047, 1052–1057, 1060–1062
 In situ monitoring, 1052

Intercalation, 756, 806, 808, 1070
 Interdigitated electrodes, 1029–1031
 Intermetallic, 792, 793
 International Agency for Research on Cancer (IARC), 942–944, 947
 International Union of Pure and Applied Chemistry (IUPAC), 751, 841, 855
 Interscan, 1050, 1052
 Iodide, 832, 834, 835, 916, 1002
 Ion(s)
 activity, 751–753
 chromatography, 857
 exchange, 730, 745, 754, 756, 758, 763, 786, 789, 805, 808, 829, 834, 844, 845, 849, 854, 908, 910, 911, 915, 917, 990, 993
 free, 841, 845
 mobility, 966
 Ion-Exchanger Membranes, 917
 Ionic
 liquid, 950, 974, 1074–1076, 1097
 strength, 843, 997, 1008
 Ion mobility spectrometry (GC-IMS), 1070
 Ionophores, 913
 Ion-pairing, 789, 792, 800, 804–806, 809, 815, 816, 828, 830, 834, 835, 990
 Ion selective electrodes (ISEs), 754, 756, 772, 790, 807, 808, 836, 842–843, 908–918, 990
 tattoo-based, 772
 Ion selective field effect transistors (ISFETs), 754, 755, 764, 914, 917, 989
 Iridium, 755, 756, 763, 808, 816, 950
 Iridium oxide, 756, 763
 Iron, 740, 796–808, 856, 1099
 Iron-manganese nodule, 797
 Iron(III)-tetra-*o*-ureaphenylporphyrino silica matrix, 740
 ISE. *See* Ion selective electrodes (ISEs)
 ISFETs. *See* Ion selective field effect transistors (ISFETs)
 Iso-propanol, 1024
 ITO. *See* Indium-tin oxide (ITO)
 IUPAC. *See* International Union of Pure and Applied Chemistry (IUPAC)

K

Keratinocytes, 897
 Ketoconazole, 896
 Ketones, 1023, 1024, 1027, 1031
 Kirishima volcano, 1061
 Kiwi fruit, 994, 999
 Krebs cycle. *See* Citric acid cycle

L

- Lab-on-a-chip, 975
Laccase, 950, 952
Lactic acid, 1031, 1039
La Fossa, 1052, 1061
Lagoon water, 994
Lake, 796, 829, 881, 917, 934, 941, 974, 1006, 1011
LAS. *See* Linear alkylbenzene sulphonates (LAS)
Laser ablation, 1033
Laser-induced fluorescence (LIF), 943, 973, 1070
Lauryl sulfate, 906, 913
Layer-by-layer (LbL) deposition, 994
L-cysteine, 892, 922
Lead (Pb), 755, 783–786, 789, 791–793, 795, 799, 828, 846–853, 886, 1091
Lead film electrode (PbFE), 795, 817
Lead oxide, 720, 721
Lead oxide, F-doped, 721–722
Least square regression, 1139–1141
Levodopa, 888
Levofloxacin, 888
Lichens, 790
LIF. *See* Laser-induced fluorescence (LIF)
Ligand, 743, 801, 802, 804, 806, 807, 843–845, 850, 913
Light addressable potentiometric sensors (LAPS), 989
Lignosulfonate, 906
Limit of detection, 730, 788, 802, 813, 831, 886, 887, 889, 891, 895, 923, 937, 950, 954, 988, 993, 1000, 1076, 1077, 1089, 1100, 1142–1144
Linear alkylbenzene sulphonates (LAS), 923
Linear range, 788, 802, 813, 831, 892, 915, 1002, 1006, 1071, 1072, 1089, 1094, 1098, 1101, 1137–1142, 1144
Linear sweep voltammetry (LSV), 802, 816, 830, 831, 885, 894
Linuron, 951, 952
Liquid crystal, 836
Liquid/liquid extraction, 943, 949, 1093
Liquid membrane, 804, 829, 908–910, 918, 990
LISICON, 1112
Lithium lanthanum titanate (LLTO), 758
Lithographically patterned nanowire electrodeposition (LPNE), 1036
Lithography, 1035–1037
LLTO. *See* Lithium lanthanum titanate (LLTO)
LSV. *See* Linear sweep voltammetry (LSV)

M

- Macrocyclic compounds, 741
Macro electrode, 873, 1074, 1075
Macroporous chalcogenides, 1034
Magnetic separation, 895
Malachite green, 816, 947, 951, 953
Malathion, 987, 991, 995, 1003, 1008
Maleic hydrazide, 951, 953
Manganese, 742, 756, 758, 796–798, 807–808, 1099
Manganese oxide, 756, 758
Manganese phthalocyanine, 742
Masaya volcano, 1051
Mass spectrometry (MS), 851, 883, 895, 933, 939, 966, 982, 983, 1025, 1069, 1096
Mass transport, 873, 938
Matrix interferences, 922
Mediator, 730–731, 739, 740, 742, 806, 896, 910, 916, 923, 992–995, 998, 1000, 1070, 1076
Medium exchange, 788, 796, 803, 813, 831, 845, 849, 943
Melatonin, 890
Meldola Blue, 993
Membrane
 covered electrode, 736–739
 porous, 736, 768, 1035
 selectivity, 911, 917, 990, 1097
Membrane-less gas sensors, 1097
Membrapor, 1050
Mercury
 electrodes, 782, 789, 831, 832, 846, 861, 862, 872, 885–886, 893, 896, 918, 921, 1091, 1093
 film, 782, 788, 794, 795, 797, 802, 813, 843, 893
 inorganic, 856
Mercury film electrode (MFE), 785, 786, 788, 789, 793–795, 798, 802, 807, 812, 831, 843, 887
Metabolites, 733, 884, 905, 999, 1010
Metal(s)
 electrocatalysts, 725, 1076
 film electrode, 792, 793
 mesoporous, 974
 nanoparticles, 724, 858, 859, 864, 866, 872
 powders, 862
Metal insulator semiconductor Field effect transistor (MISFET), 737, 738
Metallic nanoparticles, 856, 857, 974
Metalloids, 781–796
Metalloporphyrins, 740

- Metal oxides, 722, 754, 756, 757, 762, 861, 866, 1029, 1033, 1034, 1118, 1119, 1126, 1128, 1130
nanoparticles, 1039
semiconductors, 1033
- Metaupon, 923
- Methacrylamide, 987
- Methane, 932, 970
- Methylcellulose, 988
- 2(2-Methyl-4-chlorophenoxy)propionic acid, 947
- 7-Methyl-7,13-di-octyl-1,4,10-trioxo-13-aza-7-azonia-cyclopentadecane, 913
- Methylene blue, 742–743, 831
- Methylethyl ketone, 1023, 1024
- 4-Methyl-5-nitrocatechol, 950
- Methyl parathion, 936, 945, 946, 1003, 1004, 1006, 1008
- Methylprednisolone, 891
- Methyl radical, 932
- Metrohm, 921, 999
- Micelle, 909, 912, 1004
- Microbe, 729, 731–733
- Microbial biosensor, 923, 950, 1007
- Microchip
electrophoresis, 1096
HPLC, 951, 975, 1096
- Micro-contact printing, 1088
- Microdisc electrode, 863, 1076
- Microdisk, 830
- Microelectrode array, 746, 828
- Microelectrode(s), 746, 763, 770–772, 791, 863, 886, 893, 896, 897, 939, 1026, 1074, 1075, 1094, 1097
- Micro electro mechanical system (MEMS), 746
- Microemulsion, 939, 1083
- Microfabrication, 732
- Microfluidic device, 973, 1096
- Microfluidic network, 1100
- Microfluidics, 732, 973, 1096, 1102
- Micromachines, 975
- Microorganism, 729, 731–733, 735, 923, 983, 1005
- Micro-separation, 1025
- Microsystem, 732, 751
- Microwave-assisted digestion, 793
- Microwave plasma assisted chemical vapor deposition (MPCVD), 934–936
- Mineralization, 941, 948
- Miniaturization, 732, 1006, 1009, 1025, 1026, 1037
- MISFET. *See* Metal insulator semiconductor Field effect transistor (MISFET)
- Mitoxantrone, 893
- Mixed carbonates, 1112
- Modified electrode, 721–723, 725, 739–745, 761, 782, 803, 892, 949, 1002, 1139
- MOEMS. *See* Micro-optoelectro-mechanical system (MOEMS)
- Molecular imprinting, 893
- Molecular imprinting polymers (MIPs), 893
- Molluscicide, 981
- Molybdenum, 756, 797, 807, 857, 858
- Molybdenum metallic nanoparticle, 857
- Monitoring, 723, 729, 731–733, 735, 772, 773, 790, 798, 808, 832, 836, 842, 849, 855–856, 873, 874, 883, 894, 896, 897, 905, 908, 911, 923, 950, 951, 955, 982, 983, 990–992, 999, 1001, 1005, 1007, 1047, 1051–1052, 1060, 1061, 1063, 1064, 1069, 1091, 1093, 1095–1097, 1101, 1102, 1111, 1126
- Monoamine oxidase, 1095
- Monoamines, 1095
- Monochlorophenoxyacetic acid (MCPA), 947, 953, 954
- Monocrotophos, 953, 1002, 1003
- Monolayer, 744, 872, 886, 997, 1038, 1040, 1139
- Monooxon, 991
- Montmorillonite, 811, 862
- Moonflower, 816
- MPCVD. *See* Microwave plasma assisted chemical vapor deposition (MPCVD)
- Mt. Etna, 1051, 1053, 1062
- Multicomponent, 1010
- Multi-gas system, 1052–1054, 1058
- Multi walled carbon nanotubes (MWCNT), 766, 784, 788, 802, 892, 894, 895, 951, 974, 991, 1001, 1036, 1098
- MWCNT. *See* Multi walled carbon nanotubes (MWCNT)
- Myristyltrimethylammonium bromide (MTMAB), 913
- N**
- NAD. *See* Nicotinamide adenine dinucleotide (NAD)
- NAD⁺. *See* Nicotinamide adenine dinucleotide, oxidized (NAD⁺)
- NADH. *See* Nicotinamide adenine dinucleotide, reduced (NADH)
- Nafion[®], 742, 745, 758, 788, 795, 802, 888, 892, 1006, 1092, 1098, 1099, 1101, 1139
- Nanocomposites, 743, 1002, 1089, 1097, 1099, 1100

- Nanoimpact, 862, 871
Nanoimprint lithography (NIL), 1036
Nanolithography, 1035
Nanomaterials, 723, 764, 765, 855, 856, 974, 1001, 1002, 1100, 1101, 1128
Nanoparticle impacts, 861
Nanoparticles (NP), 723, 742, 764, 795, 850, 855, 887, 956, 973, 1002, 1027, 1071, 1128
Nanoparticle tracking analysis (NTA), 857, 865, 867, 869, 870
Nanopatterning, 1035
Nanorods, 761, 762, 765, 1034, 1071, 1128
Nanosized materials, 1001–1003
Nanostructure deposition, 1035
Nanostructured surfaces, 1028, 1035, 1036
Nanostructures, 724, 743, 768, 770, 891, 897, 1026, 1028, 1030, 1033–1037, 1041, 1128
Nanotechnology, 855, 892
Nanotoxicity, 856
Nanotubes, 761, 762, 891–892, 894, 895, 974, 1002, 1028, 1031, 1034, 1035, 1037, 1039, 1088, 1091, 1128
Nanowires, 763, 764, 769–770, 856, 893, 1002, 1026, 1028, 1033, 1035, 1036, 1087, 1128
Naphthalene, 943, 945, 949, 952
 α -Naphtholphthalein, 1122, 1123
Naproxen, 890, 891
NASICON, 1112, 1117
Nernst, 758, 1114, 1115
Nernst equation, 1114
Nernstian response, 843, 909, 911–913, 920
Nerve agent, 950, 975, 982, 985, 1001, 1002, 1007
Neurotoxic effects, 982
Neurotransmitters, 771, 772, 982, 984
Neutral carrier, 913, 989
Nickel, 724–725, 743–744, 755, 768, 796, 807, 864, 865, 871, 873, 921, 1040, 1091, 1092
Nickel–copper alloy, 725
Nickel nanoparticles, 724, 864, 865, 871
Nickel–salen, 743–744
Nicotinamide adenine dinucleotide (NAD), 1005
Nicotinamide adenine dinucleotide, oxidized (NAD⁺), 1005
Nicotinamide adenine dinucleotide, reduced (NADH), 1005, 1092
Nifedipine, 893
NIL. *See* Nanoimprint lithography (NIL)
Nile blue, 739–740
Nimodipine, 893
Nioximates, 803
Nitrate, 828, 832, 916, 966, 973–975, 994
Nitrene cation, 945
Nitric oxides, 1091, 1096, 1097, 1099, 1101
Nitrite, 806, 832, 947, 1097, 1098
Nitroaromatics, 908, 966, 973–975, 1024
4-Nitrobenzenediazonium tetrafluoroborate, 942
Nitrobenzenes, 908, 909, 966
Nitrocellulose, 989
Nitrofurantoin, 890
Nitrogen, 767, 771, 796, 827, 834, 897, 906, 946, 951, 995, 1039, 1048, 1069–1102
Nitrogen compound, 827, 906, 1069–1102
Nitrogen dioxide (NO₂), 799, 827, 828, 830, 848, 914, 967–972, 1033, 1038, 1056–1058, 1063, 1091, 1095, 1097, 1098, 1116, 1130
Nitrogen oxides (NO_x), 827, 832, 1069–1102, 1111, 1113, 1126
Nitro group, 940, 945, 946, 954, 955, 966
4-Nitro-*m*-xylene, 908
2-Nitrophenol, 935, 938, 940
4-Nitrophenol, 934, 935, 938, 940, 973, 1006
Nitrophenols, 937, 938, 940, 947, 950, 953, 954, 973, 1006, 1007
1-Nitropyrene, 936, 945
Nitroso group, 966
1-Nitroso-2-naphthol, 803, 807
Nitrotoluenes, 908, 966, 972, 975
N-methylcarbamate, 946
N-methylpyridinium-2-aldoxime, 998
NMOS. *See* N-type metal oxide semiconductor (NMOS)
N,N-didecylaminomethylbenzene, 989
N,N-dimethylformamide, 988
N,N-dioctadecylmethylamine, 1006
N-nitrosoamines, 947
Noble metals, 736, 886, 893, 1080, 1082, 1084
Nodularin, 802
Nonionic, polyethoxylated, 906
Nonionic surfactants, 906–908, 910, 915, 916, 921, 923
Nonylphenol, 951
Norepinephrine, 1098
N-oxides (NO_x), 827, 832, 1069–1102, 1111, 1113, 1126
NPAH. *See* Nitrated polyaromatic hydrocarbon (NPAH)
N-type metal oxide semiconductor (NMOS), 738, 1033

- Nürnberg, H.W., 845
 Nutrients, 729
 Nylon-polyamide, 988
- O**
- o*-chloranil, 939
 ODN. *See* Oligonucleotide (ODN)
 Ofloxacin, 952, 954
 Oligonucleotide (ODN), 1039
 OMD. *See* Organic metal deposition (OMD)
o-Nitrophenyl- β -D-galactopyranose, 937, 948
o-Nitrophenyloctyl ether (*o*-NPOE), 991
o-Nitrotoluene, 908
o-NPOE. *See* *o*-Nitrophenyloctyl ether (*o*-NPOE)
 Onset potentials, 861, 863, 864, 873
 On site monitoring, 955, 982, 1111
 Open-circuit, 785, 786, 789, 803, 811, 828, 829, 873
 OPH. *See* Organophosphate hydrolase (OPH)
o-Phenylenediamine, 1000, 1099
 Optical CO₂ sensors, 1124
 Orange II, 922
 Organic-inorganic hybrid material, 730, 732
 Organic ligand, 844, 845, 850
 Organic nanoparticles, 868
 Organic pollutants, 719–723, 725, 856, 883, 947–948
 Organoarsenic compounds, 846
 Organochlorine compounds, 1003
 Organophosphate hydrolase (OPH), 999, 1005–1008, 1010
 Organophosphate nerve agents, 950
 Organophosphates, 950, 953, 982, 984, 985, 990, 991, 993, 995, 999–1001, 1003, 1005–1007, 1010, 1024
 Organophosphorus, 940, 945–947, 982, 983, 988, 991, 994, 998–1000, 1002–1008, 1010, 1011, 1024
 Organophosphorus hydrolase (OPH), 983, 1005–1008, 1010
 Organophosphorus pesticide, 938, 945–947, 988, 991, 996, 998–1000, 1002, 1007, 1008, 1011
 Organosilicas, nanoporous, 974
 Organostannic compound, 846
 Orion, 921
 Osmium, 755, 808, 816, 1096
o-Tetrachlorobenzoquinone, 939
 Overall paraben index, 941
 Oxalic acid, 801, 936, 941
 Oxidation state, 763, 846–850
 Oxide ion, 1130
 Oxides, 861, 1033, 1077, 1113, 1121
- Oxygen
 equivalents, 719
 intercalation, 756
 Oxygen sensor, solid state, 745–746
 Oxytetracycline, 886
 Ozone, 832, 836, 1053, 1062, 1063, 1123
- P**
- PAH. *See* Polycyclic aromatic hydrocarbons (PAHs)
 Palladium, 808, 886, 951, 1039, 1040
p-aminophenol, 994
p-aminophenyl acetate, 994
 PANI. *See* Polyaniline (PANI)
 Parabens, 896, 941
 Paracetamol, 892
 Parachlorometacresol, 938
 Paraffin wax, 738
 Paraoxon, 987, 990, 993–995, 998–1001, 1003, 1006–1008, 1010
 Parathion, 936, 938, 945, 946, 953, 988, 990, 1003–1008
 Particulates, 942–944
 Paste electrodes, 890, 951, 973, 1091
 PbFE. *See* Lead film electrode (PbFE)
 PCP. *See* Pentachlorophenol (PCP)
p-cresol, 942
 PEDOT/PSS nanowire, 1036
 Pentachlorophenol (PCP), 934, 938, 939, 944, 949, 951, 952
 Perchlorate, 806, 831, 832, 918
 Permanganate, 719, 1040
 Peroxidase, 950, 986, 995, 1000, 1096
 Peroxodisulfate, 726, 933
 Personal Care Products (PCP), 881–897, 938, 939, 941, 944
 Personal hygiene product, 905
 Pesticides, 897, 937–940, 945–947, 949, 951, 953–955, 981–1011
 pH, 723, 739, 751, 783, 829, 843, 857, 888, 909, 953, 966, 984, 1092, 1124
 Pharmaceuticals, 808, 809, 832, 881–897, 911, 919, 932, 941, 949–951, 954
 Pharmaceuticals and Personal Care Products (PPCP), 881–897
 pH electrode, 752–755, 767, 770, 987–989, 995, 1005, 1006, 1008
 Phenanthrene, 943
 Phenanthroline, 831
 Phenol(s), 723, 906, 934, 938, 939, 941–942, 950, 952, 972, 1004, 1124
 Phenolic compounds, 934, 937–942, 950, 955, 1006

- Phenylhydrazine, 951, 952
- Phosphate, 801, 805, 810, 813, 814, 829, 831, 832, 835, 836, 857, 858, 916, 918, 946, 948, 951–953, 967–972, 990, 991, 1003, 1124
- Phospholipid, 922
- Phosphorothionate ester, 984, 985
- Phosphotungstic acid, 911, 912
- Photosynthetic activity, 735
- pH sensor(s)
solid state, 754–755
textile-based, 772–773
- Phthalates, 913
- Phthalic anhydride, 948
- p*-Hydroquinone, 922, 1077
- Physcion, 890
- Physical adsorption, 731, 997, 1123
- Picric acid, 922, 972, 973
- PIDS. *See* Poly (isophthalamide diphenylsulphone) (PIDS)
- Planar diffusion, 860
- Plant growth regulators, 951, 981
- Plasma, 722, 770, 885, 886, 889, 893, 989
- Plasticizer, 897, 909–911, 913, 915, 918, 919, 941, 991
- Platforms, 744, 768, 966, 1026, 1047, 1052, 1061–1063
- Plating
ex-situ, 795
- Platinum
electrode, 744, 985, 993, 999, 1005, 1091, 1092, 1100
metals, 757, 808, 816
nanoparticles, 895
- Platinum-based electro-catalysts, 1078
- PM2.5, 1049
- p*-Nitrocoumarin, 908
- p*-Nitrophenols, 950, 1006, 1007
- Polarography, 806, 831, 849, 885, 893, 922
- Polishing, 935
- Pollutants
inorganic, 827
organic, 719–723, 725, 856, 883, 947–948
- Pollution, 719, 725, 729, 751, 781, 881, 883, 913, 923, 937, 939, 942, 944, 983, 999, 1047, 1048, 1051, 1060, 1063, 1064
- Poly(acrylic acid), 773
- Poly(aniline), emeraldine, 767
- Polyaniline (PANI), 767, 768, 772, 1031, 1033–1036, 1088, 1089, 1091
- Polybisphenol-A, 766
- Polycarbonate, 1008, 1035
- Polycrystalline oxide nanowires, 1033
- Polycyclic aromatic amines, 949
- Polycyclic aromatic hydrocarbons (PAHs), 935, 937, 942–945, 955, 1039
- Poly(diallyldimethylammonium chloride), 974
- Polyelectrolyte, 741, 910, 922
- Polyethylenimine, 1089
- Poly(guanine), 974
- Poly(hydroxybenzene), 807
- Poly(isophthalamide diphenylsulphone) (PIDS), 738
- Poly(L-lysine), 741
- Polymer, 731, 738, 739, 742–744, 754, 755, 766–768, 772, 795, 893, 896, 909, 910, 919, 950, 952, 954, 987, 995, 997, 1001, 1007, 1030, 1033–1036, 1039, 1070, 1086–1088, 1091
- Polymeric layer, 1070
- Polymerisation, *in situ*, 1088
- Poly(methylene blue), 742–743
- Poly(methylmethacrylate) (PMMA), 910, 1039
- Polynaphthol, 946
- Polyneuropathy, 982
- Poly(nile blue), 739, 740
- Polyphenol(s), 946, 950, 953, 973
- Polyphenol oxidase (PPO), 950, 953
- Polypyrrole (PPy), 755, 915, 1030, 1031, 1033, 1034, 1036, 1039, 1086–1088, 1094, 1097, 1099, 1100
- Polysiloxane, 730
- Polystyrene, 1101, 1124, 1125
- Polytetrafluoroethylene (PTFE), 736, 745, 1074
- Poly(thiophene), 1030, 1034
- Polyurethane, 910, 1071
- Polyvinyl alcohol, 730, 732, 773, 1005, 1008
- Poly(vinyl chloride) (PVC), 889, 908–919, 988–991
- Poly(vinylpyridine), 816
- Poly (4-vinylpyridine) (PVP), 730, 732
- Pores, 742, 757, 1035
- Porous silicon (PS), 1123
- Porphyrins, 739, 740, 890, 913, 974, 1027, 1031, 1039, 1099
- Portability, 849, 857
- Potassium tetrakis (4-florophenyl) borate, 991
- Potato tissue, 1008
- Potential step, 870
- Potential window, 723, 887, 890, 891, 931, 933, 944, 945, 973, 1074
- Potentiometric detection, 983, 1007
- Potentiometric sensors, 738, 758, 772, 907, 908, 912, 913, 916, 919, 920, 987, 989–991, 1112, 1117, 1129

- Potentiometric stripping analysis (PSA), 788, 802, 813, 843
- Potentiometry, 788, 790, 796, 802, 813, 831, 833, 835, 842–844, 918, 928
- Potentiostatic electrodeposition, 1072, 1080, 1081
- Potentiostatic electrolysis, 782
- PPO. *See* Polyphenol oxidase (PPO)
- PPy. *See* Polypyrrole (PPy)
- p-Quinones, 744
- Precision, 793, 909, 911, 915, 989, 991, 1137, 1141, 1143–1146
- Preconcentration, 783, 784, 786, 787, 799, 800, 810–812, 816, 828, 831, 939, 940, 945, 946, 952, 955, 956, 973, 974
- Preconcentration, adsorptive, 799
- Pretreatment, 885, 895, 932–936, 939, 973, 995, 998, 1000, 1010, 1111
- Printing, 850, 889, 918, 919, 973, 1000, 1001, 1004, 1030, 1033, 1088
- Procaine, 889
- Propazine, 954
- Propionaldehyde, 1005
- Propoxur, 996, 1000
- Propyl gallate, 813
- Protein, 997, 1092
- Proton conductive matrix, 745
- Proximal soil sensors (PSS), 1036
- Prussian blue, 1003
- PSA. *See* Potentiometric stripping analysis (PSA)
- Pseudomonas*
- P. diminuta*, 1005
- P. rathonis*, 923
- Pseudomonas* spp., 1005
- Pseudo reference electrode, 993
- Pt-based alloy electrode, 1129
- PTFE. *See* Polytetrafluoroethylene (PTFE)
- Pulsed Amperometric Detection (PAD), 1091, 1094
- Pulsed-laser deposition, 756
- Pulse radiolysis, 858
- Purpurocatechol, 815
- PVC. *See* Poly (vinyl chloride) (PVC)
- PVP. *See* Poly (4-vinylpyridine) (PVP)
- Pyrene, 935, 943–945
- Pyridin-2-aldoxime methiodide, 988
- 2-Pyridine aldoxime, 988, 1009
- Pyrithione, 896
- Pyrolysis, 943
- Pyrolytic graphite, 809, 831, 860, 888, 889, 892, 1040, 1070, 1073, 1074, 1098
- Q**
- Quartz crystal microbalance (QCM), 1026, 1027, 1070
- Quaternary ammonium salt, 916
- Quercetin, 892
- Quinizarin, 947
- R**
- Radiometer, 1062
- Raman spectroscopy, 933
- Rare earths, 797, 802, 807, 1117, 1119
- Receptor, 982, 997, 1010, 1025
- Recognition, 731, 771, 896, 913, 985, 986, 997, 1010, 1025, 1026, 1039
- Recognition element, 731, 896, 913, 985, 1025, 1026
- Recovery, 772, 793, 895, 896, 921, 941, 946, 993, 999, 1034, 1037, 1072, 1124, 1125, 1137, 1149
- Redox potential, 755, 767, 859, 860
- Reduced graphene oxide (RGO), 1002, 1040, 1091
- Reference electrodes, 736, 739, 746, 752, 754, 763, 770, 772, 909, 914, 917, 919, 948, 989, 993, 1003, 1097, 1113, 1114, 1129, 1130
- Remote sensing, 829
- Repeatability, 764, 788, 802, 813, 831, 891, 1002, 1145
- Representative sampling, 884
- Reproducibility, 724, 731, 761, 762, 788, 793, 802, 813, 831, 886, 917, 939, 955, 996, 997, 1003, 1041, 1093, 1094, 1145
- Residual plots, 1138
- Resolution, 792, 795, 797, 816, 1062, 1087
- Resorcinol, 894, 948
- Respirometer, 732–733
- Respirometer, microfluidic, 732
- Response time, 762, 911, 912, 914–916, 918, 919, 989, 996, 1006–1008, 1034, 1059, 1060, 1086, 1115, 1117, 1119, 1120, 1128
- Rhodium, 722, 755, 808, 816
- Rhodium oxide, 722
- Rifampicine, 887
- Ring, 720–721, 742, 949–951, 1037, 1070
- Robustness, 722, 754, 770, 772, 1011, 1075
- Rodenticide, 981
- Room temperature ionic liquids (RTIL), 1071, 1074–1076
- Rosiglitazone, 886
- Rotating disc, 788, 793, 831

- Rotating ring disc electrodes (RRDE), 720, 721
Ruthenium, 808, 886, 887, 994
Ruthenium oxides (RuO₂), 738, 739, 756, 757
Rutin, 887, 892
- S**
- Salicylic acid, 948
Salinity, 746
Salmonella typhimurium, 950
SAM. *See* Self assembled monolayer (SAM)
Sample pretreatment, 998, 1010
Sample storage, 849
Sampling, 797, 849, 850, 884, 998, 1052
Sarin, 982, 1005, 1024
Saturated calomel electrode (SCE), 724, 783, 786–788, 799–802, 810, 812, 813, 816, 828–831, 849, 922, 948, 1097
Scandium, 797
Scanning electron microscopy (SEM), 857, 864–866, 868, 933, 1038, 1101
Scanning tunnelling microscopy (STM), 829, 859, 933
SCE. *See* Saturated calomel electrode (SCE)
Schiff base, 743, 829
Screen printed, 741, 767, 784, 788, 802, 805, 831, 844, 874, 886, 889, 895, 896, 908, 918–920, 923, 966, 973, 974, 986, 991, 993–995, 997, 999, 1000, 1003–1006, 1009, 1010, 1029, 1033, 1078, 1088
Screen printed carbon electrode (SPCE), 874, 895, 923, 974, 993
Screen printed electrode (SPE), 767, 805, 831, 886, 895, 896, 918–920, 973, 995, 997, 1000, 1009, 1010
Screen printing, 918, 973, 1000, 1004, 1033, 1088
SDS. *See* Sodium dodecyl sulfate (SDS)
Seawater, 783, 785–788, 797–801, 812, 813, 829, 830, 834–836, 846–848, 851, 868–870, 874, 896, 912, 917, 974
Selectivity, 724, 736, 754, 789, 803, 817, 834, 842, 896, 909–911, 913–915, 918, 922, 942, 949, 956, 987, 990, 991, 993, 996, 1001, 1011, 1025, 1028, 1034, 1039, 1077, 1097, 1111, 1121, 1124, 1126, 1128–1130, 1137, 1148
Selenium, 781, 791
Self assembled monolayer (SAM), 886, 997
SEM. *See* Scanning electron microscopy (SEM)
Semiconductors, 737, 738, 765, 770, 1006, 1026, 1033, 1034, 1111, 1118–1123, 1127–1128
Sensitivity, 723, 737, 754, 789, 843, 861, 884, 916, 923, 973, 985, 1025, 1057, 1071, 1113
Sensor(s)
 amperometric, 722, 723, 736, 804, 906, 907, 921–922, 942, 991–1003, 1117
 biological, 1008
 calibration, 1058
 chemical, 756, 1025, 1033, 1034, 1036
 electrical, 766
 electrocatalytic, 1078
 high temperature, 1004
 off line, 945
 on-line, 916, 923
 optical, 1026, 1027, 1034, 1039, 1124
 permeability, 752, 989
 physical, 724, 731
 potentiometric, 738, 758, 772, 907, 908, 912, 913, 916, 919, 920, 987, 989–991, 1112, 1117, 1129
 single-shot, 1078
 in vivo, 770, 771
Sepiolite, 954
Septonex, 800, 811, 919, 922
Serotonine, 1093
SERS. *See* Surface enhanced Raman spectroscopy (SERS)
Shampoo, 896, 941
Shochu, 731
SIA. *See* Sequential injection analysis (SIA)
Signal-to-noise ratio, 1142
Silane, 740, 742
Sildenafil, 887, 889
Silica
 functionalized, 974
 gel, 731, 999, 1007, 1123
 microspheres, 974
 nanoparticle, 742, 743, 764–765
Silicone rubber, 910
Silicon nanoparticles, 1005
Silicon nanowires, 764, 1002
Silver
 amalgam, 802, 813, 893, 896, 973
 clusters, 858
 metallic nanoparticles, 856
 spray, 874
Silver–silver chloride (Ag/AgCl)
 electrode, 752
Single-stranded DNA (ssDNA), 896
Single walled carbon nanotube (SWCNT), 765, 892, 912, 1032, 1037, 1100, 1128
Sintering technique, 1118–1120
Size distribution, 864–866, 868–870
Slope, Nernstian, 739, 910, 911, 914, 917

- Smog, 1023, 1048, 1051
 Soap, 906, 921
 Sodium dodecyl sulfate (SDS), 895, 909, 915, 916, 923, 943, 948, 1037
 Sodium tetraphenyl borate, 908, 911
 Soil, 856, 881, 897, 906, 934, 938, 939, 942, 944, 945, 953, 966, 981–983, 988, 1005, 1006, 1046, 1069
 extracts, 784, 796, 807, 988
 remediation, 906
 Soil sampling, 939, 953, 1071
 Sol, 730, 732, 756, 791, 810, 811, 828, 997, 1027
 Sol-gel, 730, 756, 997, 1027
 Sol-gel route, 756
 Solid electrolyte sensors, 1112–1118, 1128
 Solid phase extraction (SPE), 940, 945, 949, 954, 973
 Solid silver electrode, 887
 Solid state sensors, 914
 Solochrome violet, 802, 807
 Solubility product, 803, 846
 Solution phase growth, 1033
 Soman, 982, 1005
 Sorensen SPL, 751
 SPCE. *See* Screen printed carbon electrode (SPCE)
 SPE. *See* Screen printed electrode (SPE)
 Speciation, 836, 841–851
 Speciation analysis, 841, 842, 850
 Spectrophotometry, 905
 Spin-coating, 1027, 1031, 1037, 1088
 SPR. *See* Surface plasmon resonance (SPR)
 Spray-coating, 1030, 1034
 Sputter deposition, 756
 Sputtering, 756, 850, 1027, 1119, 1120
 Square wave voltammetry (SWV), 802, 831, 885, 886, 888, 939, 949, 966, 973, 974
 ssDNA. *See* Single-stranded DNA (ssDNA)
 Stability constant, conditional, 803, 846
 STM. *See* Scanning tunnelling microscopy (STM)
 Stokes-Einstein equation, 870, 871
 Streptavidin, 896, 989
 Stripping analysis, 782, 788, 789, 796, 802, 803, 813, 831, 835, 843, 849, 863, 885, 896
 Stripping potentiometry, 796, 835
 Stromboli, 1053, 1060, 1061
 Strychnos nux-vomica, 951
 Styrene, 942
 Subsoil, 944
 Sulfate, 895, 906, 909, 910, 913, 916, 943, 948, 1037
 Sulphur, 827, 1047–1064
 Sulfur dioxide (SO₂), 787, 791, 827, 831, 832, 1047–1064, 1095, 1111
 nanorod, 765, 1128
 Sulphate, 832, 834, 836, 1048, 1049, 1052, 1086
 Sulphite, 832, 836
 Sulfonamides, 948
 Sulphur, 827, 1047–1064
 Sulphur compounds, 1047–1064
 Sulfuric acid, 858, 1048, 1049
 Surface acoustic waves (SAW), 1026, 1027
 Surface acoustic wave (SAW) sensors, 1027
 Surface energy, 859, 860
 Surface enhanced Raman spectroscopy (SERS), 1027
 Surface plasmon resonance (SPR), 1026
 Surfactant(s)
 anionic, 906, 908–914, 916, 917, 919, 922, 923
 cationic, 906–908, 911–913, 915, 917, 919, 920, 922
 nonionic, 906–908, 910, 915, 916, 921, 923
 SWCNT. *See* Single walled carbon nanotube (SWCNT)
 SWV. *See* Square wave voltammetry (SWV)
 Synapse, 984
- T**
 Tabun, 1005
 Tannic acid, 846
 Tattoo, 772
 TCNQ. *See* 7,7,8,8-Tetracyanoquinodimethane (TCNQ)
 Teflon[®], 1074
 Tegaserod, 888
 Temperature, 737, 758, 759, 770, 890, 909, 919, 932, 997, 1004, 1006, 1026, 1029, 1030, 1033, 1034, 1036, 1040, 1049, 1058–1060, 1062, 1072, 1074, 1080–1086, 1096, 1097, 1112, 1115, 1120–1123, 1125–1130
 Template(s)
 deposition, 1040
 Terrestrial ecosystems, 942
 Terrorist threats, 966
 Testosterone, 887
 Tetraalkyl ammonium salts, 805
 Tetrabutyl ammonium salts, 922
 7,7,8,8-Tetracyanoquinodimethane (TCNQ), 993, 1000
 Tetracycline, 886, 891, 896
 Tetradecylammonium dodecyl sulfate, 916

- Tetradecyltrimethylammonium ions (TTA⁺), 912
- Tetrahexyldecylammonium dodecylsulfate (THDADS), 916
- Tetrakis (3,5-bis[2-methoxy-hexafluoromethyl] phenyl) borate, 990
- Tetram, 867, 937, 990
- Tetra-*n*-octylammonium bromide (TOAB), 914
- Tetrapentylammonium bromide (TPAB), 922
- Tetraphenylborate, 910, 912, 915, 921, 990
- 1,4,8,11-Tetra(*n*-octyl)-1,4,8,11-tetraazacyclotetradecane, 914
- Textile, 772–773, 923
- Thallium, 781, 792, 918
- Thallium halo complex, 918
- Theophylline, 892
- Thermistors, 1026
- Thick film, 738, 889, 919, 973, 1000, 1029, 1033, 1036
- Thin film, 744, 756, 761, 763, 764, 772, 793, 850, 918, 932–933, 935, 955, 1006, 1026–1028, 1030, 1033–1036, 1088, 1092–1094
- Thin film electrode, 932–937
- Thin layer
cell, 941
chromatography, 905
- Thiocholine, 951, 985, 986, 992, 993, 999, 1001, 1002
- Thiocyanate, 911
- Thiol(s), 816, 893, 896, 992
- Thyroid receptor, 982
- Tin, 755, 756, 768, 808, 814, 817, 858, 1030
- Tinidazole, 885
- Thioureas, 1004
- Tissues, 772, 781, 790, 796, 809, 897, 1007–908, 1093, 1096
- Titanates, 758–760
- Titania, 722, 739, 761
- Titania nanotubes, 761
- Titanium, 722, 761, 797, 807, 1088
- Titration, 829, 905, 907–913, 915–921, 991
- TOAB. *See* Tetra-*n*-octylammonium bromide (TOAB)
- Toluene, 923, 944, 1023, 1024, 1027, 1029–1031, 1040
- Toluene sulfonate, 923
- Total organic carbon (TOC), 726
- Total volatile bases (TVB), 1095
- Toxic gases, 827, 1049–1051, 1126
- Toxic heavy metals, 783
- Toxins, 985, 1025
- Trace metals, 1051
- Transducers, 983, 985–989, 995, 997, 1006, 1007, 1025
- Transduction, 986, 1006, 1025–1027
- Trazodone, 886
- Triamcinolone acetonide (TAA), 885
- Triazine, 909, 967, 970
- Trichlorfon, 988, 994
- 2,4,6-Trichlorophenols, 938, 950, 952
- Trichosporon cutaneum, 730–732
- Triclosan, 895
- Tricresyl phosphate, 805, 810, 813, 814, 831, 835, 918, 951, 953
- 2,4,6-Tri(3,5-dimethylpyrazoyl)-1,3,5-triazine, 909, 970
- Tridodecylamine, 988
- Tridodecylmethylammonium chloride (TDMAC), 910–911
- (3-Aminopropyl)triethoxysilane, 942, 974
- Trifluoperazine, 892
- Trihalomethanes (THMs), 887, 896
- Triheptyldodecylammonium iodide (THDAI), 916
- 2,4,5-Trihydroxytoluene, 950
- Trimetazidine, 888
- Trimethoprim, 887
- Trimethylamine (TMA), 1031, 1032, 1093, 1095, 1096
- 1,3,5-Trimethylbenzene, 944
- Trimethylborane, 932
- Trinitrobenzene, 911, 972, 974
- Trinitrobenzene sulfonate, 911
- 2,4,6-Trinitrotoluene, 966, 973–975
- Trinitrotoluene (TNT), 966, 967, 973–975, 1024
- Trioctylhydroxybenzene sulphonic acid, 911
- Triphenylene, 974
- Tritolyl phosphate, 916
- Triton X[®], 846
- Tropolone, 788, 813, 815
- Troposphere, 1051, 1059
- Trueness, 1137, 1146–1147, 1149
- Turrialba volcano, 1054, 1061
- Tween 80, 943
- Two-electrode cell, 1075
- Tyrosinase, 942, 950, 952, 983, 984, 1004–1005
- Tyrosinase (phenol oxidases), 950, 953

U

- Uncertainty, 1137, 1141, 1142, 1147–1148
- Unmanned aerial vehicle, 1047, 1061
- Uranium, 808, 809, 817

Uranyl ion, 815
Urban environments, 1063
UV irradiation, 796, 845

V

Vacuum evaporation, 988
Valinomycin, 755
van der Waals forces, 804, 997
Vanadium, 797, 807, 849
Vanganciclovir, 892
Vapor deposition, 722, 890, 932, 1033, 1040
Vinclozolin, 895
4-Vinylpyridine, 730, 732
Vitamin B₁₂, 741
VOCs. *See* Volatile organic compounds (VOCs)
Volatile aliphatic amines, 1096
Volatile organic compounds (VOCs), 1023–1041
Volcanic emissions, 855, 1047, 1051, 1052, 1060–1061
Volcano, 1047, 1048, 1051–1054, 1056–1058, 1060–1064
Volgonat, 923
Voltammetric sensors. *See* Sensor(s)
Voltammetry, 725, 741, 788, 794, 843, 857, 885, 921, 943, 966, 1000, 1034, 1074
VX, 1005

W

Wall-jet, 799
Wang, J., 965–975, 1006
Washing powder, 835, 909
Wastewater, 719, 720, 724, 731, 732, 735, 736, 784, 881, 883, 884, 886, 891, 894–896, 911, 923, 932, 938, 940, 941, 944, 945, 1007, 1049, 1070, 1088, 1091

Water, 719, 729, 735, 751, 783, 785, 845, 856, 881, 906, 932, 974, 981, 1037, 1049, 1069, 1112
Water pollution, 937
Wetting agent, 906
WHO. *See* World Health Organization (WHO)
Working electrode, 730, 736, 745, 746, 752, 763, 770, 782, 788, 789, 792, 809, 831, 843, 844, 921, 949, 996, 1003, 1009, 1050, 1074
World Health Organization (WHO), 939, 942–944, 946, 947, 955, 1049

X

Xenoestrogens, 941, 951
XPS. *See* X-ray photoelectron spectroscopy (XPS)
X-ray diffraction analysis, 933
X-ray photoelectron spectroscopy (XPS), 1123
Xylenes, 908, 942, 1023, 1024, 1029, 1030

Y

Yeast, 731, 732
YSZ. *See* Yttria stabilized zirconia (YSZ)
YSZ solid electrolyte, 1129
Yttria stabilized zirconia (YSZ), 1097, 1113, 1114, 1129–1131

Z

Zeolite, 742, 829, 894
Zero-current, 790, 833, 842
Zero-current measurement, 790, 833
Zinc, 755, 781, 792, 1004
Zinc oxide, 756, 761–762
Zirconia, 755, 1097, 1113
ZnO nanopencils, 1071, 1087